Site-specific Amplification Factors at Strong Motion Stations in Western US

Collaborative Effort Between GATech and the USGS Pasadena Office

Final Report Grant Award G11AP20052: 02/01/2011-07/31/2012

Dominic Assimaki*[1] Jian Shi†[1] Alan Yong‡[2]

[1]School of Civil and Environmental Engineering, Georgia Institute of Technology
[2]Earthquake Hazards Program, U.S.G.S. Pasadena Office

December 31, 2012

*dominic@gatech.edu; (404) 894-8598
†shijian@gatech.edu; (404) 894-8598
‡yong@usgs.gov; (626) 583-7816

Contents

1 Introduction **6**

2 Soil profiles, nonlinear properties and site response analyses **7**

2.1 Soil Profiles . . . 7

2.2 Estimation of 100 m shear wave velocity profiles . . . 8

2.2.1 Curve fitting: model selection . . . 9

2.2.2 Curve fitting: least square method . . . 9

2.2.3 Extrapolation . . . 11

2.3 Nonlinear dynamic soil properties . . . 12

2.4 H/V ratios from microtremor recordings . . . 14

2.5 Linear site-specific amplification factors . . . 16

2.6 Equivalent linear site response analyses . . . 17

2.7 Nonlinear analyses: Monotonic stress-strain response and hysteretic behavior . . . 18

2.8 NGA database strong ground motions . . . 20

3 Conclusions - Future Work **20**

Bibliography **23**

4 Results **25**

4.1 Class D . . . 27

4.1.1 CE.11023 . . . 28

4.1.2 CE.11625 . . . 31

4.1.3 CE.11684a . . . 34

4.1.4 CE.11684b . . . 37

4.1.5 CE.11684c . . . 40

4.1.6 CE.12076 . . . 43

4.1.7 CE.12108 . . . 46

4.1.8 CE.12952 . . . 49

4.1.9 CE.14241 . . . 52

4.1.10 CE.14395 . . . 55

4.1.11 CE.23958 . . . 58

4.1.12 CE.24965 . . . 61

4.1.13 CE.24967 . . . 64

4.1.14 CI.BAK . . . 67

4.1.15 CI.BBS 70
4.1.16 CI.BHPa 73
4.1.17 CI.BHPb 76
4.1.18 CI.BOMa 79
4.1.19 CI.BOMb 82
4.1.20 CI.BOMc 85
4.1.21 CI.CAR 88
4.1.22 CI.CHN 91
4.1.23 CI.DRE 94
4.1.24 CI.ERR 97
4.1.25 CI.LCPa 100
4.1.26 CI.LCPb 103
4.1.27 CI.MSJ 106
4.1.28 CI.NJQa 109
4.1.29 CI.NJQb 112
4.1.30 CI.NJQc 115
4.1.31 CI.RCT 118
4.1.32 CI.SAL 121
4.1.33 CI.SAN 124
4.1.34 CI.SIO 127
4.1.35 CI.SMM 130
4.1.36 CI.SMV 133
4.1.37 CI.TFT 136
4.1.38 CI.USB 139
4.1.39 CI.WES 142
4.1.40 NC.JELB 145
4.2 Class D/C 148
4.2.1 CE.12149 149
4.2.2 CE.13100 152
4.2.3 CE.24029 155
4.2.4 CI.ALP 158
4.2.5 CI.BBR 161
4.2.6 CI.CBC 164
4.2.7 CI.CRP 167

4.2.8 CI.GATRa . . . 170
4.2.9 CI.GATRb . . . 173
4.2.10 CI.LUGa . . . 176
4.2.11 CI.LUGb . . . 179
4.2.12 CI.MIKa . . . 182
4.2.13 CI.MIKb . . . 185
4.2.14 CI.NSS2a . . . 188
4.2.15 CI.NSS2b . . . 191
4.2.16 CI.NSS2c . . . 194
4.2.17 CI.PLC . . . 197
4.2.18 CI.RSBa . . . 200
4.2.19 CI.RSBb . . . 203
4.2.20 CI.SHOa . . . 206
4.2.21 CI.SHOb . . . 209
4.2.22 CI.SLBa . . . 212
4.2.23 CI.SLBb . . . 215
4.2.24 CI.VOG . . . 218
4.3 Class C . . . 221
4.3.1 CE.13096 . . . 222
4.3.2 CE.13099 . . . 225
4.3.3 CE.13929 . . . 228
4.3.4 CE.23063a . . . 231
4.3.5 CE.23063b . . . 234
4.3.6 CE.23063c . . . 237
4.3.7 CE.24644a . . . 240
4.3.8 CE.24644b . . . 243
4.3.9 CI.ADO . . . 246
4.3.10 CI.BLA . . . 249
4.3.11 CI.CAC . . . 252
4.3.12 CI.CCC . . . 255
4.3.13 CI.CGO . . . 258
4.3.14 CI.CTC . . . 261
4.3.15 CI.CWC . . . 264
4.3.16 CI.DAN . . . 267

4.3.17 CI.DNR . . . 270
4.3.18 CI.DVT . . . 273
4.3.19 CI.FHO . . . 276
4.3.20 CI.FUR . . . 279
4.3.21 CI.GORa . . . 282
4.3.22 CI.GORb . . . 285
4.3.23 CI.GORc . . . 288
4.3.24 CI.GRAa . . . 291
4.3.25 CI.GRAb . . . 294
4.3.26 CI.IDO . . . 297
4.3.27 CI.JVA . . . 300
4.3.28 CI.LDF . . . 303
4.3.29 CI.LDR . . . 306
4.3.30 CI.LPC . . . 309
4.3.31 CI.NBS . . . 312
4.3.32 CI.RRX . . . 315
4.3.33 CI.SYP . . . 318
4.3.34 CI.THM . . . 321
4.3.35 CI.VCS . . . 324
4.3.36 NC.HCABa . . . 327
4.3.37 NC.HCABb . . . 330
4.3.38 NC.JSFB . . . 333
4.3.39 NC.PHOB . . . 336
4.3.40 NC.PHSB . . . 339
4.4 Class C/B . . . 342
4.4.1 CI.GLAa . . . 343
4.4.2 CI.GLAb . . . 346
4.4.3 CI.GLAc . . . 349
4.4.4 CI.GLAd . . . 352
4.4.5 CI.HEC . . . 355
4.5 Class B . . . 358
4.5.1 CI.BEL . . . 359
4.5.2 CI.IRM . . . 362
4.6 Class B/A . . . 365

4.6.1 CI.PDM 366

Abstract

We compile H/V ambient vibration inversion data at strong motion station sites in Southern California with generic nonlinear soil properties for typical sedimentary deposits, and develop nonlinear site-specific amplification factors for implementation in ground motion simulations. Until recently, limited information existed on the soil properties and amplification effects at many of the strong motion stations in Western US. Geotechnical characterization of a large number of station sites has recently taken place as part of an ongoing effort led by the USGS. To date, site classification of a large number of station sites has been completed based on the average shear wave velocity to a depth of 30 m (V_{s30}). While V_{s30} provides a quantitative measure of the soil stiffness, however, it does not reflect the profile susceptibility to nonlinear effects during strong seismic shaking. Goal of our study is to improve the existing parameterization of nonlinear amplification factors for site-specific conditions at SC strong motion stations. We have archived available geotechnical information at more than 100 sites, conducted site-specific response analyses by means of linear, equivalent linear and validated nonlinear models available on the SCEC Broadband Simulation Platform, and computed nonlinear amplification factors for a large number of ground motions harvested from the NGA strong motion database. Our work in progress seeks to complement the existing measures of site stiffness (V_{s30}) and motion intensity (PGA) with measures of soil-bedrock impedance contrast and incident motion frequency content.

1 Introduction

Seismogram data recorded at strong motion stations in California and the Pacific North-west are invaluable for studies on seismic sources, regional wave propagation, and earthquake emergency response. Seismic monitoring in these regions is also critical for validation and refinement of ground motion models, leading to improved predictions of future earthquake scenarios. High frequency components of seismic waveforms, however, which control the response of civil infrastructure, are significantly affected by the response of near-surface soil layers. Therefore, when strong motion recordings are used for the development and refinement of broadband earthquake simulations, site effects need to be properly accounted for to allow integration of the ground motion predictions in hazard assessment and mitigation studies by the earthquake engineering and seismological communities alike.

Until recently, limited information existed on the soil properties and amplification effects at many of the strong motion stations in Western US. Acknowledging the critical role of nonlinear site response for inversion and prediction of broadband ground motions, geotechnical characterization of a large number of station sites has taken place as part of an ongoing effort led by the USGS. To date, site classification of a large number of station sites has been completed based on the average shear wave velocity to a depth of 30 m (V_{s30}). While V_{s30} provides a quantitative measure of the soil stiffness, however, it does not reflect the profile susceptibility to nonlinear effects during strong seismic shaking. Furthermore, empirical amplification factors that have been computed for a large number of stations are primarily based on weak seismic motions, thus reflecting the linear response of the sediments.

Realistic predictions of the response of soft sediments to strong ground motion, however, may only be achieved via nonlinear analyses. The limited guidance on the selection of site response model and associated input soil parameters, however, have been identified as the main sources of uncertainty in the

high-frequency range of ground motion predictions, and have in turn hindered the integration of nonlinear analyses in ground motion models.

Through this project, we seek to reduce the uncertainties associated with predictions of nonlinear site effects at strong motion station sites in the Western US. We compile available geotechnical information at selected station sites, conduct site-specific response analyses by means of approximate and nonlinear models, study the modeling uncertainty in site amplification, and identify the model and input parameters that most effectively represent nonlinear site response at the corresponding locations. We will next complement the empirical site amplification factors at the selected stations with synthetic factors computed by means of validated nonlinear models. Results indicate the sites where nonlinear effects are anticipated to be critical, and provide improved measures of site response.

The report is organized in two parts. First, we describe the methodology, assumptions, approximations and algorithms implemented for the evaluation of amplification factors at strong motion stations in Western US. Next, the stations are classified in accordance to their V_{s30}-based NEHRP site classifications (*NEHRP*, 2004; *Frankel et al.*, 2002; *Dobry et al.*, 2000). For each site class, we present the ensemble of soil profiles, and successively the empirical, and computed linear, equivalent linear and nonlinear amplification factors at each station. For stations where more than one ambient noise inversion was conducted, we compute the amplification factors separately for each measurement location to illustrate the propagation of spatial variability of soil properties to the estimation of amplification factors.

Amplification factors are computed using ground motion recordings from the NGA strong motion database, selected to span a wide range of magnitudes and distances. For each station, we compute two groups of site amplification factors per site response algorithm. The first one uses the incident NGA ground motions (half the rock-outcrop amplitude) and results are plotted as a function of PGA on rock-outctop ($\mathrm{PGA_{RO}}$). For the second, we scale all ground motions to the same $\mathrm{PGA_{RO}}$, $0.5g$ (~ 4.9 m/s^2), and plot the amplification factors as a function of the ratio of the central frequency of the ground motion to the fundamental frequency of the site (f_c/f_0). The latter reveals the deficiency of the currently established ground motion prediction equations to account for resonant phenomena in site response: two ground motions of identical PGA at one site do not necessarily elicit the same intensity of nonlinear effects, precisely due to differences in the frequency content. We note, however, that the normalized frequency we implement in this report fails in some cases to represent the effects of frequency, especially at sites with slow variation of stiffness with depth, i.e., sites with low soil-rock impedance contrast. Current and ongoing work is focused on identifying a better index to reflect the effects of site resonance using, among others, the strong motion recordings of the Japanese Strong Motion Network KiK-Net.

2 Soil profiles, nonlinear properties and site response analyses

2.1 Soil Profiles

The soil profiles used in this report were evaluated as part of the AARA-funded V_{s30} measurements at California and Central Eastern US strong motion stations, effort of the USGS. Soil layer thicknesses and shear wave velocities (V_s) were extracted from the corresponding USGS Open-File Report (*Yong et al.*, 2012),

while the low-strain damping ratio and soil mass density for each layer were determined using the following criteria:

- Damping ratio
  - when $V_s < 250$ m/s, damping ratio = 0.05
  - when 250 m/s $\leqslant V_s < 750$ m/s, damping ratio = 0.02
  - when $V_s \geqslant 750$ m/s, damping ratio = 0.01
- Mass density
  - when $V_s < 200$ m/s, mass density = 1.6 g/cm^3
  - when 200 m/s $\leqslant V_s < 800$ m/s, mass density = 1.8 g/cm^3
  - when $V_s \geqslant 800$ m/s, mass density = 2.0 g/cm^3

At some sites (for example, CE.11684), ambient noise inversion was conducted at multiple locations in the vicinity of the station, and as a result, more than one V_s profile were available in the USGS report. The V_s profiles of adjacent locations are similar but not identical, attributed to the natural spatial variability of sedimentary sites. When encountering such sites, this report uses notations such as "CE.11684a", "CE.11684b" and "CE.11684c" to distinguish between the various V_s profiles as opposed to estimating an average profile at the station.

2.2 Estimation of 100 m shear wave velocity profiles

Overarching goal of this work is the development of site-specific amplification factors at strong motion stations in the US for validation and prediction of physics-based earthquake simulations. At this time, perhaps the most well monitored and documented region in the US in terms of its crustal structure and fault system is Southern California. This information is integrated in the Southern California Broadband Ground Motion Simulation platform, and used for dynamic rupture scenaria simulations in the Los Angeles Basin. In the SCEC crustal velocity model, the soil layers are represented by a homogeneous elastic layer of 100 m thickness, and site amplification is accounted for via generic soil amplification factors evaluated as a function of the NEHRP site class at the station and PGA on rock outcrop. In this study, we seek to replace the generic amplification factors currently implemented with site-specific amplification factors, improve the currently established parameterization (V_{s30} and $\mathrm{PGA_{RO}}$), and develop a database that can be used in ground motion validation and simulation studies in Southern California.

Prompted by the existing structure of the crustal velocity model, we evaluate the amplification functions for 100 m soil profiles by extrapolating the near surface structure. The extrapolation is based on the station's NEHRP site class and its H/V ambient noise inverted velocity profile as described in *Yong et al.* (2012). The curve fitting and extrapolation criteria and algorithms are described in the foregoing sections.

Layer #	Depth of Layer Top (m)	Thickness (m)	z (m)	V_s (m/s)
1	0	2	1	151
2	2	2	3	146
3	4	2	5	162
4	6	5	8.5	214
5	11	8	15	223
6	19	12	25	255
7	31	–	37	301

Table 1: An example of measured V_s profile — CE.11023 (NEHRP class D)

2.2.1 Curve fitting: model selection

A bounded analytical shear wave velocity expression, proposed by *Vrettos* (1996), is chosen as the curve fitting model,

$$V_s(z) = V_{s0} + (V_{s\infty} - V_{s0})(1 - \mathrm{e}^{-kz}) \tag{1}$$

where V_{s0} represents the shear wave velocity at the ground surface, $V_{s\infty}$ is the upper bound of shear wave velocity (i.e., the shear wave velocity at infinite depth), and k is a positive constant defining the velocity gradient to be determined via curve fitting.

To employ curve fitting, we first select the available near surface shear wave velocity profile (an NEHRP class D site profile is shown in Table 1 and Figure 1 as an example), and use the velocity of the top layer as V_{s0}. Since the H/V ambient noise resolution yields the soil structure to a maximum depth of 30 m approximately, $V_{s\infty}$ cannot be determined solely by the near-surface velocity. For this purpose, we supplement the existing near-surface profile with a generic shear wave velocity profile corresponding to the station's site class as proposed by *Silva et al.* (1998) (see Figure 2). We next calibrate the generic profile's V_{s30} (obtained by averaging the upper and lower bounds of V_{s30} of class D, see Table 2) to match the inverted site-specific V_{s30} of the site, obtaining the V_s at 150 m depth of the example site, and assign this shear wave velocity as the extrapolated $V_{s\infty}$:

$$\frac{V_{s30}^{\langle \text{example} \rangle}}{V_{s30}^{\langle \text{example} \rangle}} = \frac{V_{s\infty}^{\langle \text{example} \rangle}}{V_{s\infty}^{\langle \text{generic} \rangle}}$$

thus

$$V_{s\infty}^{\langle \text{CE.11023} \rangle} = \frac{V_{s30}^{\langle \text{CE.11023} \rangle}}{V_{s30}^{\langle \text{Class-D} \rangle}} V_{s\infty}^{\langle \text{Class-D} \rangle} = \frac{212}{279} \times 605 = 460 \text{ m/s}$$

Having obtained both V_{s0} and $V_{s\infty}$ at each station, we then employ least squares curve fitting to obtain the proper value of k.

2.2.2 Curve fitting: least square method

Rearranging Equation (1) yields

$$k \cdot z = \ln\left(\frac{V_{s\infty} - V_{s0}}{V_{s\infty} - V_s}\right) \stackrel{\text{def}}{=} y \tag{2}$$

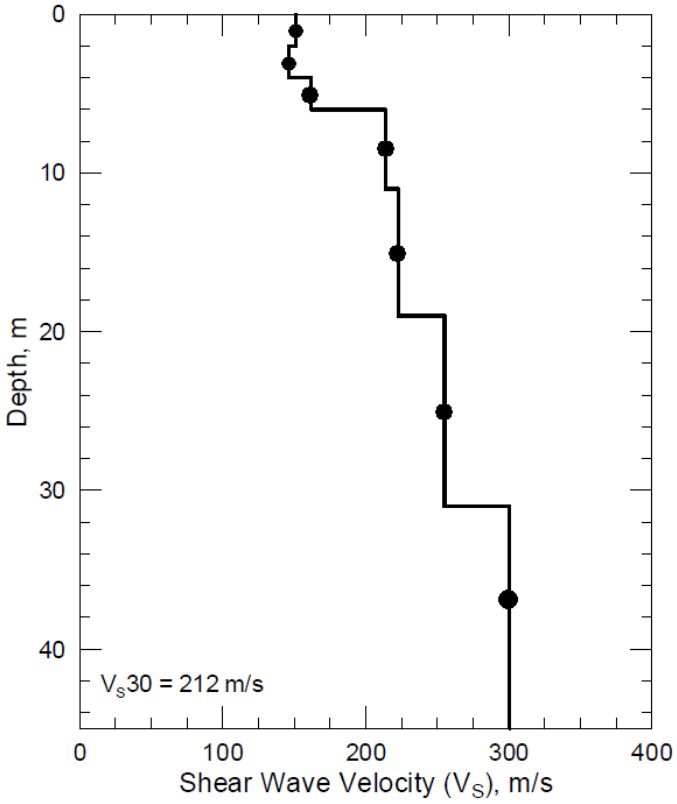

Figure 1: Shear wave velocity profile of the example site (CE.11023)

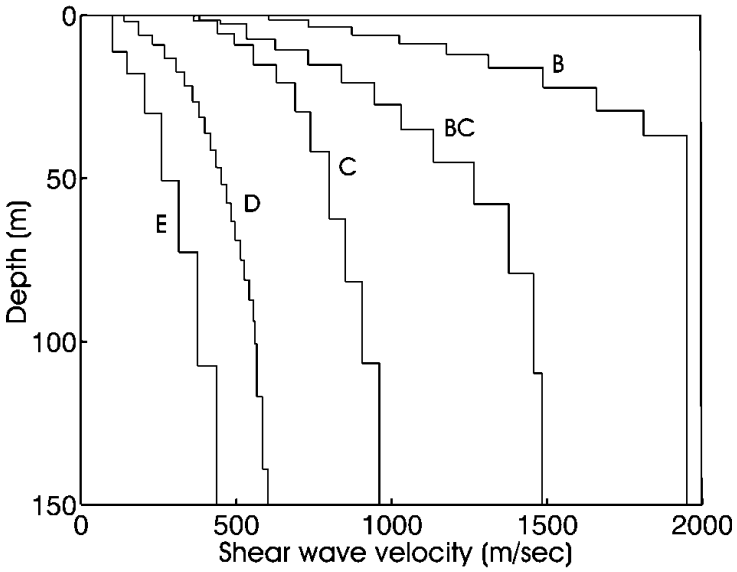

Figure 2: Average shear wave velocity profiles to 150 m depth for sites with midrange NEHRP site classifications (*Silva et al.*, 1998)

NEHRP Site Class	Description	V_{s30} (m/s)
A	Hard rock	>1500
B	Rock	760–1500
C	Very dense soil/soft rock	360–760
D	Stiff soil	180–360
E	Soft soil	<180

Table 2: NEHRP Site Classifications (*Dobry et al.*, 2000)

which becomes a simple linear least squares curve fitting problem. Note that z in Equation (2) should not be the "depth of layer top" as in Table 1, otherwise the result of curve fitting would be biased such that the whole V_s distribution becomes larger than reality. A convenient and practical way to avoid this is to use midpoint depths of every layer as z's, as shown in Table 1 and Figure 1. There is no "midpoint depth" for the last measured layer (i.e., Layer 7 in Table 1), so just assume this layer has the same thickness as the penultimate one. In some sites, there are certain layer(s) with V_s less than that of the layers above them, as for example the second layer of Site CE.11023 (in Figure 1), typically a result of overconsolidation at the corresponding site. We define such layers as "outliers" and exclude them from curve fitting.

The sum of squared residuals is

$$\Gamma = \sum_{i=1}^{n}\left(\ln\left(\frac{V_{s\infty i} - V_{s0i}}{V_{s\infty i} - V_{si}}\right) - kz_i\right)^2 \stackrel{\text{def}}{=} \sum_{i=1}^{n}(y_i - kz_i)^2 \tag{3}$$

In order for Γ to reach minimum, $\partial\Gamma/\partial k$ has to reach 0:

$$\frac{\partial\Gamma}{\partial k} = \frac{\partial}{\partial k}\left(\sum_{i=1}^{n}(y_i^2 - 2kz_i + k^2 z_i^2)\right) = 2\sum_{i=1}^{n}(kz_i^2 - y_i z_i) = 0 \tag{4}$$

thus

$$k = \frac{\sum_{i=1}^{n} y_i z_i}{\sum_{i=1}^{n} z_i^2} \tag{5}$$

Substitution of values of z's and V_s's from Table 1 into Equation (5) yields $k = 0.017697$. Therefore the analytical expression of shear wave velocity of Site CE.11023 is

$$V_s(z) = 151 + (460 - 151)(1 - \mathrm{e}^{-0.017697z}) \quad \text{(unit: m/s)} \tag{6}$$

The curve for Equation (6) and the measured profile are shown in Figure 3.

2.2.3 Extrapolation

Once curve fitting is complete, we can then extrapolate the velocity profile beyond the H/V inversion resolution depth to 100-meter depth, by discretizing the continuous shear wave velocity function Equation (6).

For simplicity, the newly constructed layers all have a thickness of 5 m, and let the layer top and bottom depths be multiples of 5. The shear wave velocity of each layer is the velocity of the layer's midpoint depth, i.e., $V_s = V_s|_{z=(z_{\text{top}}+z_{\text{bottom}})/2}$. To ensure compatibility between the extrapolated profile and the measured

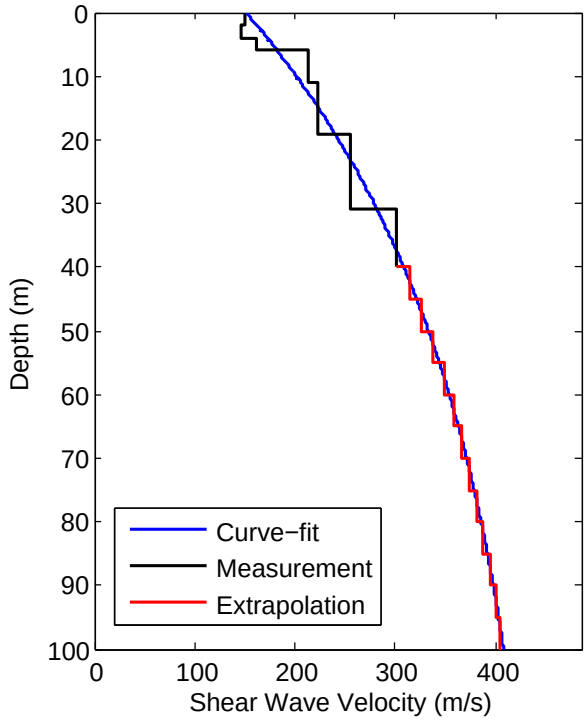

Figure 3: Result of curve fitting and extrapolation (CE.11023)

profile, the extrapolation shall start only when the first constructed layer's shear wave velocity exceeds the last measured velocity.

There exists quite a few sites in which the last measured V_s, or sometimes the last two measured velocities, is very large that they exceed the $V_{s\infty}$ of this site. We thus consider that the rock layer is reached in the measurement. In such cases, because the model of soil layers overlaying a homogeneous rock half-space is assumed, no extrapolation is necessary—we just extend the V_s of the rock layer to 100-meter depth.

The extrapolated velocity profile is shown in Figure 3, in which the analytical velocity curve and the original measured profile are also plotted.

2.3 Nonlinear dynamic soil properties

We next select the nonlinear dynamic soil properties at each site (i.e., modulus reduction and material damping curves) in accordance to the Ph.D. dissertation of *Darendeli* (2001, pp. 220–272). According to the study, soil modulus reduction is idealized as follows,

$$\frac{G}{G_{\max}} = \frac{1}{1 + \left(\frac{\gamma}{\gamma_r}\right)^a} \tag{7}$$

where G is the shear modulus of soil at strain γ, $G_{\max}$ is the initial (i.e., small-strain) shear modulus, a is the curvature coefficient describing the shape of $G/G_{\max}$ curve,

$$a = \phi_5$$

and γ_r in Equation (7) is the reference strain,

$$\gamma_r = \left(\phi_1 + \phi_2 \cdot \mathrm{PI} \cdot \mathrm{OCR}^{\phi_3}\right) \cdot \overline{\sigma_0}^{\phi_4}$$

where PI is the soil's plastic limit, OCR is the soil's over-consolidation ratio, and $\overline{\sigma_0}$ is the soil's effective vertical stress.

And the damping of soil is determined as follows,

$$D_{\text{adjusted}} = b \cdot \left(\frac{G}{G_{\max}}\right)^{0.1} \cdot D_{\text{Masing}} + D_{\min} \tag{8}$$

where D_{adjusted} is the damping ratio corresponding to the normalized shear modulus, $G/G_{\max}$, at strain γ, $D_{\min}$ is the small-strain material damping ratio,

$$D_{\min} = \left(\phi_6 + \phi_7 \cdot \mathrm{PI} \cdot \mathrm{OCR}^{\phi_8}\right) \cdot \overline{\sigma_0}^{\phi_9} \cdot (1 + \phi_{10} \cdot \ln f)$$

in which f is the representative loading frequency. In Equation (8), b is a scaling coefficient,

$$b = \phi_{11} + \phi_{12} \cdot \ln N$$

where N is the number of loading cycles. D_{Masing} in Equation (8) is the Masing damping ratio, defined as

$$D_{\text{Masing}} = c_1 D_{\text{Masing},a=1.0} + c_2 \left(D_{\text{Masing},a=1.0}\right)^2 + c_3 \left(D_{\text{Masing},a=1.0}\right)^3$$

where

$$\begin{aligned}
D_{\text{Masing},a=1.0} &= \frac{100}{\pi}\left[4 \cdot \frac{\gamma - \gamma_r \ln\left(\frac{\gamma+\gamma_r}{\gamma_r}\right)}{\frac{\gamma^2}{\gamma+\gamma_r}} - 2\right] \\
c_1 &= -1.1143a^2 + 1.8618a + 0.2523 \\
c_2 &= 0.0805a^2 - 0.0710a - 0.0095 \\
c_3 &= -0.0005a^2 + 0.0002a + 0.0003
\end{aligned}$$

Values of the ϕ coefficients are as follows,

$$\begin{array}{llll}
\phi_1 = 0.0352 & \phi_2 = 0.0010 & \phi_3 = 0.3246 & \phi_4 = 0.3483 \\
\phi_5 = 0.9190 & \phi_6 = 0.8005 & \phi_7 = 0.0129 & \phi_8 = -0.1069 \\
\phi_9 = -0.2889 & \phi_{10} = 0.2919 & \phi_{11} = 0.6329 & \phi_{12} = -0.0057
\end{array}$$

According to the equations above, soil properties such as PI and OCR, the loading conditions such as f, N and $\overline{\sigma_0}$ collectively determine the soil's damping ratio and shear modulus. The following assumptions are followed in this work in absence of a more detailed site-specific characterization at the strong motion station sites:

- PI of soil: 20%, for all layers;
- OCR of soil: 1.0, for all layers;
- N: 10 (cycles)

- f: 1 Hz
- We also disregard the water table in absence of more detailed information and therefore use total stress instead of effective stress to estimate overburden stress.

As can be readily seen from above, the only factor which affects the modulus reduction and damping curves is the soil's effective overburden stress. For each site, effective overburden stresses at the center points of each layer are calculated to obtain layer-specific modulus reduction and damping curves. The curves for Site CE.11023 are shown in Figures 4 and 5, from which we can see that the material stiffness increases and the energy absorbed per amplitude of cyclic strain decreases with the increase of overburden stress.

2.4 H/V ratios from microtremor recordings

The following steps are employed in the calculation of H/V ratio from microtremor recordings. Data processing algorithms in *Nakamura* (1989), *Theodulidis et al.* (1996), *Konno and Ohmachi* (1998), and *Yong et al.* (2012) were integrated herein to develop the following H/V estimate protocol.

1. Discard the first 15 minutes of the microtremor recording as warming-up process.
2. Use wavelet decomposition to exclude low frequency noise in the raw recordings. Discrete Meyer wavelets of decomposition level 8 were used for this purpose. Next, exclude the approximation (i.e., lowest frequency component), and reconstruct the signal. Repeat the process for all 3 channels (east-west, north-south and vertical). The filtering effects of wavelet decomposition are shown in Figure 6.
3. High-pass the signal (0.3 Hz).
4. Use 2-minute window to split the original signal into multiple sub-signals—do this to all 3 channels.
5. Taper all sub-signals with 95% Tukey window.
6. Perform fast-Fourier transforms on all three channels of all sub-signals, obtaining EW, NS and UD Fourier spectra.
7. Perform vector-summation of EW and NS Fourier spectra, obtaining the horizontal Fourier spectrum.
8. Compute the HVR, i.e., the ratio of horizontal to vertical spectra, and then smooth the HVR output using Konno-Ohmachi smoothing windows (smoothing parameter $b = 40$). Repeat for all sub-signals.
9. Calculate the geometric mean of HVR and standard deviation of $\log_{10}(\text{HVR})$, denoted σ, at all frequencies.
10. Plot the H/V ratios (geometric mean and upper/lower standard deviation envelopes). Upper/lower STD envelopes are defined as:

$$\text{Upper envelope} = \text{Mean HVR} \times 10^{\sigma}$$
$$\text{Lower envelope} = \text{Mean HVR} \div 10^{\sigma}$$

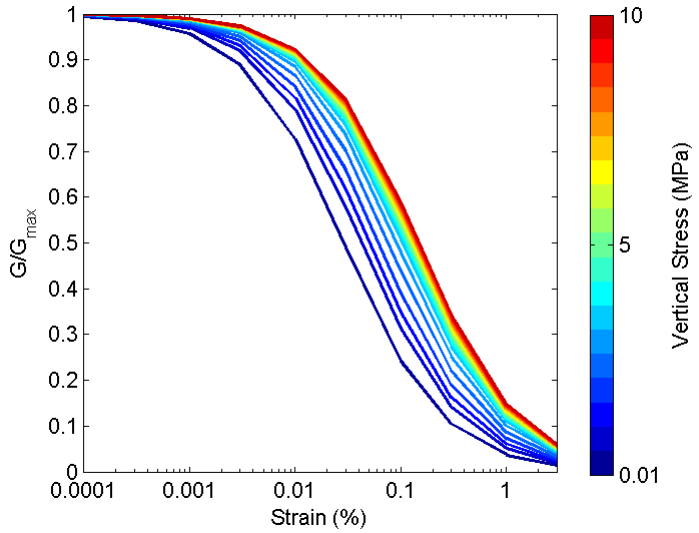

Figure 4: Modulus reduction curves of all 19 layers of Site CE.11023

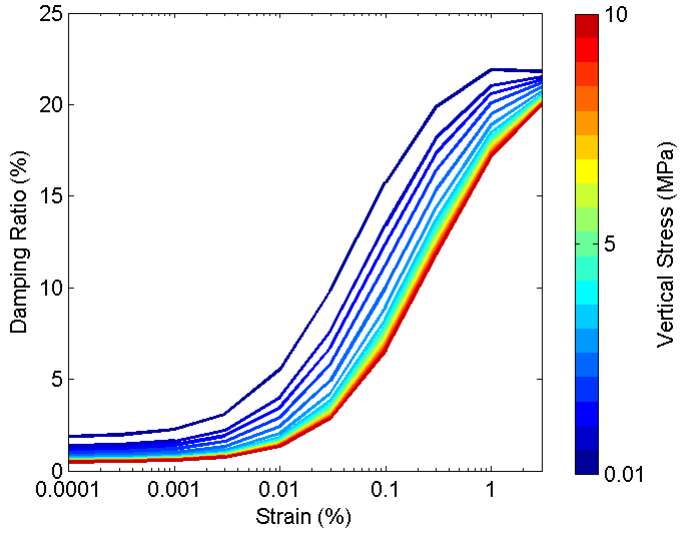

Figure 5: Damping ratio curves of all 19 layers of Site CE.11023

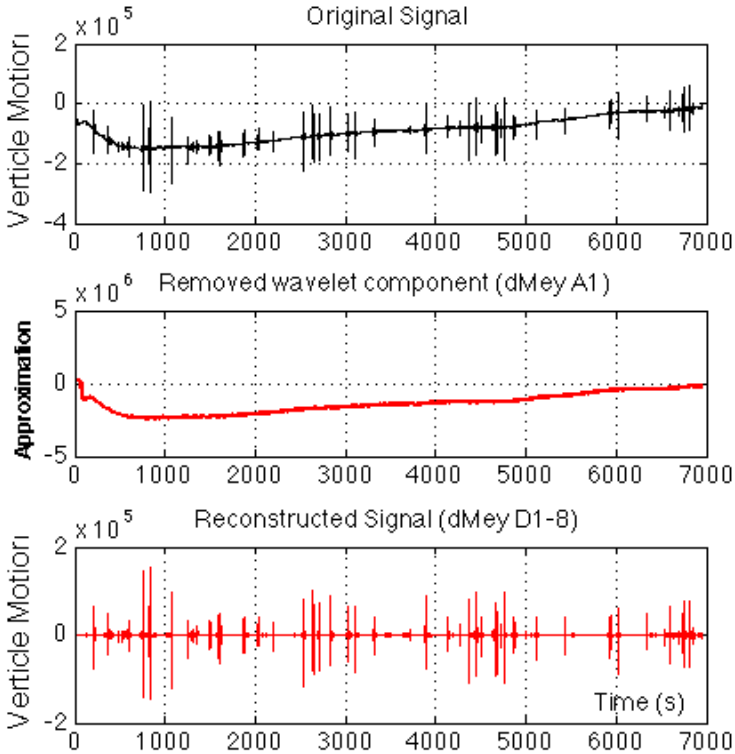

Figure 6: Effect of wavelet decomposition filtering

We next describe the algorithms used to compute the elastic and inelastic site specific response at each station. Results are plotted separately for each site class and station, and H/V empirical data are compared to the computed linear and nonlinear site amplification functions. Future extension of this work involves comparison of the frequency corresponding to the peak of the H/V function to the fundamental frequency of the site, and use of this correlation to establish a parameter that can quantify resonance phenomena when the site is subjected to a given ground motion. Using H/V ratios instead of surface to borehole transfer functions to determine the fundamental site response frequency would eliminate the need for invasive site characterization and would allow a cost-effective reparameterization of site amplification factors for ground motion prediction equations that would explicitly account for the effects of frequency and site resonance.

2.5 Linear site-specific amplification factors

Surface to rock outcrop linear transfer functions are computed as described by *Kramer* (1996). We assume the soil extending below 100m depth as the rock outcropping formation.

Let j denote the layer number, and A_j and B_j the upgoing and downgoing SH wave displacement amplitudes at the j-th layer. In this case, the following relationship holds for every j:

$$\left\{ \begin{array}{c} A_{j+1} \\ B_{j+1} \end{array} \right\} = \left[\begin{array}{cc} \frac{1}{2}(1+\alpha_j^*)\mathrm{e}^{ik_j^* h_j} & \frac{1}{2}(1-\alpha_j^*)\mathrm{e}^{-ik_j^* h_j} \\ \frac{1}{2}(1-\alpha_j^*)\mathrm{e}^{ik_j^* h_j} & \frac{1}{2}(1+\alpha_j^*)\mathrm{e}^{-ik_j^* h_j} \end{array} \right] \cdot \left\{ \begin{array}{c} A_j \\ B_j \end{array} \right\} \stackrel{\text{def}}{=} \mathbf{D}_j \cdot \left\{ \begin{array}{c} A_j \\ B_j \end{array} \right\} \tag{9}$$

where $\alpha_j^* = \dfrac{\rho_j V_{s,j}^*}{\rho_{j+1} V_{s,j+1}^*}$ is the complex impedance ratio of two successive layers j and $(j+1)$; $V_{s,j}^* = V_{s,j} \cdot \sqrt{1+2i\xi_j}$ is the complex shear wave velocity of layer j; h_j is the thickness of layer j; and $k_j^* = \dfrac{\omega}{V_{s,j}^*} = \dfrac{k_j}{1+i\xi_j}$ is the complex wave number of layer j, where ω is the angular frequency.

Hence

$$\left\{ \begin{array}{c} A_j \\ B_j \end{array} \right\} = \mathbf{D}_{j-1} \left\{ \begin{array}{c} A_{j-1} \\ B_{j-1} \end{array} \right\} = \mathbf{D}_{j-1}\mathbf{D}_{m-2} \left\{ \begin{array}{c} A_{j-2} \\ B_{j-2} \end{array} \right\} = \cdots = \mathbf{D}_{j-1}\mathbf{D}_{j-2}\cdots\mathbf{D}_1 \left\{ \begin{array}{c} A_1 \\ B_1 \end{array} \right\} \tag{10}$$

where $A_1 = B_1 = S/2$, and S is the total surface displacement amplitude.

Let $\mathbf{E}_{j-1} = \mathbf{D}_{j-1}\mathbf{D}_{j-2}\cdots\mathbf{D}_1$, thus Equation (10) becomes (substitute N, the total number of layers, for j)

$$\left\{ \begin{array}{c} A_N \\ B_N \end{array} \right\} = \mathbf{E}_{N-1} \left\{ \begin{array}{c} A_1 \\ B_1 \end{array} \right\} = \left[\begin{array}{cc} E_{N-1}^{\langle 11 \rangle} & E_{N-1}^{\langle 12 \rangle} \\ E_{N-1}^{\langle 21 \rangle} & E_{N-1}^{\langle 22 \rangle} \end{array} \right] \left\{ \begin{array}{c} S/2 \\ S/2 \end{array} \right\} \tag{11}$$

The "surface to borehole" (surface motion to total borehole motion) transfer function is

$$\mathrm{TF}_{\text{S-BH}}(\omega) = \frac{\mathrm{ampl}(u_1)}{\mathrm{ampl}(u_{N-(\text{total})})} = \frac{S/2+S/2}{A_N+B_N} = \frac{2}{E_{N-1}^{\langle 11 \rangle} + E_{N-1}^{\langle 12 \rangle} + E_{N-1}^{\langle 21 \rangle} + E_{N-1}^{\langle 22 \rangle}} \tag{12}$$

and the absolute value of the transfer function is the amplification function

$$\mathrm{AF}_{\text{S-BH}}(\omega) = |\mathrm{TF}_{\text{S-BH}}(\omega)| = \frac{2}{\left| E_{N-1}^{\langle 11 \rangle} + E_{N-1}^{\langle 12 \rangle} + E_{N-1}^{\langle 21 \rangle} + E_{N-1}^{\langle 22 \rangle} \right|} \tag{13}$$

Similarly, the "surface to incident" (surface motion to incident motion at borehole) amplification function is

$$\mathrm{AF}_{\text{S-IN}}(\omega) = |\mathrm{TF}_{\text{S-IN}}(\omega)| = \frac{S/2+S/2}{A_N} = \frac{2}{\left| E_{N-1}^{\langle 11 \rangle} + E_{N-1}^{\langle 12 \rangle} \right|} \tag{14}$$

And the "surface to rock outcrop" (motion at soil surface to motion at rock outcrop site's surface) amplification function is

$$\mathrm{AF}_{\text{S-RO}}(\omega) = |\mathrm{TF}_{\text{S-RO}}(\omega)| = \frac{S/2+S/2}{2A_N} = \frac{1}{\left| E_{n-1}^{\langle 11 \rangle} + E_{N-1}^{\langle 12 \rangle} \right|} \tag{15}$$

2.6 Equivalent linear site response analyses

The equivalent-linear approach, introduced by *Seed and Idriss* (1970a,b), approximates the second order nonlinear equation by a linear operator by defining a characteristic strain which is assumed to be constant for the duration of the excitation. Moduli and damping curves shown above are then used to define new parameters for each layer. The linear response calculation is repeated as described in the previous section,

new characteristic strains evaluated, and iterations are performed until convergence. This stepwise analysis procedure has been formalized into a computer code termed SHAKE (*Schnabel et al.*, 1972), which currently is the most widely used analysis package for 1D site-specific response calculations. The advantages of the equivalent-linear approach are that the mathematical simplicity of linear analysis is preserved and the determination of nonlinear parameters is avoided.

Despite the effectiveness of the approach for the analysis of relatively stiff sites subjected to intermediate levels of strain ($<10^{-3}$), however, the equivalent linear method has been shown to overestimate the peak ground acceleration for large events, and artificially suppress the high frequency components when applied for the analysis of deep sites. An alternative methodology that accounts for the frequency-dependence of strain amplitudes and associated dynamic soil properties has been proposed by *Assimaki and Kausel* (2002), and has been shown to yield more satisfactory results for deep sedimentary deposits; the applicability of the alternative formulation, however, is still limited to the medium strain levels (*Hartzell et al.*, 2004). The linear stress-strain material behavior and total stress approach associated with equivalent linear models, entirely prohibits their use for problems that involve large levels of strain (e.g. near-fault motions), deep and/or soft and very soft sedimentary sites. We here implement only the original formulation of the equivalent linear method for ground surface response analyses at each station to the ensemble of ground motion time-histories. Comparison of the equivalent linear analyses results to the fully nonlinear response described below reveals the drawbacks of equivalent linear analyses associated with overdamping of high frequency components, and highlights the sites and ground motion characteristics that dictate the use of nonlinear models for the computation of site-specific amplification factors.

2.7 Nonlinear analyses: Monotonic stress-strain response and hysteretic behavior

In the nonlinear formulations of transient soil behavior, the wave equation is directly integrated in the time-domain and the material properties are adjusted to the instantaneous levels of strain and loading path according to the mathematical description of nonlinear stress-strain model and hysteretic (loading and unloading) soil response. As a result, nonlinear constitutive models can simulate soil behavioral features unavailable in the equivalent linear formulation such as updated stress-strain relationships and/or cyclic modulus degradation, which are critical for the prediction of large strain problems at soft sedimentary sites.

Nonlinear simulations were evaluated by means of the central difference method as described in *Bardet and Tobita* (2001). Figure 7 illustrates schematically the geometry and boundary conditions of the response simulations conducted for a horizontally stratified system of homogeneous layers extending horizontally to infinity and subjected to vertically propagating horizontally polarized shear waves.

The constitutive law implemented for the analyses is the hysteretic nonlinear model developed by *Li and Assimaki* (2010), which is based on the modified hyperbolic model monotonic stress-strain model by *Matasovic and Vucetic* (1993, 1995) and the Muravskii hysteretic formulation (*Muravskii*, 2005).

Novel features included in this work include:

- The new hysteretic model that is capable of matching simultaneously the $G/G_{\max}$ and ξ (quality factor Q) curves by contrast to the widely employed Masing rules that have been shown to substantially

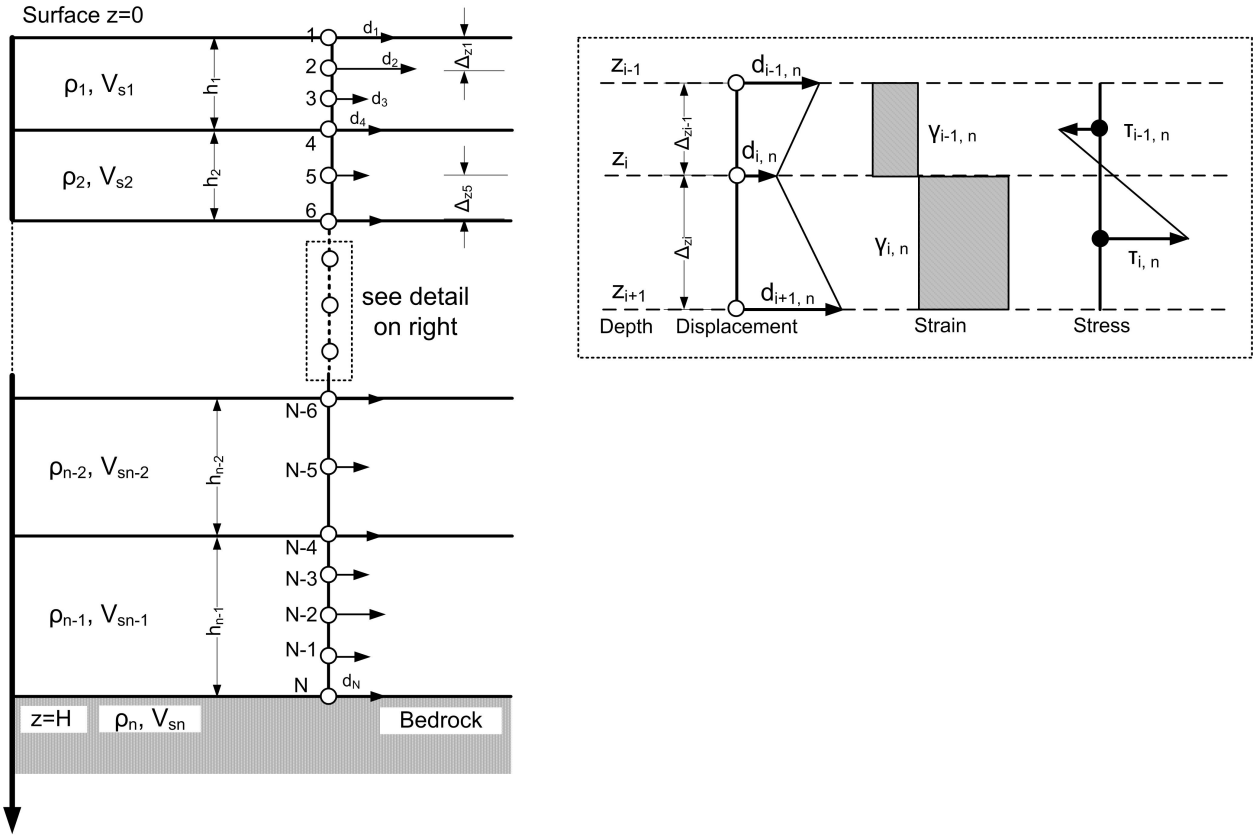

Figure 7: Schematic representation of spatial discretization for a one-dimensional soil deposit system, and detail illustrating the definition of displacement, strain and stress in the finite difference formulation. The displacement d and stress τ are evaluated at N grid nodes, which define sublayers within layers. The displacement of node i at time step t_n is denoted $d(z_i, t_n) = d_{i,n}$, where z_i is the depth of node i. Similarly, the stress and strain at node i at time step t_n are denoted $\tau_{i,n}$ and $\gamma_{i,n}$ (modified from *Bardet and Tobita*, 2001).

overestimate soil damping. The backbone curve and hysteresis function of the model are based on the same constitutive law (analytical form, here the modified hyperbolic model) but separate sets of parameters. As a result, the hysteresis function is calibrated using the same input as the equivalent linear analysis and is not updated at each stress reversal to match ξ given $G/G_{\max}$, a direct advantage relative to the original formulation by *Muravskii* (2005). We have validated the model by comparison with downhole array recordings in Southern California, and results were shown to be in excellent agreement with the observations *Assimaki et al.* (2008).

- The representation of low-strain material damping (or quality factor Q) in the time domain using the memory-variable technique originally described by *Day and Minster* (1984). This technique can be implemented to realistically represent frequency-independent ξ over a wide frequency range by using a linear combination of multiple relaxation mechanisms (see *Liu and Archuleta*, 2006), consistent with laboratory experimental data on the behavior of near-surface geologic formations at low strains.

This formulation is advantageous compared to the widely employed Rayleigh or Caughey damping models.

2.8 NGA database strong ground motions

In our equivalent linear and nonlinear analyses, 32 ground motions from the database which is used to develop the Next Generation Attenuation of Ground Motions (NGA) project (*Chiou et al.*, 2008) are chosen as input motions. These motions are all empirical (i.e., recorded) ground motions. Each ground motion is divided by 2 to produce the *incident* motion. The 32 motions were selected randomly using the following criteria:

- Minimum moment magnitude (M_w): 5.5;
- Closest distance to the rupture: 0 to 60 km;
- Fault mechanism: strike-slip, reverse, or reverse-oblique;
- Site class: C;
- Minimum usable frequency: less than 0.5 Hz (i.e., $T_{\max} > 2$ sec);
- Earthquake location: no earthquakes outside the US except for the 1995 Kobe (Japan) and 1999 Chi-Chi (Taiwan) earthquakes, and no records from the 1983 Coalinga earthquake.

The list of all 32 ground motions is shown in Table 3.

3 Conclusions - Future Work

The remaining of this report (Section 4) plots site amplification factors at each strong motion station. Sites are grouped by site class and results include the extrapolated profile, the H/V empirical frequency ratios compared to the linear computed transfer function, and surface to rock outcrop amplification factors computed via equivalent linear and nonlinear analyses. For the latter, we plot both the median inelastic response against the corresponding linear response, as well as families of amplification functions color coded as a function of PGA and ground motion frequency content.

To illustrate the effects of frequency, ground motions are scaled to the same intensity (i.e., $\mathrm{PGA_{RO}} = 0.5g$) and the amplification factors are color coded as a function of the ratio of the central frequency of the incident ground motion to the fundamental frequency of the site (f_c/f_0). This ratio is chosen as a quantitative measure how much incident energy is trapped in the near-surface soil layers: the closer to unity, the closer the ground motion frequency to the fundamental soil response, and therefore the higher the likelihood of resonance phenomena manifesting. When this ratio is combined with sufficiently high PGA, stronger nonlinear effects are anticipated to be triggered. Note that the notion of using the fundamental frequency of the soil profile in conjunction with V_{s30} to classify site amplification factors has been also reported by *Cadet et al.* (2008) based on observations from the Japanese Strong Motion Seismogram Networks K-Net and Kik-Net.

Record #	Earthquake Name	Station Name	Earthquake Magnitude (M_w)	Closest Distance to Rupture (km)
1008	Northridge-01	LA - W 15th St	6.69	29.7
1012	Northridge-01	LA 00	6.69	19.1
1013	Northridge-01	LA Dam	6.69	5.9
1014	Northridge-01	LB - City Hall	6.69	57.7
1023	Northridge-01	Lake Hughes #9	6.69	25.4
1031	Northridge-01	Leona Valley #5 - Ritter	6.69	37.8
1035	Northridge-01	Manhattan Beach – Manhattan	6.69	39.3
1055	Northridge-01	Pasadena – N Sierra Madre	6.69	36.1
1057	Northridge-01	Playa Del Rey - Saran	6.69	31.7
1085	Northridge-01	Sylmar – Converter Sta East	6.69	5.2
1086	Northridge-01	Sylmar – Olive View Med FF	6.69	5.3
1642	Sierra Madre	Cogswell Dam – Right Abutment	5.61	22.0
1794	Hector Mine	Joshua Tree	7.13	31.1
2374	Chi-Chi, Taiwan-02	TCU054	5.90	41.2
2393	Chi-Chi, Taiwan-02	TCU082	5.90	40.3
2397	Chi-Chi, Taiwan-02	TCU087	5.90	46.6
2399	Chi-Chi, Taiwan-02	TCU089	5.90	12.0
2490	Chi-Chi, Taiwan-03	CHY074	6.20	28.7
2498	Chi-Chi, Taiwan-03	CHY086	6.20	50.1
2658	Chi-Chi, Taiwan-03	TCU129	6.20	12.8
2716	Chi-Chi, Taiwan-04	CHY050	6.20	53.9
2804	Chi-Chi, Taiwan-04	KAU001	6.20	45.3
2867	Chi-Chi, Taiwan-04	TCU067	6.20	47.4
2871	Chi-Chi, Taiwan-04	TCU084	6.20	27.1
2883	Chi-Chi, Taiwan-04	TCU109	6.20	50.7
3008	Chi-Chi, Taiwan-05	HWA020	6.20	34.9
3016	Chi-Chi, Taiwan-05	HWA029	6.20	51.6
3353	Chi-Chi, Taiwan-06	HWA044	6.30	51.9
3361	Chi-Chi, Taiwan-06	HWA058	6.30	44.9
3469	Chi-Chi, Taiwan-06	TCU068	6.30	35.7
3474	Chi-Chi, Taiwan-06	TCU079	6.30	10.1
3507	Chi-Chi, Taiwan-06	TCU129	6.30	24.8

Table 3: 32 ground motions used in the equivalent linear and nonlinear simulations (time & date of each earthquake are shown in Table 4)

Earthquake Name	Magnitude	Date	Time
Northridge-01	6.69	1994-01-17	12:31
Sierra Madre	5.61	1991-06-28	n/a
Hector Mine	7.13	1999-10-16	n/a
Chi-Chi, Taiwan-02	5.90	1999-09-20	17:57
Chi-Chi, Taiwan-03	6.20	1999-09-20	18:03
Chi-Chi, Taiwan-04	6.20	1999-09-20	21:46
Chi-Chi, Taiwan-05	6.20	1999-09-22	00:14
Chi-Chi, Taiwan-06	6.30	1999-09-25	23:52

Table 4: Time, date and magnitude of all earthquakes listed in Table 3

The frequency parameterization, however, needs further investigation and our future work is directed towards identifying a more robust index. More specifically, for sites where the impedance contrast between soft soils and bedrock is not strong, namely either very stiff sites, or deep sedimentary structures with smoothly varying stiffness, resonance phenomena are very mild and the simplified frequency index proposed here cannot capture multiple modes of vibration. We plan to use the downhole array seismogram network KiK-Net to investigate alternative formulations that can be effectively used for high and low velocity gradient sites, and successively repeat the frequency parameterization of amplification functions at the US strong motion stations studied here.

Results from this work as well as future extensions stemming from our our work in progress will be archived in a database and uploaded on the SCEC Broadband Simulation Platform. Supplemental funding is requested for this purpose from the Southern California Earthquake Center. More specifically, we will develop a database of amplification functions at each strong motion station for various PGA and frequency ratios. Given a strong motion scenario, the ground motion central frequency, f_c, will be computed and in conjuction with the PGA on rock outcrop will determine the site-specific, PGA and frequency specific amplification factor that will modify the ground surface motion to account for nonlinear site response. In the future, this work is envisioned to contribute to the reparameterization of amplification factors for ground motion prediction equations that currently solely account for the near-surface soil stiffness and ground motion PGA.

Bibliography

Assimaki, D., and E. Kausel (2002), An equivalent linear algorithm with frequency- and pressure-dependent moduli and damping for the seismic analysis of deep sites, *Soil Dynamics and Earthquake Engineering*, *22*(9–12), 959–965.

Assimaki, D., W. Li, J. M. Steidl, and J. Schmedes (2008), Quantifying nonlinearity susceptibility via site response modeling uncertainty at three sites in the Los Angeles basin, *Bulletin of the Seismological Society of America*, *98*(5), 2364–2390.

Bardet, J. P., and T. Tobita (2001), *Nonlinear earthquake site response analysis: User's manual*, Department of Civil Engineering, University of Southern California.

Cadet, H., P.-Y. Bard, and A.-M. Duval (2008), A new proposal for site classification based on ambient vibration measurements and the KiK-Net strong motion data set, in *Proceedings of the 14th World Conference on Earthquake Engineering, Beijing, China*.

Chiou, B., R. Darragh, and N. Gregor (2008), NGA project strong-motion database, *Earthquake Spectra*, *24*(1), 23–44.

Darendeli, M. B. (2001), Development of a new family of normalized modulus reduction and material damping curves, Ph.D. thesis, University of Texas at Austin.

Day, S. M., and J. B. Minster (1984), Numerical simulation of attenuated wavefields using a Padé approximant method, *Geophysical Journal of the Royal Astronomical Society*, *78*(1), 105–118.

Dobry, R., R. D. Borcherdt, C. B. Crouse, I. M. Idriss, W. B. Joyner, G. R. Martin, M. S. Power, E. E. Rinne, and R. B. Seed (2000), New site coefficients and site classification system used in recent building seismic code provisions, *Earthquake Spectra*, *16*(1), 41–67.

Frankel, A., M. Petersen, C. Mueller, K. Haller, R. Wheeler, E. Leyendecker, R. Wesson, S. Harmsen, C. Cramer, D. Perkins, and K. Rukstales (2002), Documentation for the 2002 update of the national seismic hazard maps, *Open-File Report 02-420*, U.S. Geological Survey.

Hartzell, S. H., L. F. Bonilla, and R. A. Williams (2004), Prediction of nonlinear soil effects, *Bulletin of the Seismological Society of America*, *94*(5), 1609–1629.

Konno, K., and T. Ohmachi (1998), Ground-motion characteristics estimated from spectral ratio between horizontal and vertical components of microtremor, *Bulletin of the Seismological Society of America*, *88*(1), 228–241.

Kramer, S. L. (1996), *Geotechnical Earthquake Engineering*, Prentice Hall, Upper Saddle River, New Jersey.

Li, W., and D. Assimaki (2010), A hysteretic model for the simulation of soil strength degradation due to irregular loading in site response predictions, *Soil Dynamics and Earthquake Engineering*, *30*, 299–309.

Liu, P.-C., and R. J. Archuleta (2006), Efficient modeling of Q for 3D numerical simulation of wave propagation, *Bulletin of the Seismological Society of America*, *96*(4A), 1352–1358.

Matasovic, J., and M. Vucetic (1993), Analysis of seismic records obtained on November 24, 1987 at the Wildlife Liquefaction Array, *Research report*, Department of Civil Engineering, University of California at Los Angeles, (94 pages).

Matasovic, J., and M. Vucetic (1995), Generalized cyclic-degradation-pore-pressure generation model for clays, *Journal of Geotechnical Engineering*, *121*(1), 33–42.

Muravskii, G. (2005), On description of hysteretic behavior of materials, *International Journal of Solids and Structures*, *42*, 2625–2644.

Nakamura, Y. (1989), A method for dynamic characteristics estimation of subsurface using microtremor on the ground surface, *Quartly Report of Railway Technical Research Institute*, *30*(1), 25–33, (Journal based in Japan, article written in English).

NEHRP (2004), NEHRP recommended provisions for seismic regulations for new buildings, *FEMA 450-1*, Building Seismic Safety Council of the National Institute of Building Sciences, (2003 edition).

Schnabel, P. B., J. Lysmer, and H. B. Seed (1972), SHAKE: A computer program for earthquake response analyses of horizontally layered sites, *Report No. EERC 72-12*, Earthquake Engineering Research Center, University of California at Berkeley.

Seed, H. B., and I. M. Idriss (1970a), Analyses of ground motions at Union Bay, Seattle during earthquakes and distant nuclear blasts, *Bulletin of the Seismological Society of America*, *60*(1), 125–136.

Seed, H. B., and I. M. Idriss (1970b), Soil moduli and damping factors for dynamic response analyses, *UCB/EERC- 70/10*, Earthquake Engineering Research Center, University of California at Berkeley.

Silva, W. J., R. Darragh, and N. Gregor (1998), Reassessment of site coefficients and near-fault factors for building code provisions, *Pacific Engineering and Analysis Report 98-HQ-GR-1010*.

Theodulidis, N., P.-Y. Bard, R. Archuleta, and M. Bouchon (1996), Horizontal-to-vertical spectral ratio and geological conditions: the case of garner valley downhole array in Southern California, *Bulletin of the Seismological Society of America*, *86*(2), 306–319.

Vrettos, C. (1996), Simple inversion procedure for shallow seismic refraction in continuously nonhomogeneous soils, *Soil Dynamics and Earthquake Engineering*, *15*, 381–386.

Yong, A., A. Martin, K. Stokoe, and J. Diehl (2012), ARRA-funded Vs30 measurements at California and Central Eastern U.S. strong motion stations, *Open-file report*, U.S. Geological Survey, (in review).

4 Results

This section shows computation results for all 122 profiles of 86 sites (some sites have more than one version of V_s profile, which slightly differ between each other). All the results are grouped by their NEHRP site classes. And for each profile, the following are included:

- Original (measured) soil V_s profile, together with the extrapolated V_s (if applicable). The measured V_s data and extrapolated V_s data are separated by a dashed line in the profile table.
- A figure showing V_s profile, both measured and extrapolated, as well as the analytical V_s curve.
- Linear elastic transfer function, and its corresponding f_0 (fundamental frequency).
- H/V ratios of the site, calculated from microtremor recordings, usually consisting of 3 different H/V ratios, except for certain sites.
- Equivalent linear transfer functions, calculated from 32 input ground motions whose rock-outcrop PGAs vary from 0.14 m/s^2 to 8.1 m/s^2. (Their incident peak accelerations are half of their rock-outcrop PGAs.)
- Non-linear transfer functions, calculated from 32 input ground motions whose rock-out-crop PGAs vary from 0.14 m/s^2 to 8.1 m/s^2.
- Equivalent linear and non-linear transfer functions, calculated from 32 input ground motions which have the same rock-outcrop PGA: 0.5g ($\sim$ 4.9 m/s^2). Results are color-coded by each input motion's central frequency (f_c).

The V_s profiles of all the sites are plotted below, grouped by their NEHRP classes.

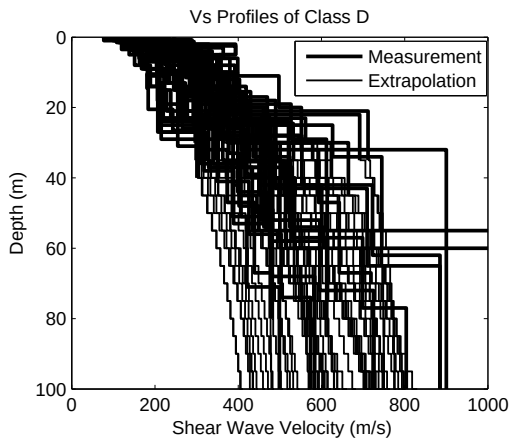

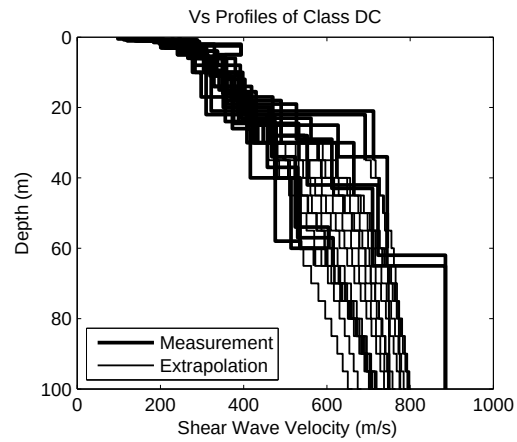

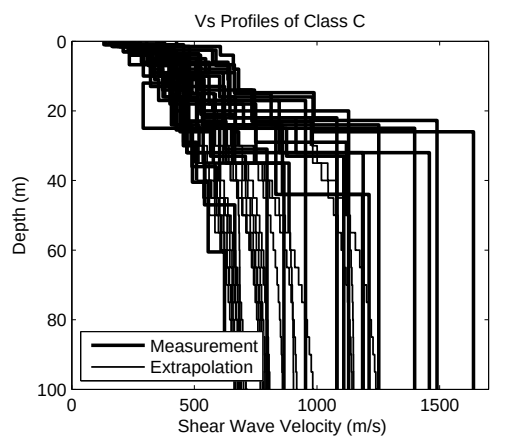

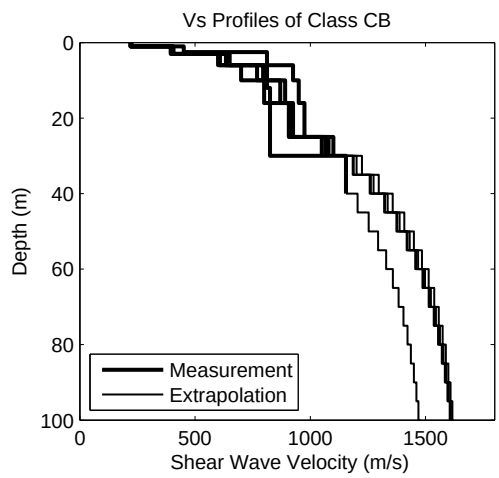

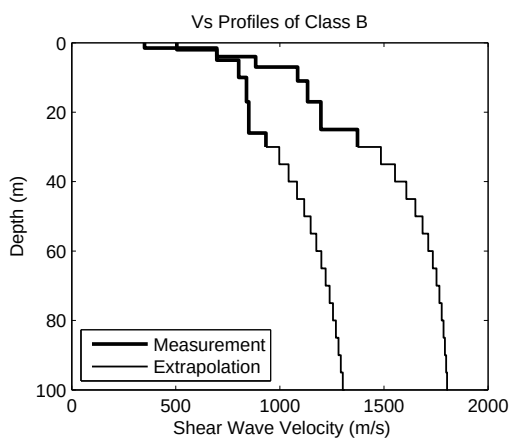

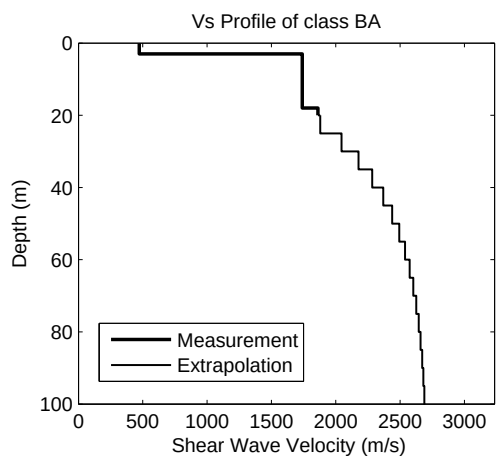

4.1 Class D

Class D sites include the following[1]:

Site Code	V_{s30}-measured (m/s)	V_{s30}-adjusted (m/s)
CE.11023	212	212
CE.11625	318	318
CE.11684	234	234
CE.12076	263	263
CE.12108	301	304
CE.12952	274	274
CE.14241	282	282
CE.14395	230	250
CE.23958	423	443
CE.24965	326	326
CE.24967	330	330
CI.BAK	275	299
CI.BBS	341	352
CI.BHP	300	323
CI.BOM	202	214
CI.CAR	310	339
CI.CHN	292	307
CI.DRE	196	216
CI.ERR	238	253
CI.LCP	259	267
CI.MSJ	244	255
CI.NJQ	297	314
CI.RCT	284	301
CI.SAL	255	255
CI.SAN	222	222
CI.SIO	249	249
CI.SMM	225	235
CI.SMV	260	278
CI.TFT	332	367
CI.USB	300	300
CI.WES	242	269
NC.JELB	323	323

[1] The "measured" and "adjusted" V_{s30} data in the table come from the report by *Yong et al.* (2012). The adjusted V_{s30} is used for curve-fitting and V_s extrapolation of all sites of all classes.

4.1.1 CE.11023

Depth (m)	Thickness (m)	V_s (m/s)	Damping ratio	Density (kg/m^3)
0	2	151	0.05	1600
2	2	146	0.05	1600
4	2	162	0.05	1600
6	5	214	0.05	1800
11	8	223	0.05	1800
19	12	255	0.02	1800
31	9	301	0.02	1800
40	5	314.2	0.02	1800
45	5	326.5	0.02	1800
50	5	337.8	0.02	1800
55	5	348.1	0.02	1800
60	5	357.6	0.02	1800
65	5	366.2	0.02	1800
70	5	374.1	0.02	1800
75	5	381.4	0.02	1800
80	5	388.0	0.02	1800
85	5	394.0	0.02	1800
90	5	399.6	0.02	1800
95	5	404.7	0.02	1800
100	–	409.4	0.02	1800

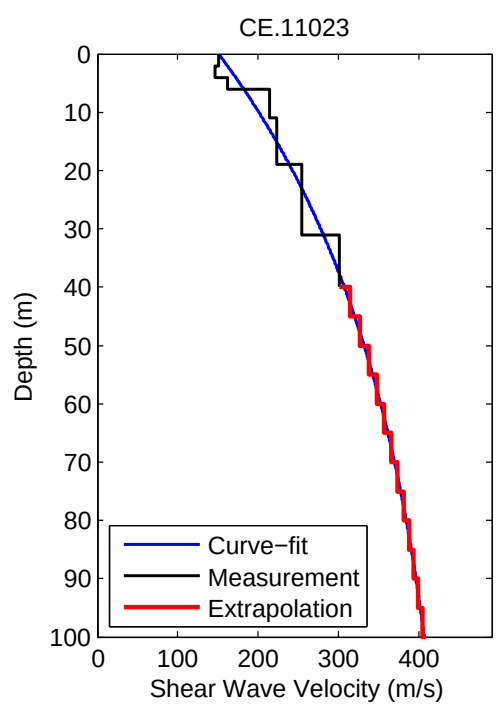

Linear Elastic Transfer Function

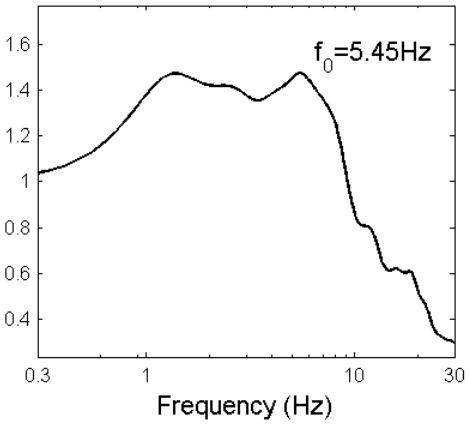

H/V Ratio – Sensor 450

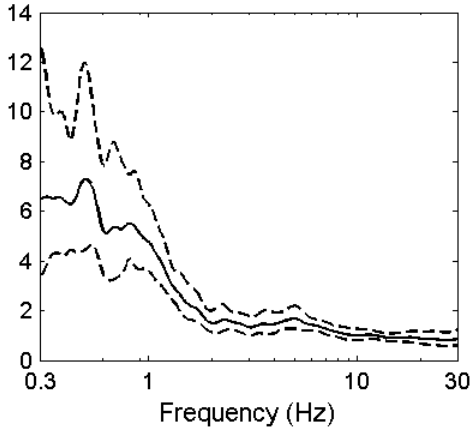

H/V Ratio – Sensor 507

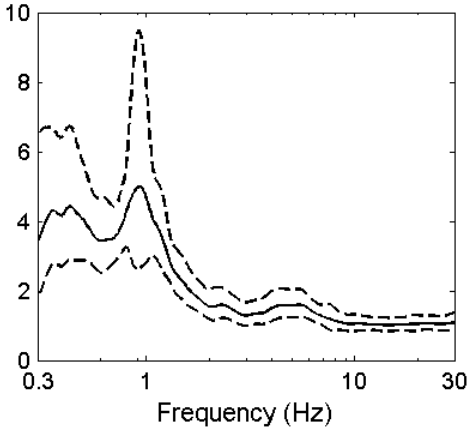

H/V Ratio – Sensor 453

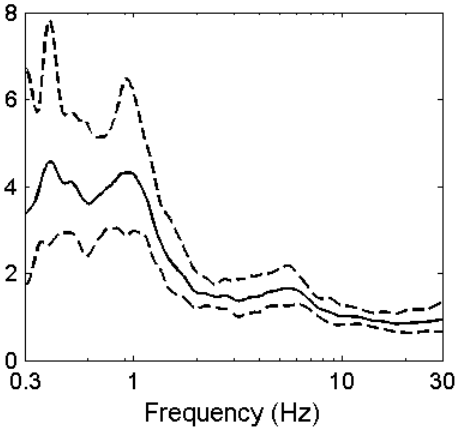

Equivalent Linear Transfer Function

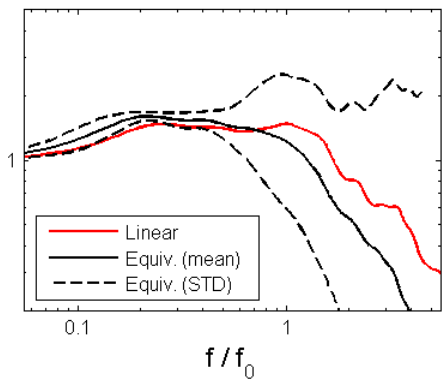

Equiv. Lin. TF (color coded by PGA_{RO})

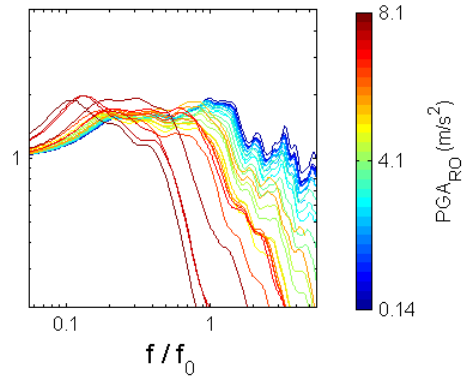

Non-linear Transfer Function

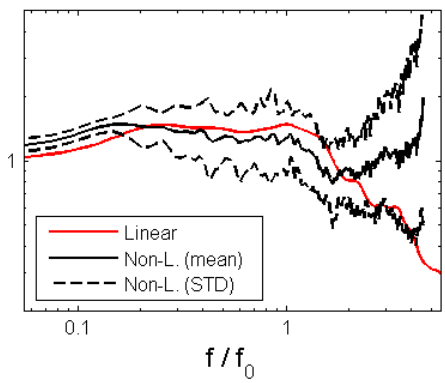

Non-linear TF (color coded by PGA_{RO})

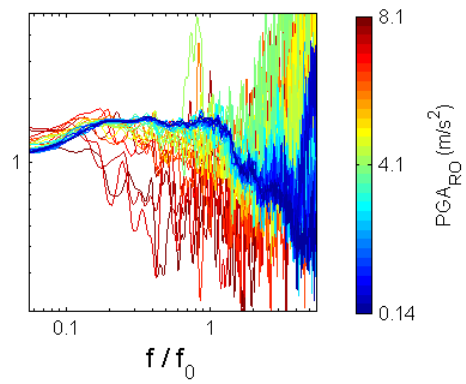

Equiv. Lin. TF (color coded by f_c)

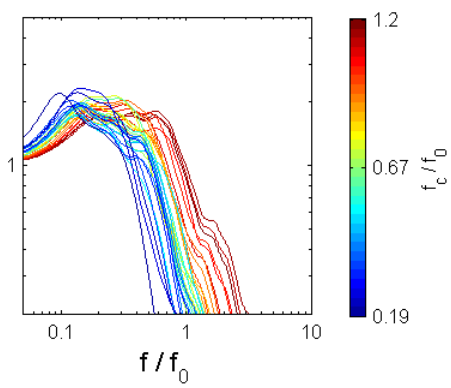

Non-linear TF (color coded by f_c)

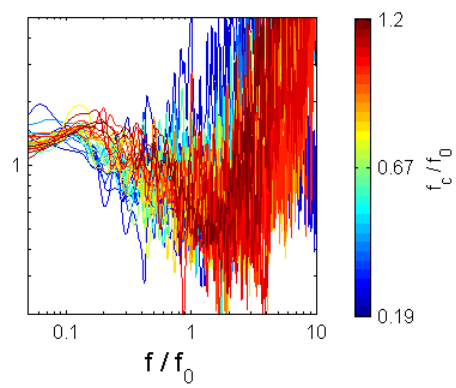

4.1.2 CE.11625

Depth (m)	Thickness (m)	V_s (m/s)	Damping ratio	Density (kg/m^3)
0	0.5	195	0.05	1600
0.5	1	197	0.05	1600
1.5	3	246	0.05	1800
4.5	6	270	0.02	1800
10.5	10	337	0.02	1800
20.5	4.5	419	0.02	1800
25	5	428.2	0.02	1800
30	5	456.8	0.02	1800
35	5	482.3	0.02	1800
40	5	505.0	0.02	1800
45	5	525.2	0.02	1800
50	5	543.2	0.02	1800
55	5	559.2	0.02	1800
60	5	573.5	0.02	1800
65	5	586.2	0.02	1800
70	5	597.5	0.02	1800
75	5	607.6	0.02	1800
80	5	616.6	0.02	1800
85	5	624.6	0.02	1800
90	5	631.7	0.02	1800
95	5	638.0	0.02	1800
100	–	643.7	0.02	1800

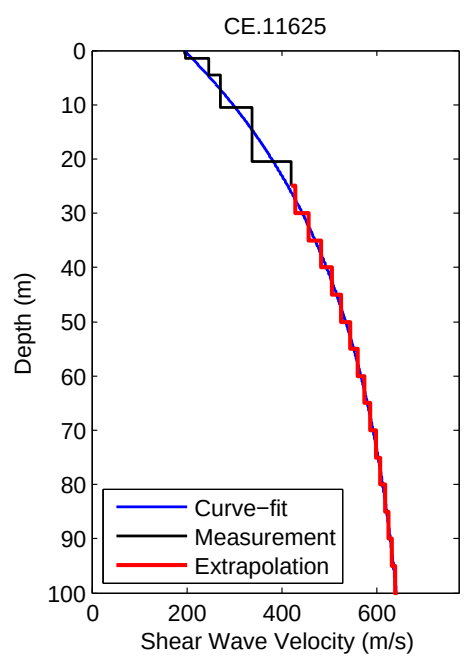

Linear Elastic Transfer Function

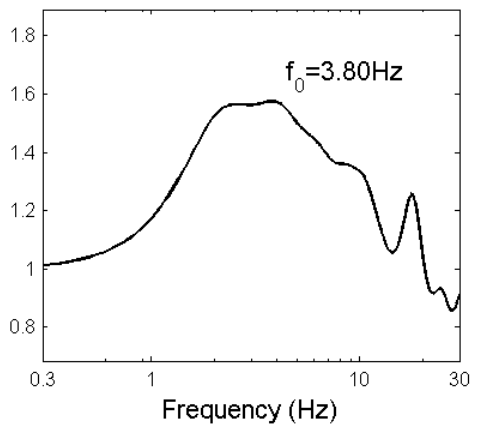

H/V Ratio – Sensor 450

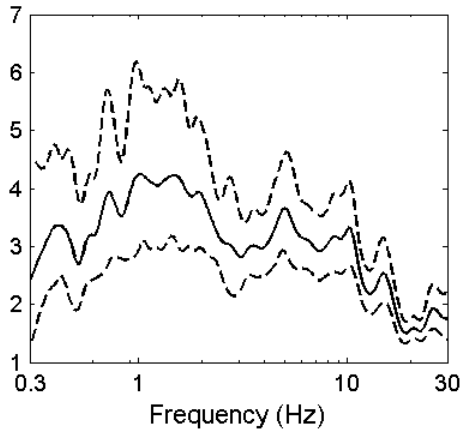

H/V Ratio – Sensor 507

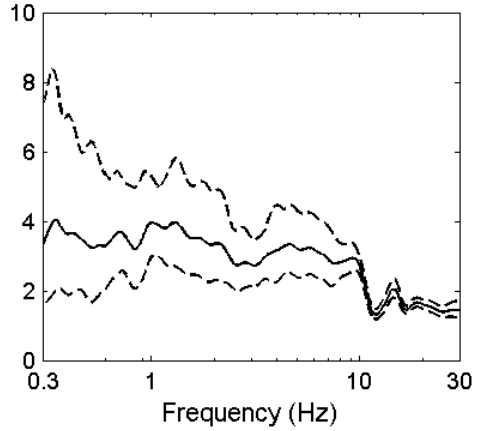

H/V Ratio – Sensor 453

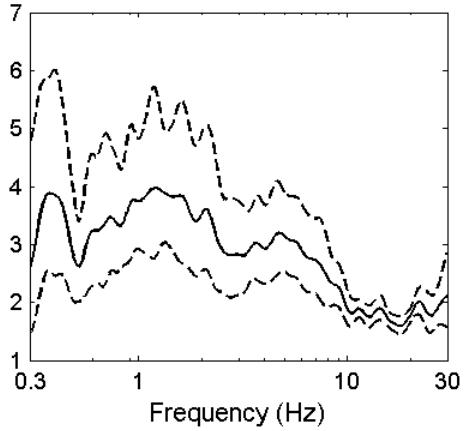

Equivalent Linear Transfer Function

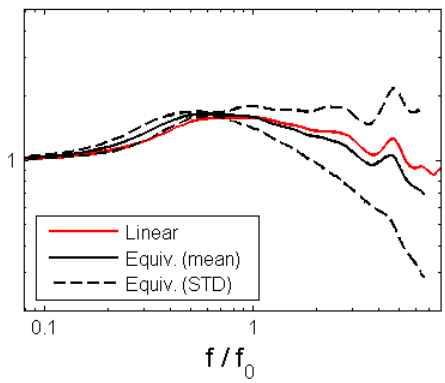

Equiv. Lin. TF (color coded by PGA_{RO})

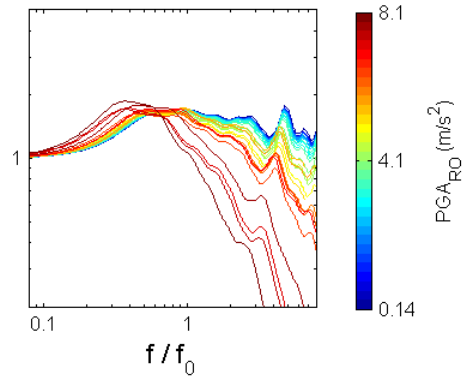

Non-linear Transfer Function

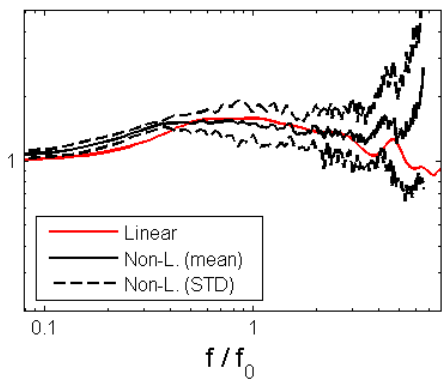

Non-linear TF (color coded by PGA_{RO})

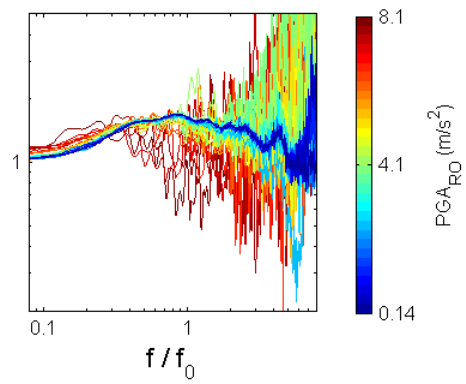

Equiv. Lin. TF (color coded by f_c)

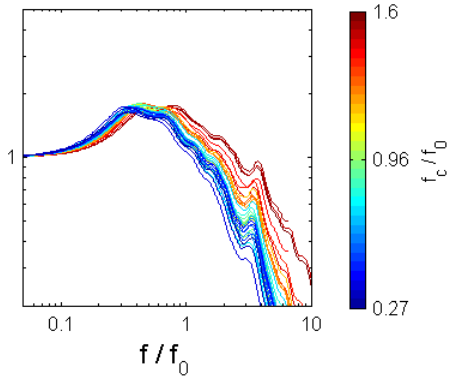

Non-linear TF (color coded by f_c)

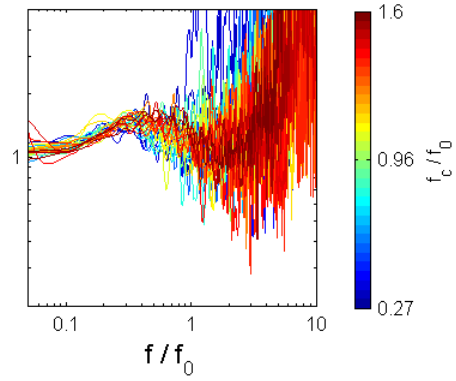

4.1.3 CE.11684a

Depth (m)	Thickness (m)	V_s (m/s)	Damping ratio	Density (kg/m^3)
0	0.75	145	0.05	1600
0.75	1.25	136	0.05	1600
2	1	170	0.05	1600
3	6	168	0.05	1600
9	7	210	0.05	1800
16	8	214	0.05	1800
24	11	299	0.02	1800
35	5	311.9	0.02	1800
40	5	327.4	0.02	1800
45	5	341.6	0.02	1800
50	5	354.7	0.02	1800
55	5	366.8	0.02	1800
60	5	377.9	0.02	1800
65	5	388.1	0.02	1800
70	5	397.5	0.02	1800
75	5	406.2	0.02	1800
80	5	414.2	0.02	1800
85	5	421.6	0.02	1800
90	5	428.4	0.02	1800
95	5	434.6	0.02	1800
100	–	440.4	0.02	1800

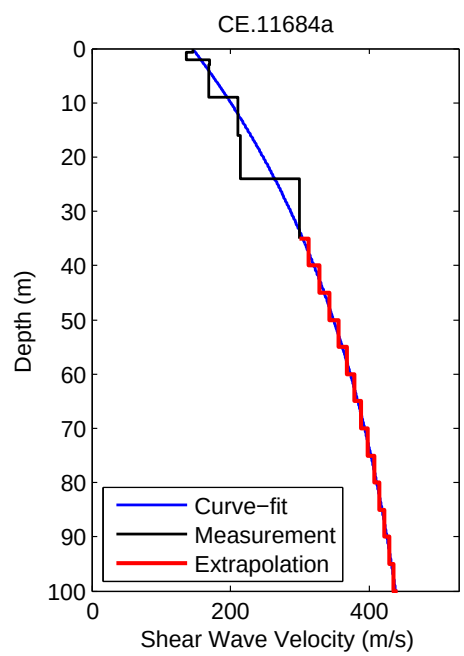

Linear Elastic Transfer Function

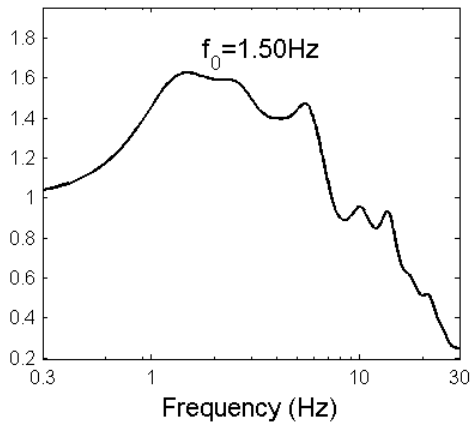

H/V Ratio – Sensor 450

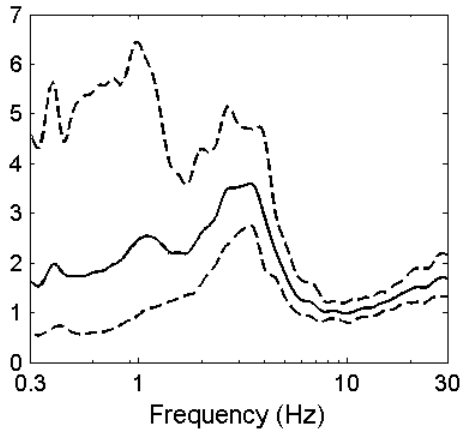

H/V Ratio – Sensor 507

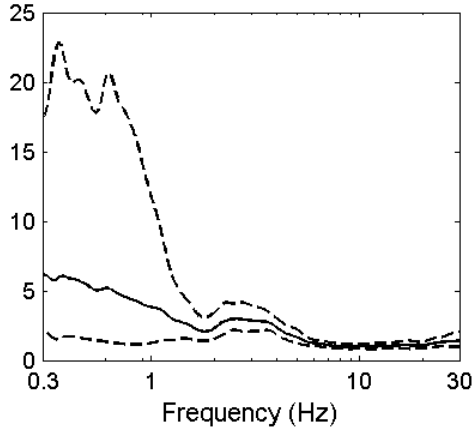

H/V Ratio – Sensor 453

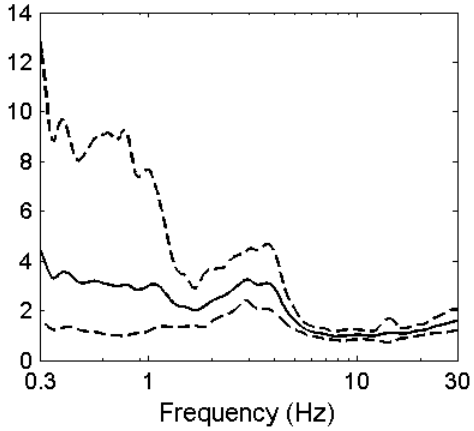

Equivalent Linear Transfer Function

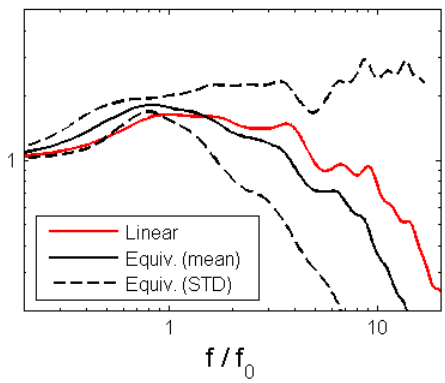

Equiv. Lin. TF (color coded by PGA_{RO})

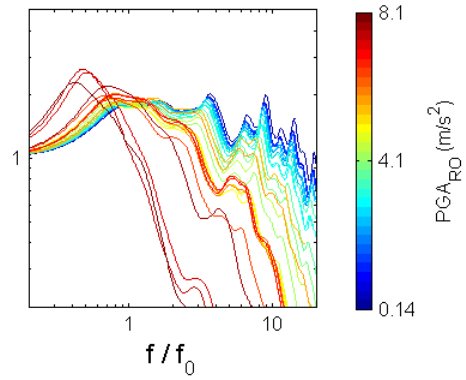

Non-linear Transfer Function

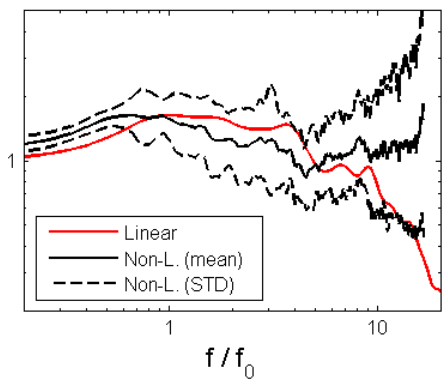

Non-linear TF (color coded by PGA_{RO})

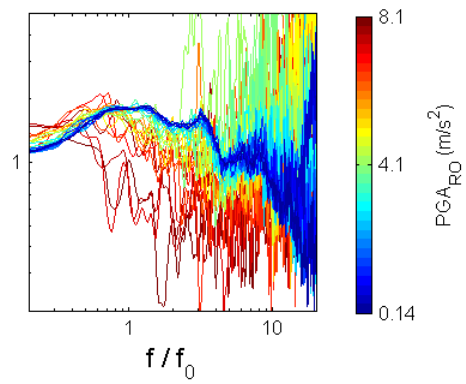

Equiv. Lin. TF (color coded by f_c)

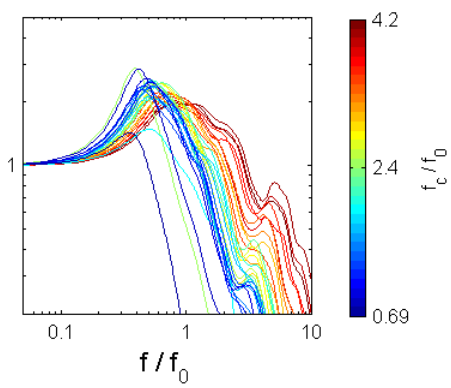

Non-linear TF (color coded by f_c)

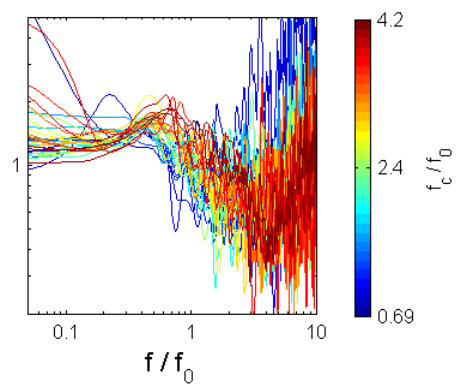

4.1.4 CE.11684b

Depth (m)	Thickness (m)	V_s (m/s)	Damping ratio	Density (kg/m^3)
0	0.75	131	0.05	1600
0.75	0.75	124	0.05	1600
1.5	1.5	160	0.05	1600
3	5	163	0.05	1600
8	6	189	0.05	1600
14	9	208	0.05	1800
23	12	347	0.02	1800
35	5	354.8	0.02	1800
40	5	372.1	0.02	1800
45	5	387.4	0.02	1800
50	5	401.0	0.02	1800
55	5	413.1	0.02	1800
60	5	423.8	0.02	1800
65	5	433.3	0.02	1800
70	5	441.7	0.02	1800
75	5	449.1	0.02	1800
80	5	455.7	0.02	1800
85	5	461.6	0.02	1800
90	5	466.8	0.02	1800
95	5	471.4	0.02	1800
100	–	475.5	0.02	1800

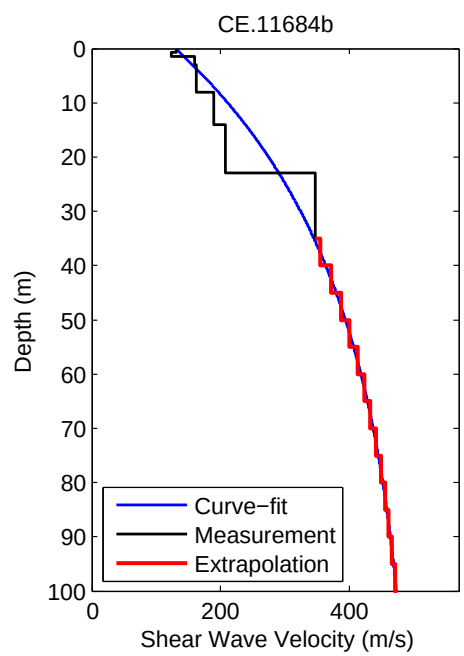

Linear Elastic Transfer Function

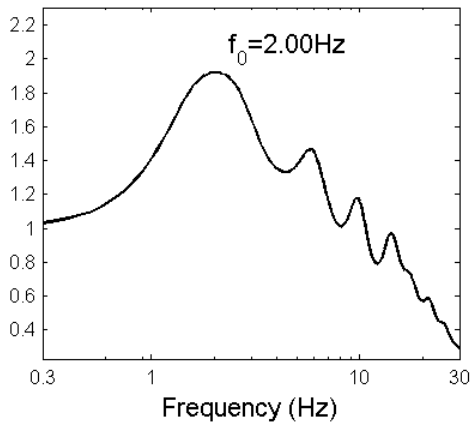

H/V Ratio – Sensor 450

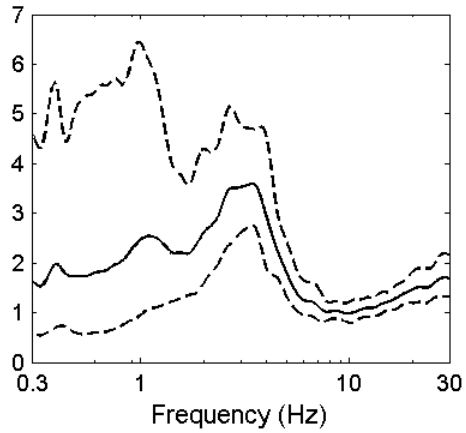

H/V Ratio – Sensor 507

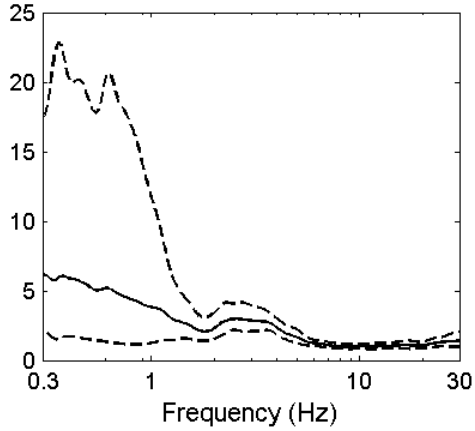

H/V Ratio – Sensor 453

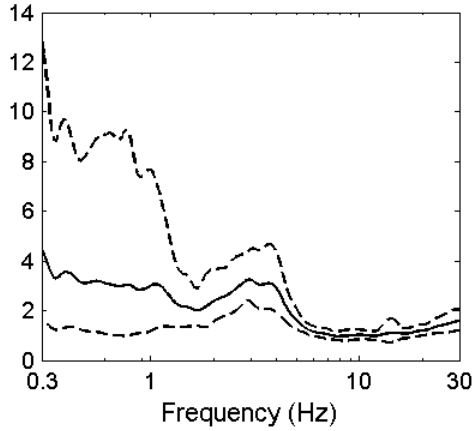

Equivalent Linear Transfer Function

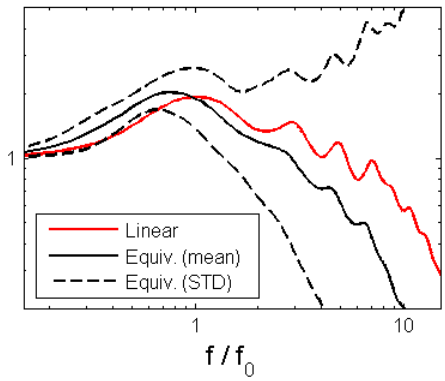

Equiv. Lin. TF (color coded by PGA_{RO})

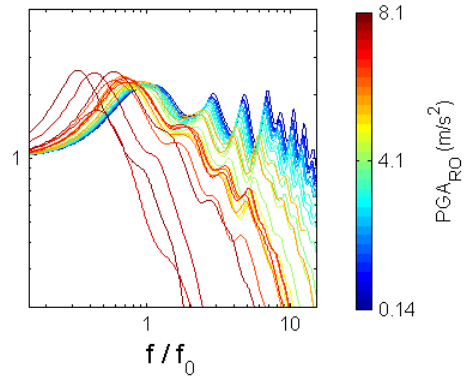

Non-linear Transfer Function

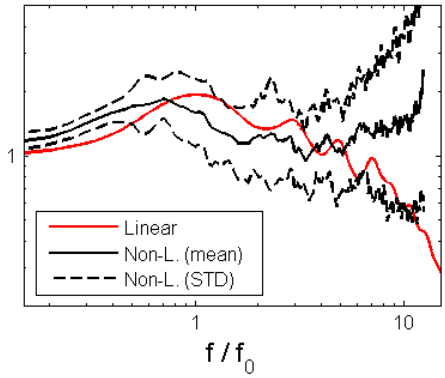

Non-linear TF (color coded by PGA_{RO})

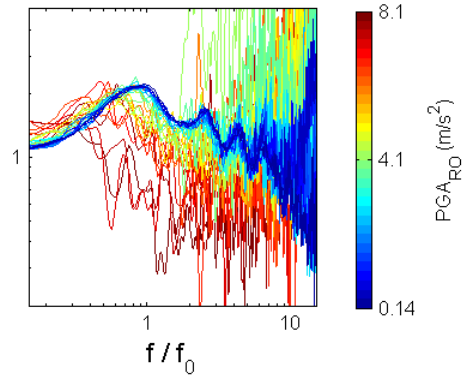

Equiv. Lin. TF (color coded by f_c)

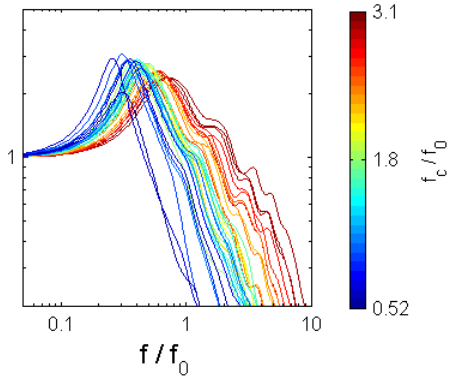

Non-linear TF (color coded by f_c)

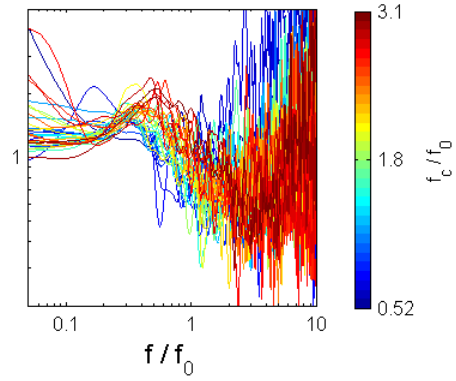

4.1.5 CE.11684c

Depth (m)	Thickness (m)	V_s (m/s)	Damping ratio	Density (kg/m^3)
0	0.75	105	0.05	1600
0.75	0.75	108	0.05	1600
1.5	1.5	156	0.05	1600
3	5	151	0.05	1600
8	6	187	0.05	1600
14	9	220	0.05	1800
23	12	352	0.02	1800
35	5	369.5	0.02	1800
40	5	387.9	0.02	1800
45	5	403.8	0.02	1800
50	5	417.6	0.02	1800
55	5	429.5	0.02	1800
60	5	439.9	0.02	1800
65	5	448.9	0.02	1800
70	5	456.7	0.02	1800
75	5	463.4	0.02	1800
80	5	469.3	0.02	1800
85	5	474.4	0.02	1800
90	5	478.8	0.02	1800
95	5	482.6	0.02	1800
100	–	485.9	0.02	1800

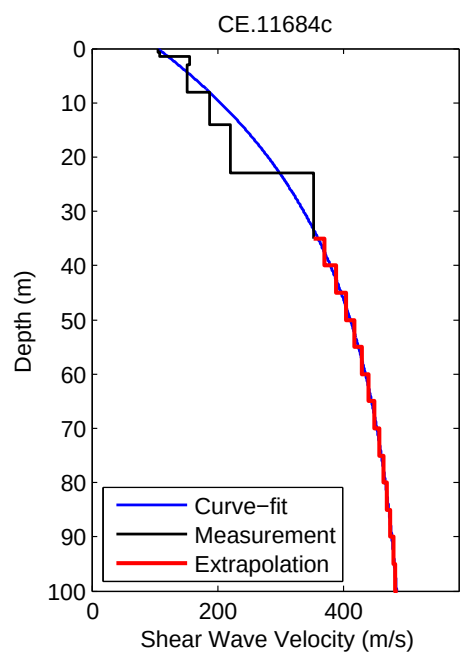

Linear Elastic Transfer Function

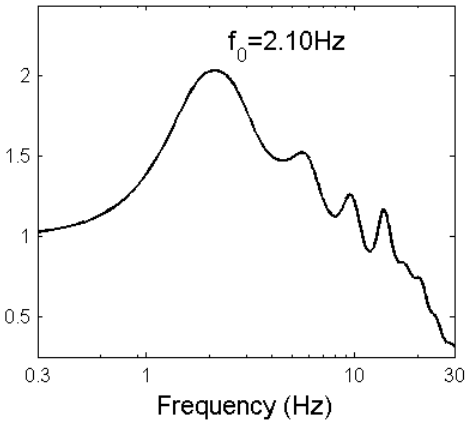

H/V Ratio – Sensor 450

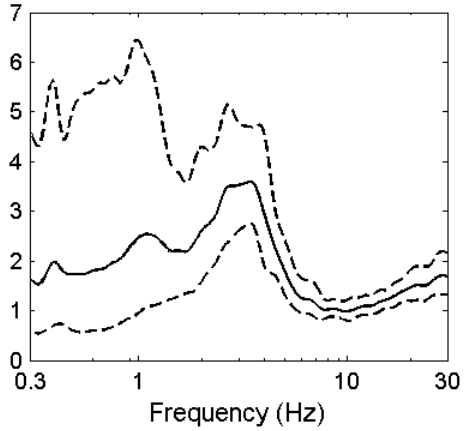

H/V Ratio – Sensor 507

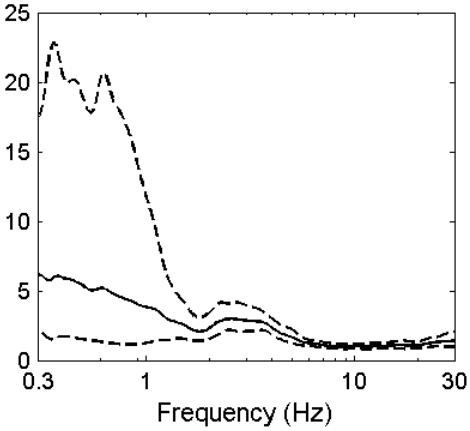

H/V Ratio – Sensor 453

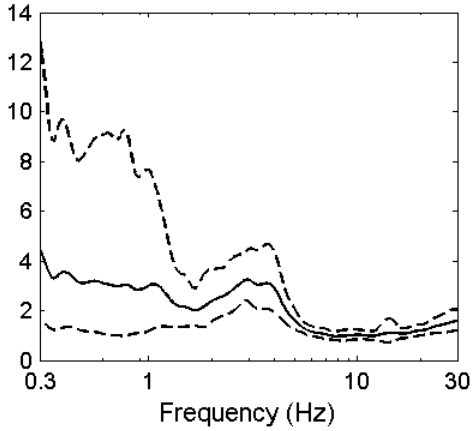

Equivalent Linear Transfer Function

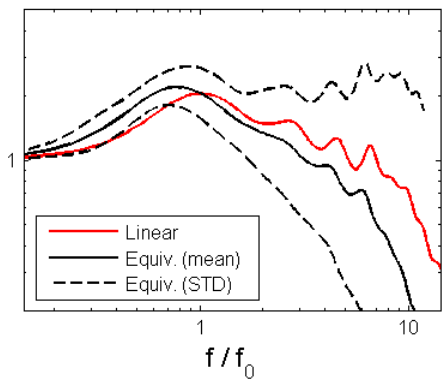

Equiv. Lin. TF (color coded by PGA_{RO})

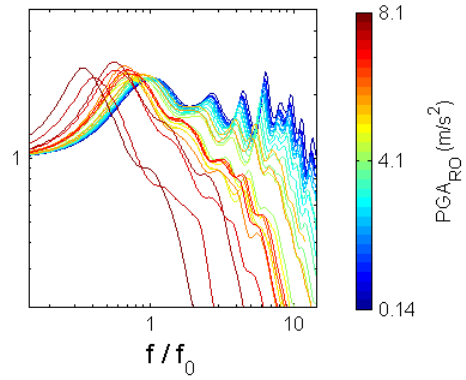

Non-linear Transfer Function

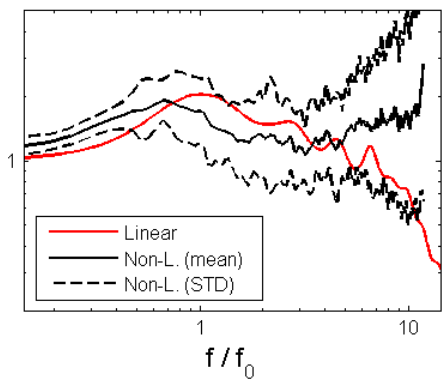

Non-linear TF (color coded by PGA_{RO})

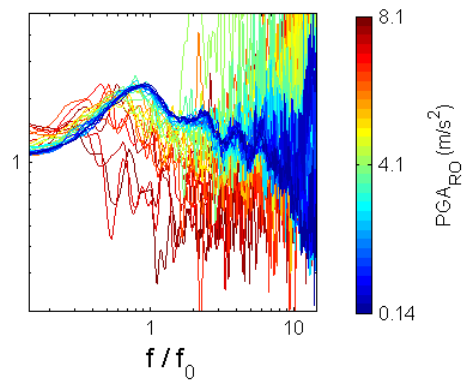

Equiv. Lin. TF (color coded by f_c)

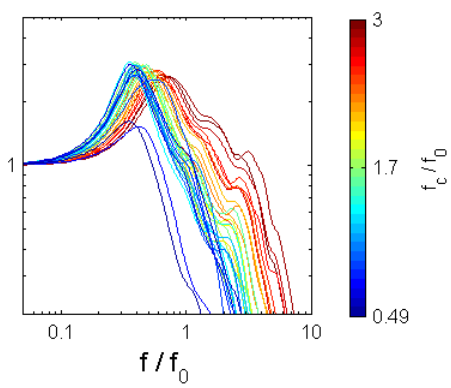

Non-linear TF (color coded by f_c)

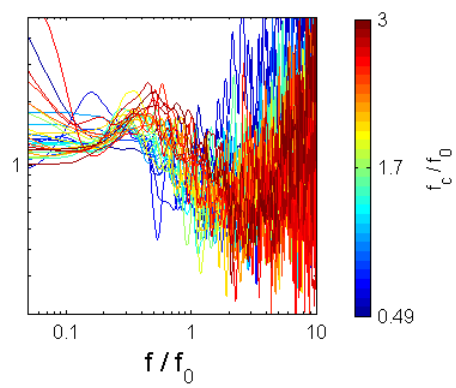

4.1.6 CE.12076

Depth (m)	Thickness (m)	V_s (m/s)	Damping ratio	Density (kg/m^3)
0	1	136	0.05	1600
1	2	211	0.05	1800
3	3	231	0.05	1800
6	6	265	0.02	1800
12	6	265	0.02	1800
18	8	295	0.02	1800
26	10	340	0.02	1800
36	12	402	0.02	1800
48	7	450	0.02	1800
55	5	454.9	0.02	1800
60	5	467.5	0.02	1800
65	5	478.6	0.02	1800
70	5	488.6	0.02	1800
75	5	497.5	0.02	1800
80	5	505.4	0.02	1800
85	5	512.5	0.02	1800
90	5	518.8	0.02	1800
95	5	524.4	0.02	1800
100	–	529.4	0.02	1800

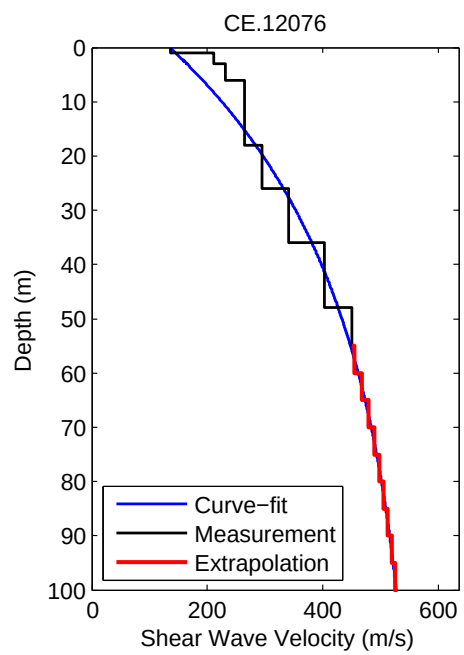

Linear Elastic Transfer Function

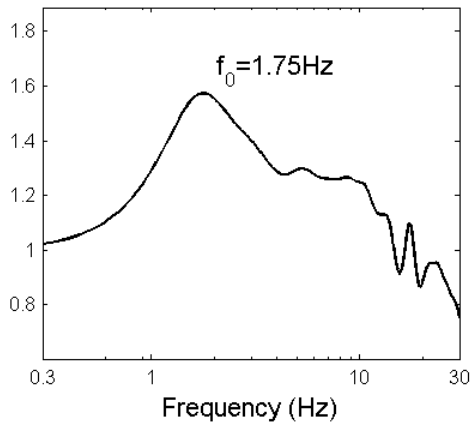

H/V Ratio – Sensor 450

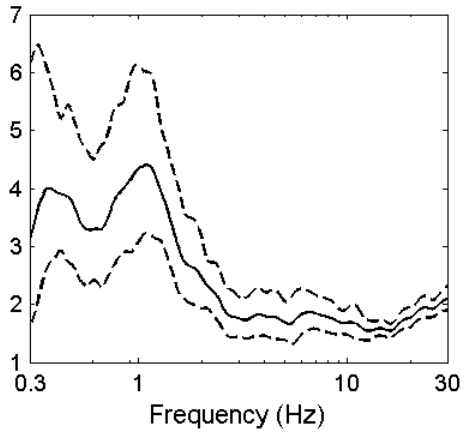

H/V Ratio – Sensor 507

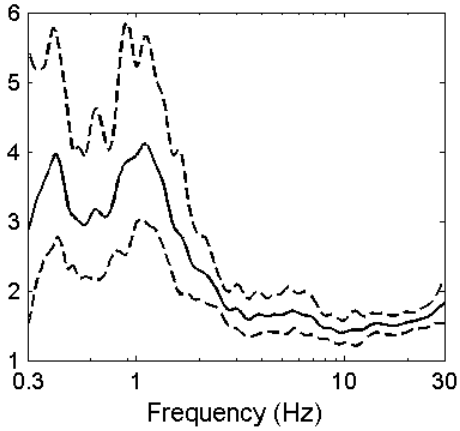

H/V Ratio – Sensor 453

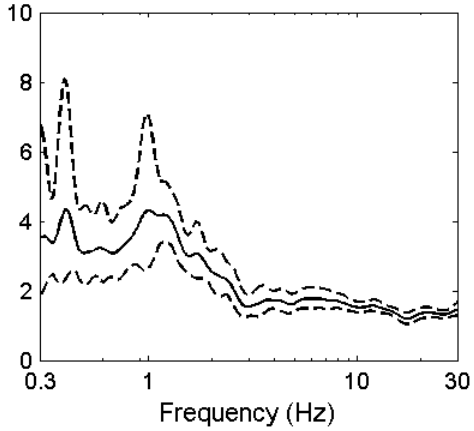

Equivalent Linear Transfer Function

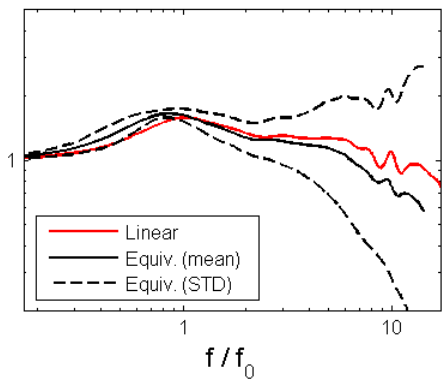

Equiv. Lin. TF (color coded by PGA_{RO})

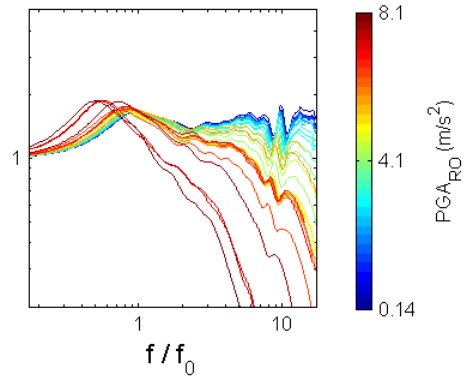

Non-linear Transfer Function

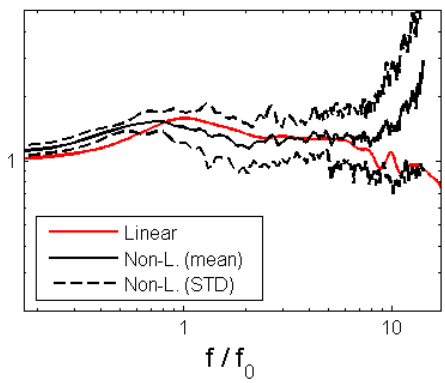

Non-linear TF (color coded by PGA_{RO})

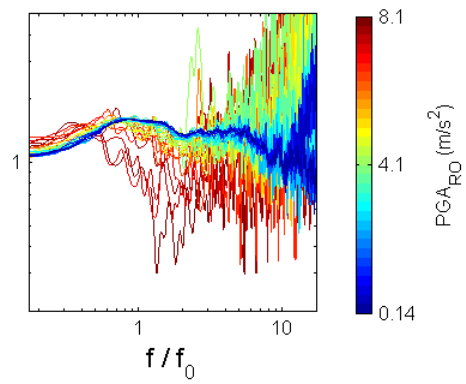

Equiv. Lin. TF (color coded by f_c)

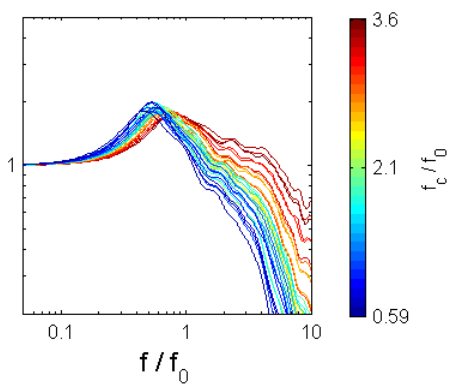

Non-linear TF (color coded by f_c)

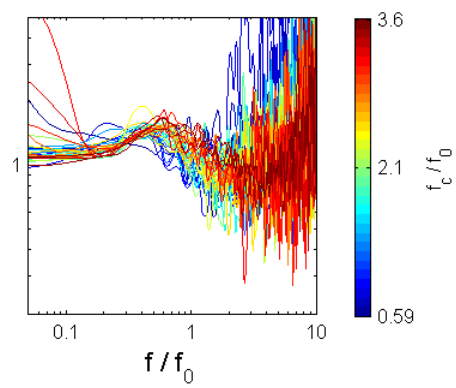

4.1.7 CE.12108

Depth (m)	Thickness (m)	V_s (m/s)	Damping ratio	Density (kg/m^3)
0	1	146	0.05	1600
1	2	210	0.05	1800
3	3	242	0.05	1800
6	4	274	0.02	1800
10	6	298	0.02	1800
16	8	359	0.02	1800
24	10	436	0.02	1800
34	15	467	0.02	1800
49	1	483	0.02	1800
50	5	501.4	0.02	1800
55	5	518.2	0.02	1800
60	5	533.2	0.02	1800
65	5	546.6	0.02	1800
70	5	558.6	0.02	1800
75	5	569.2	0.02	1800
80	5	578.8	0.02	1800
85	5	587.4	0.02	1800
90	5	595.0	0.02	1800
95	5	601.8	0.02	1800
100	–	607.9	0.02	1800

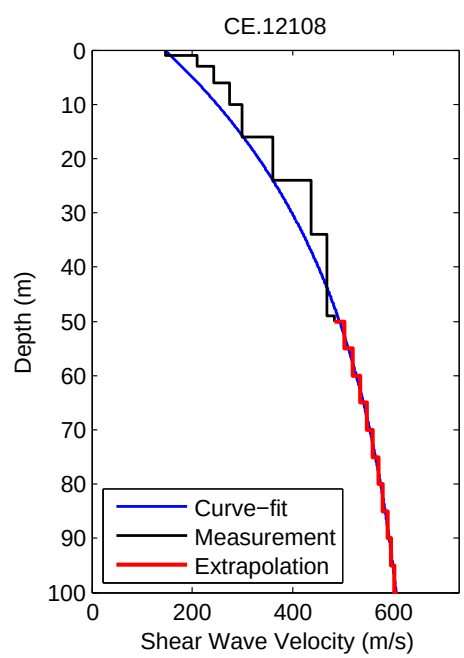

Linear Elastic Transfer Function

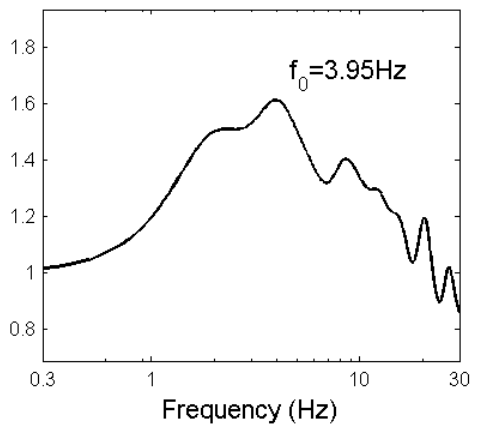

H/V Ratio – Sensor 450

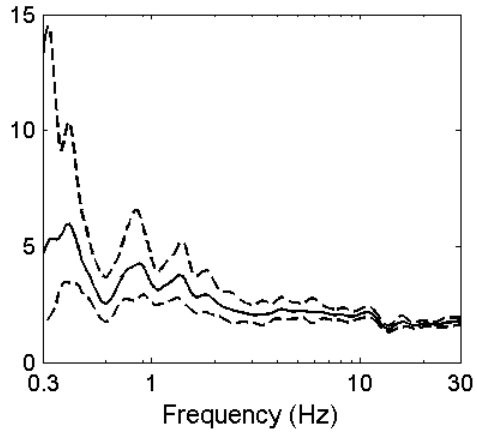

H/V Ratio – Sensor 507

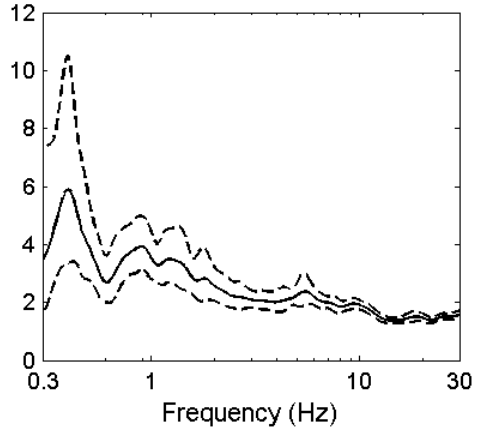

H/V Ratio – Sensor 453

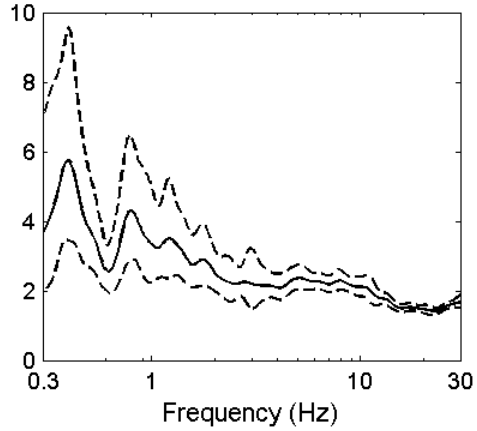

Equivalent Linear Transfer Function

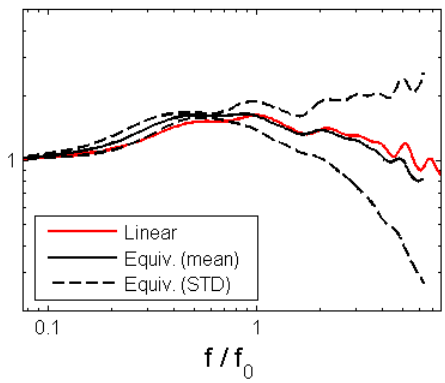

Equiv. Lin. TF (color coded by PGA_{RO})

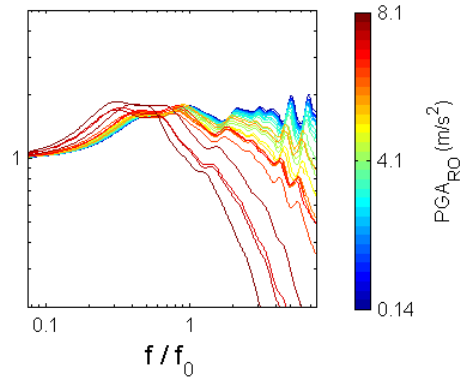

Non-linear Transfer Function

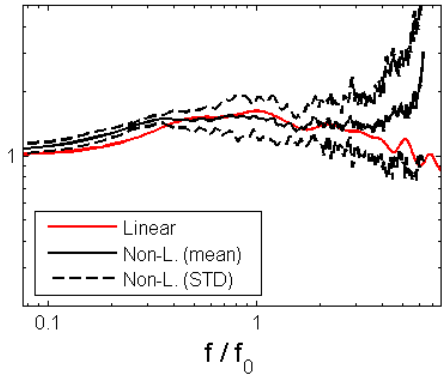

Non-linear TF (color coded by PGA_{RO})

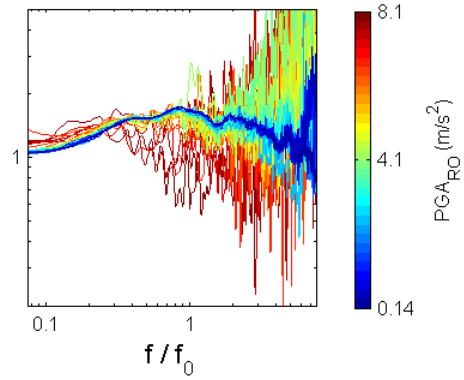

Equiv. Lin. TF (color coded by f_c)

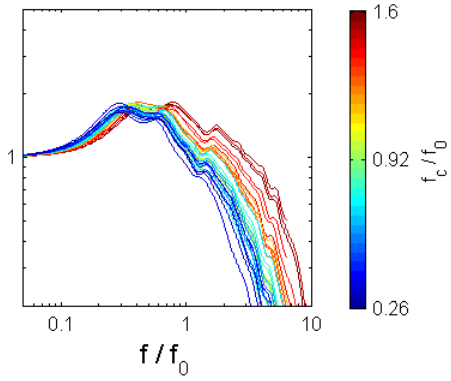

Non-linear TF (color coded by f_c)

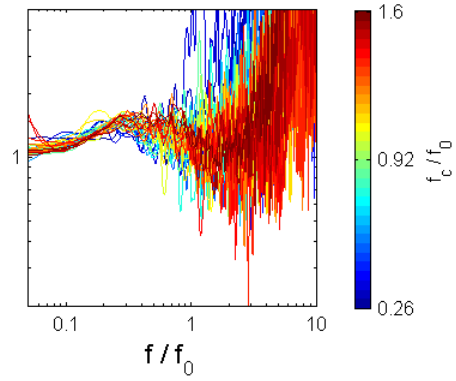

4.1.8 CE.12952

Depth (m)	Thickness (m)	V_s (m/s)	Damping ratio	Density (kg/m^3)
0	0.75	189	0.05	1600
0.75	1	219	0.05	1800
1.75	2.25	194	0.05	1600
4	5	258	0.02	1800
9	8	283	0.02	1800
17	12	307	0.02	1800
29	15	399	0.02	1800
44	11	468	0.02	1800
55	5	473.3	0.02	1800
60	5	485.3	0.02	1800
65	5	496.2	0.02	1800
70	5	506.0	0.02	1800
75	5	514.8	0.02	1800
80	5	522.7	0.02	1800
85	5	529.8	0.02	1800
90	5	536.3	0.02	1800
95	5	542.0	0.02	1800
100	–	547.2	0.02	1800

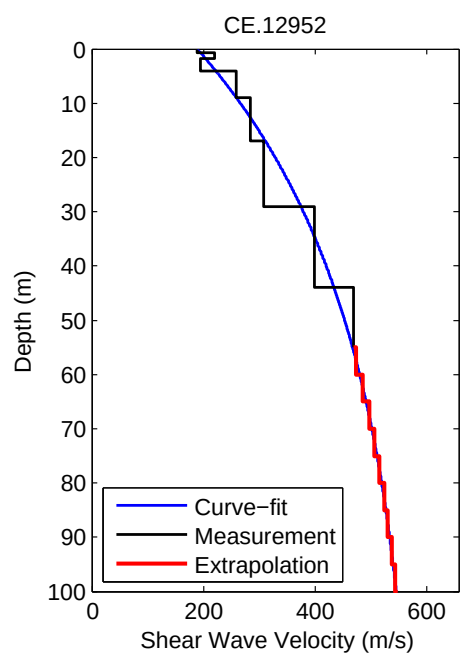

Linear Elastic Transfer Function

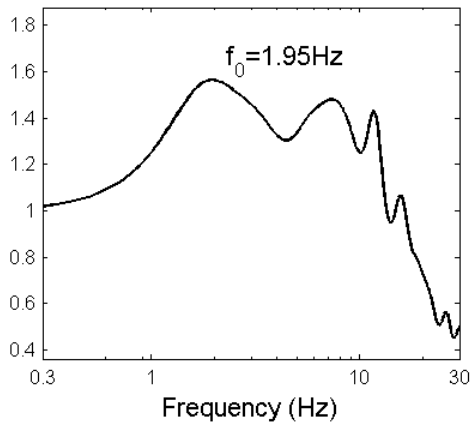

H/V Ratio – Sensor 450

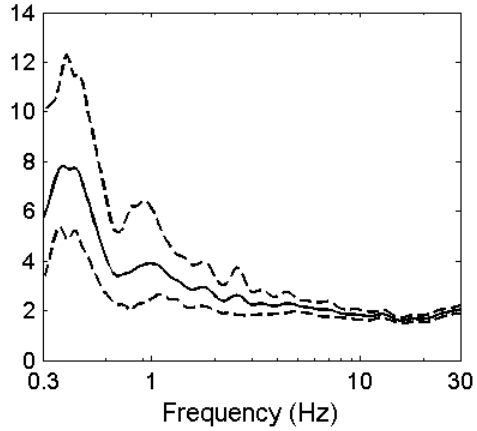

H/V Ratio – Sensor 507

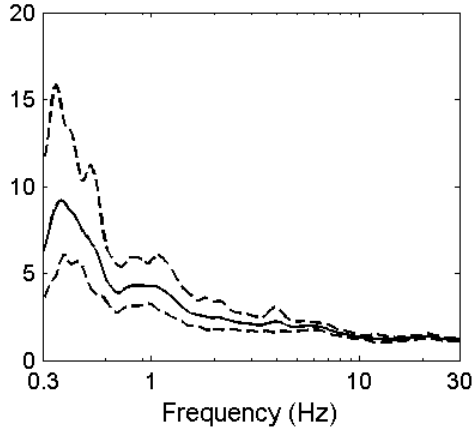

H/V Ratio – Sensor 453

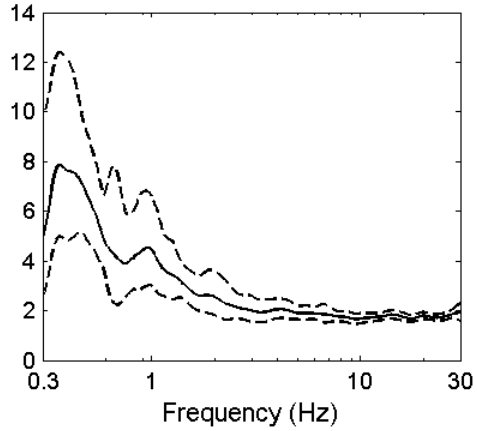

Equivalent Linear Transfer Function

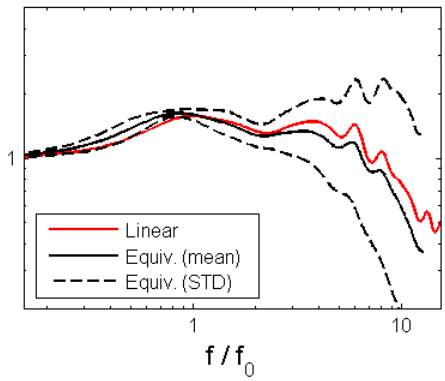

Equiv. Lin. TF (color coded by PGA_{RO})

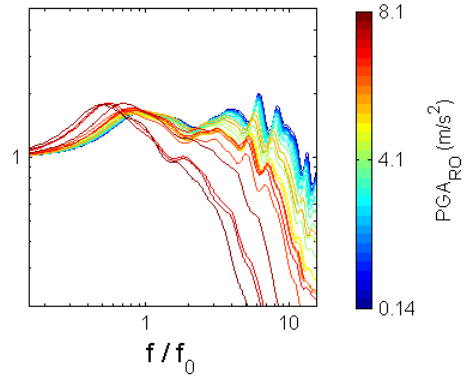

Non-linear Transfer Function

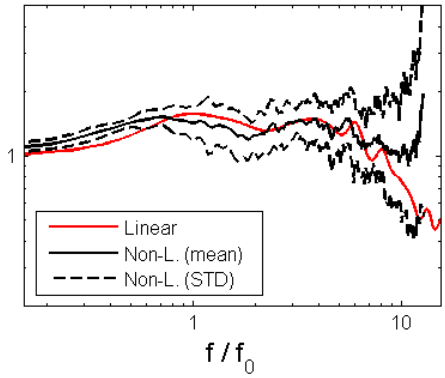

Non-linear TF (color coded by PGA_{RO})

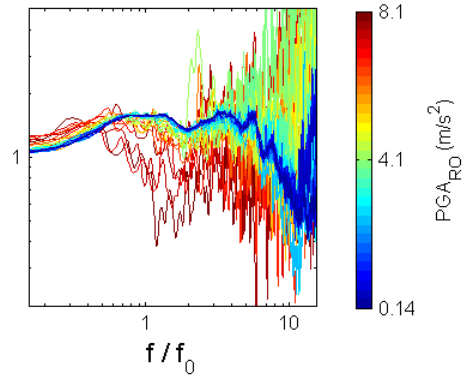

Equiv. Lin. TF (color coded by f_c)

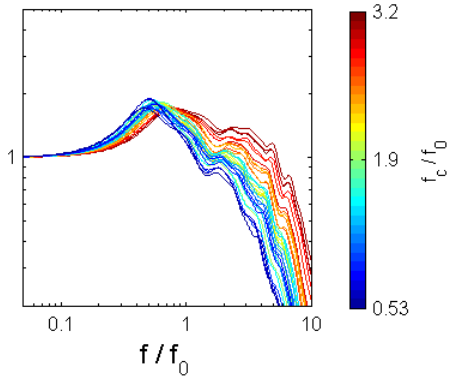

Non-linear TF (color coded by f_c)

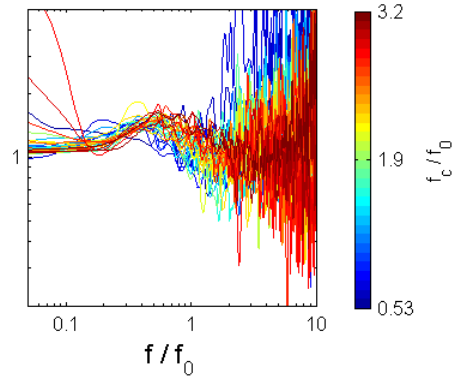

4.1.9 CE.14241

Depth (m)	Thickness (m)	V_s (m/s)	Damping ratio	Density (kg/m^3)
0	1	215	0.05	1800
1	2.5	172	0.05	1600
3.5	3.5	232	0.05	1800
7	4	273	0.02	1800
11	6	317	0.02	1800
17	9	331	0.02	1800
26	15	350	0.02	1800
41	15	426	0.02	1800
56	18	503	0.02	1800
74	–	574	0.02	1800

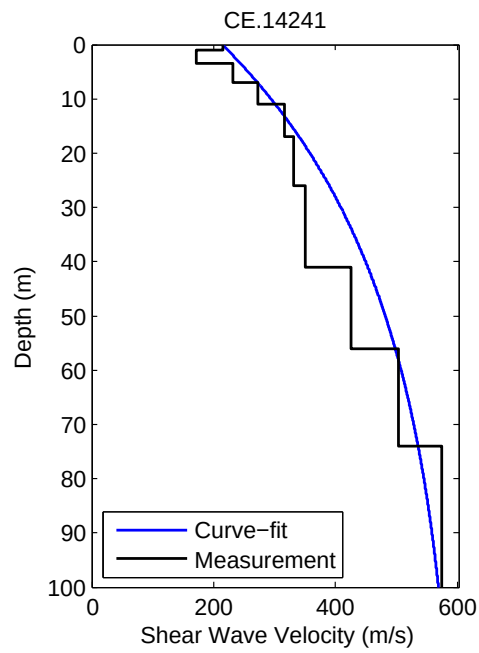

Linear Elastic Transfer Function

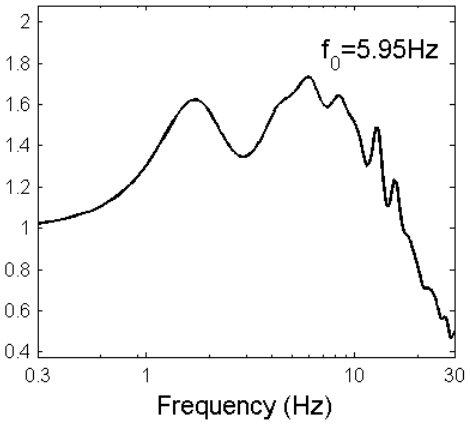

H/V Ratio – Sensor 450

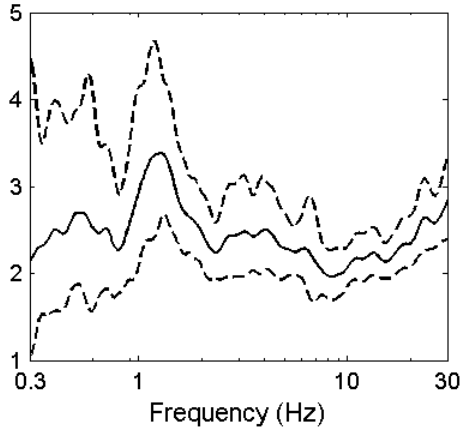

H/V Ratio – Sensor 507

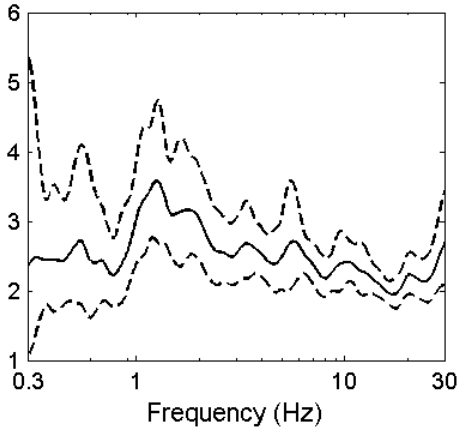

H/V Ratio – Sensor 453

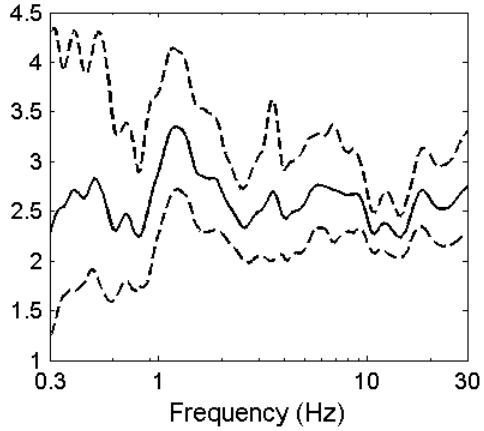

Equivalent Linear Transfer Function

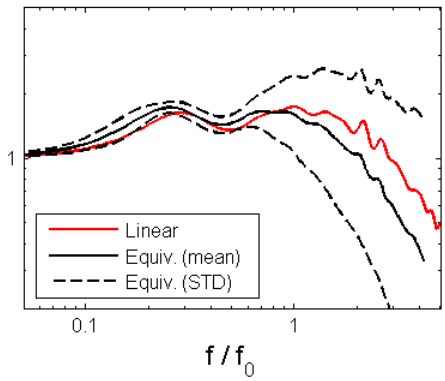

Equiv. Lin. TF (color coded by PGA_{RO})

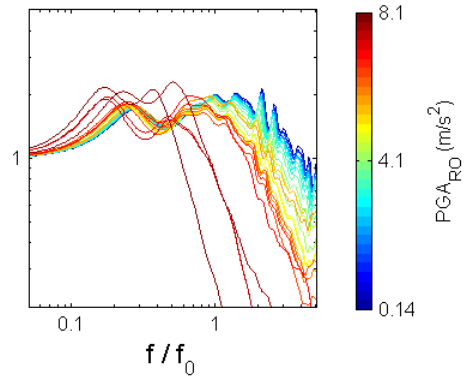

Non-linear Transfer Function

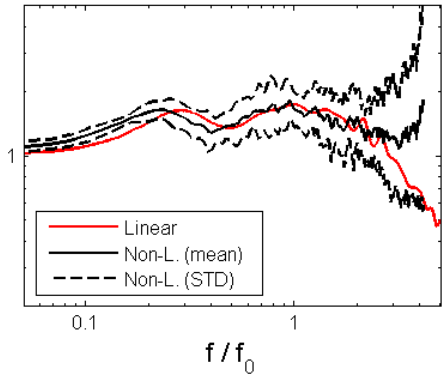

Non-linear TF (color coded by PGA_{RO})

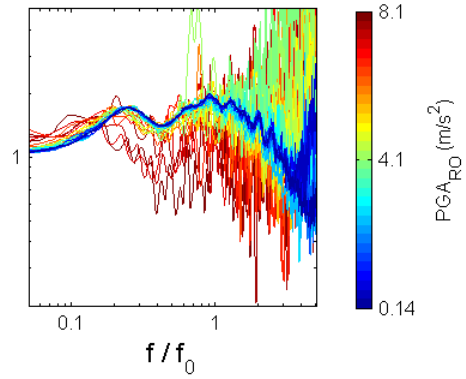

Equiv. Lin. TF (color coded by f_c)

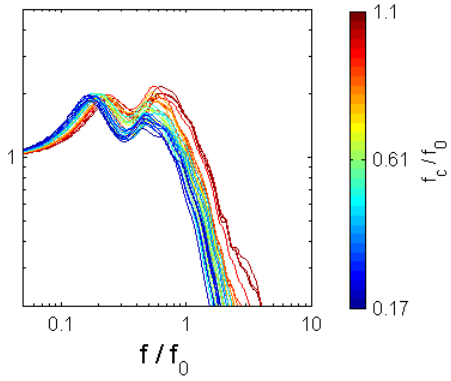

Non-linear TF (color coded by f_c)

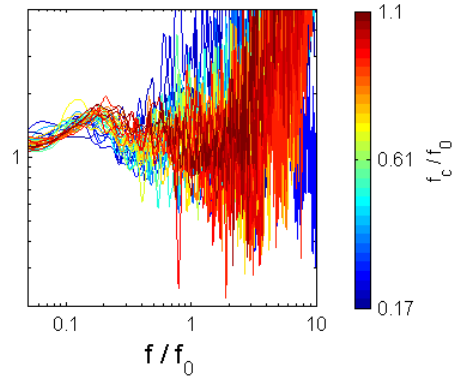

4.1.10 CE.14395

Depth (m)	Thickness (m)	V_s (m/s)	Damping ratio	Density (kg/m^3)
0	2	228	0.05	1800
2	3	203	0.05	1800
5	4	175	0.05	1600
9	6	222	0.05	1800
15	9	238	0.05	1800
24	12	312	0.02	1800
36	15	386	0.02	1800
51	20	421	0.02	1800
71	–	499	0.02	1800

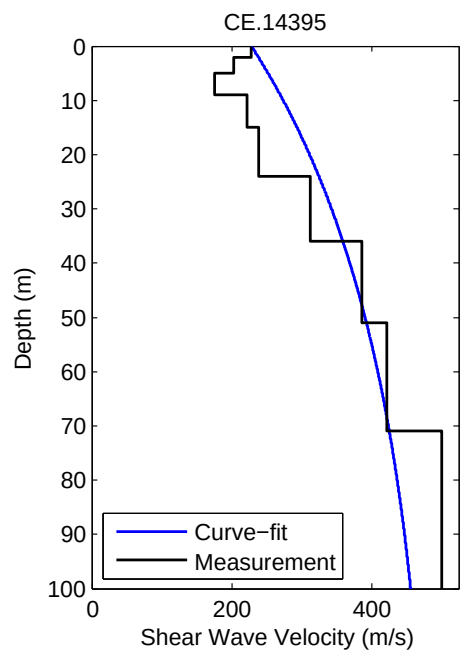

Linear Elastic Transfer Function

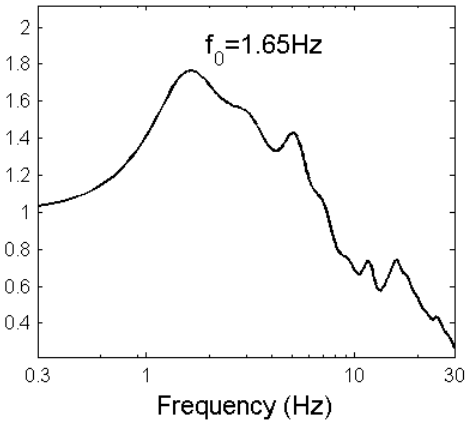

H/V Ratio – Sensor 450

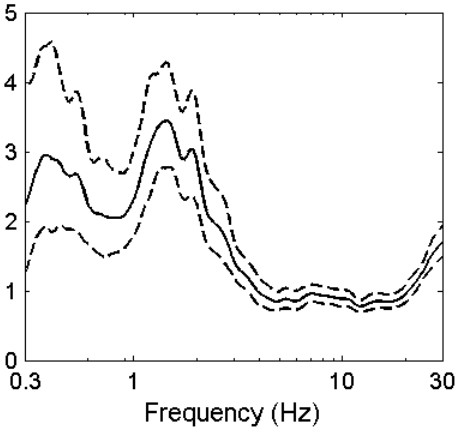

H/V Ratio – Sensor 507

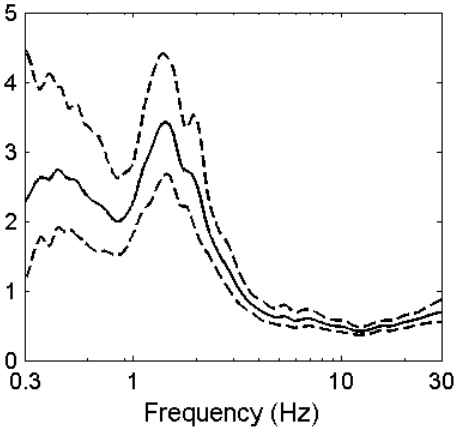

H/V Ratio – Sensor 453

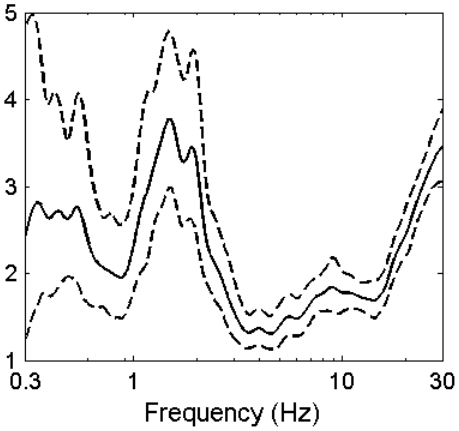

Equivalent Linear Transfer Function

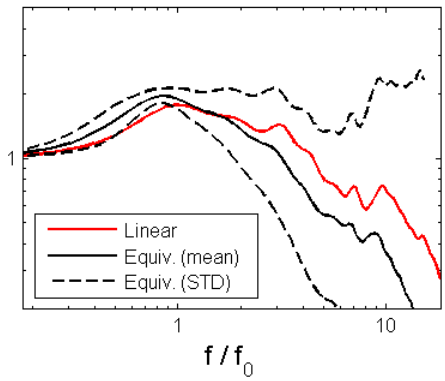

Equiv. Lin. TF (color coded by PGA_{RO})

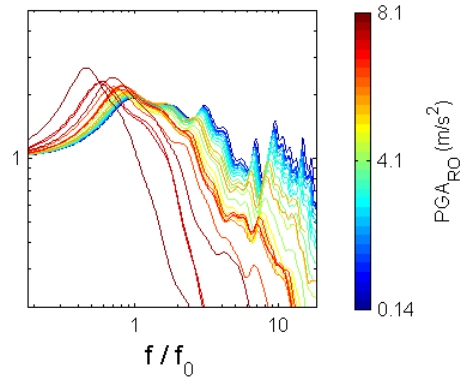

Non-linear Transfer Function

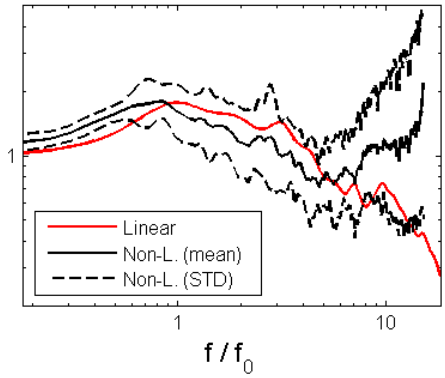

Non-linear TF (color coded by PGA_{RO})

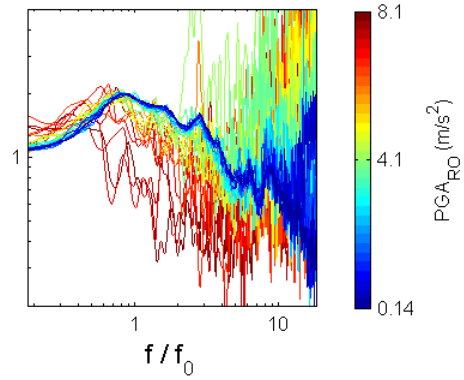

Equiv. Lin. TF (color coded by f_c)

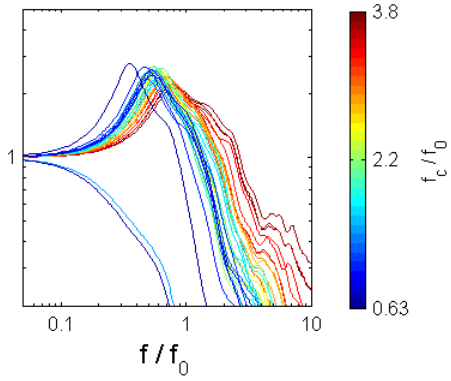

Non-linear TF (color coded by f_c)

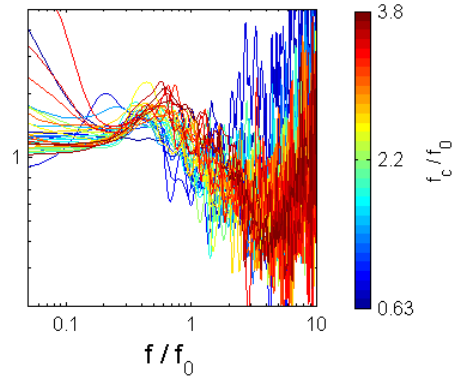

4.1.11 CE.23958

Depth (m)	Thickness (m)	V_s (m/s)	Damping ratio	Density (kg/m^3)
0	1	147	0.05	1600
1	2	280	0.02	1800
3	3	364	0.02	1800
6	5	399	0.02	1800
11	9	498	0.02	1800
20	12	552	0.02	1800
32	15	593	0.02	1800
47	20	643	0.02	1800
67	3	719	0.02	1800
70	5	738.0	0.02	1800
75	5	757.0	0.01	1800
80	5	774.4	0.01	1800
85	5	790.3	0.01	1800
90	5	804.9	0.01	2000
95	5	818.2	0.01	2000
100	–	830.4	0.01	2000

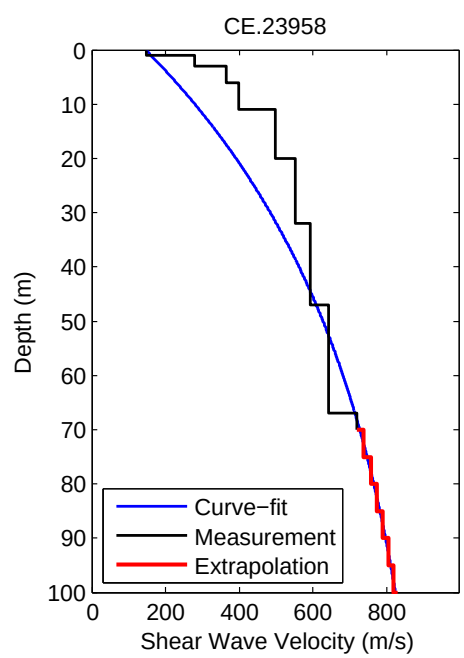

Linear Elastic Transfer Function

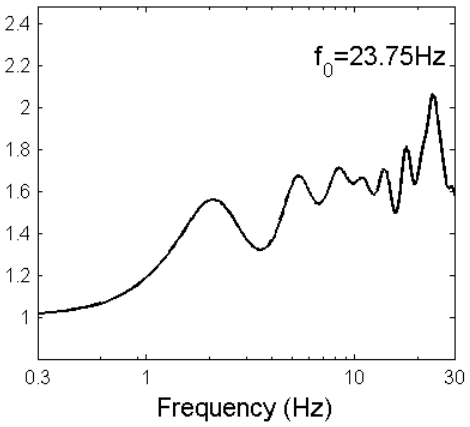

H/V Ratio – Sensor 450

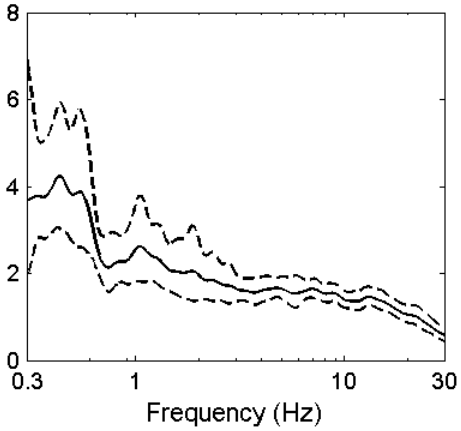

H/V Ratio – Sensor 507

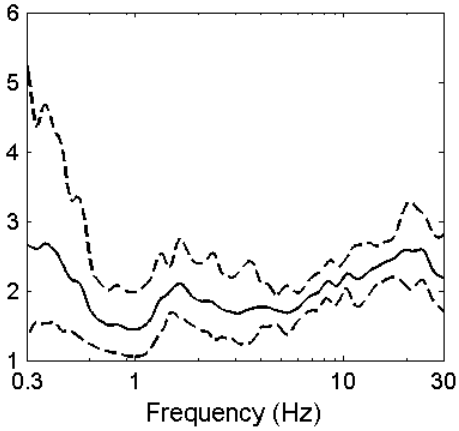

H/V Ratio – Sensor 453

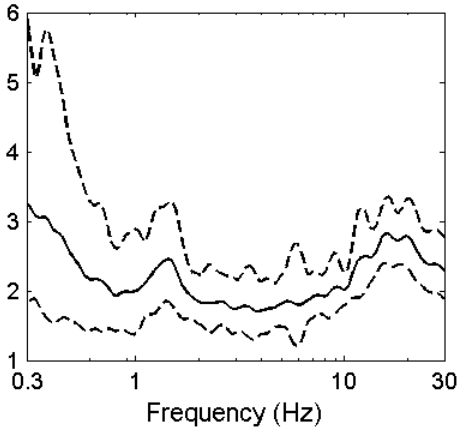

Equivalent Linear Transfer Function

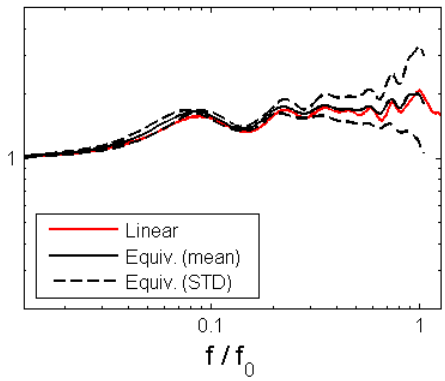

Equiv. Lin. TF (color coded by PGA_{RO})

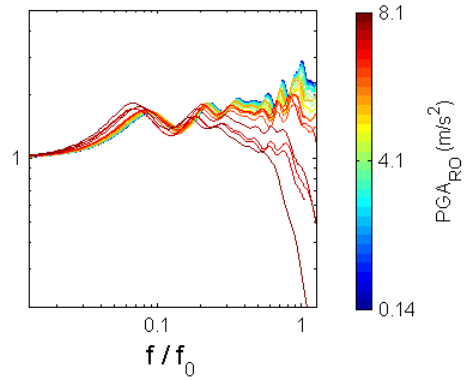

Non-linear Transfer Function

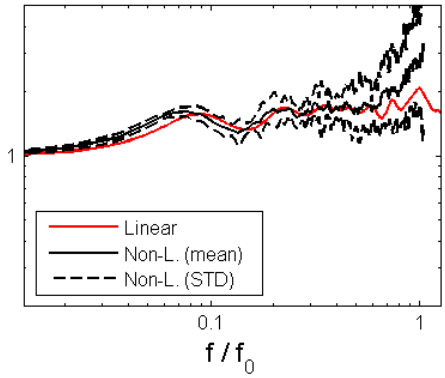

Non-linear TF (color coded by PGA_{RO})

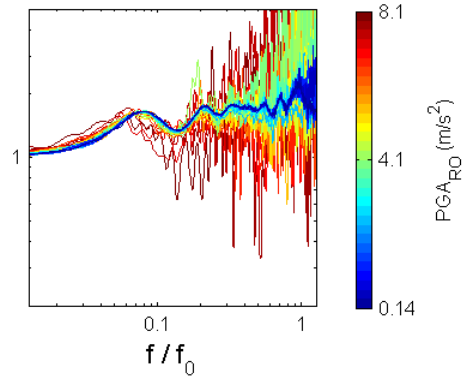

Equiv. Lin. TF (color coded by f_c)

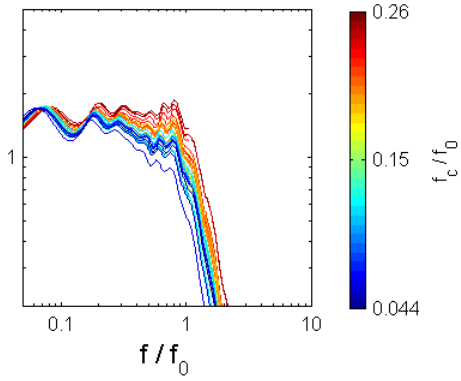

Non-linear TF (color coded by f_c)

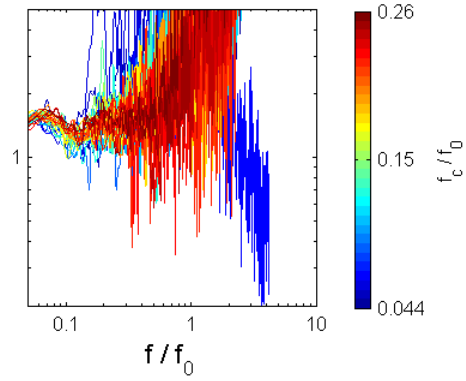

4.1.12 CE.24965

Depth (m)	Thickness (m)	V_s (m/s)	Damping ratio	Density (kg/m^3)
0	1	145	0.05	1600
1	2	182	0.05	1600
3	3	243	0.05	1800
6	4	267	0.02	1800
10	6	288	0.02	1800
16	9	292	0.02	1800
25	12	413	0.02	1800
37	18	434	0.02	1800
55	–	1342	0.01	2000

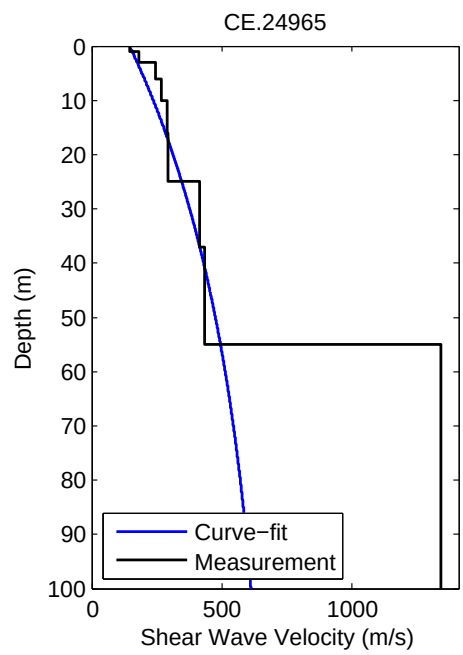

Linear Elastic Transfer Function

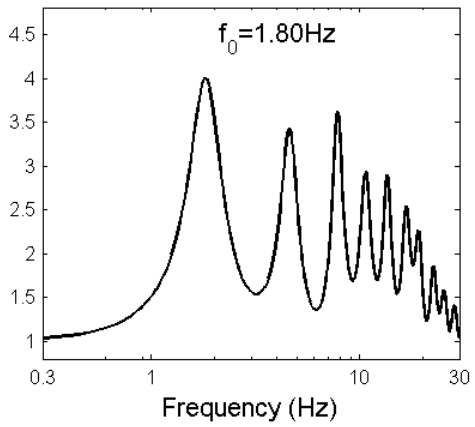

H/V Ratio – Sensor 450

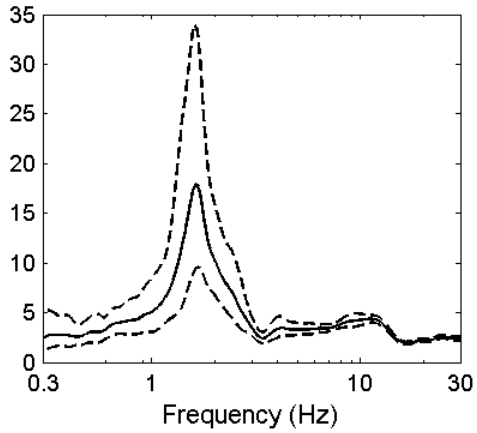

H/V Ratio – Sensor 507

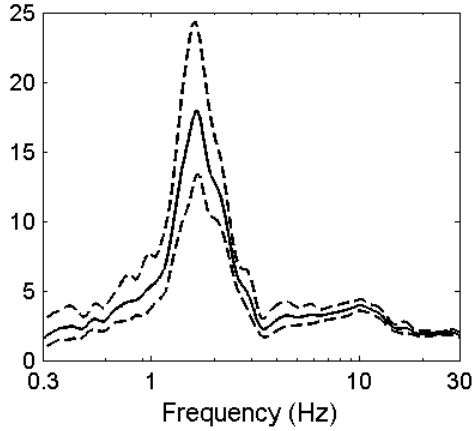

H/V Ratio – Sensor 453

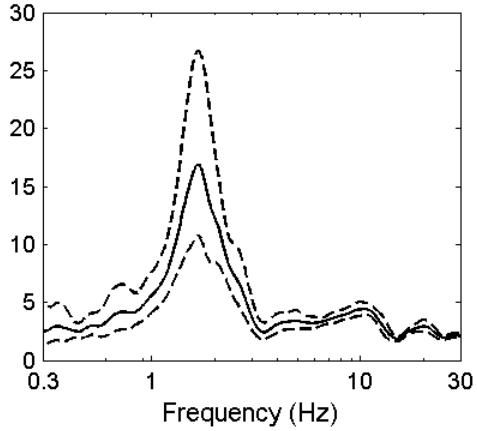

Equivalent Linear Transfer Function

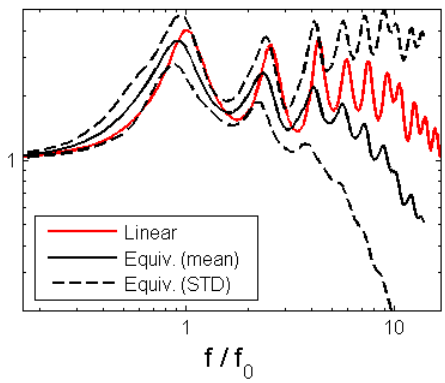

Equiv. Lin. TF (color coded by PGA_{RO})

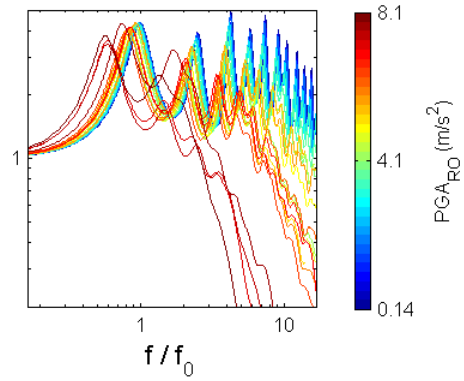

Non-linear Transfer Function

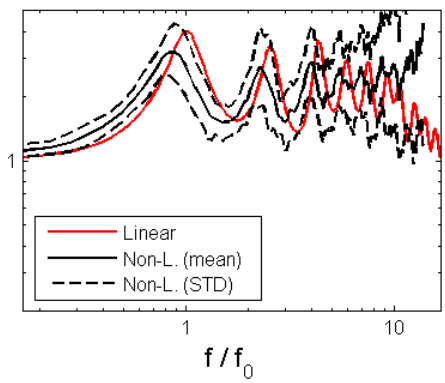

Non-linear TF (color coded by PGA_{RO})

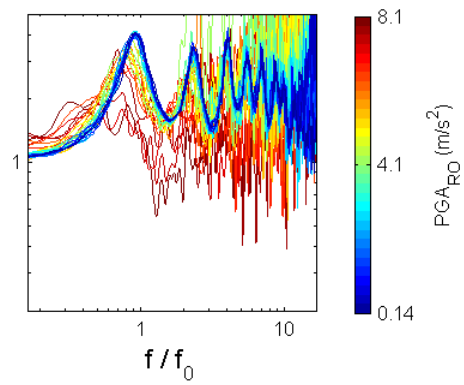

Equiv. Lin. TF (color coded by f_c)

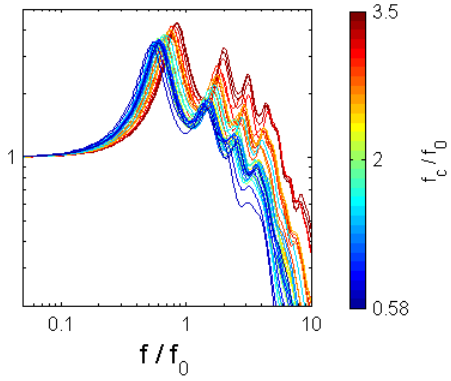

Non-linear TF (color coded by f_c)

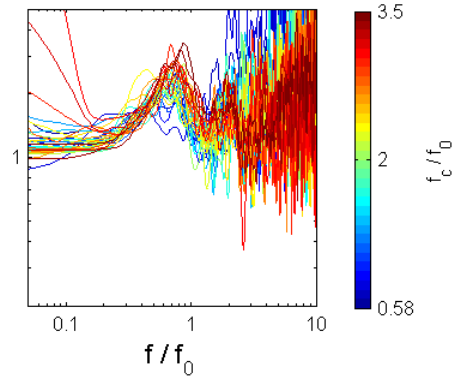

4.1.13 CE.24967

Depth (m)	Thickness (m)	V_s (m/s)	Damping ratio	Density (kg/m^3)
0	3	215	0.05	1800
3	3	248	0.05	1800
6	10	332	0.02	1800
16	12	390	0.02	1800
28	15	489	0.02	1800
43	17	614	0.02	1800
60	–	2233	0.01	2000

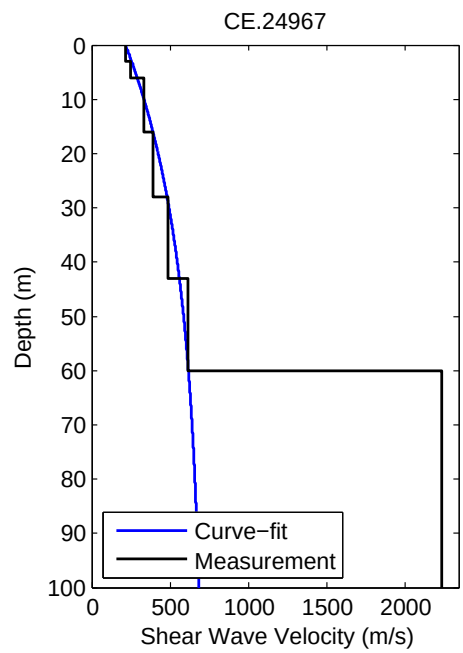

Linear Elastic Transfer Function

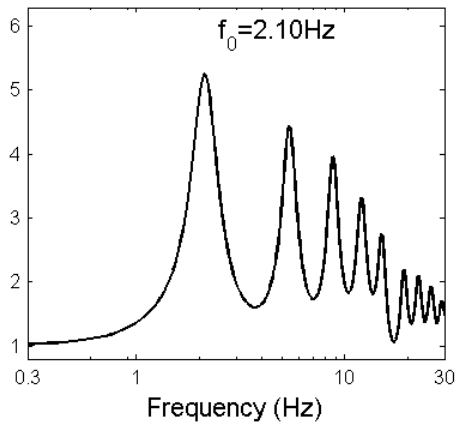

H/V Ratio – Sensor 450

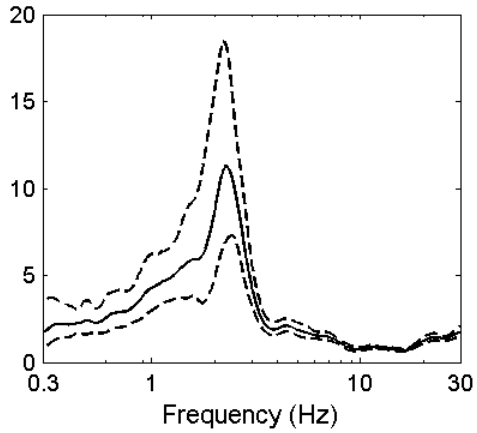

H/V Ratio – Sensor 507

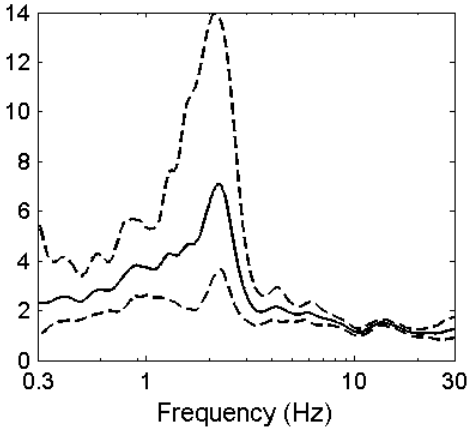

H/V Ratio – Sensor 453

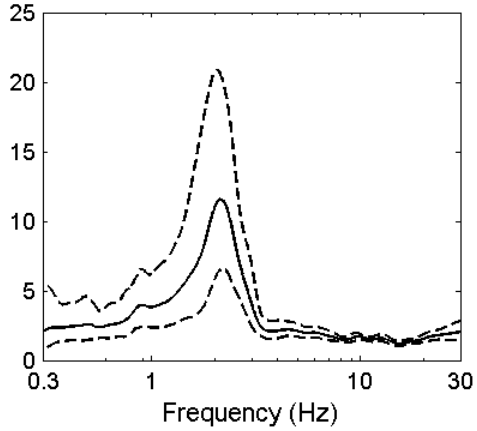

Equivalent Linear Transfer Function

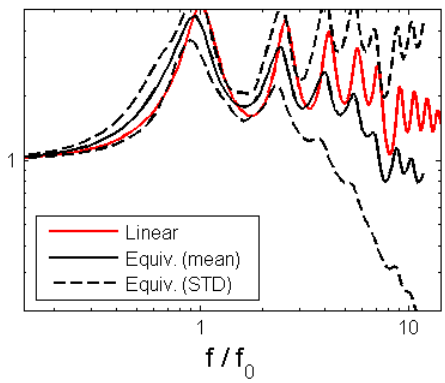

Equiv. Lin. TF (color coded by PGA_{RO})

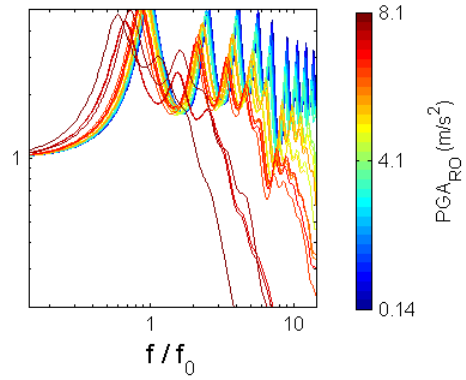

Non-linear Transfer Function

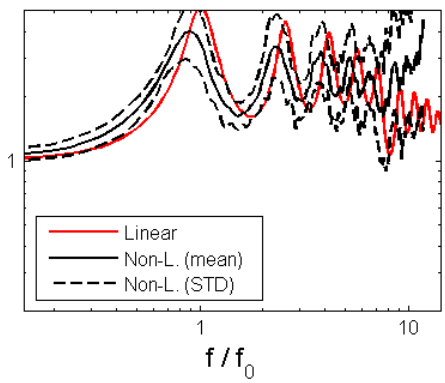

Non-linear TF (color coded by PGA_{RO})

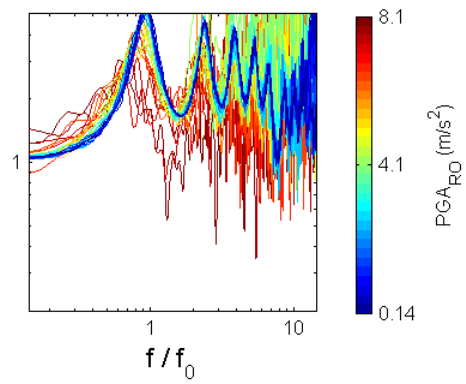

Equiv. Lin. TF (color coded by f_c)

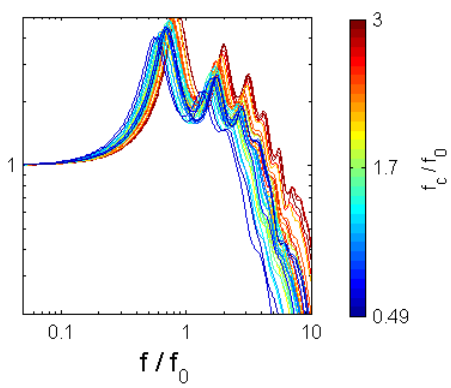

Non-linear TF (color coded by f_c)

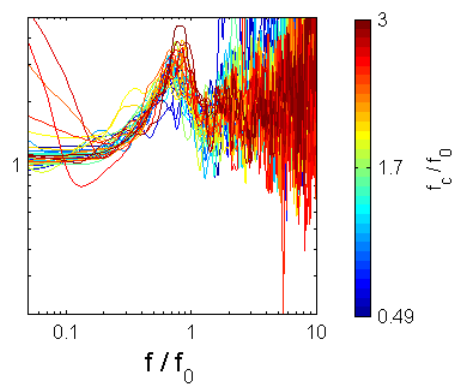

4.1.14 CI.BAK

Depth (m)	Thickness (m)	V_s (m/s)	Damping ratio	Density (kg/m^3)
0	0.5	77	0.05	1600
0.5	1	220	0.05	1800
1.5	2	221	0.05	1800
3.5	3	202	0.05	1800
6.5	5	274	0.02	1800
11.5	7.5	296	0.02	1800
19	10	353	0.02	1800
29	13	454	0.02	1800
42	16	500	0.02	1800
58	22	613	0.02	1800
80	5	617.1	0.02	1800
85	5	622.1	0.02	1800
90	5	626.4	0.02	1800
95	5	629.9	0.02	1800
100	–	632.9	0.02	1800

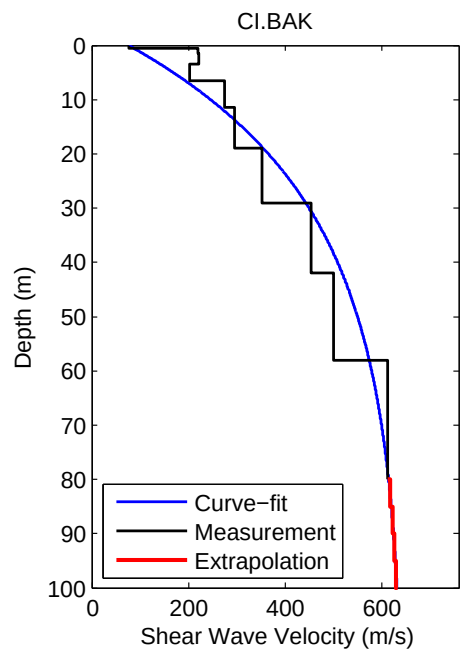

Linear Elastic Transfer Function

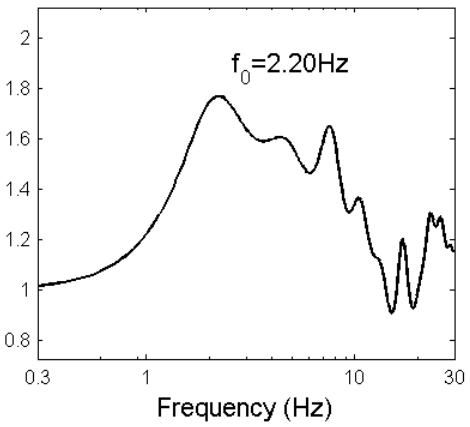

H/V Ratio – Sensor 450

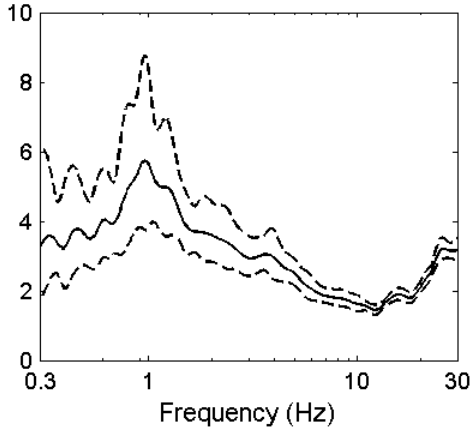

H/V Ratio – Sensor 507

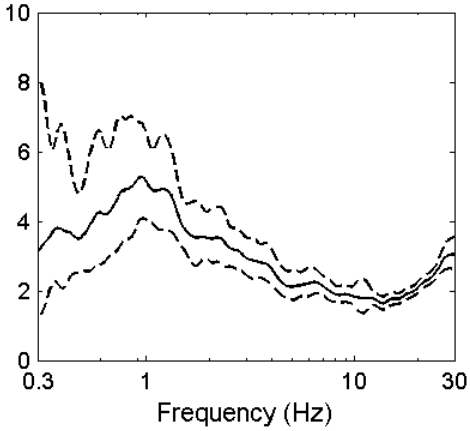

H/V Ratio – Sensor 453

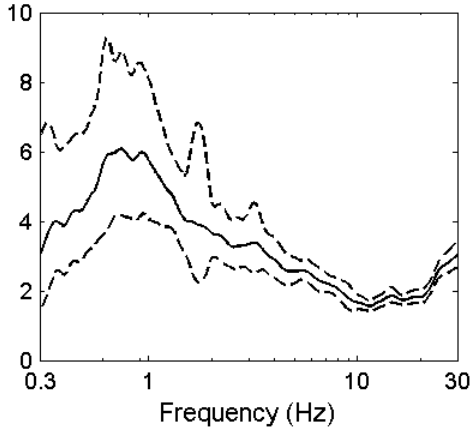

Equivalent Linear Transfer Function

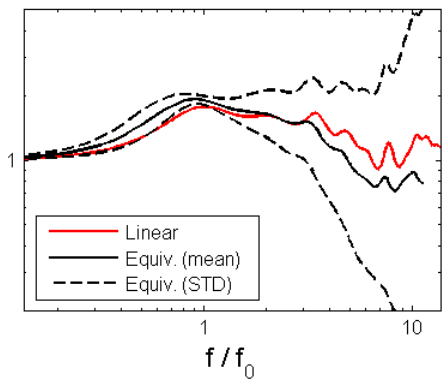

Equiv. Lin. TF (color coded by PGA_{RO})

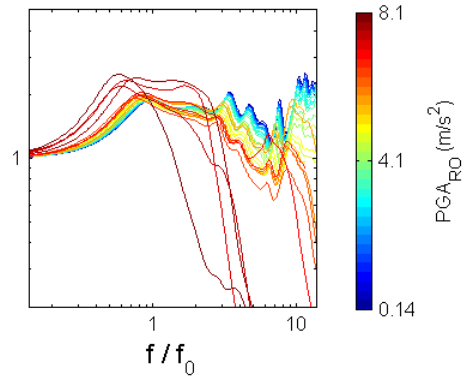

Non-linear Transfer Function

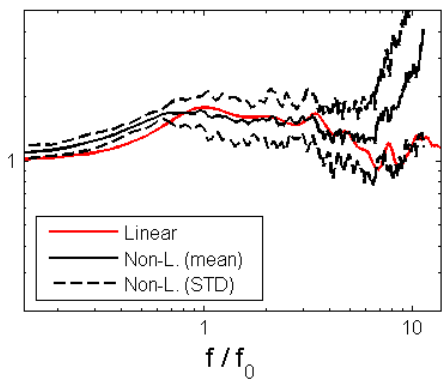

Non-linear TF (color coded by PGA_{RO})

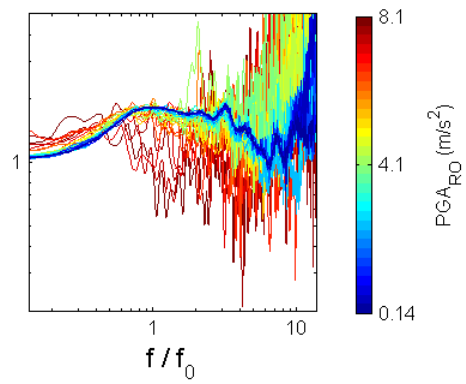

Equiv. Lin. TF (color coded by f_c)

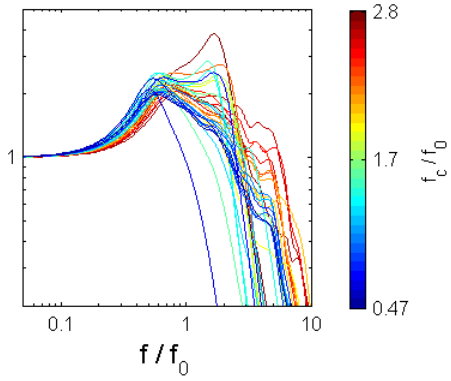

Non-linear TF (color coded by f_c)

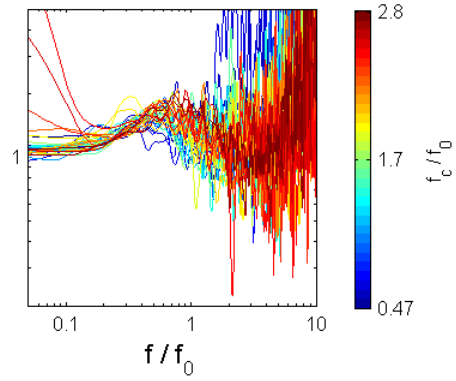

4.1.15 CI.BBS

Depth (m)	Thickness (m)	V_s (m/s)	Damping ratio	Density (kg/m^3)
0	1	233	0.05	1800
1	4	286	0.02	1800
5	7	297	0.02	1800
12	9	374	0.02	1800
21	11	407	0.02	1800
32	–	900	0.01	2000

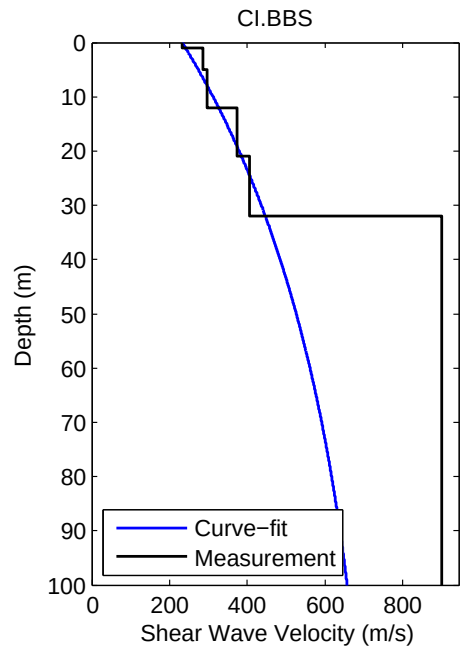

Linear Elastic Transfer Function

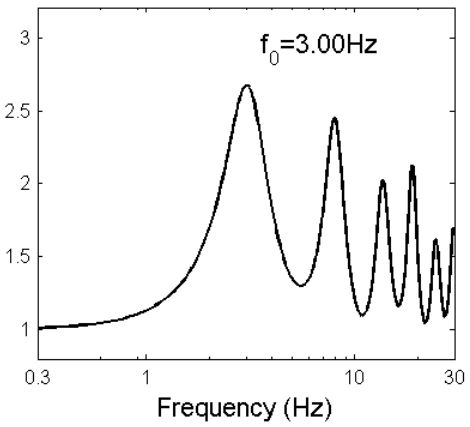

H/V Ratio – Sensor 450

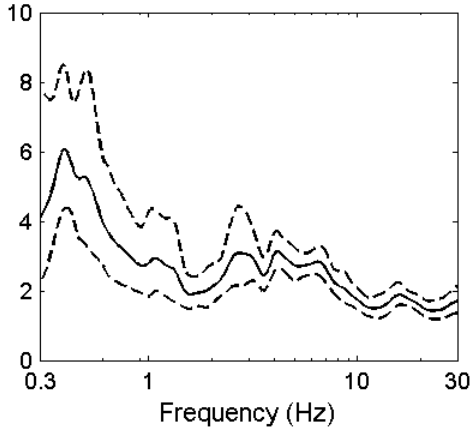

H/V Ratio – Sensor 507

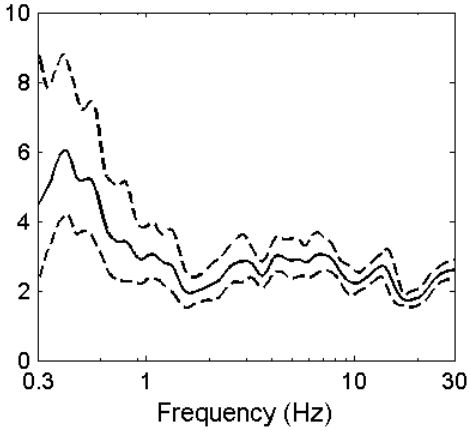

H/V Ratio – Sensor 453

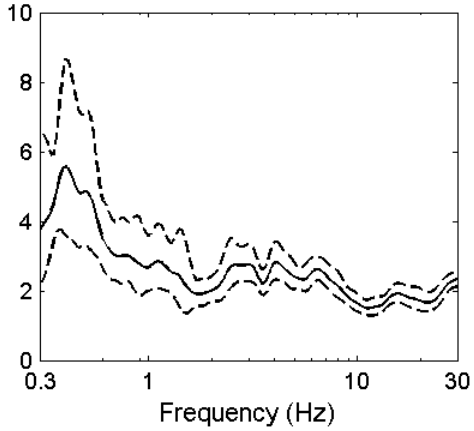

Equivalent Linear Transfer Function

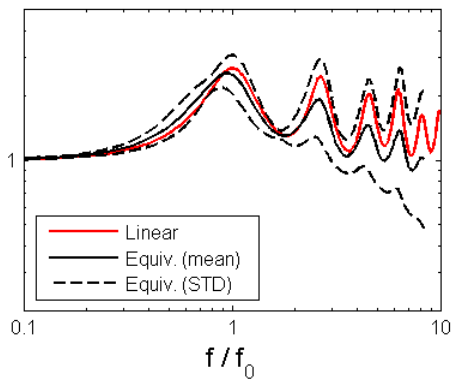

Equiv. Lin. TF (color coded by PGA_{RO})

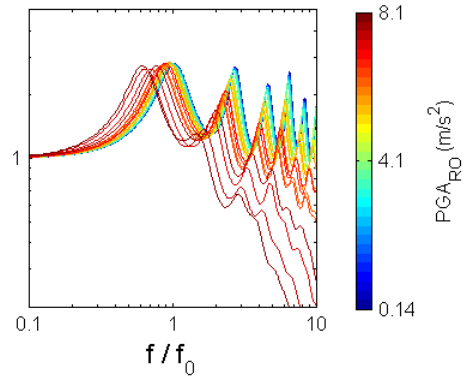

Non-linear Transfer Function

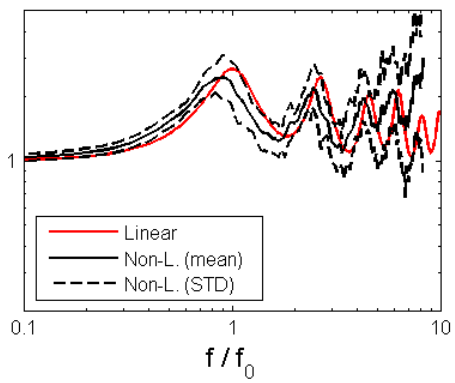

Non-linear TF (color coded by PGA_{RO})

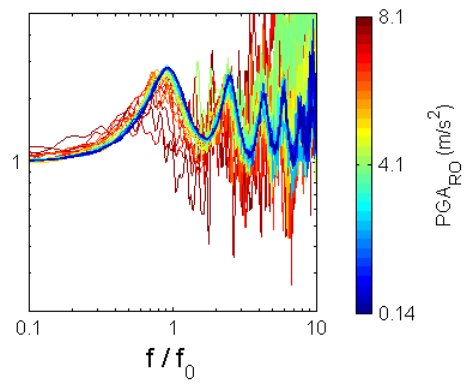

Equiv. Lin. TF (color coded by f_c)

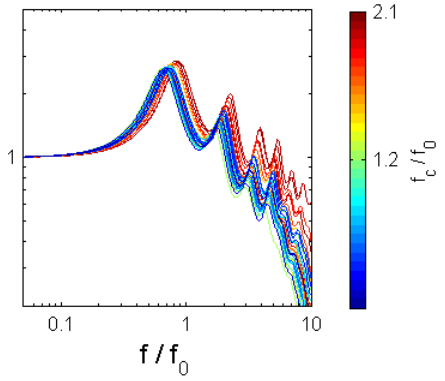

Non-linear TF (color coded by f_c)

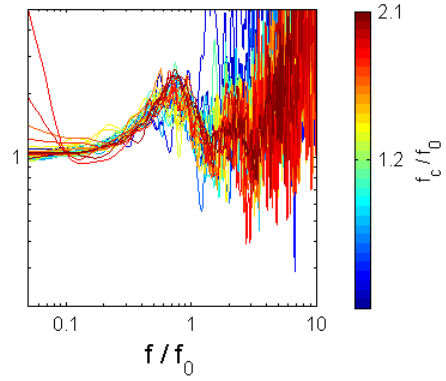

4.1.16 CI.BHPa

Depth (m)	Thickness (m)	V_s (m/s)	Damping ratio	Density (kg/m^3)
0	1	142	0.05	1600
1	2	165	0.05	1600
3	3	249	0.05	1800
6	4	322	0.02	1800
10	6	327	0.02	1800
16	9	343	0.02	1800
25	12	409	0.02	1800
37	15	455	0.02	1800
52	3	479	0.02	1800
55	5	504.4	0.02	1800
60	5	521.4	0.02	1800
65	5	537.0	0.02	1800
70	5	551.2	0.02	1800
75	5	564.2	0.02	1800
80	5	576.0	0.02	1800
85	5	586.9	0.02	1800
90	5	596.7	0.02	1800
95	5	605.8	0.02	1800
100	–	614.0	0.02	1800

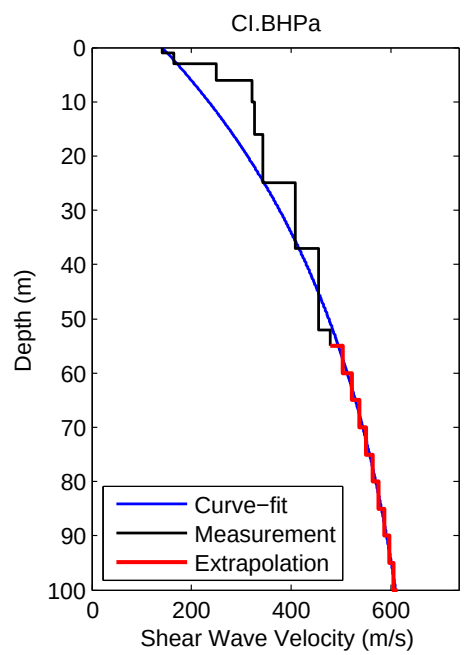

Linear Elastic Transfer Function

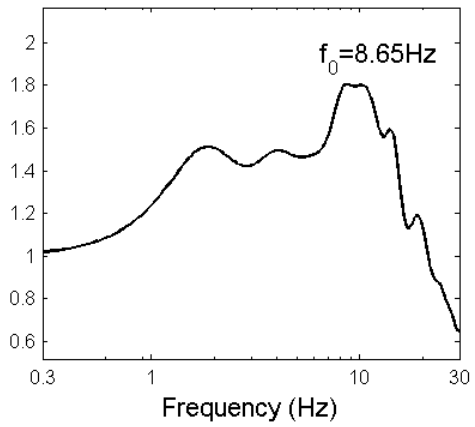

H/V Ratio – Sensor 450

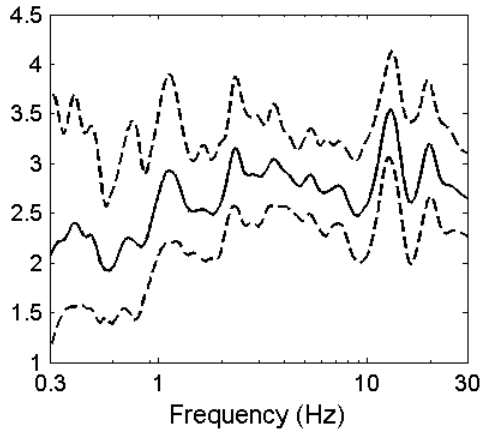

H/V Ratio – Sensor 507

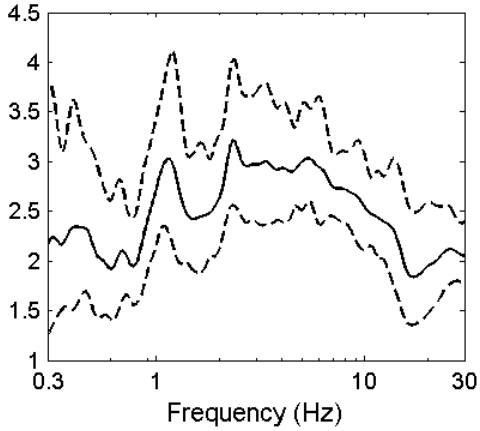

H/V Ratio – Sensor 453

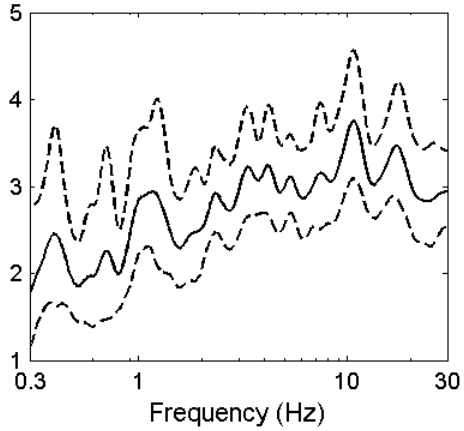

Equivalent Linear Transfer Function

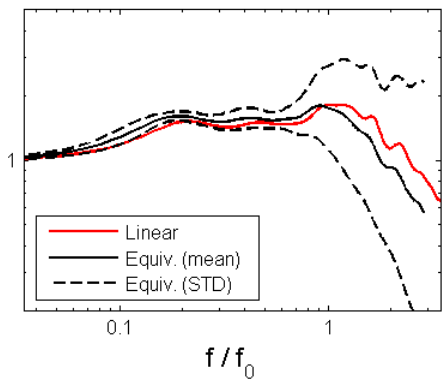

Equiv. Lin. TF (color coded by PGA_{RO})

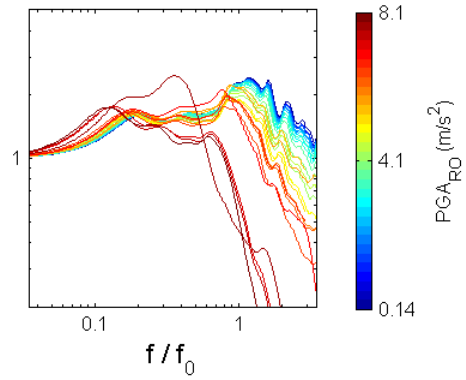

Non-linear Transfer Function

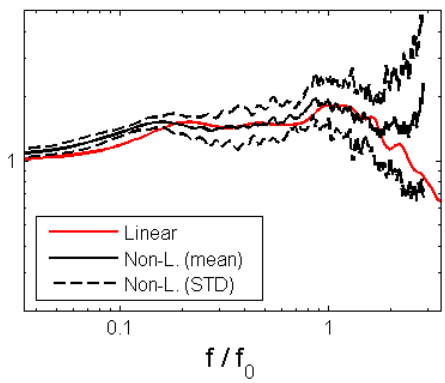

Non-linear TF (color coded by PGA_{RO})

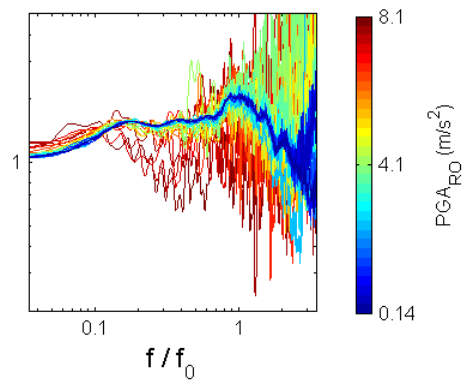

Equiv. Lin. TF (color coded by f_c)

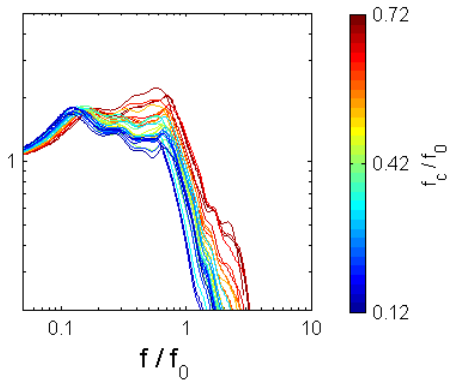

Non-linear TF (color coded by f_c)

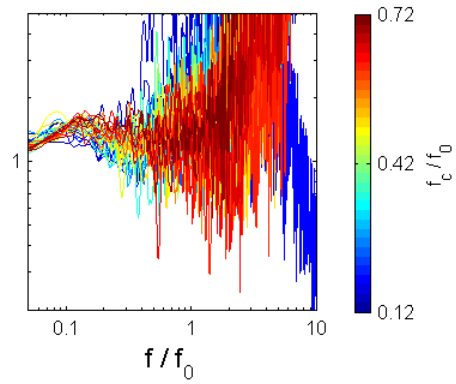

4.1.17 CI.BHPb

Depth (m)	Thickness (m)	V_s (m/s)	Damping ratio	Density (kg/m^3)
0	1	156	0.05	1600
1	2	223	0.05	1800
3	8	272	0.02	1800
11	8	326	0.02	1800
19	8	349	0.02	1800
27	12	421	0.02	1800
39	15	462	0.02	1800
54	1	472	0.02	1800
55	5	492.8	0.02	1800
60	5	509.5	0.02	1800
65	5	524.8	0.02	1800
70	5	539.0	0.02	1800
75	5	551.9	0.02	1800
80	5	563.9	0.02	1800
85	5	574.9	0.02	1800
90	5	585.0	0.02	1800
95	5	594.2	0.02	1800
100	–	602.8	0.02	1800

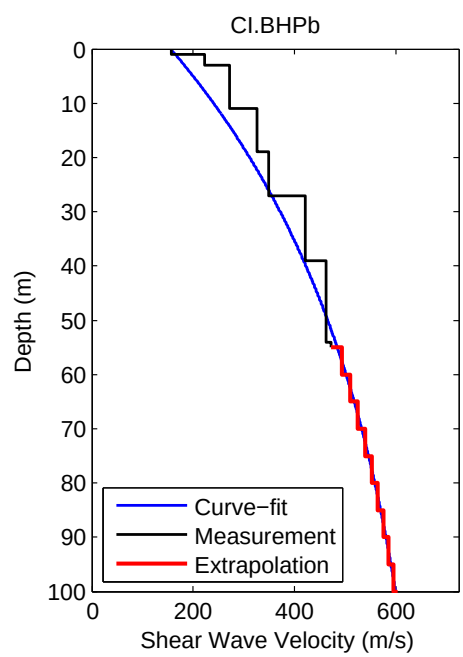

Linear Elastic Transfer Function

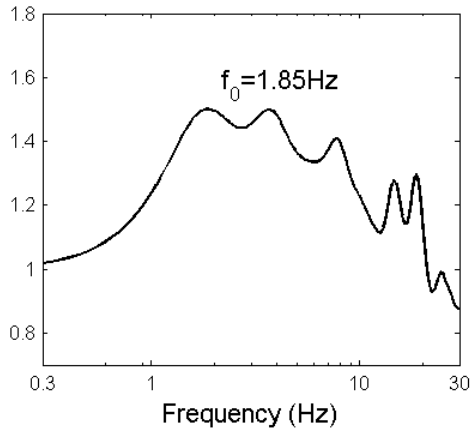

H/V Ratio – Sensor 450

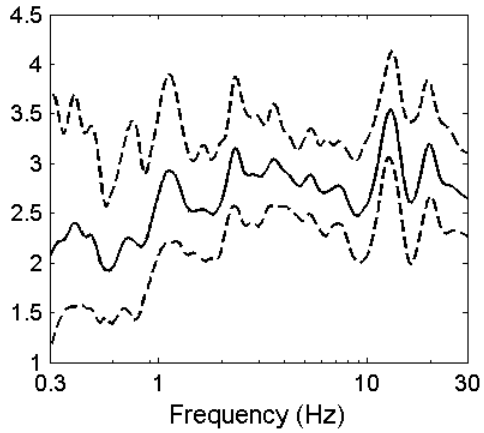

H/V Ratio – Sensor 507

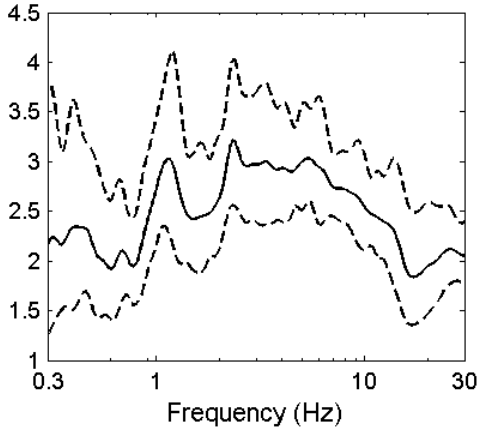

H/V Ratio – Sensor 453

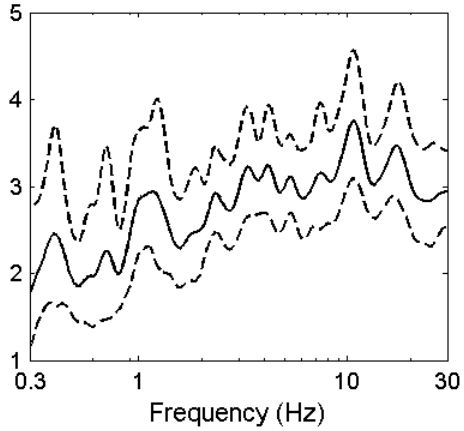

Equivalent Linear Transfer Function

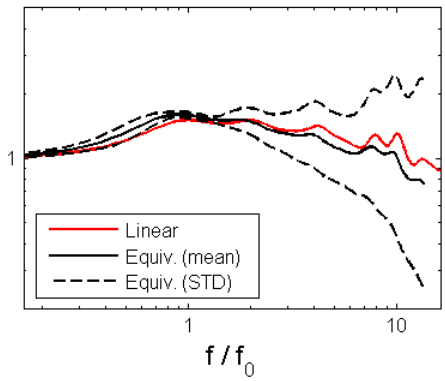

Equiv. Lin. TF (color coded by PGA_{RO})

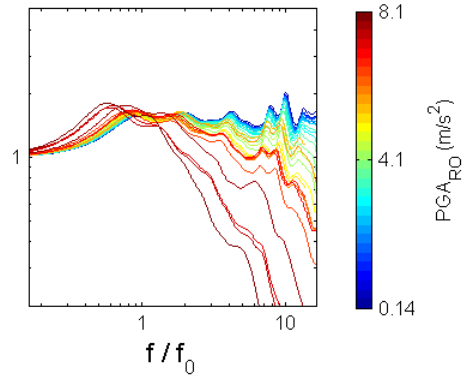

Non-linear Transfer Function

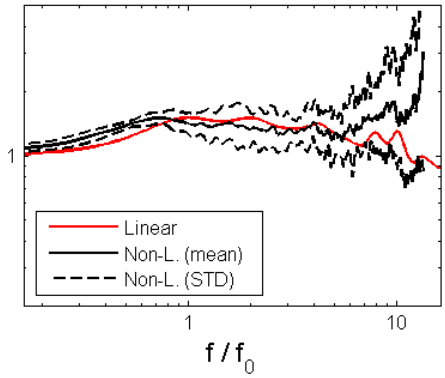

Non-linear TF (color coded by PGA_{RO})

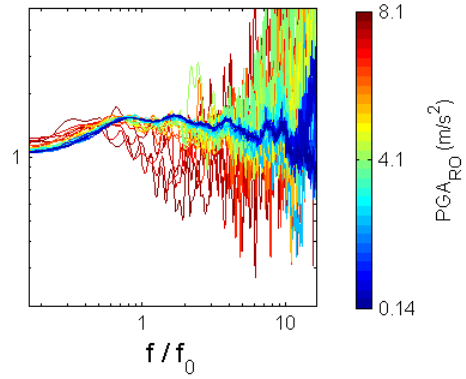

Equiv. Lin. TF (color coded by f_c)

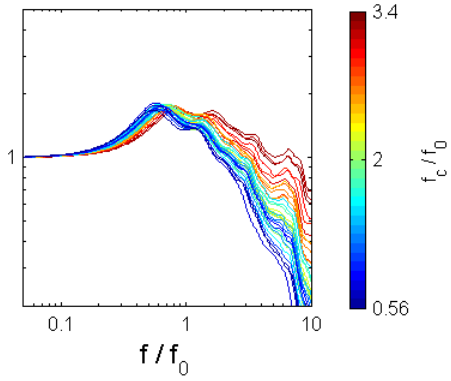

Non-linear TF (color coded by f_c)

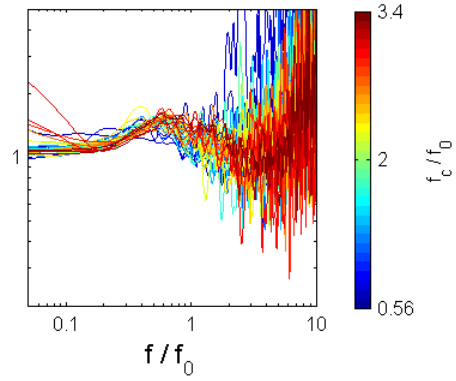

4.1.18 CI.BOMa

Depth (m)	Thickness (m)	V_s (m/s)	Damping ratio	Density (kg/m^3)
0	1	146	0.05	1600
1	2	170	0.05	1600
3	3	190	0.05	1600
6	8	212	0.05	1800
14	15	215	0.05	1800
29	11	304	0.02	1800
40	5	312.5	0.02	1800
45	5	325.2	0.02	1800
50	5	336.8	0.02	1800
55	5	347.4	0.02	1800
60	5	357.2	0.02	1800
65	5	366.1	0.02	1800
70	5	374.3	0.02	1800
75	5	381.8	0.02	1800
80	5	388.6	0.02	1800
85	5	394.9	0.02	1800
90	5	400.7	0.02	1800
95	5	406.0	0.02	1800
100	–	410.9	0.02	1800

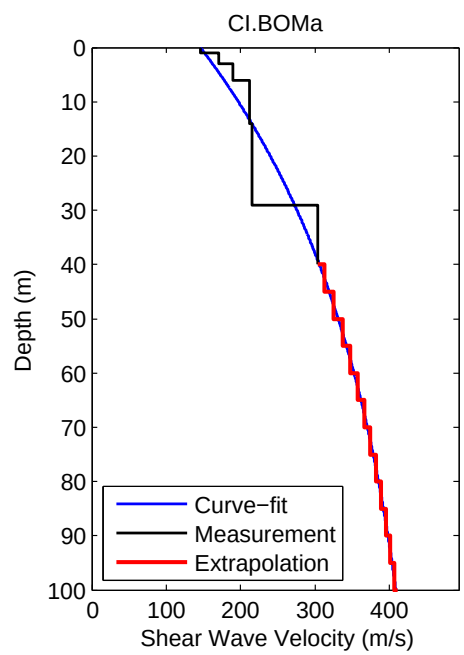

Linear Elastic Transfer Function

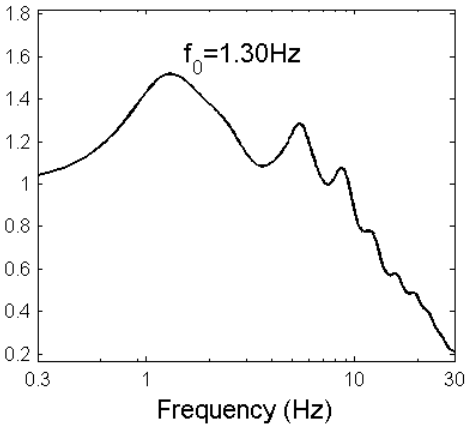

H/V Ratio – Sensor 450

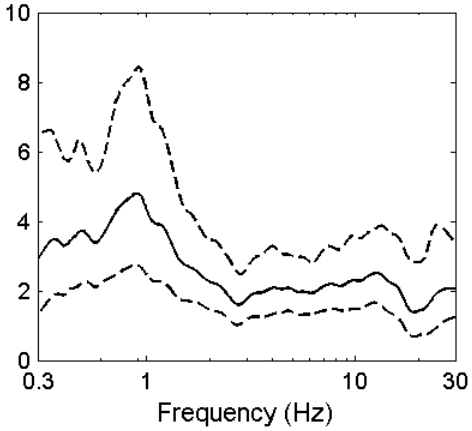

H/V Ratio – Sensor 507

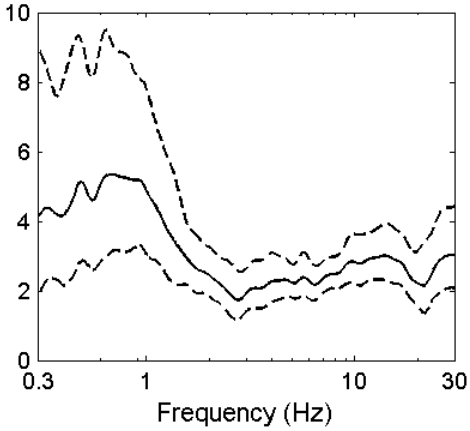

H/V Ratio – Sensor 453

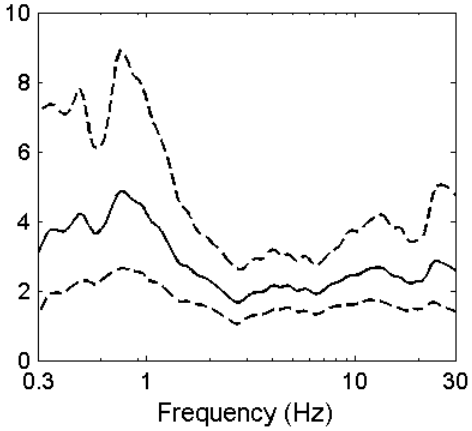

Equivalent Linear Transfer Function

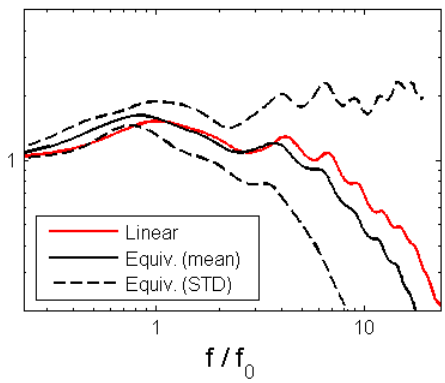

Equiv. Lin. TF (color coded by PGA_{RO})

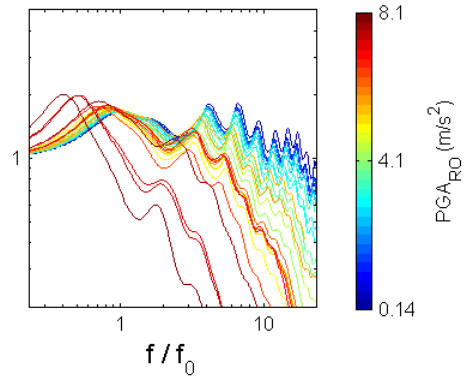

Non-linear Transfer Function

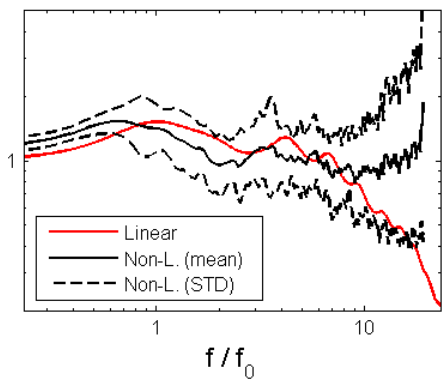

Non-linear TF (color coded by PGA_{RO})

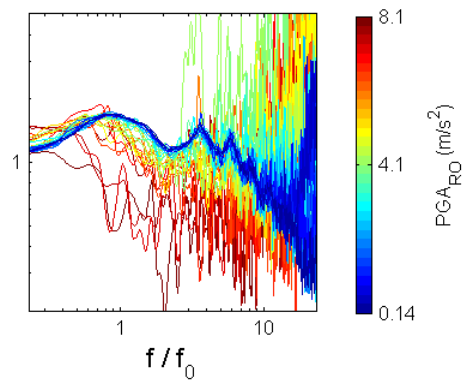

Equiv. Lin. TF (color coded by f_c)

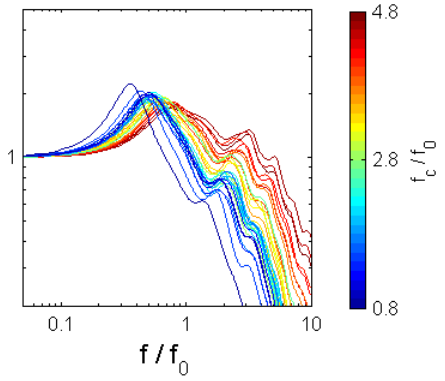

Non-linear TF (color coded by f_c)

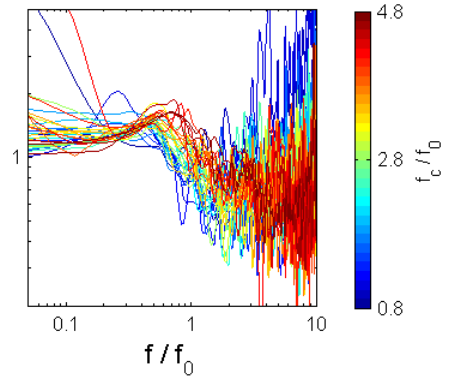

4.1.19 CI.BOMb

Depth (m)	Thickness (m)	V_s (m/s)	Damping ratio	Density (kg/m^3)
0	1	110	0.05	1600
1	5	166	0.05	1600
6	5	182	0.05	1600
11	7	206	0.05	1800
18	9	214	0.05	1800
27	8	314	0.02	1800
35	5	316.9	0.02	1800
40	5	333.2	0.02	1800
45	5	347.6	0.02	1800
50	5	360.5	0.02	1800
55	5	371.9	0.02	1800
60	5	382.1	0.02	1800
65	5	391.2	0.02	1800
70	5	399.2	0.02	1800
75	5	406.4	0.02	1800
80	5	412.7	0.02	1800
85	5	418.4	0.02	1800
90	5	423.5	0.02	1800
95	5	427.9	0.02	1800
100	–	431.9	0.02	1800

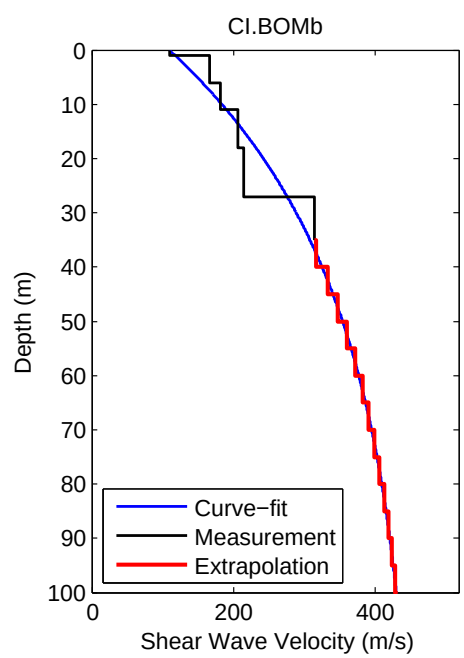

Linear Elastic Transfer Function

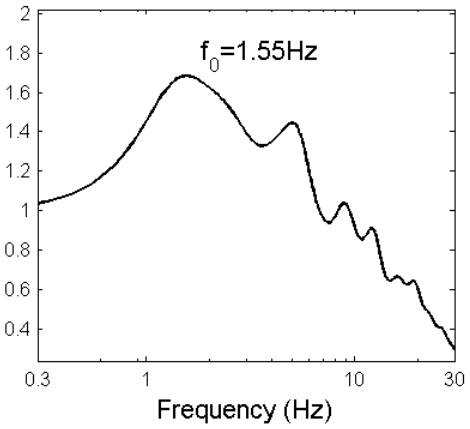

H/V Ratio – Sensor 450

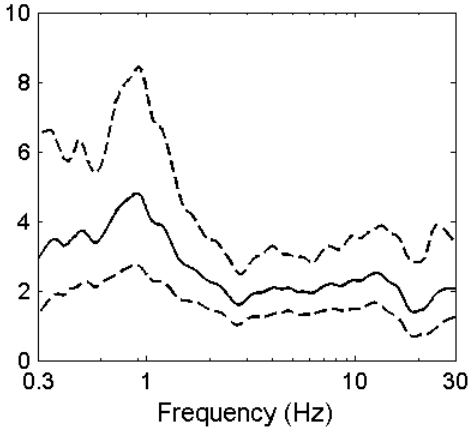

H/V Ratio – Sensor 507

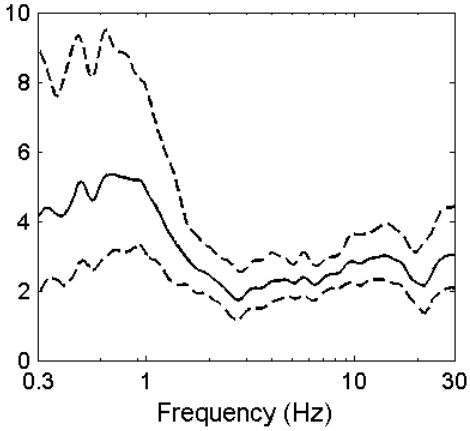

H/V Ratio – Sensor 453

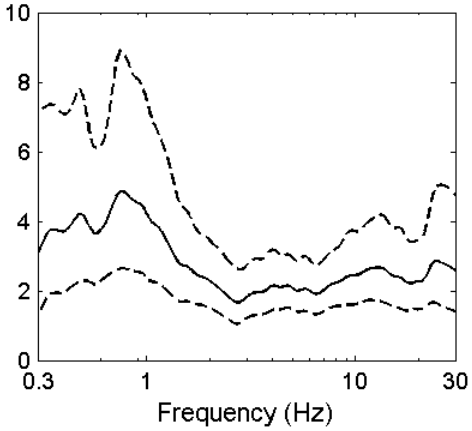

Equivalent Linear Transfer Function

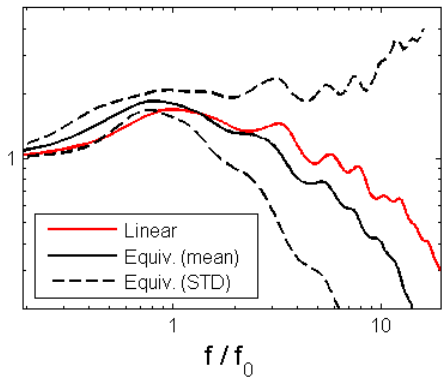

Equiv. Lin. TF (color coded by PGA_{RO})

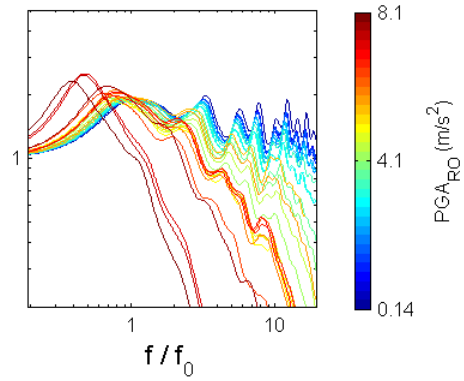

Non-linear Transfer Function

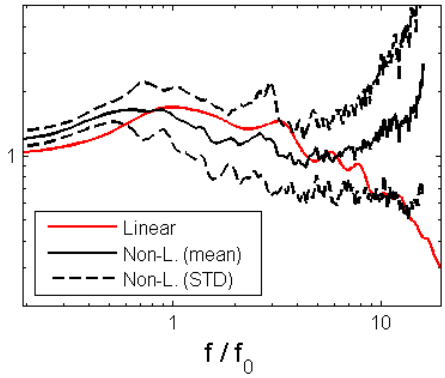

Non-linear TF (color coded by PGA_{RO})

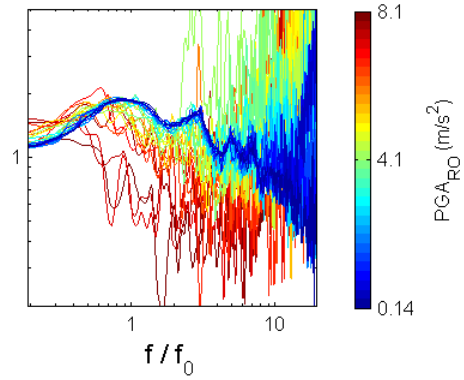

Equiv. Lin. TF (color coded by f_c)

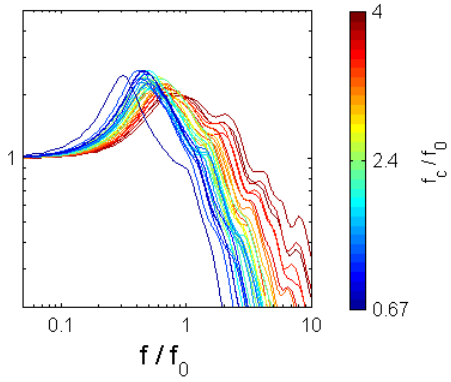

Non-linear TF (color coded by f_c)

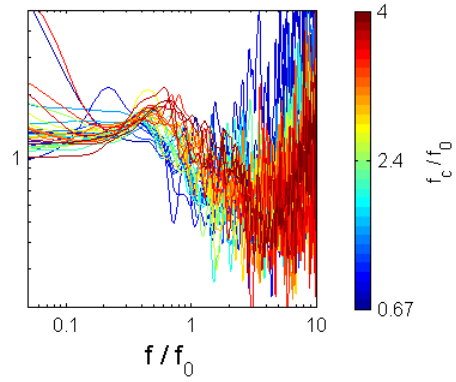

4.1.20 CI.BOMc

Depth (m)	Thickness (m)	V_s (m/s)	Damping ratio	Density (kg/m^3)
0	0.75	100	0.05	1600
0.75	2.25	160	0.05	1600
3	3	196	0.05	1600
6	8	205	0.05	1800
14	13	207	0.05	1800
27	8	322	0.02	1800
35	5	328.1	0.02	1800
40	5	344.9	0.02	1800
45	5	359.5	0.02	1800
50	5	372.4	0.02	1800
55	5	383.7	0.02	1800
60	5	393.6	0.02	1800
65	5	402.3	0.02	1800
70	5	409.9	0.02	1800
75	5	416.5	0.02	1800
80	5	422.4	0.02	1800
85	5	427.5	0.02	1800
90	5	432.0	0.02	1800
95	5	436.0	0.02	1800
100	–	439.4	0.02	1800

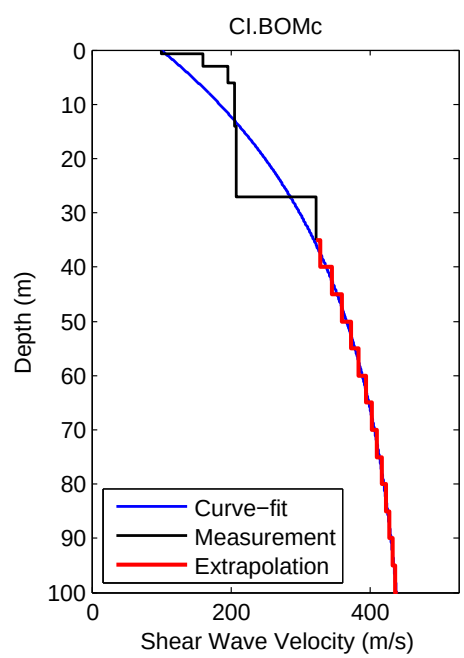

Linear Elastic Transfer Function

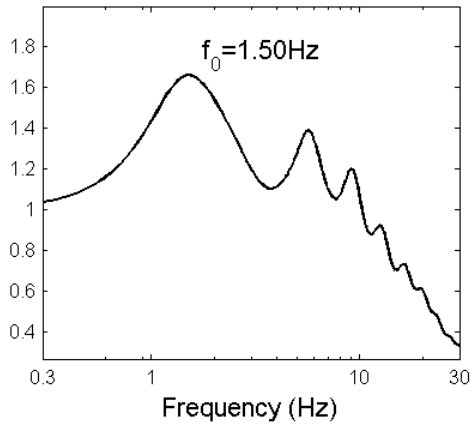

H/V Ratio – Sensor 450

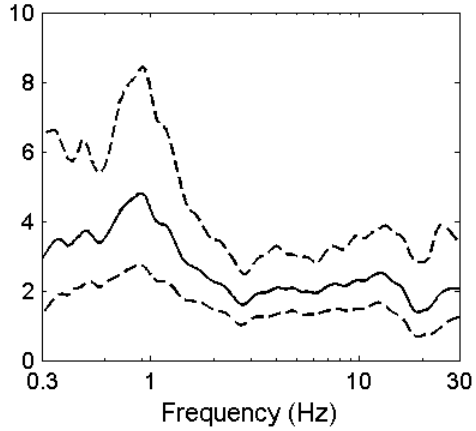

H/V Ratio – Sensor 507

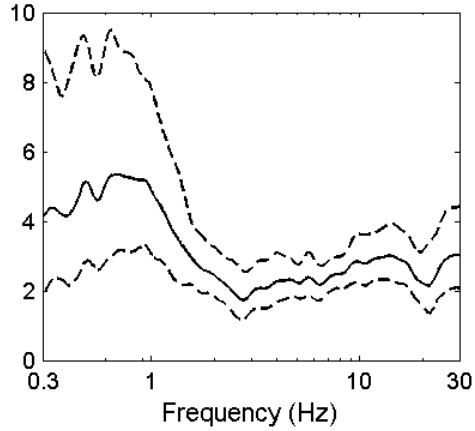

H/V Ratio – Sensor 453

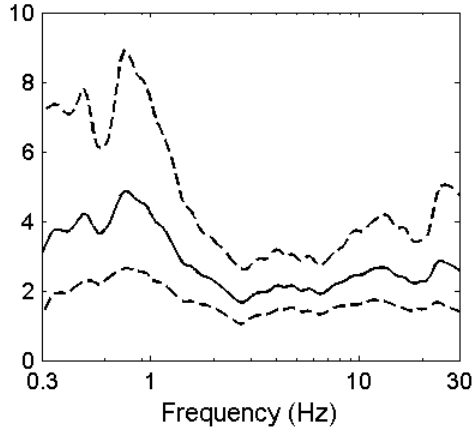

Equivalent Linear Transfer Function

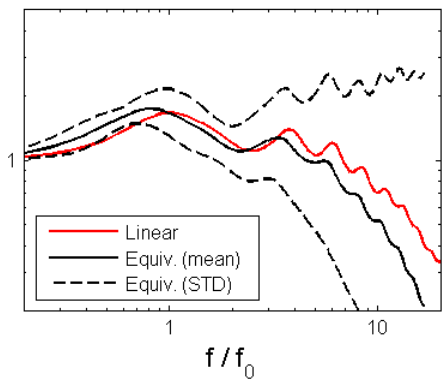

Equiv. Lin. TF (color coded by PGA_{RO})

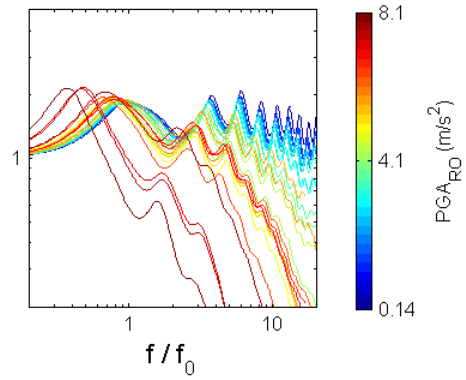

Non-linear Transfer Function

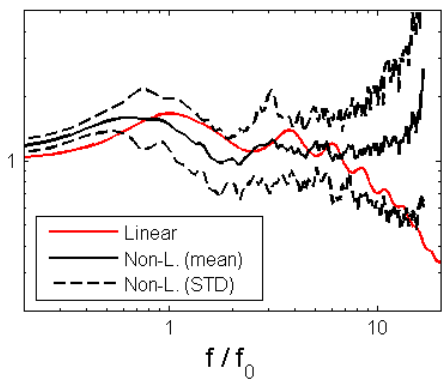

Non-linear TF (color coded by PGA_{RO})

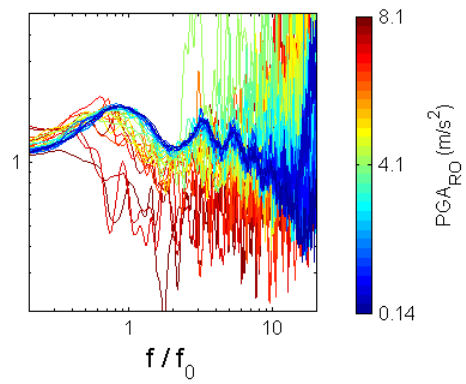

Equiv. Lin. TF (color coded by f_c)

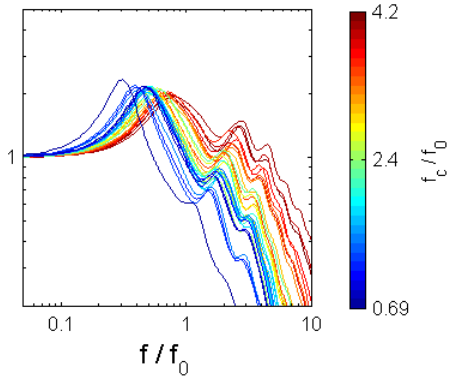

Non-linear TF (color coded by f_c)

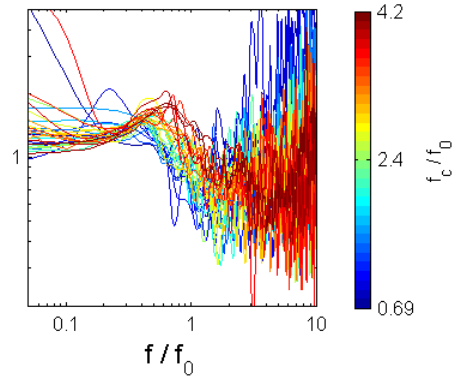

4.1.21 CI.CAR

Depth (m)	Thickness (m)	V_s (m/s)	Damping ratio	Density (kg/m^3)
0	1	123	0.05	1600
1	2	187	0.05	1600
3	3	258	0.02	1800
6	4	303	0.02	1800
10	8	373	0.02	1800
18	12	378	0.02	1800
30	12	388	0.02	1800
42	3	402	0.02	1800
45	5	456.9	0.02	1800
50	5	479.0	0.02	1800
55	5	499.4	0.02	1800
60	5	518.2	0.02	1800
65	5	535.5	0.02	1800
70	5	551.4	0.02	1800
75	5	566.0	0.02	1800
80	5	579.5	0.02	1800
85	5	591.9	0.02	1800
90	5	603.3	0.02	1800
95	5	613.8	0.02	1800
100	–	623.4	0.02	1800

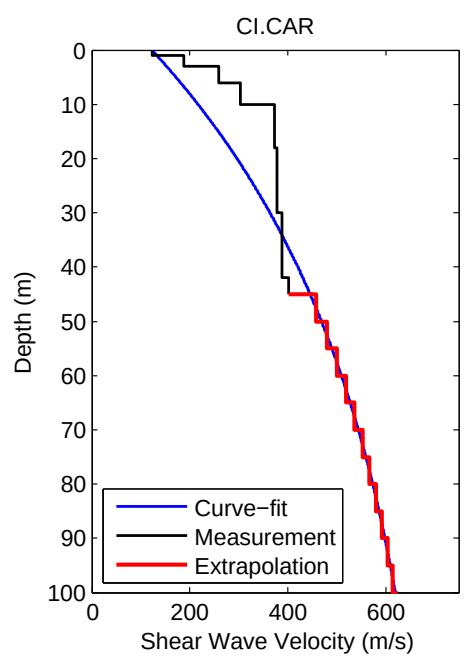

Linear Elastic Transfer Function

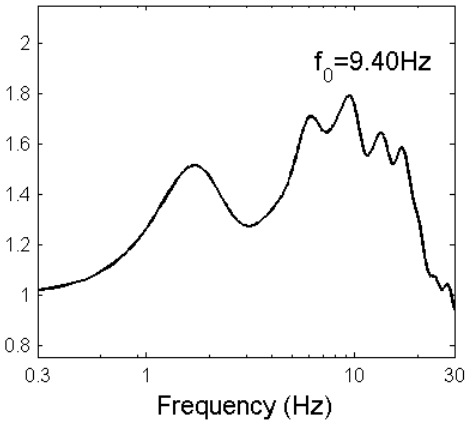

H/V Ratio – Sensor 450

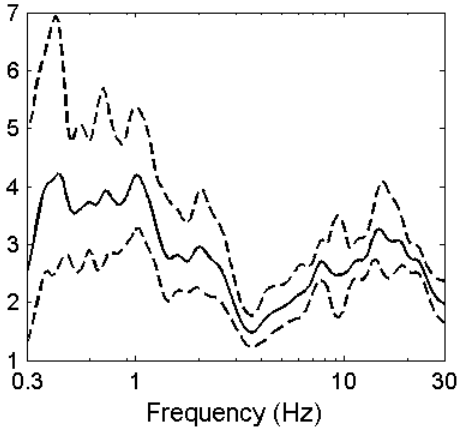

H/V Ratio – Sensor 507

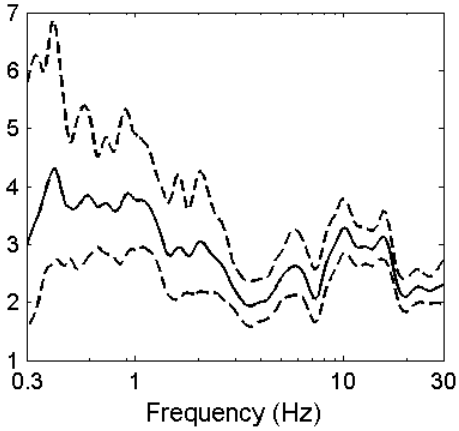

H/V Ratio – Sensor 453

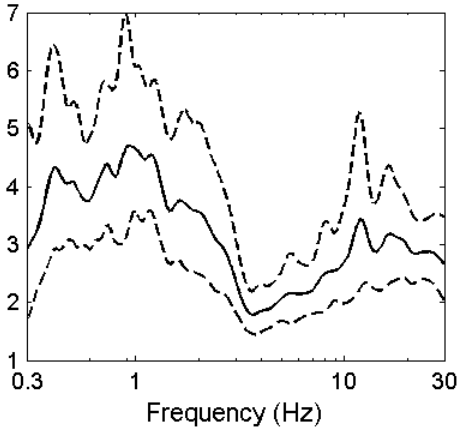

Equivalent Linear Transfer Function

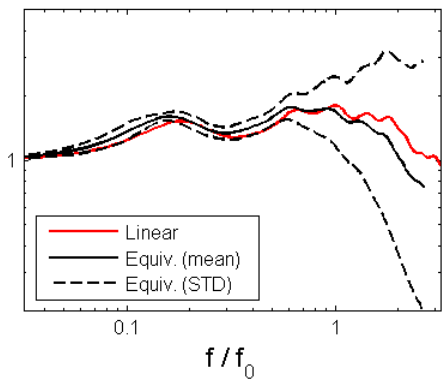

Equiv. Lin. TF (color coded by PGA_{RO})

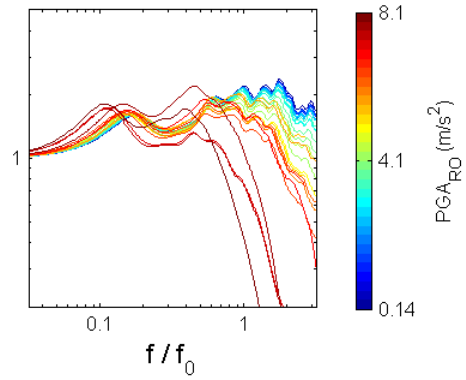

Non-linear Transfer Function

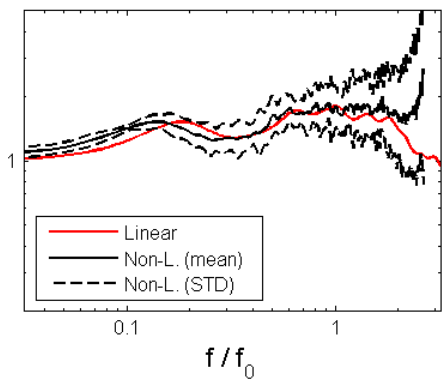

Non-linear TF (color coded by PGA_{RO})

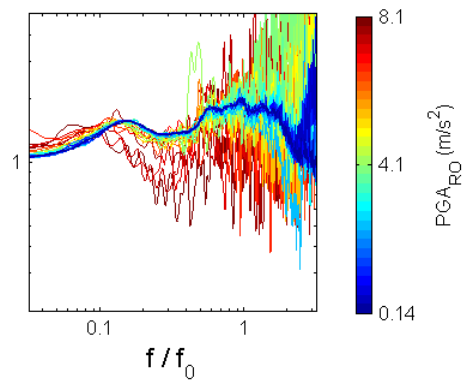

Equiv. Lin. TF (color coded by f_c)

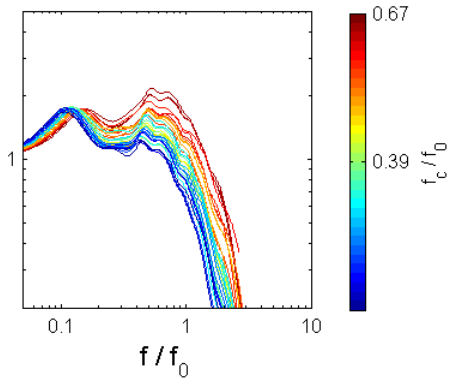

Non-linear TF (color coded by f_c)

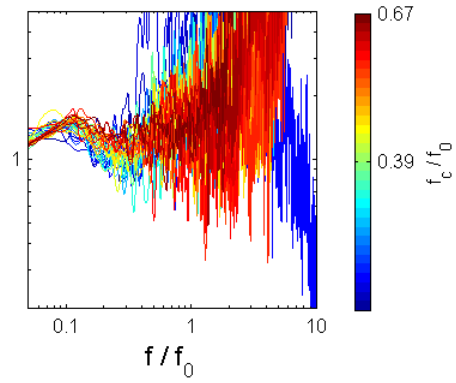

4.1.22 CI.CHN

Depth (m)	Thickness (m)	V_s (m/s)	Damping ratio	Density (kg/m^3)
0	2	220	0.05	1800
2	6	226	0.05	1800
8	6	261	0.02	1800
14	8	351	0.02	1800
22	8	375	0.02	1800
30	12	501	0.02	1800
42	15	601	0.02	1800
57	20	699	0.02	1800
77	–	804	0.01	2000

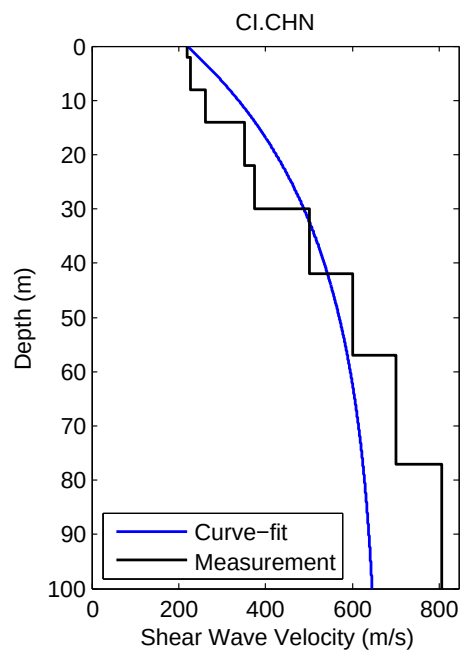

Linear Elastic Transfer Function

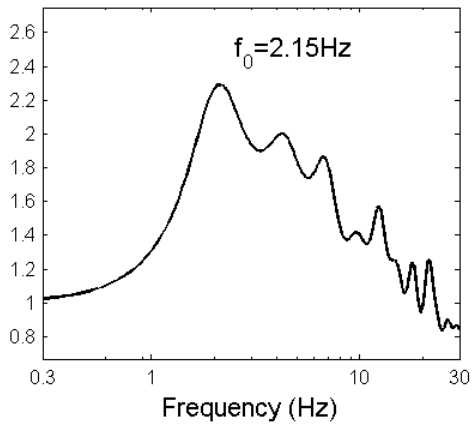

H/V Ratio – Sensor 450

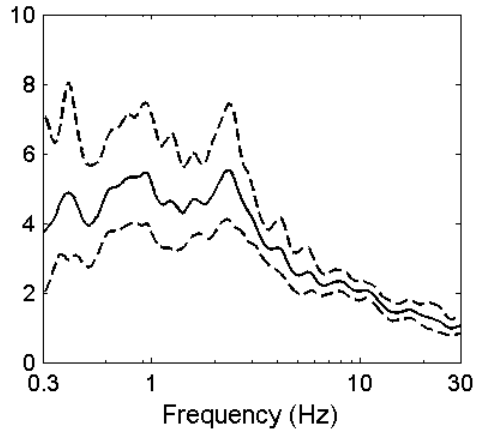

H/V Ratio – Sensor 507

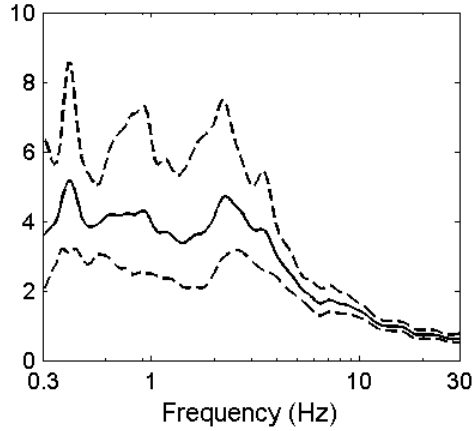

H/V Ratio – Sensor 453

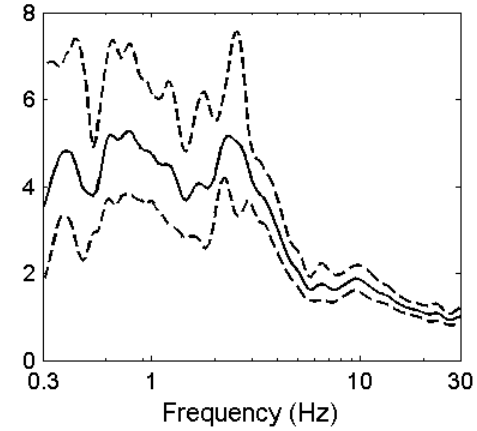

Equivalent Linear Transfer Function

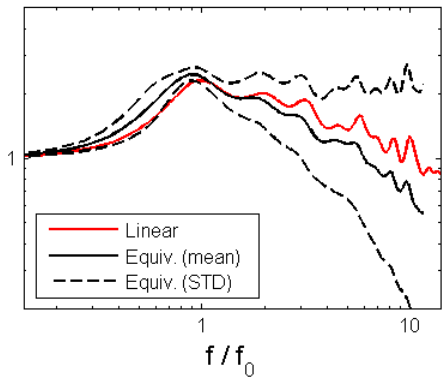

Equiv. Lin. TF (color coded by PGA_{RO})

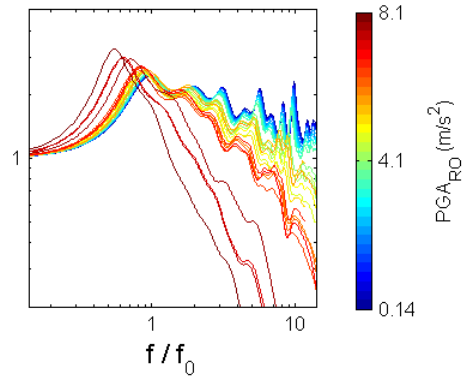

Non-linear Transfer Function

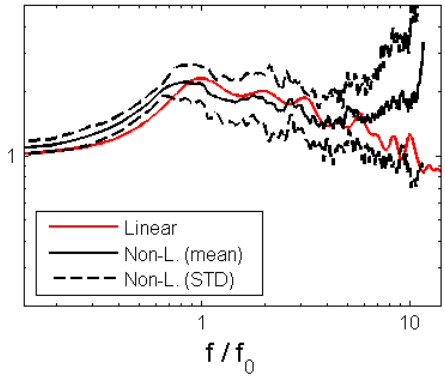

Non-linear TF (color coded by PGA_{RO})

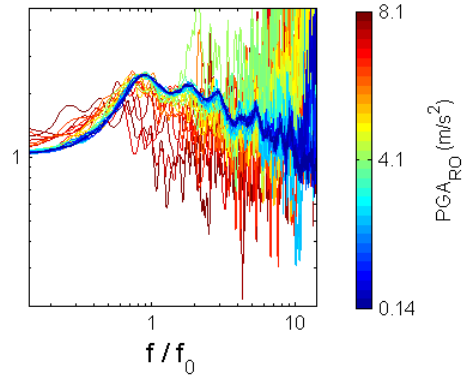

Equiv. Lin. TF (color coded by f_c)

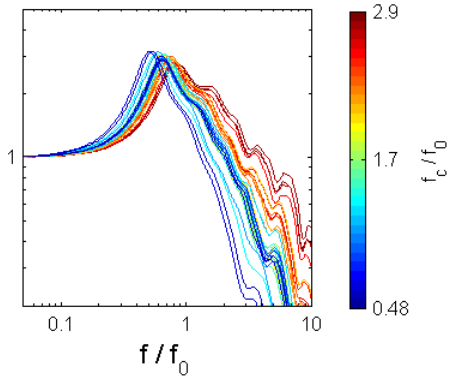

Non-linear TF (color coded by f_c)

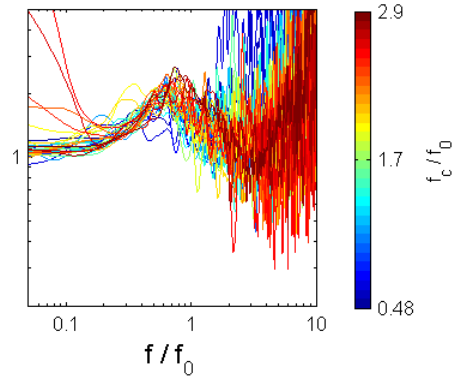

4.1.23 CI.DRE

Depth (m)	Thickness (m)	V_s (m/s)	Damping ratio	Density (kg/m^3)
0	1	77	0.05	1600
1	2	126	0.05	1600
3	2.5	170	0.05	1600
5.5	5	258	0.02	1800
10.5	4	181	0.05	1600
14.5	6	184	0.05	1600
20.5	6	243	0.05	1800
26.5	3.5	313	0.02	1800
30	5	313.1	0.02	1800
35	5	333.7	0.02	1800
40	5	351.5	0.02	1800
45	5	367.0	0.02	1800
50	5	380.5	0.02	1800
55	5	392.1	0.02	1800
60	5	402.2	0.02	1800
65	5	411.0	0.02	1800
70	5	418.6	0.02	1800
75	5	425.2	0.02	1800
80	5	430.9	0.02	1800
85	5	435.9	0.02	1800
90	5	440.2	0.02	1800
95	5	443.9	0.02	1800
100	–	447.2	0.02	1800

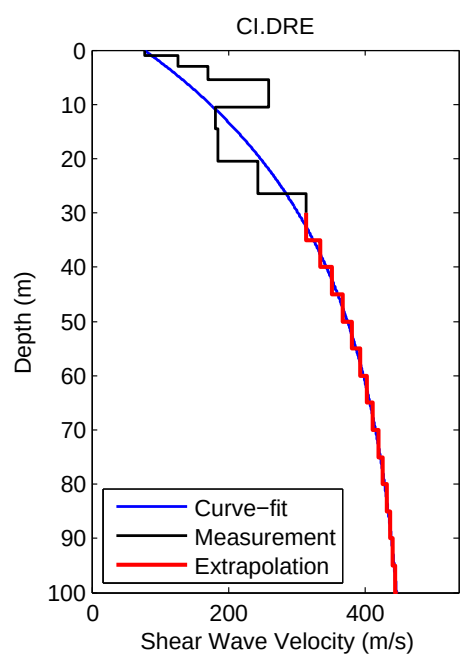

Linear Elastic Transfer Function

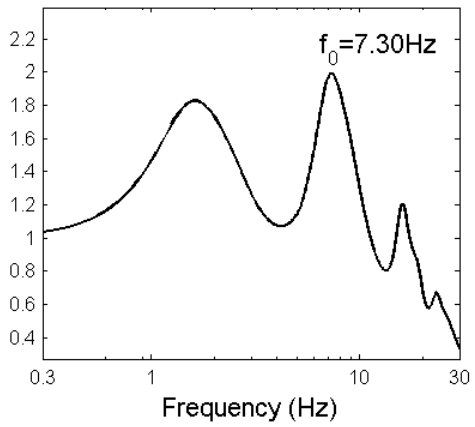

H/V Ratio – Sensor 450

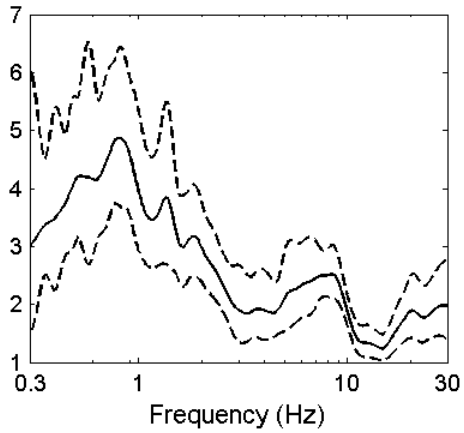

H/V Ratio – Sensor 507

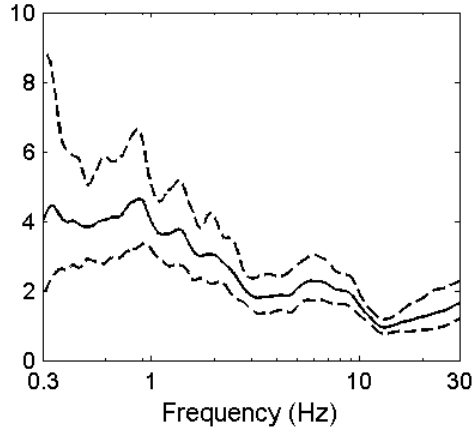

H/V Ratio – Sensor 453

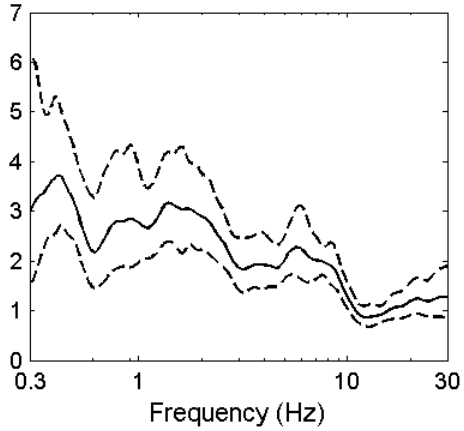

Equivalent Linear Transfer Function

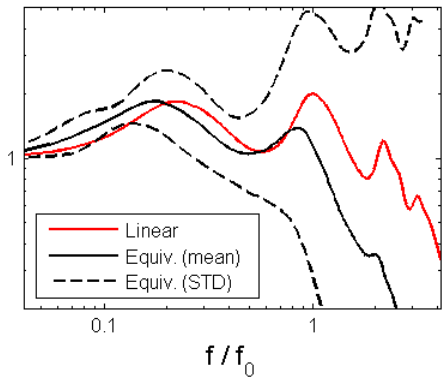

Equiv. Lin. TF (color coded by PGA_{RO})

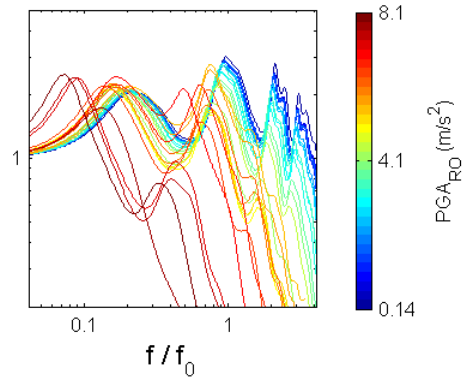

Non-linear Transfer Function

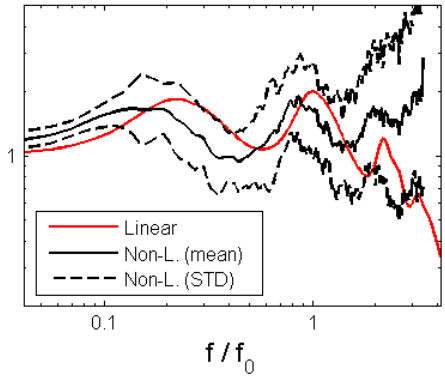

Non-linear TF (color coded by PGA_{RO})

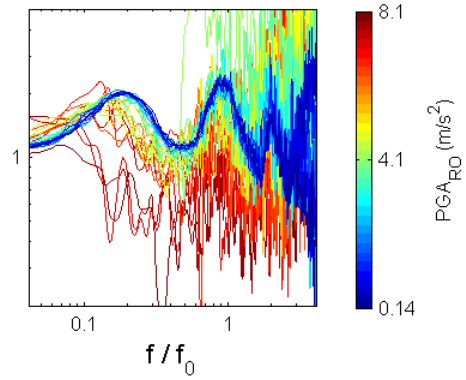

Equiv. Lin. TF (color coded by f_c)

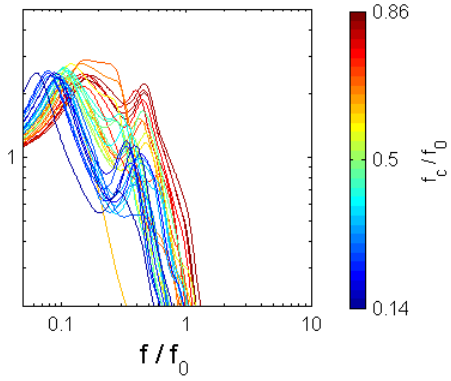

Non-linear TF (color coded by f_c)

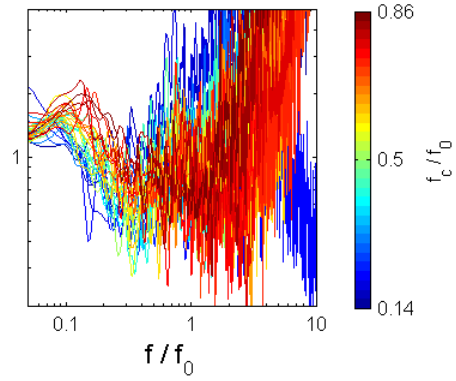

4.1.24 CI.ERR

Depth (m)	Thickness (m)	V_s (m/s)	Damping ratio	Density (kg/m^3)
0	0.5	132	0.05	1600
0.5	1.5	150	0.05	1600
2	2	185	0.05	1600
4	5	215	0.05	1800
9	6	223	0.05	1800
15	6	228	0.05	1800
21	9	366	0.02	1800
30	5	374.1	0.02	1800
35	5	396.0	0.02	1800
40	5	415.1	0.02	1800
45	5	431.9	0.02	1800
50	5	446.5	0.02	1800
55	5	459.3	0.02	1800
60	5	470.5	0.02	1800
65	5	480.3	0.02	1800
70	5	488.8	0.02	1800
75	5	496.3	0.02	1800
80	5	502.9	0.02	1800
85	5	508.6	0.02	1800
90	5	513.6	0.02	1800
95	5	518.0	0.02	1800
100	–	521.9	0.02	1800

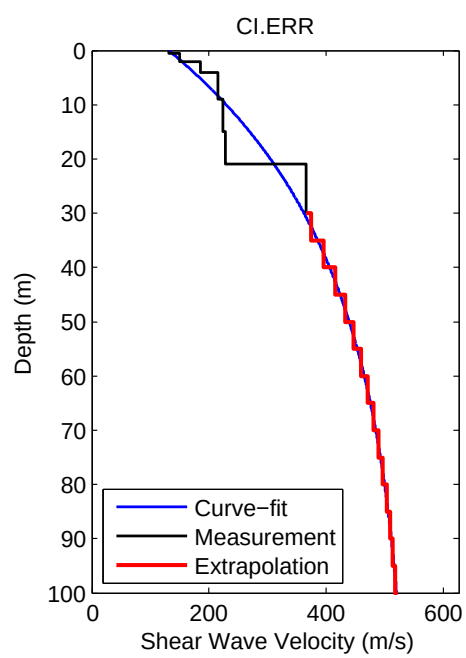

Linear Elastic Transfer Function

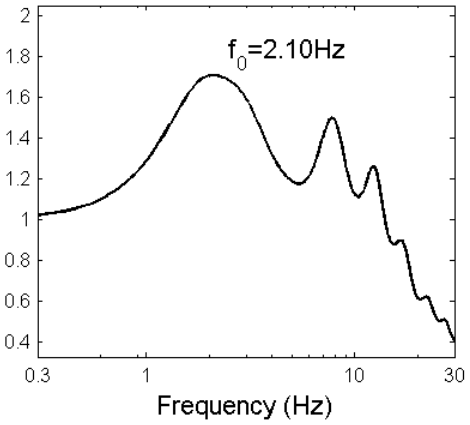

H/V Ratio – Sensor 450

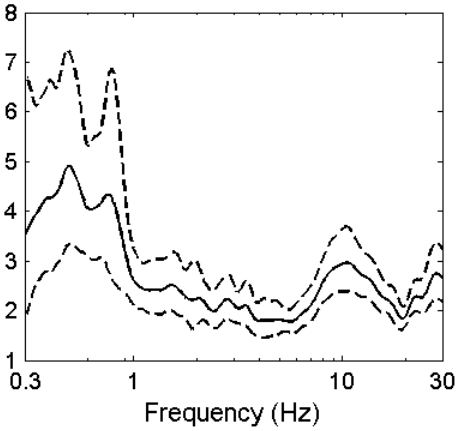

H/V Ratio – Sensor 507

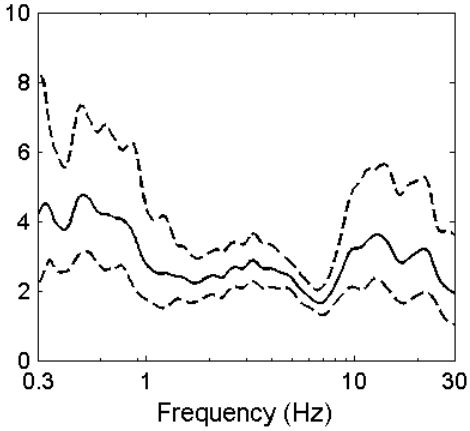

H/V Ratio – Sensor 453

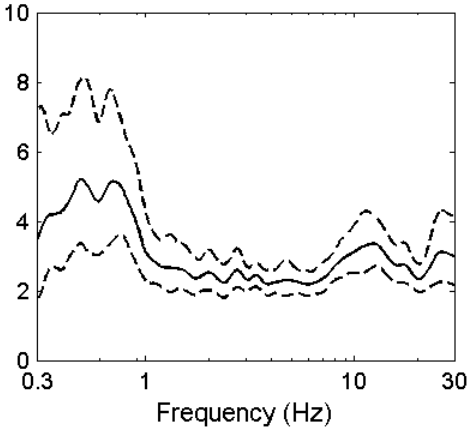

Equivalent Linear Transfer Function

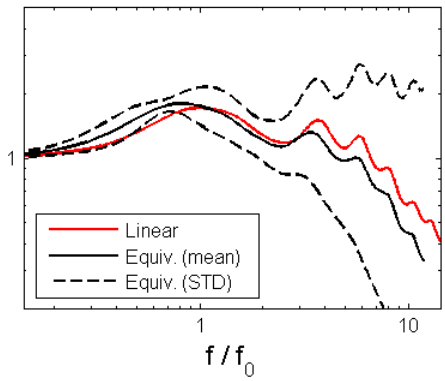

Equiv. Lin. TF (color coded by PGA_{RO})

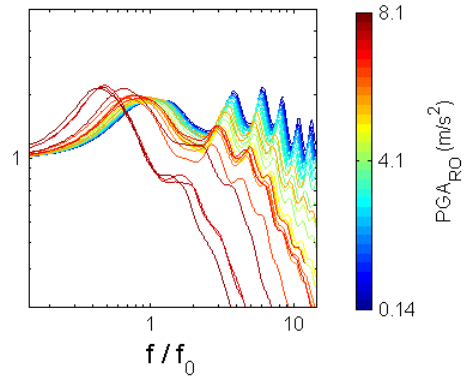

Non-linear Transfer Function

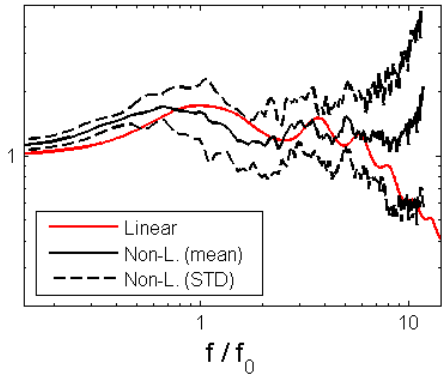

Non-linear TF (color coded by PGA_{RO})

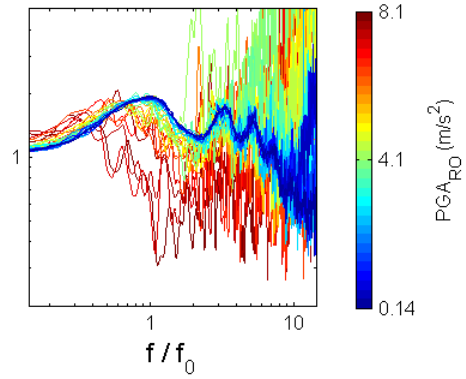

Equiv. Lin. TF (color coded by f_c)

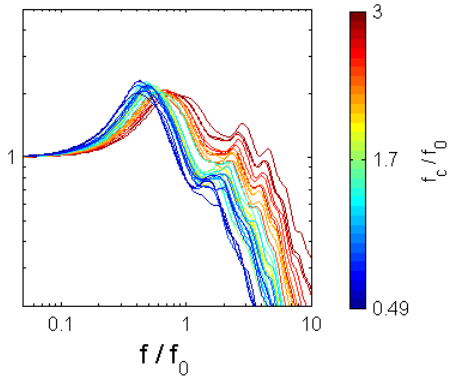

Non-linear TF (color coded by f_c)

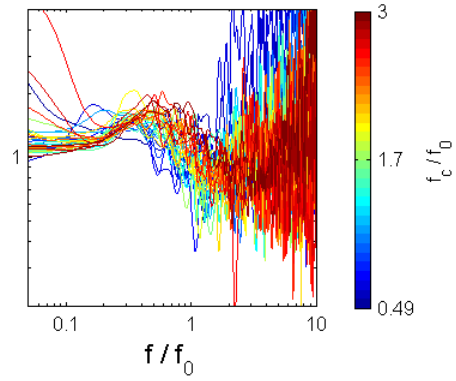

4.1.25 CI.LCPa

Depth (m)	Thickness (m)	V_s (m/s)	Damping ratio	Density (kg/m^3)
0	1.5	160	0.05	1600
1.5	2.5	175	0.05	1600
4	3	186	0.05	1600
7	5	246	0.05	1800
12	12	259	0.02	1800
24	16	486	0.02	1800
40	5	498.9	0.02	1800
45	5	513.1	0.02	1800
50	5	524.7	0.02	1800
55	5	534.3	0.02	1800
60	5	542.2	0.02	1800
65	5	548.7	0.02	1800
70	5	554.1	0.02	1800
75	5	558.5	0.02	1800
80	5	562.1	0.02	1800
85	5	565.1	0.02	1800
90	5	567.6	0.02	1800
95	5	569.6	0.02	1800
100	–	571.2	0.02	1800

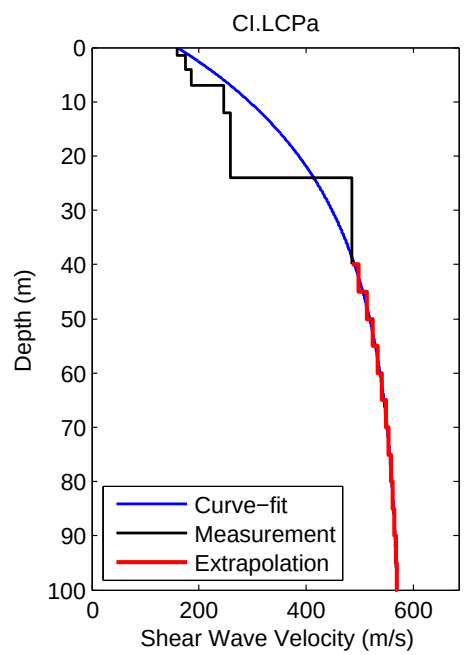

Linear Elastic Transfer Function

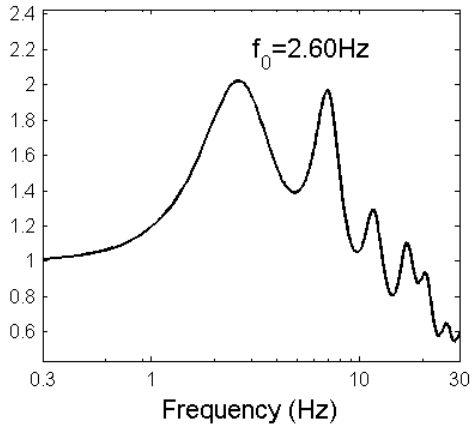

H/V Ratio – Sensor 450

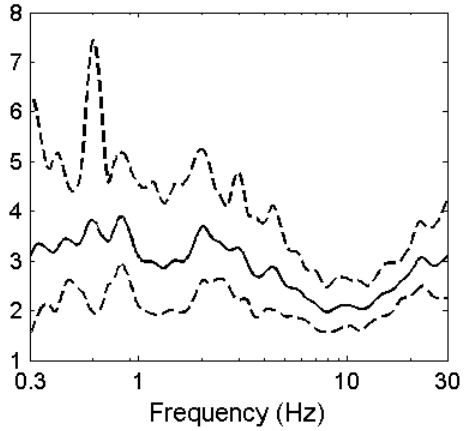

H/V Ratio – Sensor 507

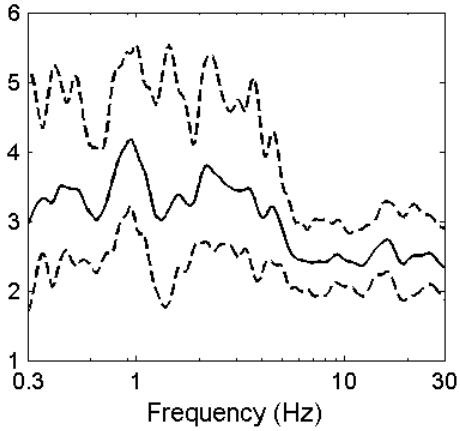

H/V Ratio – Sensor 453

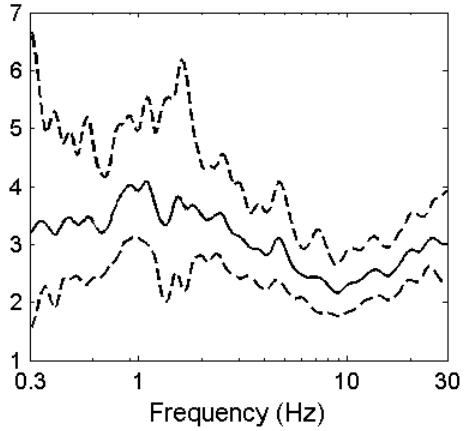

Equivalent Linear Transfer Function

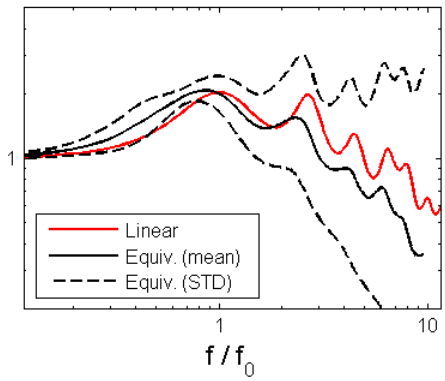

Equiv. Lin. TF (color coded by PGA_{RO})

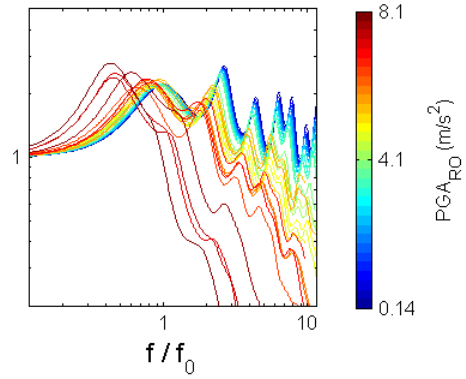

Non-linear Transfer Function

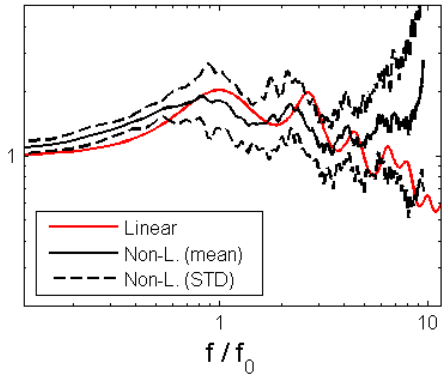

Non-linear TF (color coded by PGA_{RO})

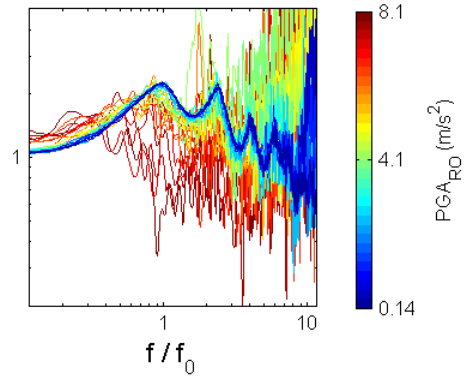

Equiv. Lin. TF (color coded by f_c)

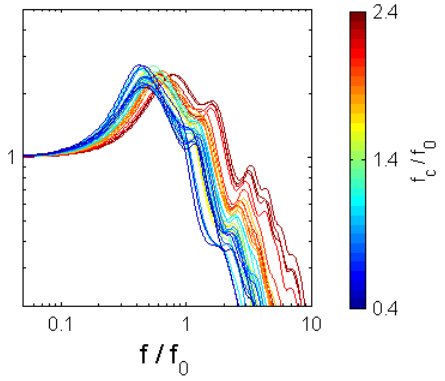

Non-linear TF (color coded by f_c)

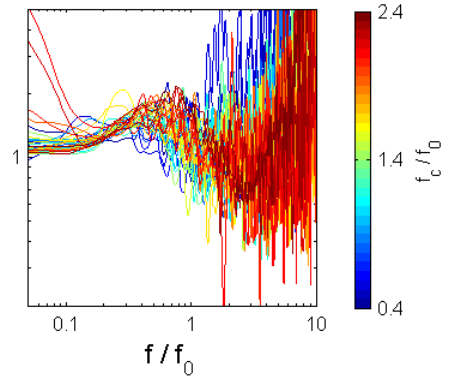

4.1.26 CI.LCPb

Depth (m)	Thickness (m)	V_s (m/s)	Damping ratio	Density (kg/m^3)
0	1.5	181	0.05	1600
1.5	2	174	0.05	1600
3.5	4	214	0.05	1800
7.5	5.5	230	0.05	1800
13	11	273	0.02	1800
24	16	521	0.02	1800
40	5	524.8	0.02	1800
45	5	536.1	0.02	1800
50	5	545.1	0.02	1800
55	5	552.2	0.02	1800
60	5	557.8	0.02	1800
65	5	562.2	0.02	1800
70	5	565.7	0.02	1800
75	5	568.5	0.02	1800
80	5	570.7	0.02	1800
85	5	572.4	0.02	1800
90	5	573.8	0.02	1800
95	5	574.9	0.02	1800
100	–	575.7	0.02	1800

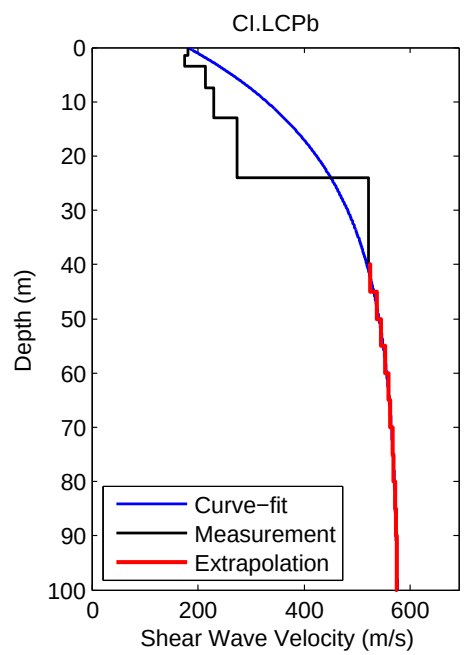

Linear Elastic Transfer Function

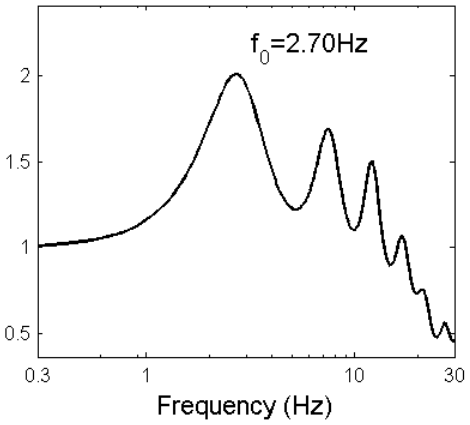

H/V Ratio – Sensor 450

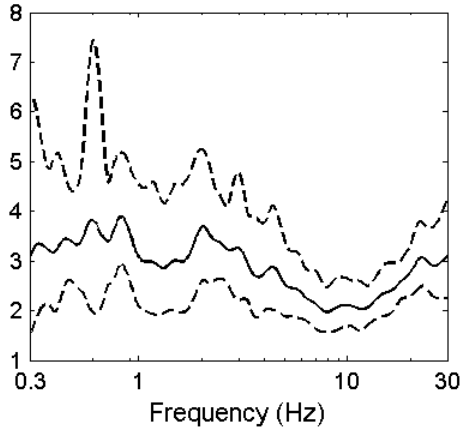

H/V Ratio – Sensor 507

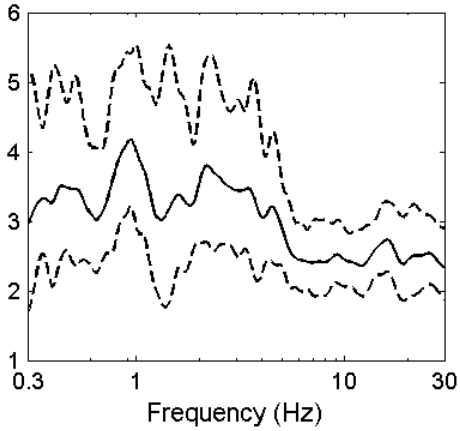

H/V Ratio – Sensor 453

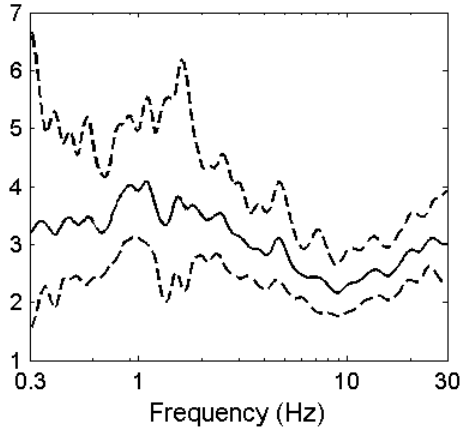

Equivalent Linear Transfer Function

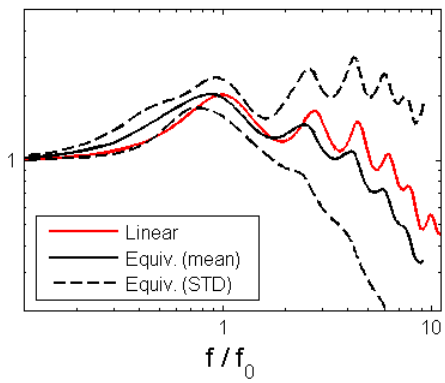

Equiv. Lin. TF (color coded by PGA_{RO})

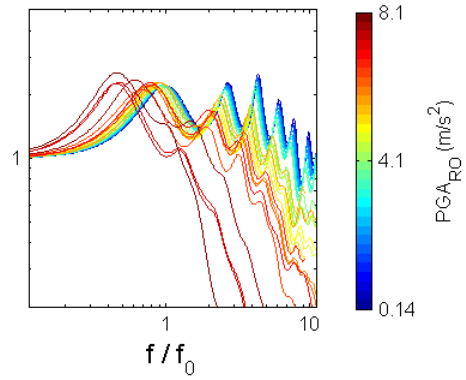

Non-linear Transfer Function

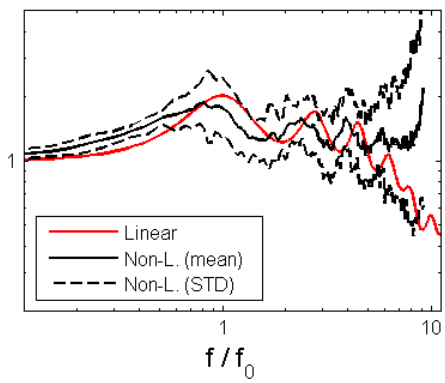

Non-linear TF (color coded by PGA_{RO})

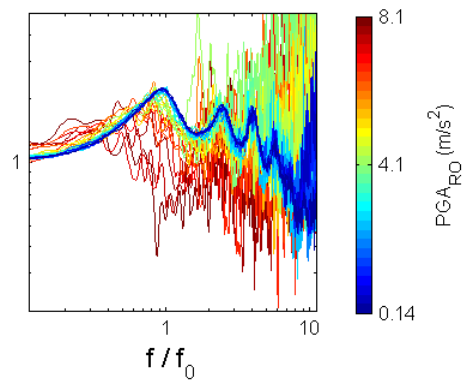

Equiv. Lin. TF (color coded by f_c)

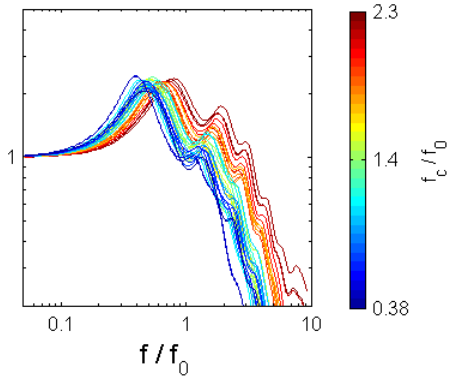

Non-linear TF (color coded by f_c)

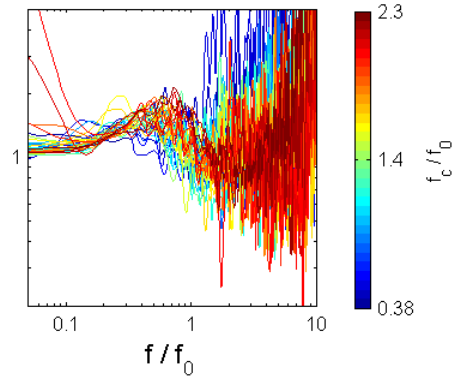

4.1.27 CI.MSJ

Depth (m)	Thickness (m)	V_s (m/s)	Damping ratio	Density (kg/m^3)
0	1	170	0.05	1600
1	2	177	0.05	1600
3	2	213	0.05	1800
5	3	228	0.05	1800
8	5	230	0.05	1800
13	8	255	0.02	1800
21	11	301	0.02	1800
32	15	374	0.02	1800
47	20	439	0.02	1800
67	13	482	0.02	1800
80	5	484.2	0.02	1800
85	5	491.0	0.02	1800
90	5	497.1	0.02	1800
95	5	502.6	0.02	1800
100	–	507.6	0.02	1800

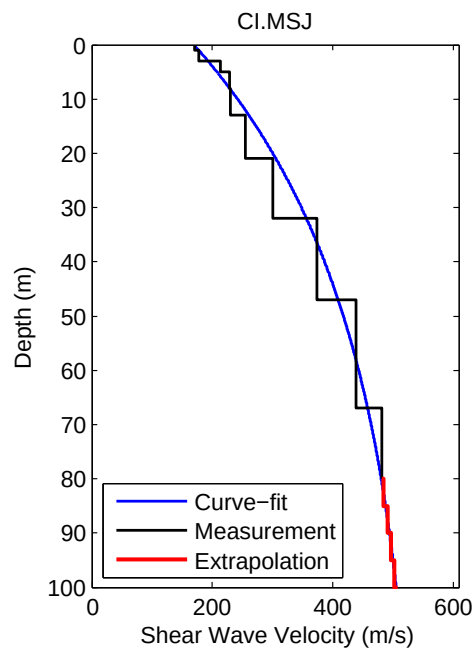

Linear Elastic Transfer Function

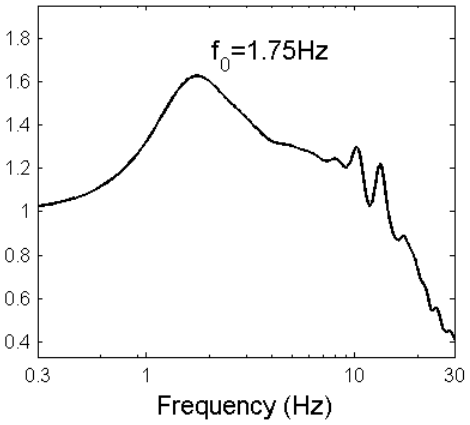

H/V Ratio – Sensor 450

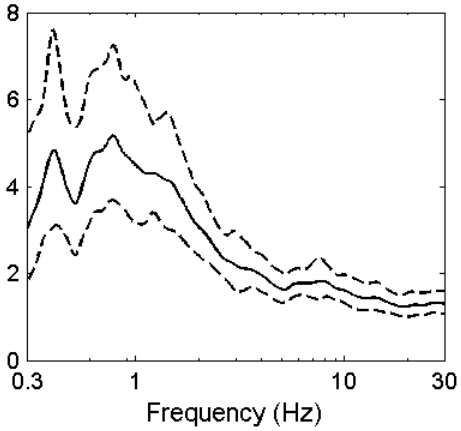

H/V Ratio – Sensor 507

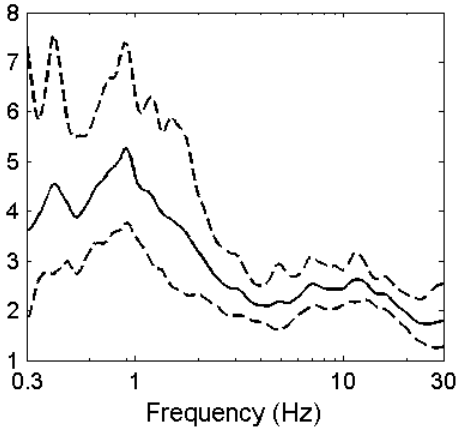

H/V Ratio – Sensor 453

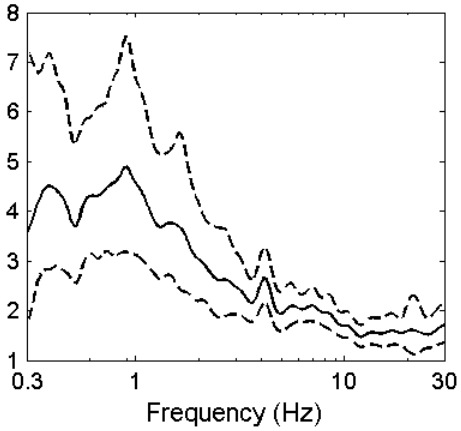

Equivalent Linear Transfer Function

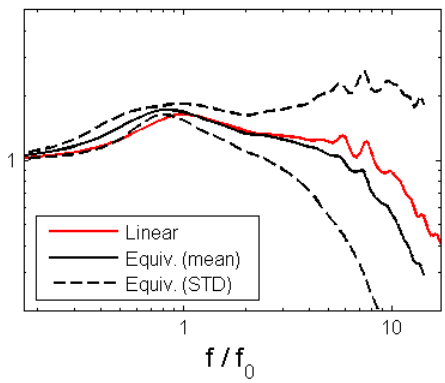

Equiv. Lin. TF (color coded by PGA_{RO})

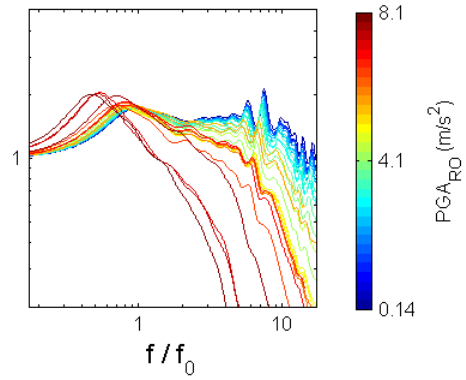

Non-linear Transfer Function

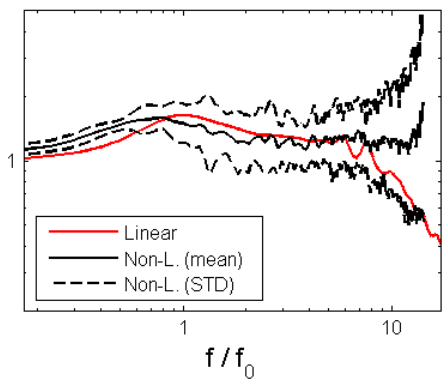

Non-linear TF (color coded by PGA_{RO})

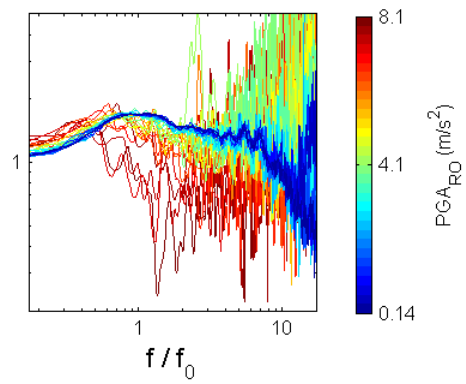

Equiv. Lin. TF (color coded by f_c)

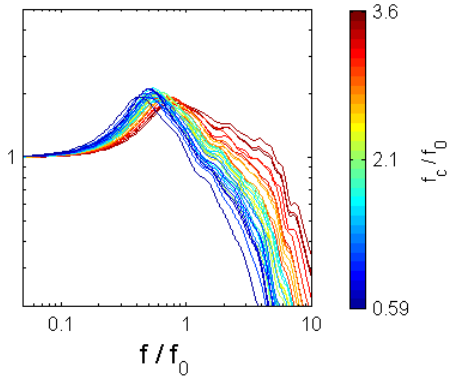

Non-linear TF (color coded by f_c)

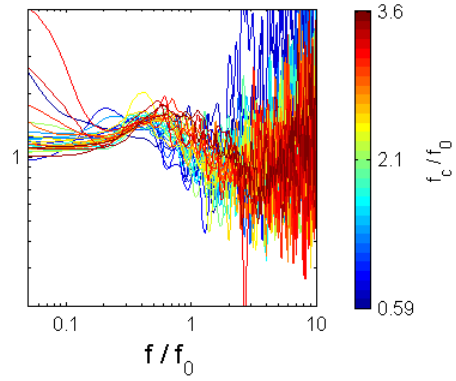

4.1.28 CI.NJQa

Depth (m)	Thickness (m)	V_s (m/s)	Damping ratio	Density (kg/m^3)
0	0.5	234	0.05	1800
0.5	1	193	0.05	1600
1.5	4.5	227	0.05	1800
6	5	262	0.02	1800
11	7	306	0.02	1800
18	10	359	0.02	1800
28	7	427	0.02	1800
35	5	429.2	0.02	1800
40	5	447.7	0.02	1800
45	5	464.9	0.02	1800
50	5	480.8	0.02	1800
55	5	495.5	0.02	1800
60	5	509.2	0.02	1800
65	5	521.8	0.02	1800
70	5	533.6	0.02	1800
75	5	544.4	0.02	1800
80	5	554.5	0.02	1800
85	5	563.8	0.02	1800
90	5	572.4	0.02	1800
95	5	580.4	0.02	1800
100	–	587.8	0.02	1800

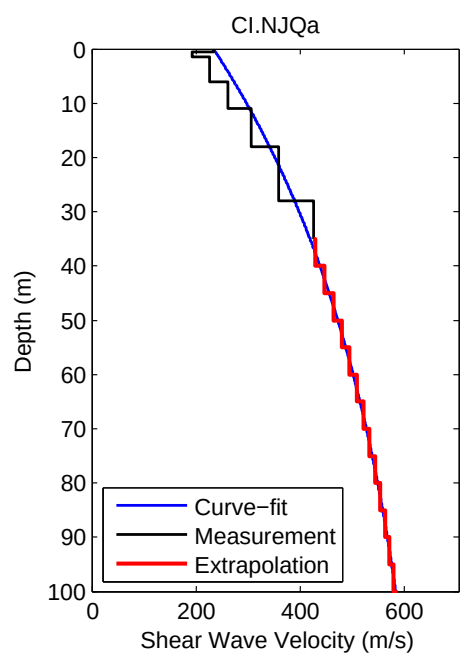

Linear Elastic Transfer Function

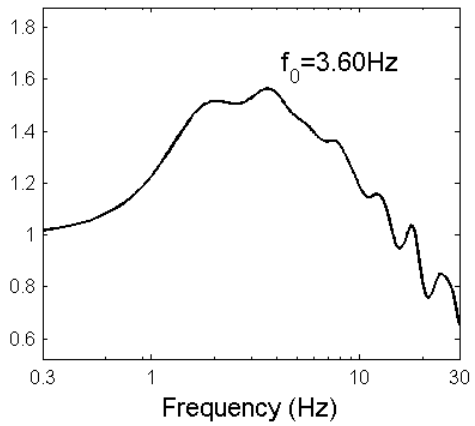

H/V Ratio – Sensor 450

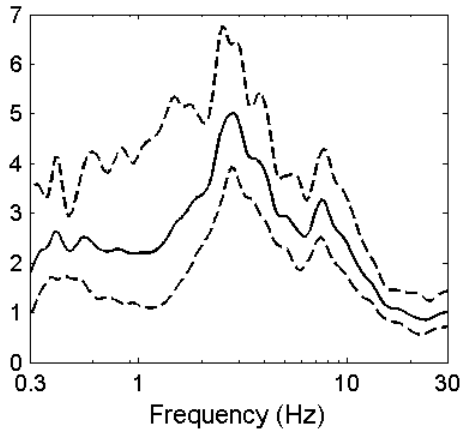

H/V Ratio – Sensor 507

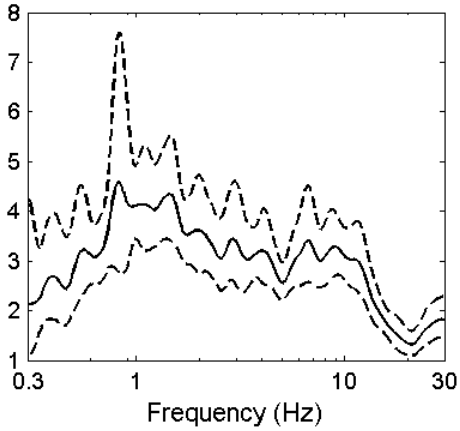

H/V Ratio – Sensor 453

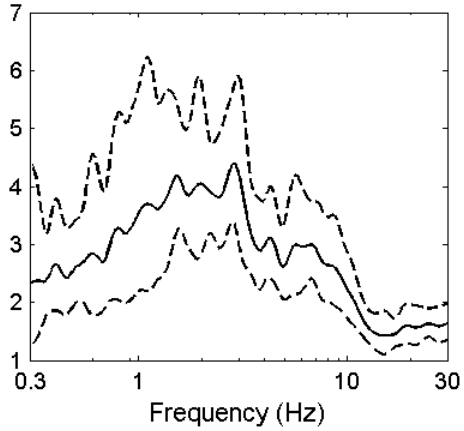

Equivalent Linear Transfer Function

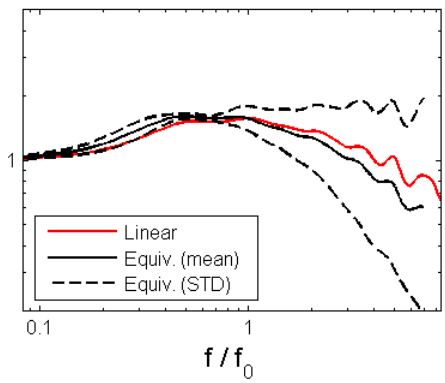

Equiv. Lin. TF (color coded by PGA_{RO})

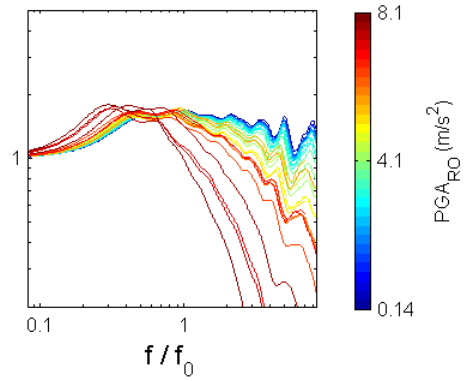

Non-linear Transfer Function

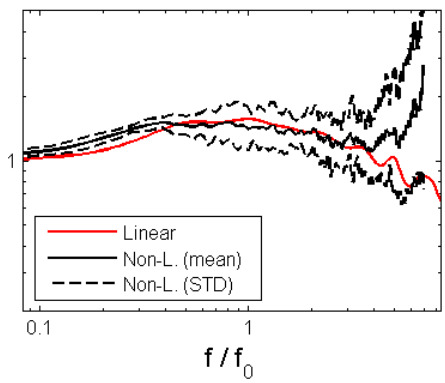

Non-linear TF (color coded by PGA_{RO})

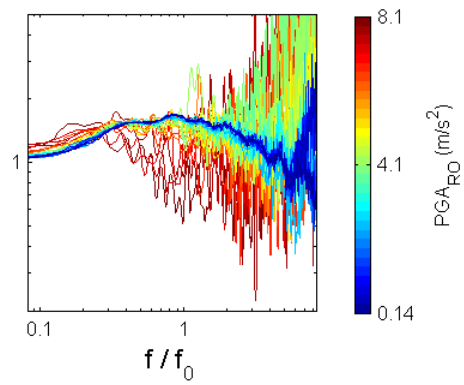

Equiv. Lin. TF (color coded by f_c)

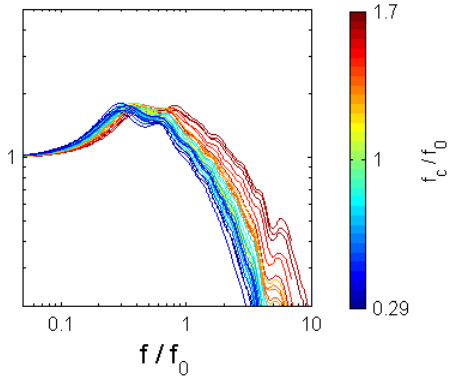

Non-linear TF (color coded by f_c)

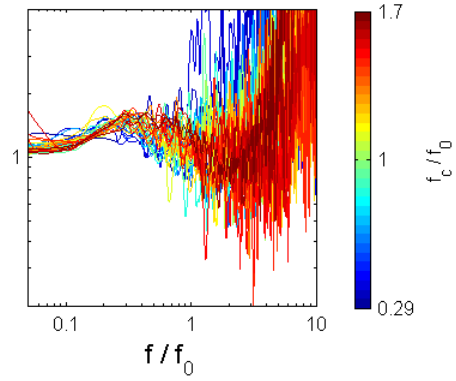

4.1.29 CI.NJQb

Depth (m)	Thickness (m)	V_s (m/s)	Damping ratio	Density (kg/m^3)
0	1	225	0.05	1800
1	2	211	0.05	1800
3	3	227	0.05	1800
6	5	290	0.02	1800
11	7	293	0.02	1800
18	10	362	0.02	1800
28	12	462	0.02	1800
40	5	475.8	0.02	1800
45	5	494.2	0.02	1800
50	5	510.9	0.02	1800
55	5	526.2	0.02	1800
60	5	540.1	0.02	1800
65	5	552.7	0.02	1800
70	5	564.2	0.02	1800
75	5	574.7	0.02	1800
80	5	584.2	0.02	1800
85	5	592.9	0.02	1800
90	5	600.8	0.02	1800
95	5	607.9	0.02	1800
100	–	614.5	0.02	1800

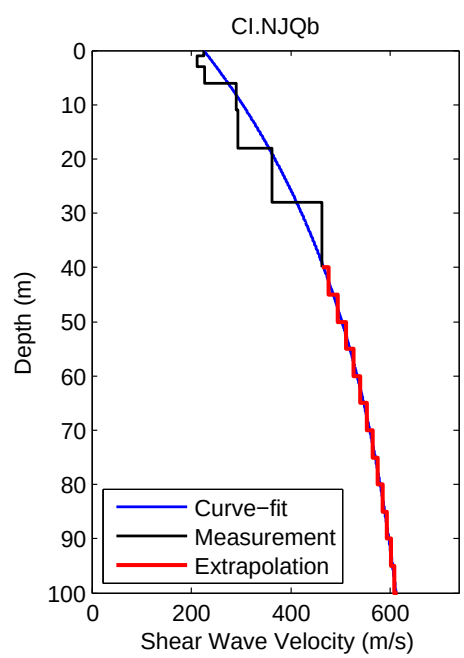

Linear Elastic Transfer Function

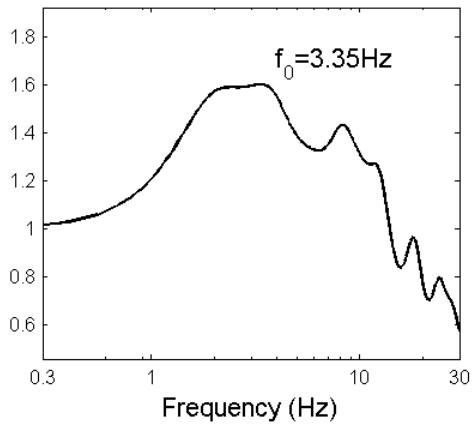

H/V Ratio – Sensor 450

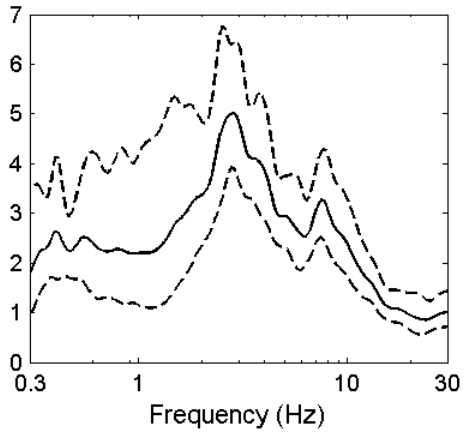

H/V Ratio – Sensor 507

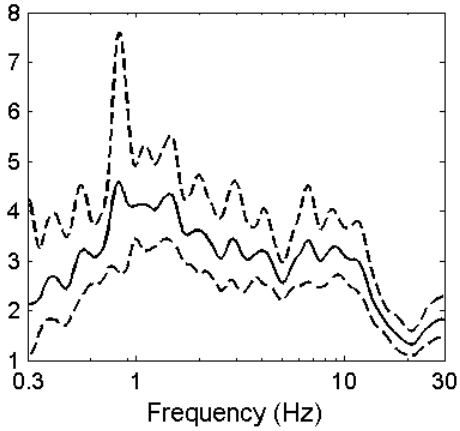

H/V Ratio – Sensor 453

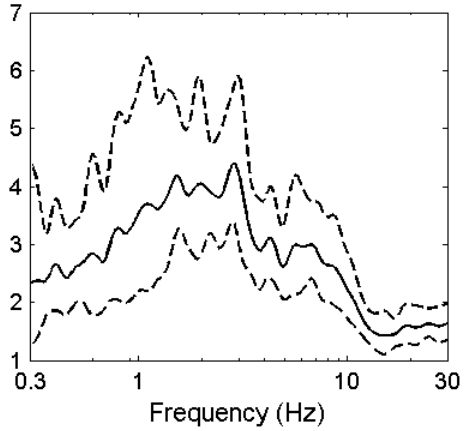

Equivalent Linear Transfer Function

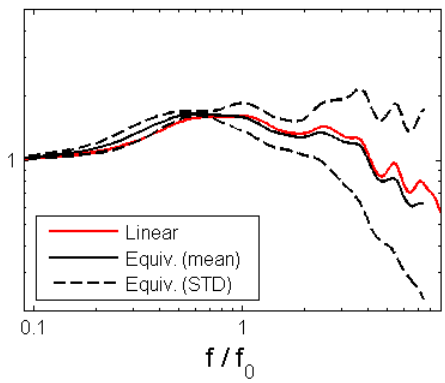

Equiv. Lin. TF (color coded by PGA_{RO})

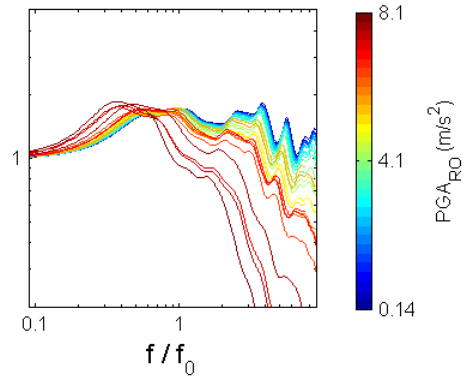

Non-linear Transfer Function

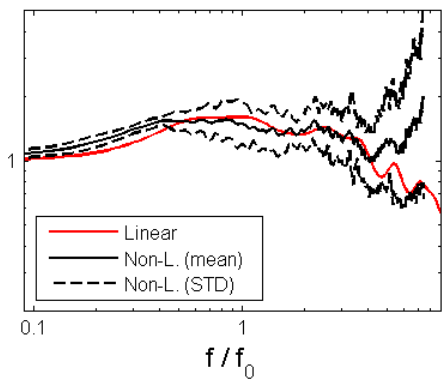

Non-linear TF (color coded by PGA_{RO})

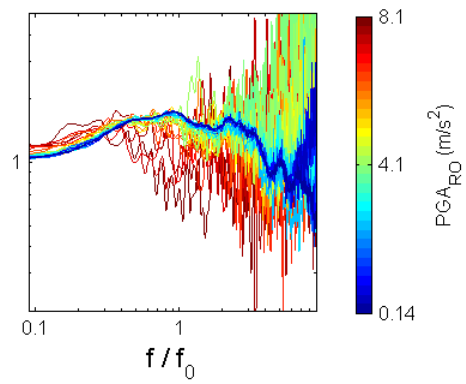

Equiv. Lin. TF (color coded by f_c)

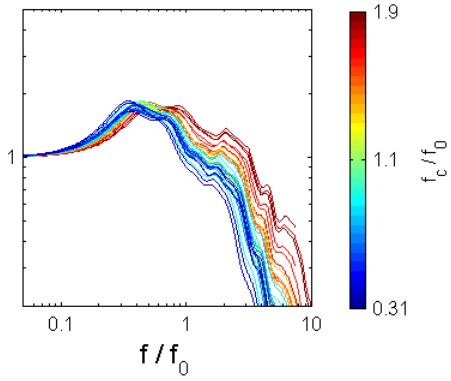

Non-linear TF (color coded by f_c)

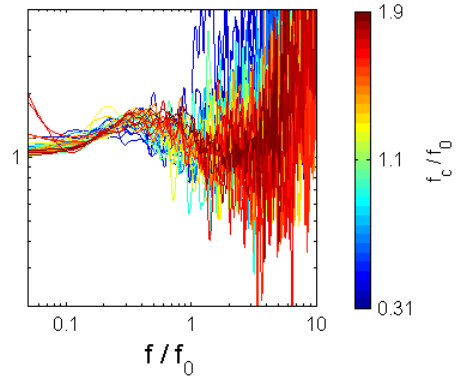

4.1.30 CI.NJQc

Depth (m)	Thickness (m)	V_s (m/s)	Damping ratio	Density (kg/m^3)
0	1	172	0.05	1600
1	2	202	0.05	1800
3	3	248	0.05	1800
6	10	290	0.02	1800
16	12	349	0.02	1800
28	7	466	0.02	1800
35	5	472.2	0.02	1800
40	5	495.6	0.02	1800
45	5	516.4	0.02	1800
50	5	534.8	0.02	1800
55	5	551.2	0.02	1800
60	5	565.7	0.02	1800
65	5	578.6	0.02	1800
70	5	590.1	0.02	1800
75	5	600.3	0.02	1800
80	5	609.3	0.02	1800
85	5	617.3	0.02	1800
90	5	624.4	0.02	1800
95	5	630.8	0.02	1800
100	–	636.4	0.02	1800

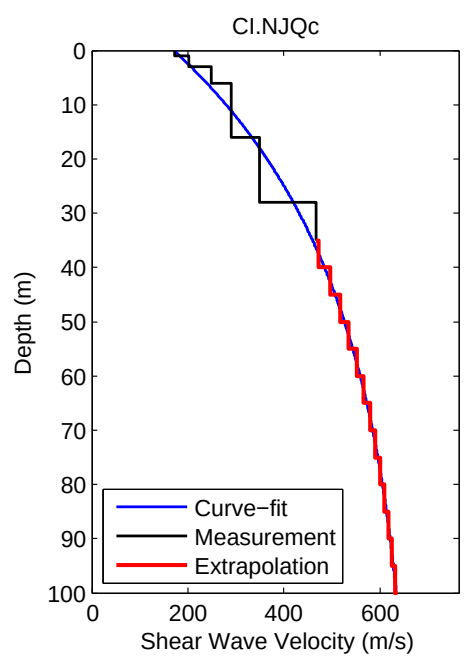

Linear Elastic Transfer Function

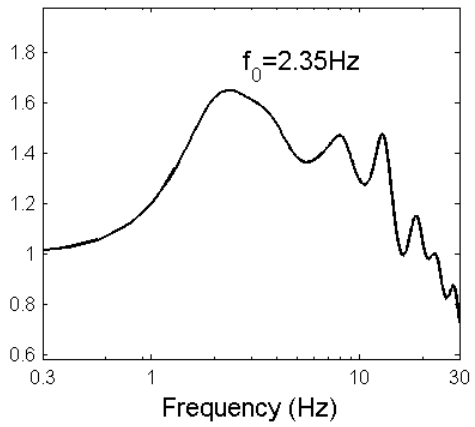

H/V Ratio – Sensor 450

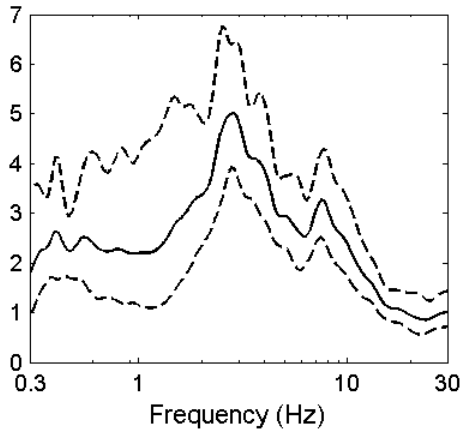

H/V Ratio – Sensor 507

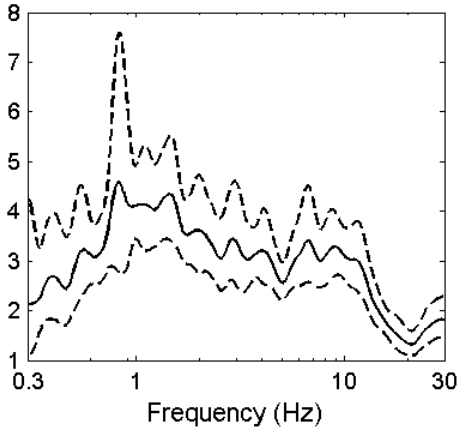

H/V Ratio – Sensor 453

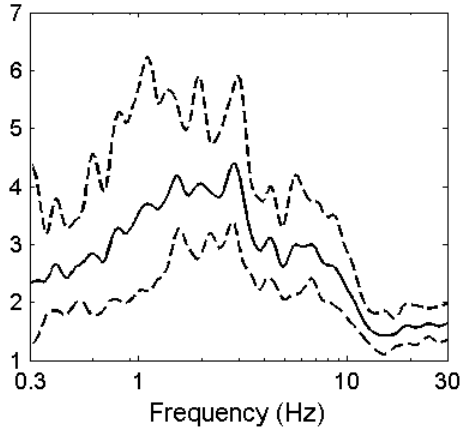

Equivalent Linear Transfer Function

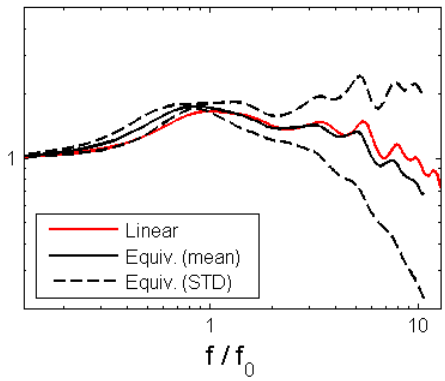

Equiv. Lin. TF (color coded by PGA_{RO})

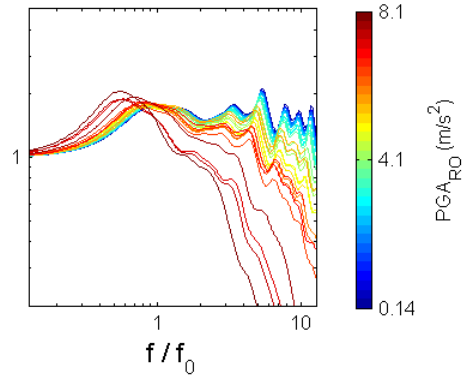

Non-linear Transfer Function

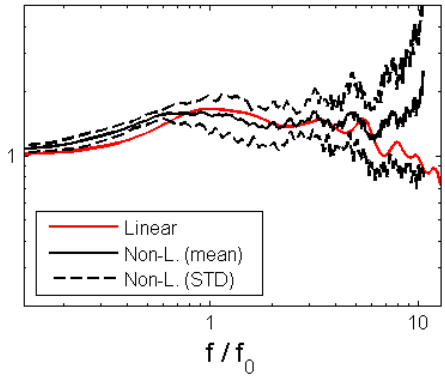

Non-linear TF (color coded by PGA_{RO})

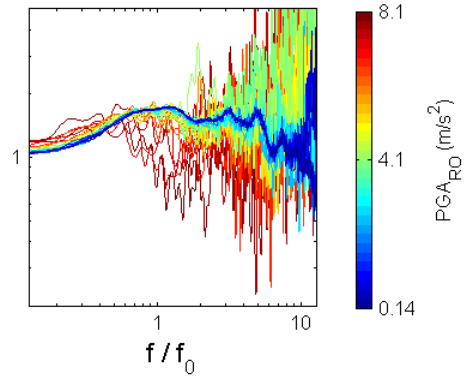

Equiv. Lin. TF (color coded by f_c)

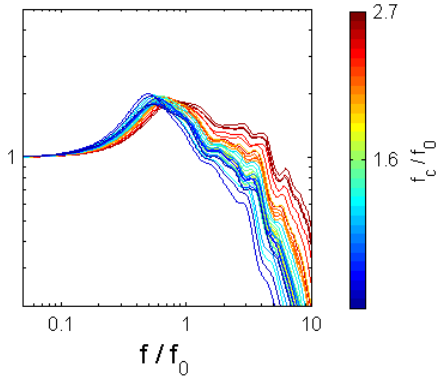

Non-linear TF (color coded by f_c)

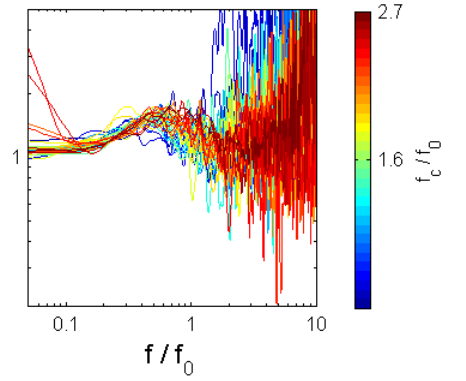

4.1.31 CI.RCT

Depth (m)	Thickness (m)	V_s (m/s)	Damping ratio	Density (kg/m^3)
0	2.3	176	0.05	1600
2.3	2.4	218	0.05	1800
4.7	5.7	217	0.05	1800
10.4	6.7	303	0.02	1800
17.1	18.3	388	0.02	1800
35.4	14.6	517	0.02	1800
50	5	531.9	0.02	1800
55	5	546.7	0.02	1800
60	5	559.7	0.02	1800
65	5	571.1	0.02	1800
70	5	581.1	0.02	1800
75	5	589.9	0.02	1800
80	5	597.6	0.02	1800
85	5	604.3	0.02	1800
90	5	610.3	0.02	1800
95	5	615.5	0.02	1800
100	–	620.0	0.02	1800

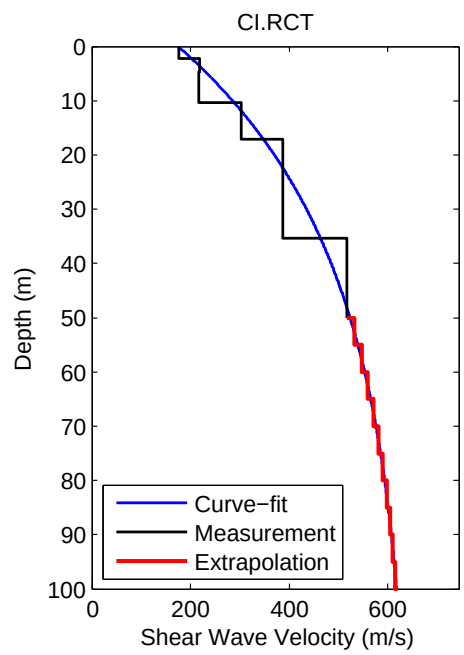

Linear Elastic Transfer Function

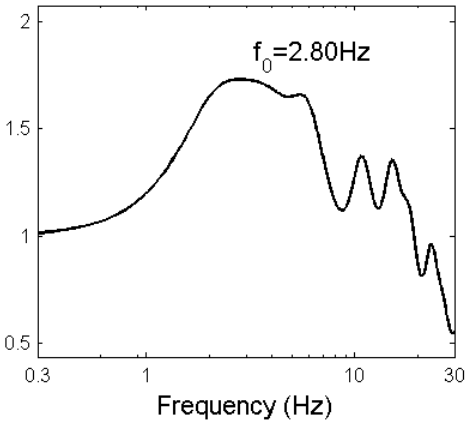

H/V Ratio – Sensor 450

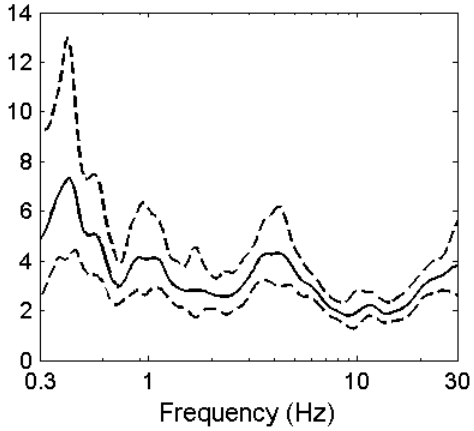

H/V Ratio – Sensor 507

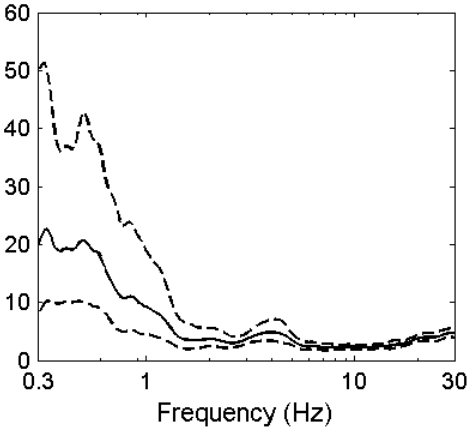

H/V Ratio – Sensor 453

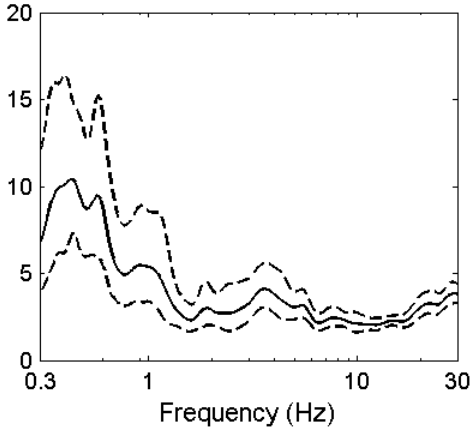

Equivalent Linear Transfer Function

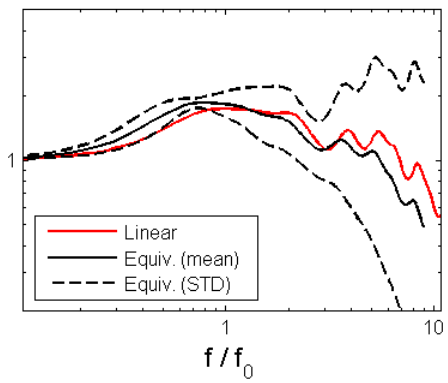

Equiv. Lin. TF (color coded by PGA_{RO})

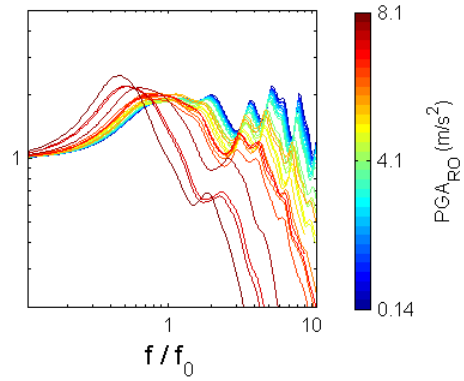

Non-linear Transfer Function

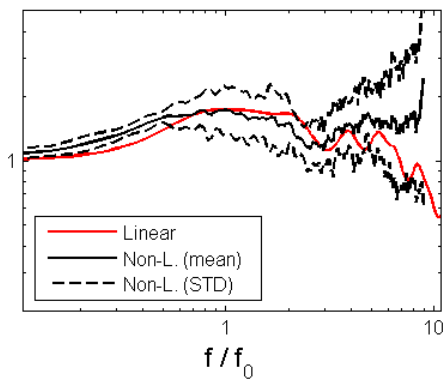

Non-linear TF (color coded by PGA_{RO})

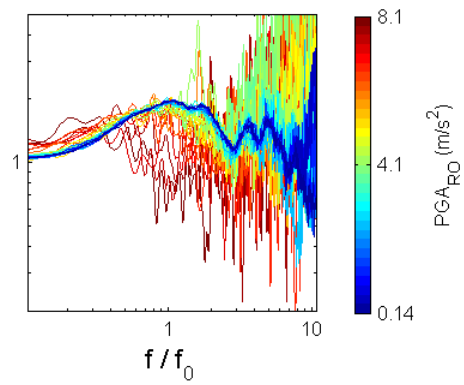

Equiv. Lin. TF (color coded by f_c)

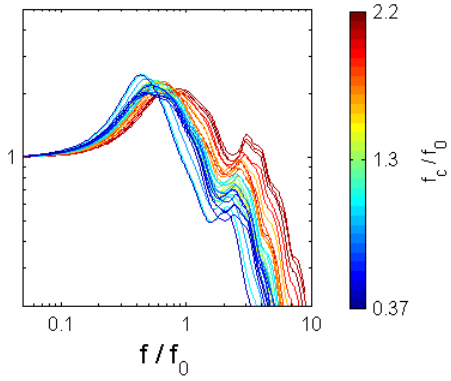

Non-linear TF (color coded by f_c)

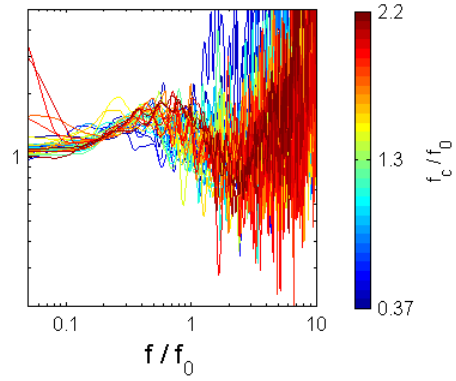

4.1.32 CI.SAL

Depth (m)	Thickness (m)	V_s (m/s)	Damping ratio	Density (kg/m^3)
0	1	133	0.05	1600
1	2	183	0.05	1600
3	2	204	0.05	1800
5	4	233	0.05	1800
9	6	247	0.05	1800
15	8	278	0.02	1800
23	12	363	0.02	1800
35	10	450	0.02	1800
45	5	455.8	0.02	1800
50	5	469.6	0.02	1800
55	5	481.5	0.02	1800
60	5	491.7	0.02	1800
65	5	500.5	0.02	1800
70	5	508.0	0.02	1800
75	5	514.4	0.02	1800
80	5	519.9	0.02	1800
85	5	524.6	0.02	1800
90	5	528.7	0.02	1800
95	5	532.1	0.02	1800
100	–	535.1	0.02	1800

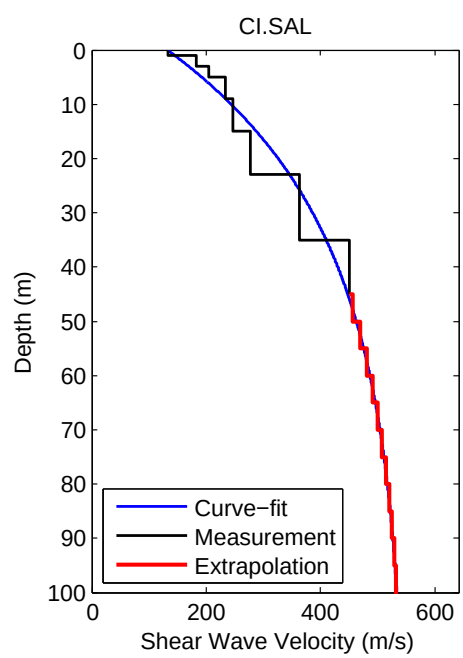

Linear Elastic Transfer Function

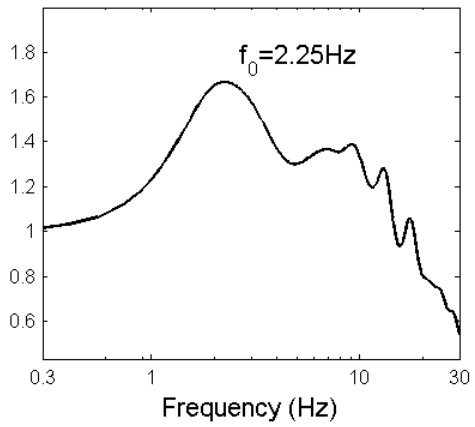

H/V Ratio – Sensor 450

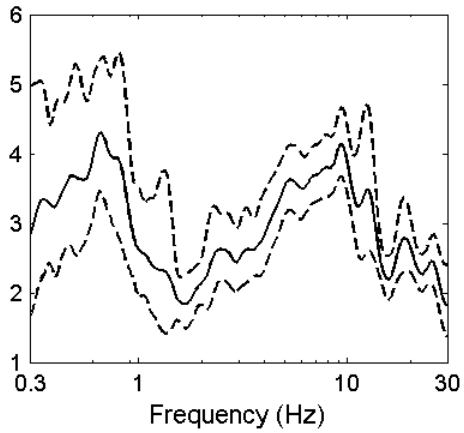

H/V Ratio – Sensor 507

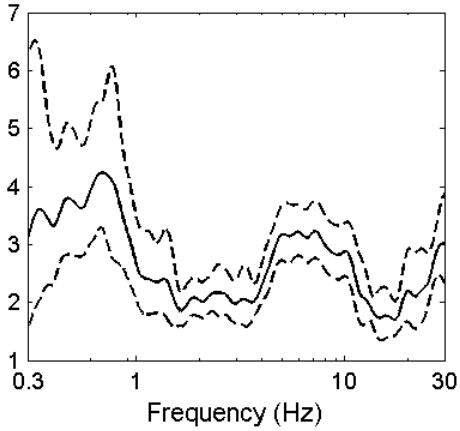

H/V Ratio – Sensor 453

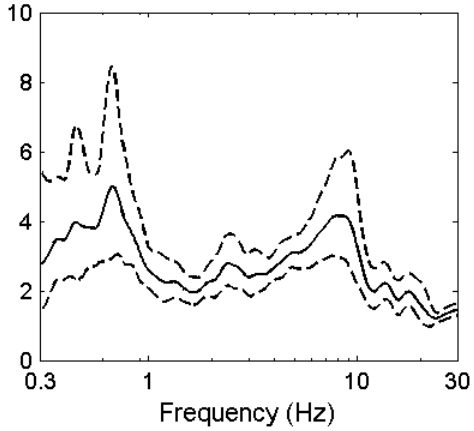

Equivalent Linear Transfer Function

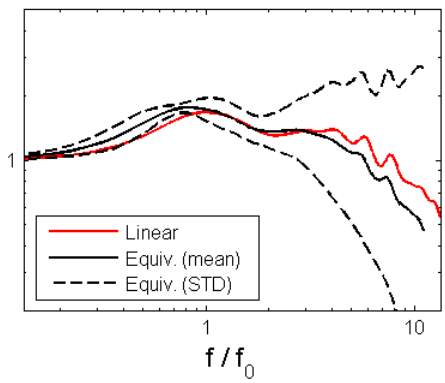

Equiv. Lin. TF (color coded by PGA_{RO})

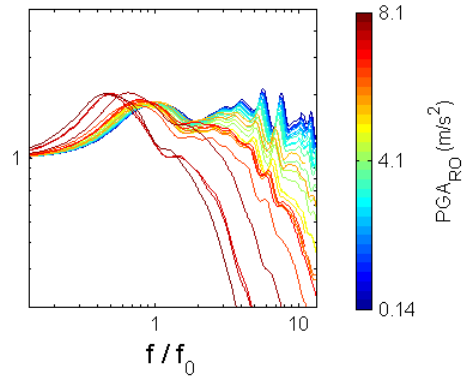

Non-linear Transfer Function

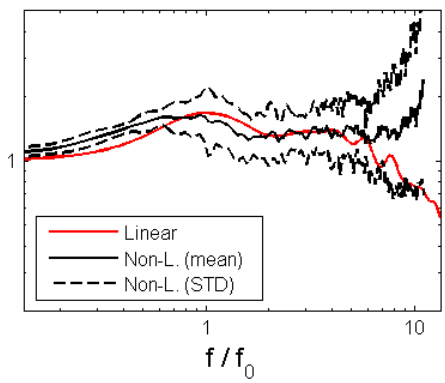

Non-linear TF (color coded by PGA_{RO})

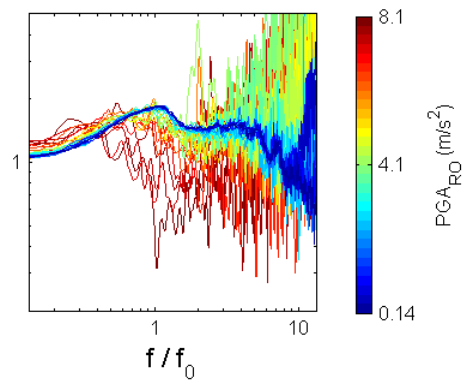

Equiv. Lin. TF (color coded by f_c)

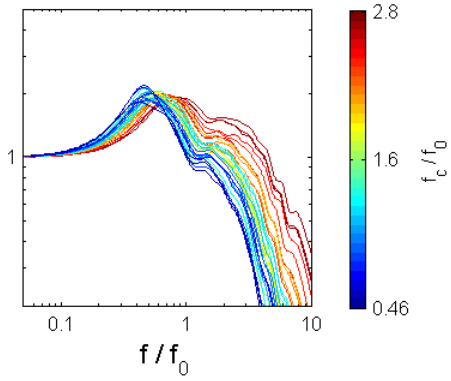

Non-linear TF (color coded by f_c)

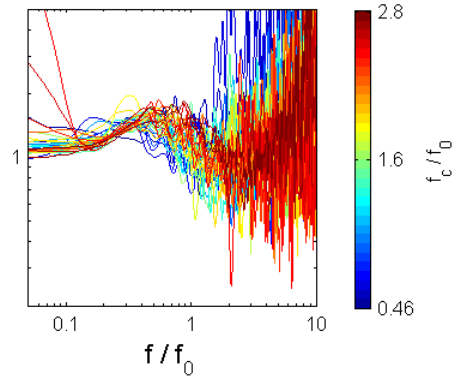

4.1.33 CI.SAN

Depth (m)	Thickness (m)	V_s (m/s)	Damping ratio	Density (kg/m^3)
0	1	99	0.05	1600
1	1.5	133	0.05	1600
2.5	2.5	138	0.05	1600
5	4	171	0.05	1600
9	6	245	0.05	1800
15	9	301	0.02	1800
24	12	340	0.02	1800
36	15	407	0.02	1800
51	29	477	0.02	1800
80	5	477.8	0.02	1800
85	5	478.7	0.02	1800
90	5	479.4	0.02	1800
95	5	479.9	0.02	1800
100	–	480.2	0.02	1800

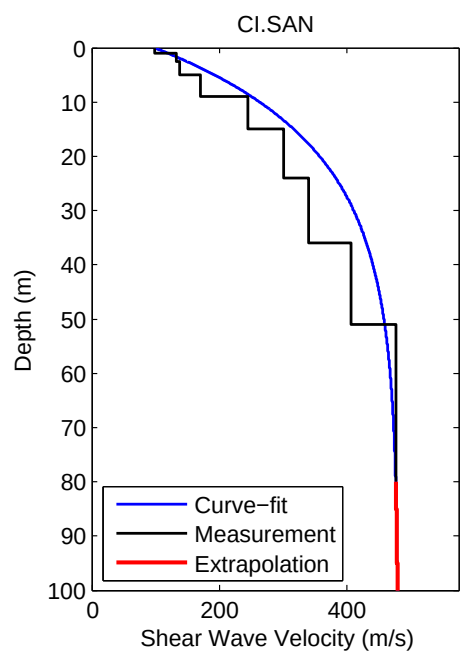

Linear Elastic Transfer Function

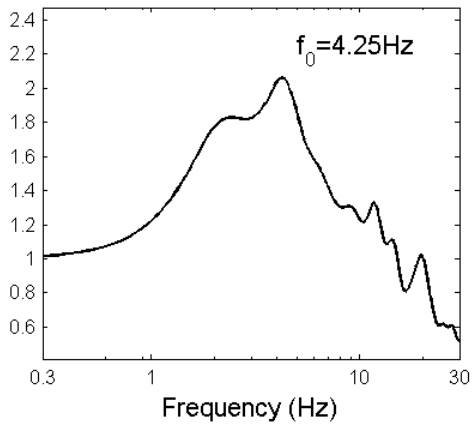

H/V Ratio – Sensor 450

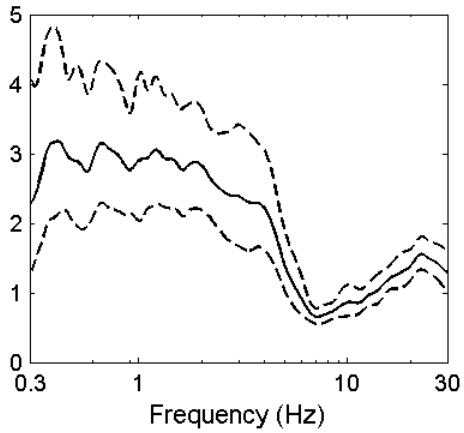

H/V Ratio – Sensor 507

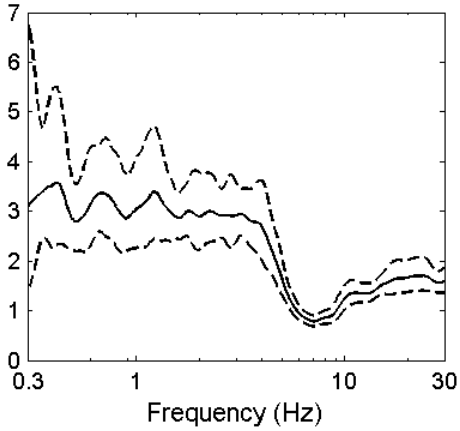

H/V Ratio – Sensor 453

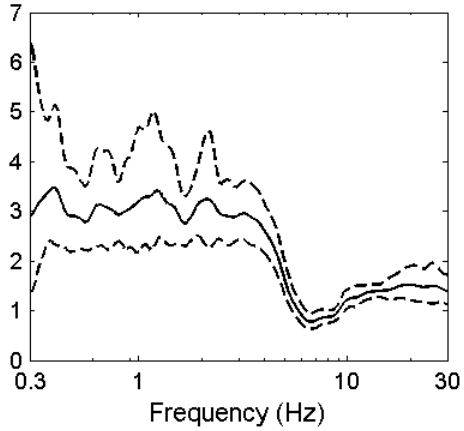

Equivalent Linear Transfer Function

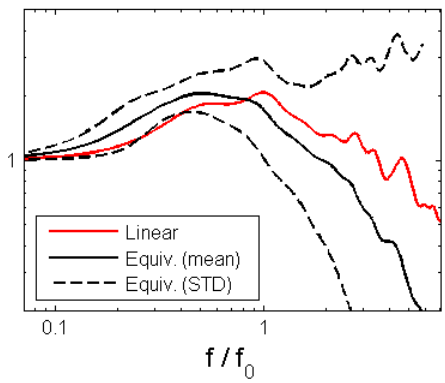

Equiv. Lin. TF (color coded by PGA_{RO})

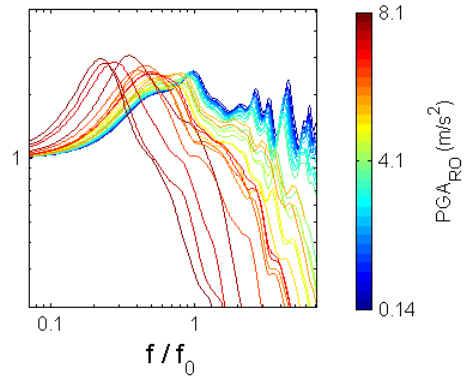

Non-linear Transfer Function

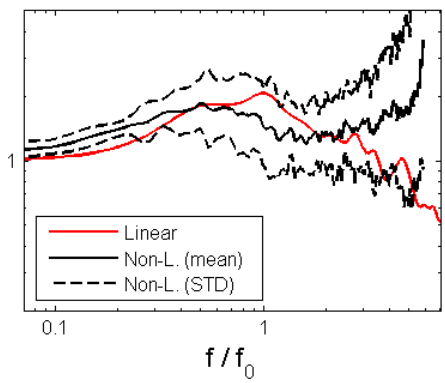

Non-linear TF (color coded by PGA_{RO})

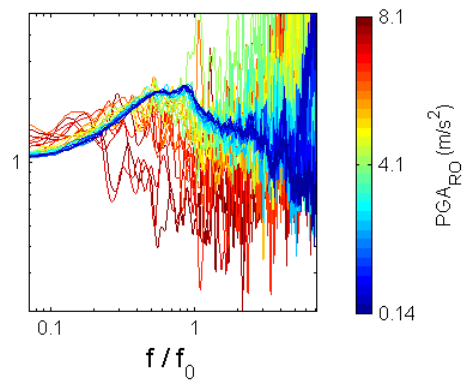

Equiv. Lin. TF (color coded by f_c)

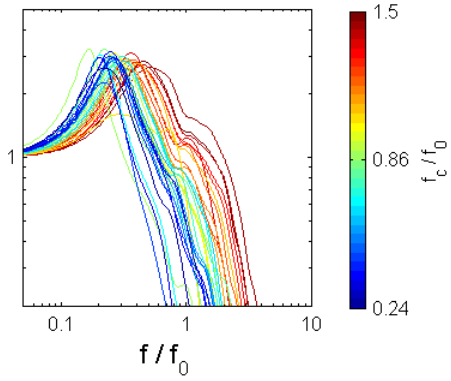

Non-linear TF (color coded by f_c)

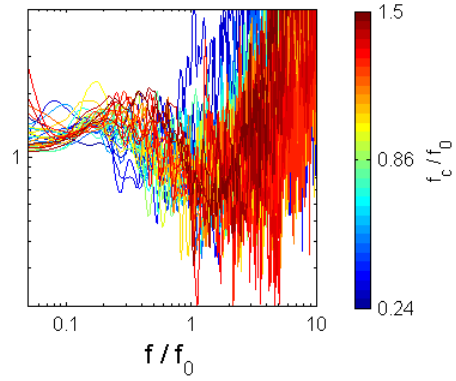

4.1.34 CI.SIO

Depth (m)	Thickness (m)	V_s (m/s)	Damping ratio	Density (kg/m^3)
0	1.5	122	0.05	1600
1.5	2	189	0.05	1600
3.5	4.5	261	0.02	1800
8	8	265	0.02	1800
16	10	266	0.02	1800
26	12	318	0.02	1800
38	15	389	0.02	1800
53	15	482	0.02	1800
68	–	584	0.02	1800

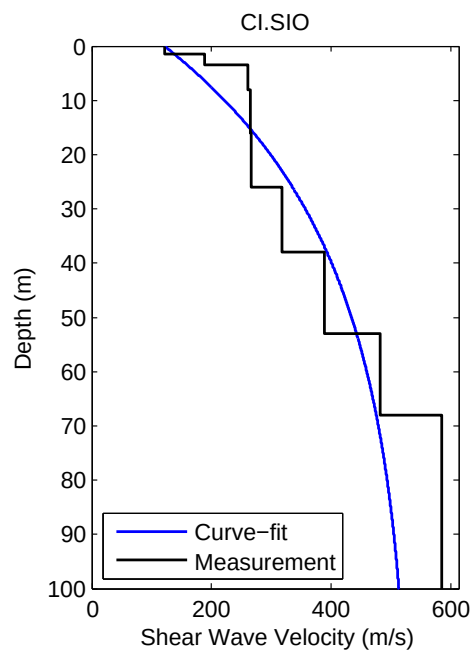

Linear Elastic Transfer Function

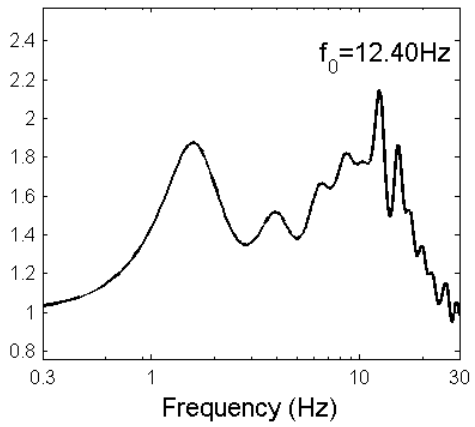

H/V Ratio – Sensor 450

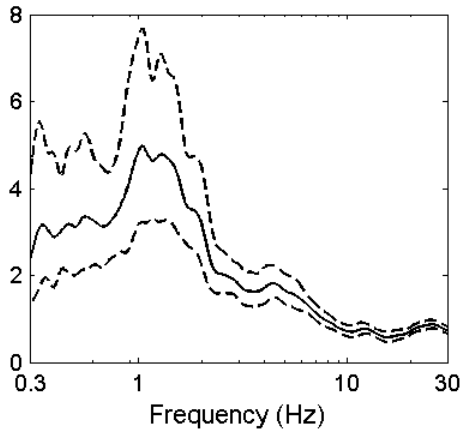

H/V Ratio – Sensor 507

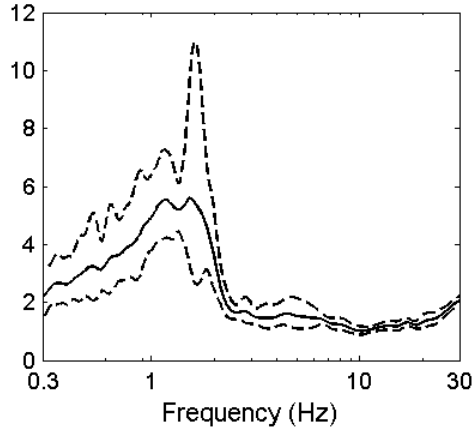

H/V Ratio – Sensor 453

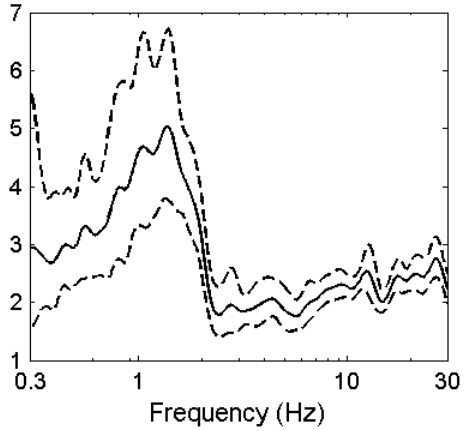

Equivalent Linear Transfer Function

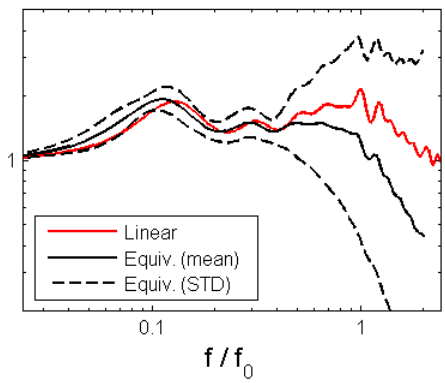

Equiv. Lin. TF (color coded by PGA_{RO})

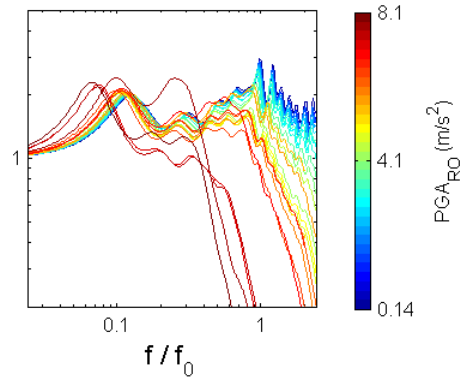

Non-linear Transfer Function

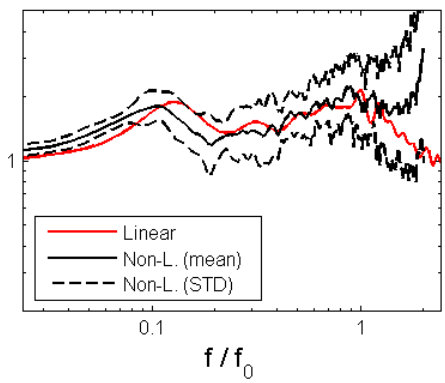

Non-linear TF (color coded by PGA_{RO})

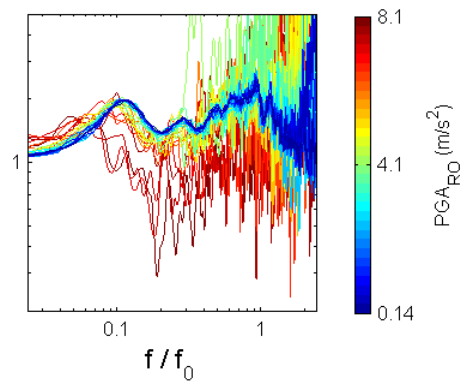

Equiv. Lin. TF (color coded by f_c)

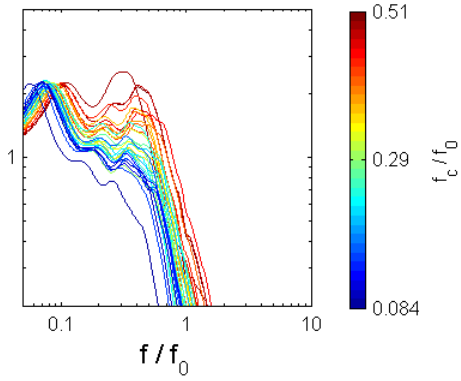

Non-linear TF (color coded by f_c)

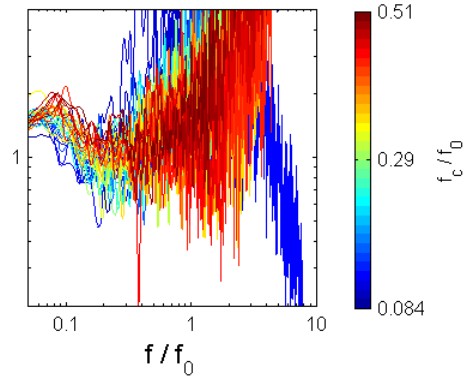

4.1.35 CI.SMM

Depth (m)	Thickness (m)	V_s (m/s)	Damping ratio	Density (kg/m^3)
0	1	128	0.05	1600
1	4	223	0.05	1800
5	8	235	0.05	1800
13	12	211	0.05	1800
25	5	297	0.02	1800
30	5	316.1	0.02	1800
35	5	335.3	0.02	1800
40	5	352.5	0.02	1800
45	5	368.1	0.02	1800
50	5	382.1	0.02	1800
55	5	394.8	0.02	1800
60	5	406.2	0.02	1800
65	5	416.4	0.02	1800
70	5	425.7	0.02	1800
75	5	434.0	0.02	1800
80	5	441.5	0.02	1800
85	5	448.2	0.02	1800
90	5	454.3	0.02	1800
95	5	459.8	0.02	1800
100	–	464.7	0.02	1800

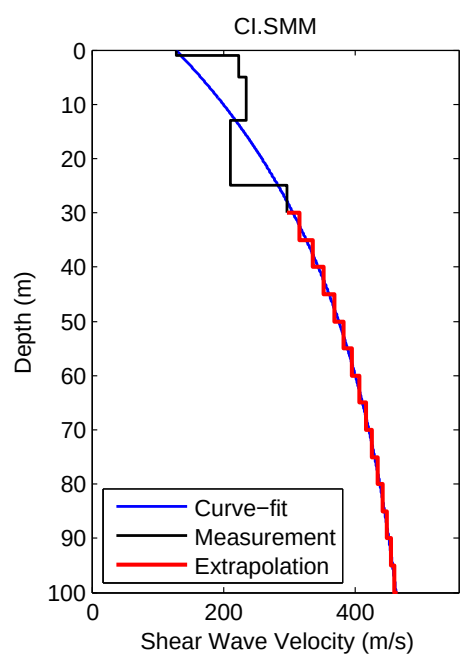

Linear Elastic Transfer Function

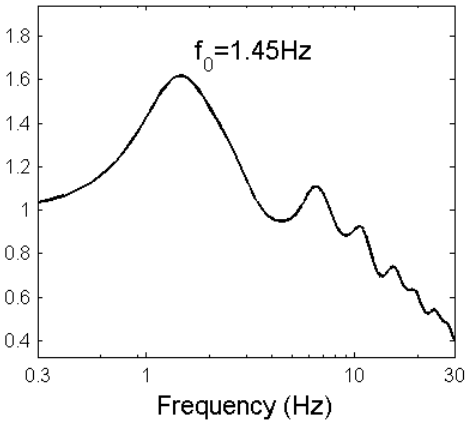

H/V Ratio – Sensor 450

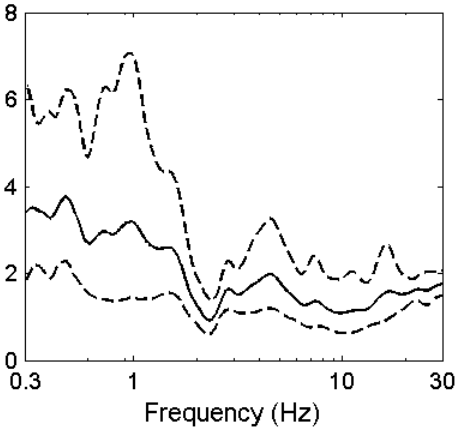

H/V Ratio – Sensor 507

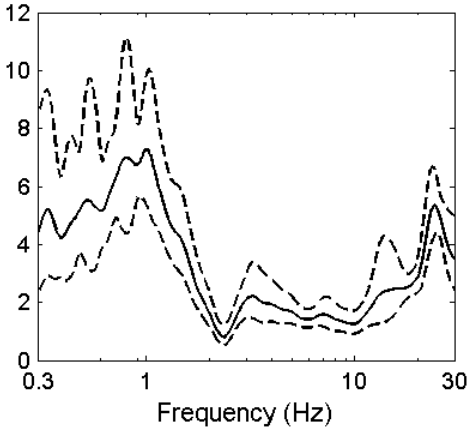

H/V Ratio – Sensor 453

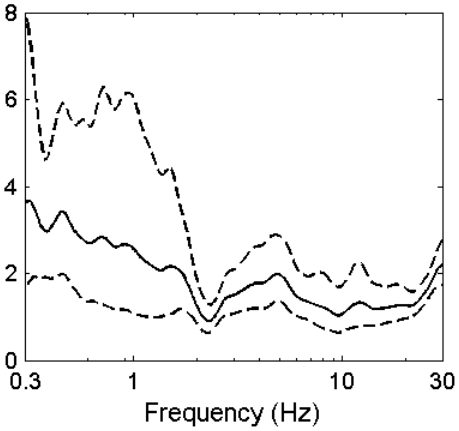

Equivalent Linear Transfer Function

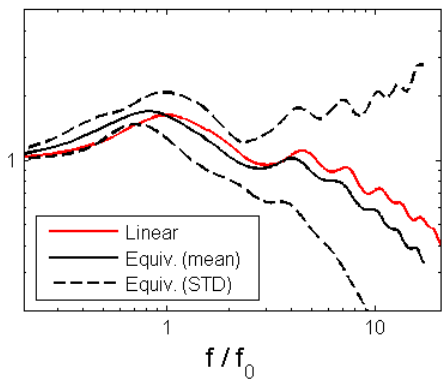

Equiv. Lin. TF (color coded by PGA_{RO})

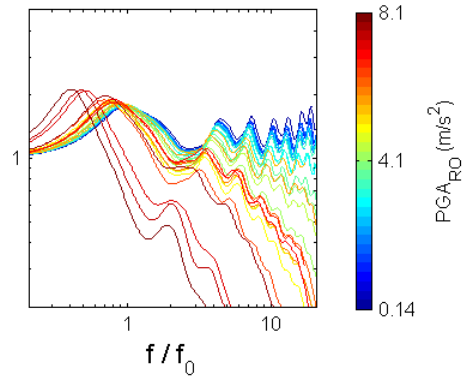

Non-linear Transfer Function

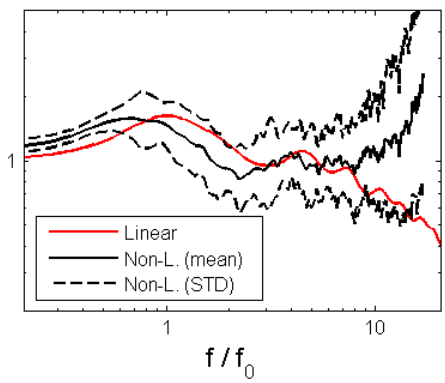

Non-linear TF (color coded by PGA_{RO})

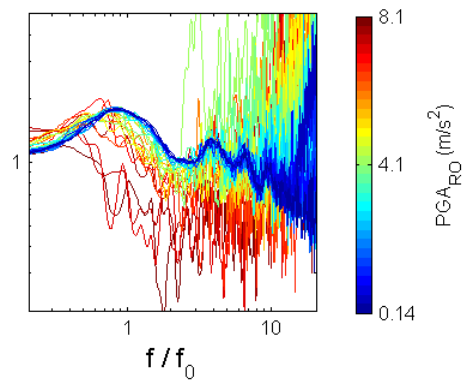

Equiv. Lin. TF (color coded by f_c)

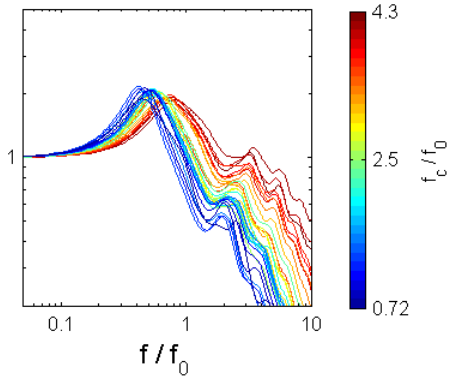

Non-linear TF (color coded by f_c)

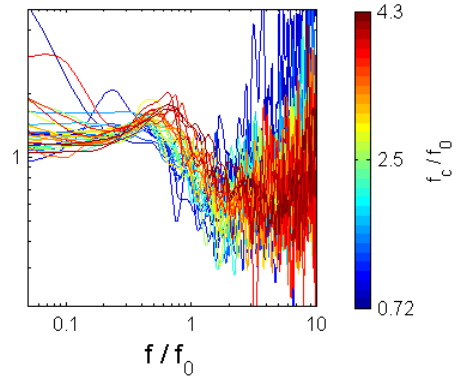

4.1.36 CI.SMV

Depth (m)	Thickness (m)	V_s (m/s)	Damping ratio	Density (kg/m^3)
0	1	144	0.05	1600
1	2	203	0.05	1800
3	3	208	0.05	1800
6	4	229	0.05	1800
10	6	266	0.02	1800
16	9	309	0.02	1800
25	12	329	0.02	1800
37	15	483	0.02	1800
52	20	596	0.02	1800
72	–	725	0.02	1800

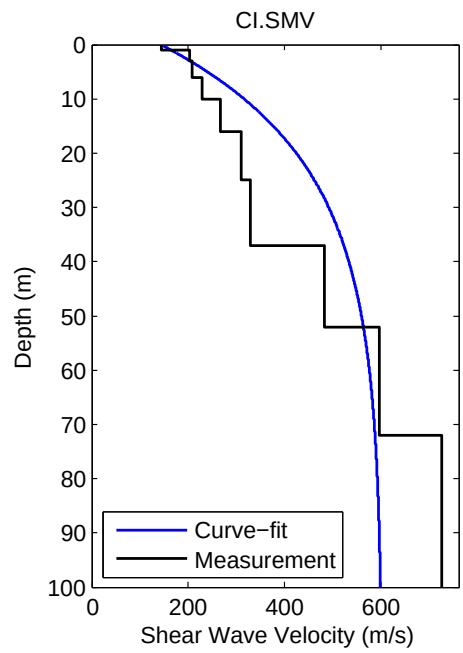

Linear Elastic Transfer Function

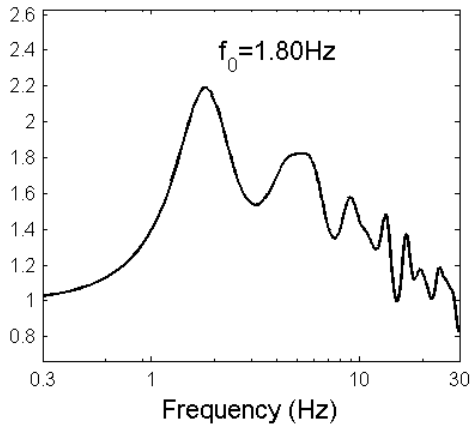

H/V Ratio – Sensor 450

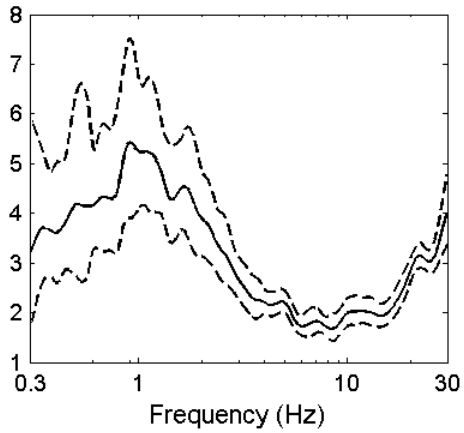

H/V Ratio – Sensor 507

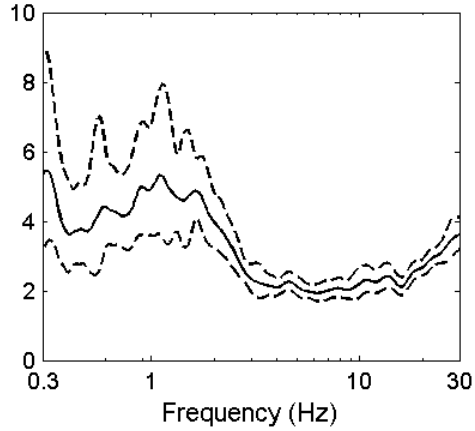

H/V Ratio – Sensor 453

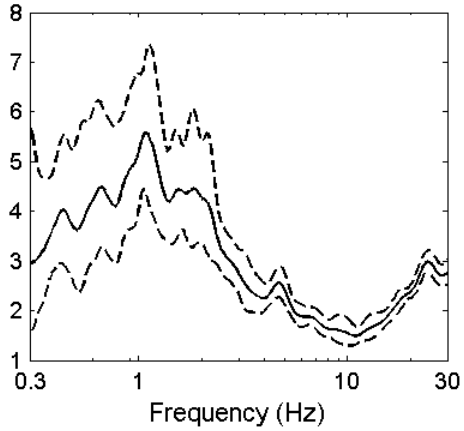

Equivalent Linear Transfer Function

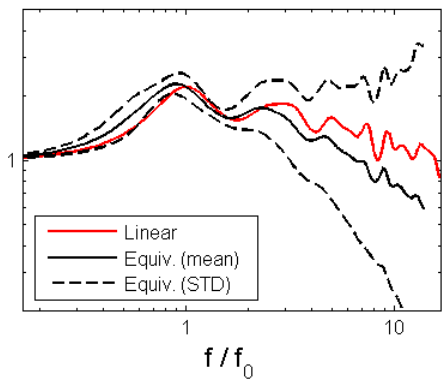

Equiv. Lin. TF (color coded by PGA_{RO})

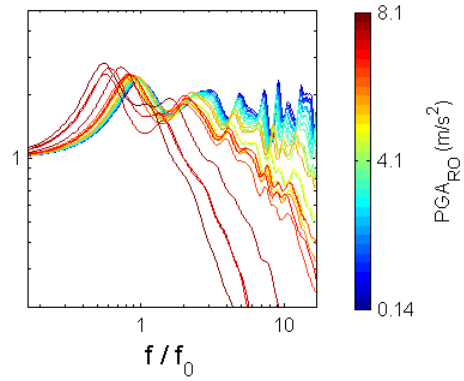

Non-linear Transfer Function

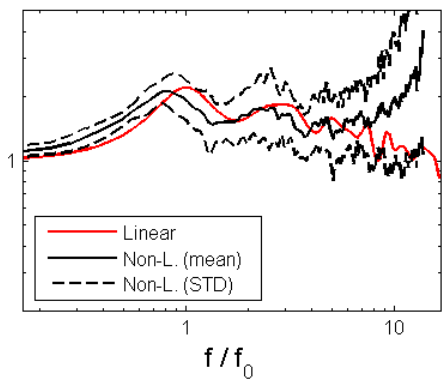

Non-linear TF (color coded by PGA_{RO})

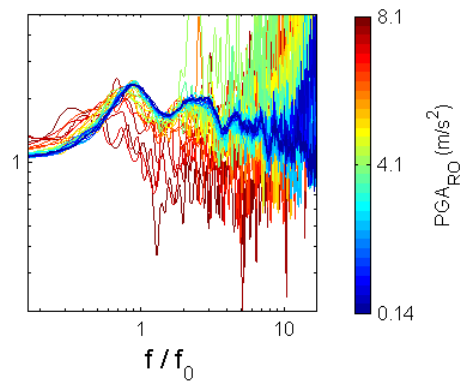

Equiv. Lin. TF (color coded by f_c)

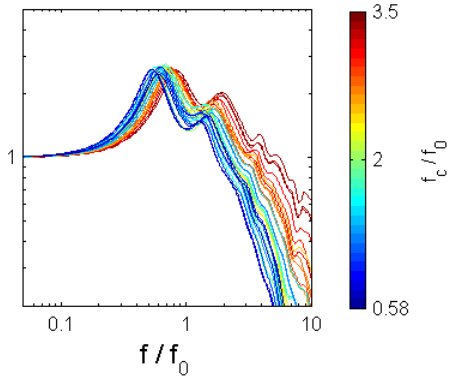

Non-linear TF (color coded by f_c)

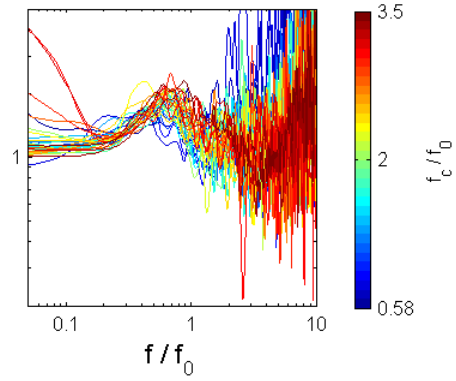

4.1.37 CI.TFT

Depth (m)	Thickness (m)	V_s (m/s)	Damping ratio	Density (kg/m^3)
0	1	147	0.05	1600
1	2	213	0.05	1800
3	3	283	0.02	1800
6	4	333	0.02	1800
10	6	363	0.02	1800
16	9	379	0.02	1800
25	5	445	0.02	1800
30	5	494.0	0.02	1800
35	5	527.5	0.02	1800
40	5	557.3	0.02	1800
45	5	583.8	0.02	1800
50	5	607.4	0.02	1800
55	5	628.3	0.02	1800
60	5	646.9	0.02	1800
65	5	663.5	0.02	1800
70	5	678.2	0.02	1800
75	5	691.2	0.02	1800
80	5	702.8	0.02	1800
85	5	713.2	0.02	1800
90	5	722.4	0.02	1800
95	5	730.5	0.02	1800
100	–	737.8	0.02	1800

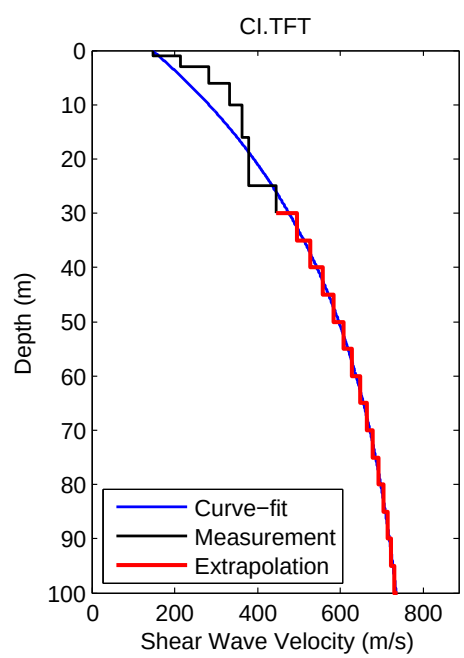

Linear Elastic Transfer Function

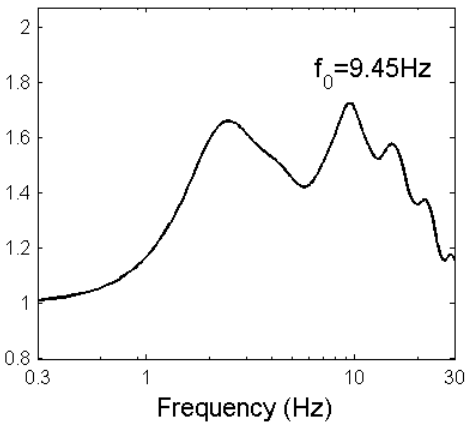

H/V Ratio – Sensor 450

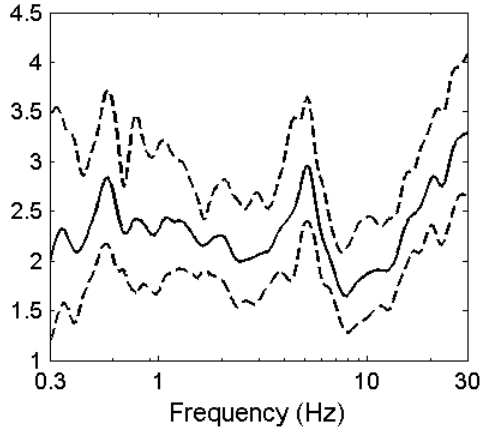

H/V Ratio – Sensor 507

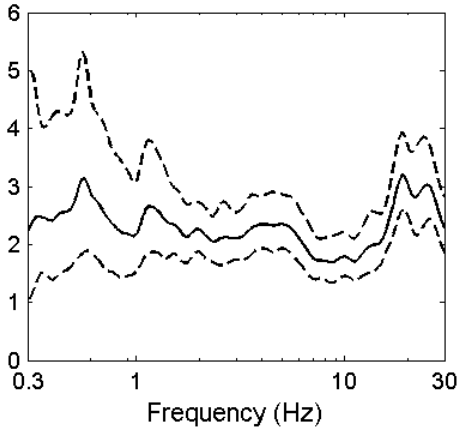

H/V Ratio – Sensor 453

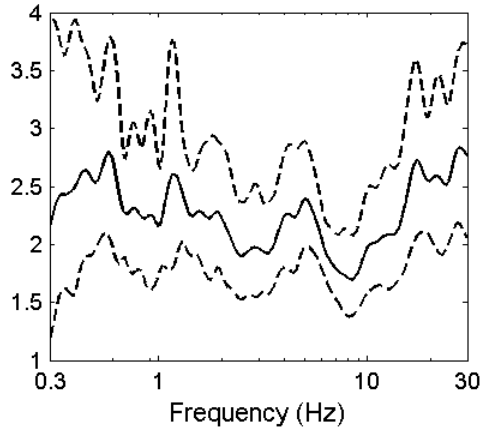

Equivalent Linear Transfer Function

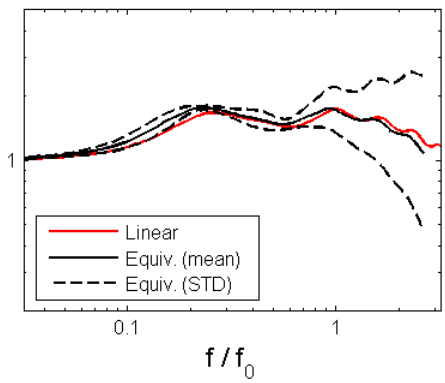

Equiv. Lin. TF (color coded by PGA_{RO})

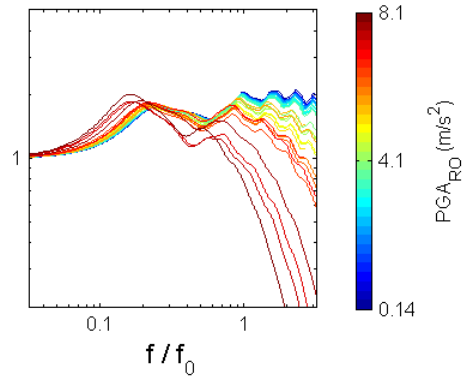

Non-linear Transfer Function

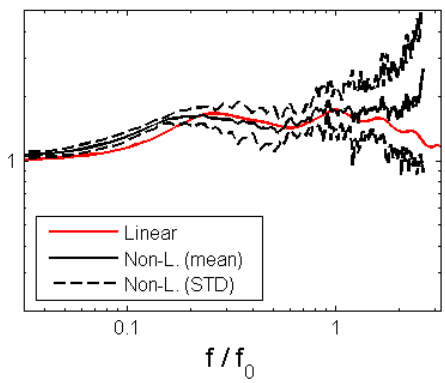

Non-linear TF (color coded by PGA_{RO})

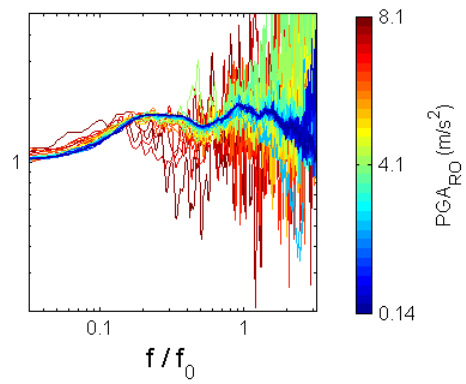

Equiv. Lin. TF (color coded by f_c)

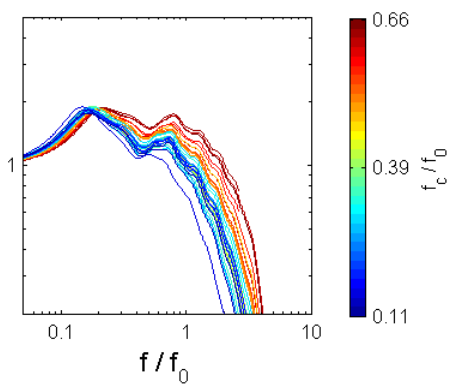

Non-linear TF (color coded by f_c)

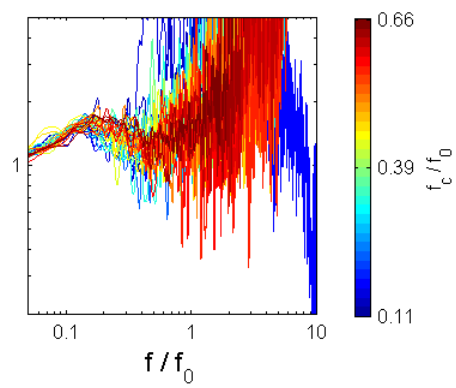

4.1.38 CI.USB

Depth (m)	Thickness (m)	V_s (m/s)	Damping ratio	Density (kg/m^3)
0	1	104	0.05	1600
1	1.5	156	0.05	1600
2.5	2.5	228	0.05	1800
5	4	317	0.02	1800
9	6	358	0.02	1800
15	8	366	0.02	1800
23	10	378	0.02	1800
33	12	403	0.02	1800
45	5	445	0.02	1800
50	5	485.2	0.02	1800
55	5	503.0	0.02	1800
60	5	518.9	0.02	1800
65	5	533.1	0.02	1800
70	5	545.7	0.02	1800
75	5	557.0	0.02	1800
80	5	567.1	0.02	1800
85	5	576.0	0.02	1800
90	5	584.1	0.02	1800
95	5	591.2	0.02	1800
100	–	597.6	0.02	1800

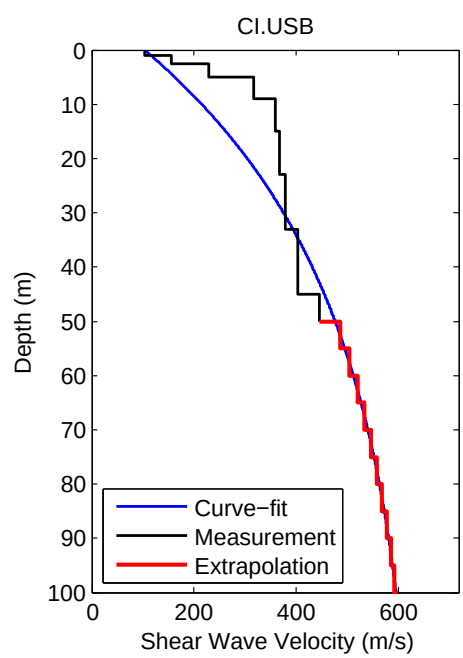

Linear Elastic Transfer Function

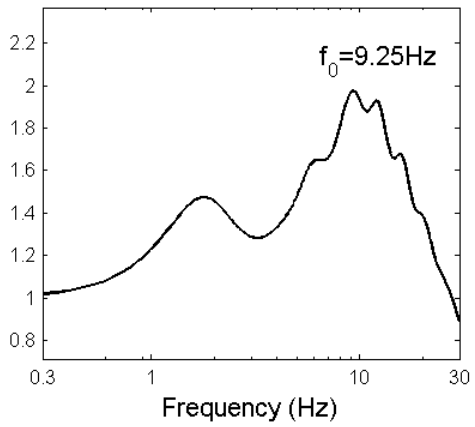

H/V Ratio – Sensor 450

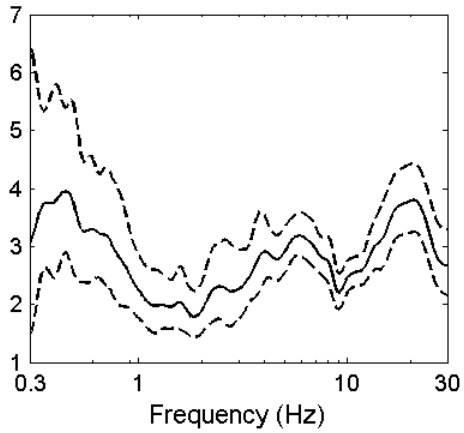

H/V Ratio – Sensor 507

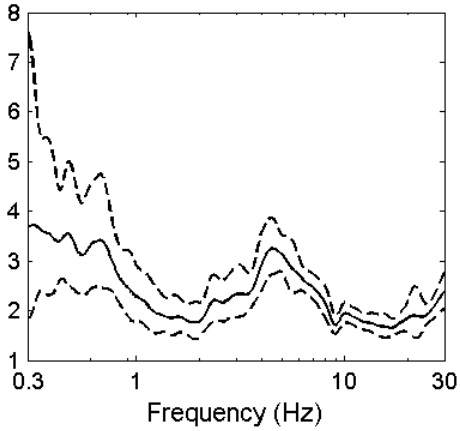

H/V Ratio – Sensor 453

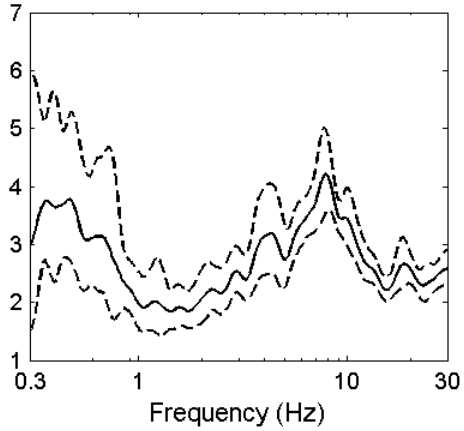

Equivalent Linear Transfer Function

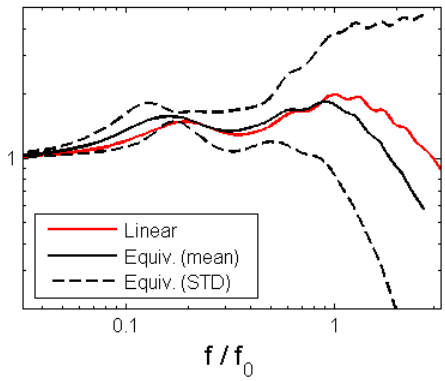

Equiv. Lin. TF (color coded by PGA_{RO})

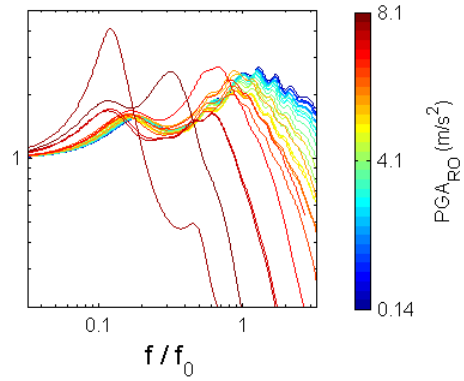

Non-linear Transfer Function

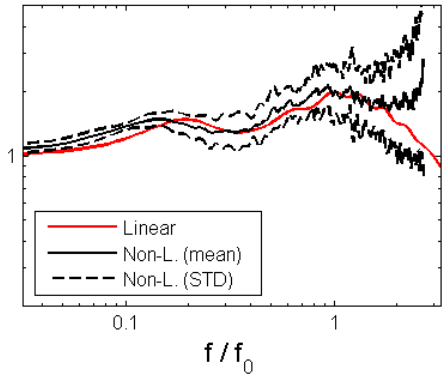

Non-linear TF (color coded by PGA_{RO})

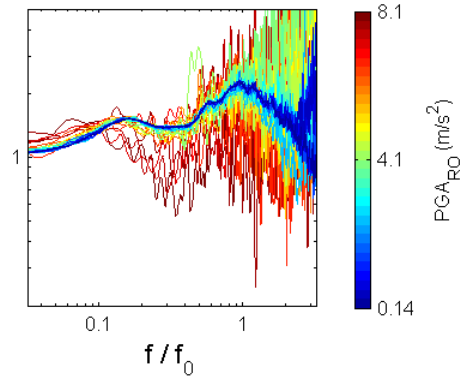

Equiv. Lin. TF (color coded by f_c)

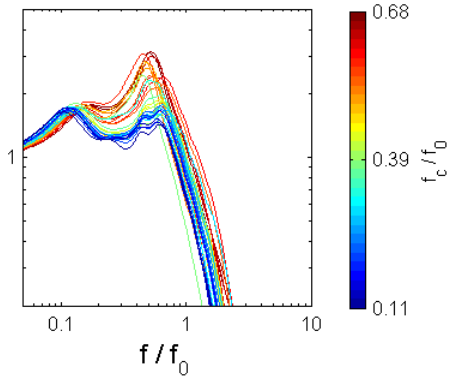

Non-linear TF (color coded by f_c)

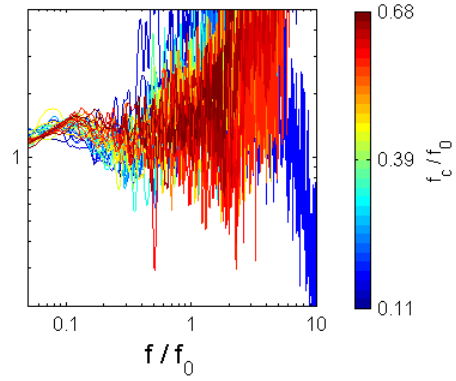

4.1.39 CI.WES

Depth (m)	Thickness (m)	V_s (m/s)	Damping ratio	Density (kg/m^3)
0	0.5	125	0.05	1600
0.5	1	112	0.05	1600
1.5	2	120	0.05	1600
3.5	2	181	0.05	1600
5.5	4	204	0.05	1800
9.5	6	254	0.02	1800
15.5	8	313	0.02	1800
23.5	11.5	443	0.02	1800
35	5	463.5	0.02	1800
40	5	483.1	0.02	1800
45	5	499.5	0.02	1800
50	5	513.2	0.02	1800
55	5	524.7	0.02	1800
60	5	534.3	0.02	1800
65	5	542.3	0.02	1800
70	5	549.1	0.02	1800
75	5	554.7	0.02	1800
80	5	559.4	0.02	1800
85	5	563.3	0.02	1800
90	5	566.6	0.02	1800
95	5	569.3	0.02	1800
100	–	571.6	0.02	1800

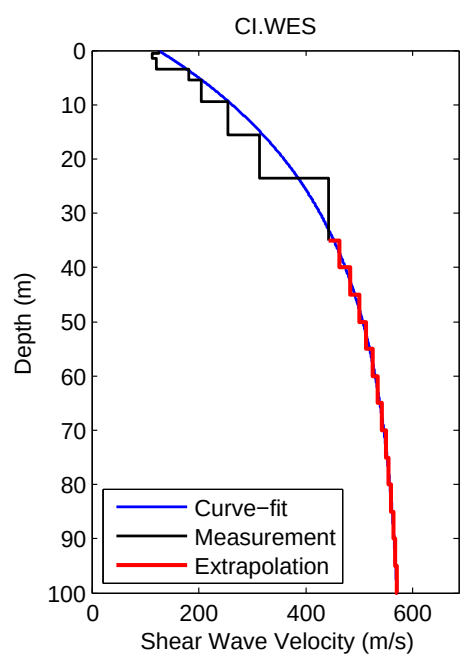

Linear Elastic Transfer Function

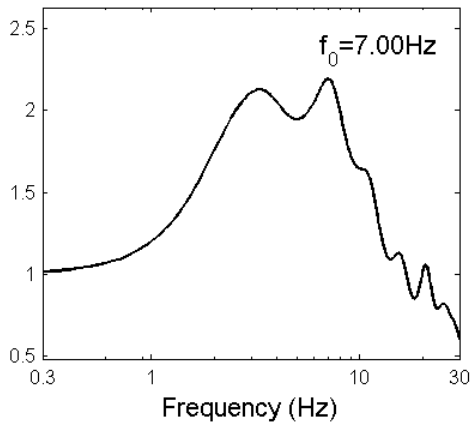

H/V Ratio – Sensor 450

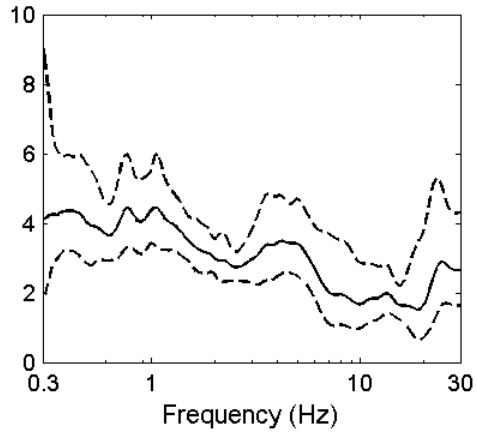

H/V Ratio – Sensor 507

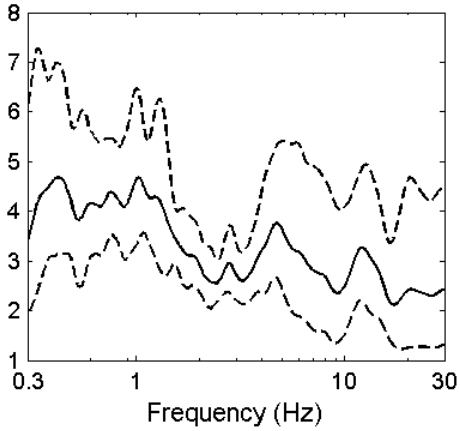

H/V Ratio – Sensor 453

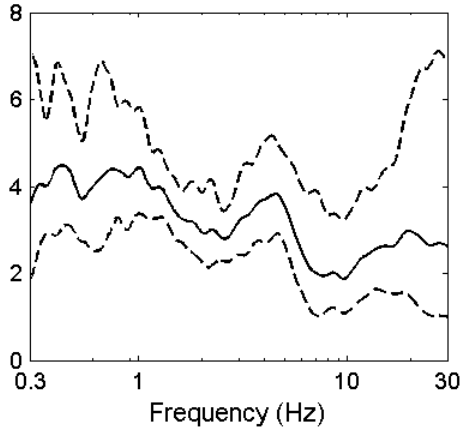

Equivalent Linear Transfer Function

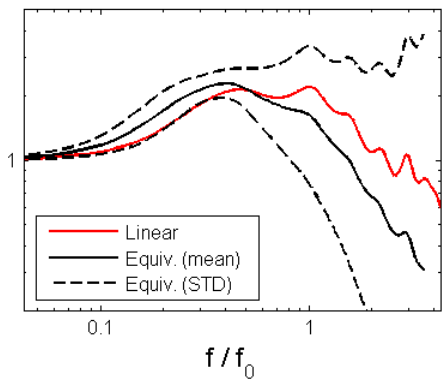

Equiv. Lin. TF (color coded by PGA_{RO})

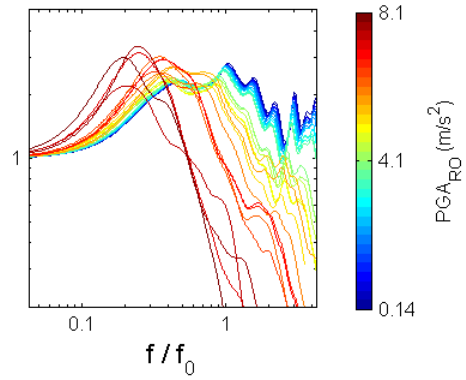

Non-linear Transfer Function

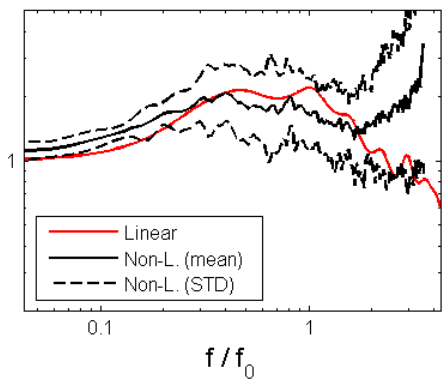

Non-linear TF (color coded by PGA_{RO})

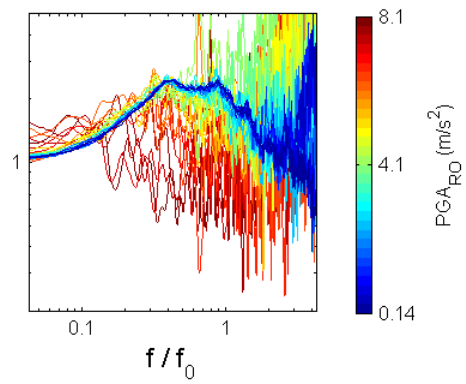

Equiv. Lin. TF (color coded by f_c)

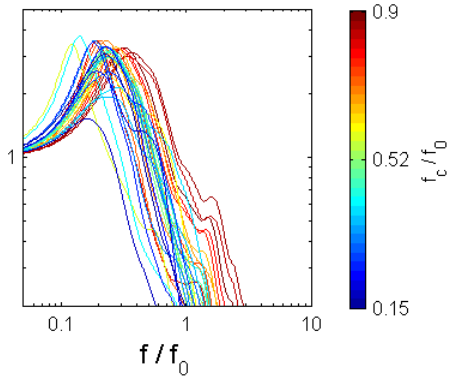

Non-linear TF (color coded by f_c)

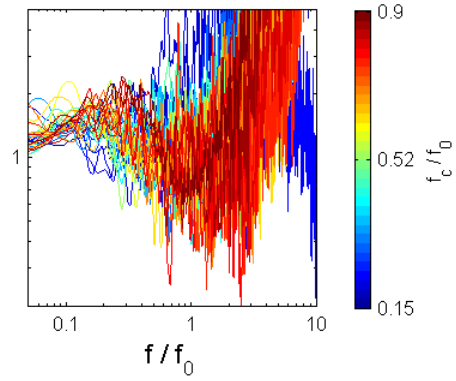

4.1.40 NC.JELB

Depth (m)	Thickness (m)	V_s (m/s)	Damping ratio	Density (kg/m^3)
0	1	201	0.05	1800
1	1.5	227	0.05	1800
2.5	2	283	0.02	1800
4.5	10.5	326	0.02	1800
15	10	322	0.02	1800
25	10	453	0.02	1800
35	5	476.4	0.02	1800
40	5	499.1	0.02	1800
45	5	519.5	0.02	1800
50	5	537.8	0.02	1800
55	5	554.3	0.02	1800
60	5	569.1	0.02	1800
65	5	582.4	0.02	1800
70	5	594.4	0.02	1800
75	5	605.1	0.02	1800
80	5	614.8	0.02	1800
85	5	623.5	0.02	1800
90	5	631.3	0.02	1800
95	5	638.3	0.02	1800
100	–	644.6	0.02	1800

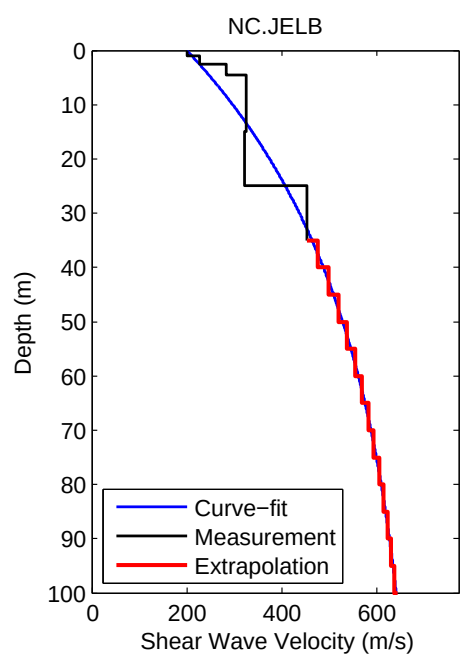

Linear Elastic Transfer Function

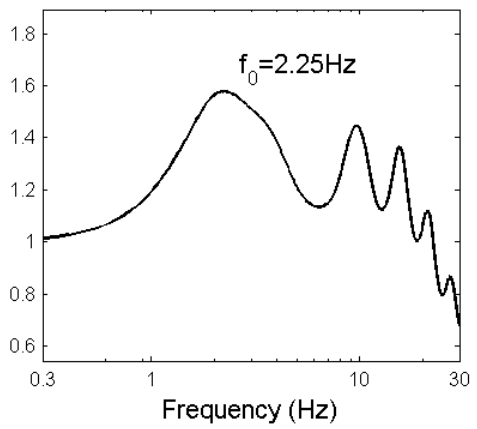

H/V Ratio – Sensor 507

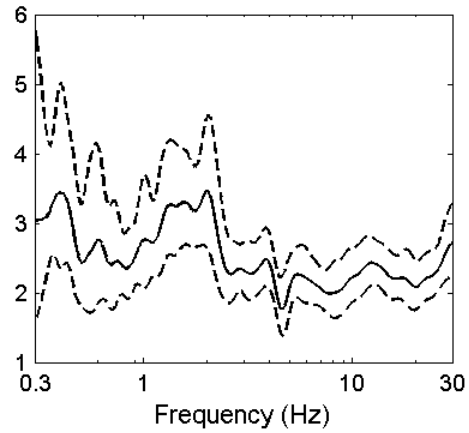

H/V Ratio – Sensor 453a

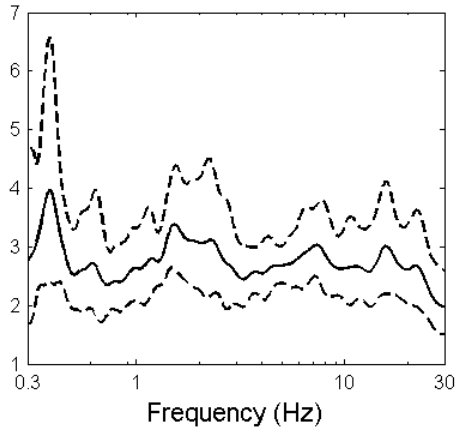

H/V Ratio – Sensor 453b

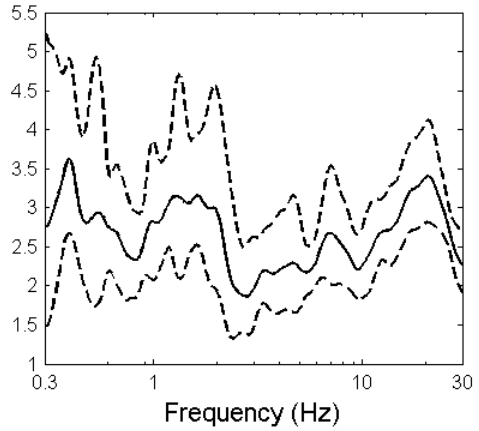

Equivalent Linear Transfer Function

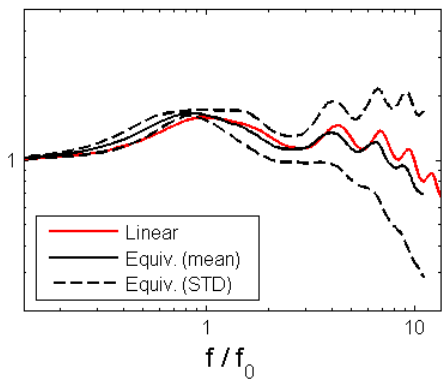

Equiv. Lin. TF (color coded by PGA_{RO})

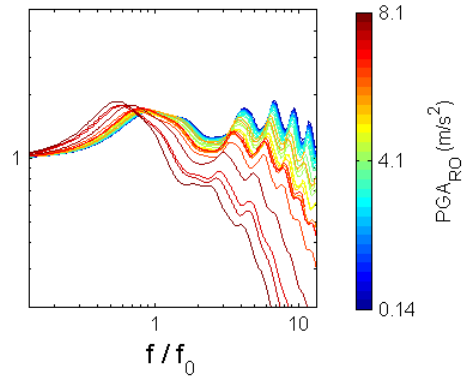

Non-linear Transfer Function

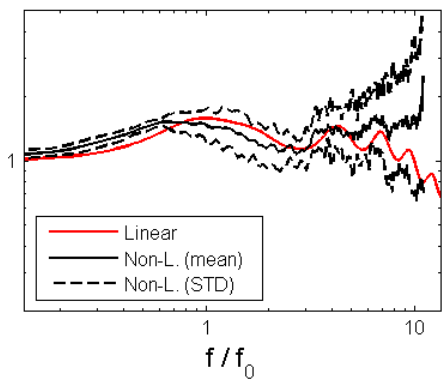

Non-linear TF (color coded by PGA_{RO})

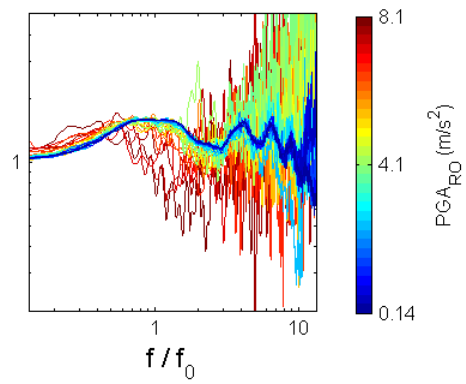

Equiv. Lin. TF (color coded by f_c)

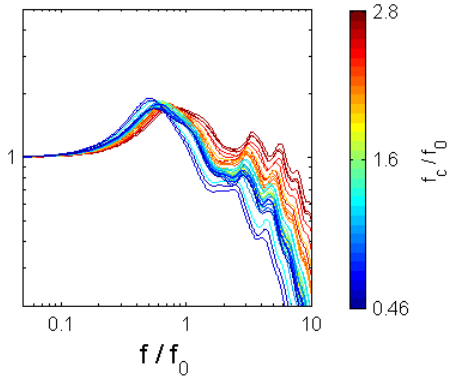

Non-linear TF (color coded by f_c)

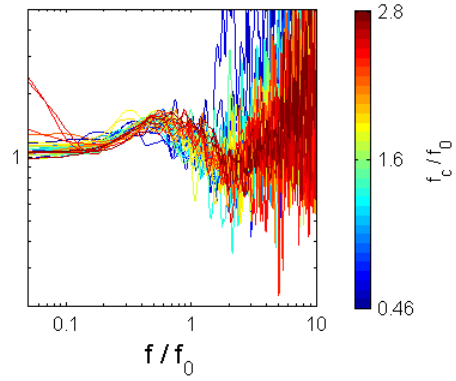

4.2 Class D/C

Class D/C sites include the following:

Site Code	V_{s30}-measured (m/s)	V_{s30}-adjusted (m/s)
CE.12149	359	385
CE.13100	341	357
CE.24029	369	377
CI.ALP	347	362
CI.BBR	356	380
CI.CBC	361	437
CI.CRP	340	385
CI.GATR	338	345
CI.LUG	365	381
CI.MIK	333	376
CI.NSS2	352	377
CI.PLC	346	371
CI.RSB	360	360
CI.SHO	356	377
CI.SLB	336	377
CI.VOG	341	358

4.2.1 CE.12149

Depth (m)	Thickness (m)	V_s (m/s)	Damping ratio	Density (kg/m^3)
0	1.25	183	0.05	1600
1.25	1.75	294	0.02	1800
3	7	307	0.02	1800
10	12	389	0.02	1800
22	12	468	0.02	1800
34	20	524	0.02	1800
54	6	604	0.02	1800
60	5	613.6	0.02	1800
65	5	632.0	0.02	1800
70	5	648.9	0.02	1800
75	5	664.4	0.02	1800
80	5	678.6	0.02	1800
85	5	691.7	0.02	1800
90	5	703.7	0.02	1800
95	5	714.6	0.02	1800
100	–	724.7	0.02	1800

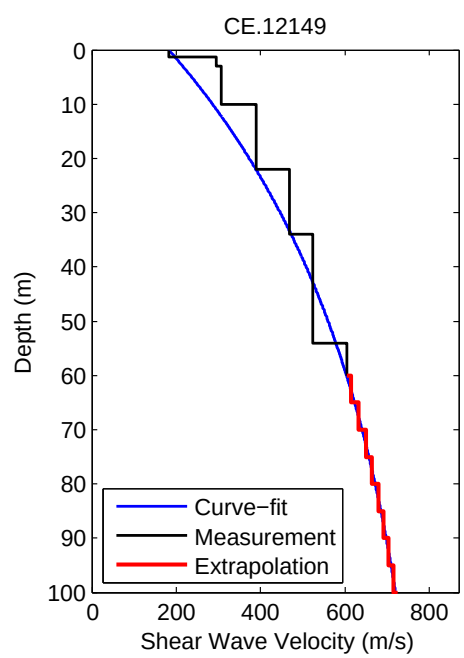

Linear Elastic Transfer Function

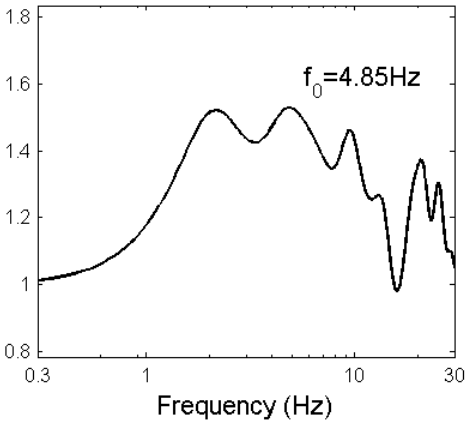

H/V Ratio – Sensor 450

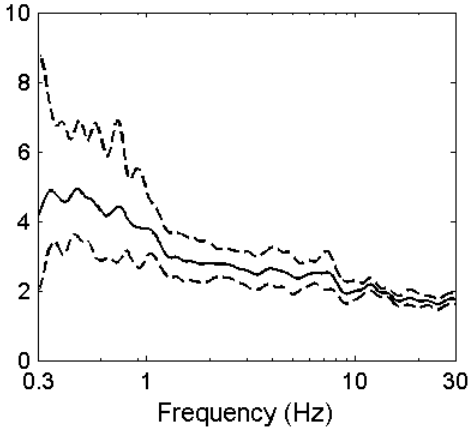

H/V Ratio – Sensor 507

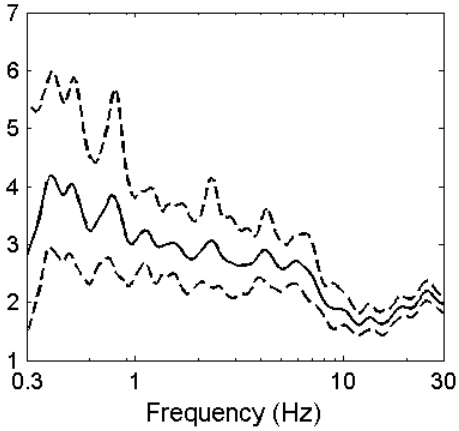

H/V Ratio – Sensor 453

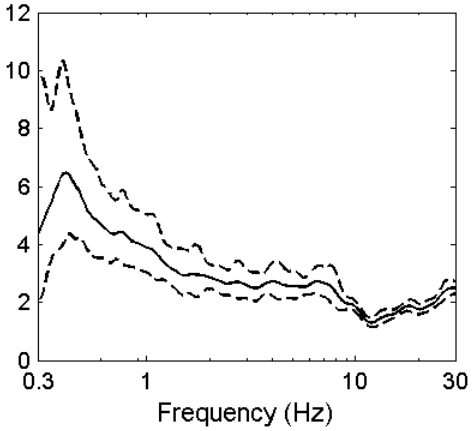

Equivalent Linear Transfer Function

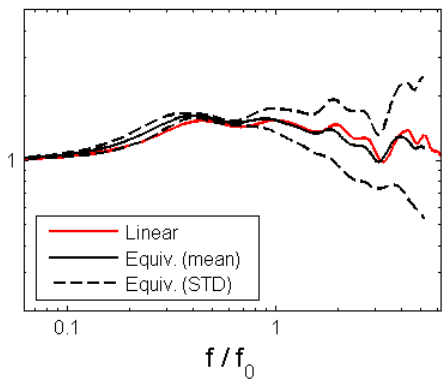

Equiv. Lin. TF (color coded by PGA_{RO})

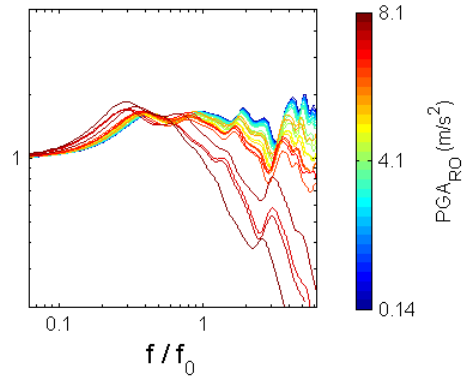

Non-linear Transfer Function

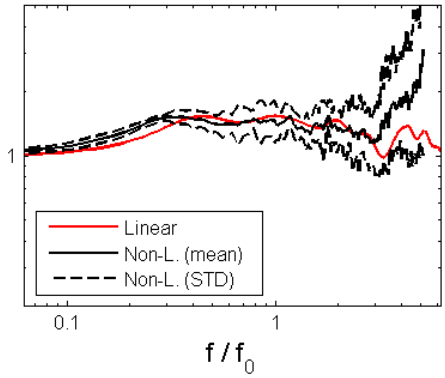

Non-linear TF (color coded by PGA_{RO})

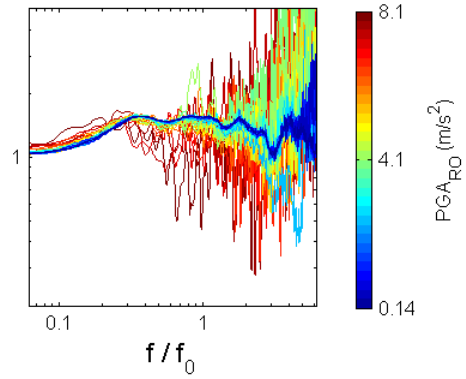

Equiv. Lin. TF (color coded by f_c)

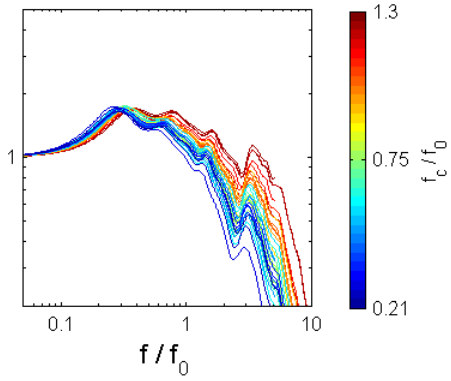

Non-linear TF (color coded by f_c)

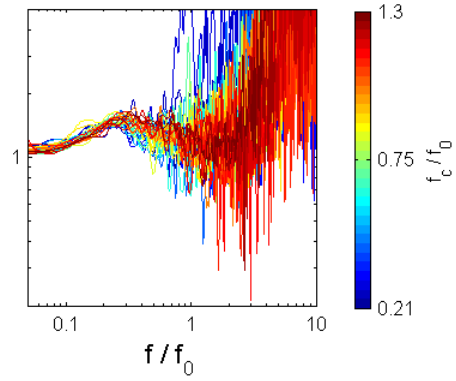

4.2.2 CE.13100

Depth (m)	Thickness (m)	V_s (m/s)	Damping ratio	Density (kg/m^3)
0	1	120	0.05	1600
1	1.5	224	0.05	1800
2.5	2.5	288	0.02	1800
5	4	314	0.02	1800
9	5	328	0.02	1800
14	6	388	0.02	1800
20	8	466	0.02	1800
28	2	547	0.02	1800
30	5	551.5	0.02	1800
35	5	585.6	0.02	1800
40	5	614.6	0.02	1800
45	5	639.2	0.02	1800
50	5	660.0	0.02	1800
55	5	677.7	0.02	1800
60	5	692.7	0.02	1800
65	5	705.4	0.02	1800
70	5	716.2	0.02	1800
75	5	725.4	0.02	1800
80	5	733.1	0.02	1800
85	5	739.7	0.02	1800
90	5	745.3	0.02	1800
95	5	750.0	0.01	1800
100	–	754.1	0.01	1800

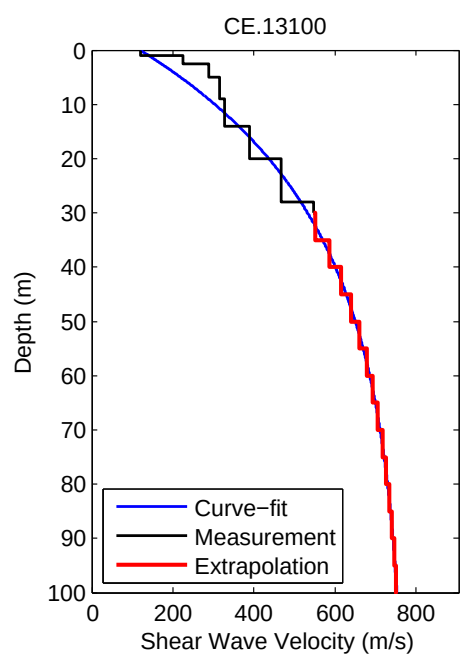

Linear Elastic Transfer Function

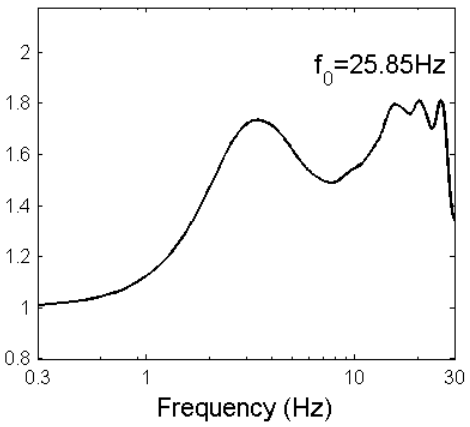

H/V Ratio – Sensor 450

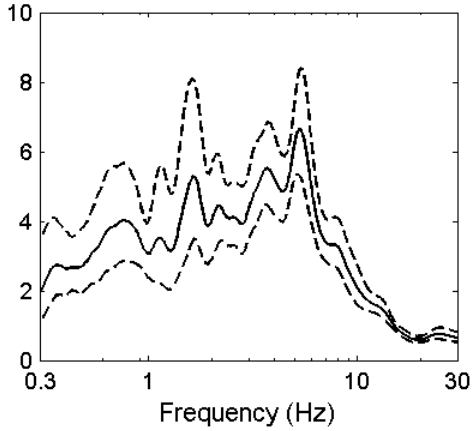

H/V Ratio – Sensor 507

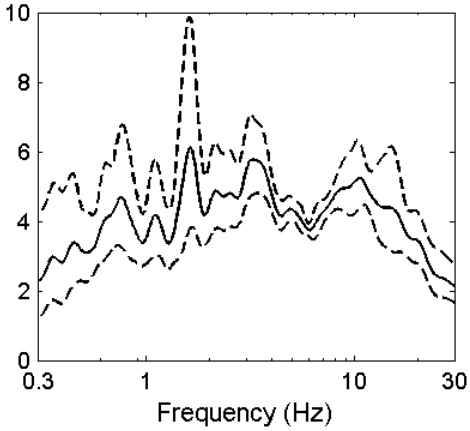

H/V Ratio – Sensor 453

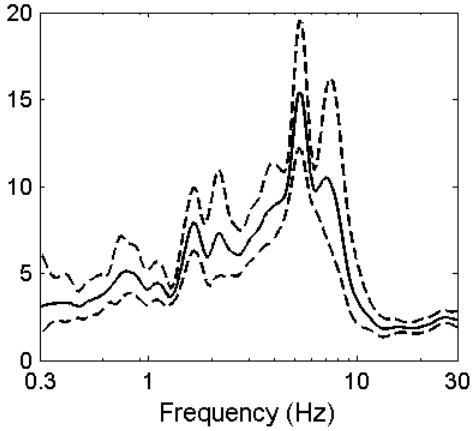

Equivalent Linear Transfer Function

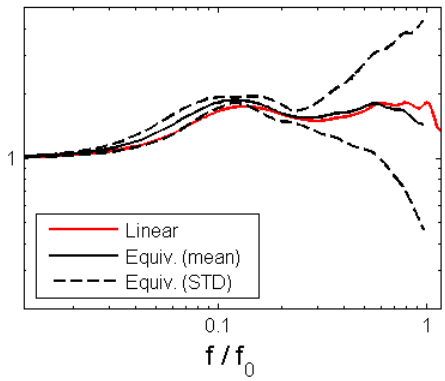

Equiv. Lin. TF (color coded by PGA_{RO})

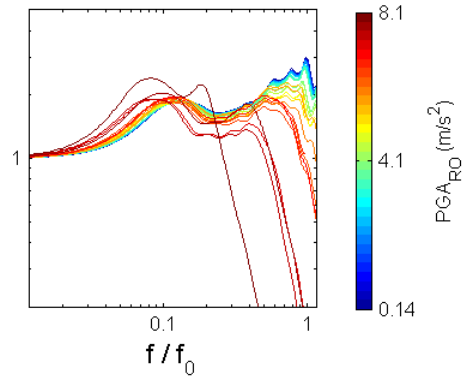

Non-linear Transfer Function

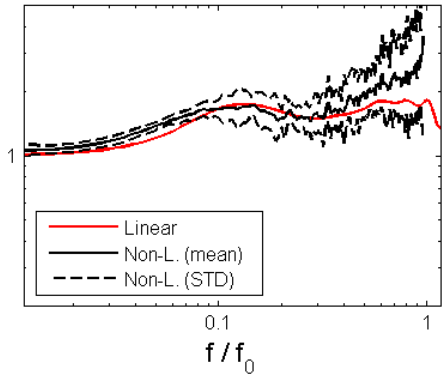

Non-linear TF (color coded by PGA_{RO})

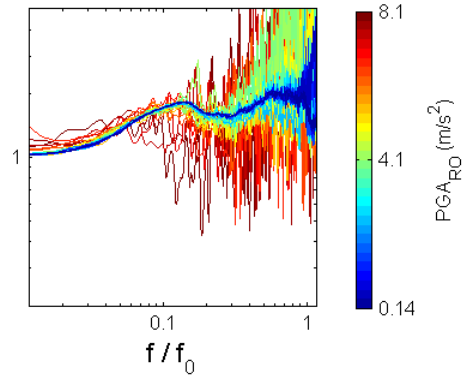

Equiv. Lin. TF (color coded by f_c)

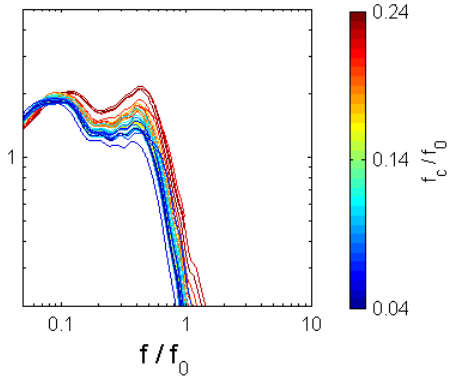

Non-linear TF (color coded by f_c)

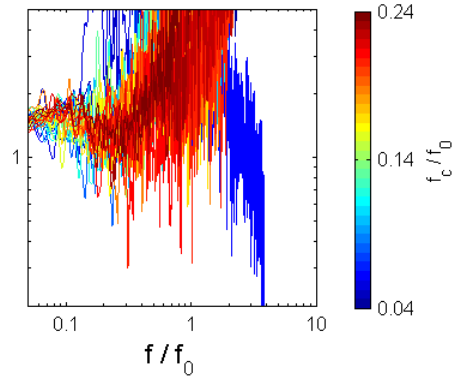

4.2.3 CE.24029

Depth (m)	Thickness (m)	V_s (m/s)	Damping ratio	Density (kg/m^3)
0	0.75	172	0.05	1600
0.75	1.75	289	0.02	1800
2.5	3.5	296	0.02	1800
6	6	359	0.02	1800
12	10	403	0.02	1800
22	15	457	0.02	1800
37	20	530	0.02	1800
57	8	615	0.02	1800
65	5	628.6	0.02	1800
70	5	645.1	0.02	1800
75	5	660.2	0.02	1800
80	5	674.0	0.02	1800
85	5	686.6	0.02	1800
90	5	698.1	0.02	1800
95	5	708.7	0.02	1800
100	–	718.3	0.02	1800

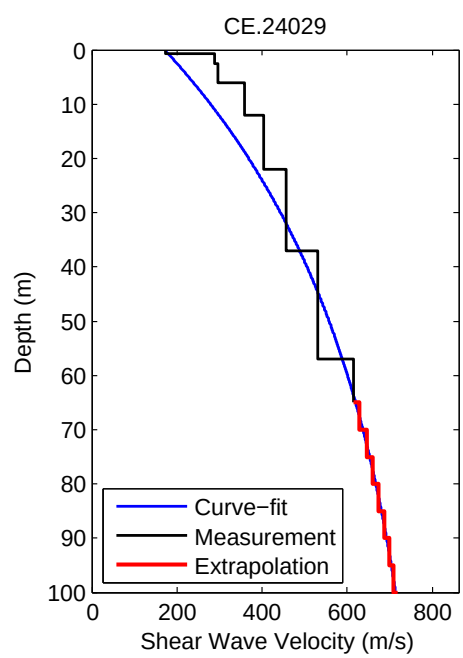

Linear Elastic Transfer Function

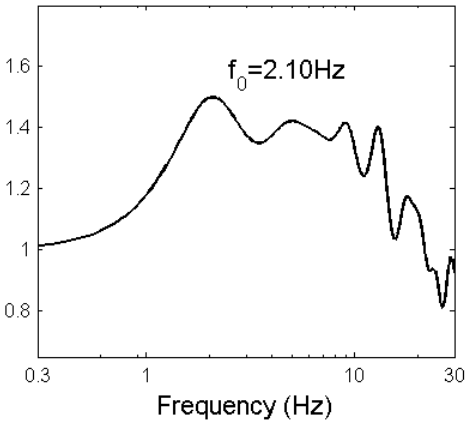

H/V Ratio – Sensor 450

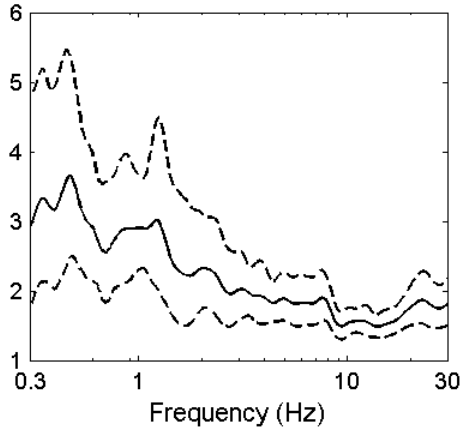

H/V Ratio – Sensor 507

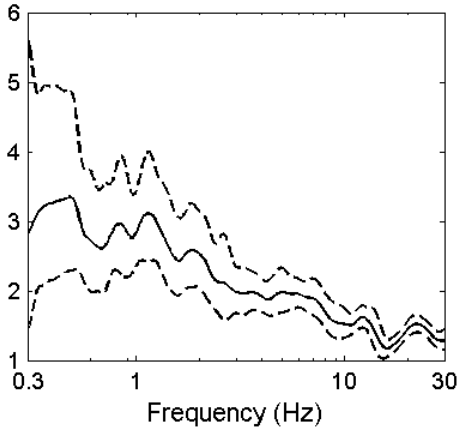

H/V Ratio – Sensor 453

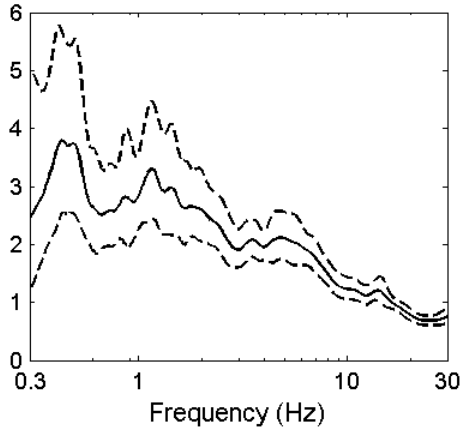

Equivalent Linear Transfer Function

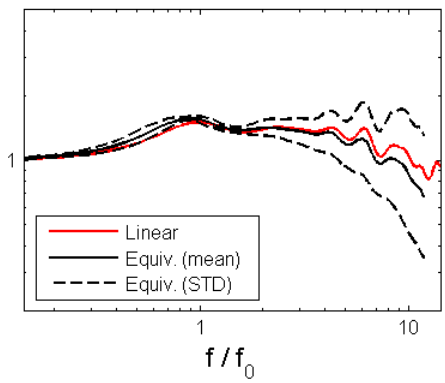

Equiv. Lin. TF (color coded by PGA_{RO})

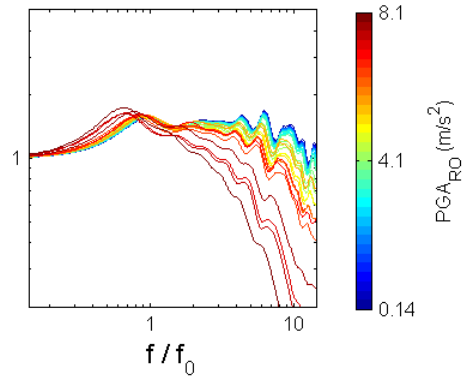

Non-linear Transfer Function

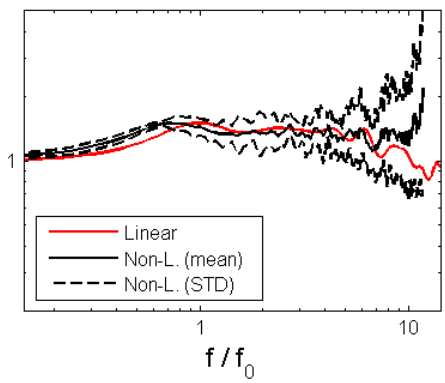

Non-linear TF (color coded by PGA_{RO})

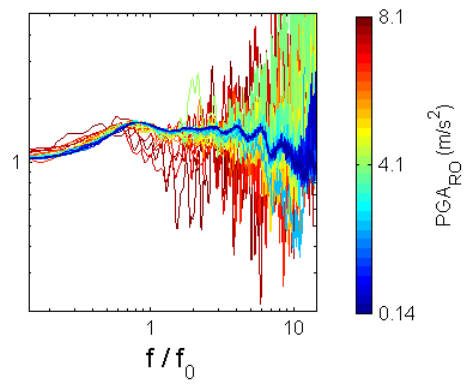

Equiv. Lin. TF (color coded by f_c)

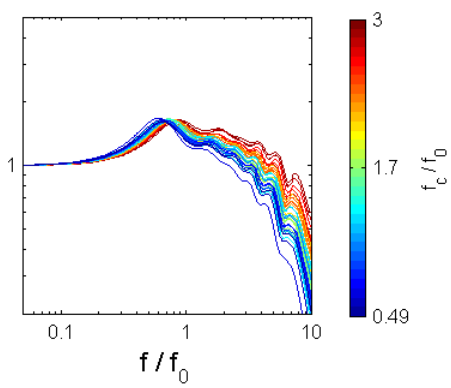

Non-linear TF (color coded by f_c)

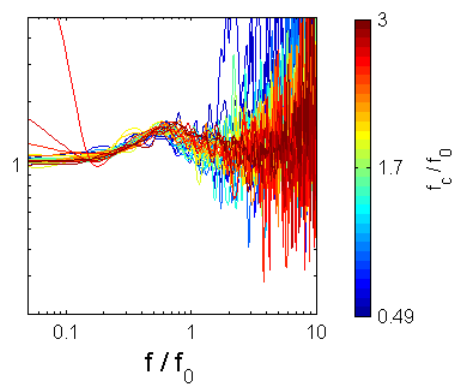

4.2.4 CI.ALP

Depth (m)	Thickness (m)	V_s (m/s)	Damping ratio	Density (kg/m^3)
0	1.5	229	0.05	1800
1.5	2.5	282	0.02	1800
4	4	337	0.02	1800
8	8	350	0.02	1800
16	8	356	0.02	1800
24	6	434	0.02	1800
30	5	459.5	0.02	1800
35	5	485.3	0.02	1800
40	5	509.0	0.02	1800
45	5	530.9	0.02	1800
50	5	551.1	0.02	1800
55	5	569.7	0.02	1800
60	5	586.8	0.02	1800
65	5	602.5	0.02	1800
70	5	617.1	0.02	1800
75	5	630.5	0.02	1800
80	5	642.8	0.02	1800
85	5	654.2	0.02	1800
90	5	664.6	0.02	1800
95	5	674.3	0.02	1800
100	–	683.2	0.02	1800

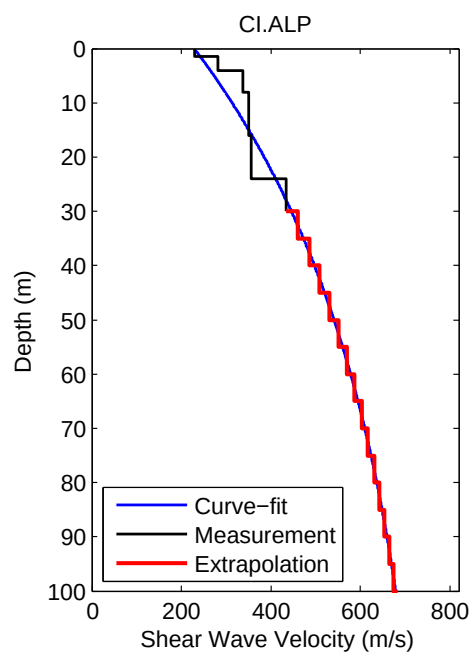

Linear Elastic Transfer Function

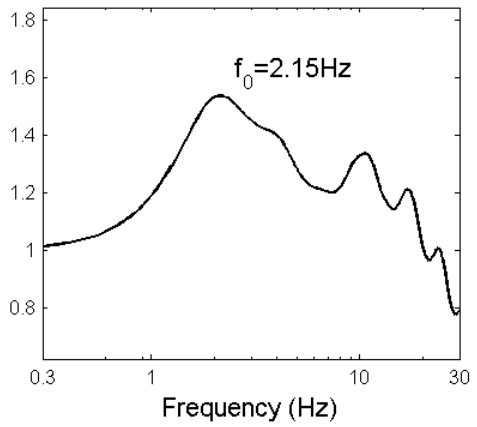

H/V Ratio – Sensor 450

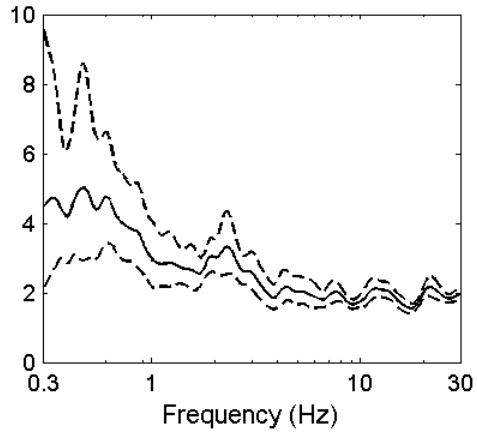

H/V Ratio – Sensor 507

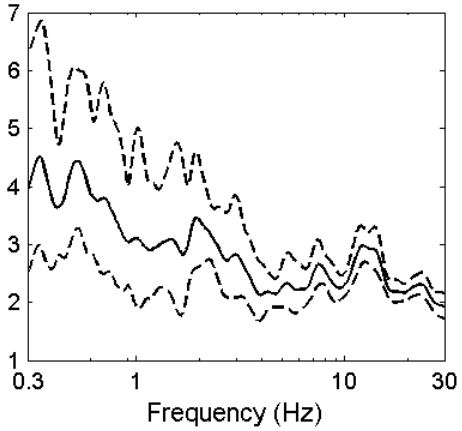

H/V Ratio – Sensor 453

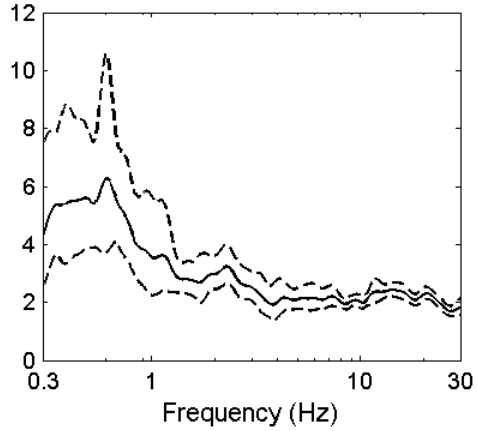

Equivalent Linear Transfer Function

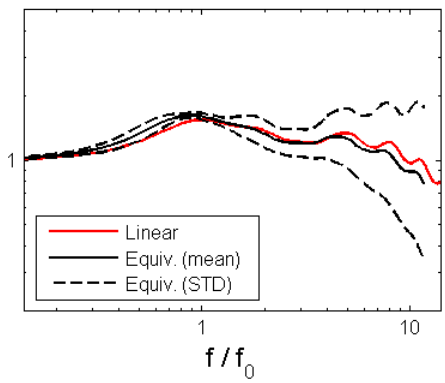

Equiv. Lin. TF (color coded by PGA_{RO})

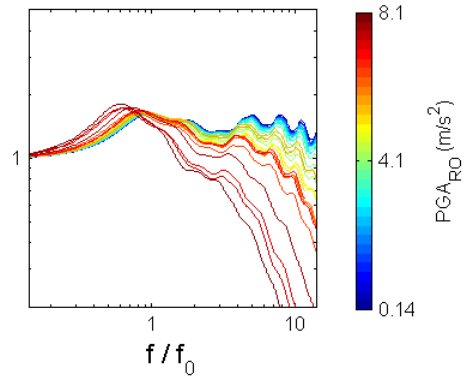

Non-linear Transfer Function

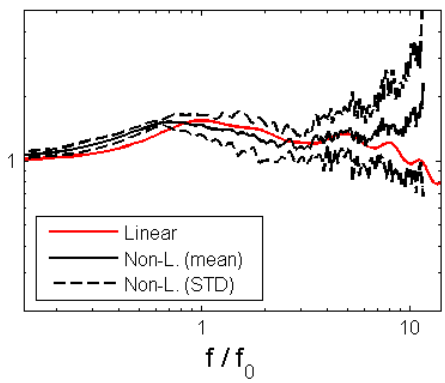

Non-linear TF (color coded by PGA_{RO})

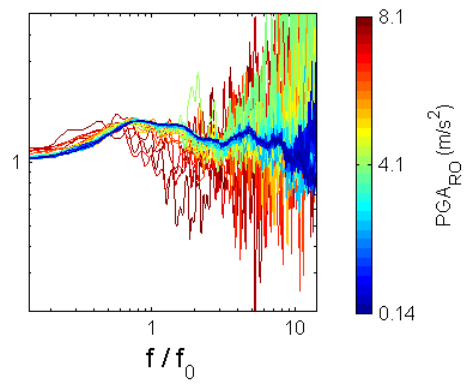

Equiv. Lin. TF (color coded by f_c)

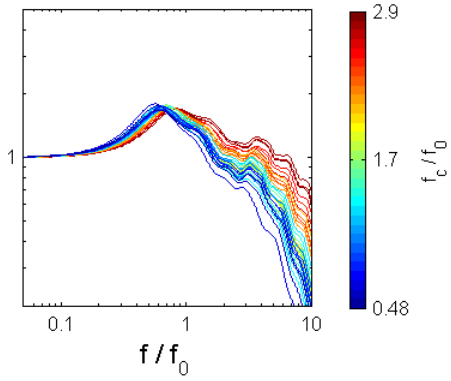

Non-linear TF (color coded by f_c)

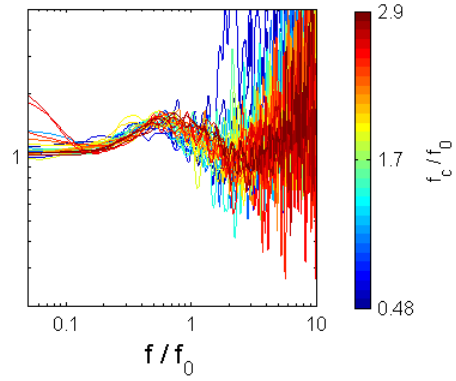

4.2.5 CI.BBR

Depth (m)	Thickness (m)	V_s (m/s)	Damping ratio	Density (kg/m^3)
0	1	142	0.05	1600
1	2	204	0.05	1800
3	3	266	0.02	1800
6	5	380	0.02	1800
11	12	394	0.02	1800
23	7	562	0.02	1800
30	5	590.0	0.02	1800
35	5	625.6	0.02	1800
40	5	655.9	0.02	1800
45	5	681.7	0.02	1800
50	5	703.5	0.02	1800
55	5	722.0	0.02	1800
60	5	737.8	0.02	1800
65	5	751.2	0.01	1800
70	5	762.5	0.01	1800
75	5	772.2	0.01	1800
80	5	780.4	0.01	1800
85	5	787.3	0.01	1800
90	5	793.2	0.01	1800
95	5	798.3	0.01	1800
100	–	802.5	0.01	2000

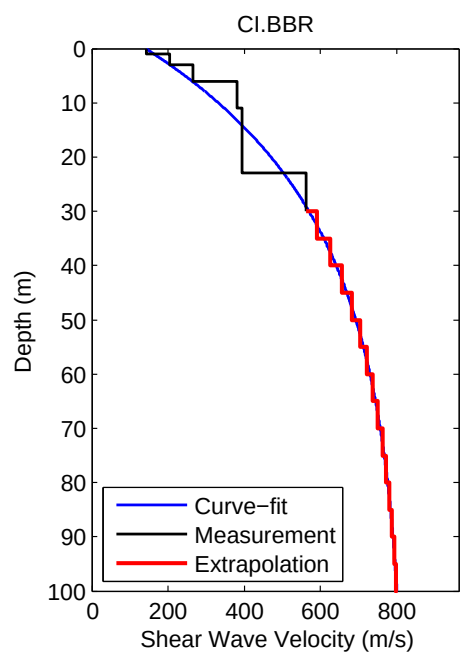

Linear Elastic Transfer Function

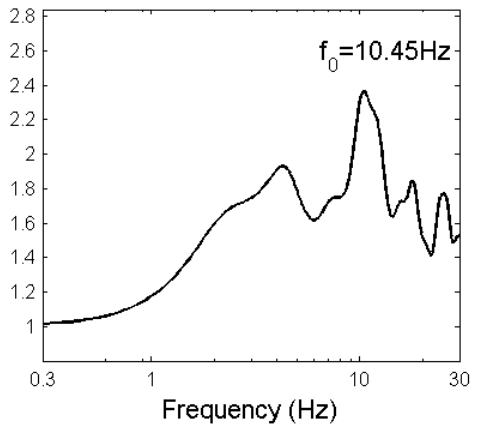

H/V Ratio – Sensor 450

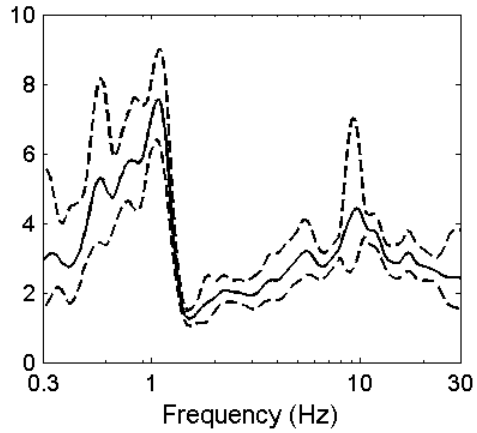

H/V Ratio – Sensor 507

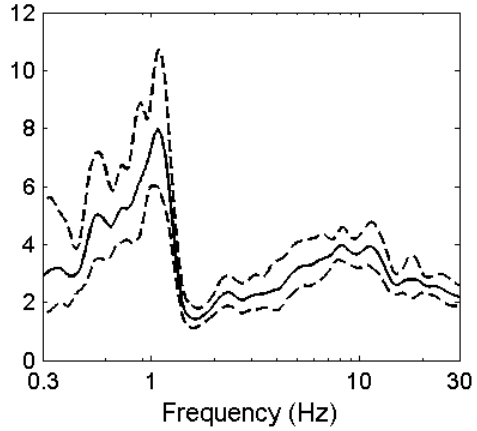

H/V Ratio – Sensor 453

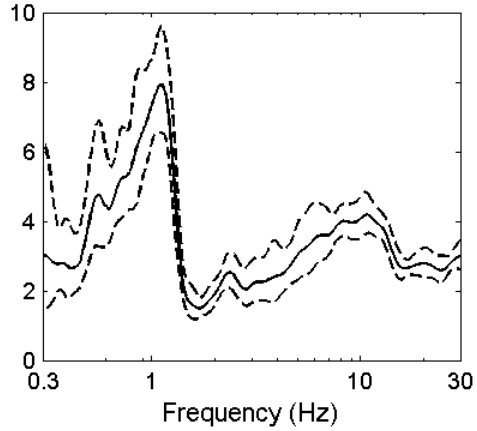

Equivalent Linear Transfer Function

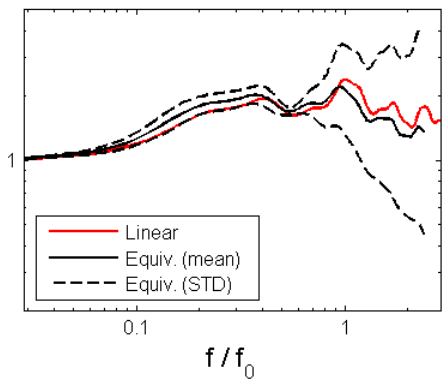

Equiv. Lin. TF (color coded by PGA_{RO})

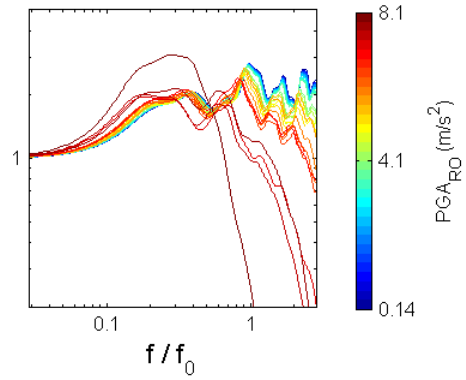

Non-linear Transfer Function

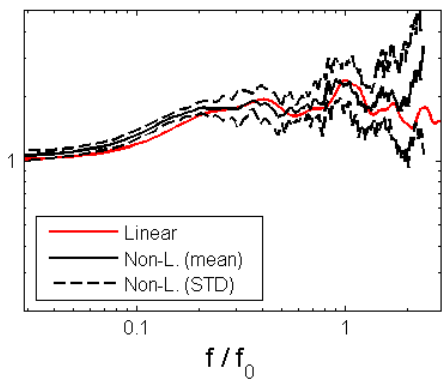

Non-linear TF (color coded by PGA_{RO})

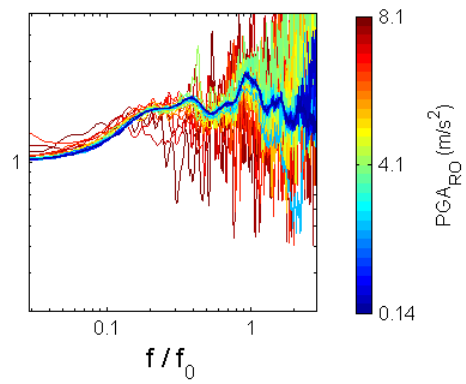

Equiv. Lin. TF (color coded by f_c)

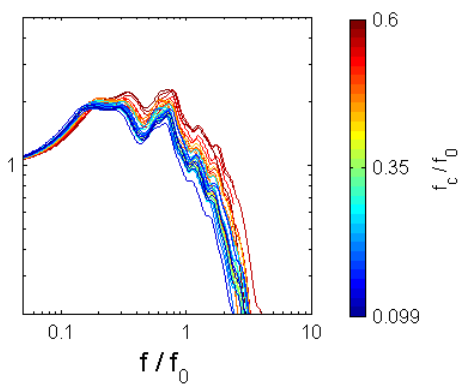

Non-linear TF (color coded by f_c)

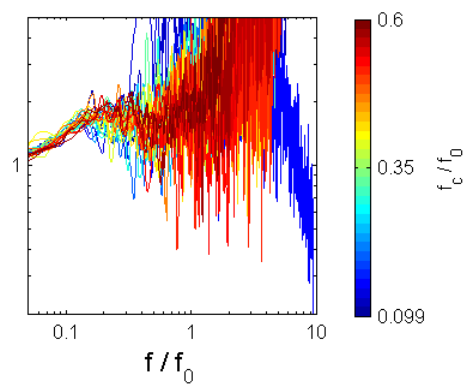

4.2.6 CI.CBC

Depth (m)	Thickness (m)	V_s (m/s)	Damping ratio	Density (kg/m^3)
0	0.75	140	0.05	1600
0.75	1.25	207	0.05	1800
2	2	246	0.05	1800
4	4	337	0.02	1800
8	6	392	0.02	1800
14	10	419	0.02	1800
24	16	475	0.02	1800
40	20	514	0.02	1800
60	5	570	0.02	1800
65	5	610.6	0.02	1800
70	5	631.8	0.02	1800
75	5	651.7	0.02	1800
80	5	670.3	0.02	1800
85	5	687.8	0.02	1800
90	5	704.1	0.02	1800
95	5	719.5	0.02	1800
100	–	733.9	0.02	1800

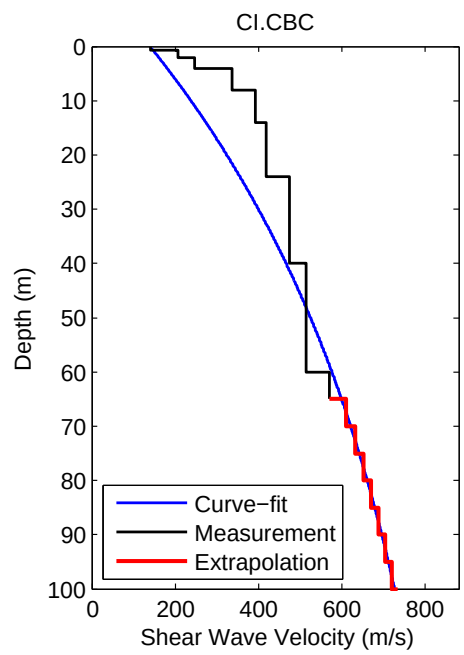

Linear Elastic Transfer Function

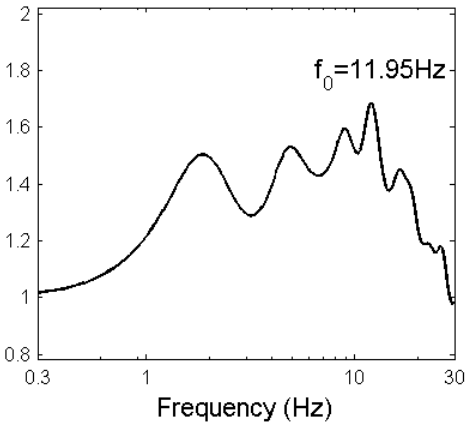

H/V Ratio – Sensor 450

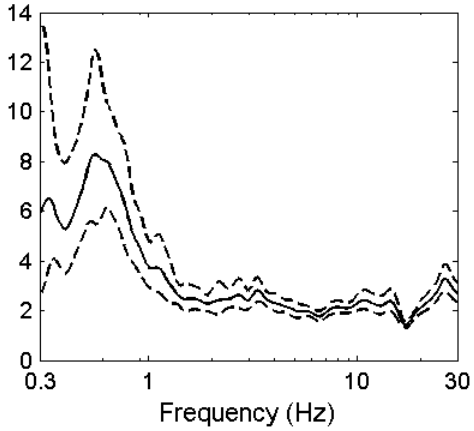

H/V Ratio – Sensor 507

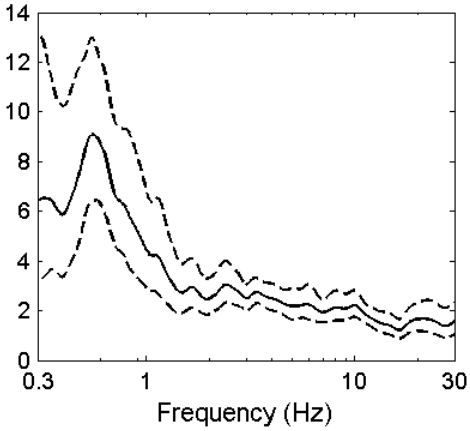

H/V Ratio – Sensor 453

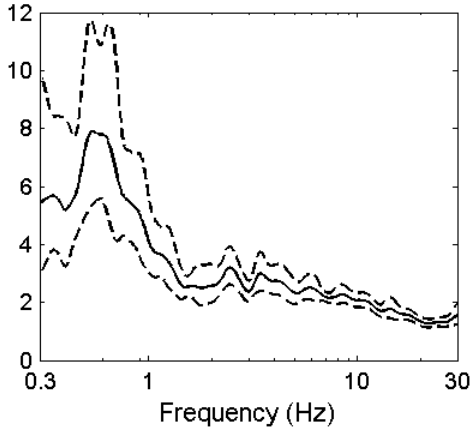

Equivalent Linear Transfer Function

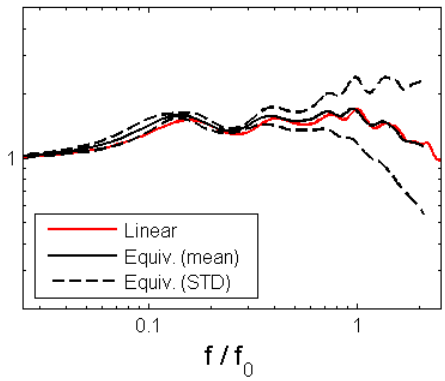

Equiv. Lin. TF (color coded by PGA_{RO})

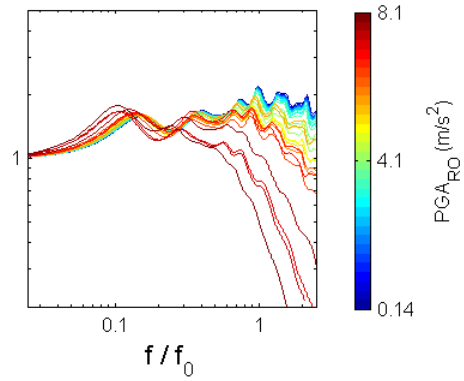

Non-linear Transfer Function

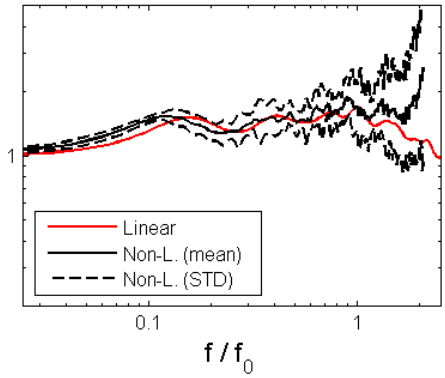

Non-linear TF (color coded by PGA_{RO})

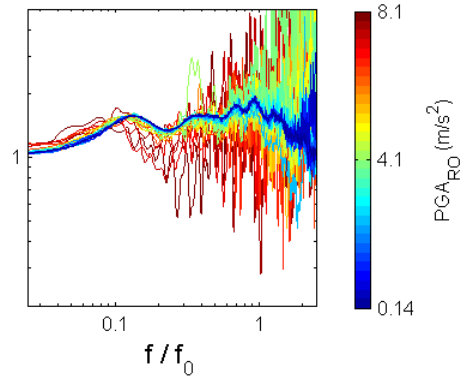

Equiv. Lin. TF (color coded by f_c)

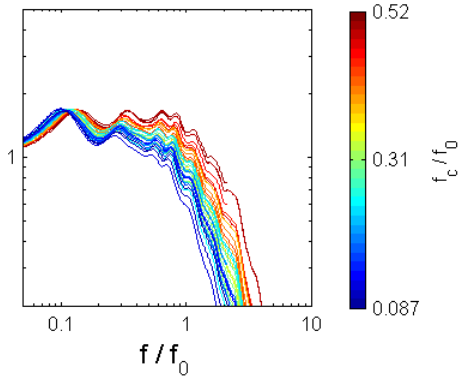

Non-linear TF (color coded by f_c)

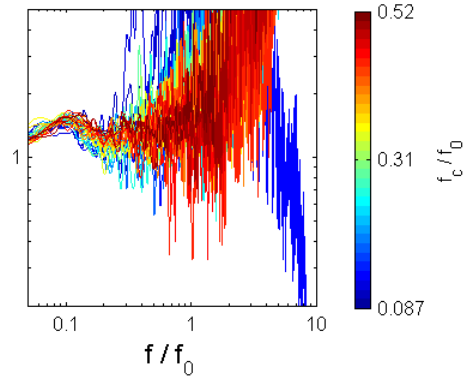

4.2.7 CI.CRP

Depth (m)	Thickness (m)	V_s (m/s)	Damping ratio	Density (kg/m^3)
0	1	139	0.05	1600
1	2	211	0.05	1800
3	3	304	0.02	1800
6	4	324	0.02	1800
10	6	352	0.02	1800
16	9	411	0.02	1800
25	15	478	0.02	1800
40	20	535	0.02	1800
60	5	599	0.02	1800
65	5	619.2	0.02	1800
70	5	637.2	0.02	1800
75	5	653.7	0.02	1800
80	5	668.9	0.02	1800
85	5	682.8	0.02	1800
90	5	695.6	0.02	1800
95	5	707.3	0.02	1800
100	–	718.0	0.02	1800

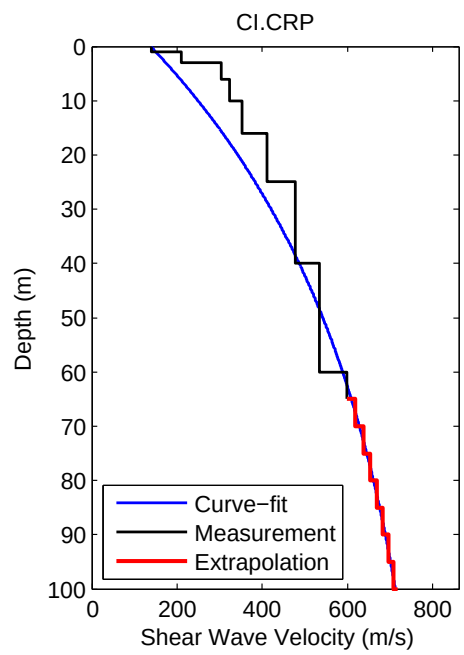

Linear Elastic Transfer Function

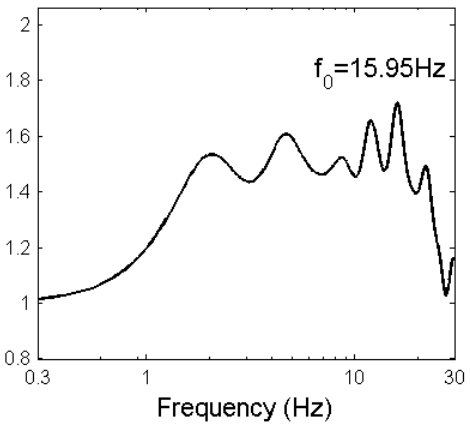

H/V Ratio – Sensor 507

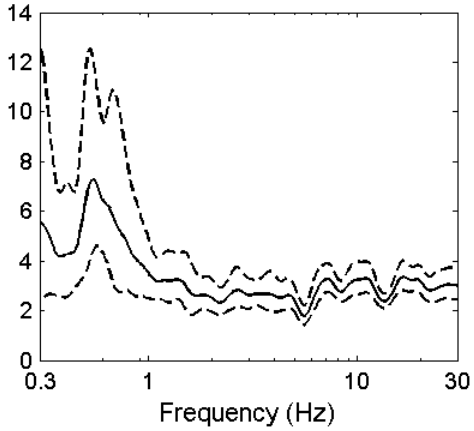

Equivalent Linear Transfer Function

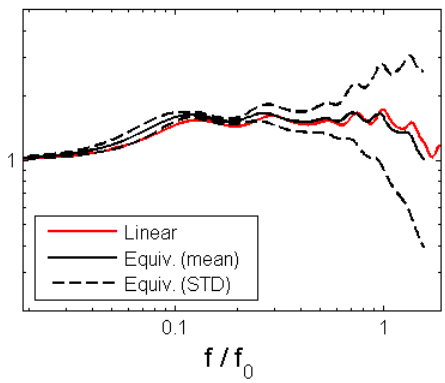

Equiv. Lin. TF (color coded by PGA_{RO})

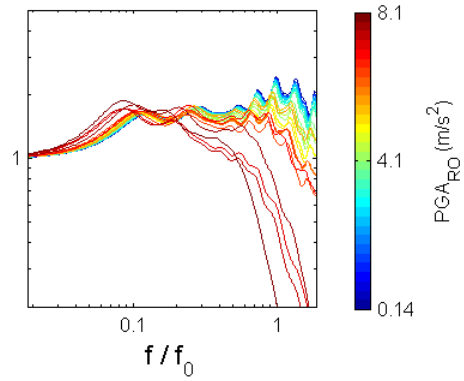

Non-linear Transfer Function

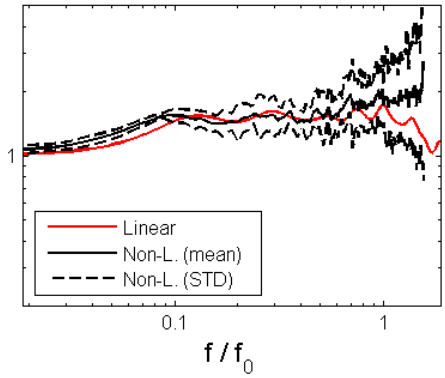

Non-linear TF (color coded by PGA_{RO})

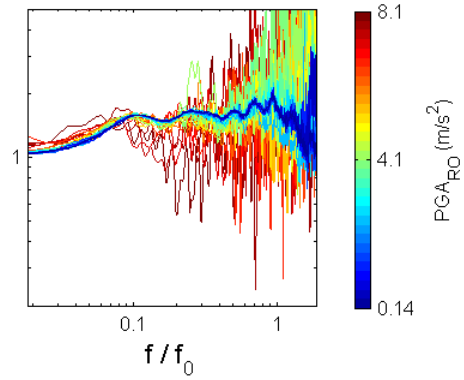

Equiv. Lin. TF (color coded by f_c)

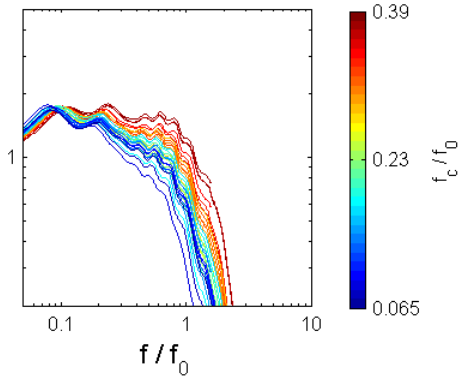

Non-linear TF (color coded by f_c)

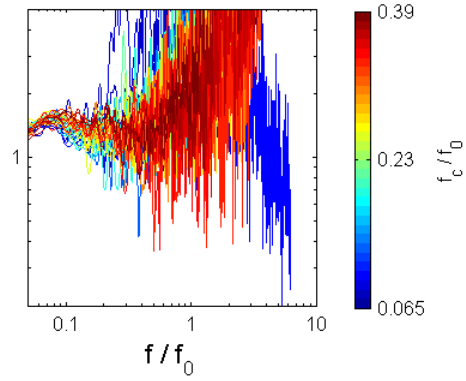

4.2.8 CI.GATRa

Depth (m)	Thickness (m)	V_s (m/s)	Damping ratio	Density (kg/m^3)
0	2	199	0.05	1600
2	3	241	0.05	1800
5	5	283	0.02	1800
10	7	298	0.02	1800
17	8	470	0.02	1800
25	9	627	0.02	1800
34	26	745	0.02	1800
60	5	746.4	0.02	1800
65	5	747.7	0.02	1800
70	5	748.6	0.02	1800
75	5	749.2	0.02	1800
80	5	749.6	0.02	1800
85	5	749.8	0.02	1800
90	5	750.0	0.01	1800
95	5	750.1	0.01	1800
100	–	750.2	0.01	1800

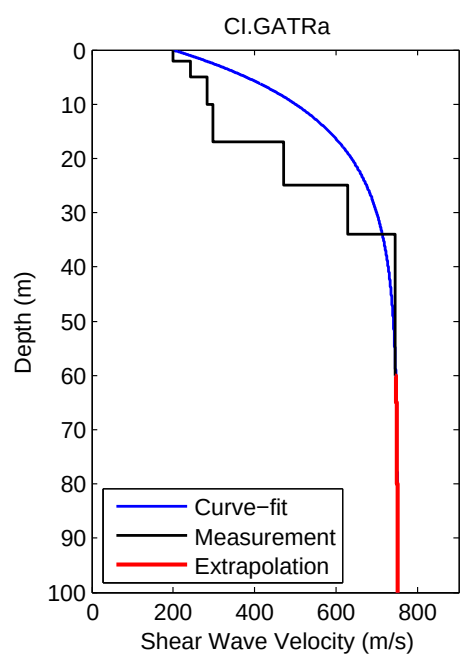

Linear Elastic Transfer Function

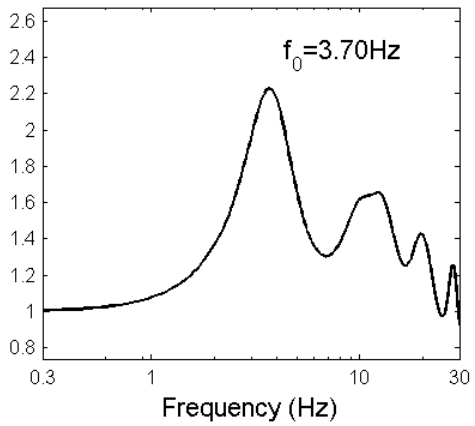

H/V Ratio – Sensor 450

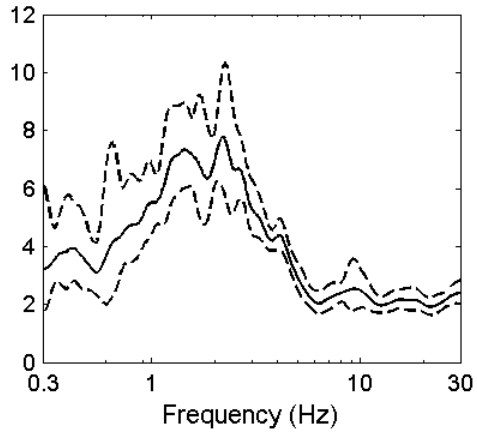

H/V Ratio – Sensor 507

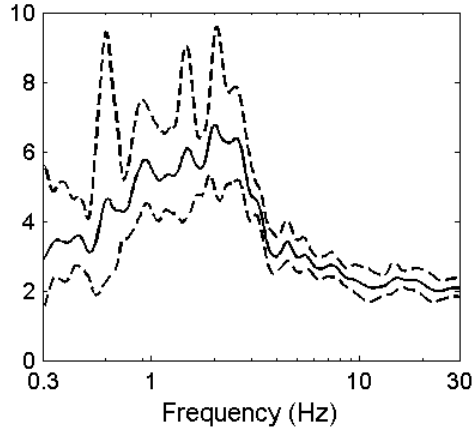

H/V Ratio – Sensor 453

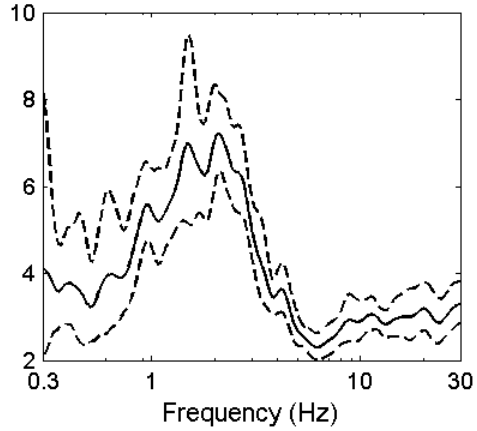

Equivalent Linear Transfer Function

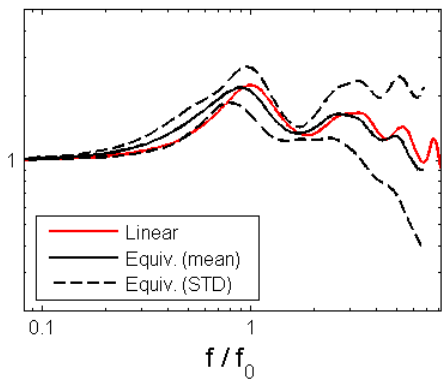

Equiv. Lin. TF (color coded by PGA_{RO})

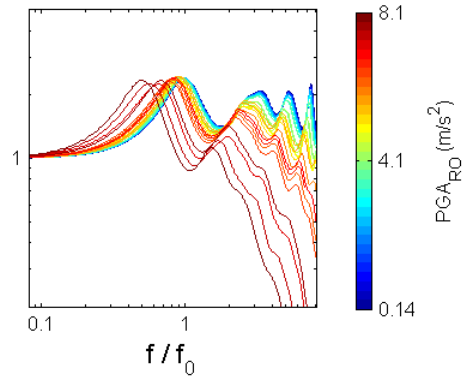

Non-linear Transfer Function

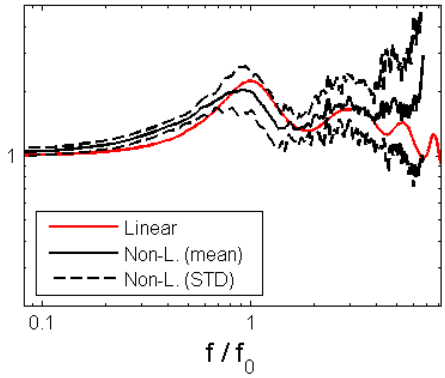

Non-linear TF (color coded by PGA_{RO})

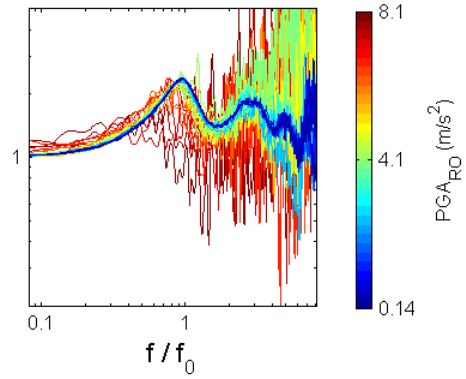

Equiv. Lin. TF (color coded by f_c)

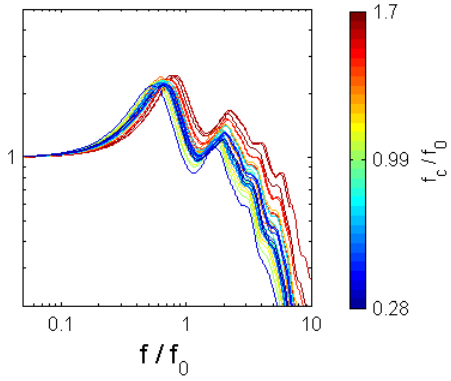

Non-linear TF (color coded by f_c)

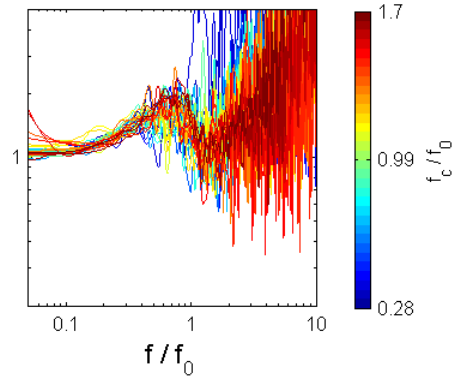

4.2.9 CI.GATRb

Depth (m)	Thickness (m)	V_s (m/s)	Damping ratio	Density (kg/m^3)
0	2	199	0.05	1600
2	3	242	0.05	1800
5	5	277	0.02	1800
10	11	322	0.02	1800
21	14	712	0.02	1800
35	5	717.4	0.02	1800
40	5	727.7	0.02	1800
45	5	734.8	0.02	1800
50	5	739.7	0.02	1800
55	5	743.0	0.02	1800
60	5	745.3	0.02	1800
65	5	746.9	0.02	1800
70	5	748.0	0.02	1800
75	5	748.7	0.02	1800
80	5	749.3	0.02	1800
85	5	749.6	0.02	1800
90	5	749.8	0.02	1800
95	5	750.0	0.01	1800
100	–	750.1	0.01	1800

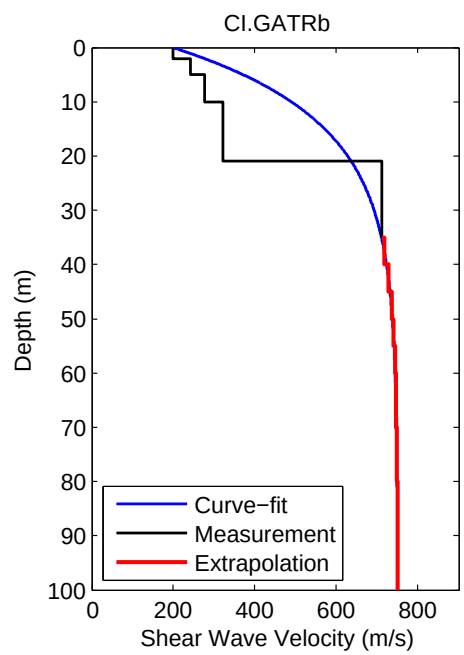

Linear Elastic Transfer Function

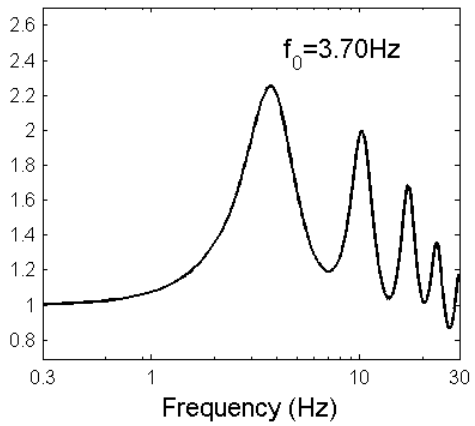

H/V Ratio – Sensor 450

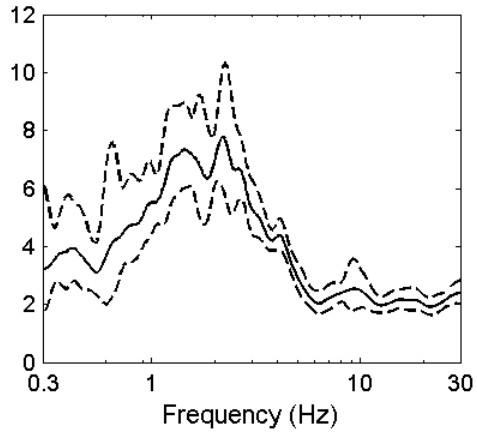

H/V Ratio – Sensor 507

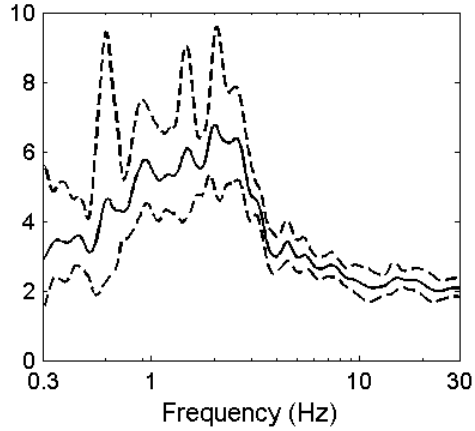

H/V Ratio – Sensor 453

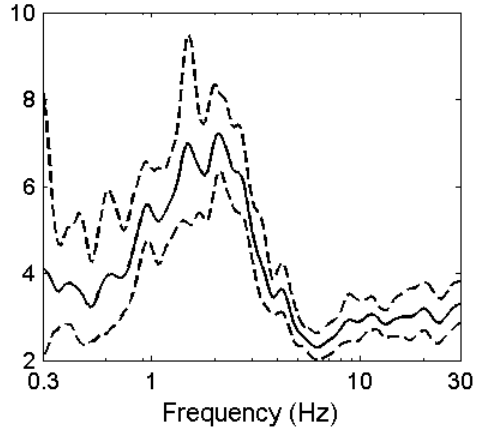

Equivalent Linear Transfer Function

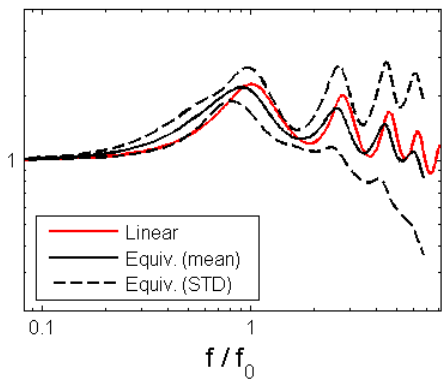

Equiv. Lin. TF (color coded by PGA_{RO})

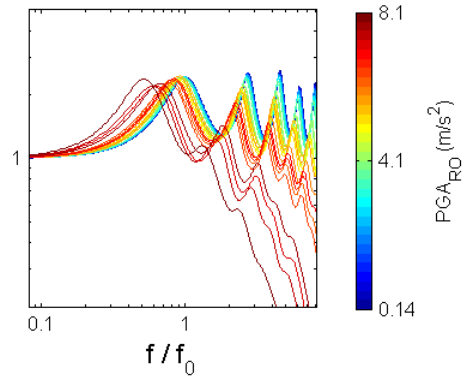

Non-linear Transfer Function

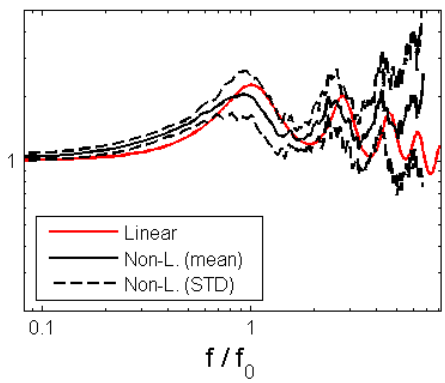

Non-linear TF (color coded by PGA_{RO})

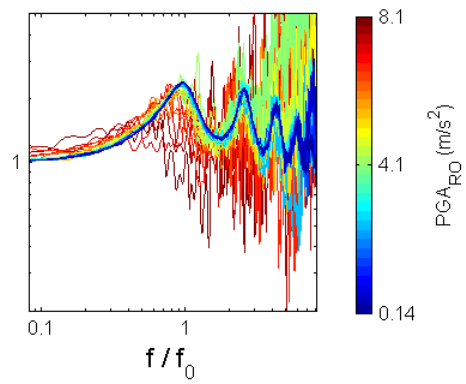

Equiv. Lin. TF (color coded by f_c)

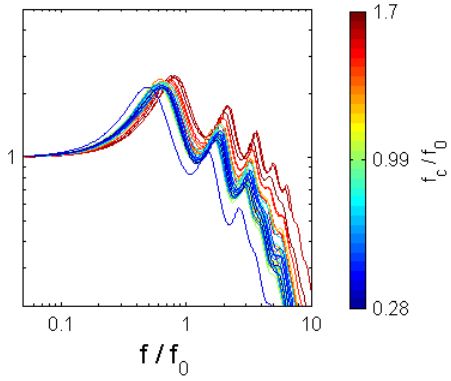

Non-linear TF (color coded by f_c)

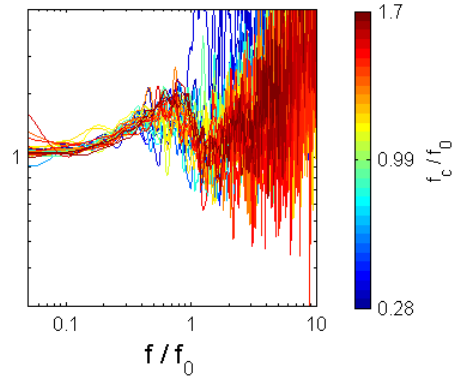

4.2.10 CI.LUGa

Depth (m)	Thickness (m)	V_s (m/s)	Damping ratio	Density (kg/m^3)
0	1	247	0.05	1800
1	2	247	0.05	1800
3	3	277	0.02	1800
6	4	305	0.02	1800
10	6	398	0.02	1800
16	9	419	0.02	1800
25	5	447	0.02	1800
30	5	481.7	0.02	1800
35	5	508.2	0.02	1800
40	5	532.7	0.02	1800
45	5	555.3	0.02	1800
50	5	576.2	0.02	1800
55	5	595.5	0.02	1800
60	5	613.3	0.02	1800
65	5	629.7	0.02	1800
70	5	644.9	0.02	1800
75	5	659.0	0.02	1800
80	5	671.9	0.02	1800
85	5	683.9	0.02	1800
90	5	695.0	0.02	1800
95	5	705.2	0.02	1800
100	–	714.6	0.02	1800

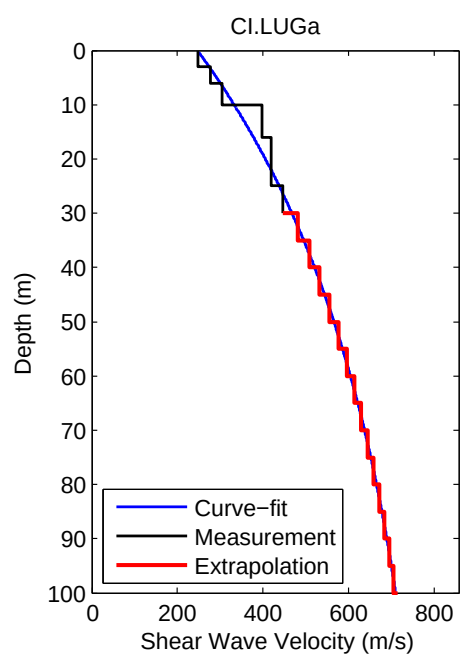

Linear Elastic Transfer Function

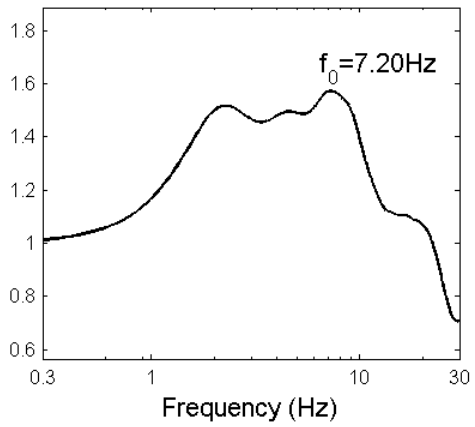

H/V Ratio – Sensor 450

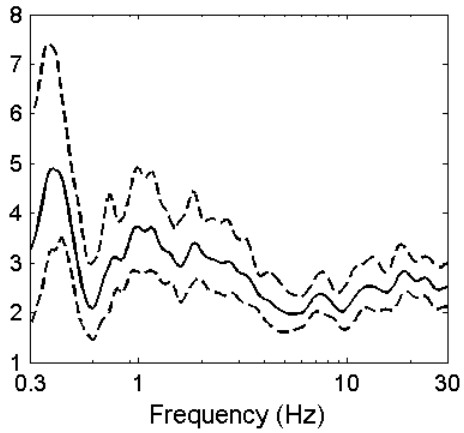

H/V Ratio – Sensor 507

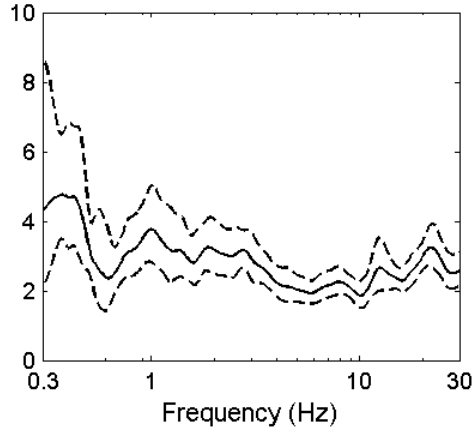

H/V Ratio – Sensor 453

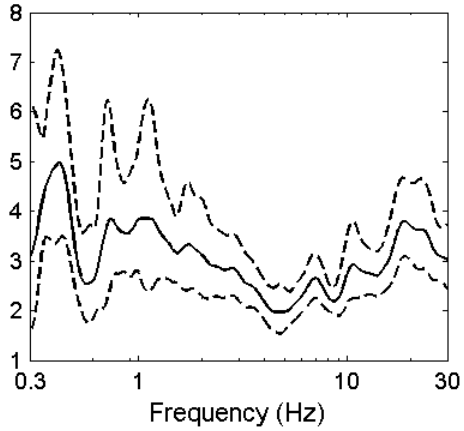

Equivalent Linear Transfer Function

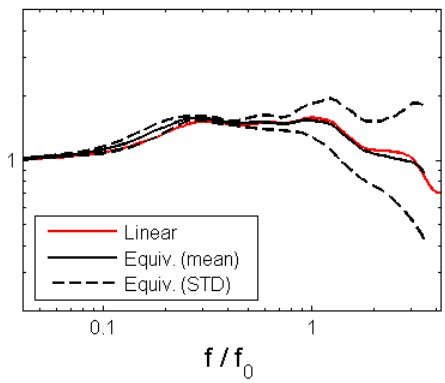

Equiv. Lin. TF (color coded by PGA_{RO})

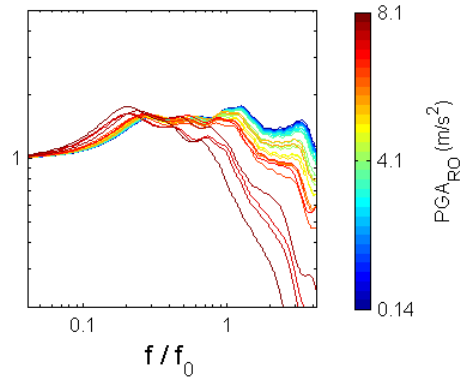

Non-linear Transfer Function

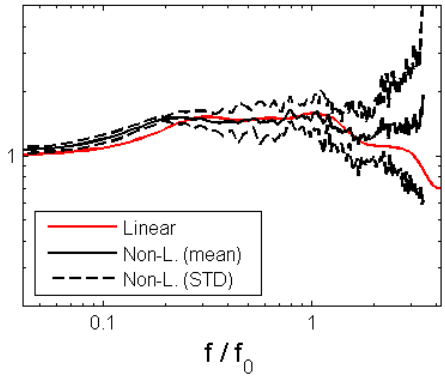

Non-linear TF (color coded by PGA_{RO})

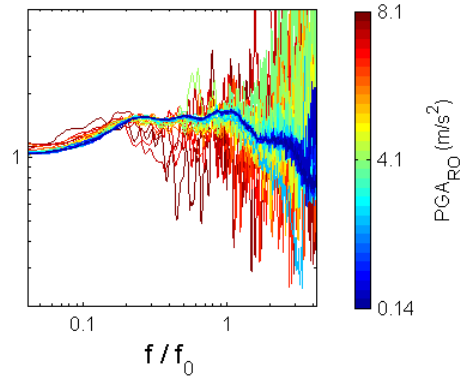

Equiv. Lin. TF (color coded by f_c)

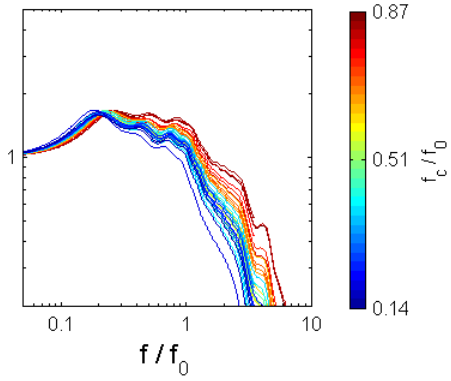

Non-linear TF (color coded by f_c)

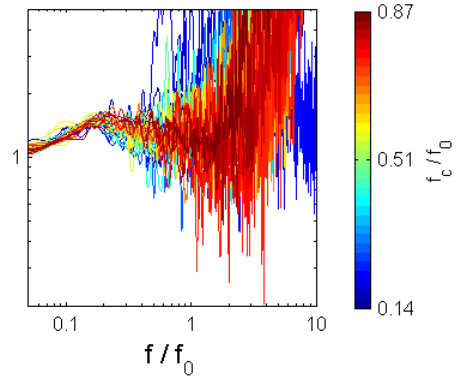

4.2.11 CI.LUGb

Depth (m)	Thickness (m)	V_s (m/s)	Damping ratio	Density (kg/m^3)
0	1	245	0.05	1800
1	1	283	0.02	1800
2	8	330	0.02	1800
10	14	388	0.02	1800
24	6	464	0.02	1800
30	5	479.8	0.02	1800
35	5	506.4	0.02	1800
40	5	530.9	0.02	1800
45	5	553.6	0.02	1800
50	5	574.5	0.02	1800
55	5	593.9	0.02	1800
60	5	611.8	0.02	1800
65	5	628.3	0.02	1800
70	5	643.5	0.02	1800
75	5	657.6	0.02	1800
80	5	670.7	0.02	1800
85	5	682.7	0.02	1800
90	5	693.8	0.02	1800
95	5	704.1	0.02	1800
100	–	713.6	0.02	1800

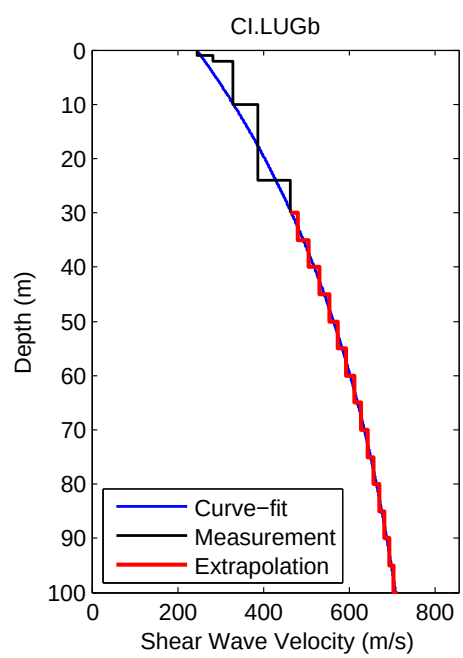

Linear Elastic Transfer Function

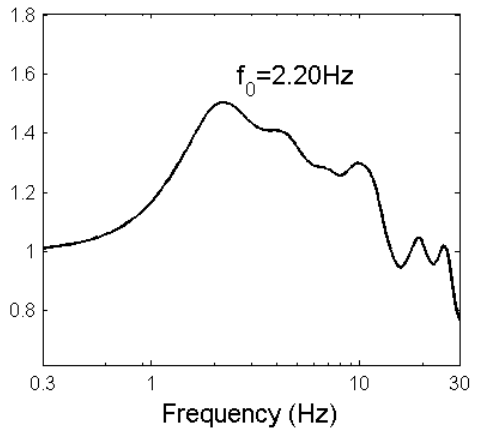

H/V Ratio – Sensor 450

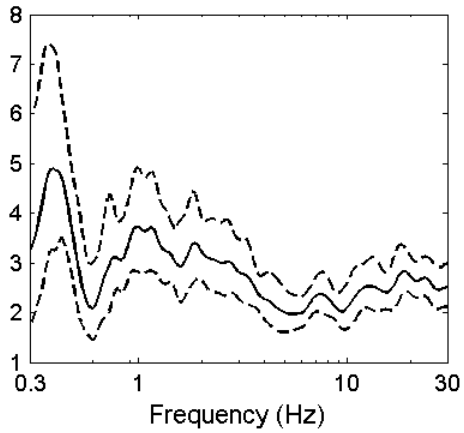

H/V Ratio – Sensor 507

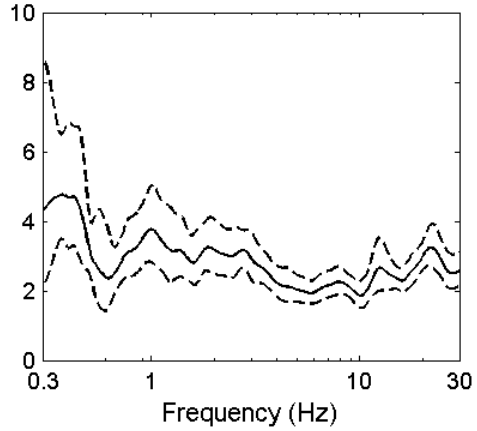

H/V Ratio – Sensor 453

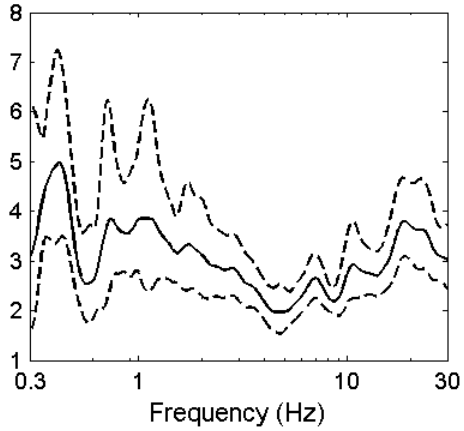

Equivalent Linear Transfer Function

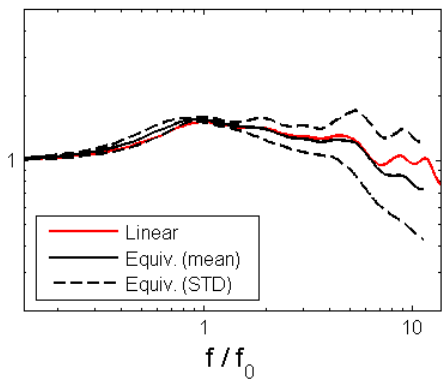

Equiv. Lin. TF (color coded by PGA_{RO})

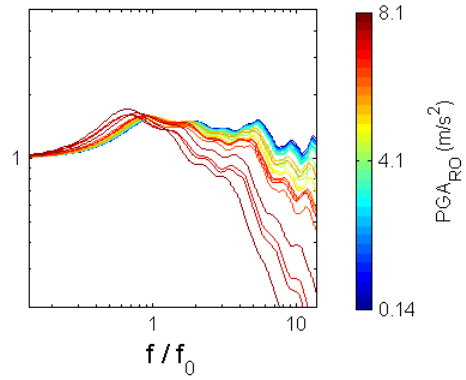

Non-linear Transfer Function

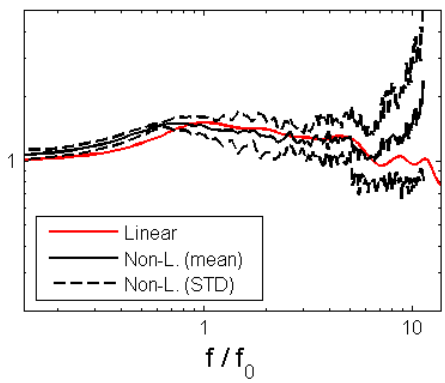

Non-linear TF (color coded by PGA_{RO})

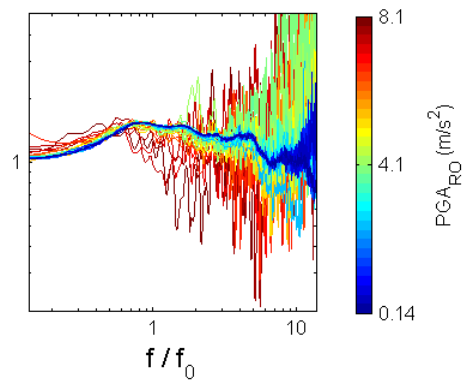

Equiv. Lin. TF (color coded by f_c)

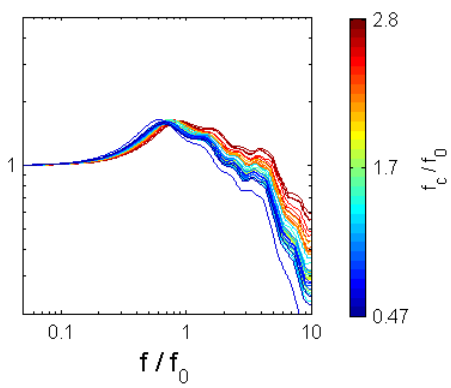

Non-linear TF (color coded by f_c)

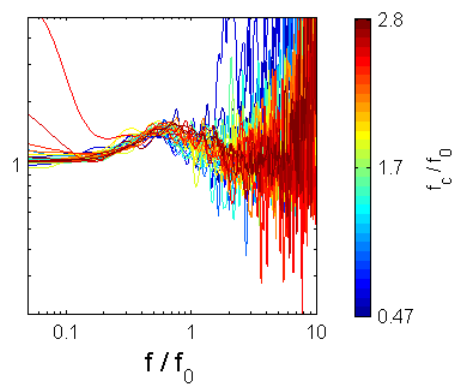

4.2.12 CI.MIKa

Depth (m)	Thickness (m)	V_s (m/s)	Damping ratio	Density (kg/m^3)
0	1	158	0.05	1600
1	2	232	0.05	1800
3	3	279	0.02	1800
6	4	304	0.02	1800
10	6	360	0.02	1800
16	10	373	0.02	1800
26	14	416	0.02	1800
40	18	476	0.02	1800
58	2	537	0.02	1800
60	5	543.8	0.02	1800
65	5	562.4	0.02	1800
70	5	579.8	0.02	1800
75	5	595.9	0.02	1800
80	5	611.0	0.02	1800
85	5	625.0	0.02	1800
90	5	638.1	0.02	1800
95	5	650.3	0.02	1800
100	–	661.7	0.02	1800

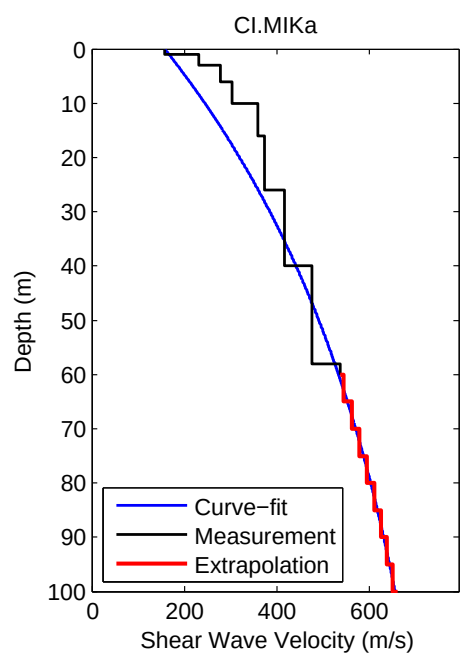

Linear Elastic Transfer Function

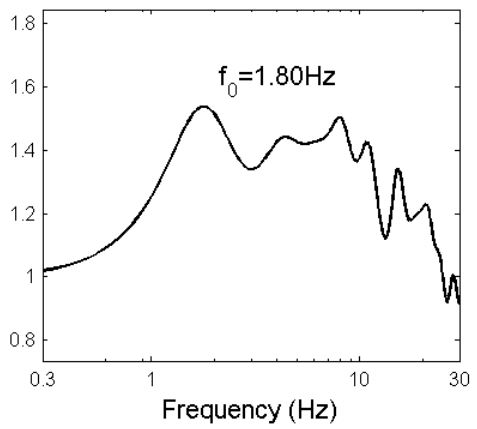

H/V Ratio – Sensor 450

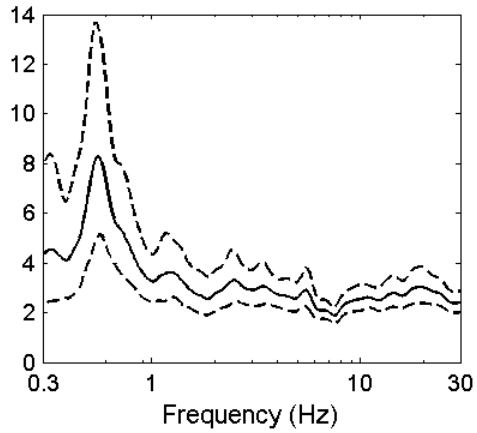

Equivalent Linear Transfer Function

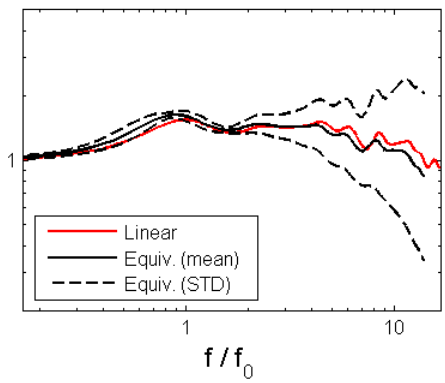

Equiv. Lin. TF (color coded by PGA_{RO})

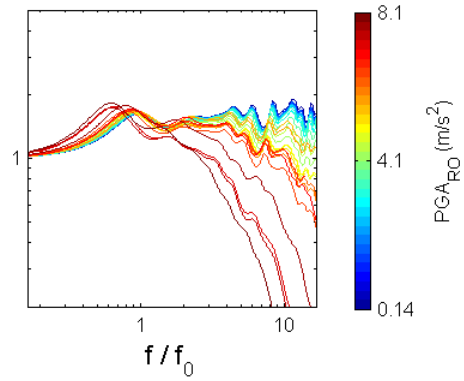

Non-linear Transfer Function

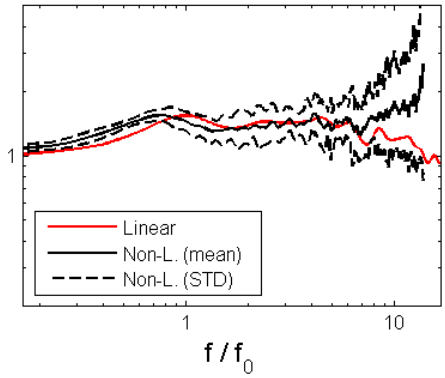

Non-linear TF (color coded by PGA_{RO})

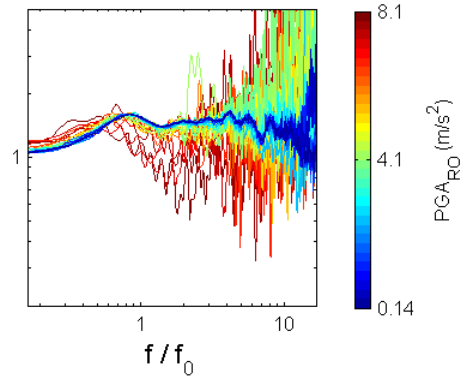

Equiv. Lin. TF (color coded by f_c)

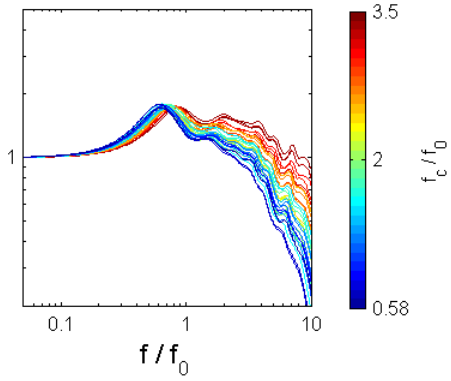

Non-linear TF (color coded by f_c)

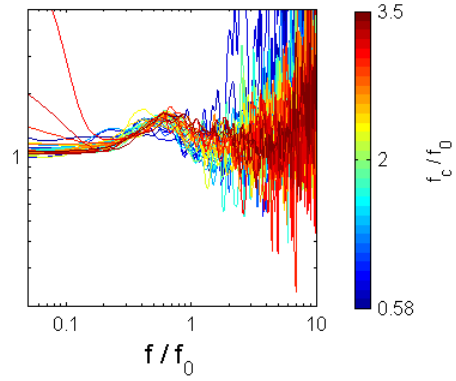

4.2.13 CI.MIKb

Depth (m)	Thickness (m)	V_s (m/s)	Damping ratio	Density (kg/m^3)
0	1	139	0.05	1600
1	2	211	0.05	1800
3	3	304	0.02	1800
6	4	324	0.02	1800
10	6	352	0.02	1800
16	9	411	0.02	1800
25	15	478	0.02	1800
40	20	535	0.02	1800
60	5	599	0.02	1800
65	5	617.2	0.02	1800
70	5	634.5	0.02	1800
75	5	650.3	0.02	1800
80	5	664.8	0.02	1800
85	5	678.0	0.02	1800
90	5	690.1	0.02	1800
95	5	701.1	0.02	1800
100	–	711.2	0.02	1800

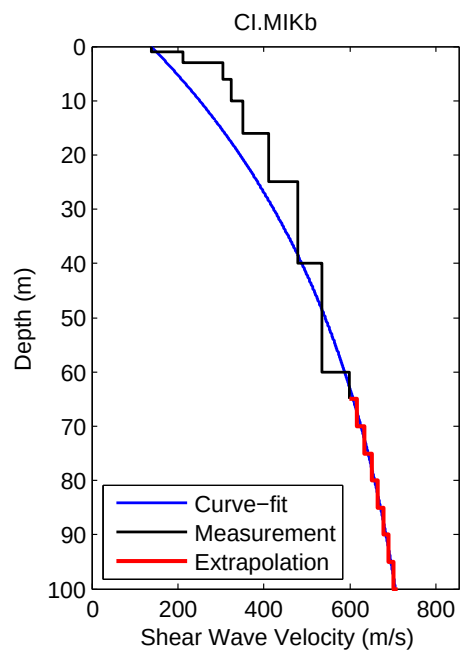

Linear Elastic Transfer Function

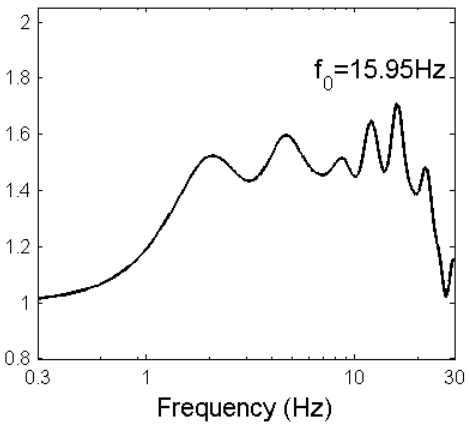

H/V Ratio – Sensor 450

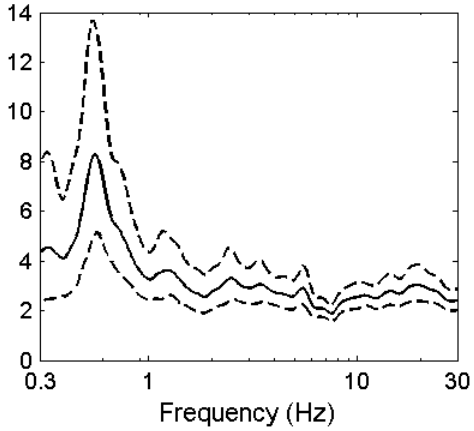

Equivalent Linear Transfer Function

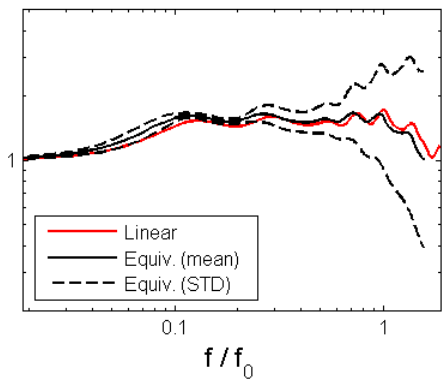

Equiv. Lin. TF (color coded by PGA_{RO})

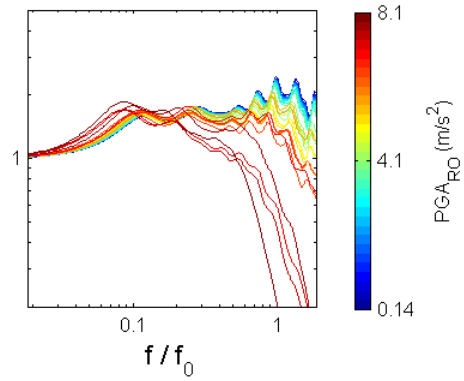

Non-linear Transfer Function

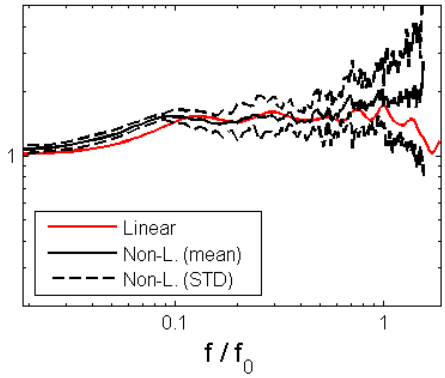

Non-linear TF (color coded by PGA_{RO})

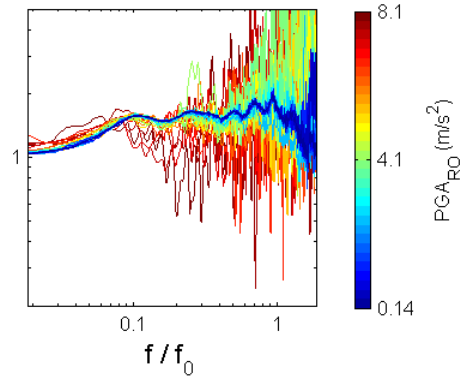

Equiv. Lin. TF (color coded by f_c)

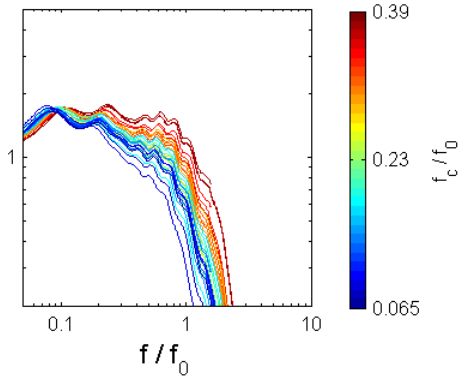

Non-linear TF (color coded by f_c)

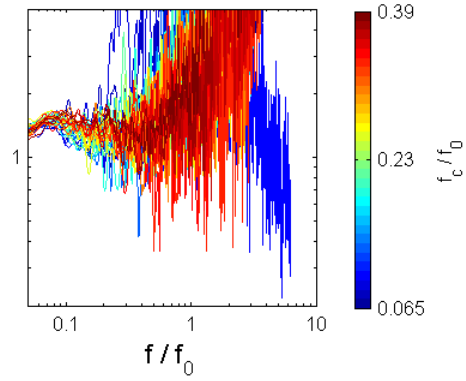

4.2.14 CI.NSS2a

Depth (m)	Thickness (m)	V_s (m/s)	Damping ratio	Density (kg/m^3)
0	0.5	177	0.05	1600
0.5	1	200	0.05	1800
1.5	1.5	240	0.05	1800
3	2.5	273	0.02	1800
5.5	4	331	0.02	1800
9.5	6	358	0.02	1800
15.5	9	409	0.02	1800
24.5	5.5	490	0.02	1800
30	5	525.1	0.02	1800
35	5	558.4	0.02	1800
40	5	588.0	0.02	1800
45	5	614.2	0.02	1800
50	5	637.4	0.02	1800
55	5	658.1	0.02	1800
60	5	676.4	0.02	1800
65	5	692.6	0.02	1800
70	5	707.0	0.02	1800
75	5	719.8	0.02	1800
80	5	731.1	0.02	1800
85	5	741.1	0.02	1800
90	5	750.0	0.01	1800
95	5	757.9	0.01	1800
100	–	764.9	0.01	1800

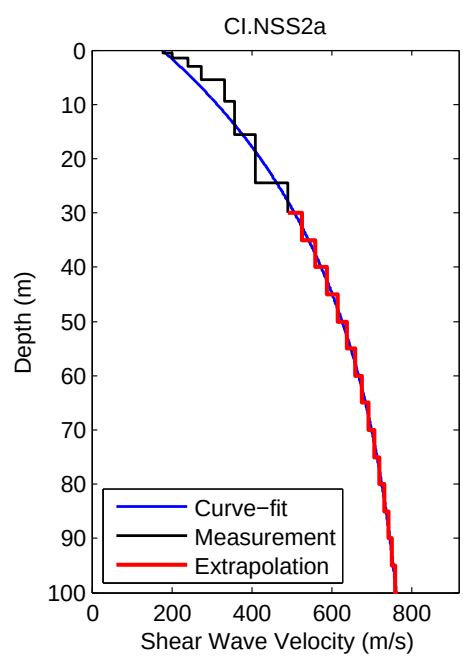

Linear Elastic Transfer Function

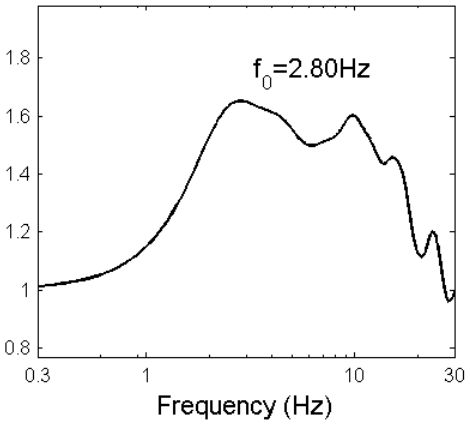

H/V Ratio – Sensor 450

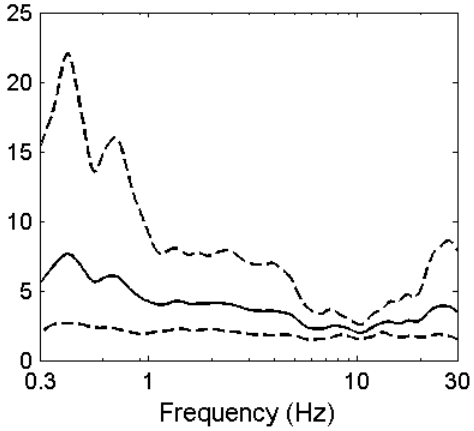

H/V Ratio – Sensor 507

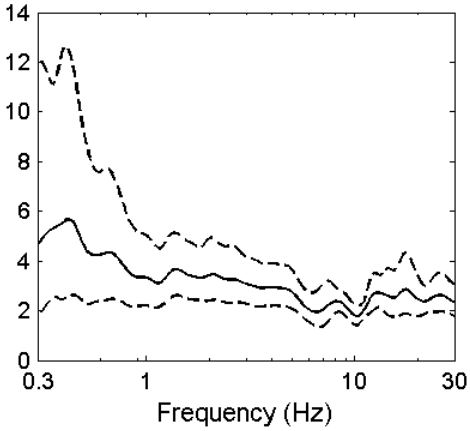

H/V Ratio – Sensor 453

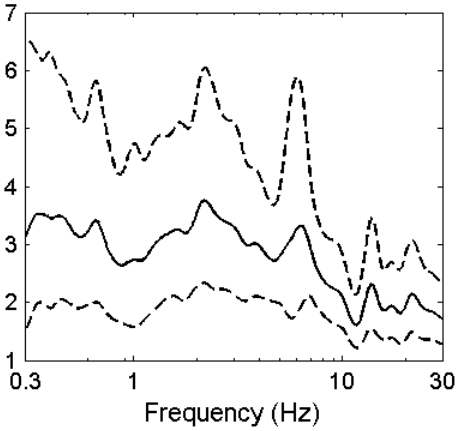

Equivalent Linear Transfer Function

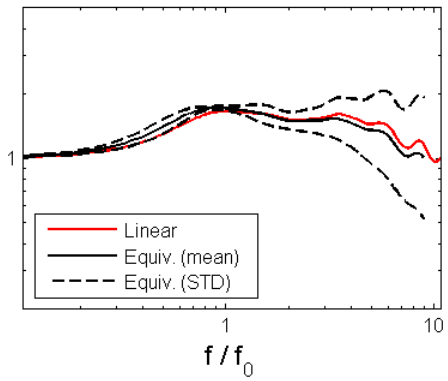

Equiv. Lin. TF (color coded by PGA_{RO})

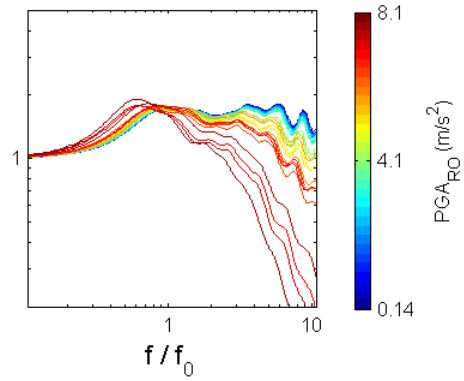

Non-linear Transfer Function

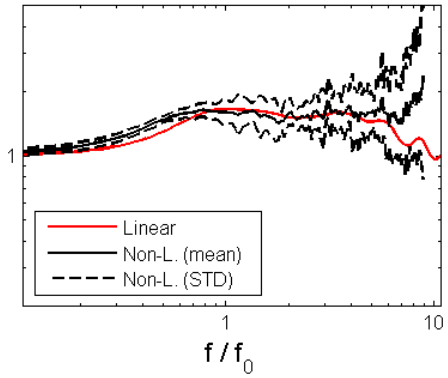

Non-linear TF (color coded by PGA_{RO})

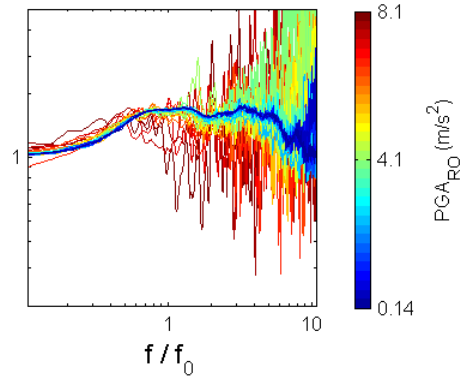

Equiv. Lin. TF (color coded by f_c)

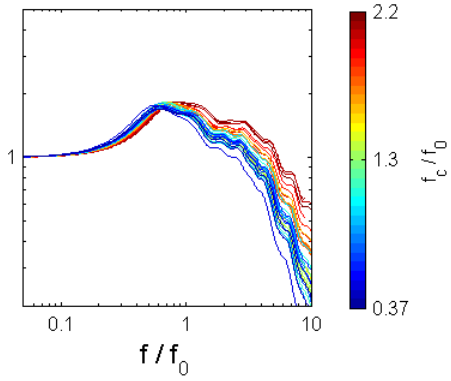

Non-linear TF (color coded by f_c)

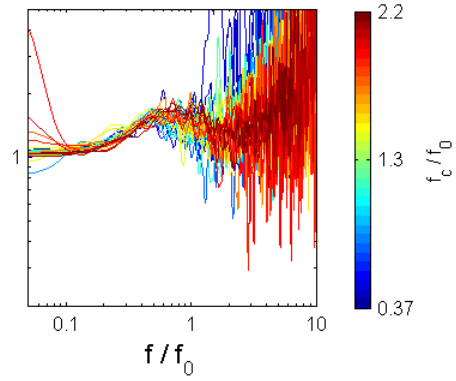

4.2.15 CI.NSS2b

Depth (m)	Thickness (m)	V_s (m/s)	Damping ratio	Density (kg/m^3)
0	0.5	178	0.05	1600
0.5	1	193	0.05	1600
1.5	1.5	236	0.05	1800
3	2.5	268	0.02	1800
5.5	4	335	0.02	1800
9.5	6	351	0.02	1800
15.5	9	430	0.02	1800
24.5	5.5	532	0.02	1800
30	5	554.4	0.02	1800
35	5	588.1	0.02	1800
40	5	617.5	0.02	1800
45	5	643.2	0.02	1800
50	5	665.7	0.02	1800
55	5	685.3	0.02	1800
60	5	702.4	0.02	1800
65	5	717.3	0.02	1800
70	5	730.3	0.02	1800
75	5	741.7	0.02	1800
80	5	751.7	0.01	1800
85	5	760.3	0.01	1800
90	5	767.9	0.01	1800
95	5	774.5	0.01	1800
100	–	780.3	0.01	1800

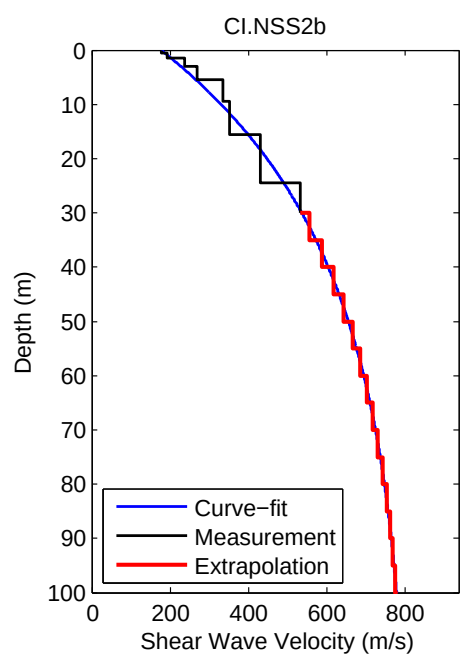

Linear Elastic Transfer Function

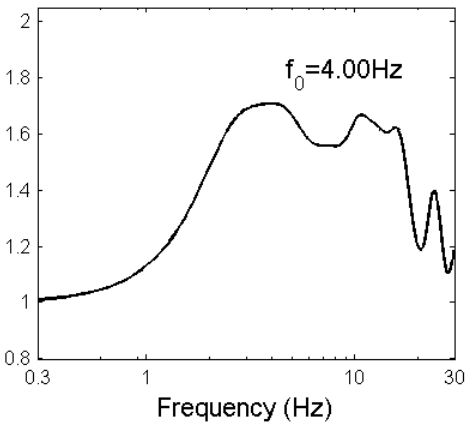

H/V Ratio – Sensor 450

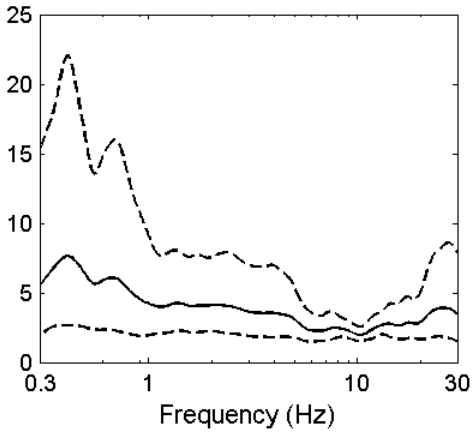

H/V Ratio – Sensor 507

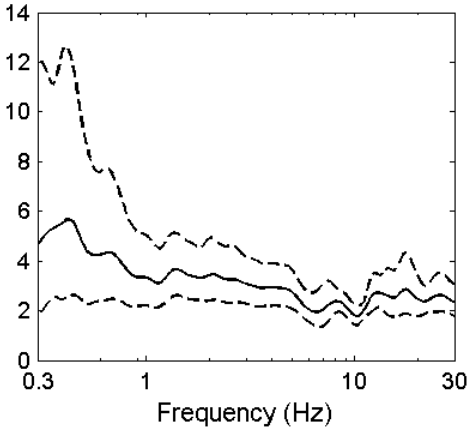

H/V Ratio – Sensor 453

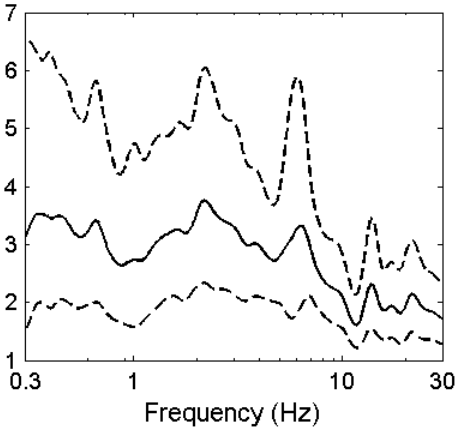

Equivalent Linear Transfer Function

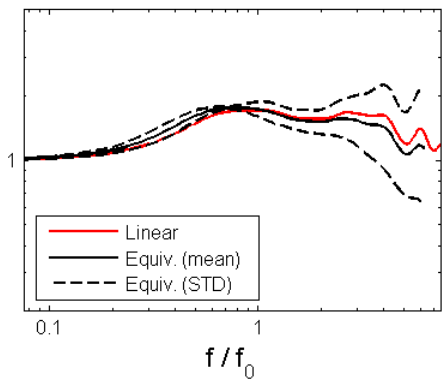

Equiv. Lin. TF (color coded by PGA_{RO})

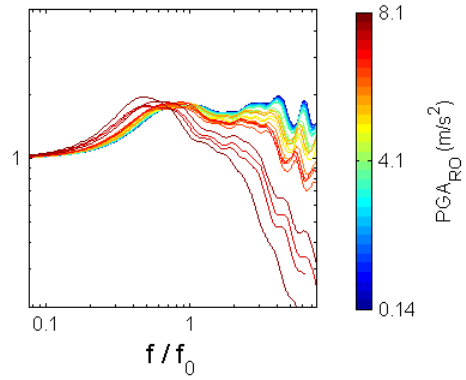

Non-linear Transfer Function

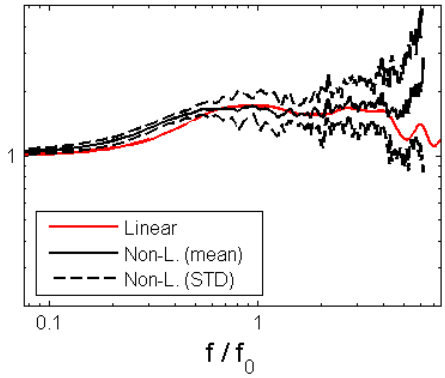

Non-linear TF (color coded by PGA_{RO})

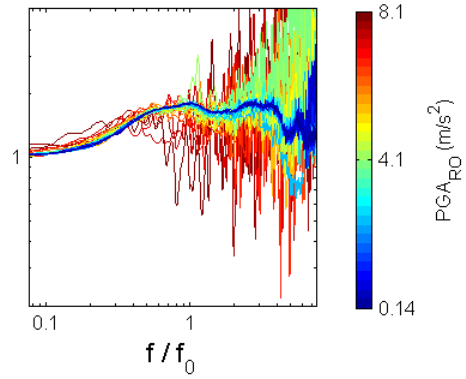

Equiv. Lin. TF (color coded by f_c)

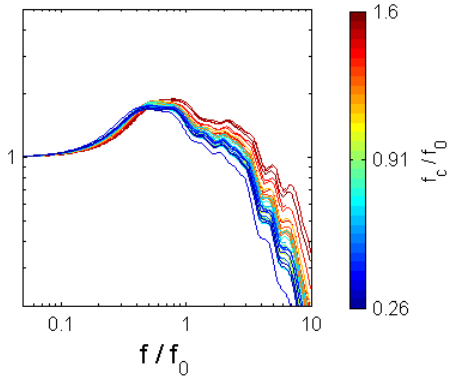

Non-linear TF (color coded by f_c)

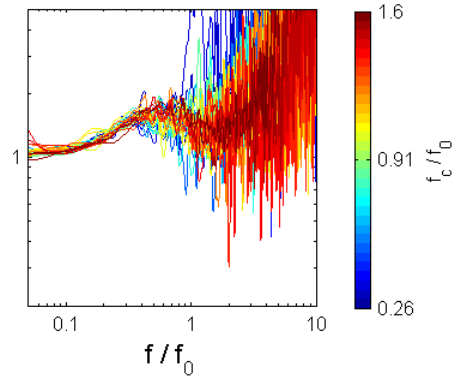

4.2.16 CI.NSS2c

Depth (m)	Thickness (m)	V_s (m/s)	Damping ratio	Density (kg/m^3)
0	0.5	191	0.05	1600
0.5	1	208	0.05	1800
1.5	1.5	251	0.02	1800
3	2.5	276	0.02	1800
5.5	4	334	0.02	1800
9.5	6	358	0.02	1800
15.5	9	376	0.02	1800
24.5	5.5	472	0.02	1800
30	5	500.5	0.02	1800
35	5	532.1	0.02	1800
40	5	560.6	0.02	1800
45	5	586.2	0.02	1800
50	5	609.4	0.02	1800
55	5	630.2	0.02	1800
60	5	649.0	0.02	1800
65	5	665.9	0.02	1800
70	5	681.2	0.02	1800
75	5	694.9	0.02	1800
80	5	707.3	0.02	1800
85	5	718.4	0.02	1800
90	5	728.5	0.02	1800
95	5	737.5	0.02	1800
100	–	745.7	0.02	1800

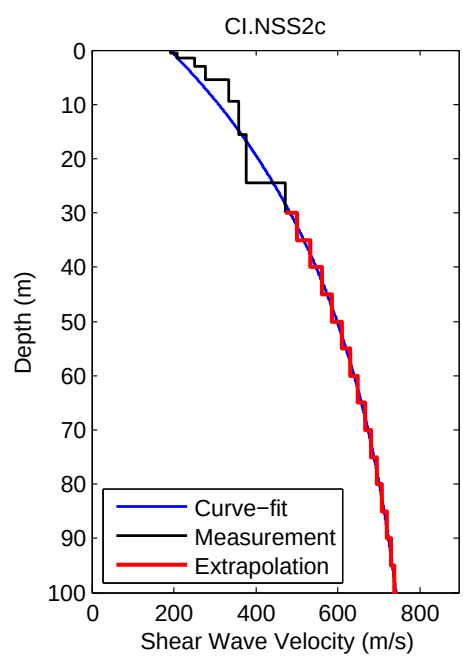

Linear Elastic Transfer Function

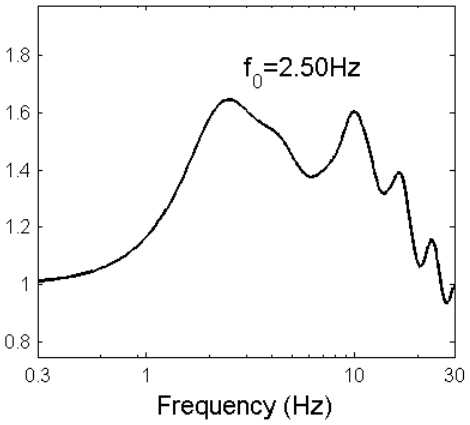

H/V Ratio – Sensor 450

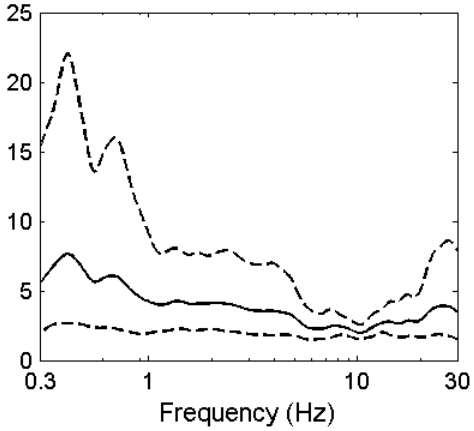

H/V Ratio – Sensor 507

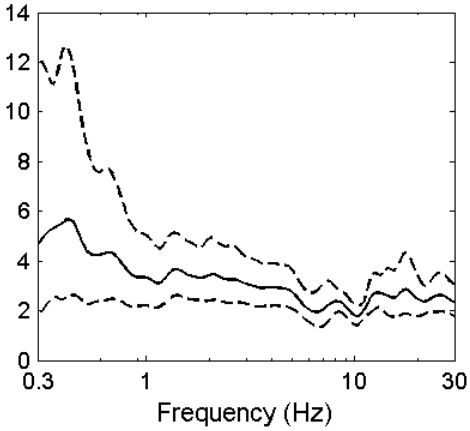

H/V Ratio – Sensor 453

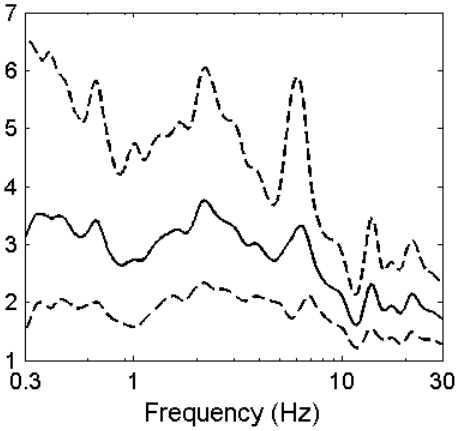

Equivalent Linear Transfer Function

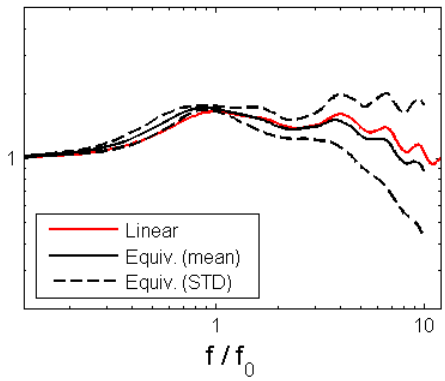

Equiv. Lin. TF (color coded by PGA_{RO})

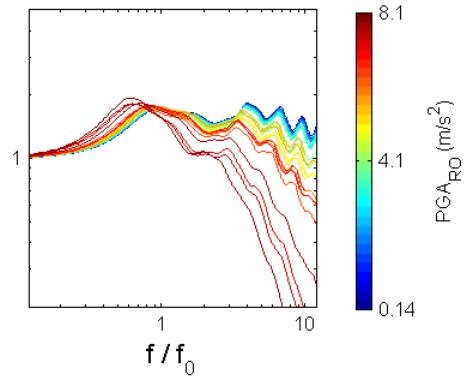

Non-linear Transfer Function

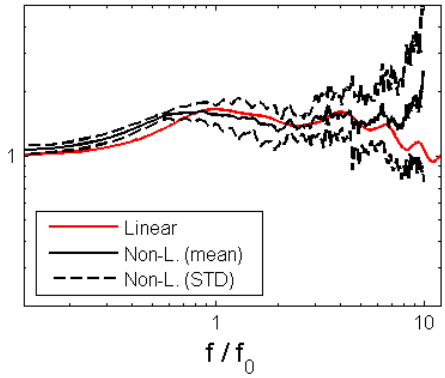

Non-linear TF (color coded by PGA_{RO})

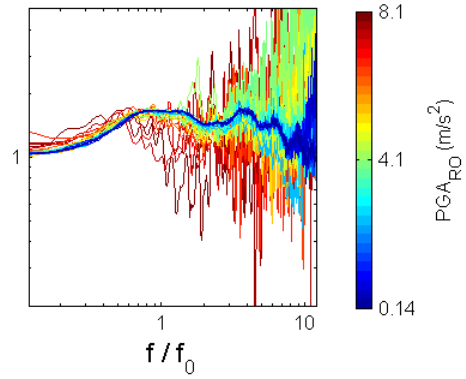

Equiv. Lin. TF (color coded by f_c)

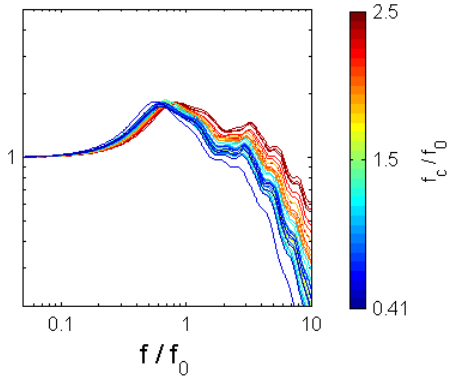

Non-linear TF (color coded by f_c)

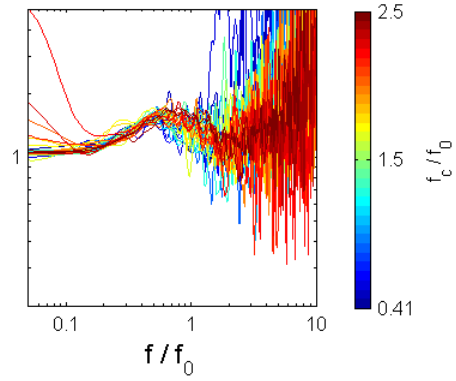

4.2.17 CI.PLC

Depth (m)	Thickness (m)	V_s (m/s)	Damping ratio	Density (kg/m^3)
0	1	192	0.05	1600
1	2	213	0.05	1800
3	3	301	0.02	1800
6	4	323	0.02	1800
10	5	341	0.02	1800
15	7	386	0.02	1800
22	12	475	0.02	1800
34	1	498	0.02	1800
35	5	511.8	0.02	1800
40	5	539.3	0.02	1800
45	5	564.2	0.02	1800
50	5	586.9	0.02	1800
55	5	607.4	0.02	1800
60	5	626.0	0.02	1800
65	5	642.8	0.02	1800
70	5	658.1	0.02	1800
75	5	672.0	0.02	1800
80	5	684.6	0.02	1800
85	5	696.0	0.02	1800
90	5	706.3	0.02	1800
95	5	715.7	0.02	1800
100	–	724.2	0.02	1800

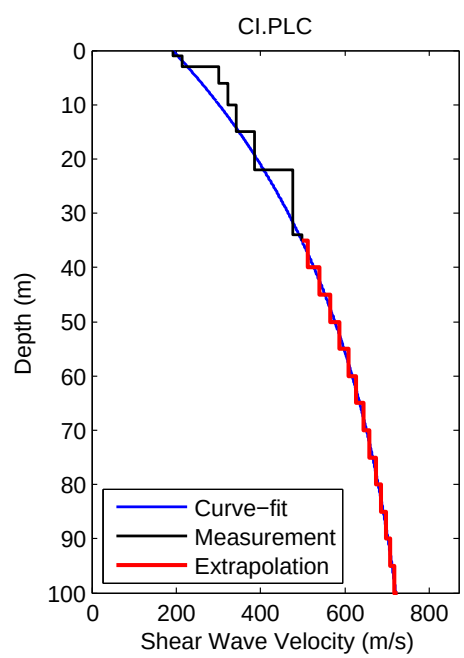

Linear Elastic Transfer Function

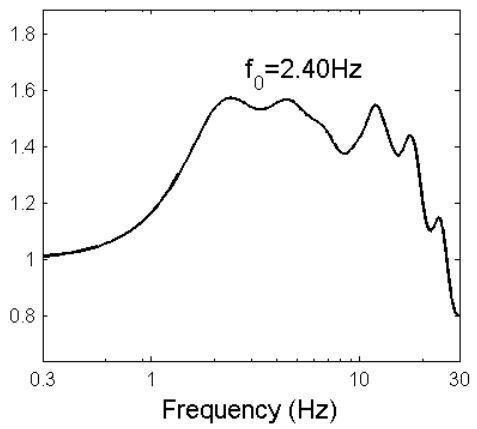

H/V Ratio – Sensor 450

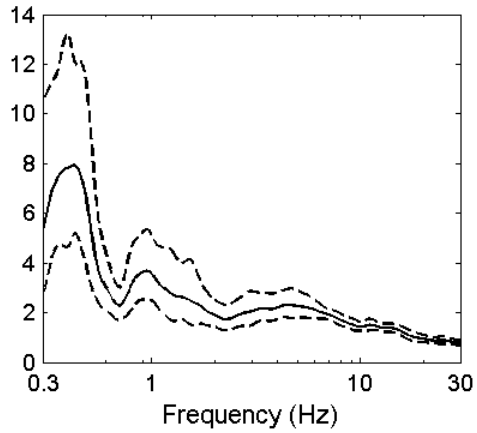

H/V Ratio – Sensor 507

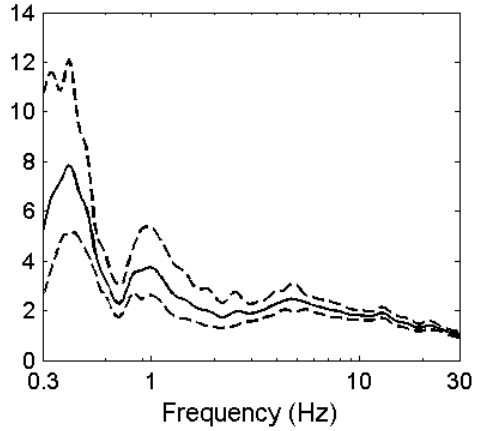

H/V Ratio – Sensor 453

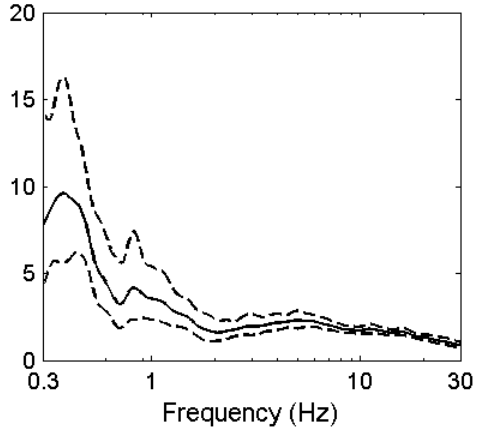

Equivalent Linear Transfer Function

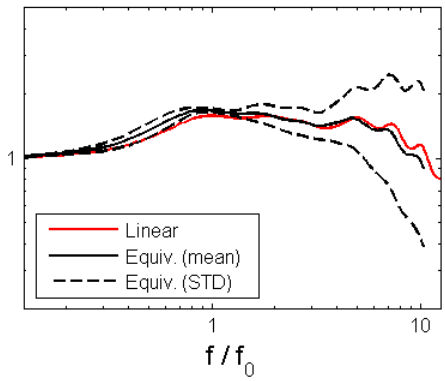

Equiv. Lin. TF (color coded by PGA_{RO})

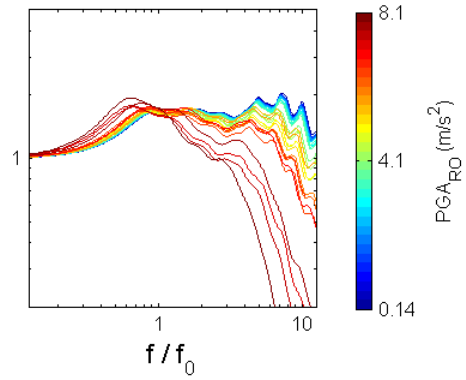

Non-linear Transfer Function

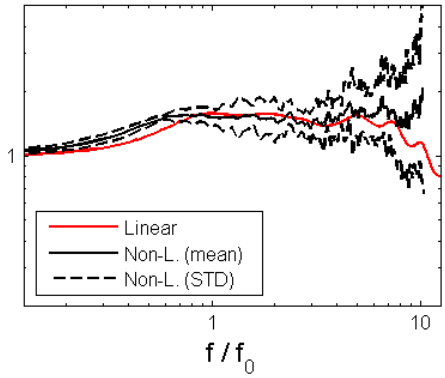

Non-linear TF (color coded by PGA_{RO})

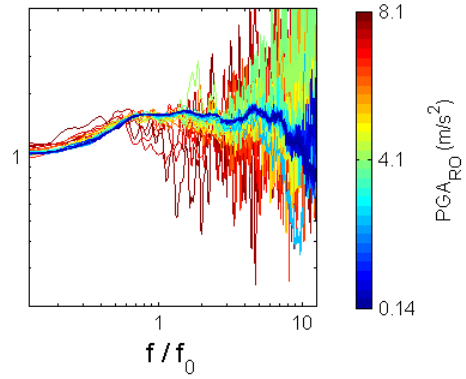

Equiv. Lin. TF (color coded by f_c)

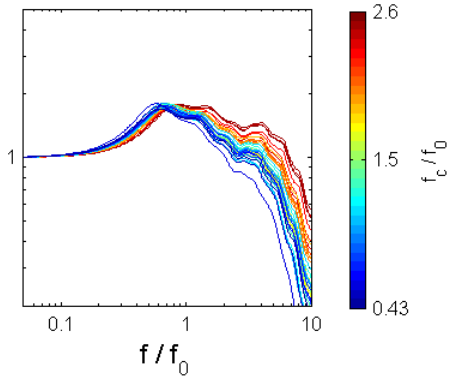

Non-linear TF (color coded by f_c)

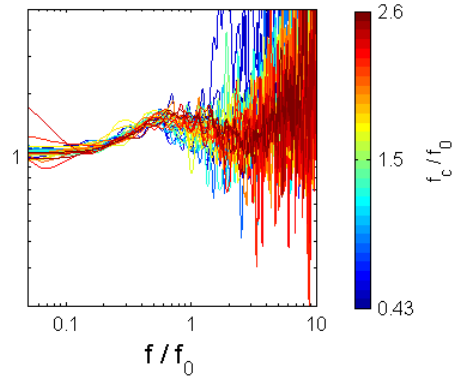

4.2.18 CI.RSBa

Depth (m)	Thickness (m)	V_s (m/s)	Damping ratio	Density (kg/m^3)
0	3	202	0.05	1800
3	3	272	0.02	1800
6	5	351	0.02	1800
11	7	357	0.02	1800
18	10	490	0.02	1800
28	14	553	0.02	1800
42	20	723	0.02	1800
62	–	885	0.01	2000

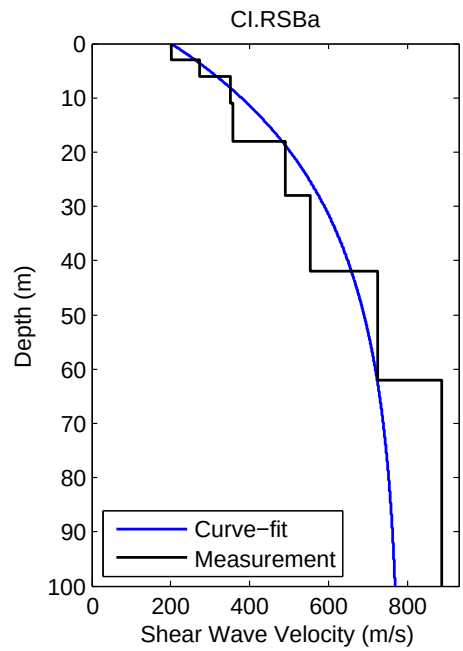

Linear Elastic Transfer Function

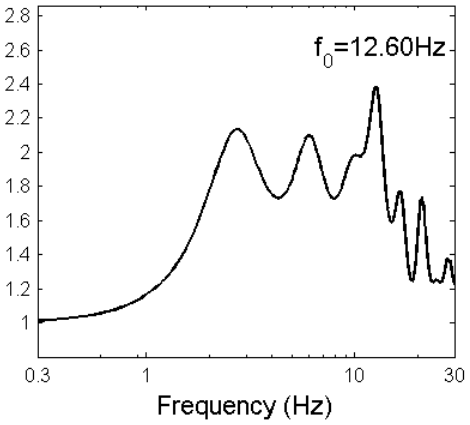

H/V Ratio – Sensor 450

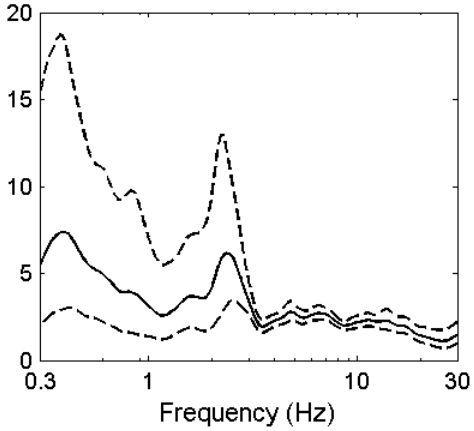

H/V Ratio – Sensor 507

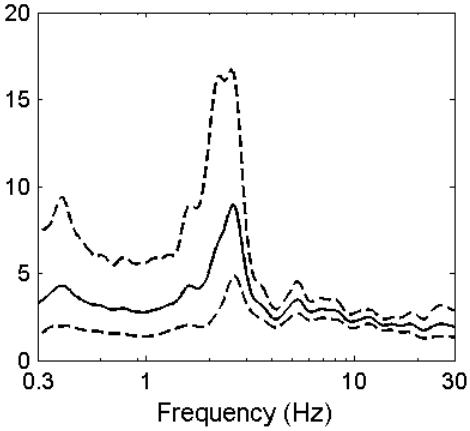

H/V Ratio – Sensor 453

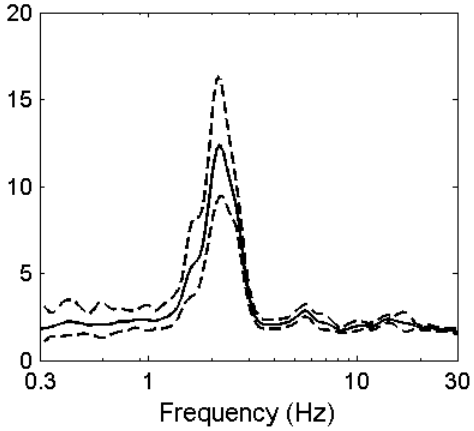

Equivalent Linear Transfer Function

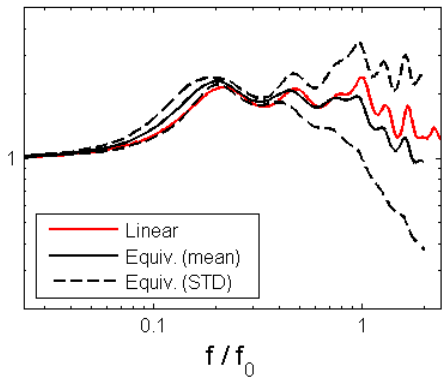

Equiv. Lin. TF (color coded by PGA_{RO})

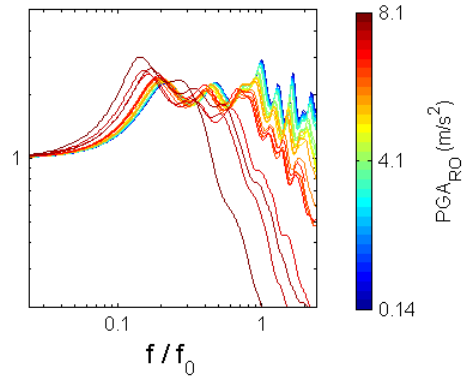

Non-linear Transfer Function

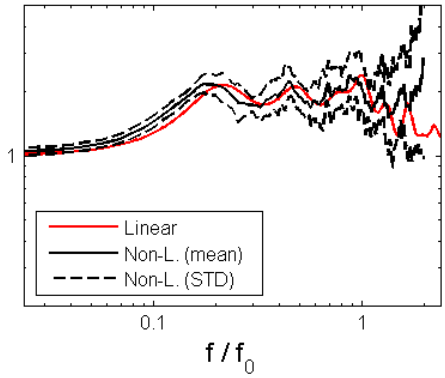

Non-linear TF (color coded by PGA_{RO})

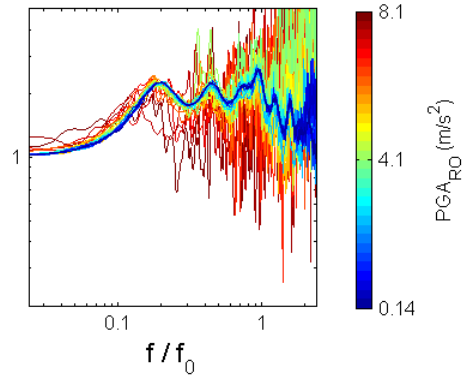

Equiv. Lin. TF (color coded by f_c)

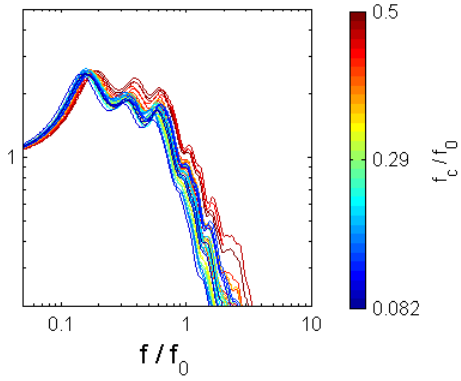

Non-linear TF (color coded by f_c)

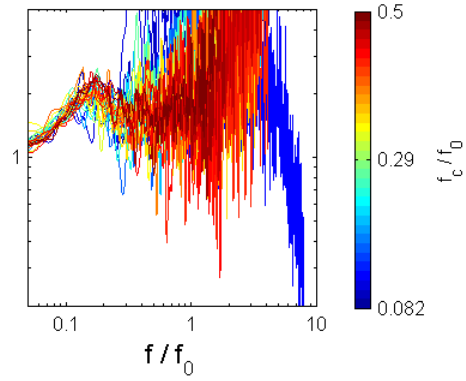

4.2.19 CI.RSBb

Depth (m)	Thickness (m)	V_s (m/s)	Damping ratio	Density (kg/m^3)
0	3	201	0.05	1800
3	3	274	0.02	1800
6	5	352	0.02	1800
11	8	359	0.02	1800
19	10	527	0.02	1800
29	14	612	0.02	1800
43	22	710	0.02	1800
65	–	885	0.01	2000

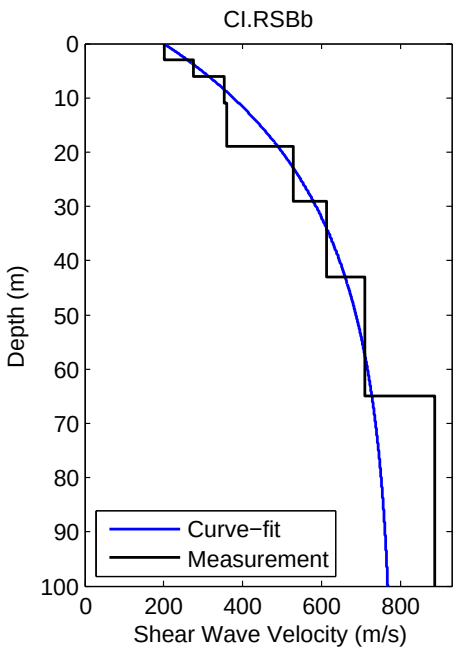

Linear Elastic Transfer Function

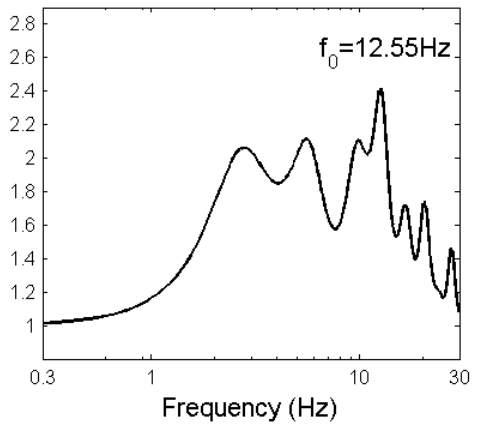

H/V Ratio – Sensor 450

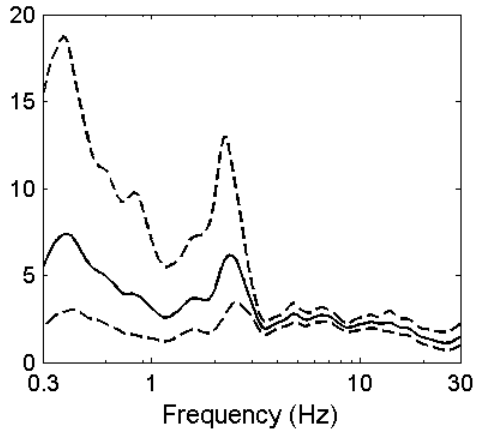

H/V Ratio – Sensor 507

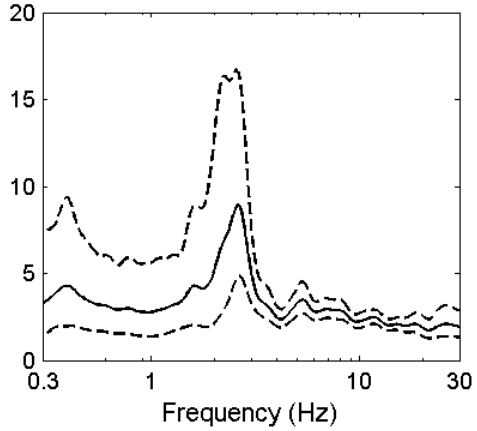

H/V Ratio – Sensor 453

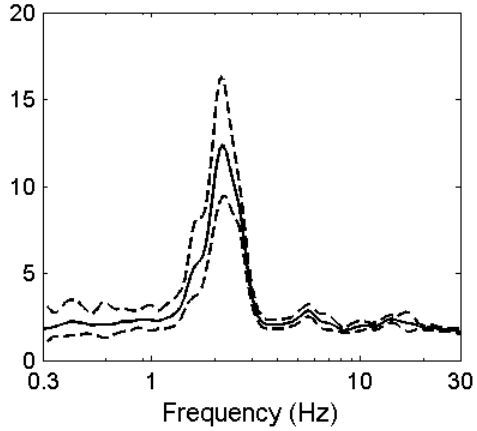

Equivalent Linear Transfer Function

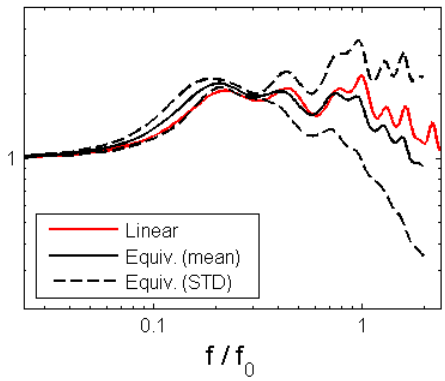

Equiv. Lin. TF (color coded by PGA_{RO})

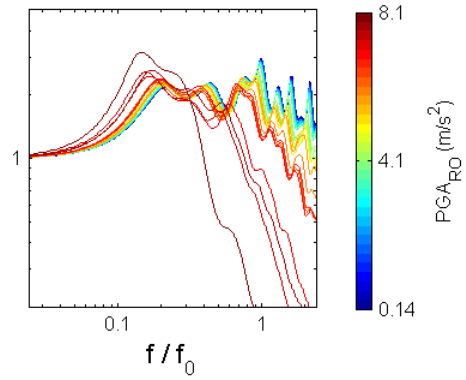

Non-linear Transfer Function

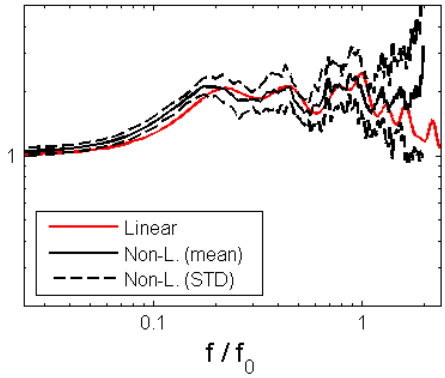

Non-linear TF (color coded by PGA_{RO})

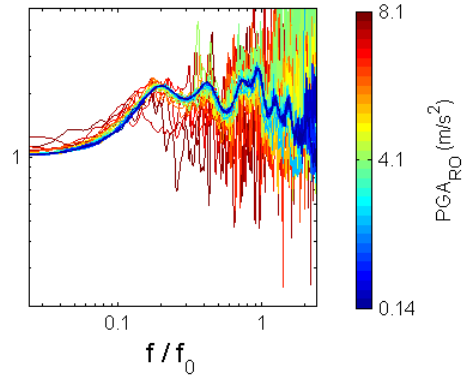

Equiv. Lin. TF (color coded by f_c)

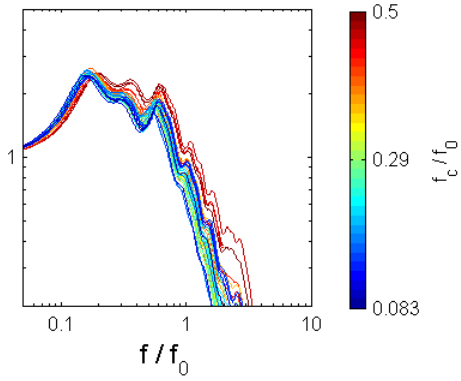

Non-linear TF (color coded by f_c)

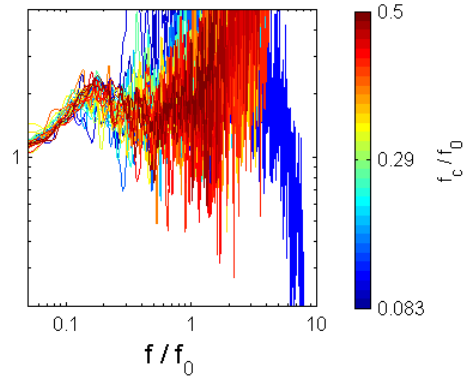

4.2.20 CI.SHOa

Depth (m)	Thickness (m)	V_s (m/s)	Damping ratio	Density (kg/m^3)
0	0.75	112	0.05	1600
0.75	1.75	243	0.05	1800
2.5	2.5	394	0.02	1800
5	15	355	0.02	1800
20	10	461	0.02	1800
30	5	579	0.02	1800
35	5	596.4	0.02	1800
40	5	628.3	0.02	1800
45	5	655.6	0.02	1800
50	5	679.0	0.02	1800
55	5	699.1	0.02	1800
60	5	716.3	0.02	1800
65	5	731.1	0.02	1800
70	5	743.8	0.02	1800
75	5	754.6	0.01	1800
80	5	763.9	0.01	1800
85	5	771.9	0.01	1800
90	5	778.8	0.01	1800
95	5	784.6	0.01	1800
100	–	789.7	0.01	1800

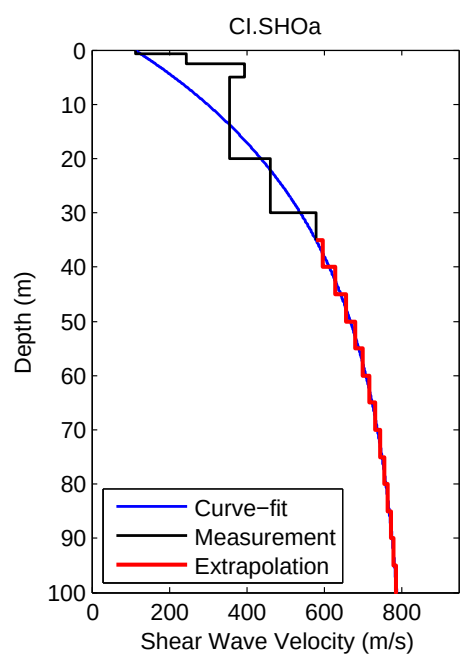

Linear Elastic Transfer Function

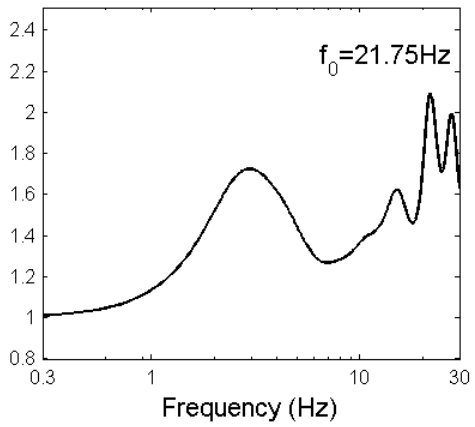

H/V Ratio – Sensor 450

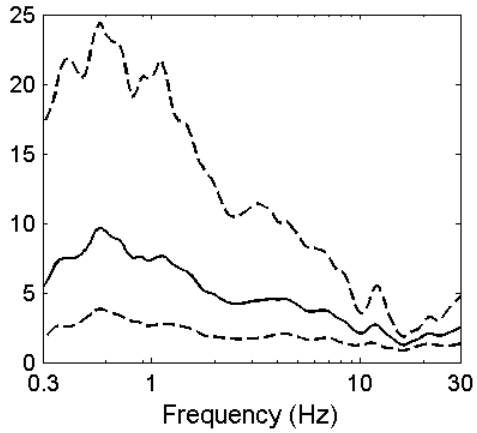

H/V Ratio – Sensor 507

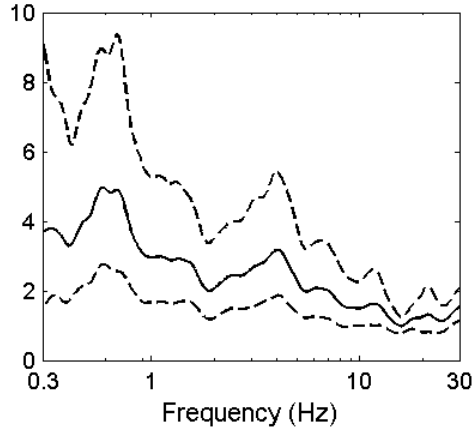

H/V Ratio – Sensor 453

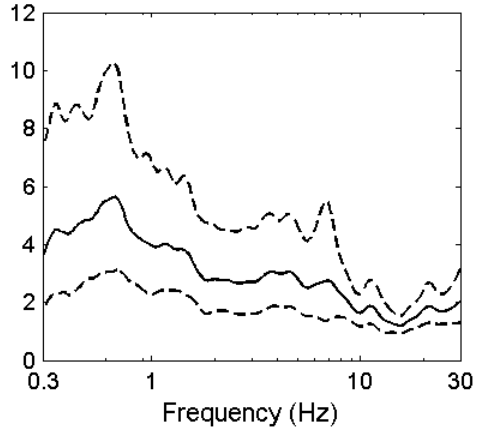

Equivalent Linear Transfer Function

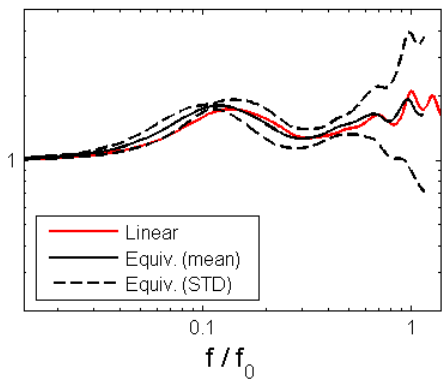

Equiv. Lin. TF (color coded by PGA_{RO})

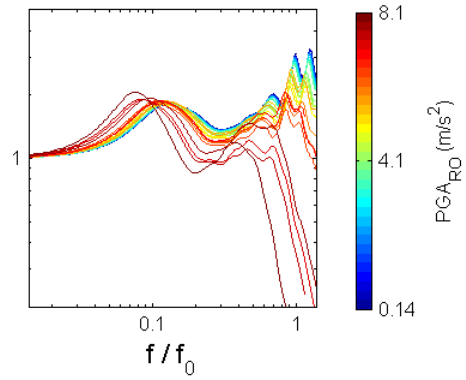

Non-linear Transfer Function

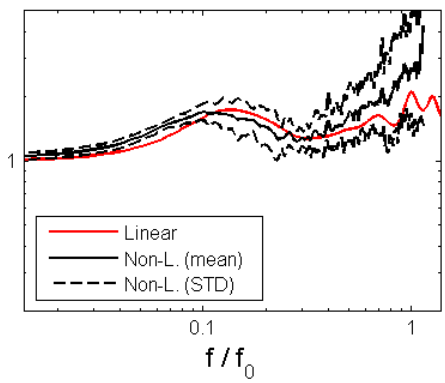

Non-linear TF (color coded by PGA_{RO})

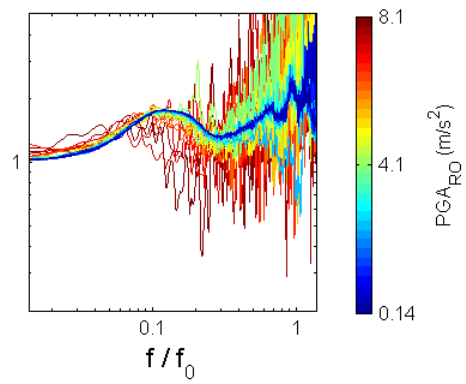

Equiv. Lin. TF (color coded by f_c)

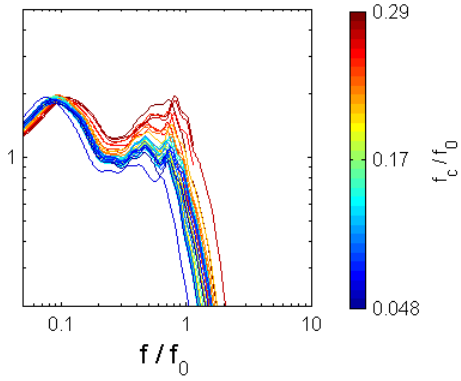

Non-linear TF (color coded by f_c)

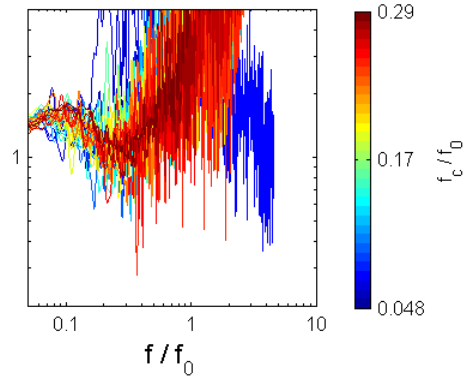

4.2.21 CI.SHOb

Depth (m)	Thickness (m)	V_s (m/s)	Damping ratio	Density (kg/m^3)
0	1	183	0.05	1600
1	1	266	0.02	1800
2	3	394	0.02	1800
5	6	330	0.02	1800
11	9	351	0.02	1800
20	10	422	0.02	1800
30	5	533	0.02	1800
35	5	542.8	0.02	1800
40	5	571.9	0.02	1800
45	5	598.0	0.02	1800
50	5	621.3	0.02	1800
55	5	642.2	0.02	1800
60	5	660.8	0.02	1800
65	5	677.6	0.02	1800
70	5	692.5	0.02	1800
75	5	705.9	0.02	1800
80	5	717.9	0.02	1800
85	5	728.6	0.02	1800
90	5	738.2	0.02	1800
95	5	746.8	0.02	1800
100	–	754.5	0.01	1800

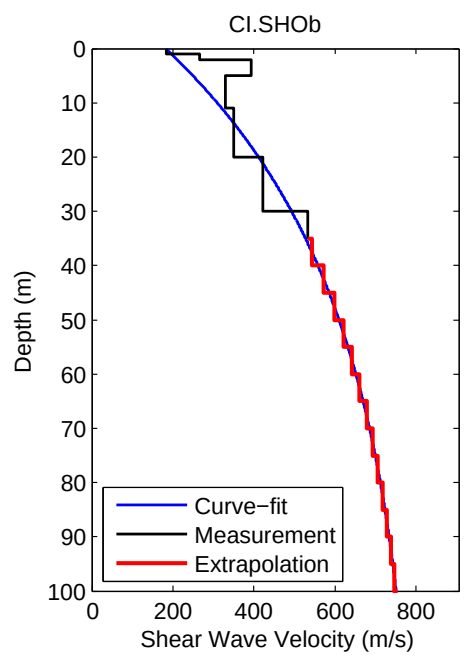

Linear Elastic Transfer Function

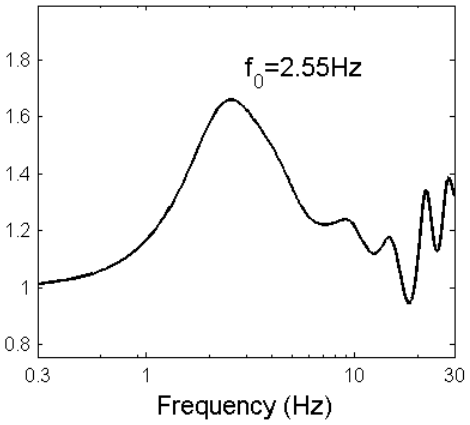

H/V Ratio – Sensor 450

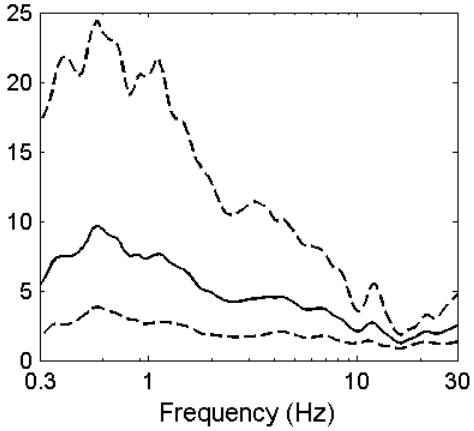

H/V Ratio – Sensor 507

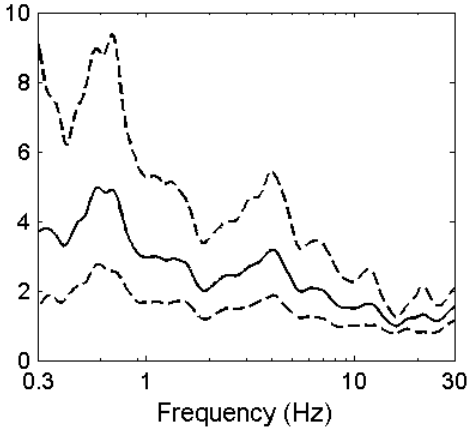

H/V Ratio – Sensor 453

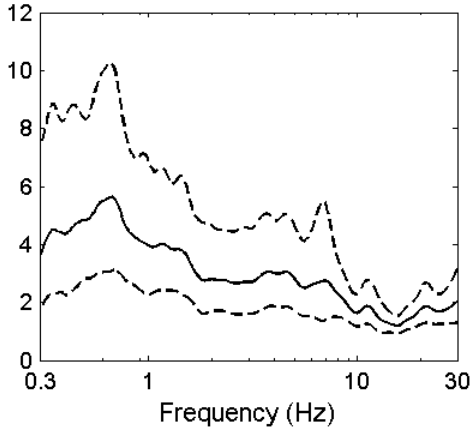

Equivalent Linear Transfer Function

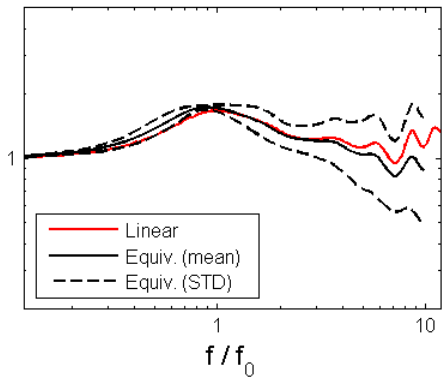

Equiv. Lin. TF (color coded by PGA_{RO})

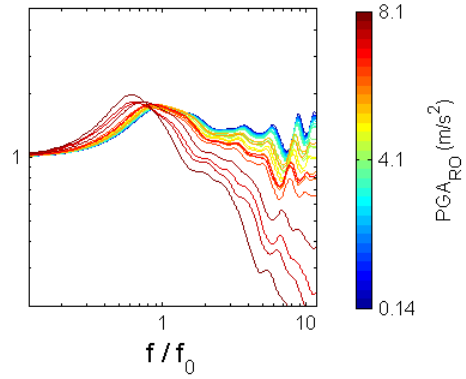

Non-linear Transfer Function

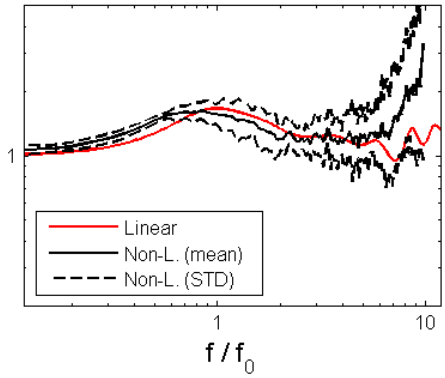

Non-linear TF (color coded by PGA_{RO})

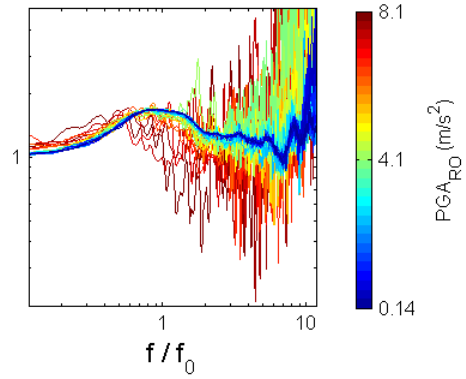

Equiv. Lin. TF (color coded by f_c)

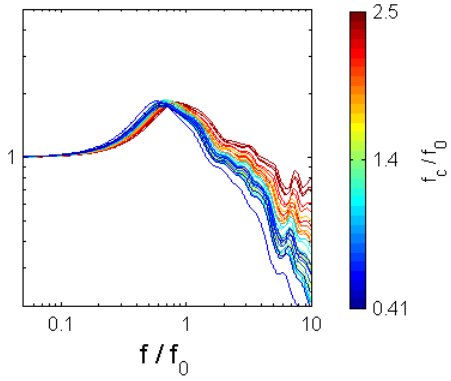

Non-linear TF (color coded by f_c)

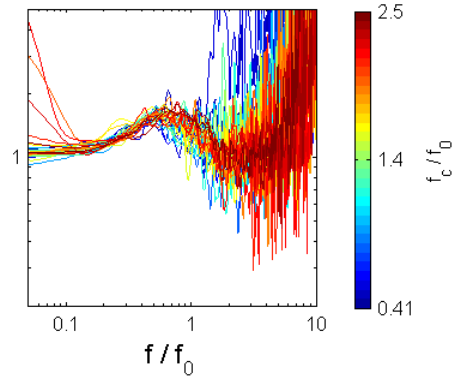

4.2.22 CI.SLBa

Depth (m)	Thickness (m)	V_s (m/s)	Damping ratio	Density (kg/m^3)
0	0.5	98	0.05	1600
0.5	1	184	0.05	1600
1.5	1.5	226	0.05	1800
3	3	311	0.02	1800
6	5	319	0.02	1800
11	7	379	0.02	1800
18	12	426	0.02	1800
30	10	624	0.02	1800
40	5	648.9	0.02	1800
45	5	675.5	0.02	1800
50	5	698.0	0.02	1800
55	5	717.0	0.02	1800
60	5	733.1	0.02	1800
65	5	746.6	0.02	1800
70	5	758.0	0.01	1800
75	5	767.7	0.01	1800
80	5	775.8	0.01	1800
85	5	782.7	0.01	1800
90	5	788.5	0.01	1800
95	5	793.4	0.01	1800
100	–	797.6	0.01	1800

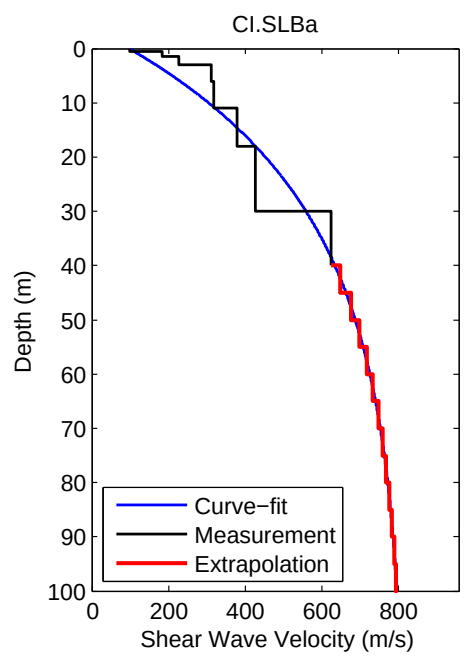

Linear Elastic Transfer Function

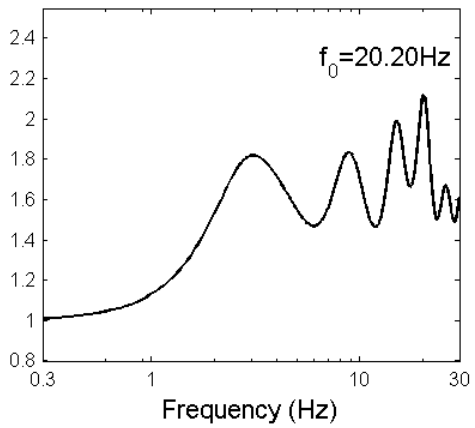

H/V Ratio – Sensor 450

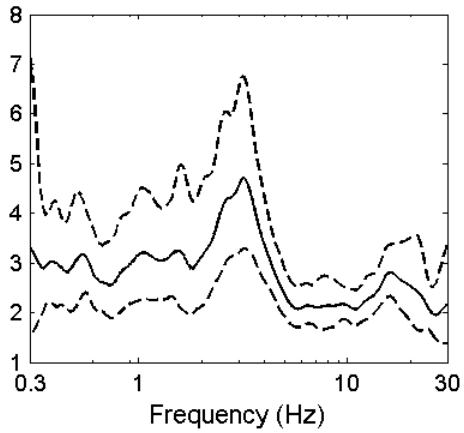

H/V Ratio – Sensor 507

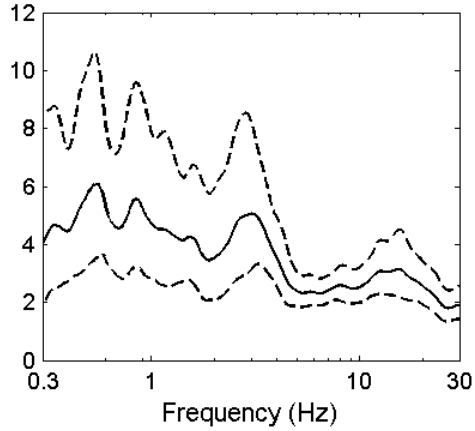

H/V Ratio – Sensor 453

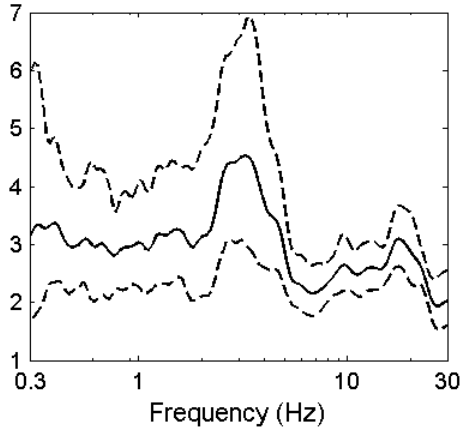

Equivalent Linear Transfer Function

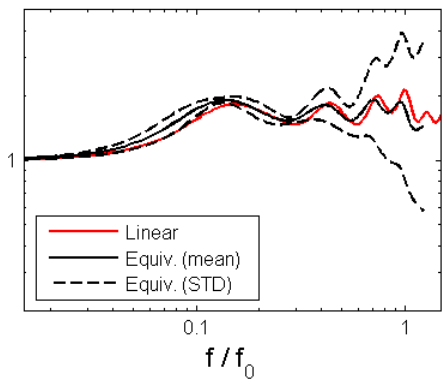

Equiv. Lin. TF (color coded by PGA_{RO})

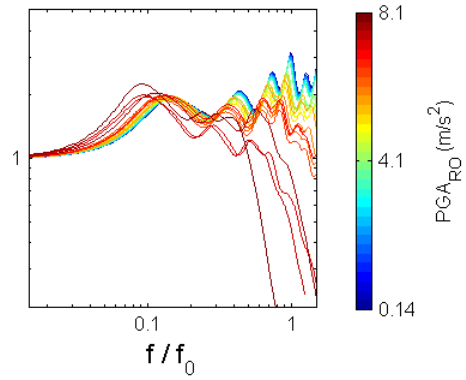

Non-linear Transfer Function

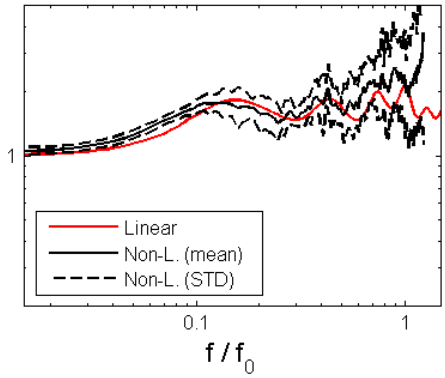

Non-linear TF (color coded by PGA_{RO})

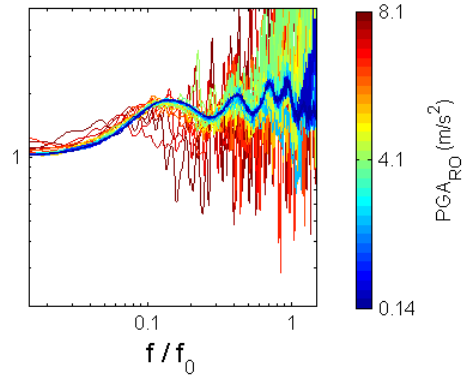

Equiv. Lin. TF (color coded by f_c)

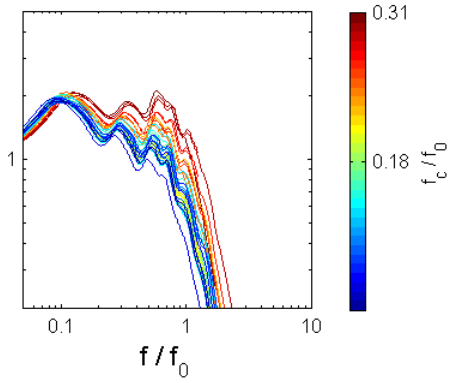

Non-linear TF (color coded by f_c)

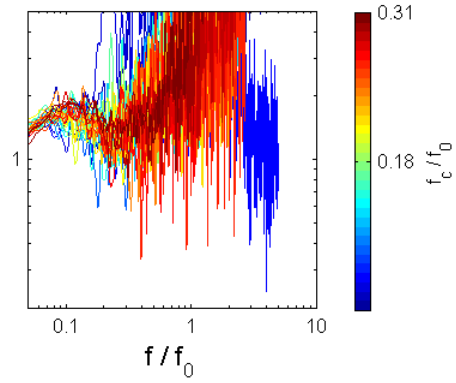

4.2.23 CI.SLBb

Depth (m)	Thickness (m)	V_s (m/s)	Damping ratio	Density (kg/m^3)
0	1	144	0.05	1600
1	2	219	0.05	1800
3	3	304	0.02	1800
6	5	349	0.02	1800
11	7	370	0.02	1800
18	12	408	0.02	1800
30	15	665	0.02	1800
45	5	689.2	0.02	1800
50	5	709.9	0.02	1800
55	5	727.4	0.02	1800
60	5	742.1	0.02	1800
65	5	754.5	0.01	1800
70	5	764.9	0.01	1800
75	5	773.6	0.01	1800
80	5	781.0	0.01	1800
85	5	787.2	0.01	1800
90	5	792.4	0.01	1800
95	5	796.8	0.01	1800
100	–	800.4	0.01	2000

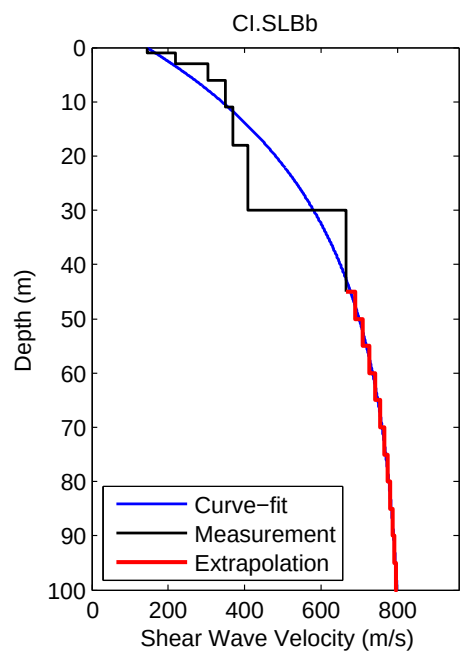

Linear Elastic Transfer Function

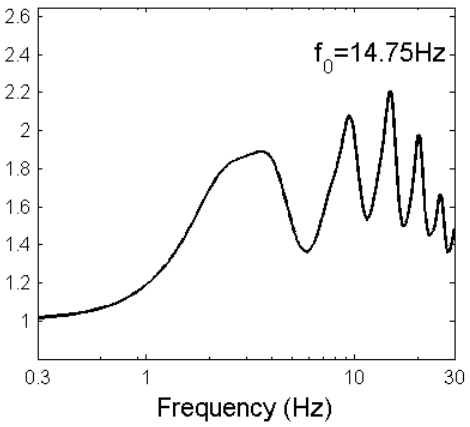

H/V Ratio – Sensor 450

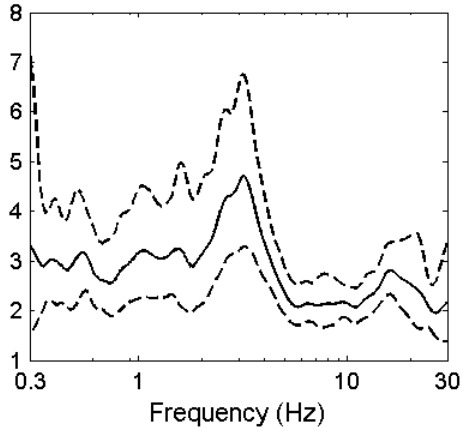

H/V Ratio – Sensor 507

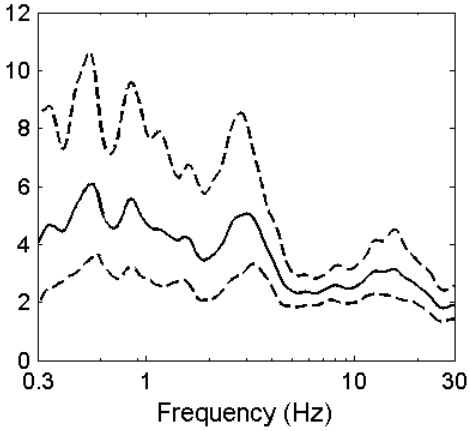

H/V Ratio – Sensor 453

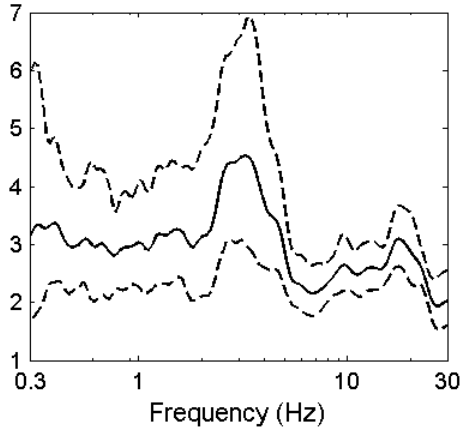

Equivalent Linear Transfer Function

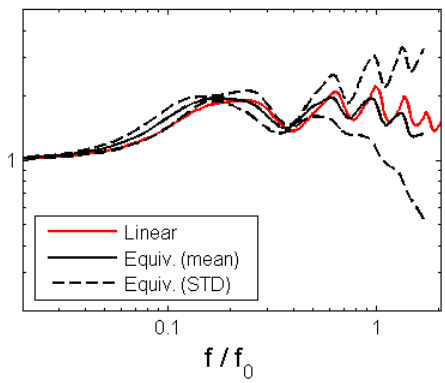

Equiv. Lin. TF (color coded by PGA_{RO})

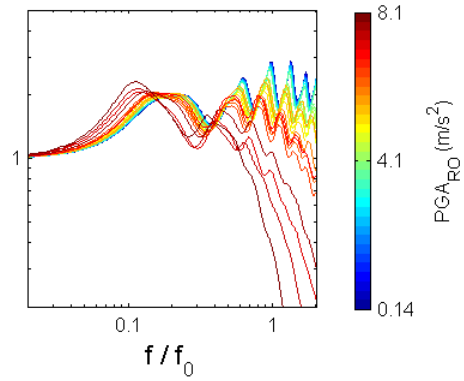

Non-linear Transfer Function

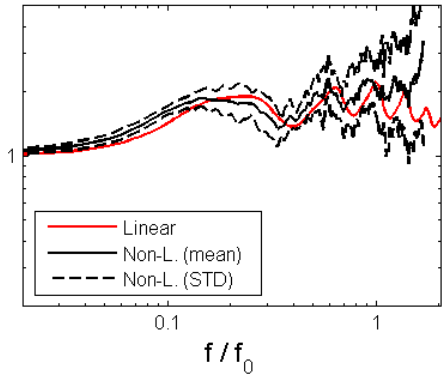

Non-linear TF (color coded by PGA_{RO})

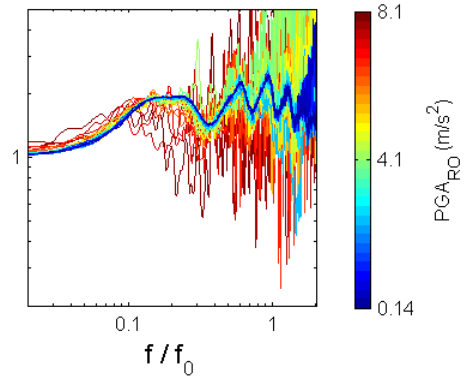

Equiv. Lin. TF (color coded by f_c)

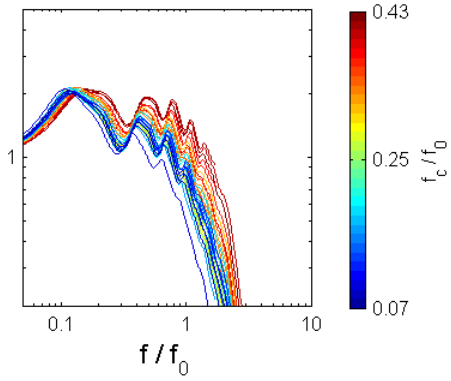

Non-linear TF (color coded by f_c)

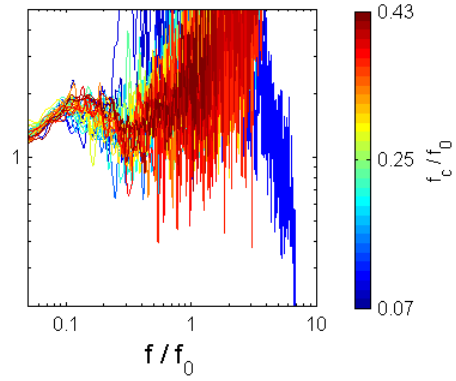

4.2.24 CI.VOG

Depth (m)	Thickness (m)	V_s (m/s)	Damping ratio	Density (kg/m^3)
0	0.75	163	0.05	1600
0.75	1.75	245	0.05	1800
2.5	5.5	283	0.02	1800
8	14	310	0.02	1800
22	13	692	0.02	1800
35	5	705.6	0.02	1800
40	5	723.7	0.02	1800
45	5	737.3	0.02	1800
50	5	747.5	0.02	1800
55	5	755.2	0.01	1800
60	5	761.0	0.01	1800
65	5	765.4	0.01	1800
70	5	768.7	0.01	1800
75	5	771.1	0.01	1800
80	5	773.0	0.01	1800
85	5	774.4	0.01	1800
90	5	775.4	0.01	1800
95	5	776.2	0.01	1800
100	–	776.8	0.01	1800

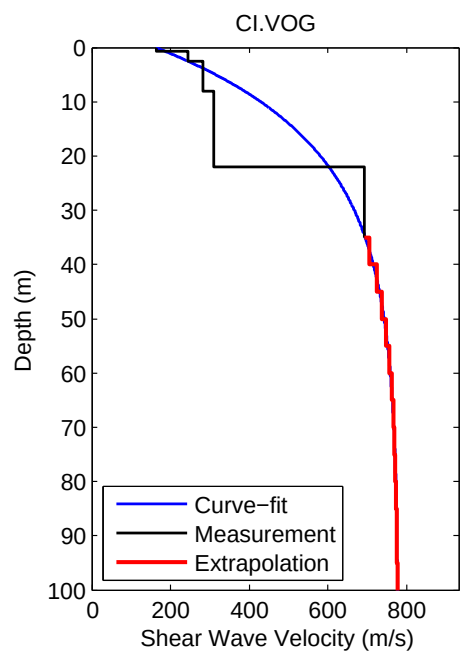

Linear Elastic Transfer Function

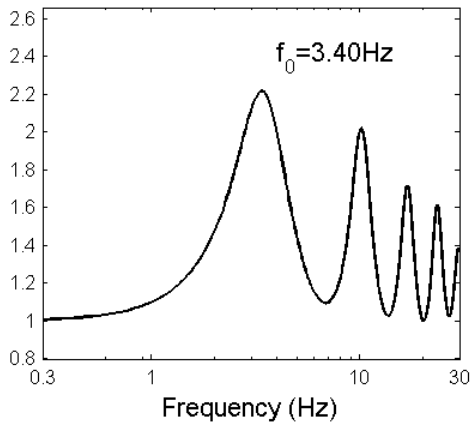

H/V Ratio – Sensor 450

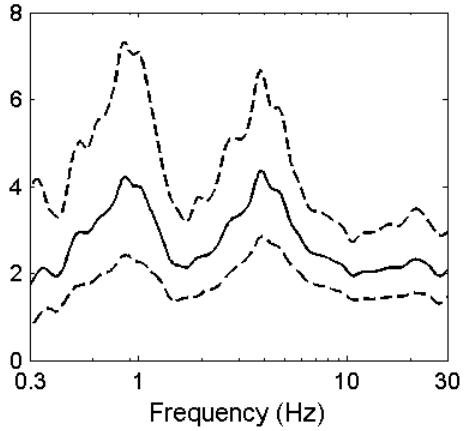

H/V Ratio – Sensor 507

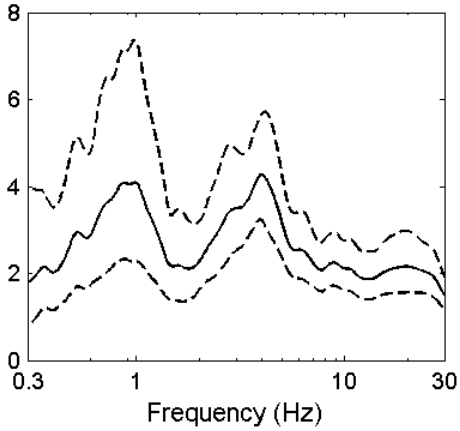

H/V Ratio – Sensor 453

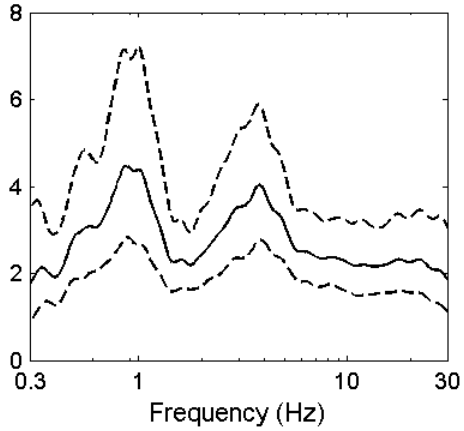

Equivalent Linear Transfer Function

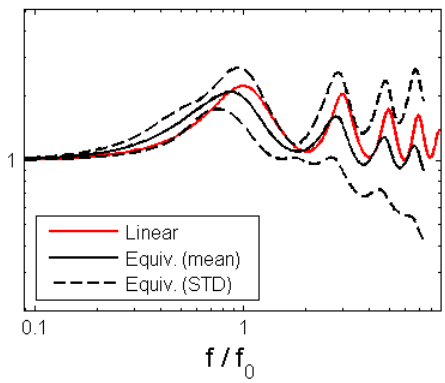

Equiv. Lin. TF (color coded by PGA_{RO})

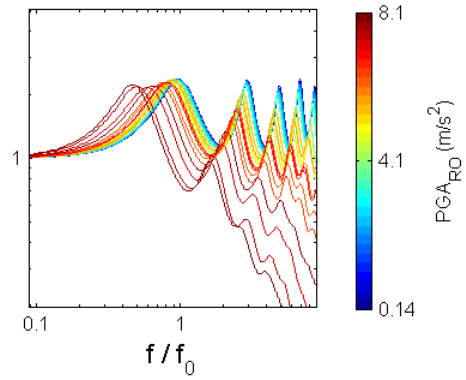

Non-linear Transfer Function

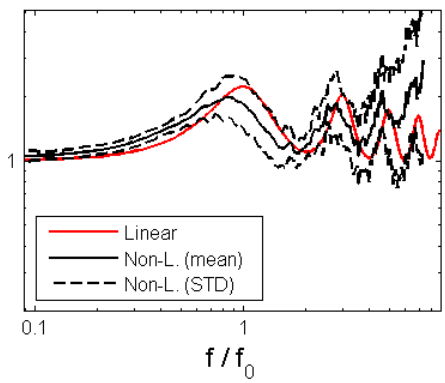

Non-linear TF (color coded by PGA_{RO})

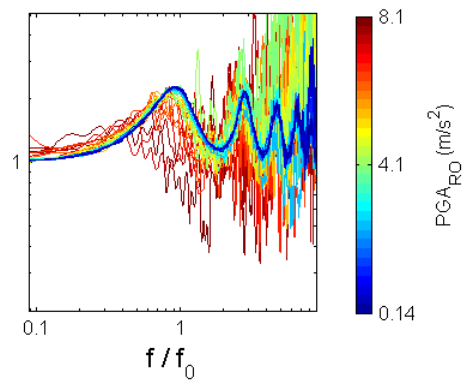

Equiv. Lin. TF (color coded by f_c)

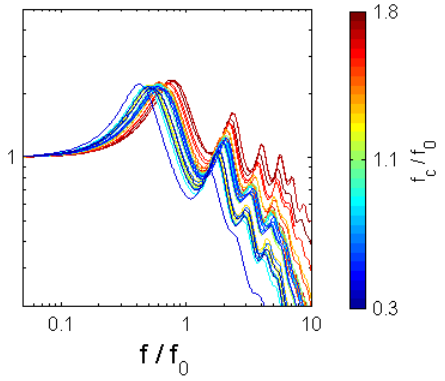

Non-linear TF (color coded by f_c)

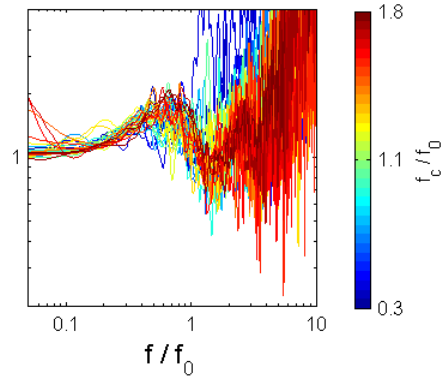

4.3 Class C

Class C sites include the following:

Site Code	V_{s30}-measured (m/s)	V_{s30}-adjusted (m/s)
CE.13096	646	699
CE.13099	420	420
CE.13929	542	542
CE.23063	506	506
CE.24644	421	421
CI.ADO	375	400
CI.BLA	524	613
CI.CAC	399	433
CI.CCC	432	461
CI.CGO	715	739
CI.CTC	370	396
CI.CWC	580	580
CI.DAN	477	528
CI.DNR	361	411
CI.DVT	625	625
CI.FHO	416	460
CI.FUR	433	456
CI.GOR	559	623
CI.GRA	386	407
CI.IDO	557	597
CI.JVA	388	423
CI.LDF	448	477
CI.LDR	378	415
CI.LPC	506	542
CI.NBS	419	461
CI.RRX	372	396
CI.SYP	440	470
CI.THM	452	480
CI.VCS	402	433
NC.HCAB	646	671
NC.JSFB	432	463
NC.PHOB	376	404
NC.PHSB	422	422

4.3.1 CE.13096

Depth (m)	Thickness (m)	V_s (m/s)	Damping ratio	Density (kg/m^3)
0	1.5	204	0.05	1800
1.5	2.5	394	0.02	1800
4	4	525	0.02	1800
8	8	639	0.02	1800
16	10	984	0.01	2000
26	–	1638	0.01	2000

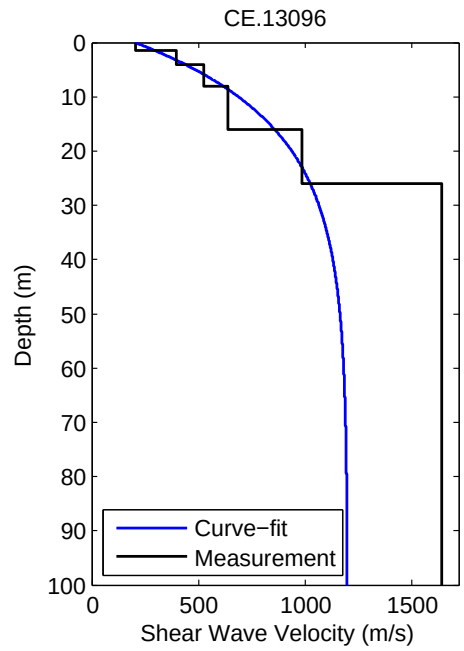

Linear Elastic Transfer Function

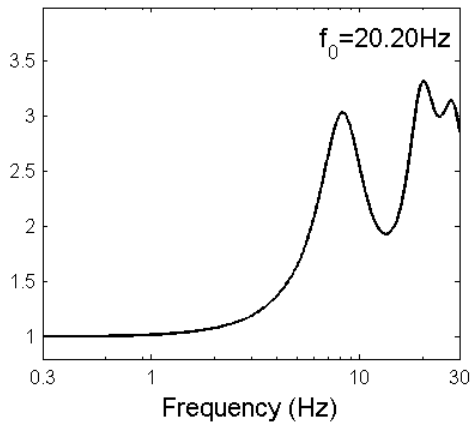

H/V Ratio – Sensor 450

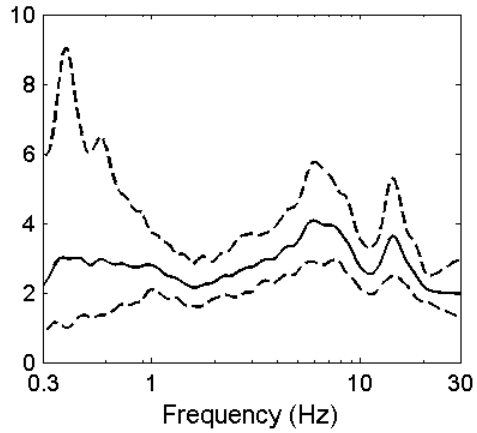

H/V Ratio – Sensor 507

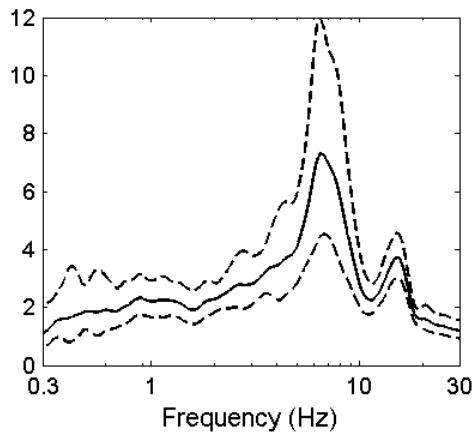

H/V Ratio – Sensor 453

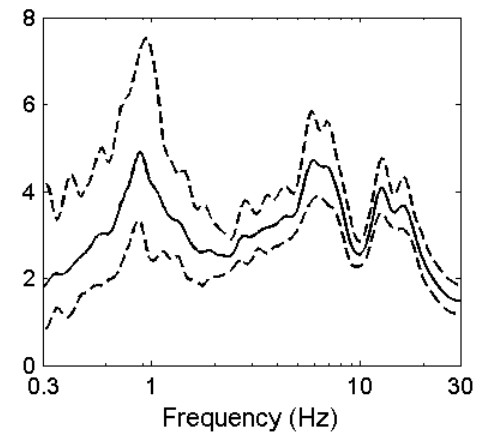

Equivalent Linear Transfer Function

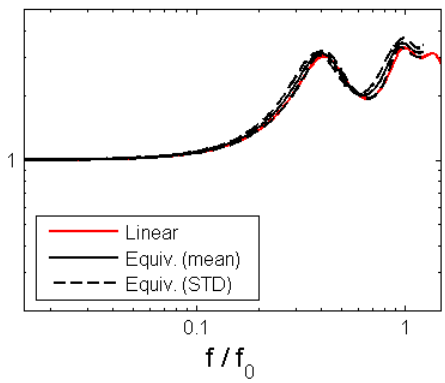

Equiv. Lin. TF (color coded by PGA_{RO})

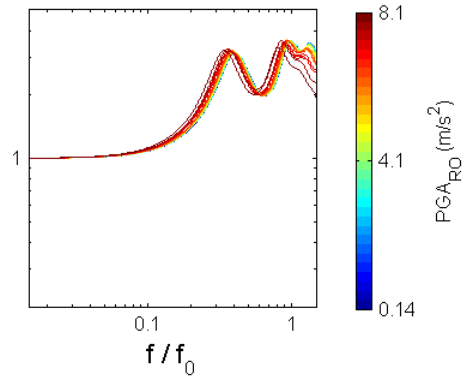

Non-linear Transfer Function

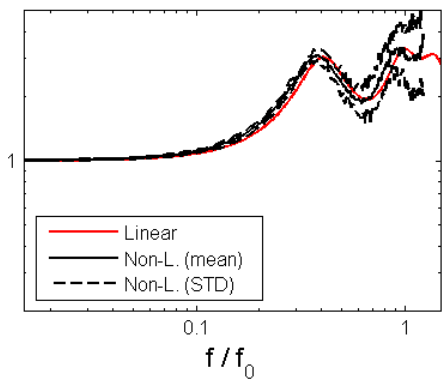

Non-linear TF (color coded by PGA_{RO})

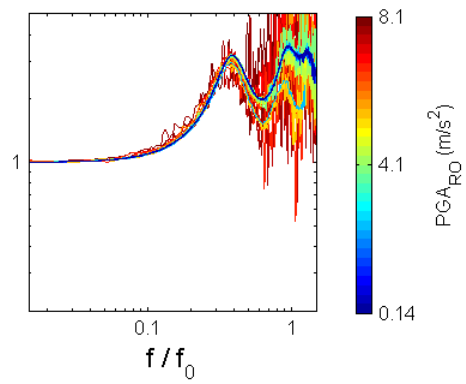

Equiv. Lin. TF (color coded by f_c)

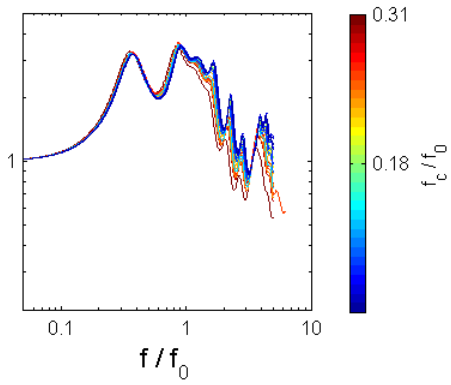

Non-linear TF (color coded by f_c)

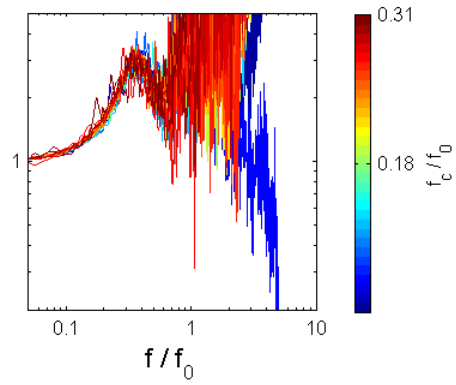

4.3.2 CE.13099

Depth (m)	Thickness (m)	V_s (m/s)	Damping ratio	Density (kg/m^3)
0	1	278	0.02	1800
1	2	336	0.02	1800
3	4	345	0.02	1800
7	5	429	0.02	1800
12	8	460	0.02	1800
20	12	470	0.02	1800
32	15	541	0.02	1800
47	18	665	0.02	1800
65	5	668.4	0.02	1800
70	5	676.0	0.02	1800
75	5	682.5	0.02	1800
80	5	688.0	0.02	1800
85	5	692.7	0.02	1800
90	5	696.7	0.02	1800
95	5	700.2	0.02	1800
100	–	703.1	0.02	1800

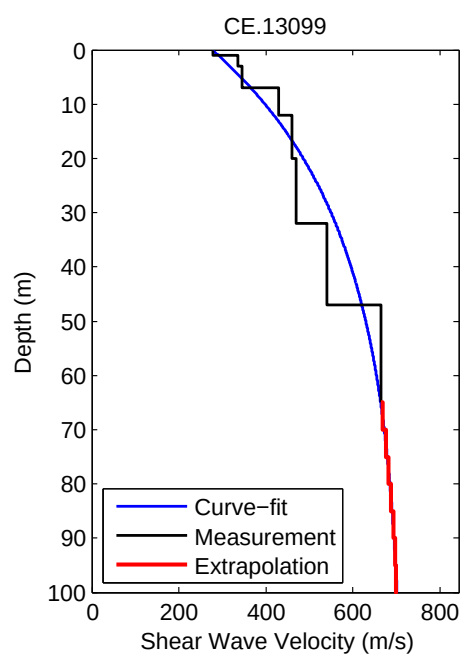

Linear Elastic Transfer Function

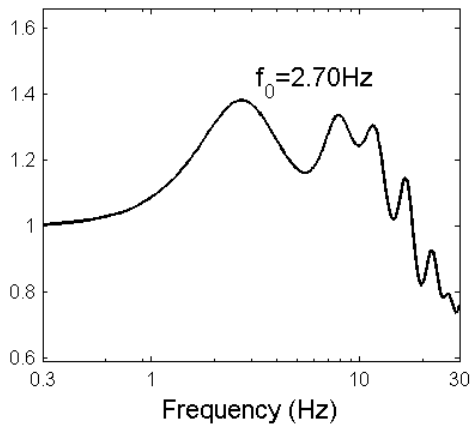

H/V Ratio – Sensor 450

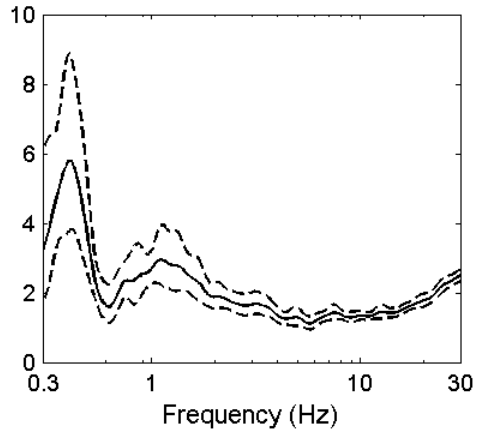

H/V Ratio – Sensor 507

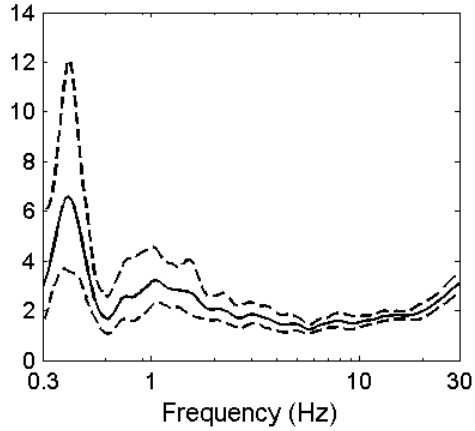

H/V Ratio – Sensor 453

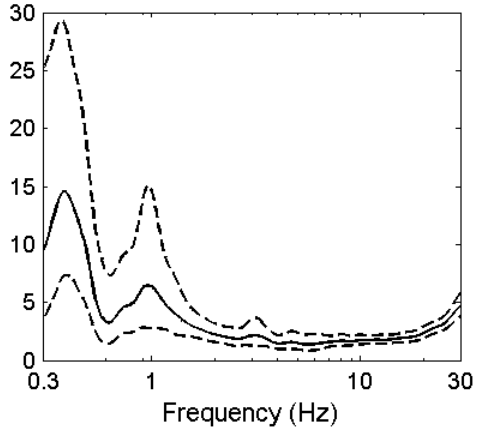

Equivalent Linear Transfer Function

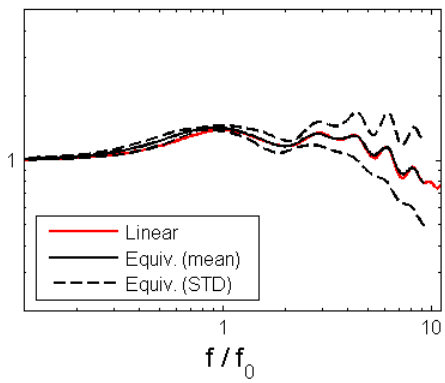

Equiv. Lin. TF (color coded by PGA_{RO})

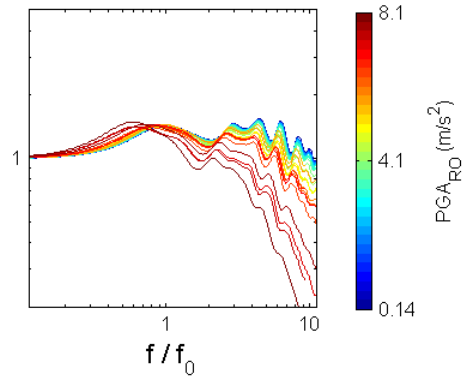

Non-linear Transfer Function

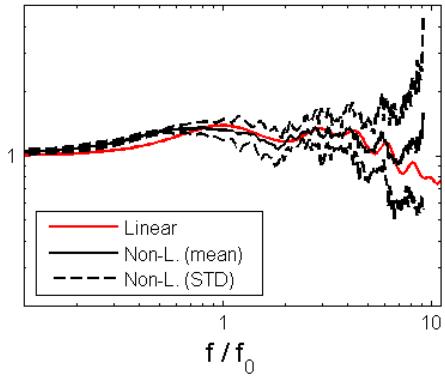

Non-linear TF (color coded by PGA_{RO})

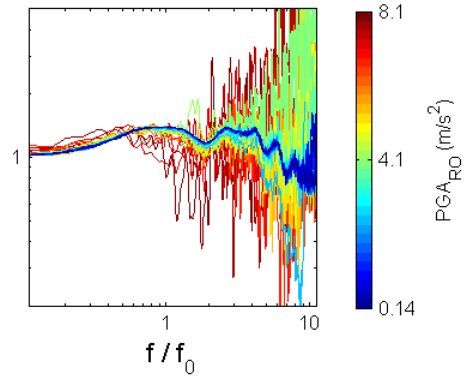

Equiv. Lin. TF (color coded by f_c)

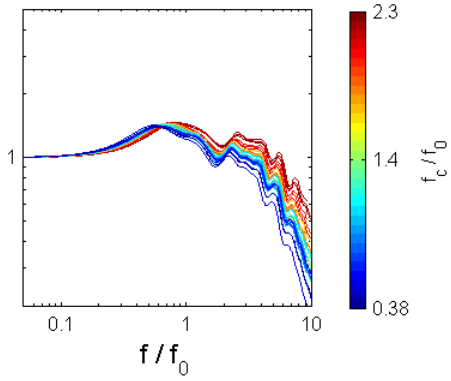

Non-linear TF (color coded by f_c)

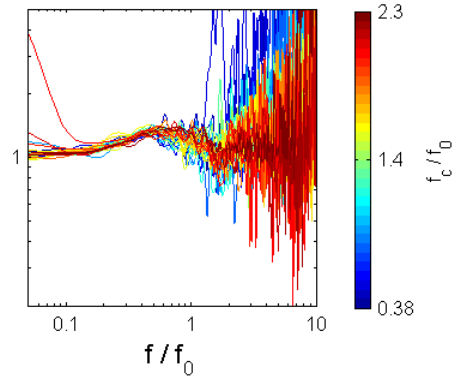

4.3.3 CE.13929

Depth (m)	Thickness (m)	V_s (m/s)	Damping ratio	Density (kg/m^3)
0	1	170	0.05	1600
1	5.75	235	0.05	1800
6.75	8	663	0.02	1800
14.75	8	988	0.01	2000
22.75	–	1489	0.01	2000

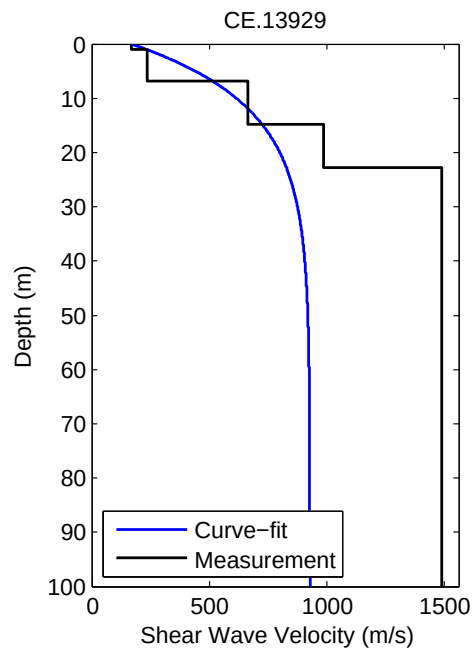

Linear Elastic Transfer Function

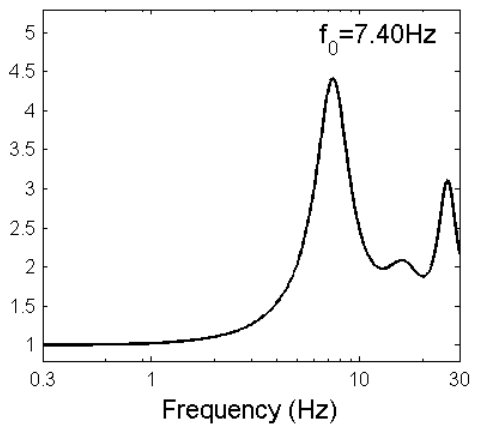

H/V Ratio – Sensor 450

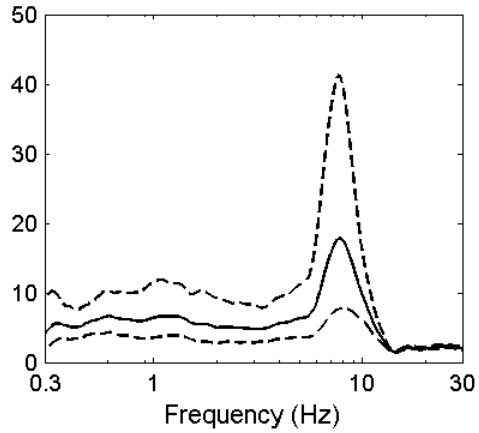

H/V Ratio – Sensor 507

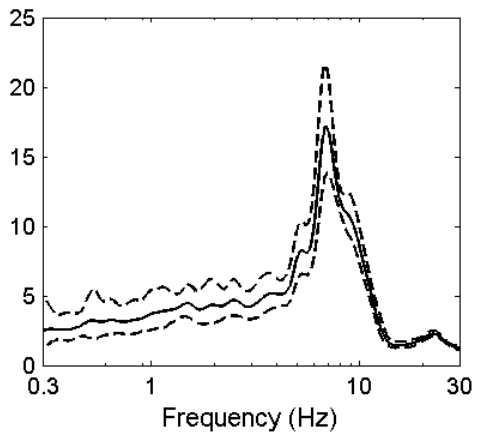

H/V Ratio – Sensor 453

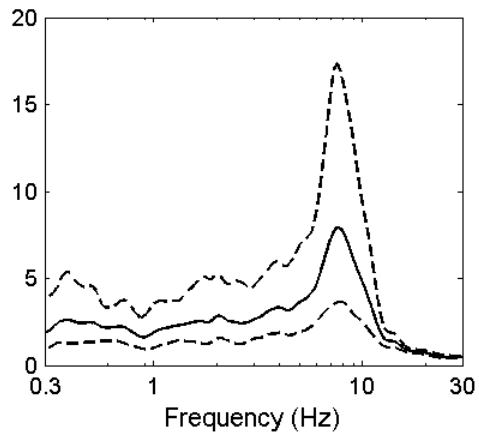

Equivalent Linear Transfer Function

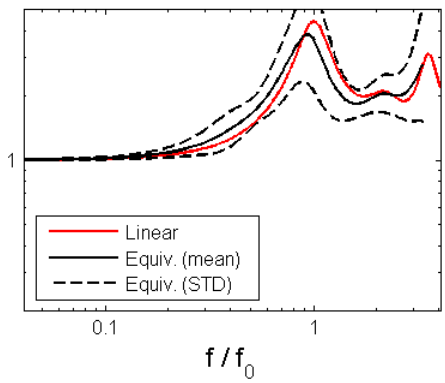

Equiv. Lin. TF (color coded by PGA_{RO})

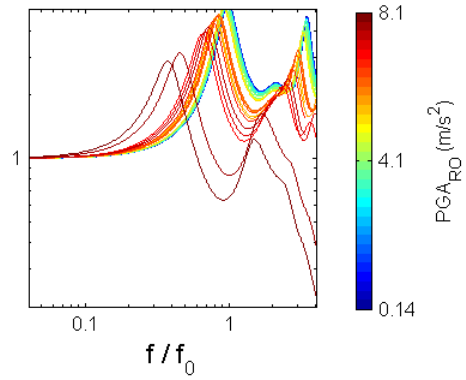

Non-linear Transfer Function

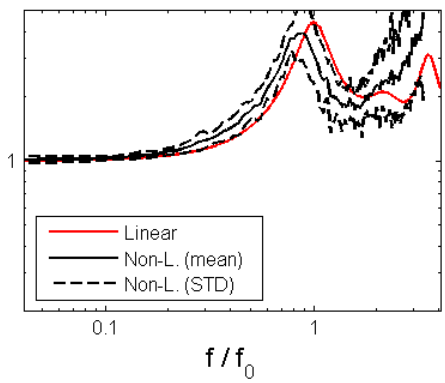

Non-linear TF (color coded by PGA_{RO})

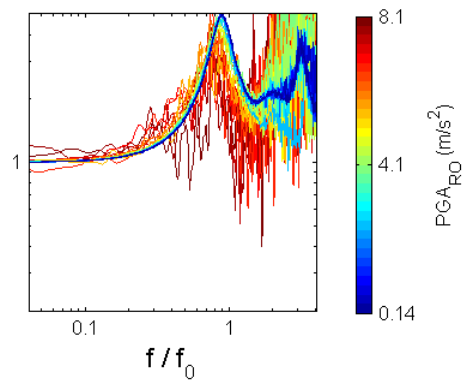

Equiv. Lin. TF (color coded by f_c)

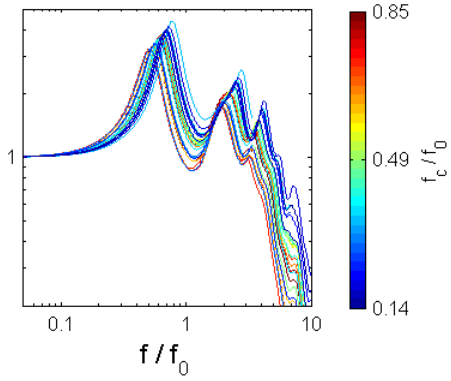

Non-linear TF (color coded by f_c)

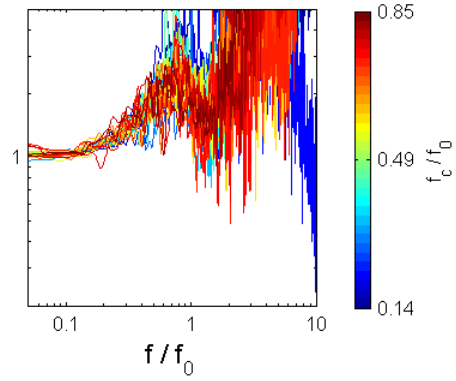

4.3.4 CE.23063a

Depth (m)	Thickness (m)	V_s (m/s)	Damping ratio	Density (kg/m^3)
0	4	349	0.02	1800
4	6	421	0.02	1800
10	14	533	0.02	1800
24	11	751	0.01	1800
35	5	760.9	0.01	1800
40	5	781.1	0.01	1800
45	5	797.5	0.01	1800
50	5	810.8	0.01	2000
55	5	821.6	0.01	2000
60	5	830.3	0.01	2000
65	5	837.4	0.01	2000
70	5	843.1	0.01	2000
75	5	847.7	0.01	2000
80	5	851.5	0.01	2000
85	5	854.5	0.01	2000
90	5	857.0	0.01	2000
95	5	858.9	0.01	2000
100	–	860.6	0.01	2000

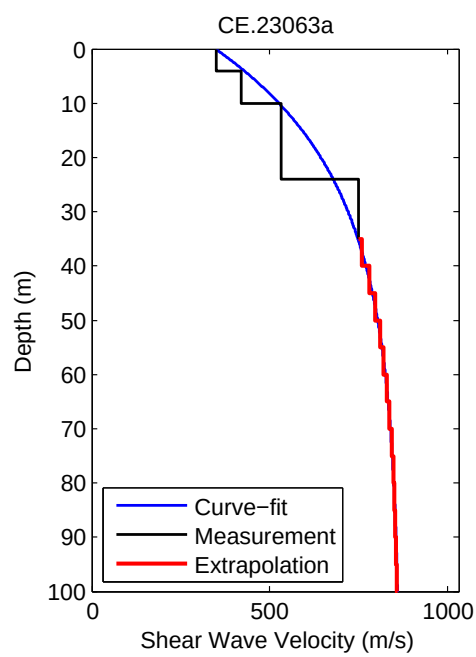

Linear Elastic Transfer Function

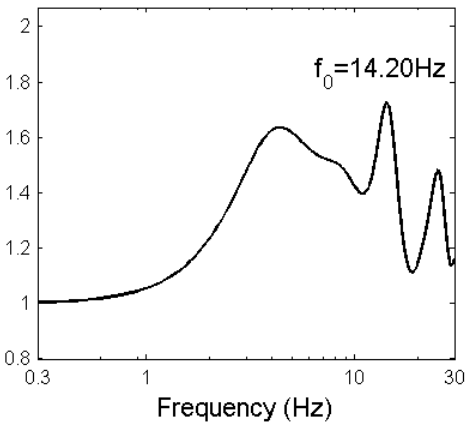

H/V Ratio – Sensor 450

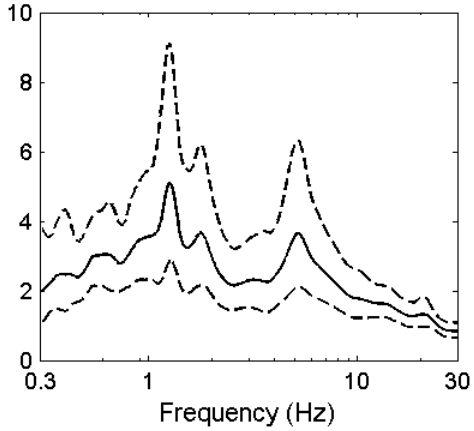

H/V Ratio – Sensor 507

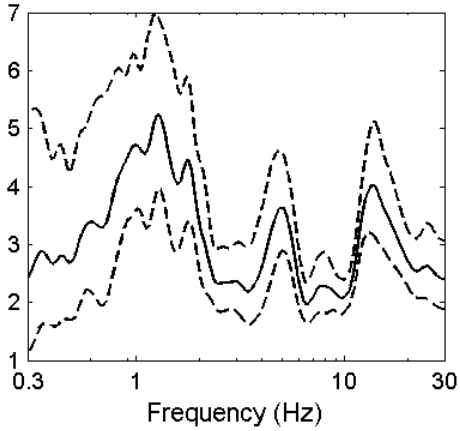

H/V Ratio – Sensor 453

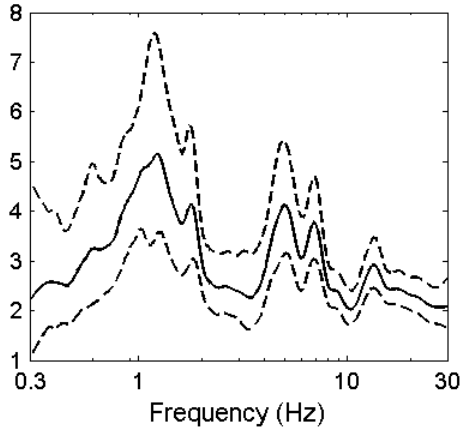

Equivalent Linear Transfer Function

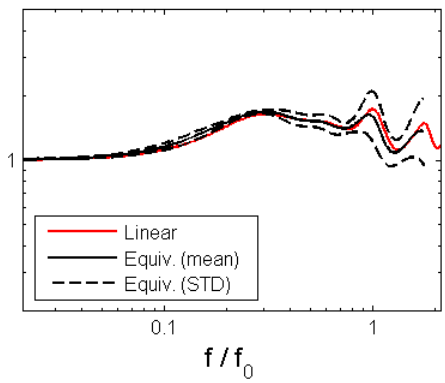

Equiv. Lin. TF (color coded by PGA_{RO})

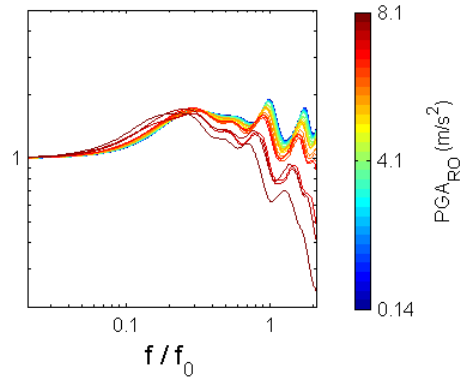

Non-linear Transfer Function

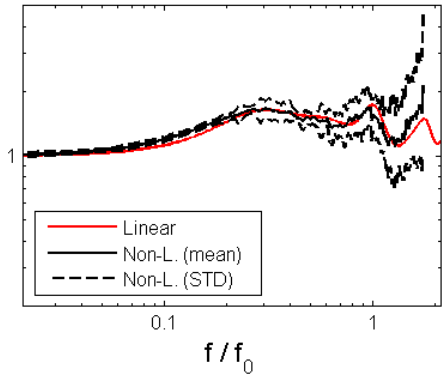

Non-linear TF (color coded by PGA_{RO})

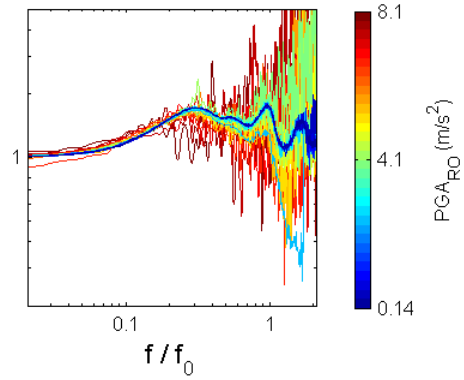

Equiv. Lin. TF (color coded by f_c)

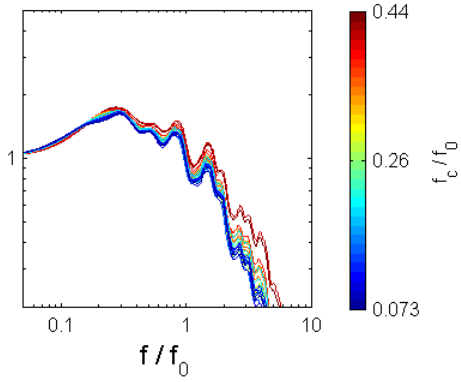

Non-linear TF (color coded by f_c)

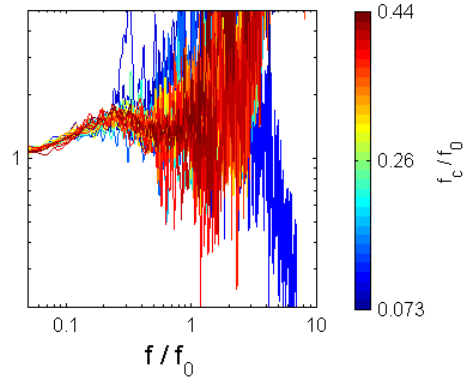

4.3.5 CE.23063b

Depth (m)	Thickness (m)	V_s (m/s)	Damping ratio	Density (kg/m^3)
0	4	348	0.02	1800
4	6	421	0.02	1800
10	14	536	0.02	1800
24	20	859	0.01	2000
44	–	1186	0.01	2000

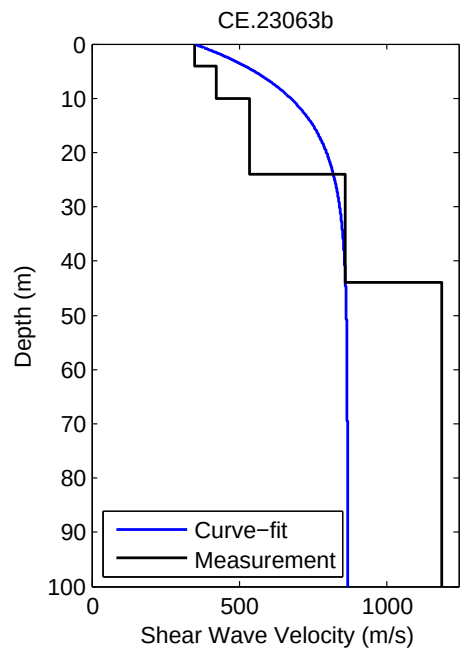

Linear Elastic Transfer Function

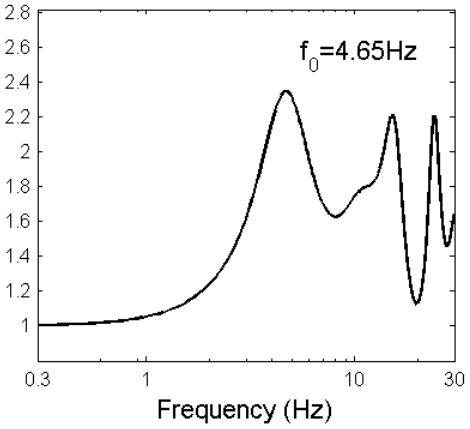

H/V Ratio – Sensor 450

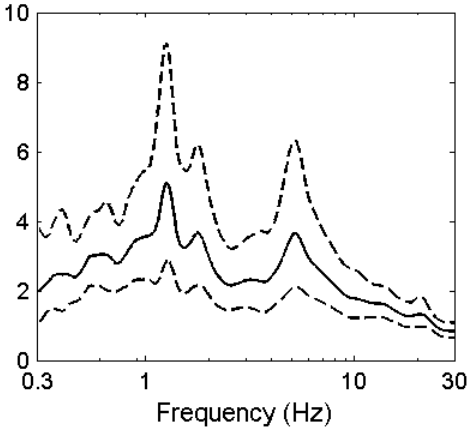

H/V Ratio – Sensor 507

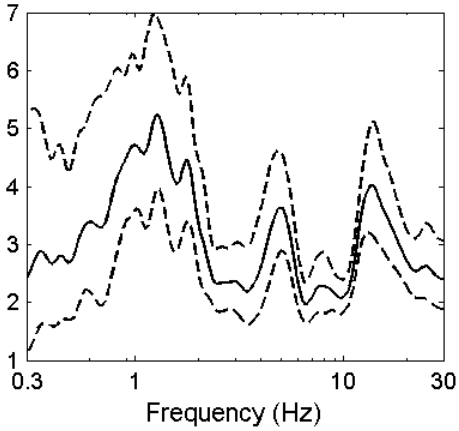

H/V Ratio – Sensor 453

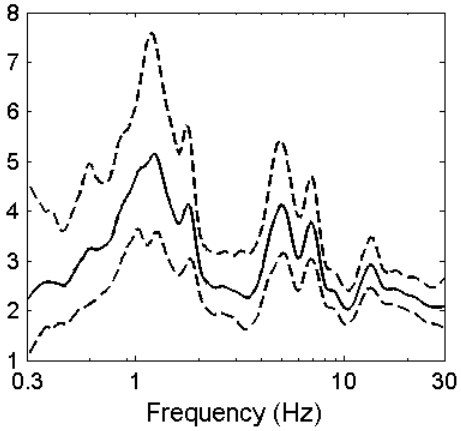

Equivalent Linear Transfer Function

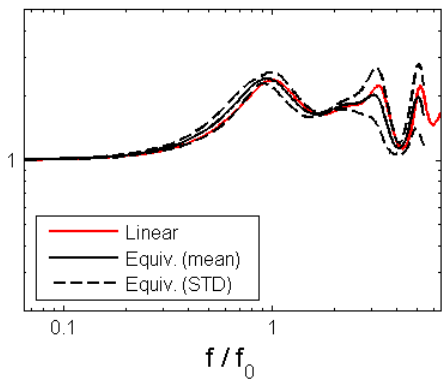

Equiv. Lin. TF (color coded by PGA_{RO})

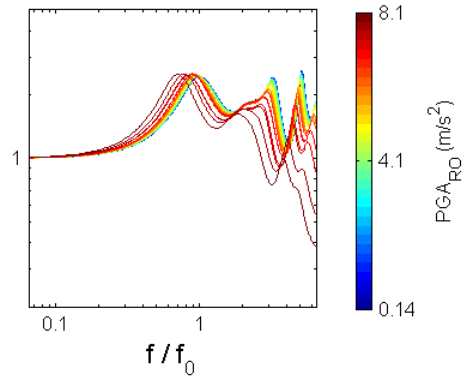

Non-linear Transfer Function

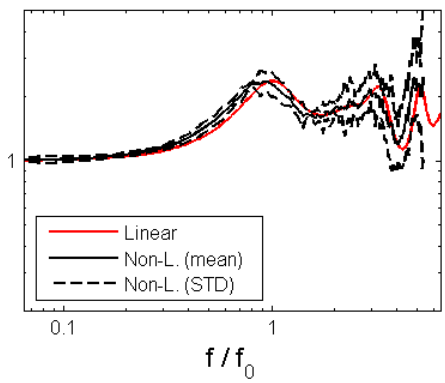

Non-linear TF (color coded by PGA_{RO})

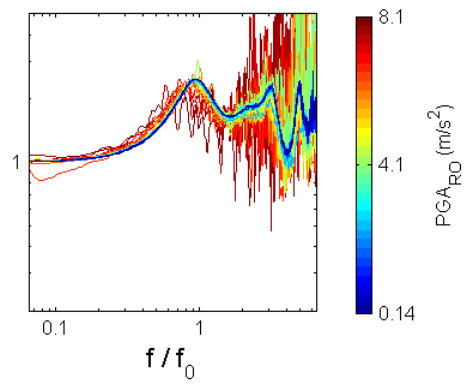

Equiv. Lin. TF (color coded by f_c)

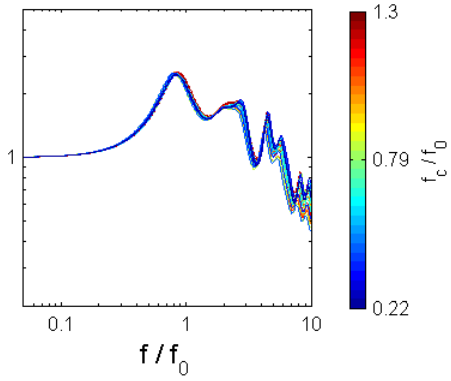

Non-linear TF (color coded by f_c)

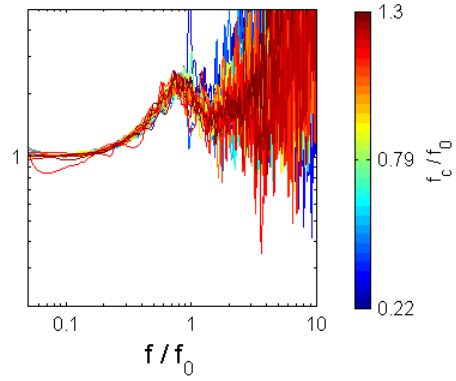

4.3.6 CE.23063c

Depth (m)	Thickness (m)	V_s (m/s)	Damping ratio	Density (kg/m^3)
0	4	348	0.02	1800
4	6	420	0.02	1800
10	14	538	0.02	1800
24	20	832	0.01	2000
44	70	1212	0.01	2000
114	–	1890	0.01	2000

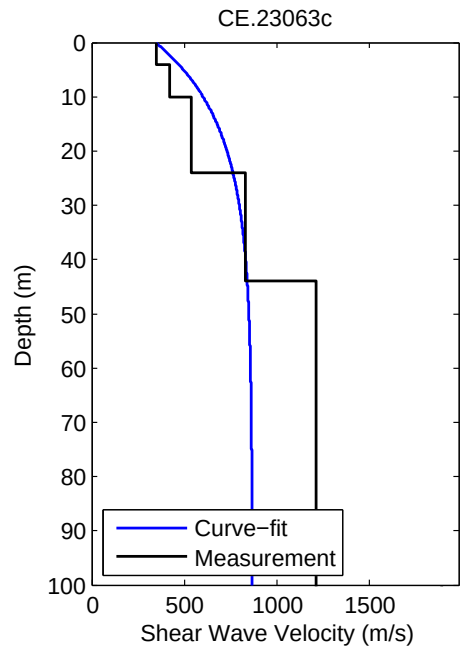

Linear Elastic Transfer Function

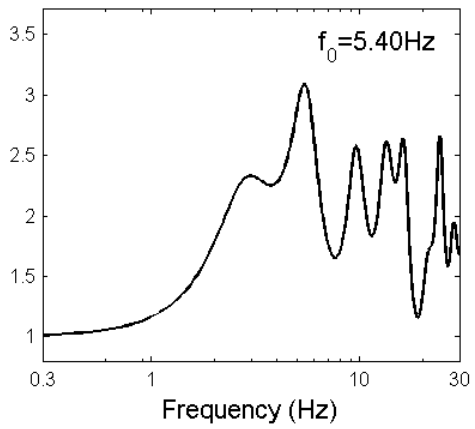

H/V Ratio – Sensor 450

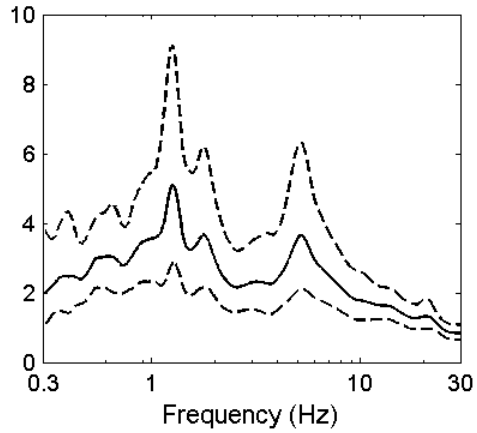

H/V Ratio – Sensor 507

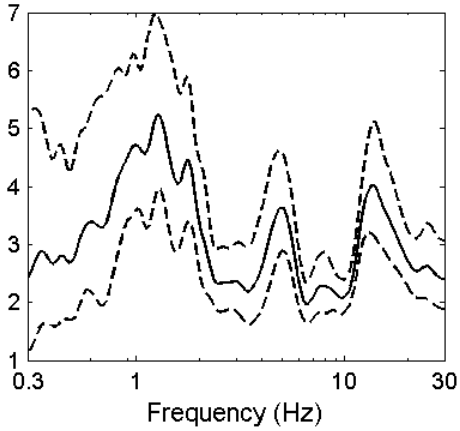

H/V Ratio – Sensor 453

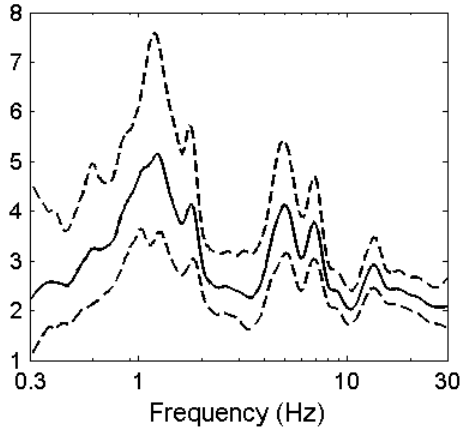

Equivalent Linear Transfer Function

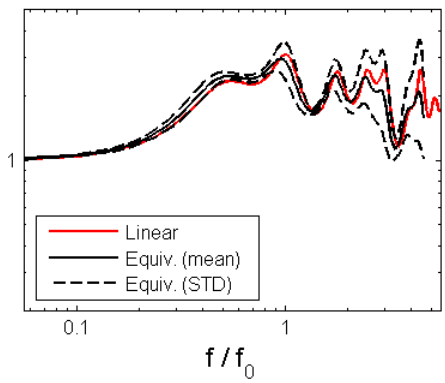

Equiv. Lin. TF (color coded by PGA_{RO})

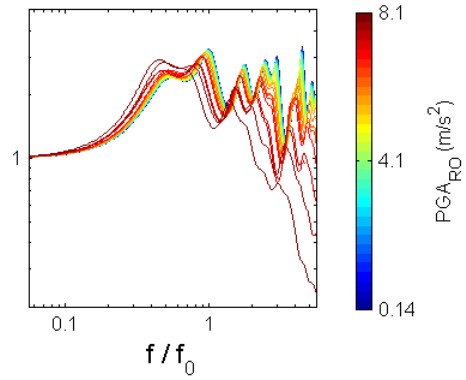

Non-linear Transfer Function

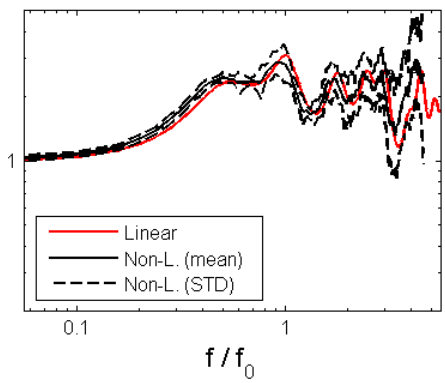

Non-linear TF (color coded by PGA_{RO})

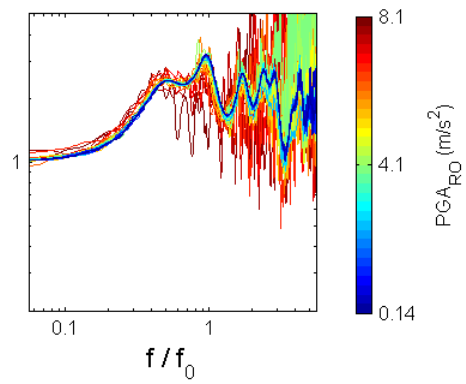

Equiv. Lin. TF (color coded by f_c)

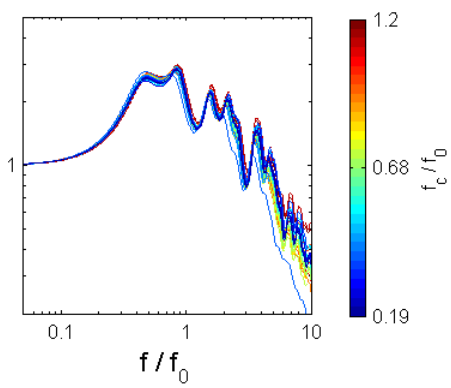

Non-linear TF (color coded by f_c)

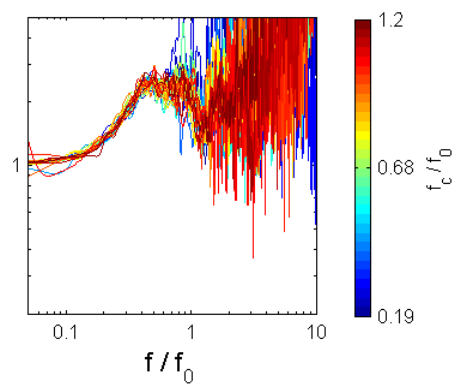

4.3.7 CE.24644a

Depth (m)	Thickness (m)	V_s (m/s)	Damping ratio	Density (kg/m^3)
0	1.5	194	0.05	1600
1.5	2.5	244	0.05	1800
4	3	312	0.02	1800
7	4	338	0.02	1800
11	6	354	0.02	1800
17	–	953	0.01	2000

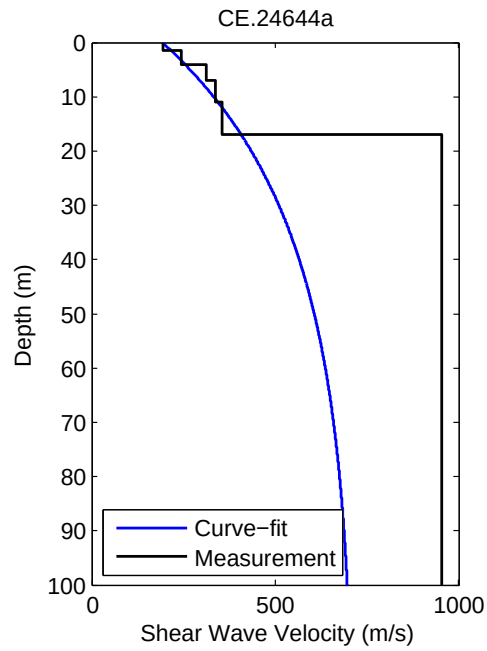

Linear Elastic Transfer Function

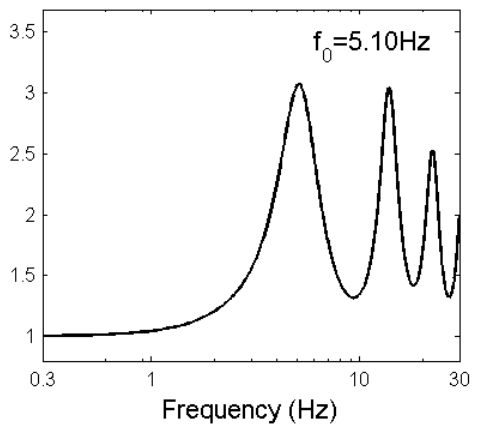

H/V Ratio – Sensor 450

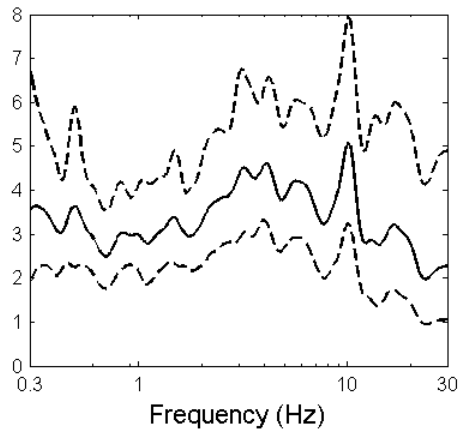

H/V Ratio – Sensor 507

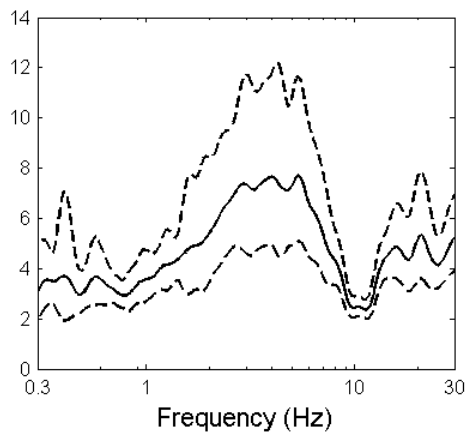

Equivalent Linear Transfer Function

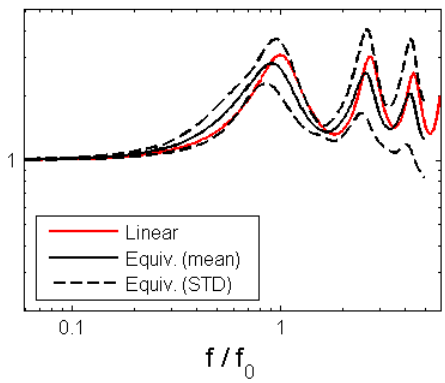

Equiv. Lin. TF (color coded by PGA_{RO})

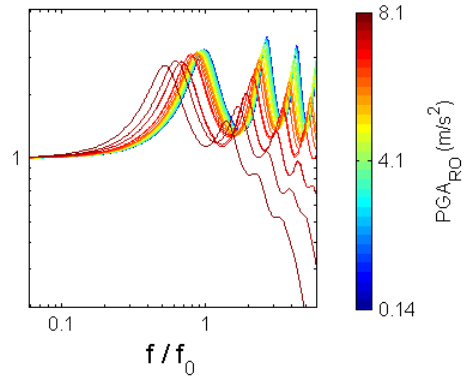

Non-linear Transfer Function

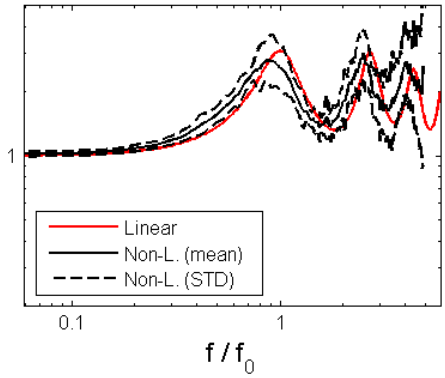

Non-linear TF (color coded by PGA_{RO})

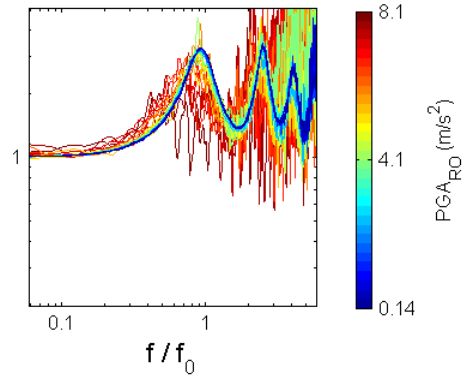

Equiv. Lin. TF (color coded by f_c)

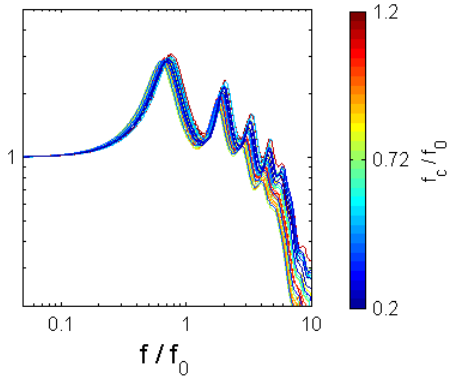

Non-linear TF (color coded by f_c)

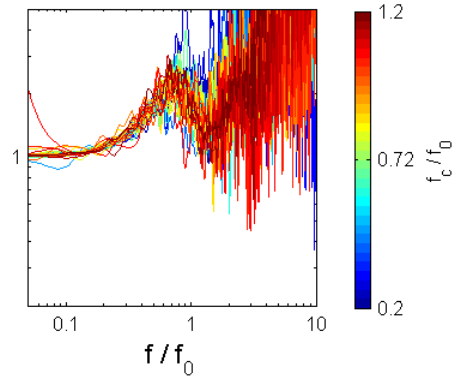

4.3.8 CE.24644b

Depth (m)	Thickness (m)	V_s (m/s)	Damping ratio	Density (kg/m^3)
0	1.5	196	0.05	1600
1.5	2.5	241	0.05	1800
4	9	321	0.02	1800
13	5	464	0.02	1800
18	7	700	0.02	1800
25	8	876	0.01	2000
33	–	1109	0.01	2000

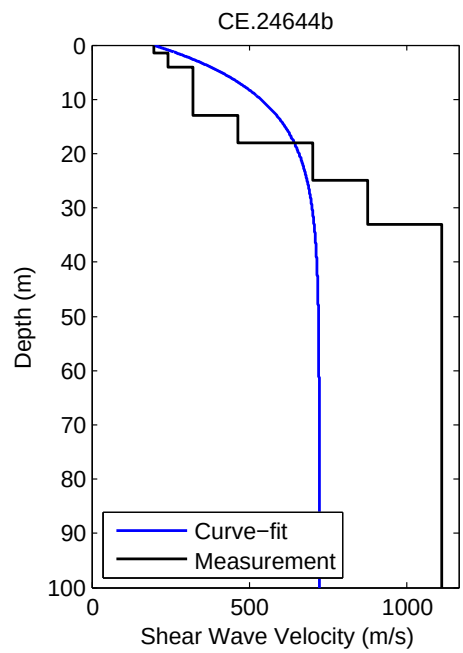

Linear Elastic Transfer Function

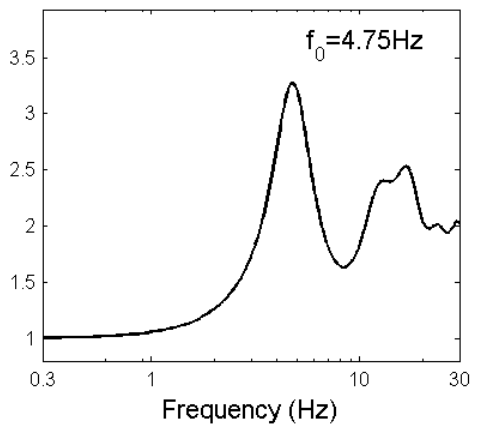

H/V Ratio – Sensor 450

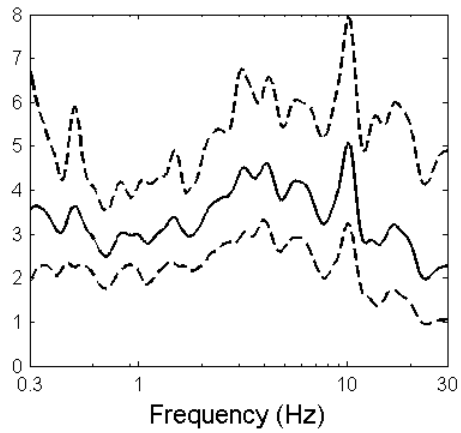

H/V Ratio – Sensor 507

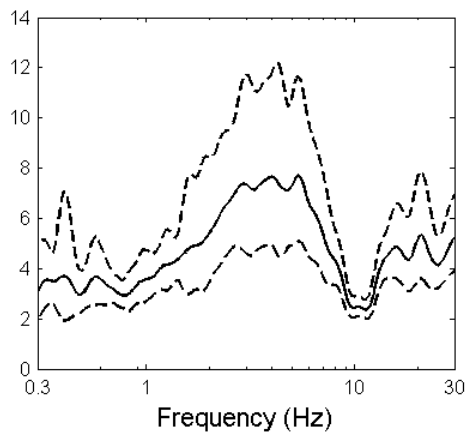

Equivalent Linear Transfer Function

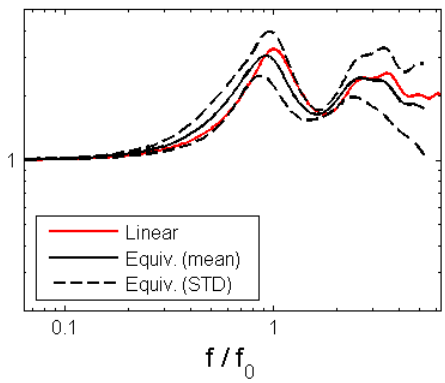

Equiv. Lin. TF (color coded by PGA_{RO})

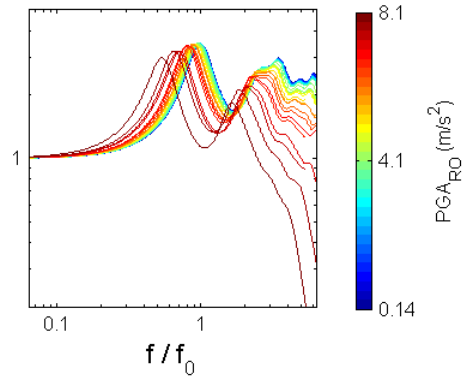

Non-linear Transfer Function

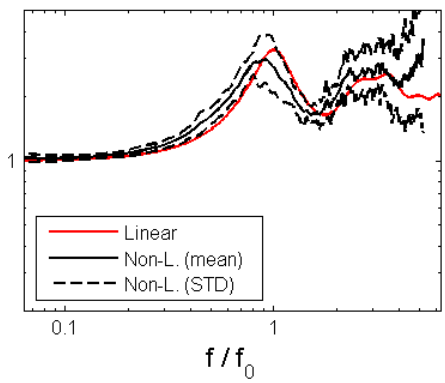

Non-linear TF (color coded by PGA_{RO})

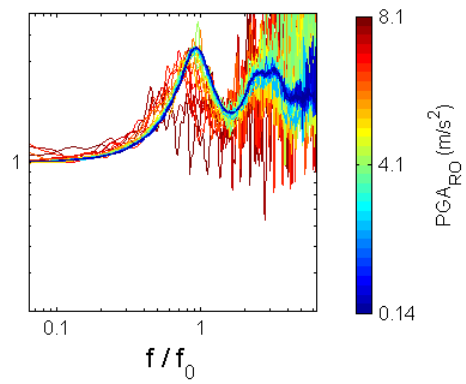

Equiv. Lin. TF (color coded by f_c)

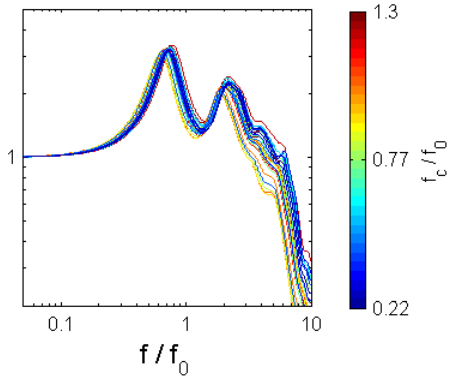

Non-linear TF (color coded by f_c)

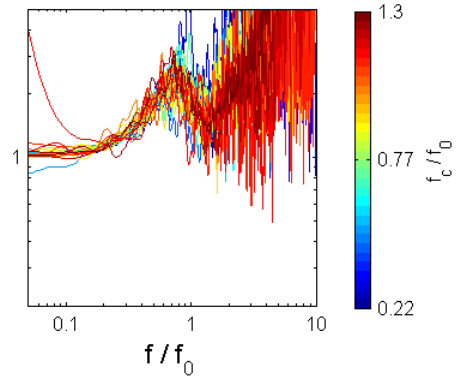

4.3.9 CI.ADO

Depth (m)	Thickness (m)	V_s (m/s)	Damping ratio	Density (kg/m^3)
0	1	187	0.05	1600
1	2	230	0.05	1800
3	2	326	0.02	1800
5	5	419	0.02	1800
10	5	531.0	0.02	1800
15	5	588.8	0.02	1800
20	5	625.0	0.02	1800
25	5	647.7	0.02	1800
30	5	661.9	0.02	1800
35	5	670.8	0.02	1800
40	5	676.4	0.02	1800
45	5	679.9	0.02	1800
50	5	682.1	0.02	1800
55	5	683.4	0.02	1800
60	5	684.3	0.02	1800
65	5	684.8	0.02	1800
70	5	685.2	0.02	1800
75	5	685.4	0.02	1800
80	5	685.5	0.02	1800
85	5	685.6	0.02	1800
90	5	685.6	0.02	1800
95	5	685.7	0.02	1800
100	–	685.7	0.02	1800

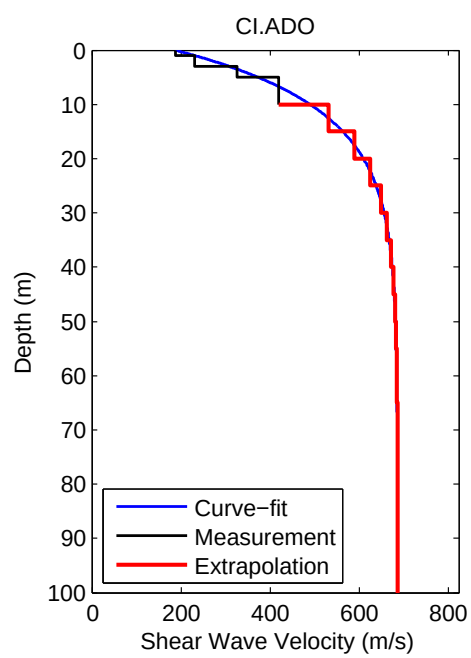

Linear Elastic Transfer Function

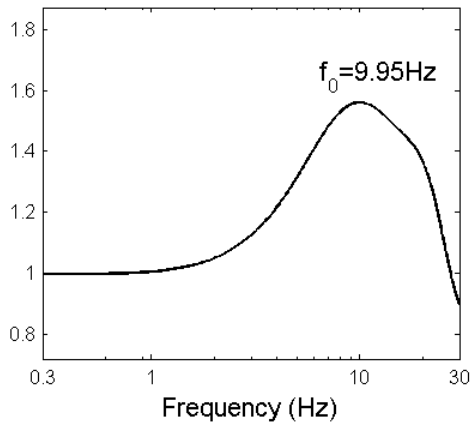

H/V Ratio – Sensor 450

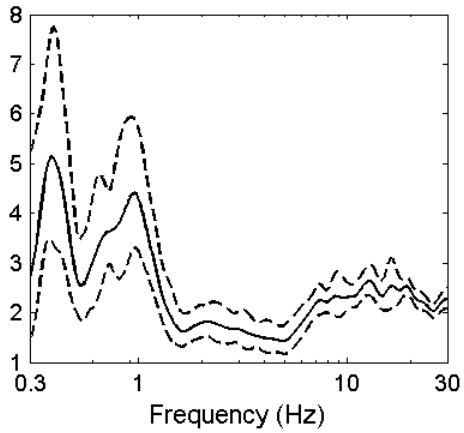

H/V Ratio – Sensor 507

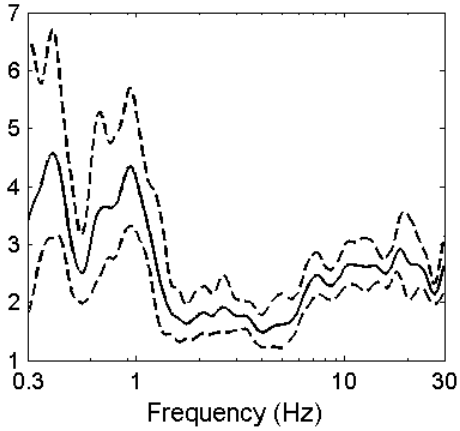

H/V Ratio – Sensor 453

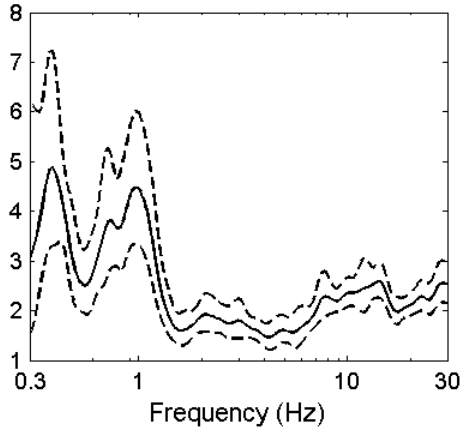

Equivalent Linear Transfer Function

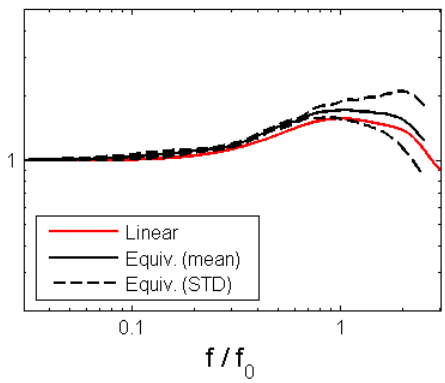

Equiv. Lin. TF (color coded by PGA_{RO})

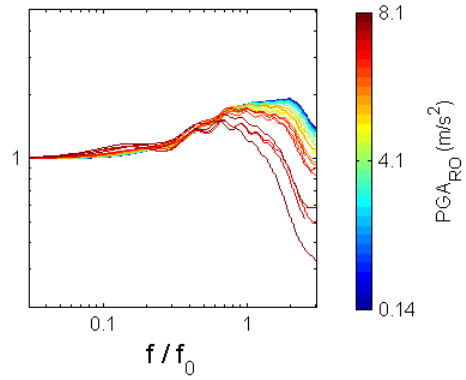

Non-linear Transfer Function

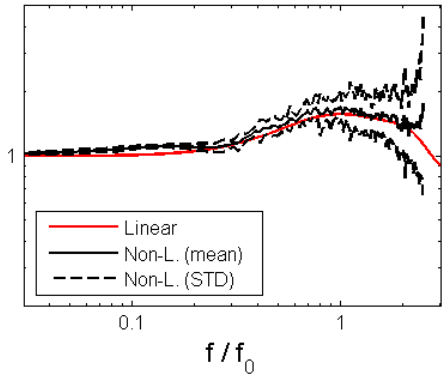

Non-linear TF (color coded by PGA_{RO})

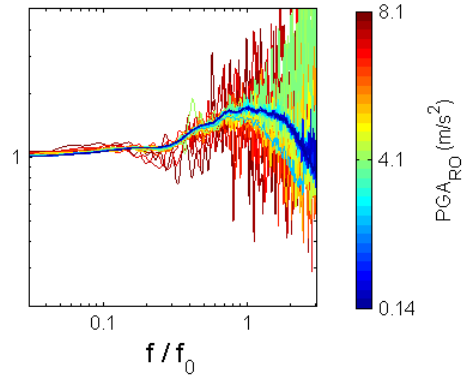

Equiv. Lin. TF (color coded by f_c)

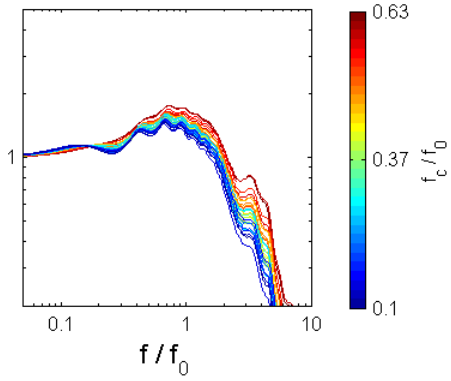

Non-linear TF (color coded by f_c)

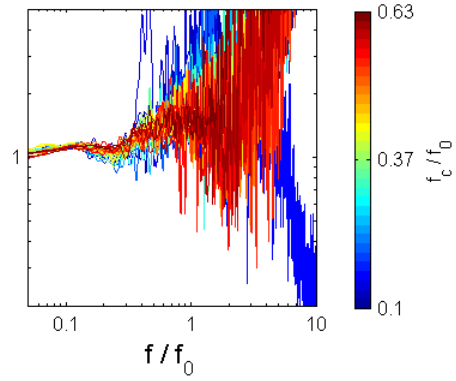

4.3.10 CI.BLA

Depth (m)	Thickness (m)	V_s (m/s)	Damping ratio	Density (kg/m^3)
0	1.5	167	0.05	1600
1.5	2	320	0.02	1800
3.5	4.5	404	0.02	1800
8	6	523	0.02	1800
14	8	745	0.02	1800
22	10	914	0.01	2000
32	–	1081	0.01	2000

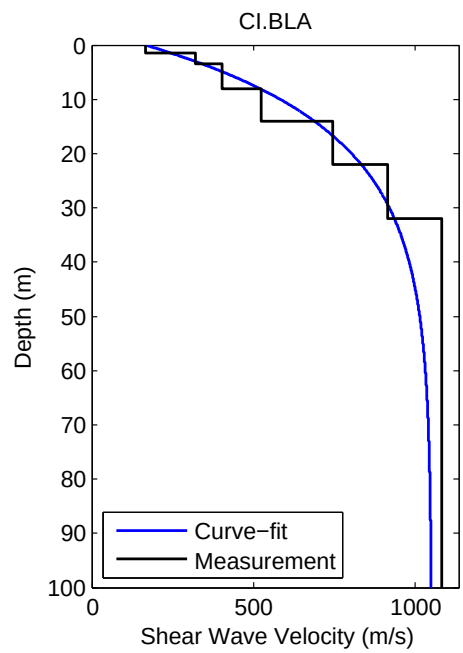

Linear Elastic Transfer Function

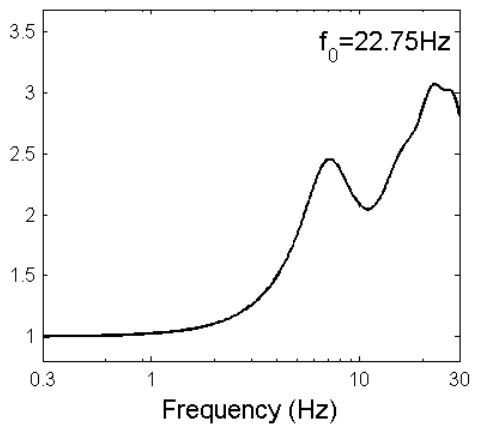

H/V Ratio – Sensor 450

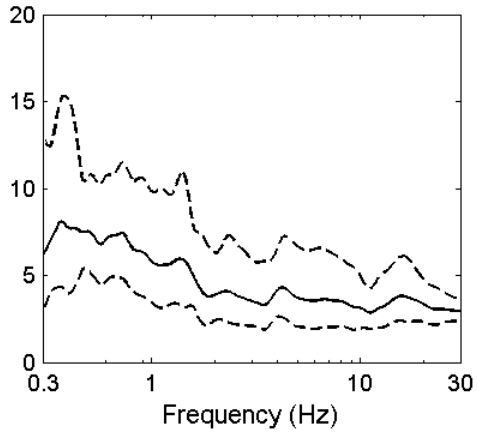

H/V Ratio – Sensor 507

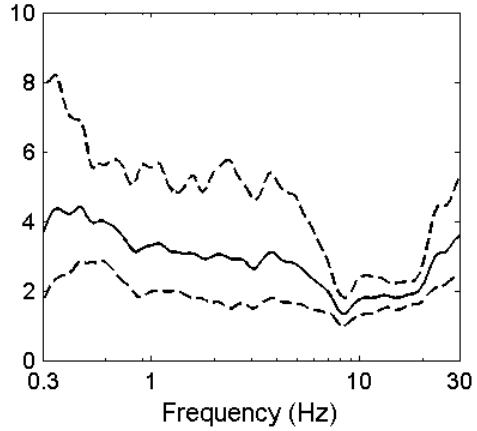

H/V Ratio – Sensor 453

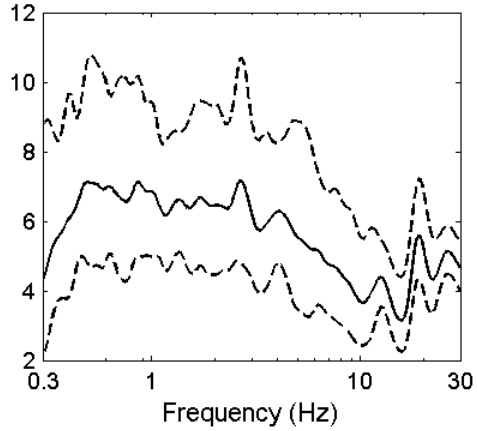

Equivalent Linear Transfer Function

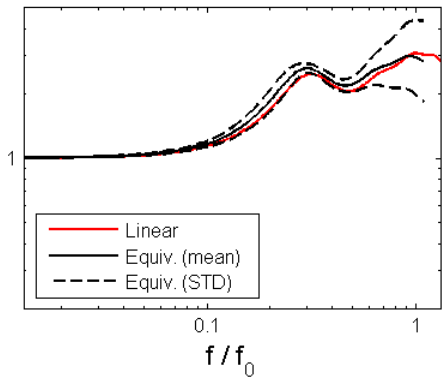

Equiv. Lin. TF (color coded by PGA_{RO})

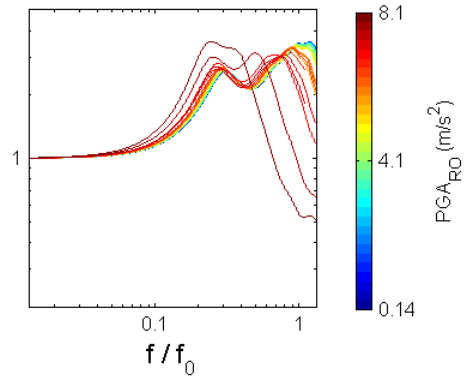

Non-linear Transfer Function

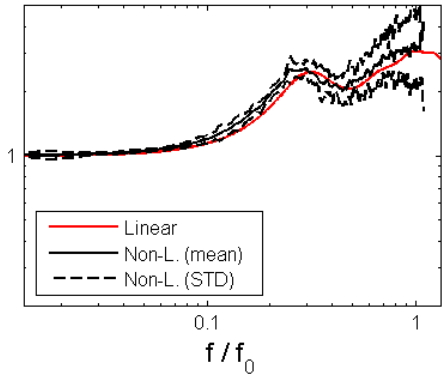

Non-linear TF (color coded by PGA_{RO})

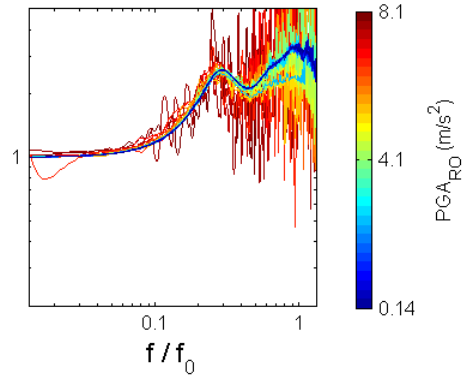

Equiv. Lin. TF (color coded by f_c)

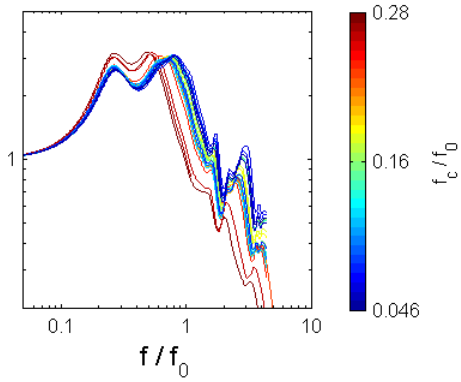

Non-linear TF (color coded by f_c)

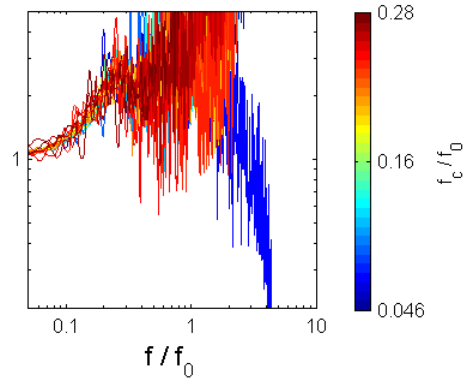

4.3.11 CI.CAC

Depth (m)	Thickness (m)	V_s (m/s)	Damping ratio	Density (kg/m^3)
0	1.5	186	0.05	1600
1.5	4	379	0.02	1800
5.5	8	416	0.02	1800
13.5	12	426	0.02	1800
25.5	15	492	0.02	1800
40.5	20	556	0.02	1800
60.5	25.3	623	0.02	1800
85.8	14.2	679	0.02	1800
100	–	685.2	0.02	1800

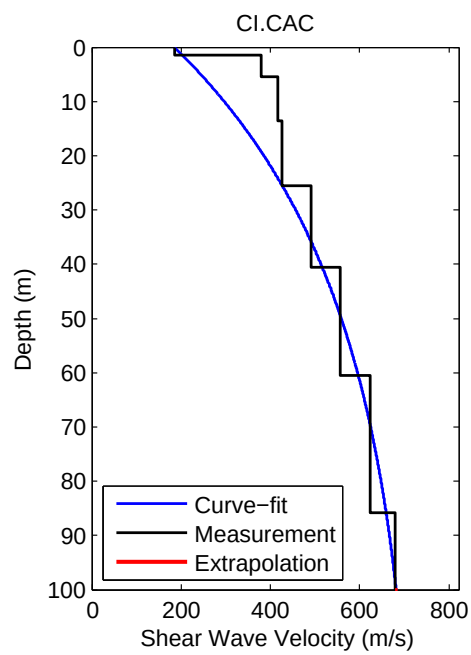

Linear Elastic Transfer Function

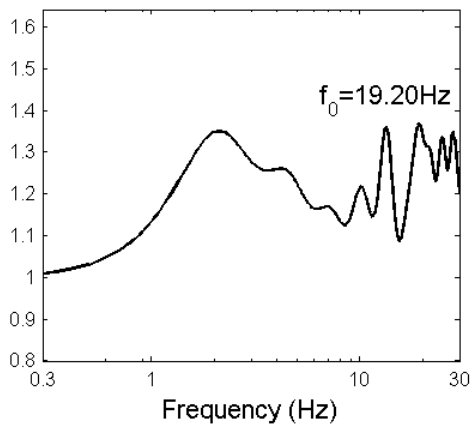

H/V Ratio – Sensor 453

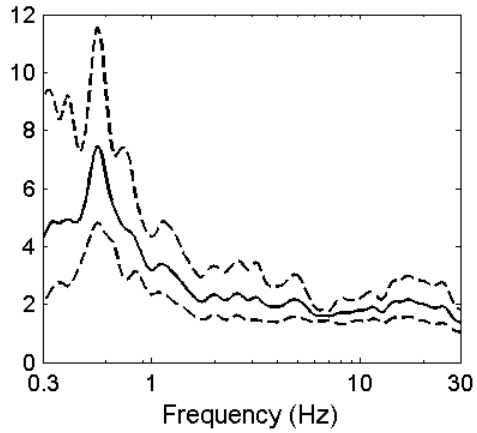

Equivalent Linear Transfer Function

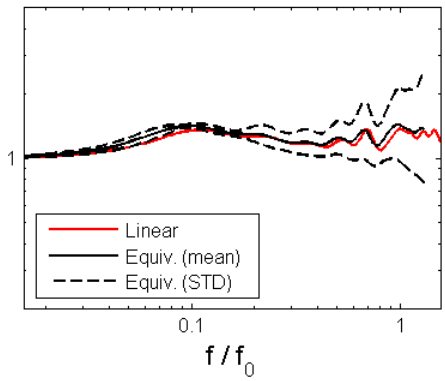

Equiv. Lin. TF (color coded by PGA_{RO})

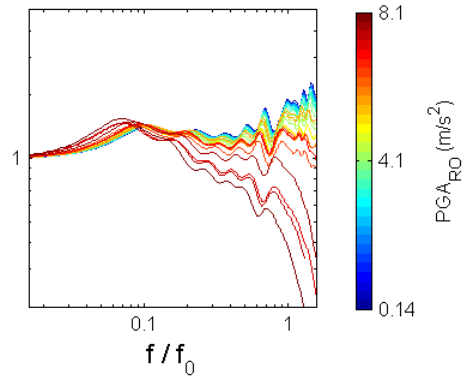

Non-linear Transfer Function

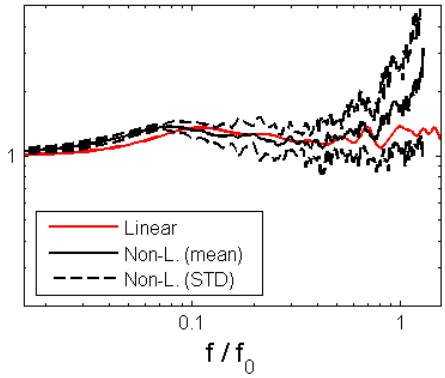

Non-linear TF (color coded by PGA_{RO})

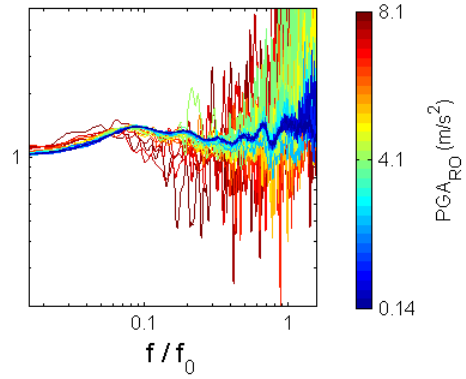

Equiv. Lin. TF (color coded by f_c)

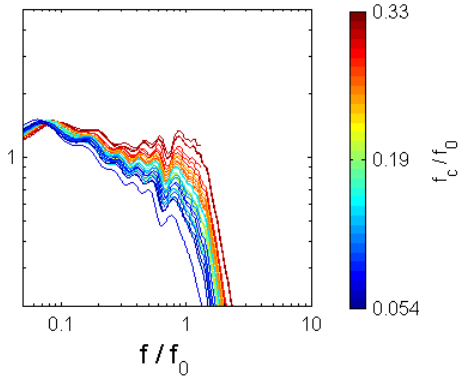

Non-linear TF (color coded by f_c)

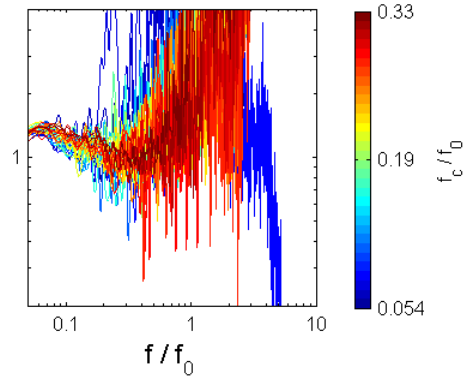

4.3.12 CI.CCC

Depth (m)	Thickness (m)	V_s (m/s)	Damping ratio	Density (kg/m^3)
0	1	164	0.05	1600
1	28	456	0.02	1800
29	11	509	0.02	1800
40	5	535.2	0.02	1800
45	5	560.8	0.02	1800
50	5	583.8	0.02	1800
55	5	604.5	0.02	1800
60	5	623.1	0.02	1800
65	5	639.9	0.02	1800
70	5	655.0	0.02	1800
75	5	668.6	0.02	1800
80	5	680.8	0.02	1800
85	5	691.8	0.02	1800
90	5	701.6	0.02	1800
95	5	710.5	0.02	1800
100	–	718.5	0.02	1800

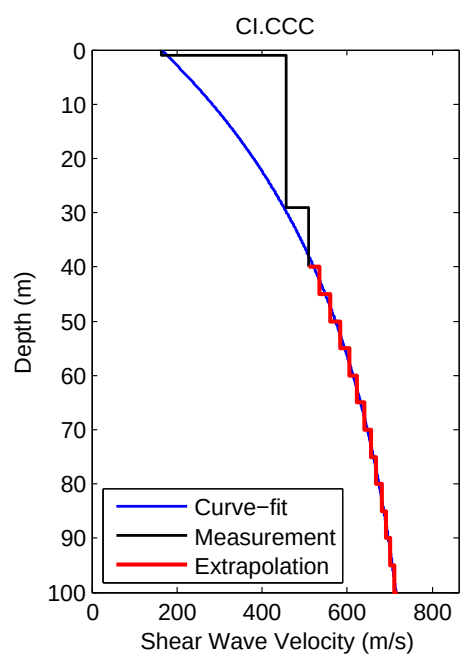

Linear Elastic Transfer Function

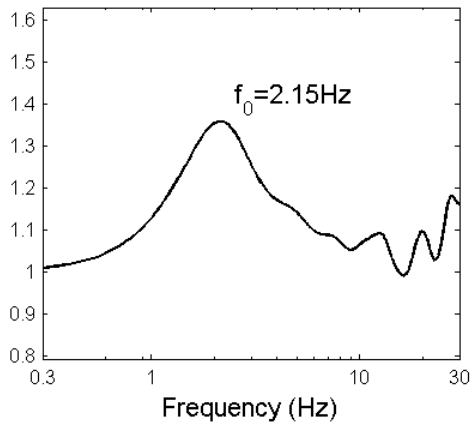

H/V Ratio – Sensor 450

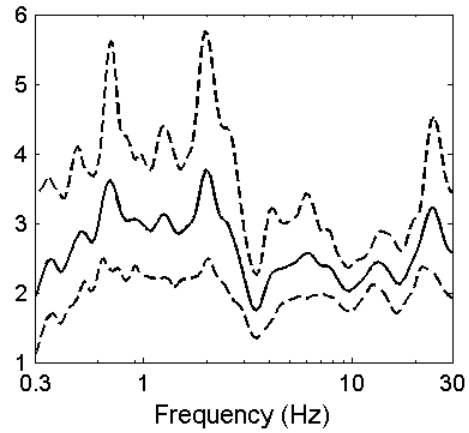

H/V Ratio – Sensor 507

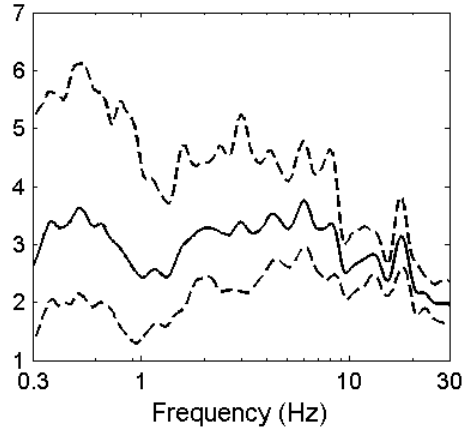

H/V Ratio – Sensor 453

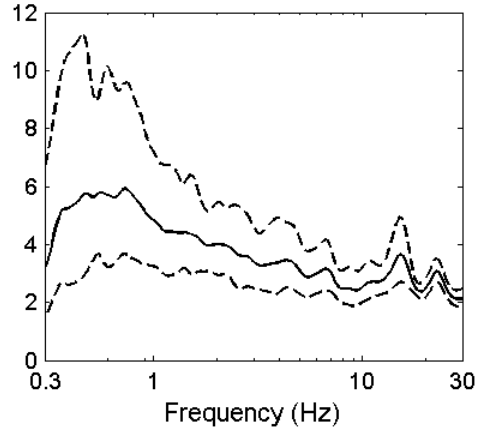

Equivalent Linear Transfer Function

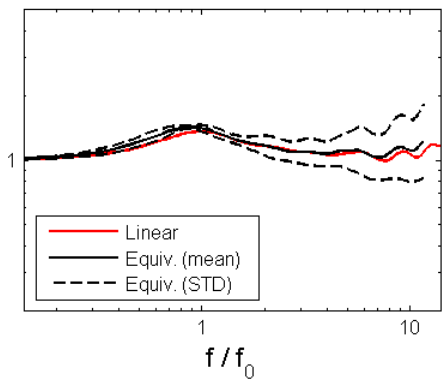

Equiv. Lin. TF (color coded by PGA_{RO})

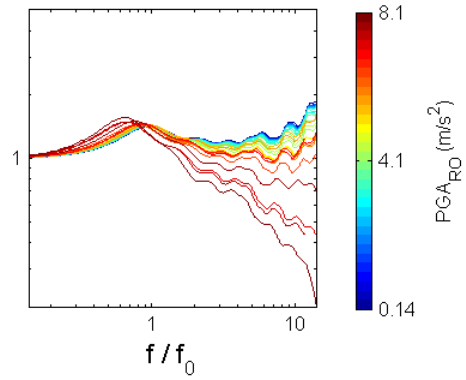

Non-linear Transfer Function

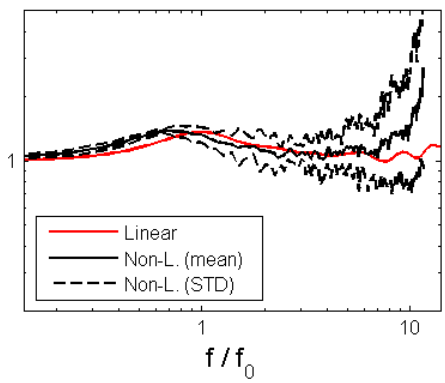

Non-linear TF (color coded by PGA_{RO})

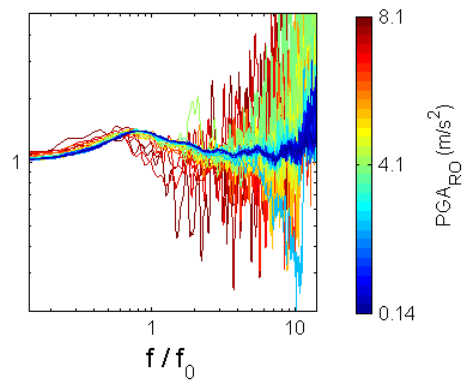

Equiv. Lin. TF (color coded by f_c)

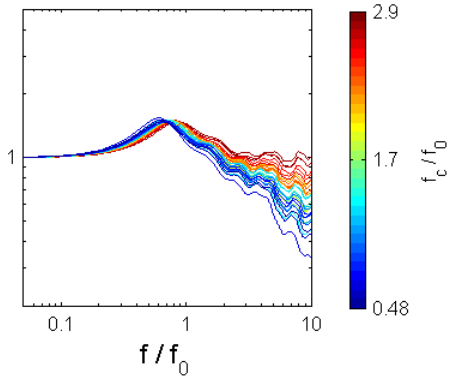

Non-linear TF (color coded by f_c)

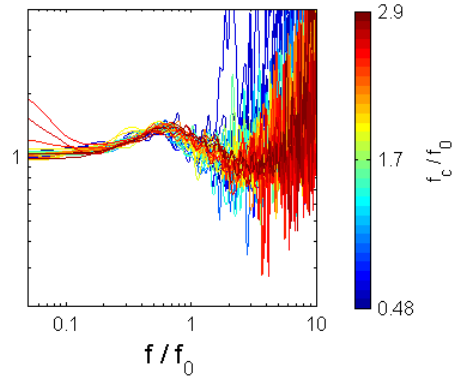

4.3.13 CI.CGO

Depth (m)	Thickness (m)	V_s (m/s)	Damping ratio	Density (kg/m^3)
0	1.5	427	0.02	1800
1.5	2.5	606	0.02	1800
4	4	659	0.02	1800
8	6	680	0.02	1800
14	9	734	0.02	1800
23	7	981	0.01	2000
30	5	1000.3	0.01	2000
35	5	1043.4	0.01	2000
40	5	1079.6	0.01	2000
45	5	1109.9	0.01	2000
50	5	1135.3	0.01	2000
55	5	1156.6	0.01	2000
60	5	1174.4	0.01	2000
65	5	1189.4	0.01	2000
70	5	1201.9	0.01	2000
75	5	1212.4	0.01	2000
80	5	1221.2	0.01	2000
85	5	1228.6	0.01	2000
90	5	1234.8	0.01	2000
95	5	1240.0	0.01	2000
100	–	1244.3	0.01	2000

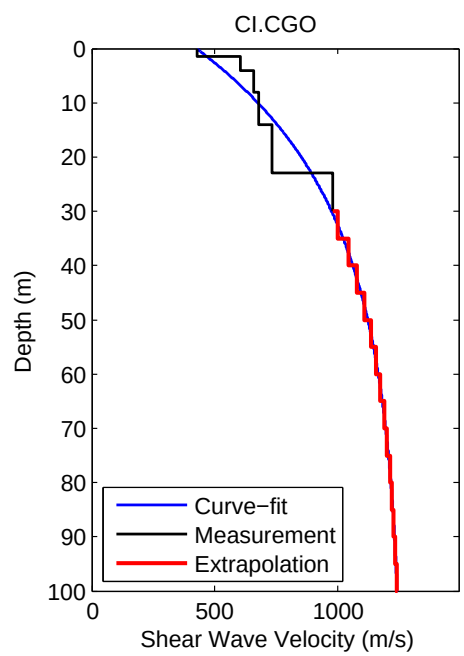

Linear Elastic Transfer Function

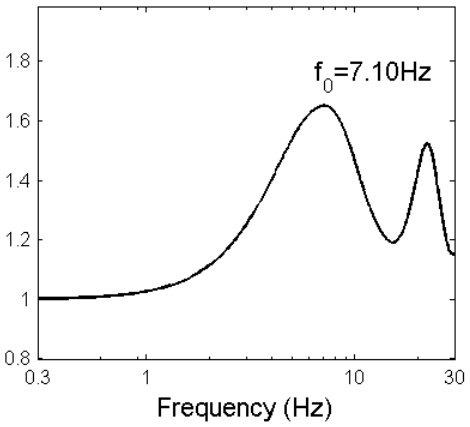

H/V Ratio – Sensor 450

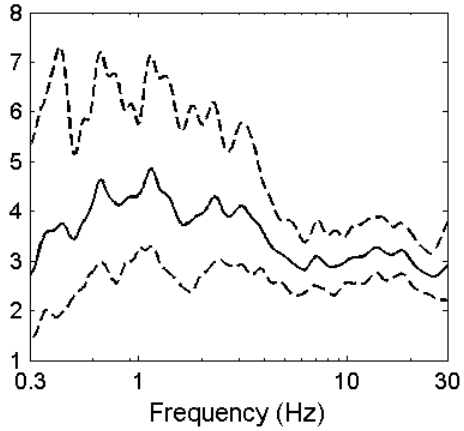

H/V Ratio – Sensor 507

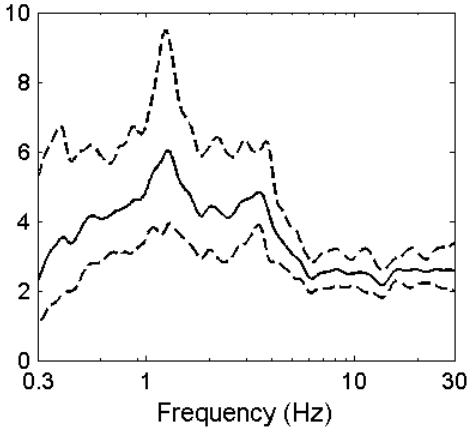

H/V Ratio – Sensor 453

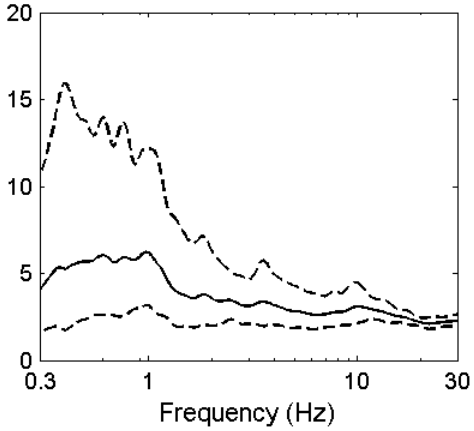

Equivalent Linear Transfer Function

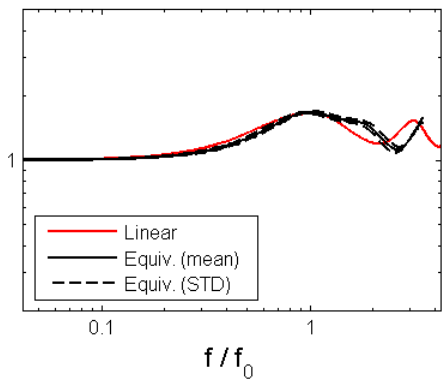

Equiv. Lin. TF (color coded by PGA_{RO})

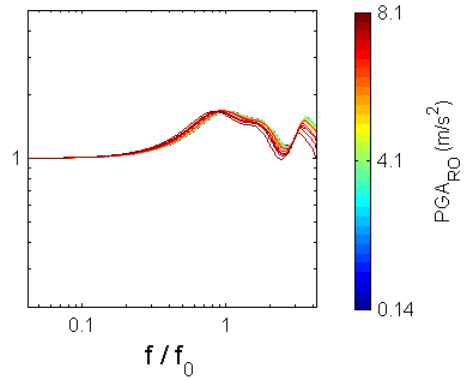

Non-linear Transfer Function

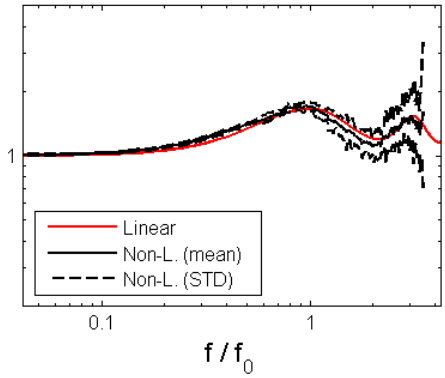

Non-linear TF (color coded by PGA_{RO})

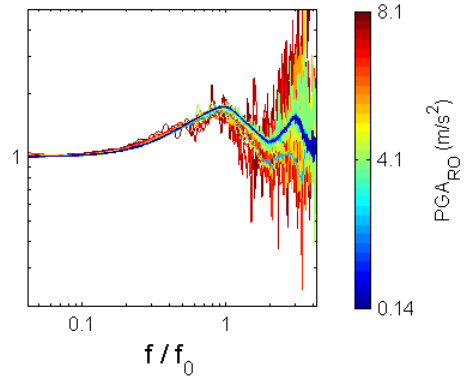

Equiv. Lin. TF (color coded by f_c)

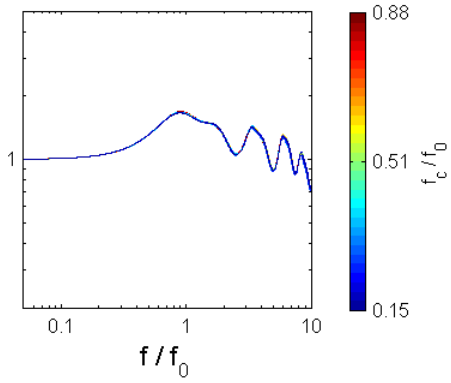

Non-linear TF (color coded by f_c)

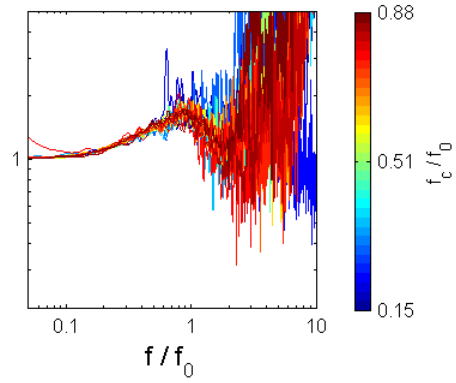

4.3.14 CI.CTC

Depth (m)	Thickness (m)	V_s (m/s)	Damping ratio	Density (kg/m^3)
0	1	185	0.05	1600
1	2	276	0.02	1800
3	3	310	0.02	1800
6	4	356	0.02	1800
10	6	372	0.02	1800
16	8	406	0.02	1800
24	6	519	0.02	1800
30	5	535.2	0.02	1800
35	5	560.0	0.02	1800
40	5	580.6	0.02	1800
45	5	597.6	0.02	1800
50	5	611.7	0.02	1800
55	5	623.3	0.02	1800
60	5	632.9	0.02	1800
65	5	640.8	0.02	1800
70	5	647.4	0.02	1800
75	5	652.9	0.02	1800
80	5	657.4	0.02	1800
85	5	661.1	0.02	1800
90	5	664.2	0.02	1800
95	5	666.7	0.02	1800
100	–	668.8	0.02	1800

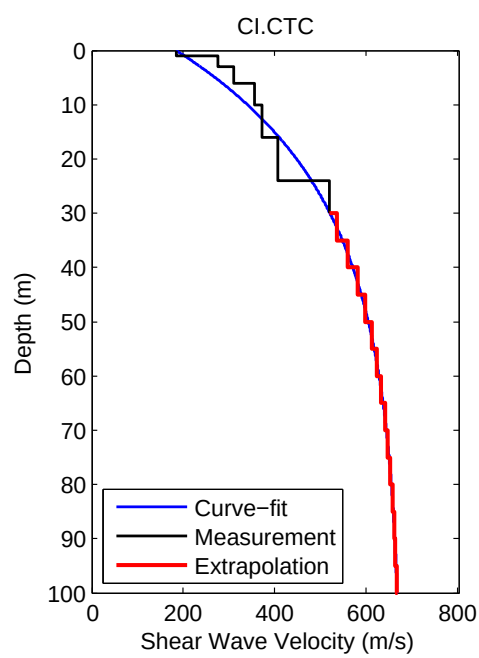

Linear Elastic Transfer Function

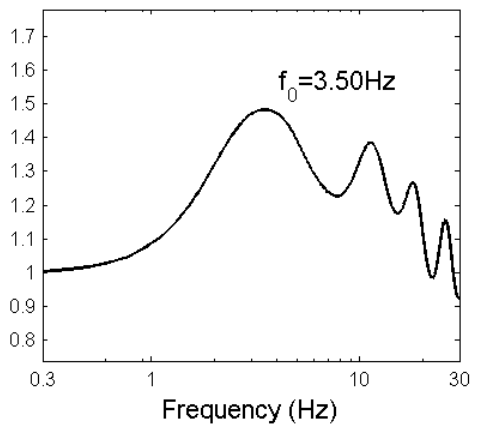

H/V Ratio – Sensor 450

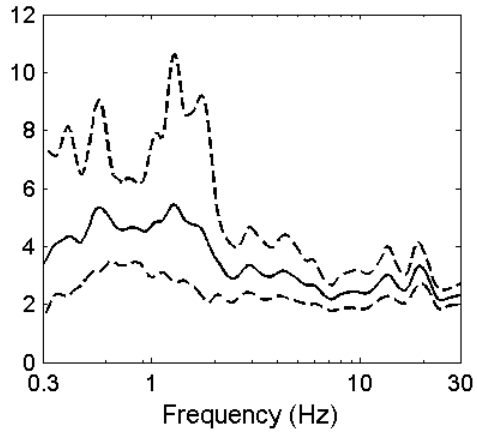

H/V Ratio – Sensor 507

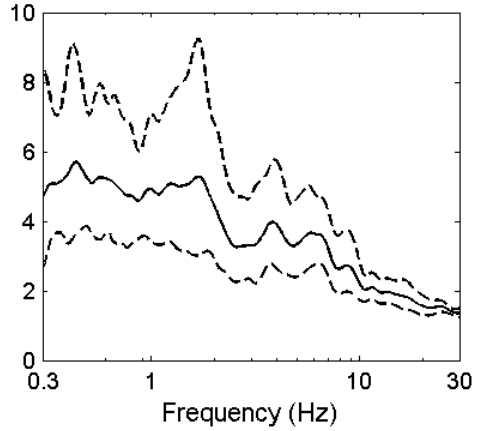

H/V Ratio – Sensor 453

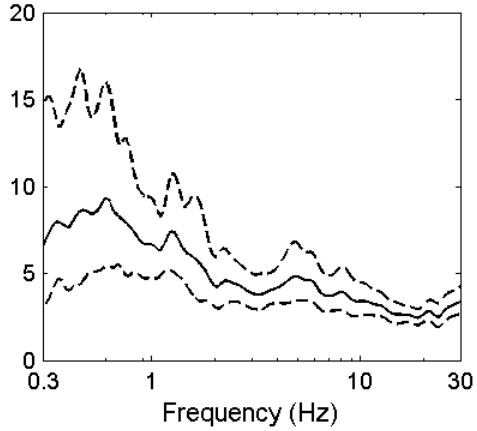

Equivalent Linear Transfer Function

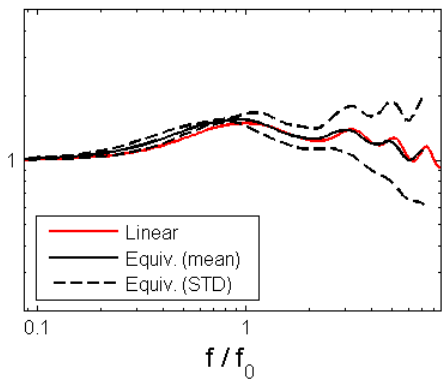

Equiv. Lin. TF (color coded by PGA_{RO})

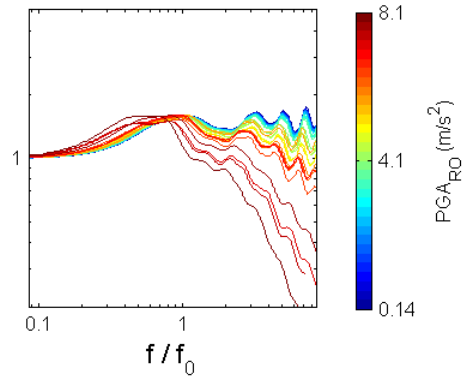

Non-linear Transfer Function

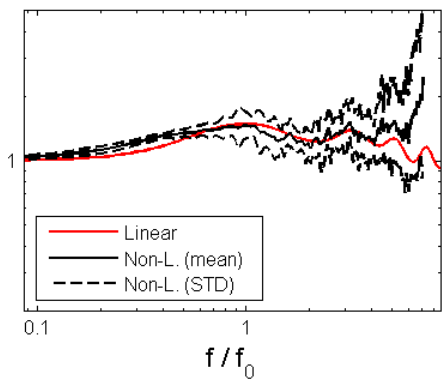

Non-linear TF (color coded by PGA_{RO})

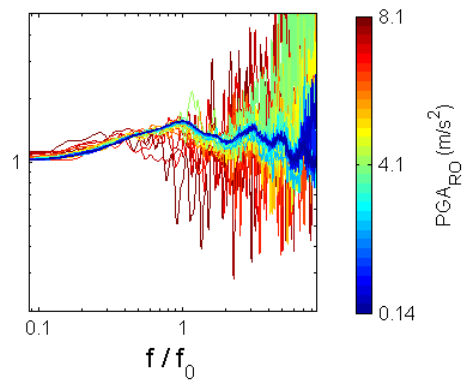

Equiv. Lin. TF (color coded by f_c)

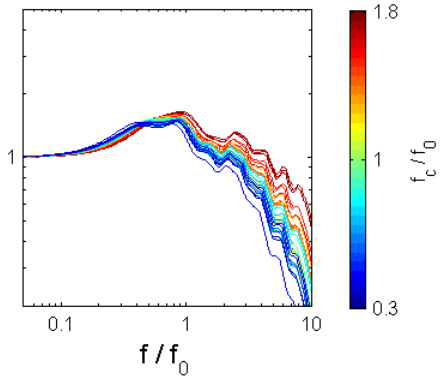

Non-linear TF (color coded by f_c)

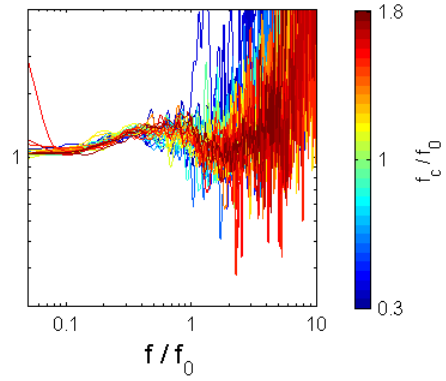

4.3.15 CI.CWC

Depth (m)	Thickness (m)	V_s (m/s)	Damping ratio	Density (kg/m^3)
0	1.5	361	0.02	1800
1.5	9.5	480	0.02	1800
11	11	539	0.02	1800
22	–	1081	0.01	2000

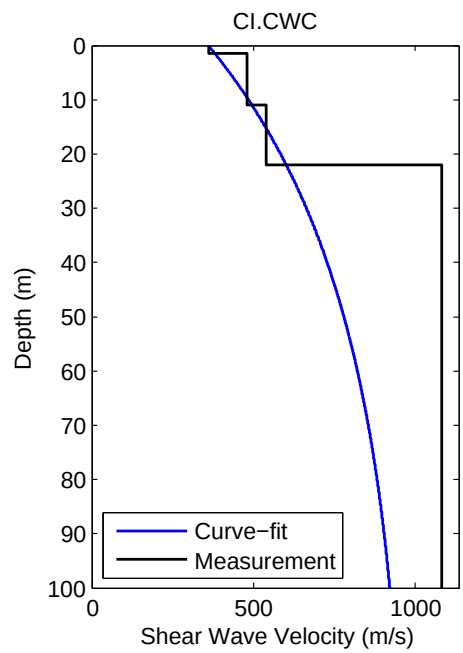

Linear Elastic Transfer Function

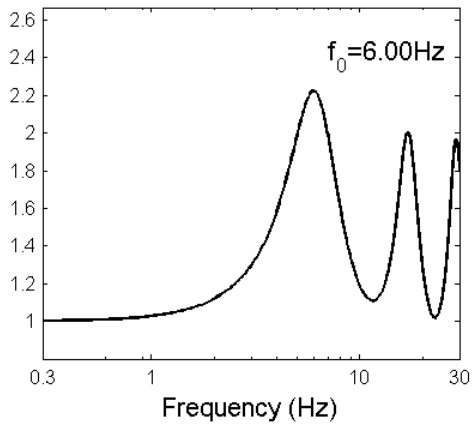

H/V Ratio – Sensor 450

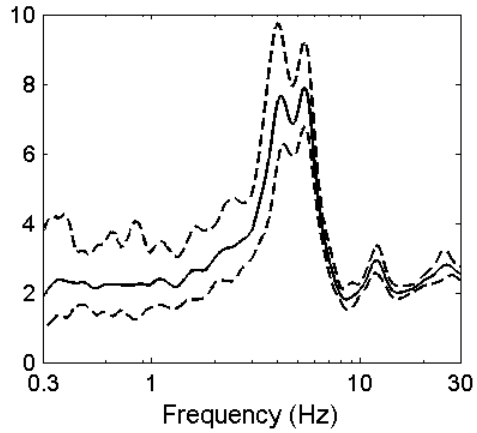

H/V Ratio – Sensor 507

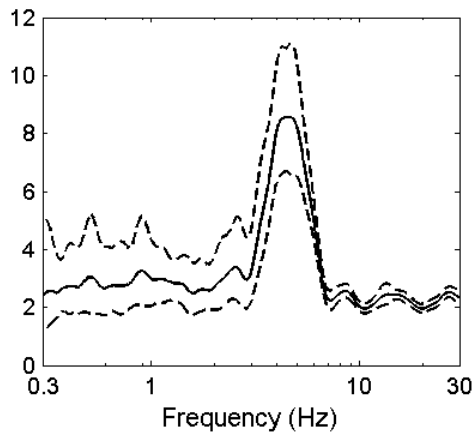

H/V Ratio – Sensor 453

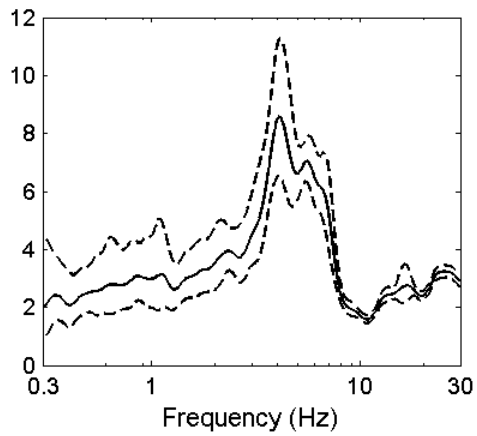

Equivalent Linear Transfer Function

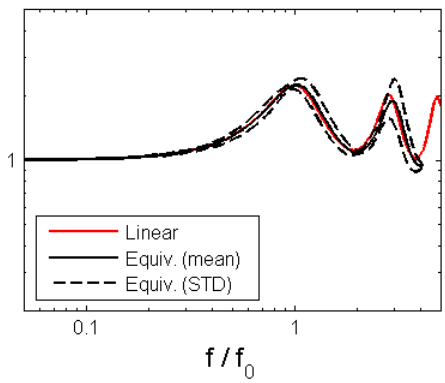

Equiv. Lin. TF (color coded by PGA_{RO})

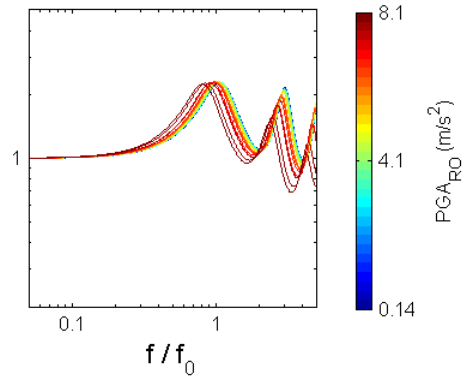

Non-linear Transfer Function

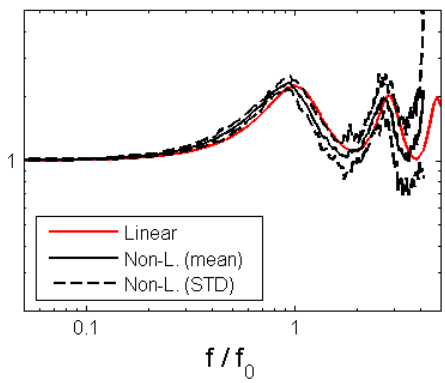

Non-linear TF (color coded by PGA_{RO})

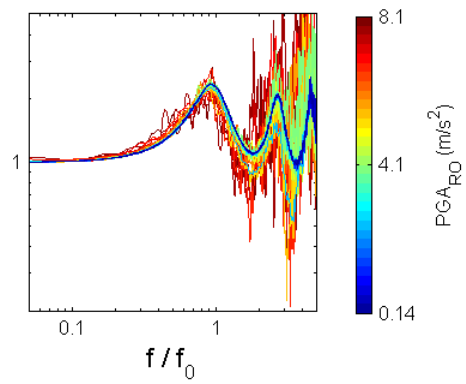

Equiv. Lin. TF (color coded by f_c)

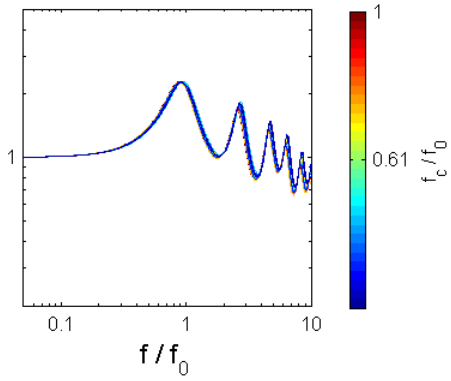

Non-linear TF (color coded by f_c)

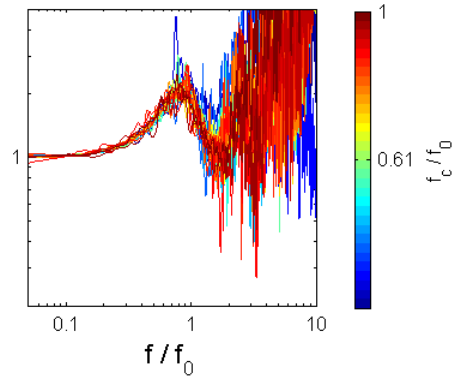

4.3.16 CI.DAN

Depth (m)	Thickness (m)	V_s (m/s)	Damping ratio	Density (kg/m^3)
0	0.5	154	0.05	1600
0.5	1.5	249	0.05	1800
2	3	361	0.02	1800
5	4	467	0.02	1800
9	6	508	0.02	1800
15	8	581	0.02	1800
23	12	629	0.02	1800
35	20	886	0.01	2000
55	5	889.5	0.01	2000
60	5	894.0	0.01	2000
65	5	897.2	0.01	2000
70	5	899.5	0.01	2000
75	5	901.1	0.01	2000
80	5	902.2	0.01	2000
85	5	903.1	0.01	2000
90	5	903.7	0.01	2000
95	5	904.1	0.01	2000
100	–	904.4	0.01	2000

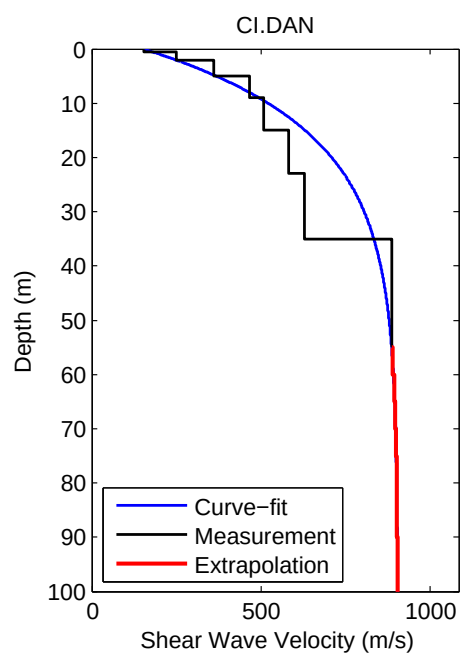

Linear Elastic Transfer Function

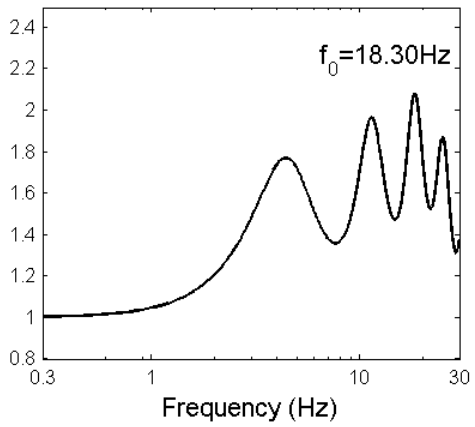

H/V Ratio – Sensor 450

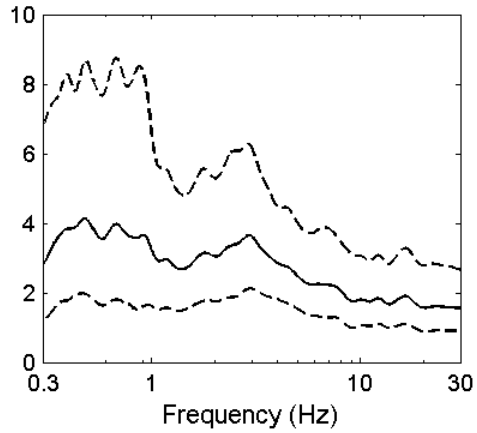

H/V Ratio – Sensor 507

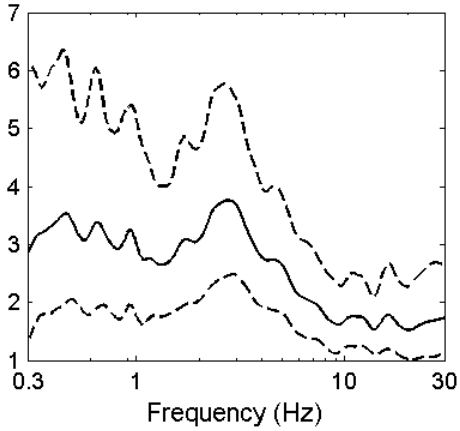

H/V Ratio – Sensor 453

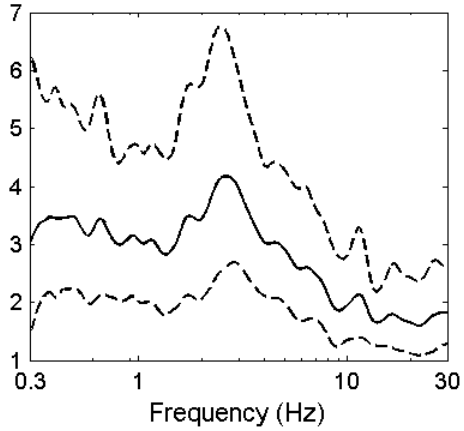

Equivalent Linear Transfer Function

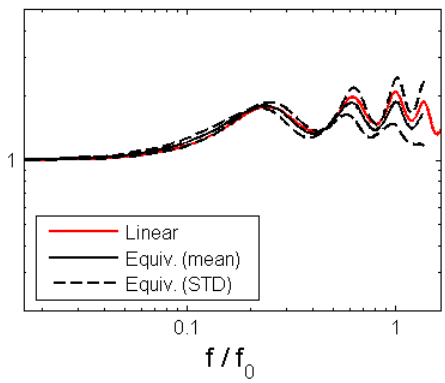

Equiv. Lin. TF (color coded by PGA_{RO})

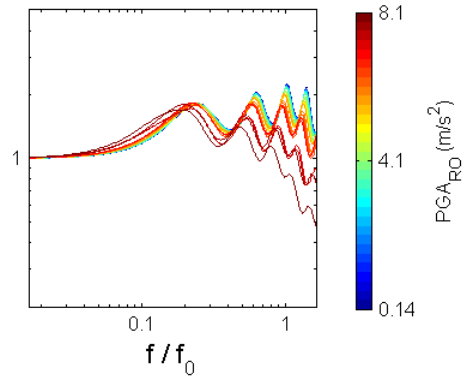

Non-linear Transfer Function

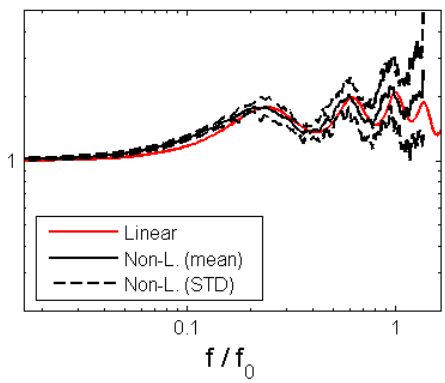

Non-linear TF (color coded by PGA_{RO})

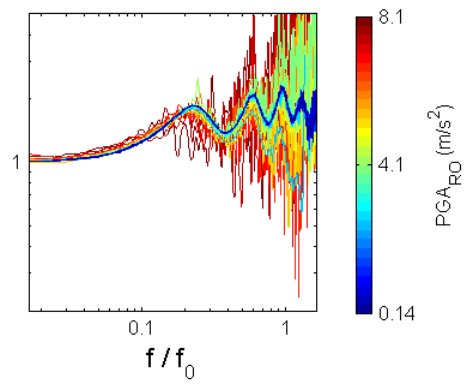

Equiv. Lin. TF (color coded by f_c)

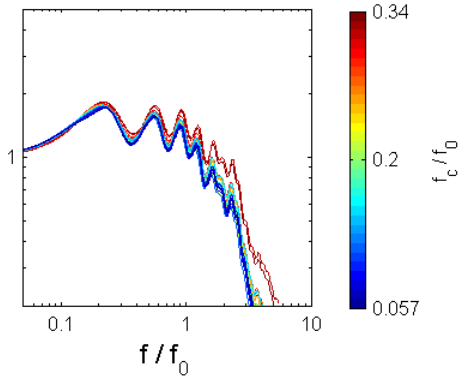

Non-linear TF (color coded by f_c)

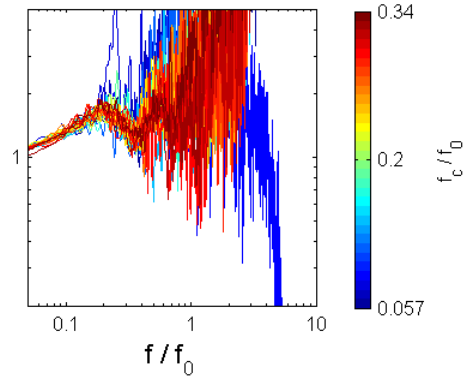

4.3.17 CI.DNR

Depth (m)	Thickness (m)	V_s (m/s)	Damping ratio	Density (kg/m^3)
0	1	174	0.05	1600
1	2	211	0.05	1800
3	3	319	0.02	1800
6	4	321	0.02	1800
10	6	379	0.02	1800
16	8	443	0.02	1800
24	12	490	0.02	1800
36	9	589	0.02	1800
45	5	603.4	0.02	1800
50	5	619.6	0.02	1800
55	5	633.2	0.02	1800
60	5	644.6	0.02	1800
65	5	654.2	0.02	1800
70	5	662.3	0.02	1800
75	5	669.0	0.02	1800
80	5	674.7	0.02	1800
85	5	679.5	0.02	1800
90	5	683.5	0.02	1800
95	5	686.9	0.02	1800
100	–	689.7	0.02	1800

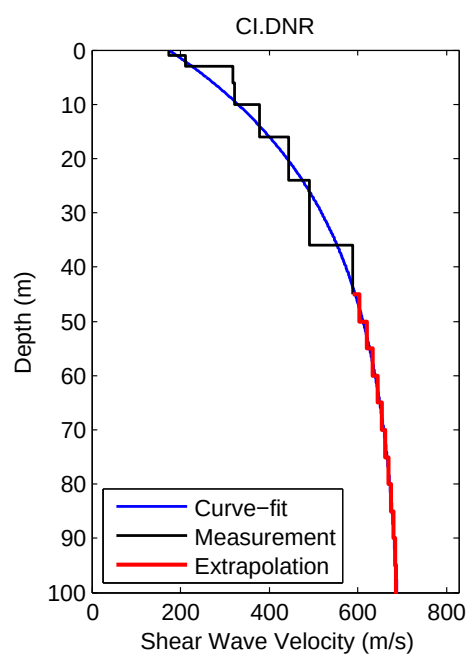

Linear Elastic Transfer Function

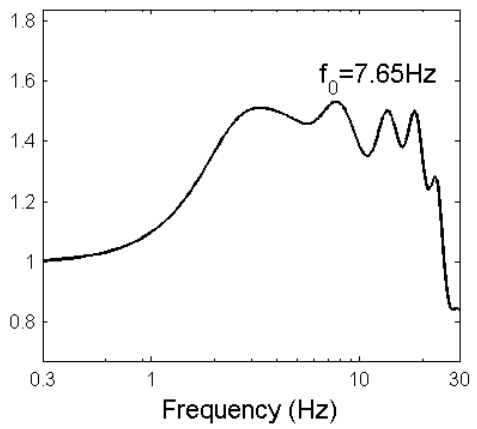

H/V Ratio – Sensor 450

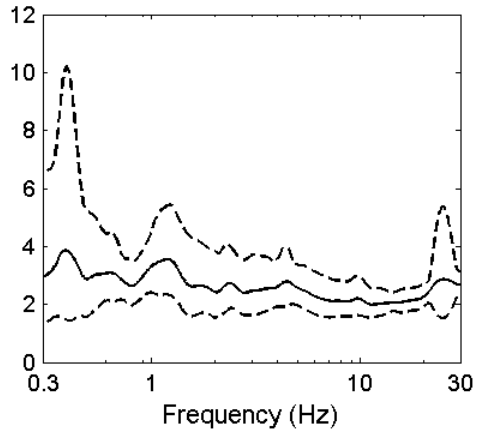

H/V Ratio – Sensor 507

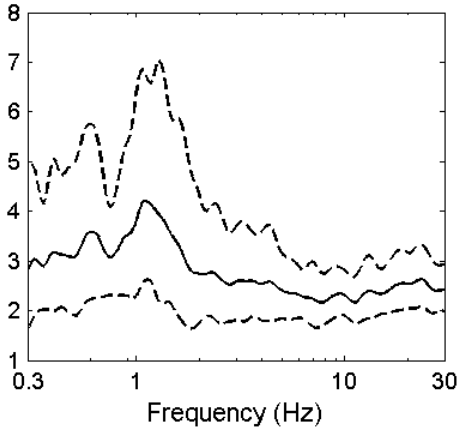

H/V Ratio – Sensor 453

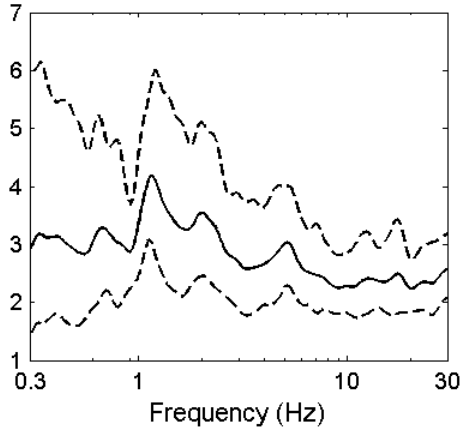

Equivalent Linear Transfer Function

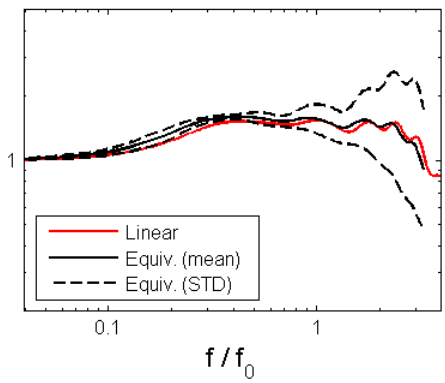

Equiv. Lin. TF (color coded by PGA_{RO})

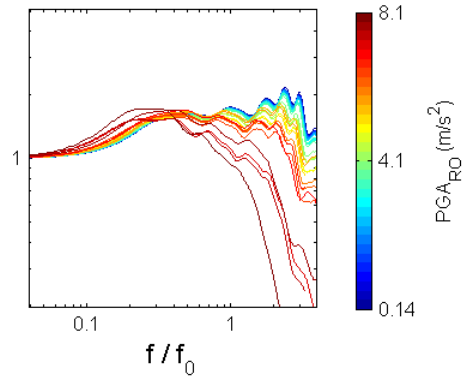

Non-linear Transfer Function

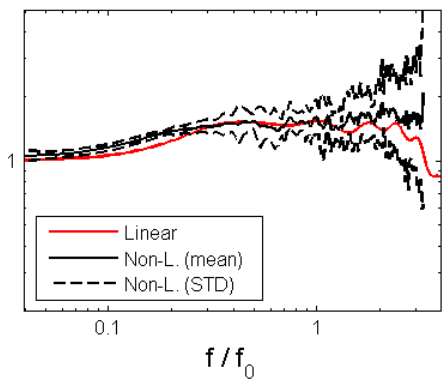

Non-linear TF (color coded by PGA_{RO})

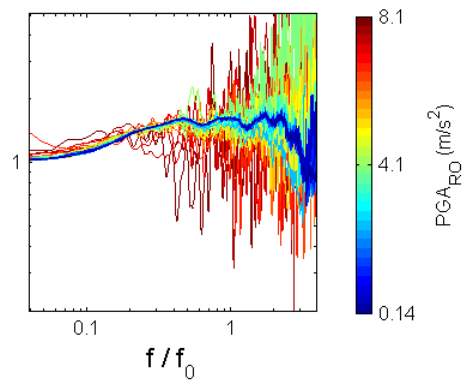

Equiv. Lin. TF (color coded by f_c)

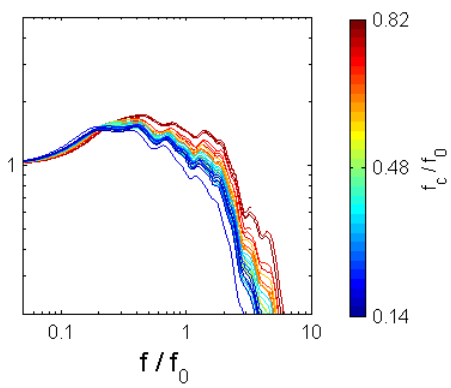

Non-linear TF (color coded by f_c)

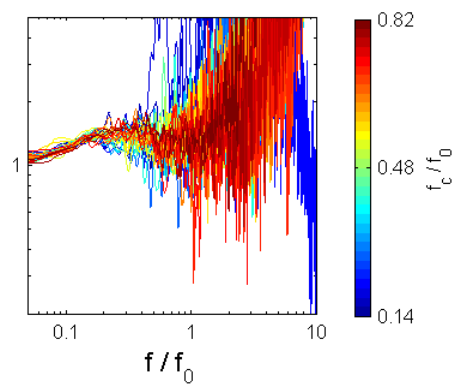

4.3.18 CI.DVT

Depth (m)	Thickness (m)	V_s (m/s)	Damping ratio	Density (kg/m^3)
0	2	233	0.05	1800
2	3	417	0.02	1800
5	4	546	0.02	1800
9	6	665	0.02	1800
15	9	813	0.01	2000
24	–	1252	0.01	2000

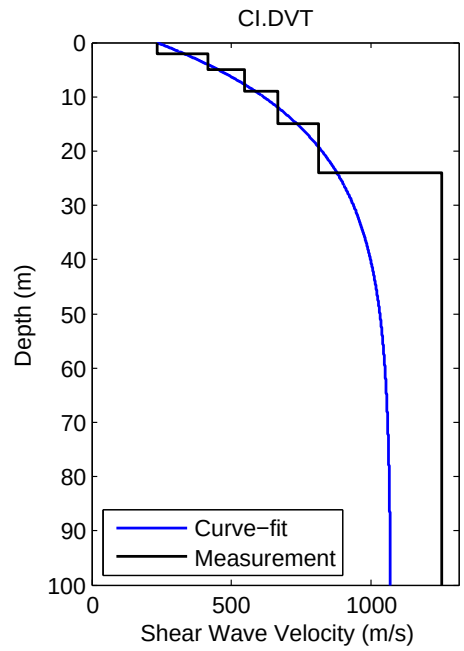

Linear Elastic Transfer Function

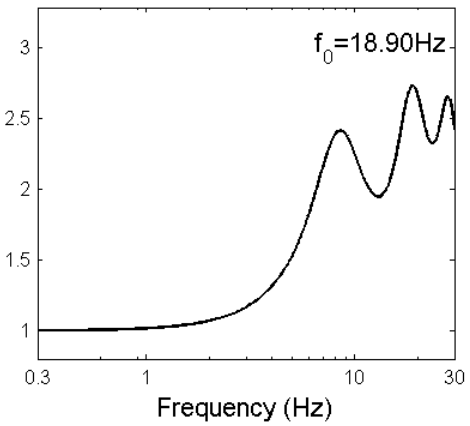

H/V Ratio – Sensor 450

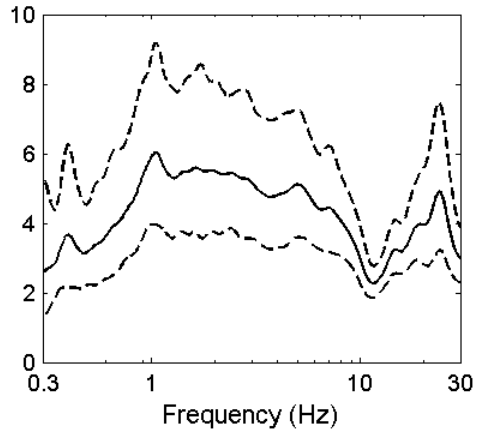

H/V Ratio – Sensor 507

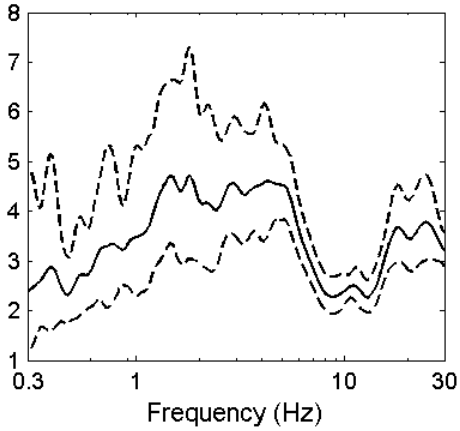

H/V Ratio – Sensor 453

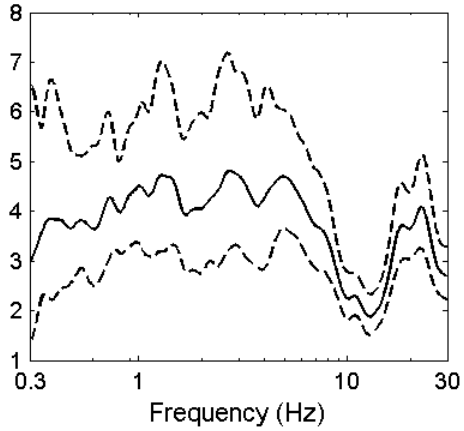

Equivalent Linear Transfer Function

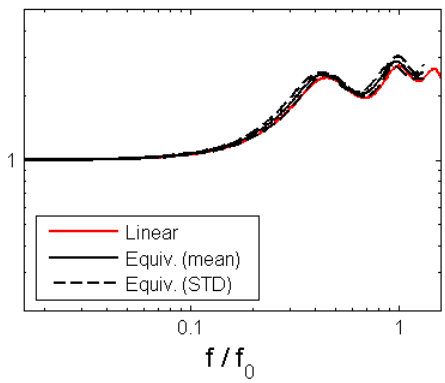

Equiv. Lin. TF (color coded by PGA_{RO})

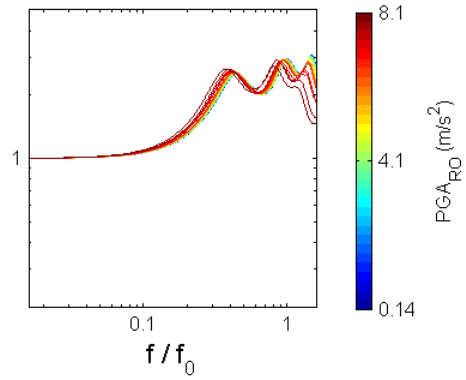

Non-linear Transfer Function

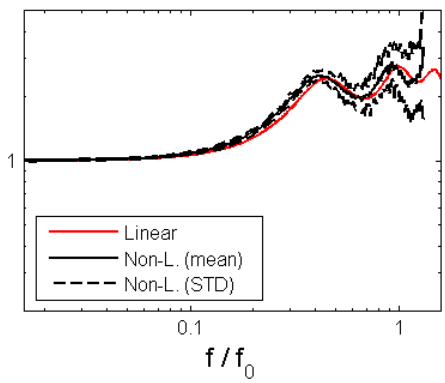

Non-linear TF (color coded by PGA_{RO})

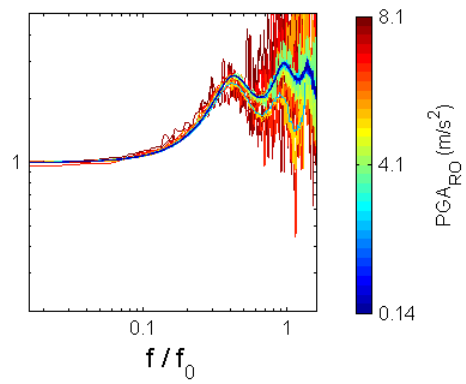

Equiv. Lin. TF (color coded by f_c)

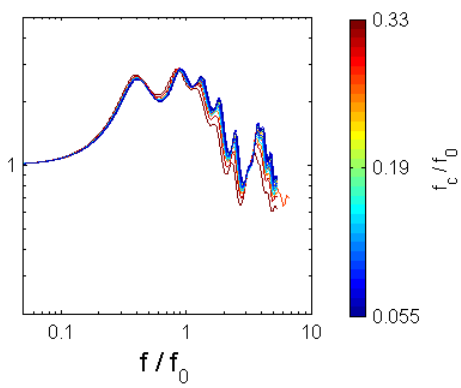

Non-linear TF (color coded by f_c)

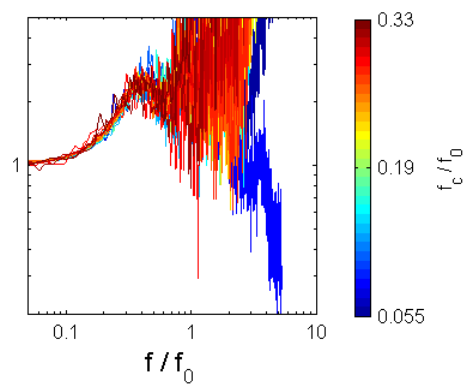

4.3.19 CI.FHO

Depth (m)	Thickness (m)	V_s (m/s)	Damping ratio	Density (kg/m^3)
0	1	166	0.05	1600
1	2	242	0.05	1800
3	3	364	0.02	1800
6	4	396	0.02	1800
10	6	431	0.02	1800
16	9	512	0.02	1800
25	5	622	0.02	1800
30	5	640.5	0.02	1800
35	5	669.9	0.02	1800
40	5	693.4	0.02	1800
45	5	712.3	0.02	1800
50	5	727.4	0.02	1800
55	5	739.5	0.02	1800
60	5	749.3	0.02	1800
65	5	757.1	0.01	1800
70	5	763.3	0.01	1800
75	5	768.3	0.01	1800
80	5	772.3	0.01	1800
85	5	775.6	0.01	1800
90	5	778.1	0.01	1800
95	5	780.2	0.01	1800
100	–	781.9	0.01	1800

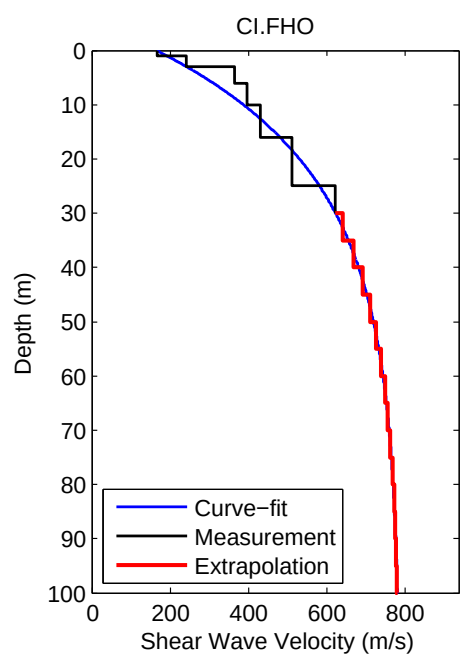

Linear Elastic Transfer Function

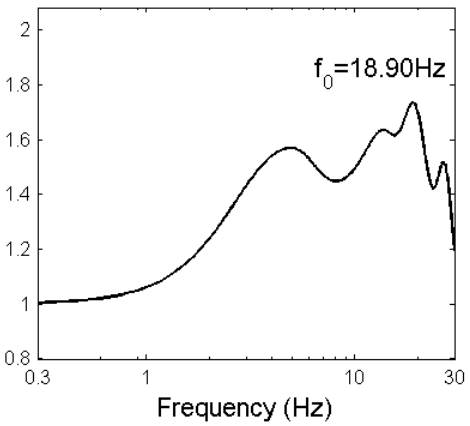

H/V Ratio – Sensor 450

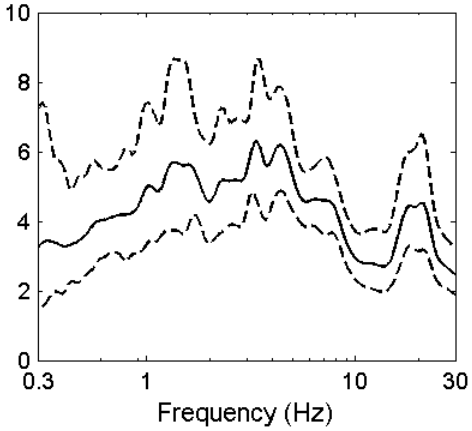

H/V Ratio – Sensor 507

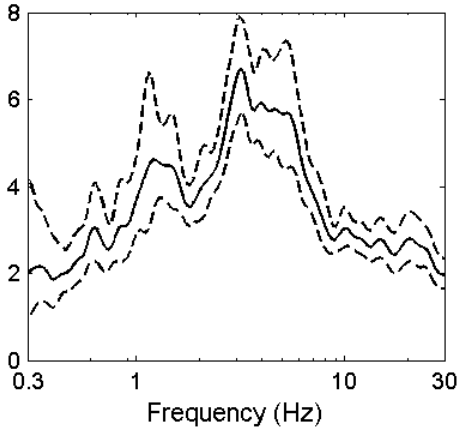

H/V Ratio – Sensor 453

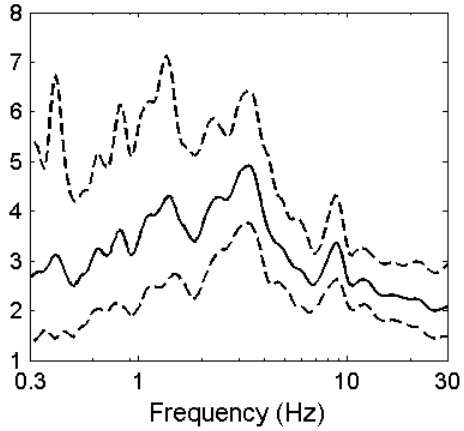

Equivalent Linear Transfer Function

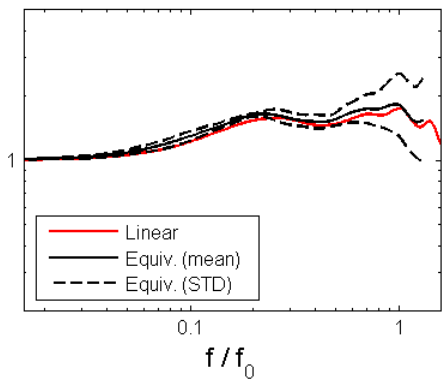

Equiv. Lin. TF (color coded by PGA_{RO})

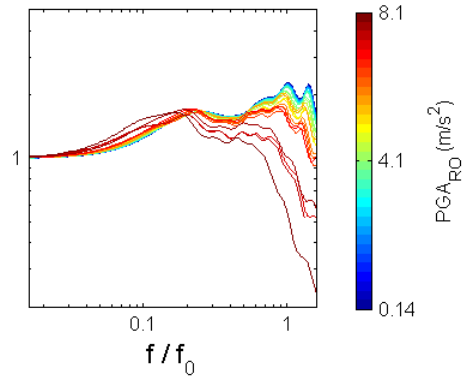

Non-linear Transfer Function

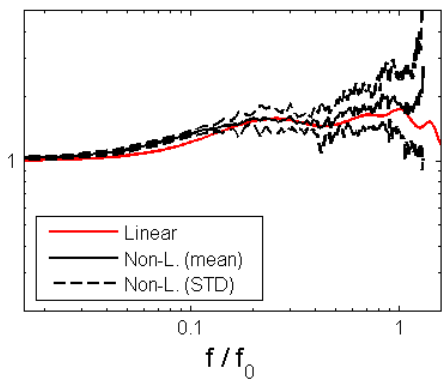

Non-linear TF (color coded by PGA_{RO})

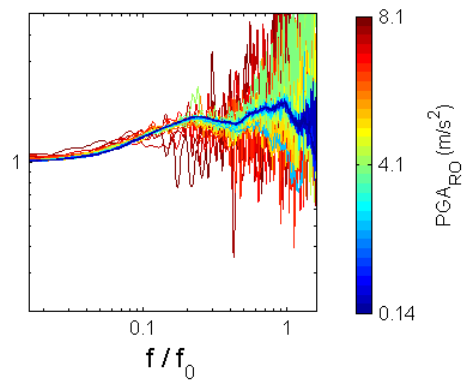

Equiv. Lin. TF (color coded by f_c)

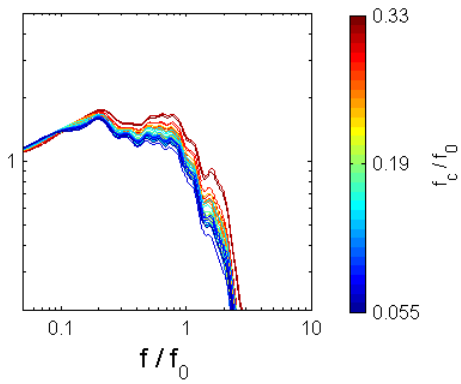

Non-linear TF (color coded by f_c)

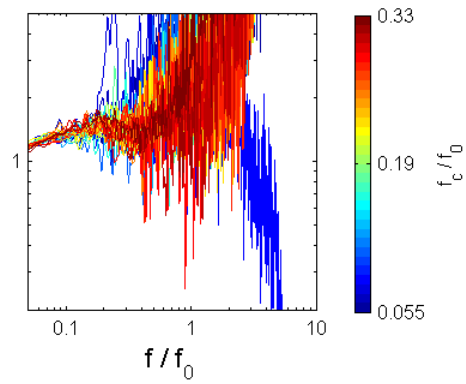

4.3.20 CI.FUR

Depth (m)	Thickness (m)	V_s (m/s)	Damping ratio	Density (kg/m^3)
0	1	278	0.02	1800
1	5	326	0.02	1800
6	3	561	0.02	1800
9	4	390	0.02	1800
13	5	400	0.02	1800
18	7	477	0.02	1800
25	10	655	0.02	1800
35	5	657.8	0.02	1800
40	5	679.0	0.02	1800
45	5	696.5	0.02	1800
50	5	711.0	0.02	1800
55	5	723.1	0.02	1800
60	5	733.1	0.02	1800
65	5	741.4	0.02	1800
70	5	748.3	0.02	1800
75	5	754.0	0.01	1800
80	5	758.7	0.01	1800
85	5	762.6	0.01	1800
90	5	765.9	0.01	1800
95	5	768.6	0.01	1800
100	–	770.8	0.01	1800

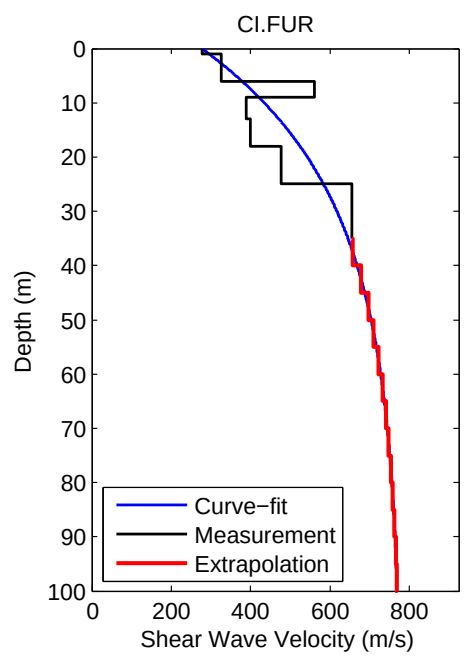

Linear Elastic Transfer Function

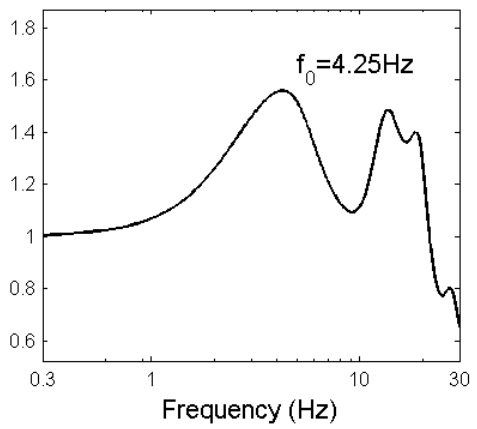

H/V Ratio – Sensor 450

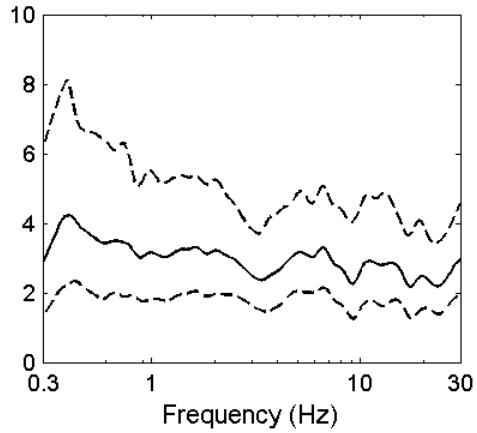

H/V Ratio – Sensor 507

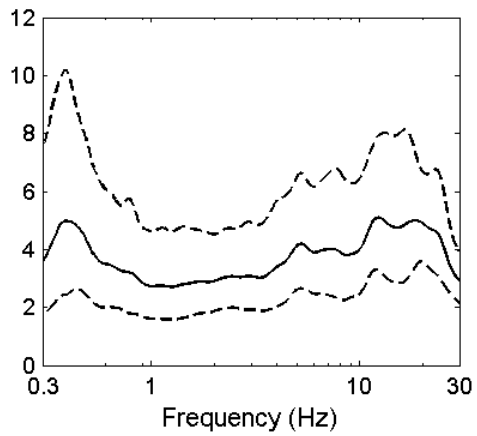

H/V Ratio – Sensor 453

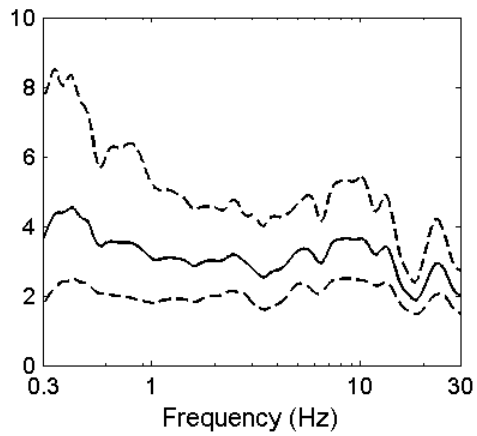

Equivalent Linear Transfer Function

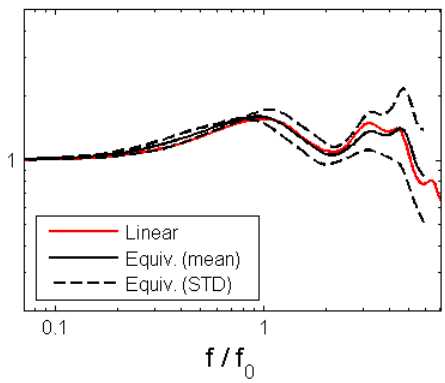

Equiv. Lin. TF (color coded by PGA_{RO})

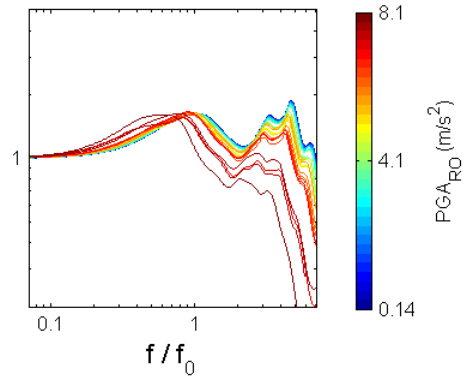

Non-linear Transfer Function

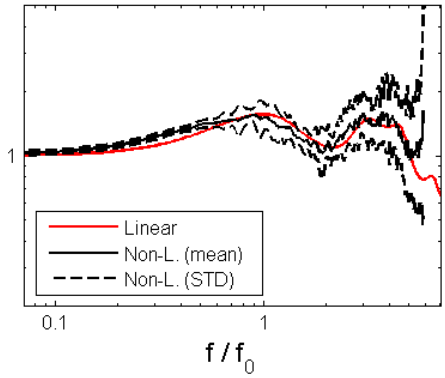

Non-linear TF (color coded by PGA_{RO})

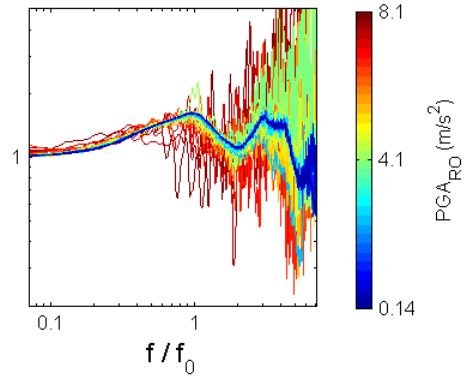

Equiv. Lin. TF (color coded by f_c)

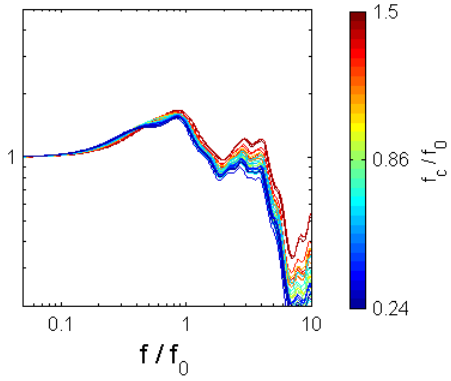

Non-linear TF (color coded by f_c)

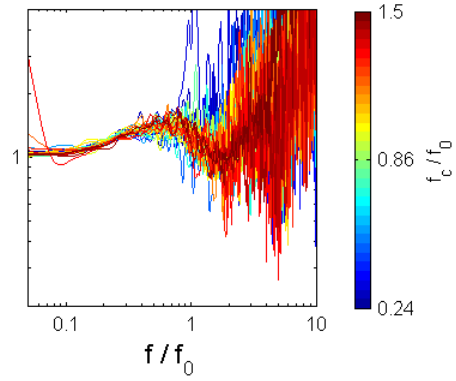

4.3.21 CI.GORa

Depth (m)	Thickness (m)	V_s (m/s)	Damping ratio	Density (kg/m^3)
0	1.5	253	0.02	1800
1.5	2.5	380	0.02	1800
4	6	468	0.02	1800
10	10	514	0.02	1800
20	–	1129	0.01	2000

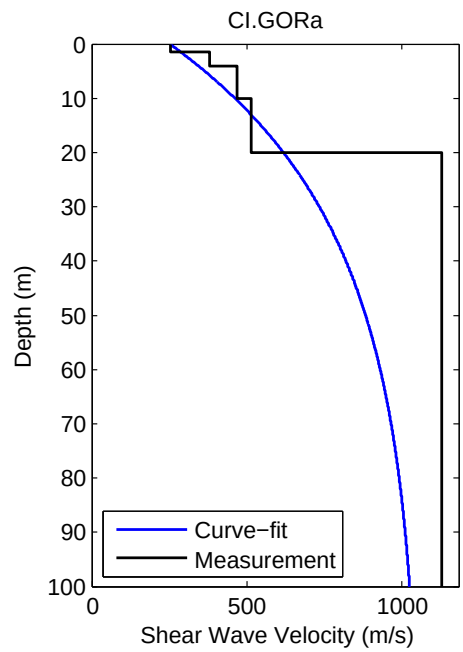

Linear Elastic Transfer Function

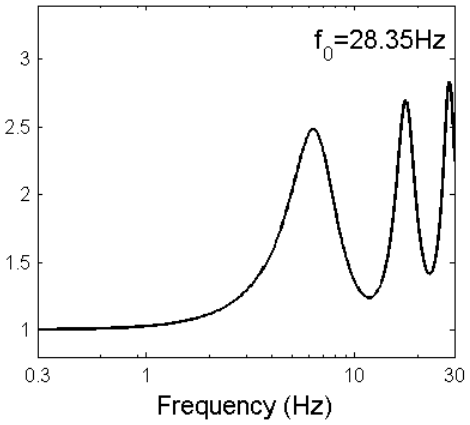

H/V Ratio – Sensor 450

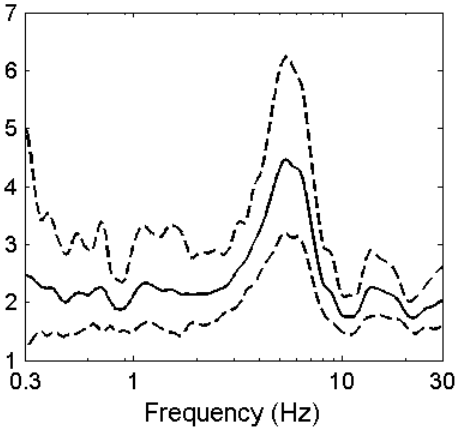

H/V Ratio – Sensor 507

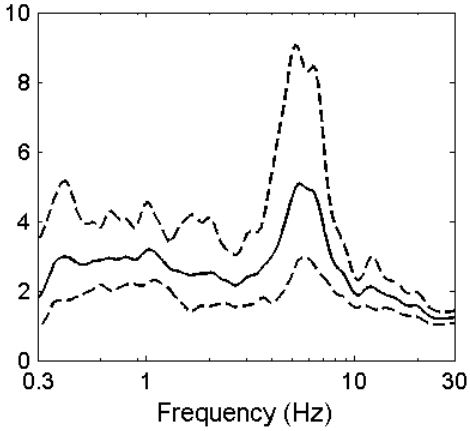

H/V Ratio – Sensor 453

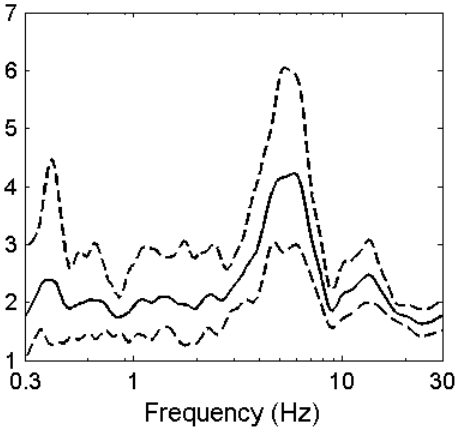

Equivalent Linear Transfer Function

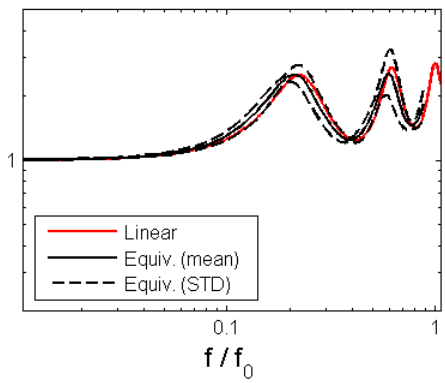

Equiv. Lin. TF (color coded by PGA_{RO})

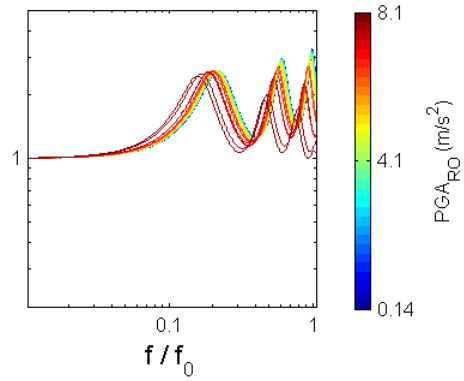

Non-linear Transfer Function

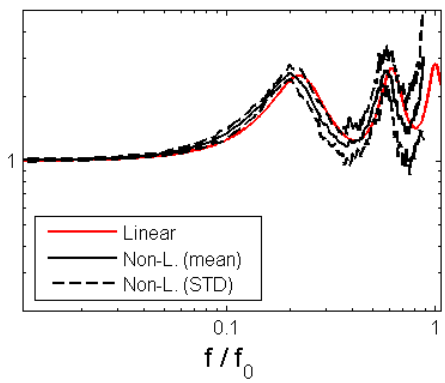

Non-linear TF (color coded by PGA_{RO})

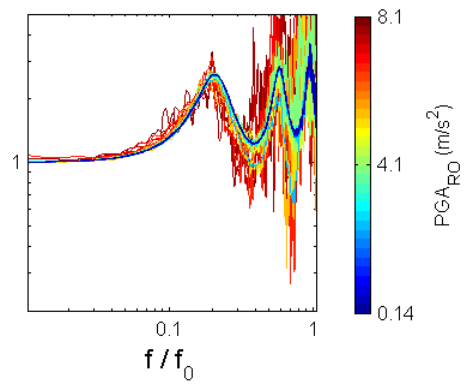

Equiv. Lin. TF (color coded by f_c)

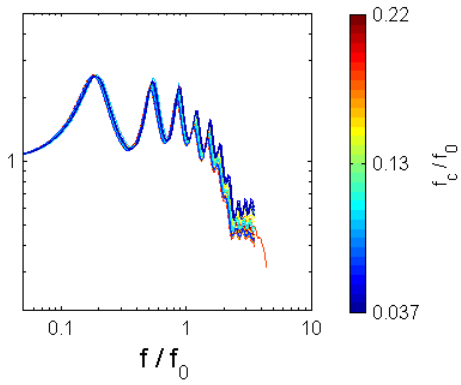

Non-linear TF (color coded by f_c)

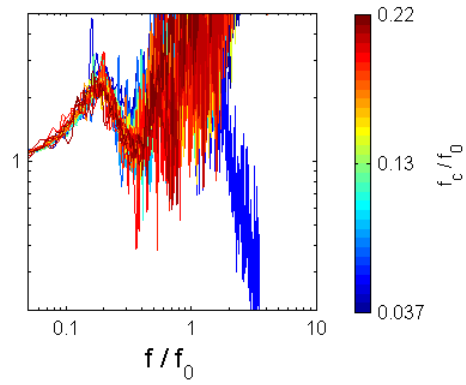

4.3.22 CI.GORb

Depth (m)	Thickness (m)	V_s (m/s)	Damping ratio	Density (kg/m^3)
0	1.5	251	0.02	1800
1.5	2.5	384	0.02	1800
4	9	465	0.02	1800
13	12	623	0.02	1800
25	–	1398	0.01	2000

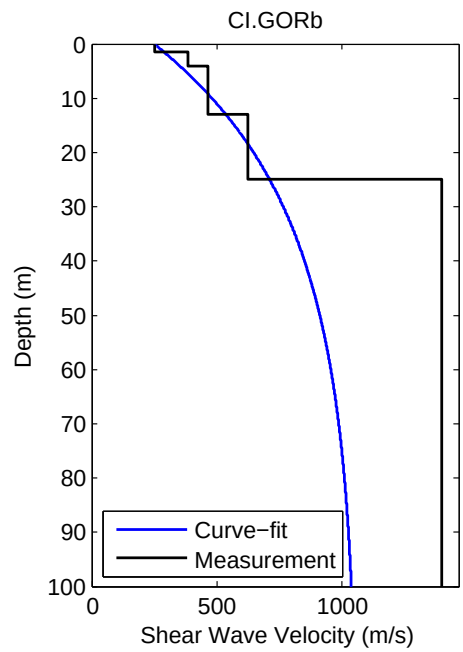

Linear Elastic Transfer Function

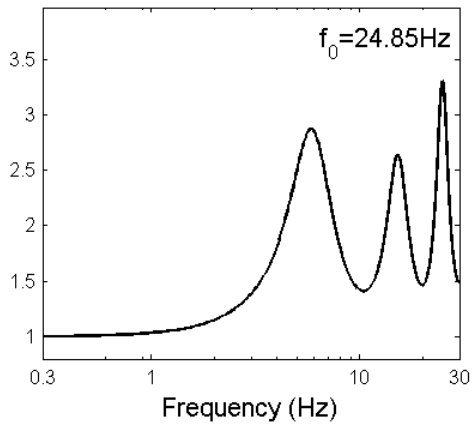

H/V Ratio – Sensor 450

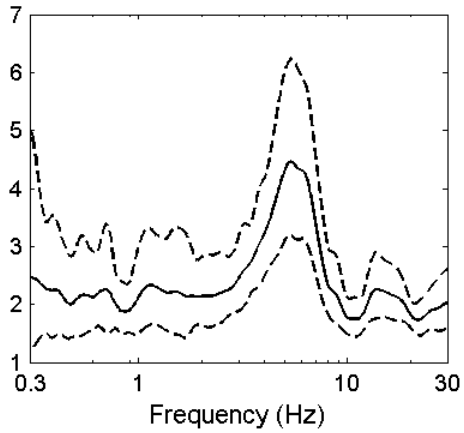

H/V Ratio – Sensor 507

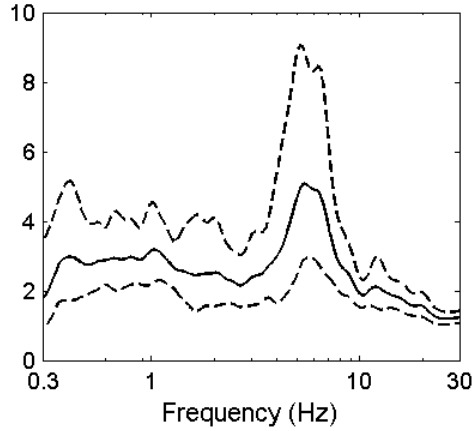

H/V Ratio – Sensor 453

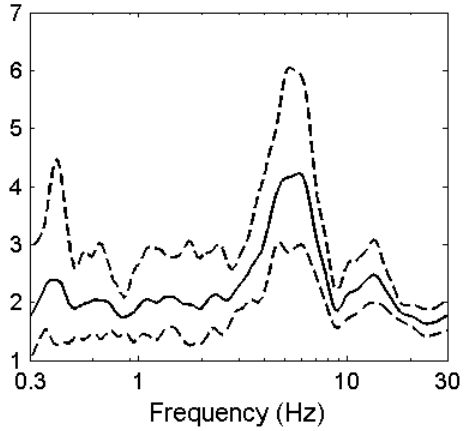

Equivalent Linear Transfer Function

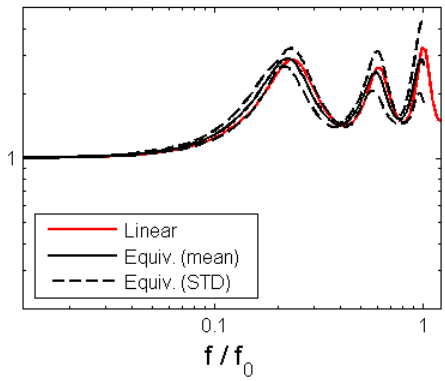

Equiv. Lin. TF (color coded by PGA_{RO})

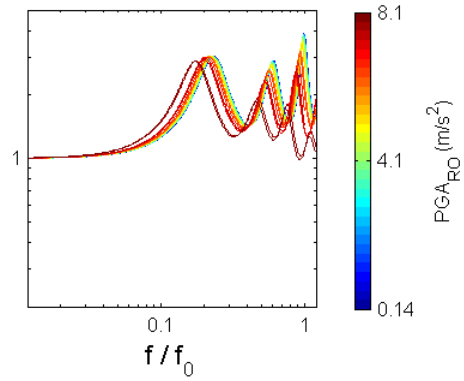

Non-linear Transfer Function

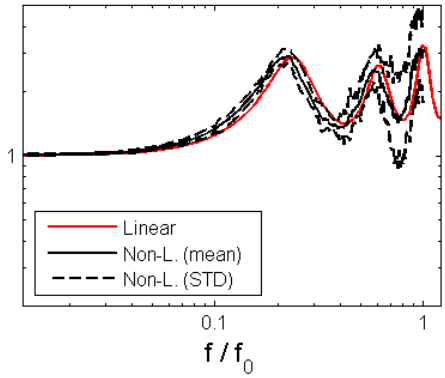

Non-linear TF (color coded by PGA_{RO})

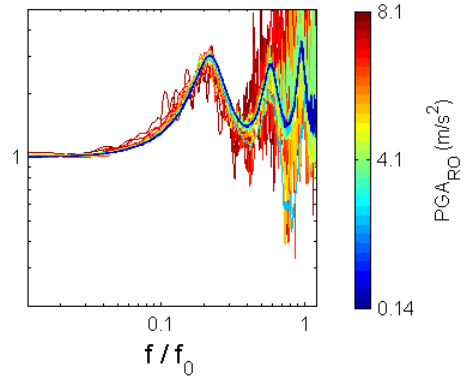

Equiv. Lin. TF (color coded by f_c)

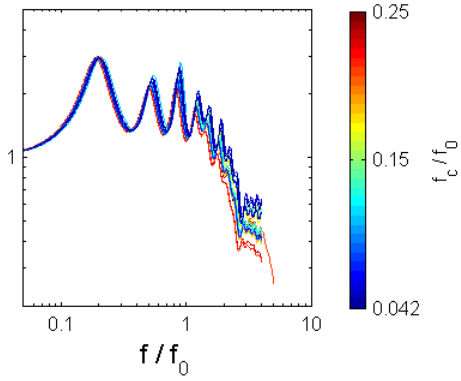

Non-linear TF (color coded by f_c)

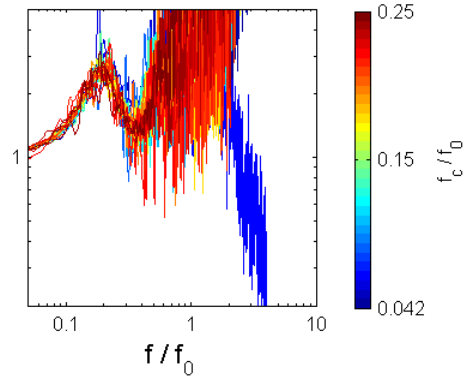

4.3.23 CI.GORc

Depth (m)	Thickness (m)	V_s (m/s)	Damping ratio	Density (kg/m^3)
0	1.5	253	0.02	1800
1.5	2.5	379	0.02	1800
4	5	472	0.02	1800
9	8	483	0.02	1800
17	15	846	0.01	2000
32	–	1458	0.01	2000

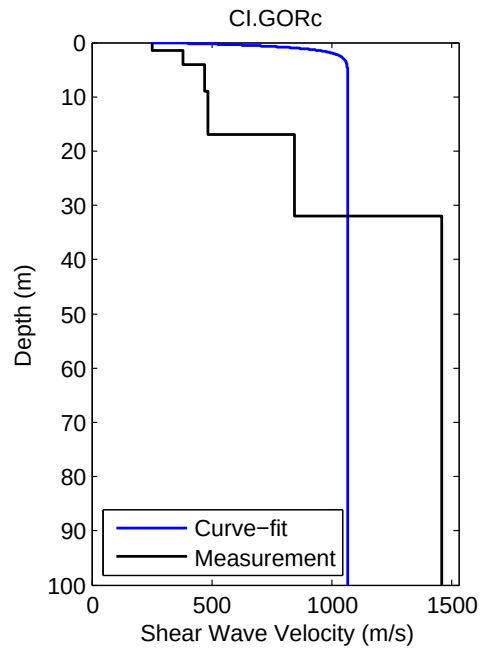

Linear Elastic Transfer Function

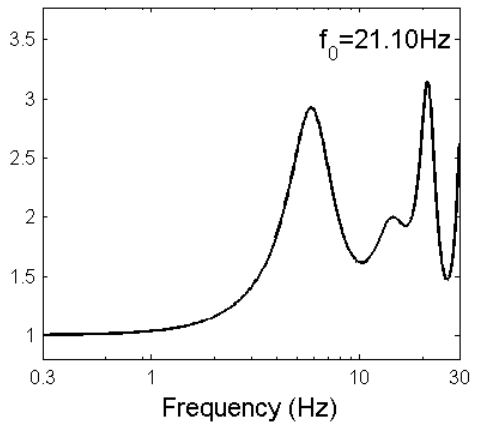

H/V Ratio – Sensor 450

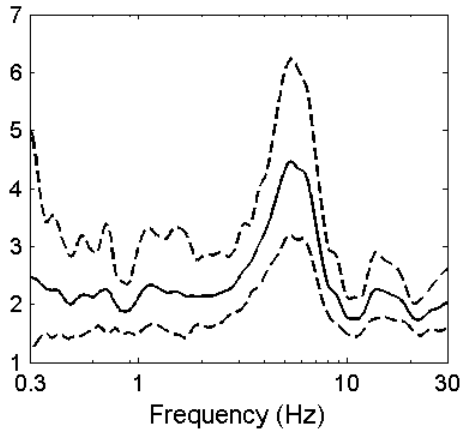

H/V Ratio – Sensor 507

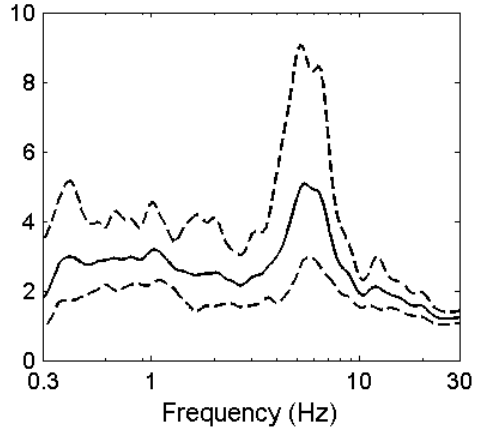

H/V Ratio – Sensor 453

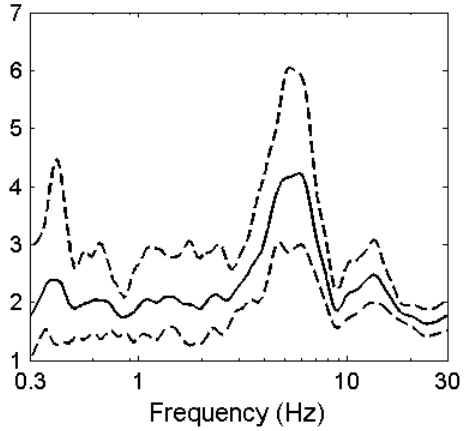

Equivalent Linear Transfer Function

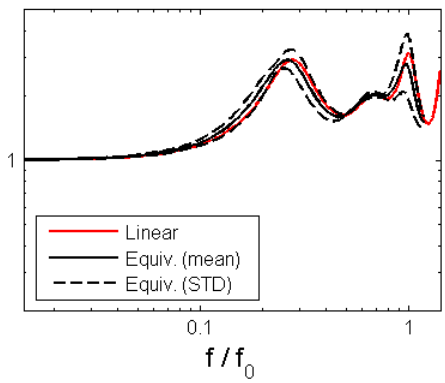

Equiv. Lin. TF (color coded by PGA_{RO})

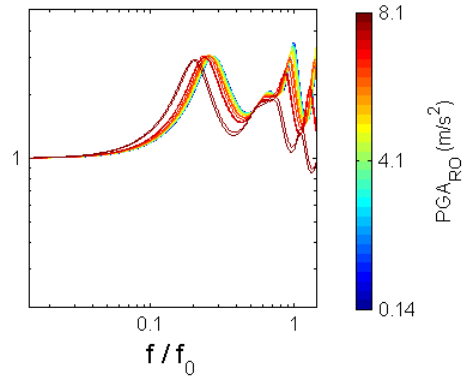

Non-linear Transfer Function

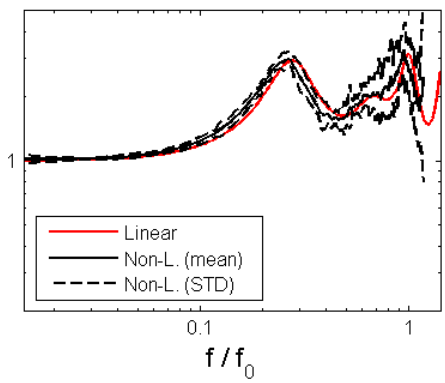

Non-linear TF (color coded by PGA_{RO})

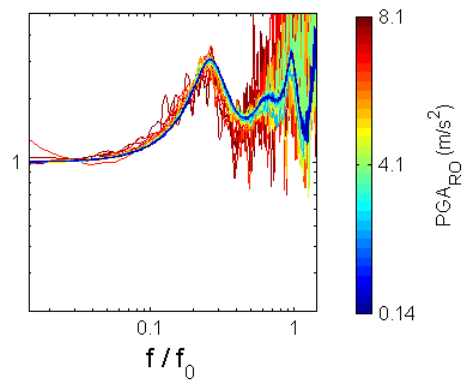

Equiv. Lin. TF (color coded by f_c)

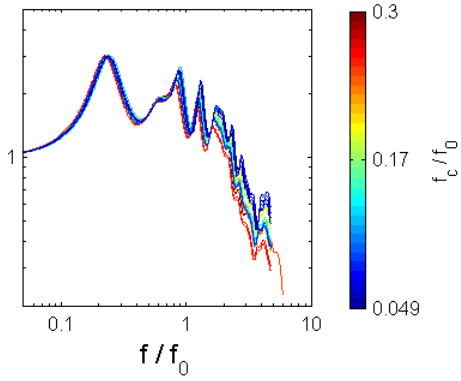

Non-linear TF (color coded by f_c)

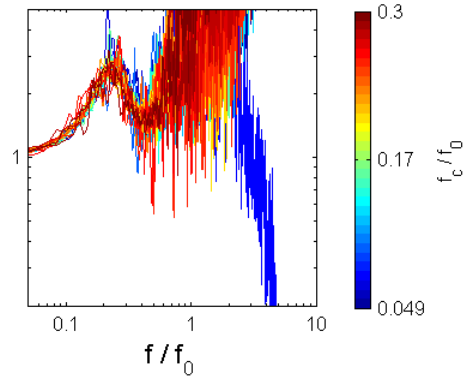

4.3.24 CI.GRAa

Depth (m)	Thickness (m)	V_s (m/s)	Damping ratio	Density (kg/m^3)
0	1.5	254	0.02	1800
1.5	2.5	316	0.02	1800
4	6	292	0.02	1800
10	2	429	0.02	1800
12	14	441	0.02	1800
26	9	577	0.02	1800
35	5	586.1	0.02	1800
40	5	604.9	0.02	1800
45	5	620.5	0.02	1800
50	5	633.5	0.02	1800
55	5	644.3	0.02	1800
60	5	653.3	0.02	1800
65	5	660.7	0.02	1800
70	5	666.9	0.02	1800
75	5	672.1	0.02	1800
80	5	676.4	0.02	1800
85	5	680.0	0.02	1800
90	5	683.0	0.02	1800
95	5	685.5	0.02	1800
100	–	687.5	0.02	1800

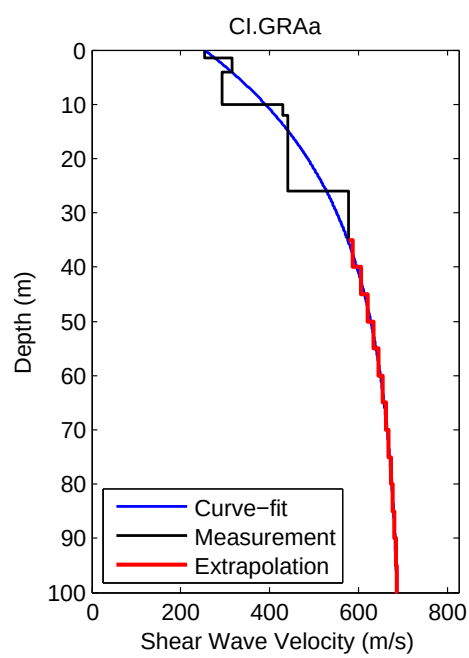

Linear Elastic Transfer Function

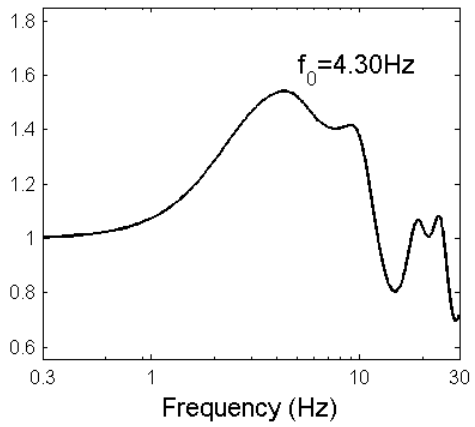

H/V Ratio – Sensor 450

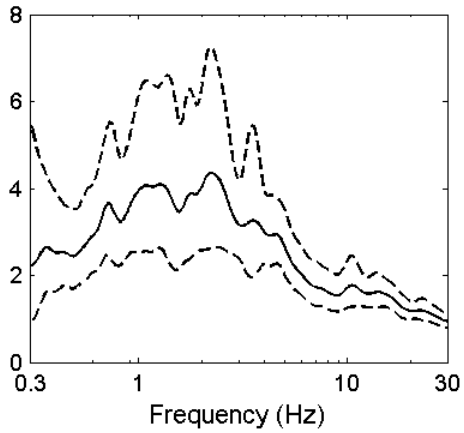

H/V Ratio – Sensor 507

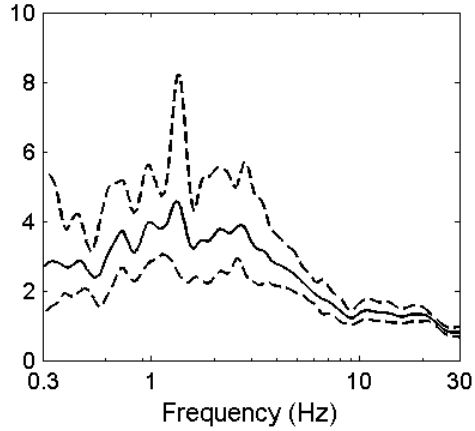

H/V Ratio – Sensor 453

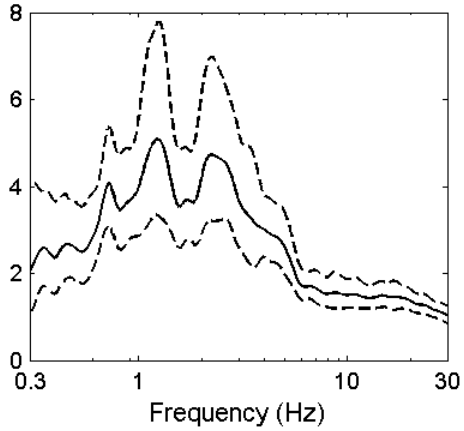

Equivalent Linear Transfer Function

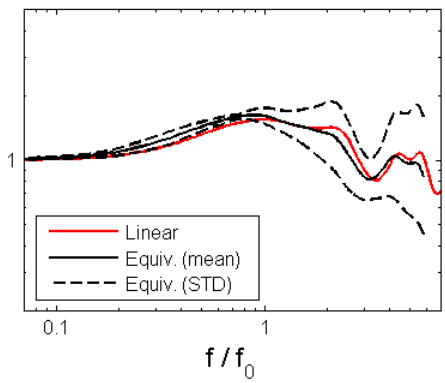

Equiv. Lin. TF (color coded by PGA_{RO})

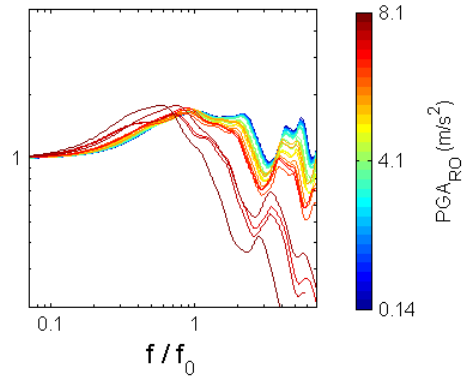

Non-linear Transfer Function

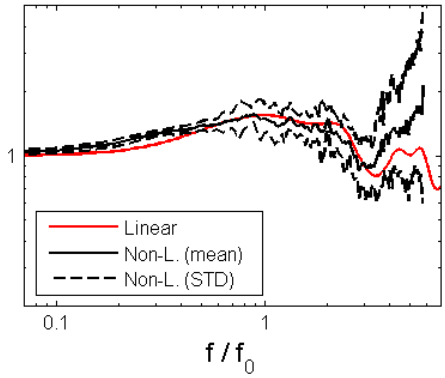

Non-linear TF (color coded by PGA_{RO})

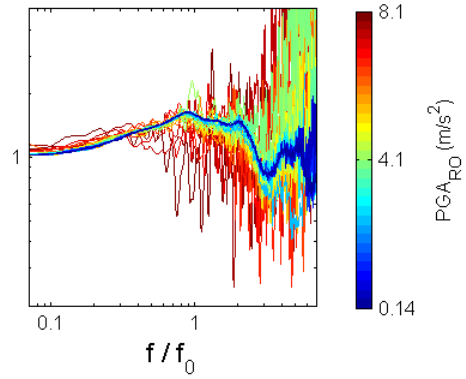

Equiv. Lin. TF (color coded by f_c)

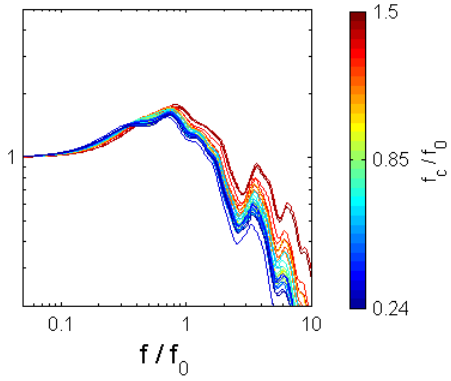

Non-linear TF (color coded by f_c)

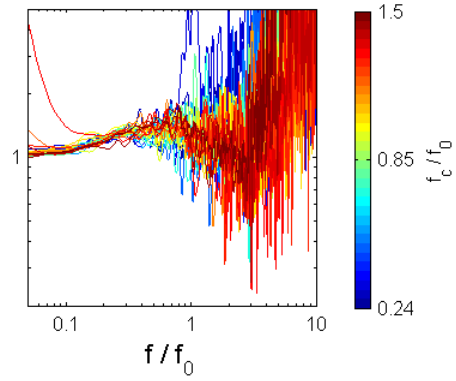

4.3.25 CI.GRAb

Depth (m)	Thickness (m)	V_s (m/s)	Damping ratio	Density (kg/m^3)
0	0.75	202	0.05	1800
0.75	4.25	349	0.02	1800
5	7	442	0.02	1800
12	13	291	0.02	1800
25	15	603	0.02	1800
40	5	621.7	0.02	1800
45	5	636.8	0.02	1800
50	5	648.8	0.02	1800
55	5	658.5	0.02	1800
60	5	666.3	0.02	1800
65	5	672.5	0.02	1800
70	5	677.5	0.02	1800
75	5	681.5	0.02	1800
80	5	684.7	0.02	1800
85	5	687.3	0.02	1800
90	5	689.3	0.02	1800
95	5	691.0	0.02	1800
100	–	692.3	0.02	1800

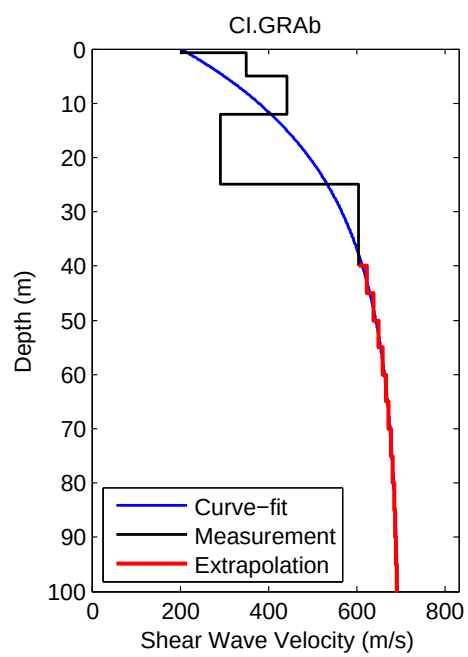

Linear Elastic Transfer Function

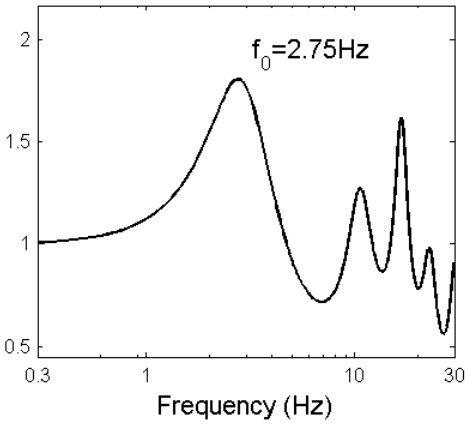

H/V Ratio – Sensor 450

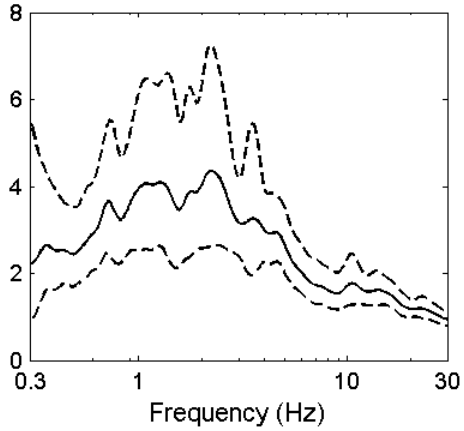

H/V Ratio – Sensor 507

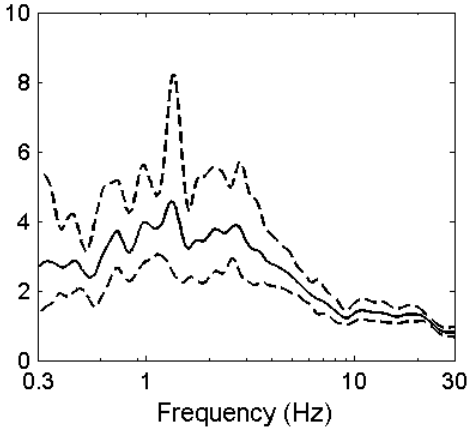

H/V Ratio – Sensor 453

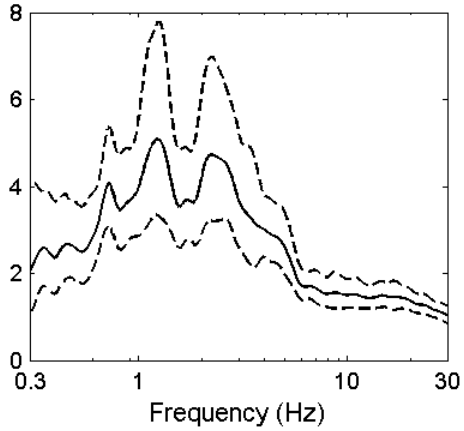

Equivalent Linear Transfer Function

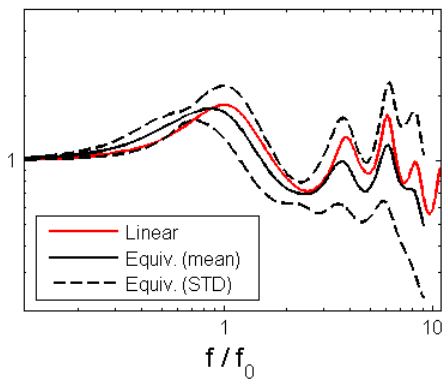

Equiv. Lin. TF (color coded by PGA_{RO})

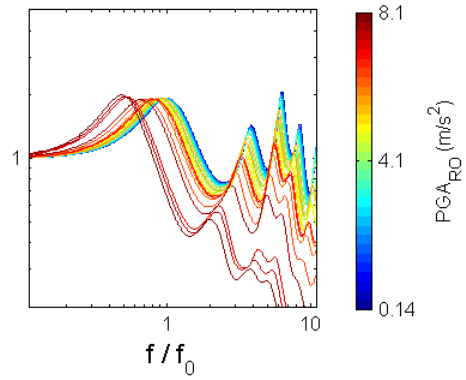

Non-linear Transfer Function

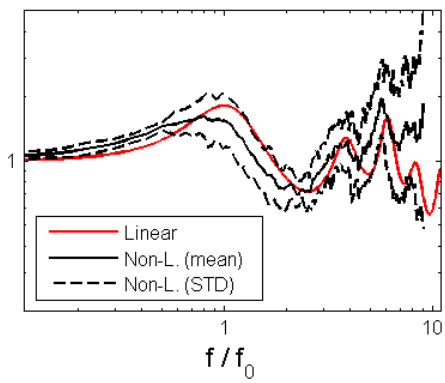

Non-linear TF (color coded by PGA_{RO})

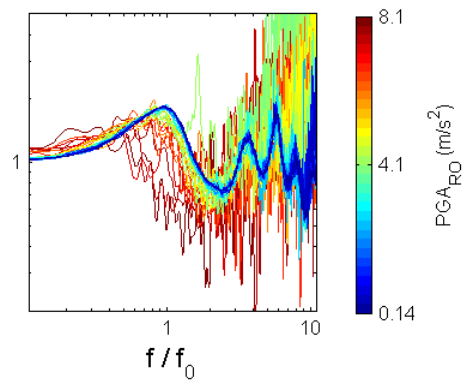

Equiv. Lin. TF (color coded by f_c)

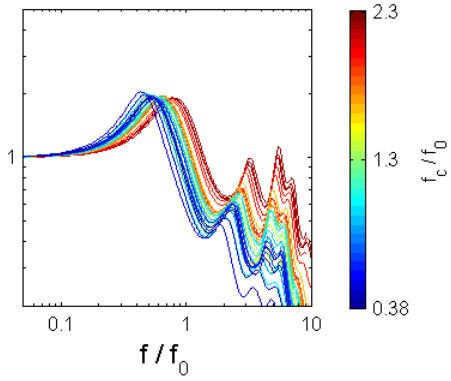

Non-linear TF (color coded by f_c)

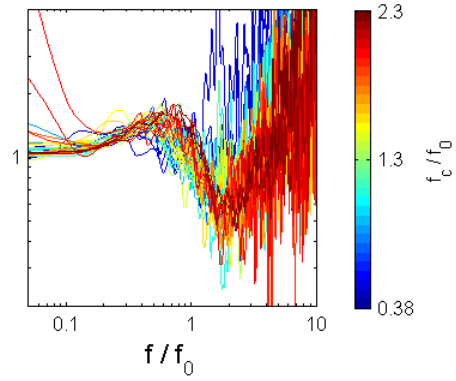

4.3.26 CI.IDO

Depth (m)	Thickness (m)	V_s (m/s)	Damping ratio	Density (kg/m^3)
0	2	305	0.02	1800
2	3	415	0.02	1800
5	4	509	0.02	1800
9	7	618	0.02	1800
16	10	667	0.02	1800
26	4	680	0.02	1800
30	5	747.4	0.02	1800
35	5	785.2	0.01	1800
40	5	817.8	0.01	2000
45	5	845.9	0.01	2000
50	5	870.2	0.01	2000
55	5	891.2	0.01	2000
60	5	909.3	0.01	2000
65	5	924.9	0.01	2000
70	5	938.4	0.01	2000
75	5	950.0	0.01	2000
80	5	960.1	0.01	2000
85	5	968.8	0.01	2000
90	5	976.2	0.01	2000
95	5	982.7	0.01	2000
100	–	988.3	0.01	2000

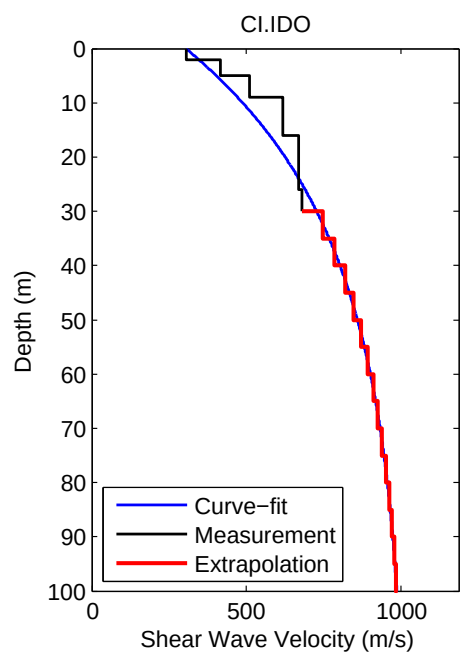

Linear Elastic Transfer Function

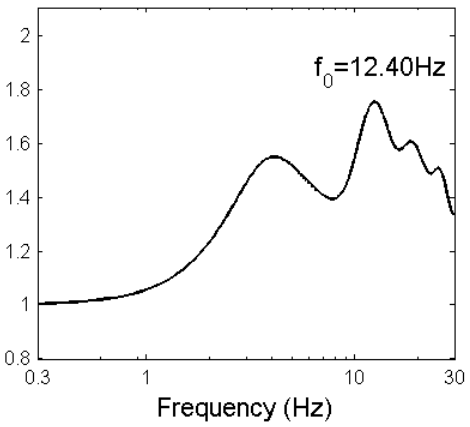

H/V Ratio – Sensor 450

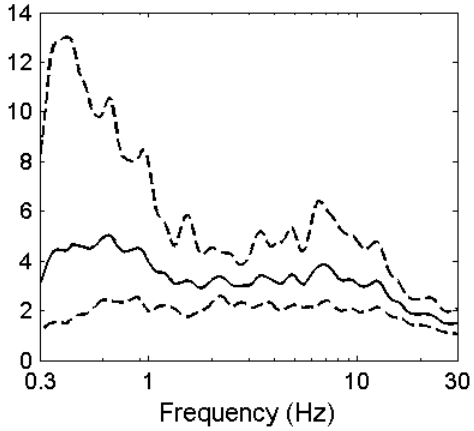

H/V Ratio – Sensor 507

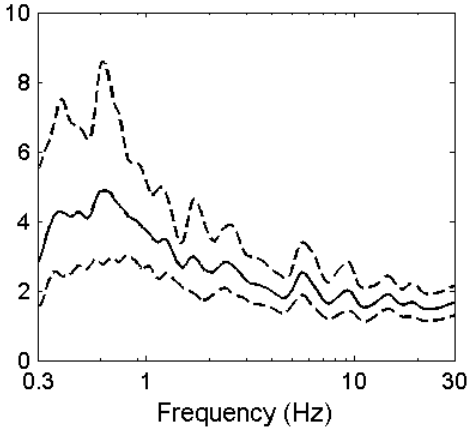

H/V Ratio – Sensor 453

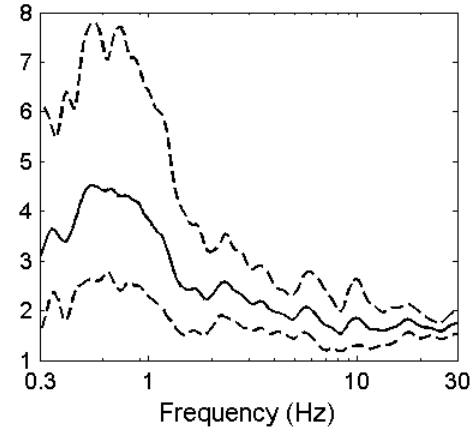

Equivalent Linear Transfer Function

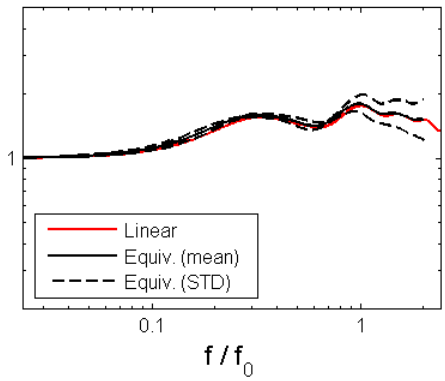

Equiv. Lin. TF (color coded by PGA_{RO})

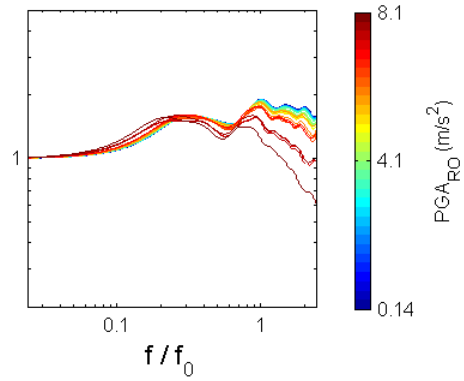

Non-linear Transfer Function

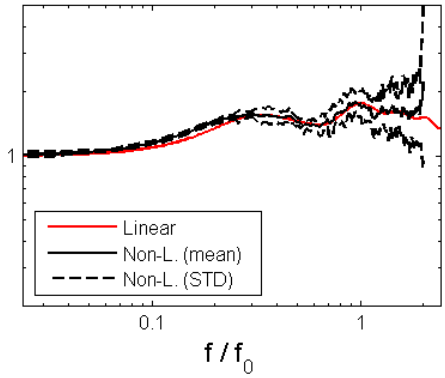

Non-linear TF (color coded by PGA_{RO})

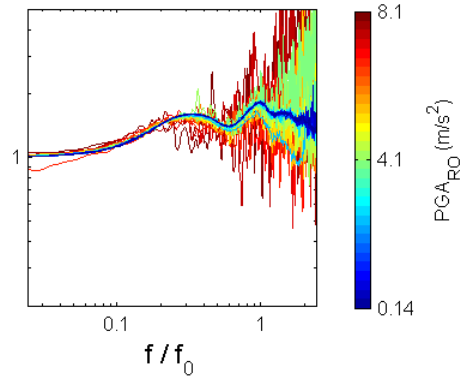

Equiv. Lin. TF (color coded by f_c)

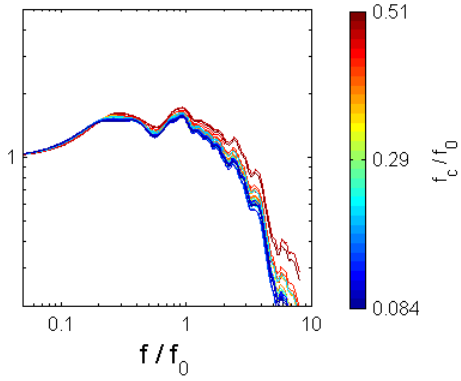

Non-linear TF (color coded by f_c)

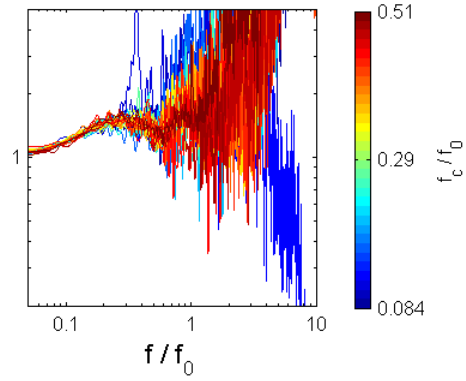

4.3.27 CI.JVA

Depth (m)	Thickness (m)	V_s (m/s)	Damping ratio	Density (kg/m^3)
0	1	159	0.05	1600
1	2	231	0.05	1800
3	3	332	0.02	1800
6	4	402	0.02	1800
10	6	432	0.02	1800
16	9	467	0.02	1800
25	5	486	0.02	1800
30	5	552.2	0.02	1800
35	5	581.0	0.02	1800
40	5	605.1	0.02	1800
45	5	625.1	0.02	1800
50	5	641.8	0.02	1800
55	5	655.7	0.02	1800
60	5	667.3	0.02	1800
65	5	676.9	0.02	1800
70	5	685.0	0.02	1800
75	5	691.7	0.02	1800
80	5	697.2	0.02	1800
85	5	701.9	0.02	1800
90	5	705.8	0.02	1800
95	5	709.0	0.02	1800
100	–	711.7	0.02	1800

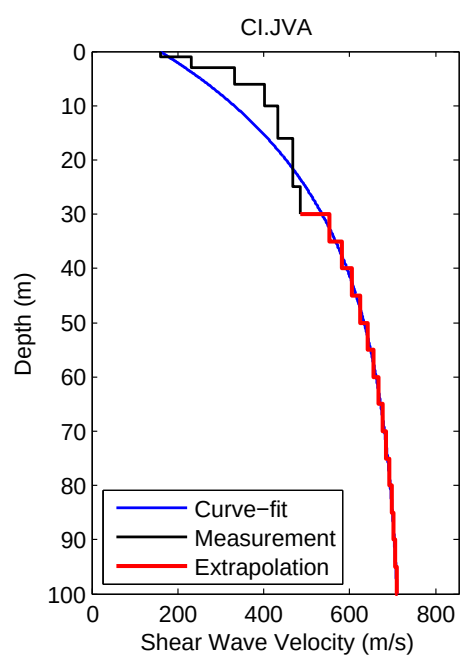

Linear Elastic Transfer Function

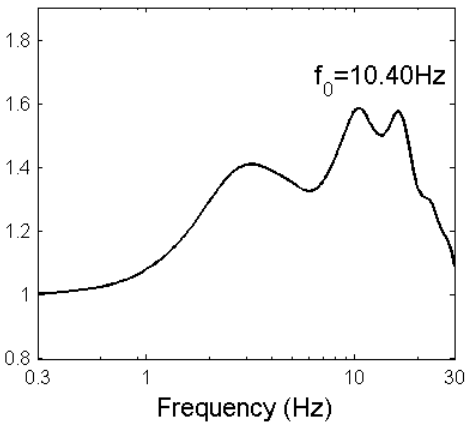

H/V Ratio – Sensor 450

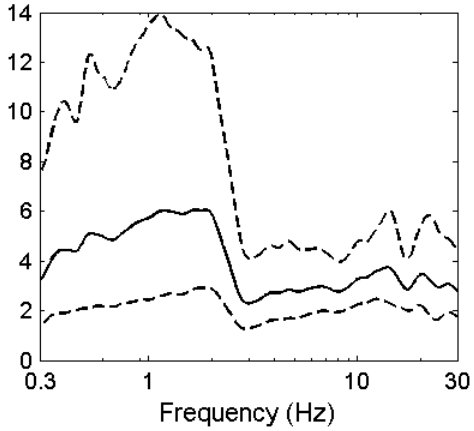

H/V Ratio – Sensor 507

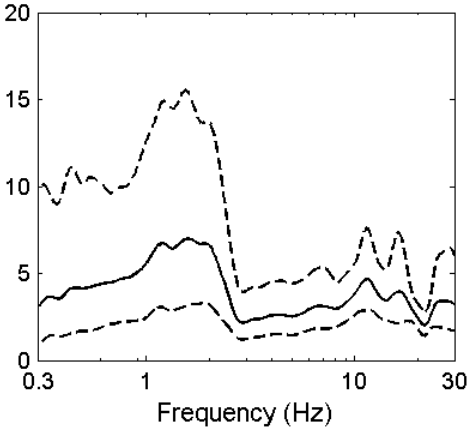

H/V Ratio – Sensor 453

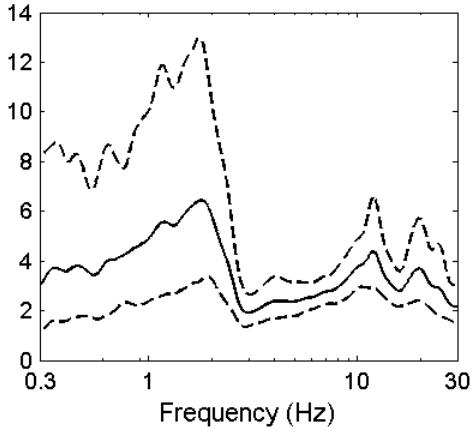

Equivalent Linear Transfer Function

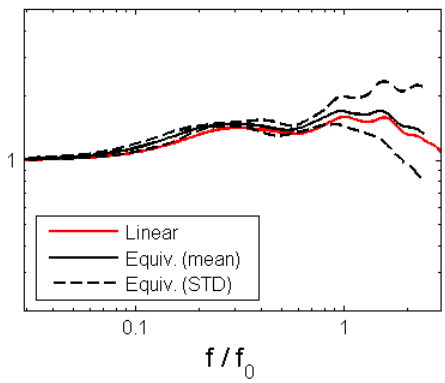

Equiv. Lin. TF (color coded by PGA_{RO})

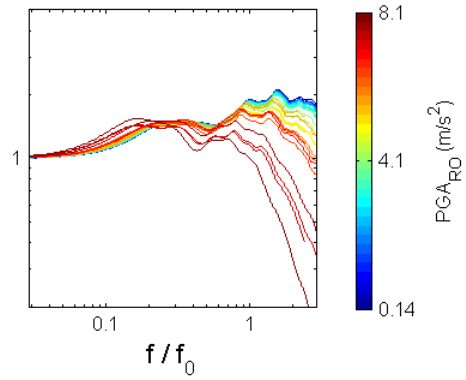

Non-linear Transfer Function

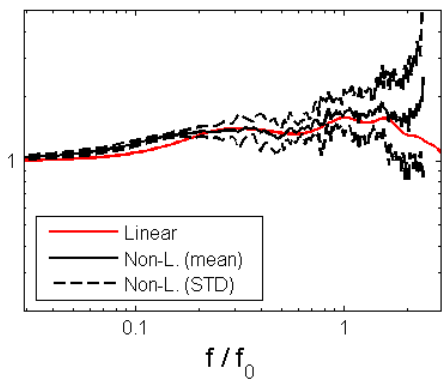

Non-linear TF (color coded by PGA_{RO})

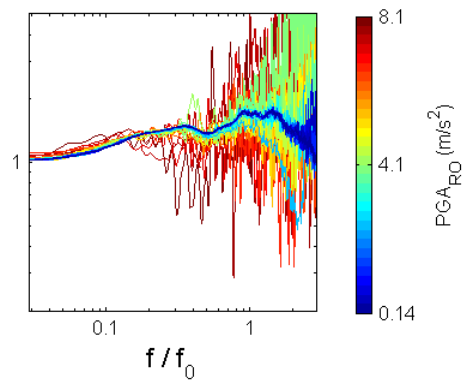

Equiv. Lin. TF (color coded by f_c)

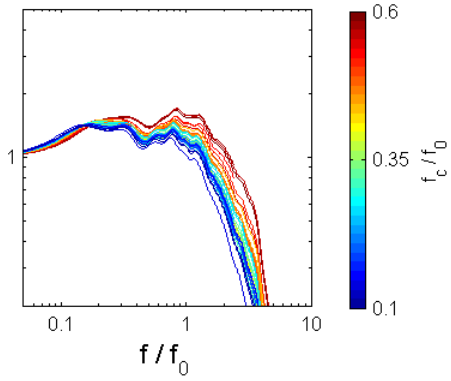

Non-linear TF (color coded by f_c)

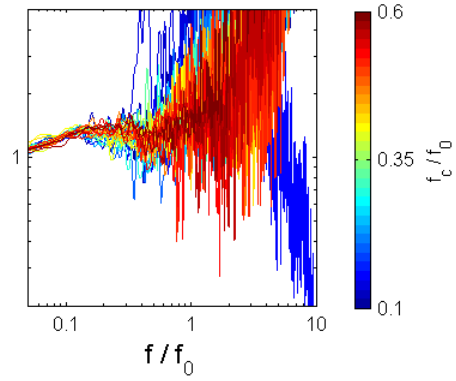

4.3.28 CI.LDF

Depth (m)	Thickness (m)	V_s (m/s)	Damping ratio	Density (kg/m^3)
0	1	263	0.02	1800
1	2	271	0.02	1800
3	3	321	0.02	1800
6	4	355	0.02	1800
10	8	560	0.02	1800
18	2	575	0.02	1800
20	5	593.3	0.02	1800
25	5	634.1	0.02	1800
30	5	667.6	0.02	1800
35	5	694.9	0.02	1800
40	5	717.3	0.02	1800
45	5	735.6	0.02	1800
50	5	750.5	0.01	1800
55	5	762.8	0.01	1800
60	5	772.8	0.01	1800
65	5	781.0	0.01	1800
70	5	787.7	0.01	1800
75	5	793.1	0.01	1800
80	5	797.6	0.01	1800
85	5	801.3	0.01	2000
90	5	804.3	0.01	2000
95	5	806.7	0.01	2000
100	–	808.7	0.01	2000

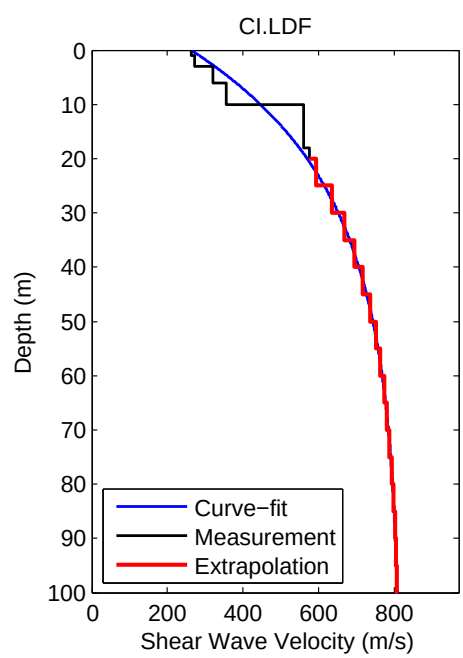

Linear Elastic Transfer Function

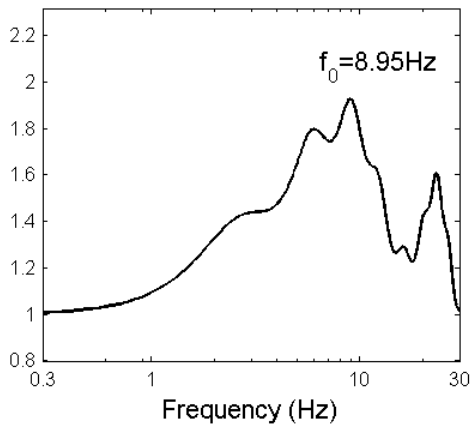

H/V Ratio – Sensor 450

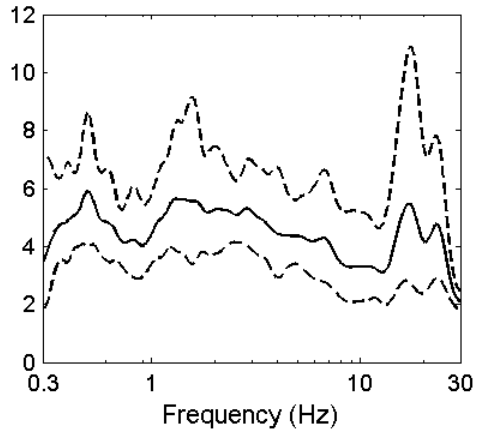

H/V Ratio – Sensor 507

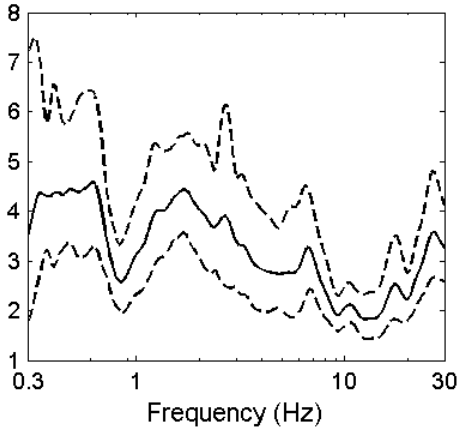

H/V Ratio – Sensor 453

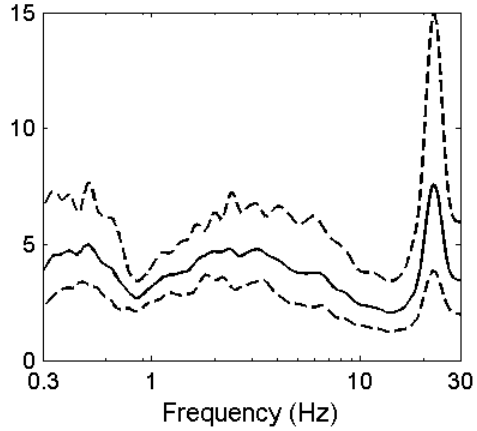

Equivalent Linear Transfer Function

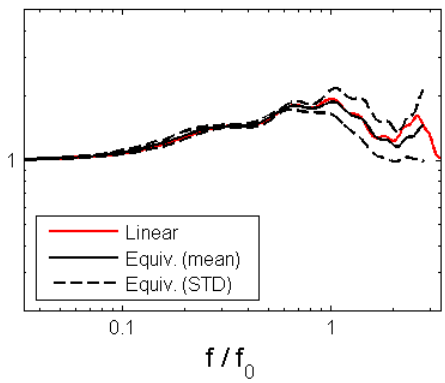

Equiv. Lin. TF (color coded by PGA_{RO})

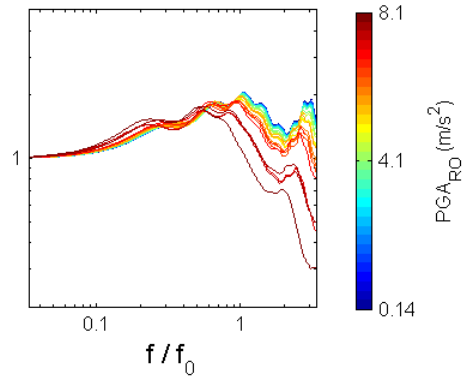

Non-linear Transfer Function

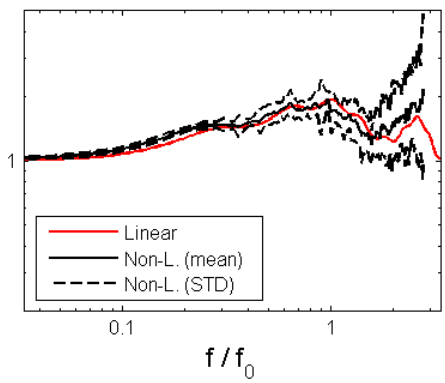

Non-linear TF (color coded by PGA_{RO})

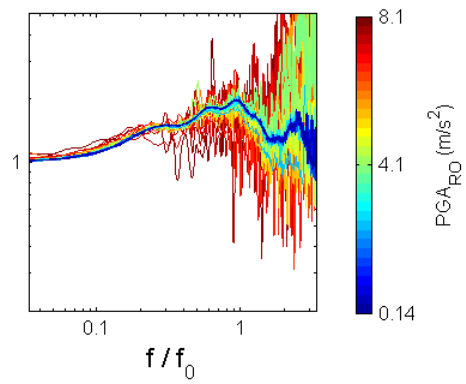

Equiv. Lin. TF (color coded by f_c)

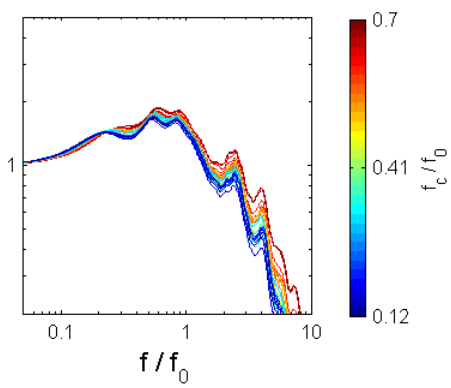

Non-linear TF (color coded by f_c)

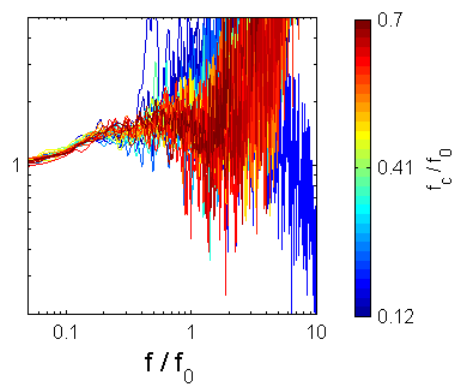

4.3.29 CI.LDR

Depth (m)	Thickness (m)	V_s (m/s)	Damping ratio	Density (kg/m^3)
0	1.5	164	0.05	1600
1.5	2.5	275	0.02	1800
4	4	328	0.02	1800
8	6	370	0.02	1800
14	9	455	0.02	1800
23	12	536	0.02	1800
35	–	865	0.01	2000

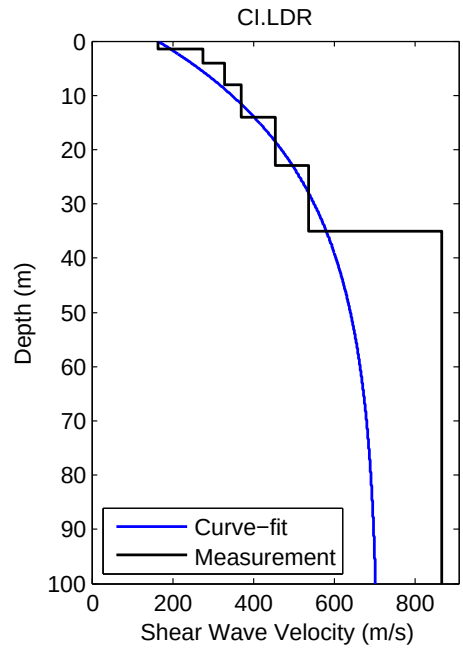

Linear Elastic Transfer Function

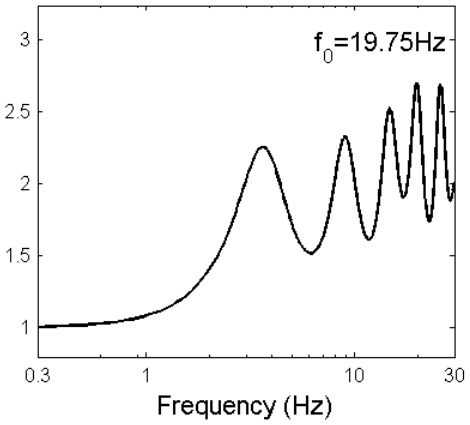

H/V Ratio – Sensor 450

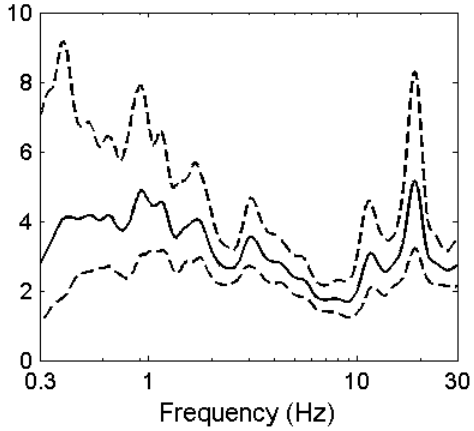

H/V Ratio – Sensor 507

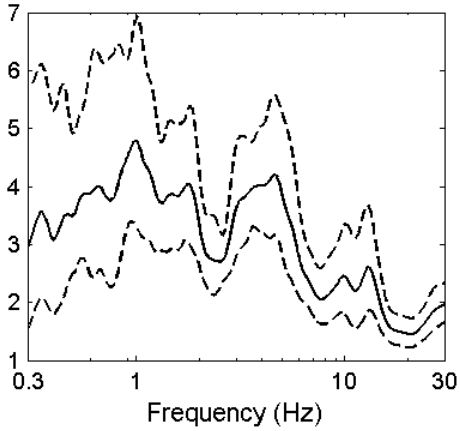

H/V Ratio – Sensor 453

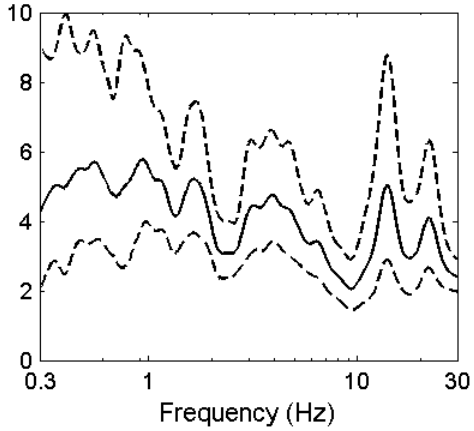

Equivalent Linear Transfer Function

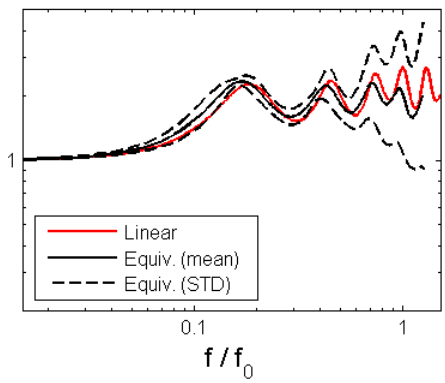

Equiv. Lin. TF (color coded by PGA_{RO})

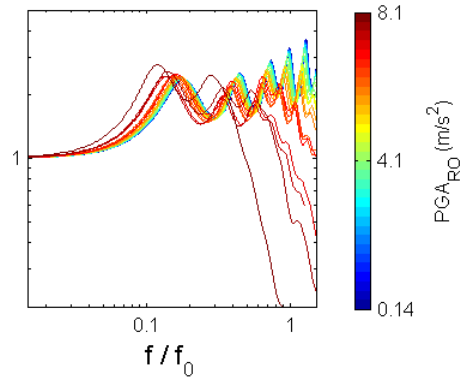

Non-linear Transfer Function

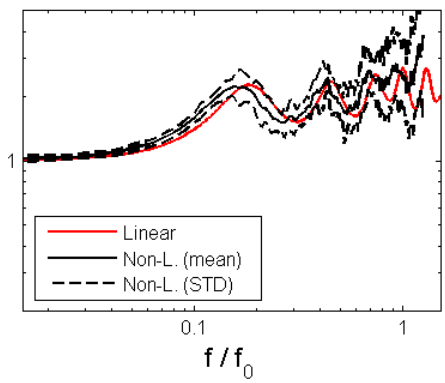

Non-linear TF (color coded by PGA_{RO})

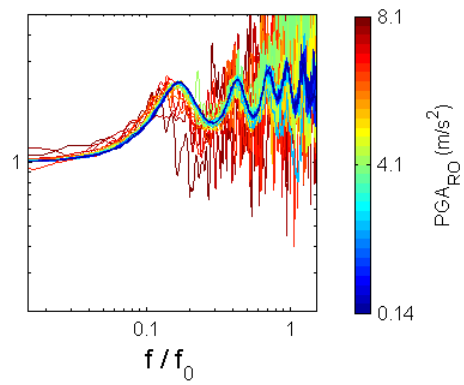

Equiv. Lin. TF (color coded by f_c)

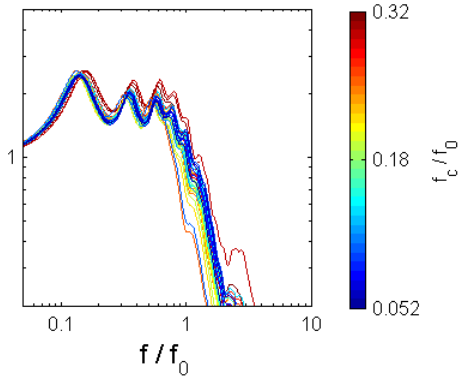

Non-linear TF (color coded by f_c)

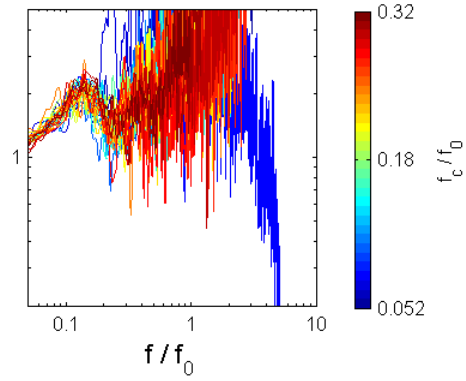

4.3.30 CI.LPC

Depth (m)	Thickness (m)	V_s (m/s)	Damping ratio	Density (kg/m^3)
0	1	184	0.05	1600
1	2	294	0.02	1800
3	3	427	0.02	1800
6	4	505	0.02	1800
10	6	603	0.02	1800
16	9	616	0.02	1800
25	5	664	0.02	1800
30	5	741.2	0.02	1800
35	5	777.1	0.01	1800
40	5	806.1	0.01	2000
45	5	829.6	0.01	2000
50	5	848.6	0.01	2000
55	5	864.0	0.01	2000
60	5	876.4	0.01	2000
65	5	886.5	0.01	2000
70	5	894.6	0.01	2000
75	5	901.2	0.01	2000
80	5	906.6	0.01	2000
85	5	910.9	0.01	2000
90	5	914.4	0.01	2000
95	5	917.2	0.01	2000
100	–	919.5	0.01	2000

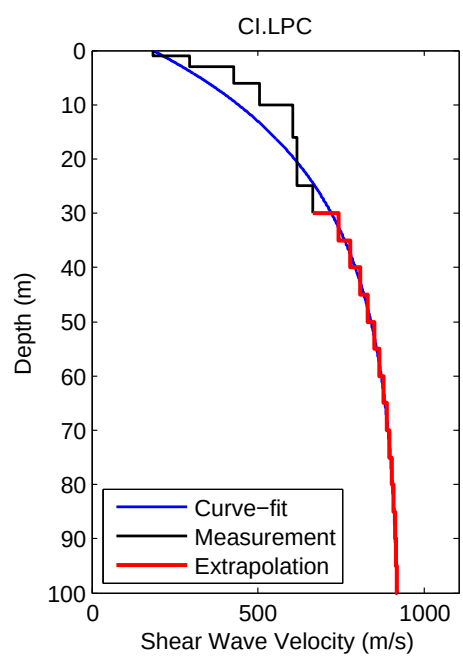

Linear Elastic Transfer Function

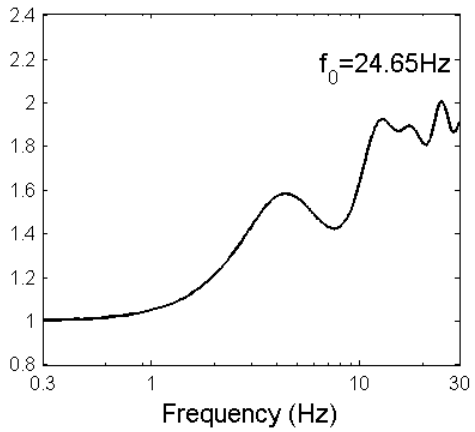

H/V Ratio – Sensor 450

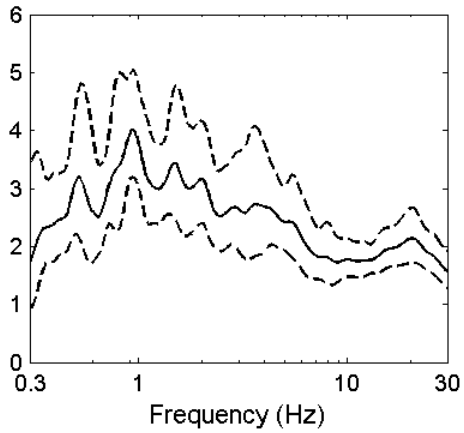

H/V Ratio – Sensor 507

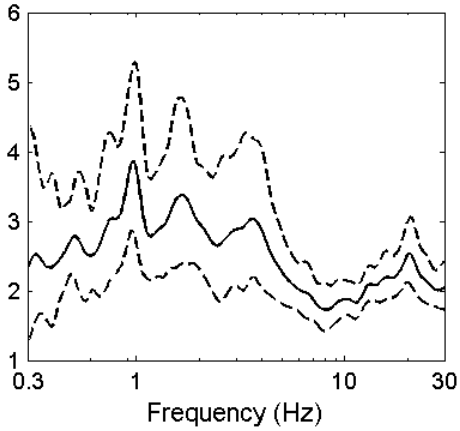

H/V Ratio – Sensor 453

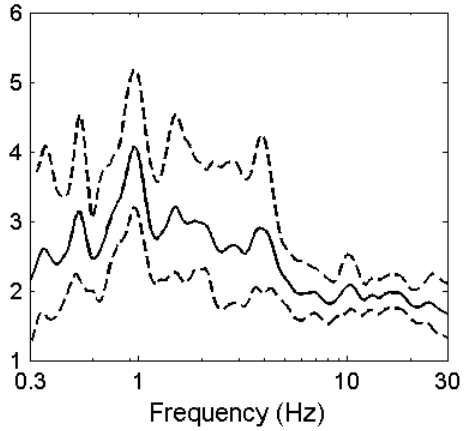

Equivalent Linear Transfer Function

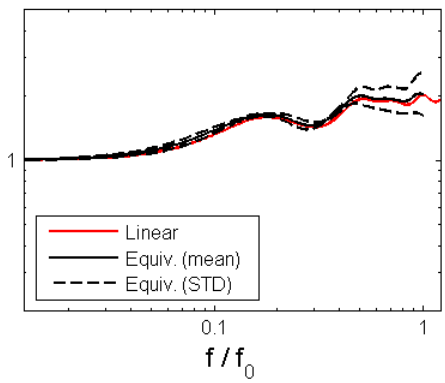

Equiv. Lin. TF (color coded by PGA_{RO})

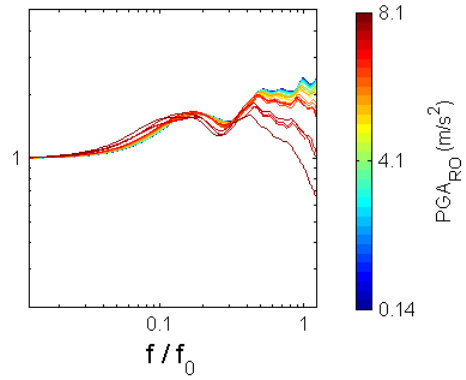

Non-linear Transfer Function

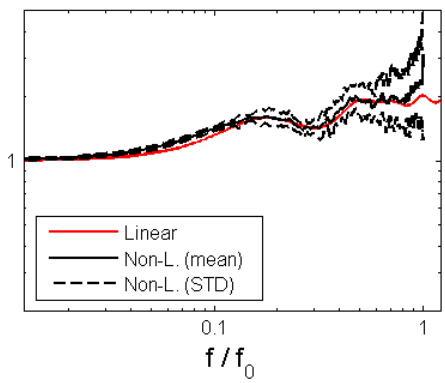

Non-linear TF (color coded by PGA_{RO})

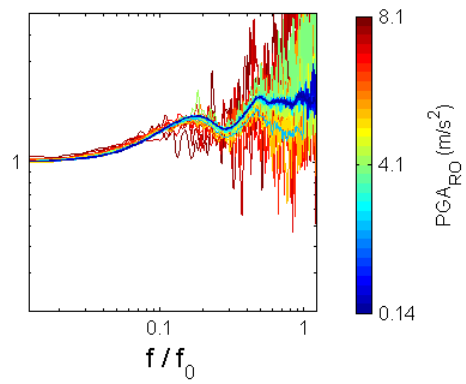

Equiv. Lin. TF (color coded by f_c)

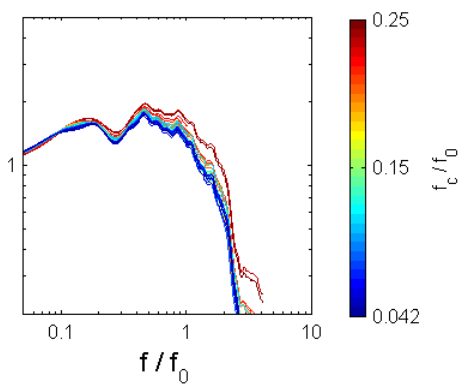

Non-linear TF (color coded by f_c)

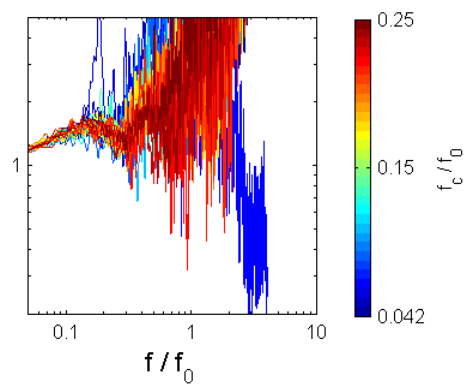

4.3.31 CI.NBS

Depth (m)	Thickness (m)	V_s (m/s)	Damping ratio	Density (kg/m^3)
0	0.5	166	0.05	1600
0.5	1	196	0.05	1600
1.5	2	276	0.02	1800
3.5	3	351	0.02	1800
6.5	4	424	0.02	1800
10.5	6	475	0.02	1800
16.5	9	509	0.02	1800
25.5	4.5	570	0.02	1800
30	5	616.5	0.02	1800
35	5	647.5	0.02	1800
40	5	673.0	0.02	1800
45	5	693.9	0.02	1800
50	5	711.1	0.02	1800
55	5	725.3	0.02	1800
60	5	736.9	0.02	1800
65	5	746.4	0.02	1800
70	5	754.3	0.01	1800
75	5	760.7	0.01	1800
80	5	766.0	0.01	1800
85	5	770.3	0.01	1800
90	5	773.9	0.01	1800
95	5	776.8	0.01	1800
100	–	779.2	0.01	1800

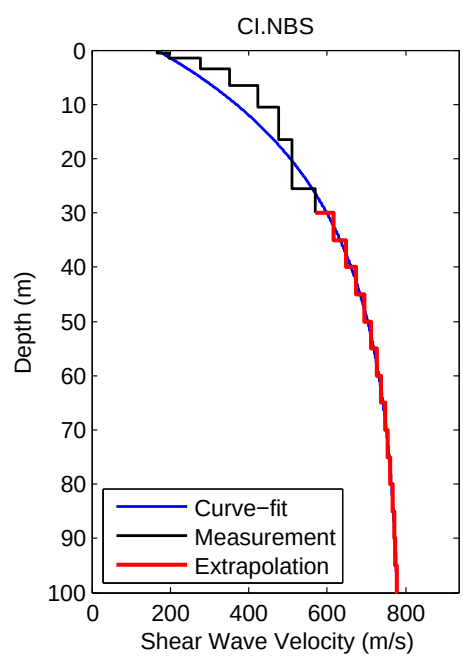

Linear Elastic Transfer Function

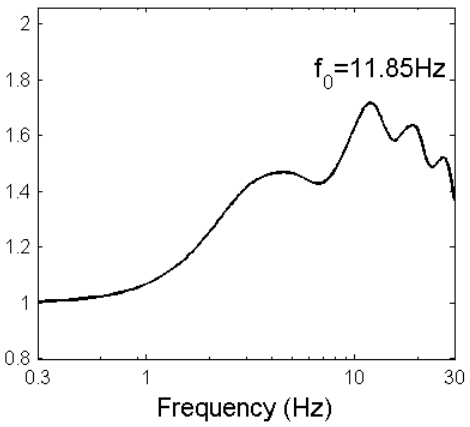

H/V Ratio – Sensor 450

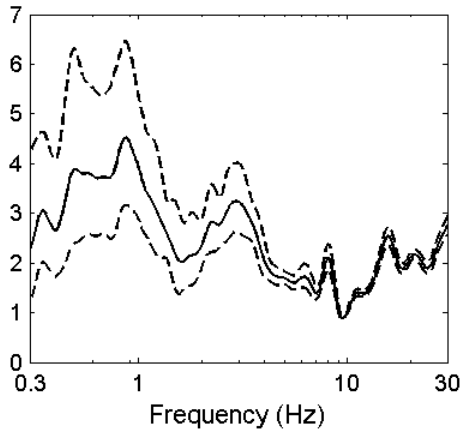

H/V Ratio – Sensor 507

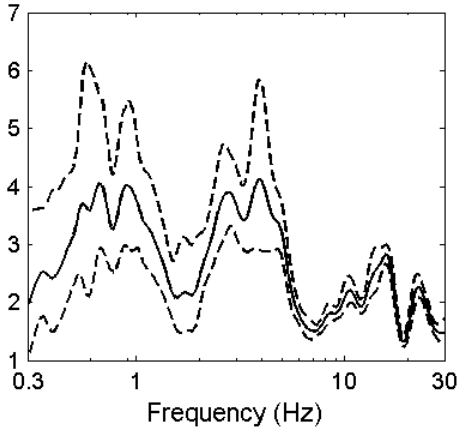

H/V Ratio – Sensor 453

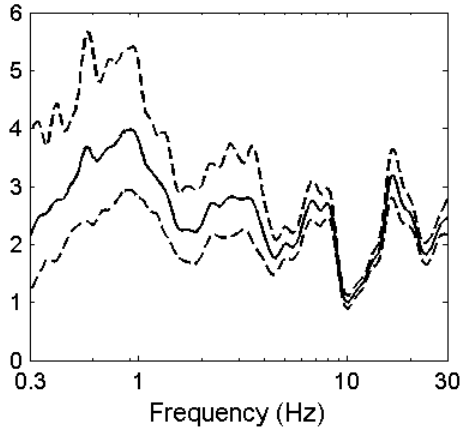

Equivalent Linear Transfer Function

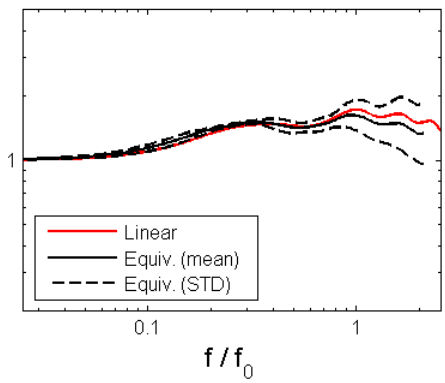

Equiv. Lin. TF (color coded by PGA_{RO})

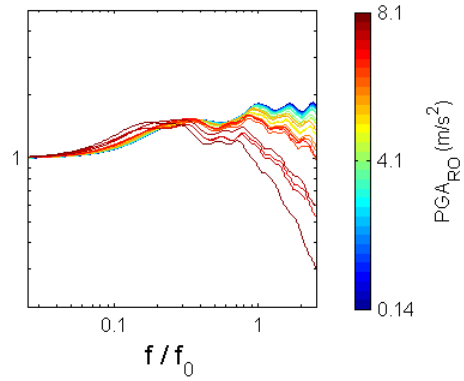

Non-linear Transfer Function

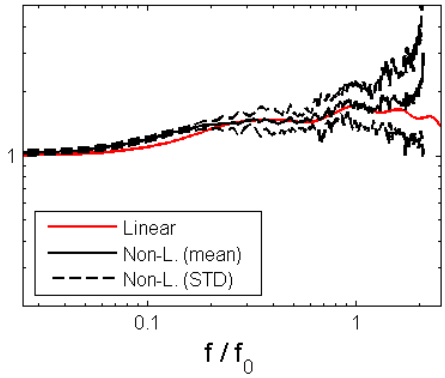

Non-linear TF (color coded by PGA_{RO})

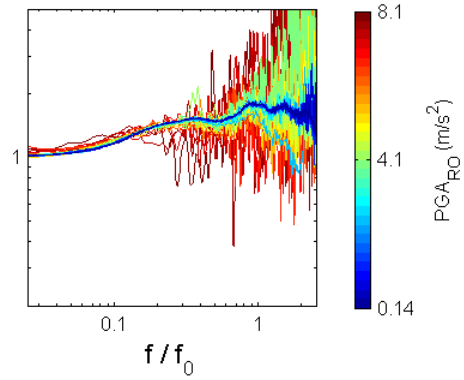

Equiv. Lin. TF (color coded by f_c)

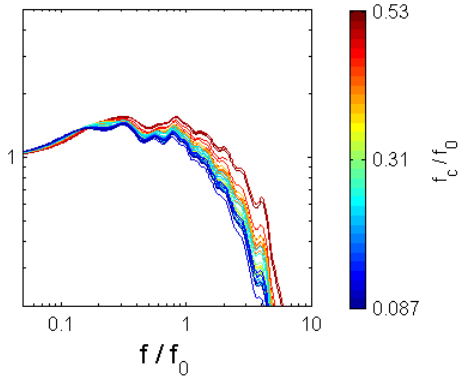

Non-linear TF (color coded by f_c)

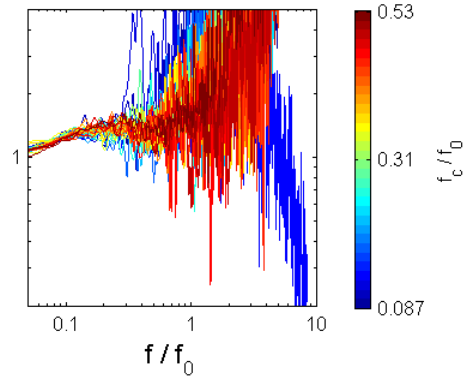

4.3.32 CI.RRX

Depth (m)	Thickness (m)	V_s (m/s)	Damping ratio	Density (kg/m^3)
0	1	189	0.05	1600
1	2	266	0.02	1800
3	3	307	0.02	1800
6	3	326	0.02	1800
9	6	410	0.02	1800
15	9	416	0.02	1800
24	1	477	0.02	1800
25	5	488.3	0.02	1800
30	5	518.3	0.02	1800
35	5	543.7	0.02	1800
40	5	565.0	0.02	1800
45	5	583.0	0.02	1800
50	5	598.1	0.02	1800
55	5	610.8	0.02	1800
60	5	621.6	0.02	1800
65	5	630.6	0.02	1800
70	5	638.2	0.02	1800
75	5	644.6	0.02	1800
80	5	650.0	0.02	1800
85	5	654.6	0.02	1800
90	5	658.4	0.02	1800
95	5	661.6	0.02	1800
100	–	664.3	0.02	1800

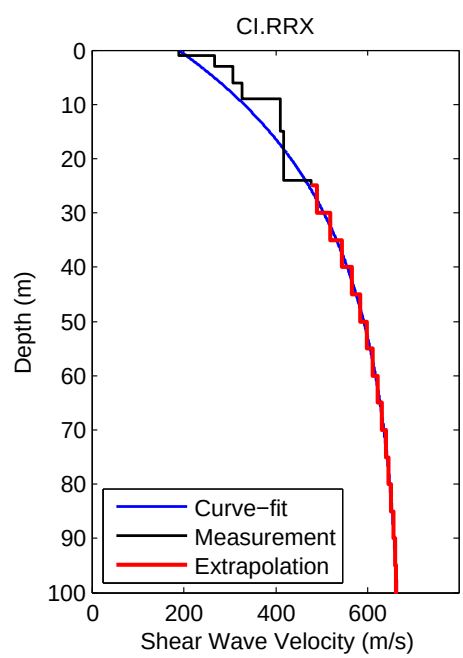

Linear Elastic Transfer Function

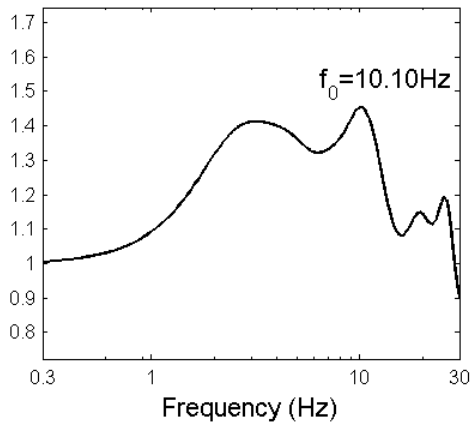

H/V Ratio – Sensor 450

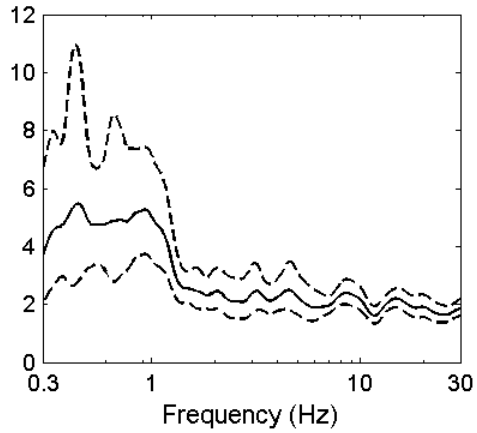

H/V Ratio – Sensor 507

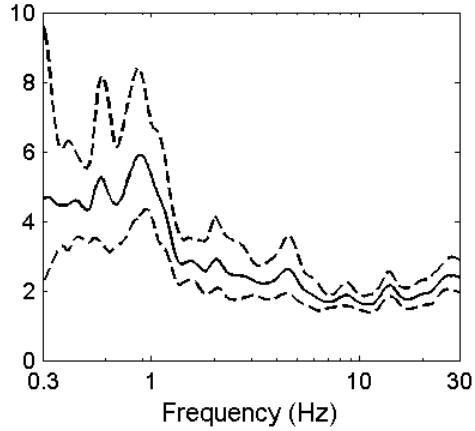

H/V Ratio – Sensor 453

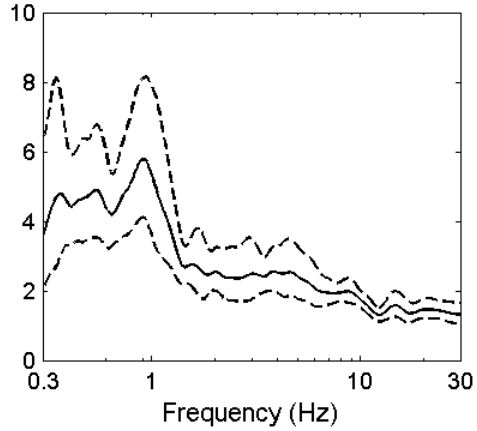

Equivalent Linear Transfer Function

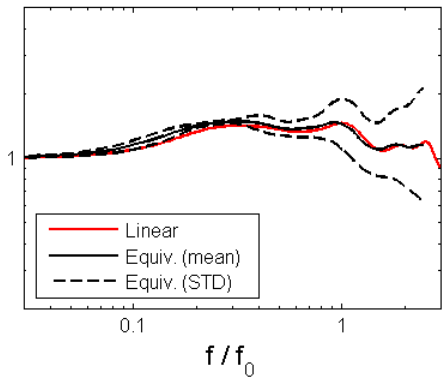

Equiv. Lin. TF (color coded by PGA_{RO})

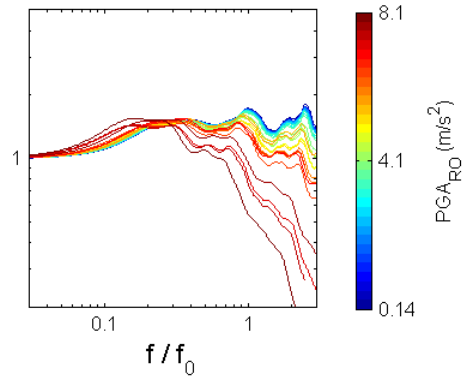

Non-linear Transfer Function

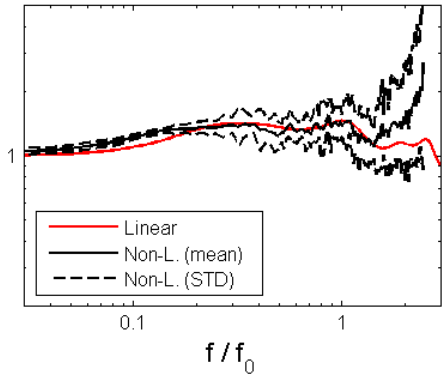

Non-linear TF (color coded by PGA_{RO})

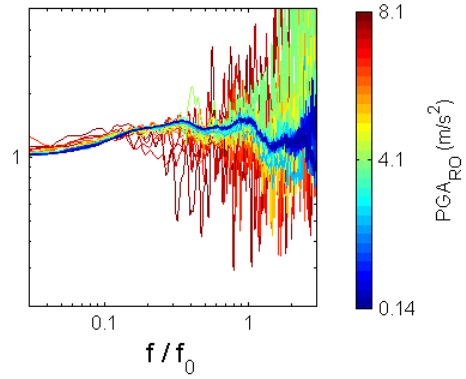

Equiv. Lin. TF (color coded by f_c)

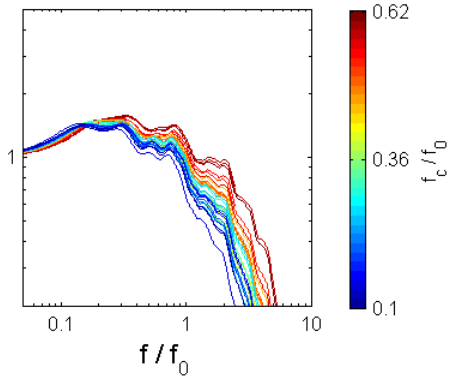

Non-linear TF (color coded by f_c)

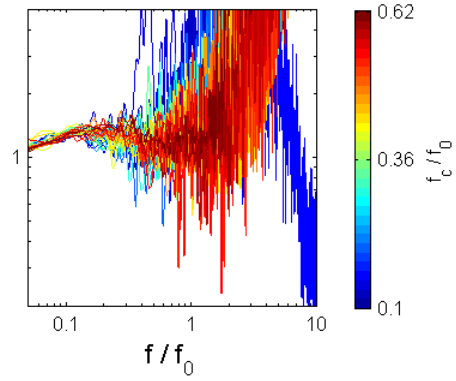

4.3.33 CI.SYP

Depth (m)	Thickness (m)	V_s (m/s)	Damping ratio	Density (kg/m^3)
0	1	216	0.05	1800
1	2	266	0.02	1800
3	3	284	0.02	1800
6	4	403	0.02	1800
10	5	473	0.02	1800
15	6	526	0.02	1800
21	9	666	0.02	1800
30	5	695.1	0.02	1800
35	5	720.2	0.02	1800
40	5	739.6	0.02	1800
45	5	754.6	0.01	1800
50	5	766.2	0.01	1800
55	5	775.2	0.01	1800
60	5	782.1	0.01	1800
65	5	787.5	0.01	1800
70	5	791.6	0.01	1800
75	5	794.8	0.01	1800
80	5	797.3	0.01	1800
85	5	799.2	0.01	1800
90	5	800.7	0.01	2000
95	5	801.8	0.01	2000
100	–	802.7	0.01	2000

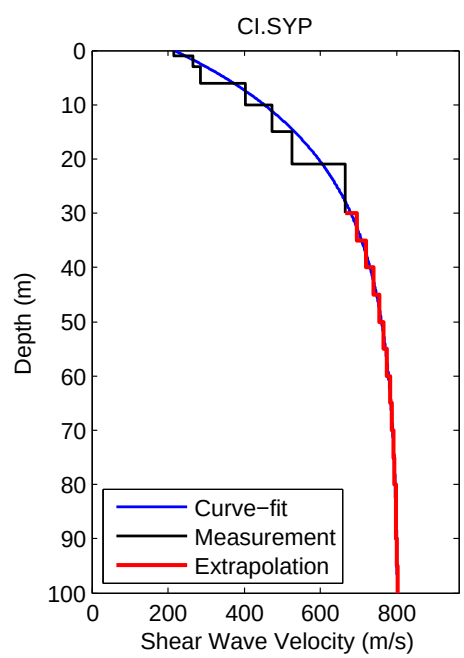

Linear Elastic Transfer Function

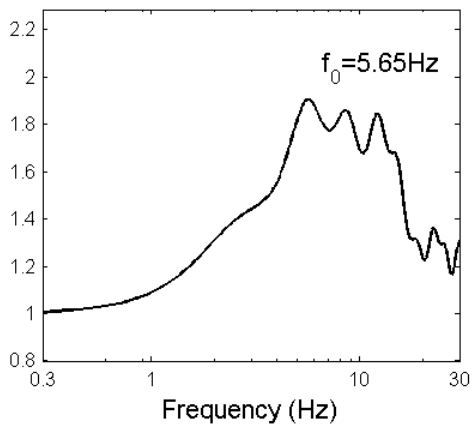

H/V Ratio – Sensor 507

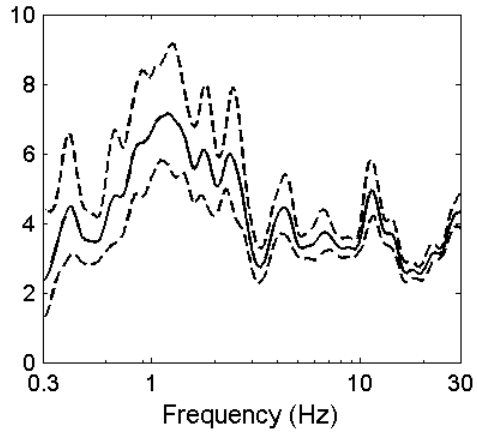

H/V Ratio – Sensor 453a

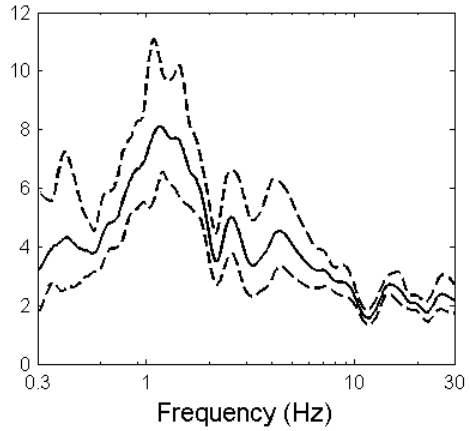

H/V Ratio – Sensor 453b

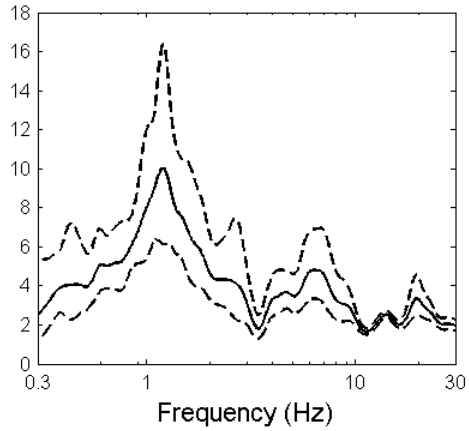

Equivalent Linear Transfer Function

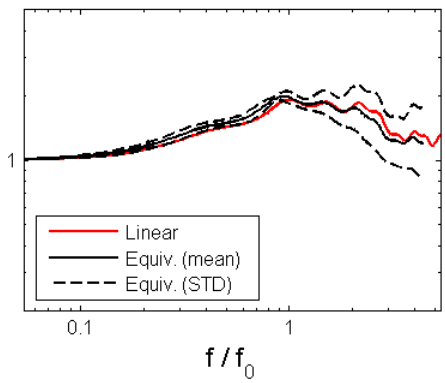

Equiv. Lin. TF (color coded by PGA_{RO})

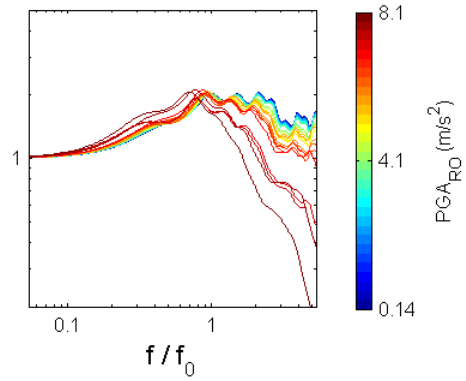

Non-linear Transfer Function

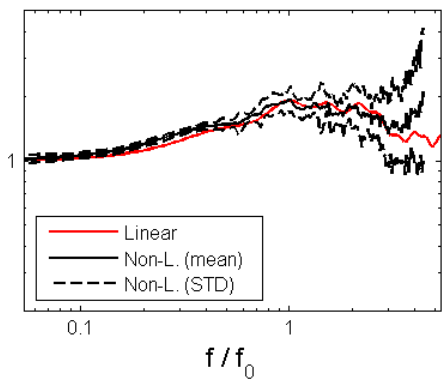

Non-linear TF (color coded by PGA_{RO})

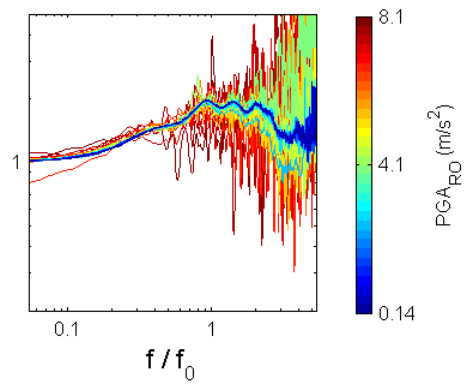

Equiv. Lin. TF (color coded by f_c)

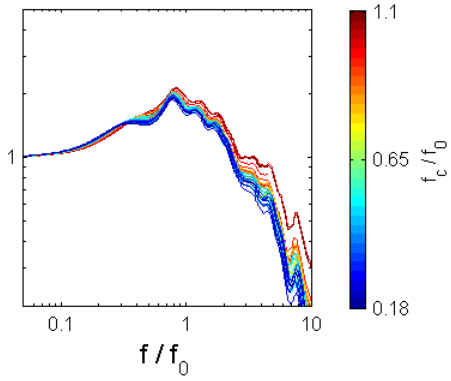

Non-linear TF (color coded by f_c)

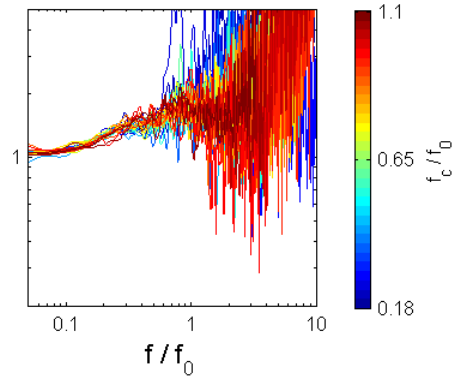

4.3.34 CI.THM

Depth (m)	Thickness (m)	V_s (m/s)	Damping ratio	Density (kg/m^3)
0	1.5	243	0.05	1800
1.5	2	406	0.02	1800
3.5	5.5	517	0.02	1800
9	7	409	0.02	1800
16	7	450	0.02	1800
23	7	582	0.02	1800
30	5	617.1	0.02	1800
35	5	647.4	0.02	1800
40	5	673.3	0.02	1800
45	5	695.3	0.02	1800
50	5	714.1	0.02	1800
55	5	730.1	0.02	1800
60	5	743.8	0.02	1800
65	5	755.4	0.01	1800
70	5	765.4	0.01	1800
75	5	773.8	0.01	1800
80	5	781.1	0.01	1800
85	5	787.2	0.01	1800
90	5	792.5	0.01	1800
95	5	796.9	0.01	1800
100	–	800.8	0.01	2000

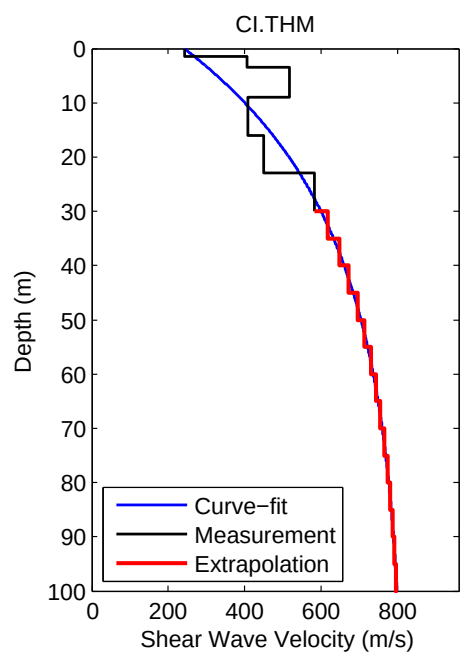

Linear Elastic Transfer Function

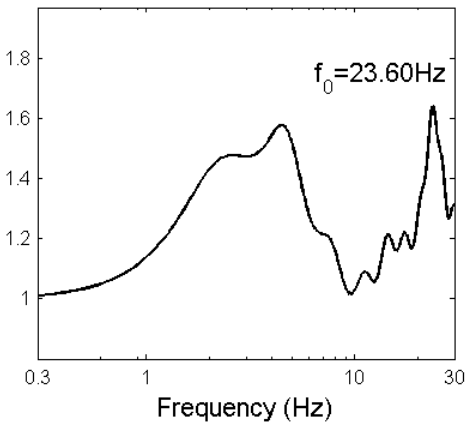

H/V Ratio – Sensor 450

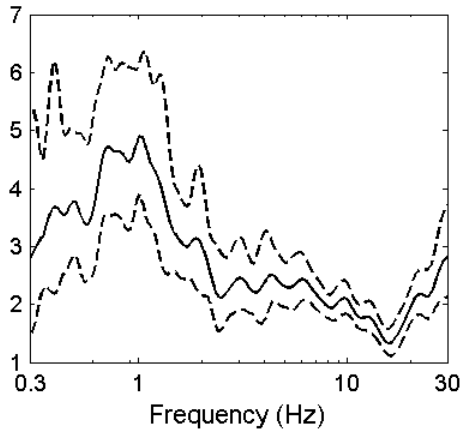

H/V Ratio – Sensor 507

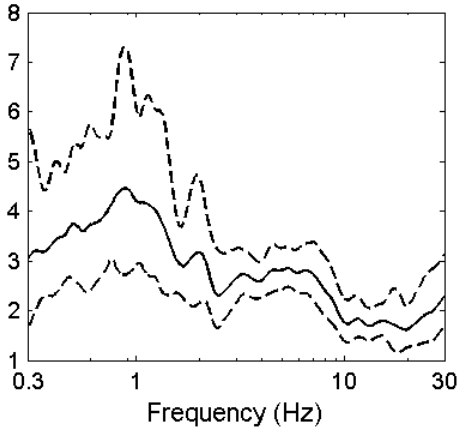

H/V Ratio – Sensor 453

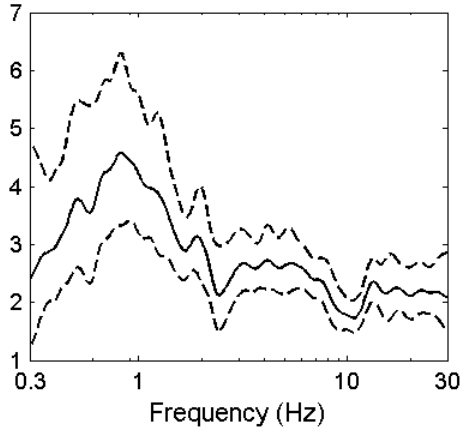

Equivalent Linear Transfer Function

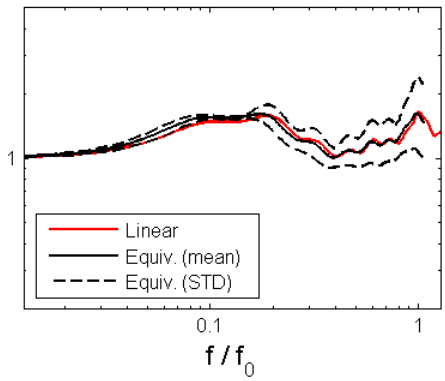

Equiv. Lin. TF (color coded by PGA_{RO})

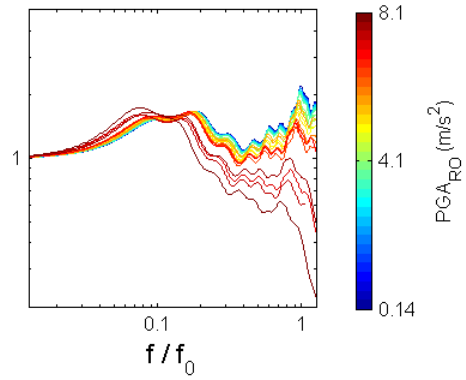

Non-linear Transfer Function

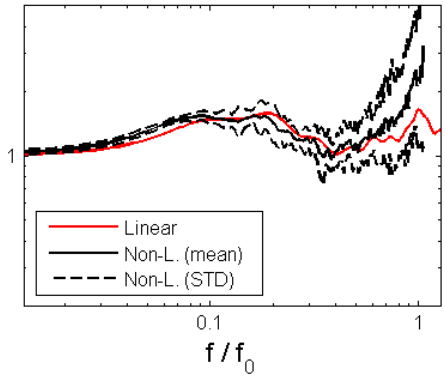

Non-linear TF (color coded by PGA_{RO})

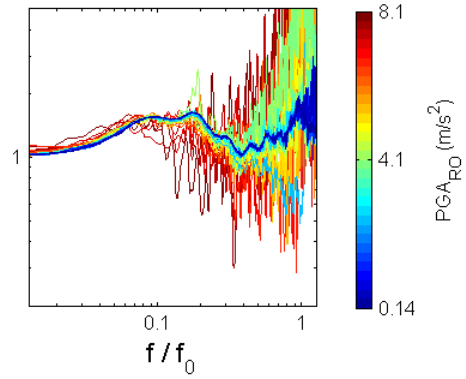

Equiv. Lin. TF (color coded by f_c)

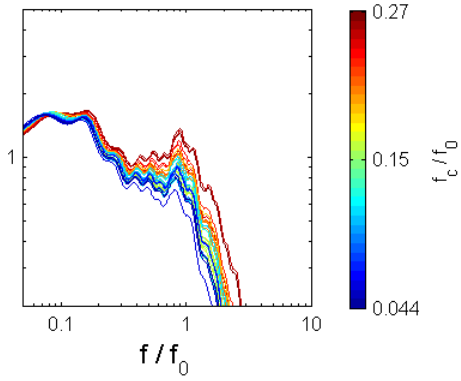

Non-linear TF (color coded by f_c)

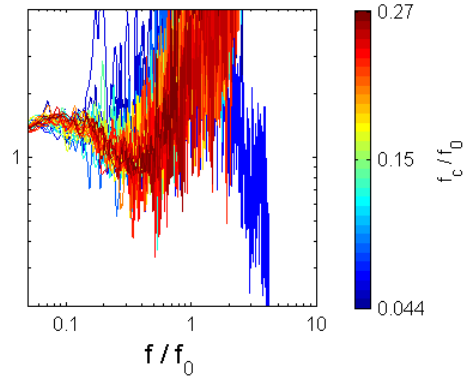

4.3.35 CI.VCS

Depth (m)	Thickness (m)	V_s (m/s)	Damping ratio	Density (kg/m^3)
0	1.5	193	0.05	1600
1.5	4.5	365	0.02	1800
6	8	403	0.02	1800
14	18	469	0.02	1800
32	–	1188	0.01	2000

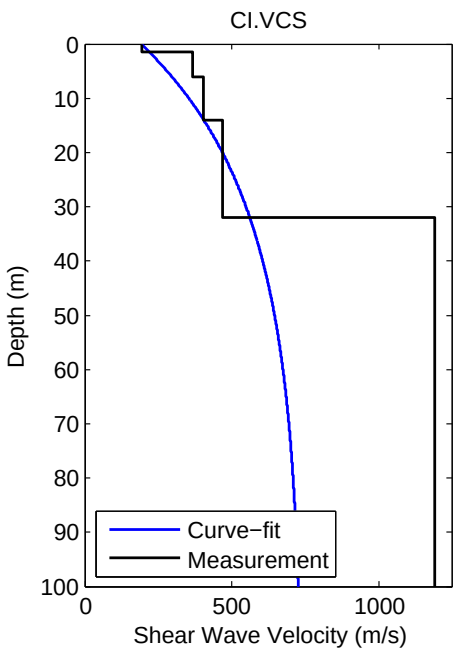

Linear Elastic Transfer Function

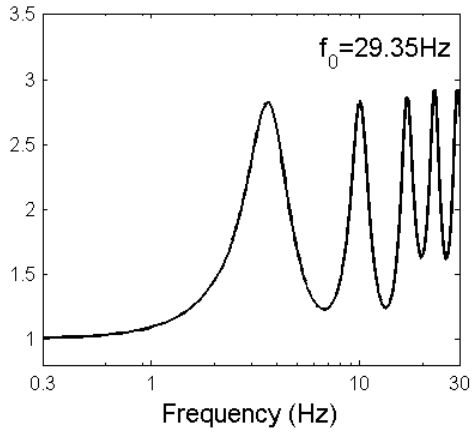

H/V Ratio – Sensor 507

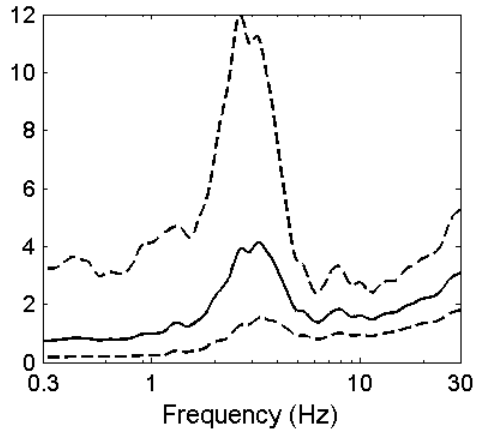

H/V Ratio – Sensor 453a

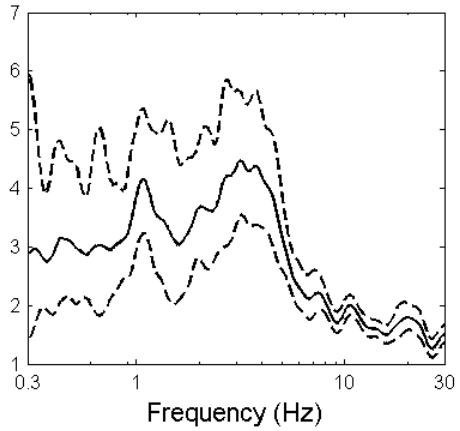

H/V Ratio – Sensor 453b

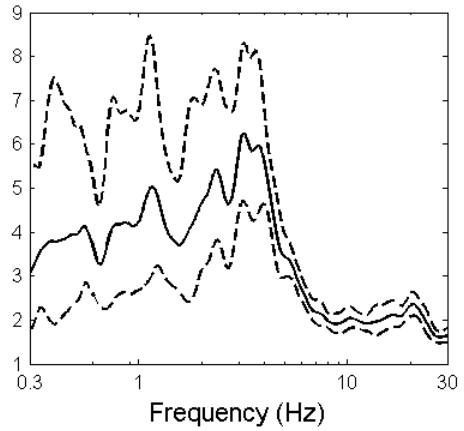

Equivalent Linear Transfer Function

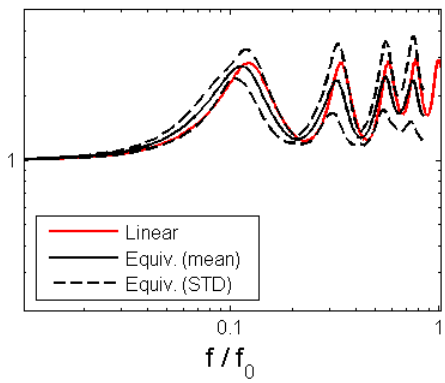

Equiv. Lin. TF (color coded by PGA_{RO})

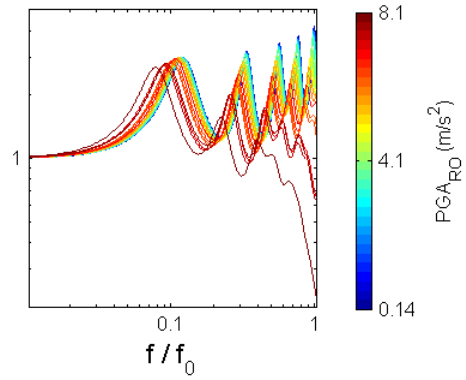

Non-linear Transfer Function

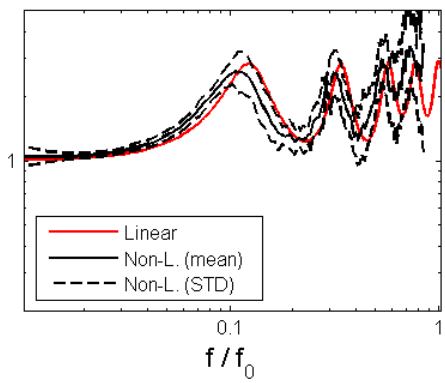

Non-linear TF (color coded by PGA_{RO})

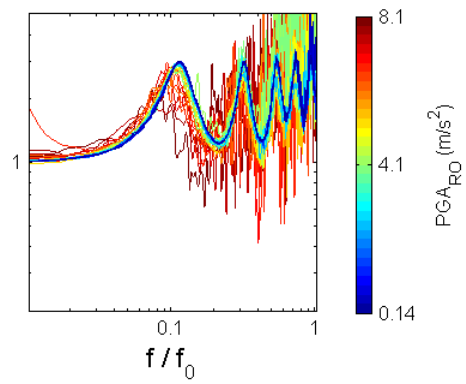

Equiv. Lin. TF (color coded by f_c)

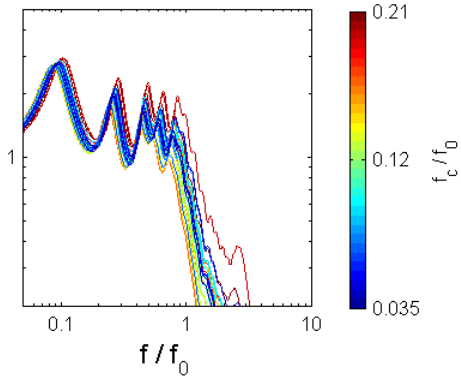

Non-linear TF (color coded by f_c)

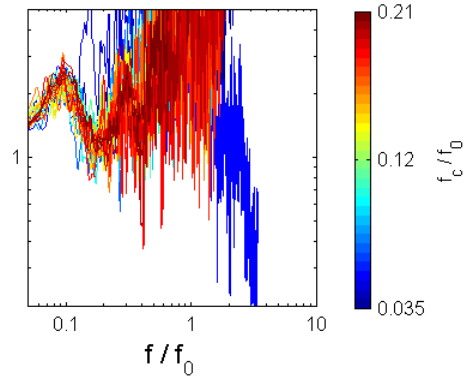

4.3.36 NC.HCABa

Depth (m)	Thickness (m)	V_s (m/s)	Damping ratio	Density (kg/m^3)
0	2.5	373	0.02	1800
2.5	4.5	588	0.02	1800
7	15	645	0.02	1800
22	8	977	0.01	2000
30	5	982.6	0.01	2000
35	5	1017.9	0.01	2000
40	5	1045.7	0.01	2000
45	5	1067.7	0.01	2000
50	5	1085.0	0.01	2000
55	5	1098.8	0.01	2000
60	5	1109.6	0.01	2000
65	5	1118.1	0.01	2000
70	5	1124.9	0.01	2000
75	5	1130.2	0.01	2000
80	5	1134.5	0.01	2000
85	5	1137.8	0.01	2000
90	5	1140.4	0.01	2000
95	5	1142.5	0.01	2000
100	–	1144.1	0.01	2000

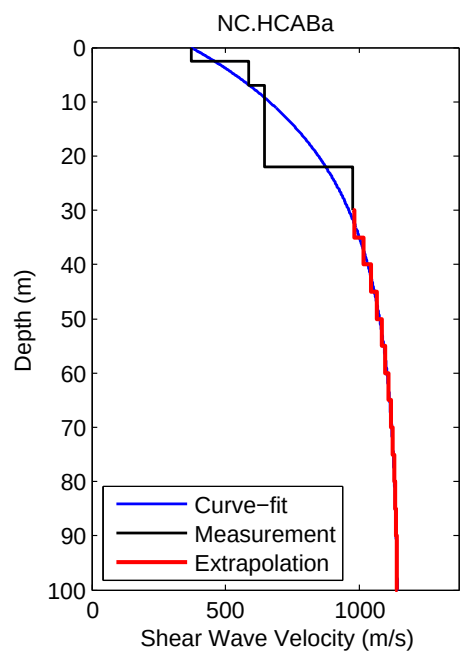

Linear Elastic Transfer Function

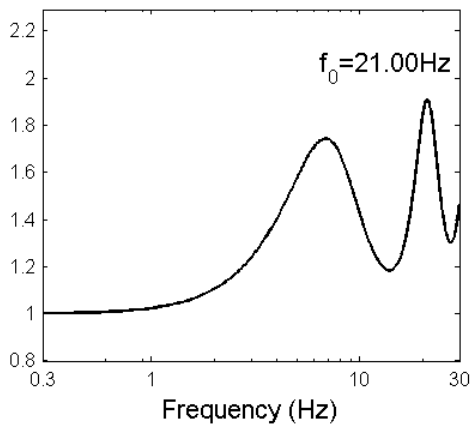

H/V Ratio – Sensor 450

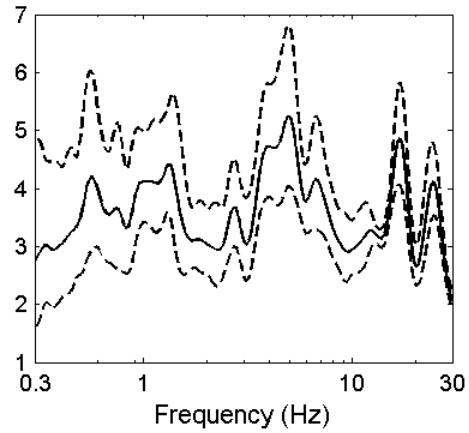

H/V Ratio – Sensor 507

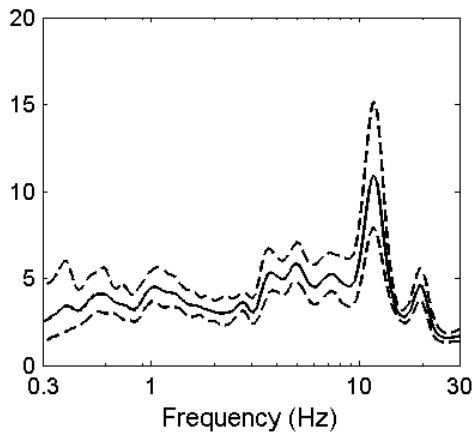

H/V Ratio – Sensor 453

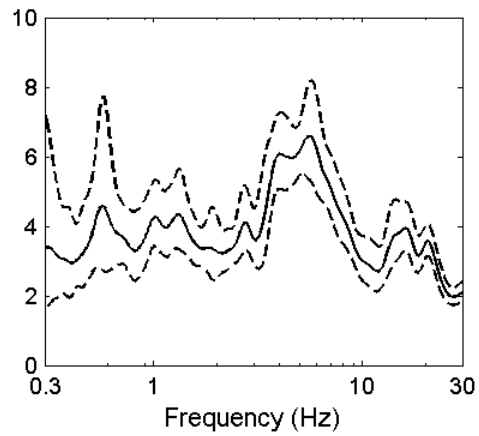

Equivalent Linear Transfer Function

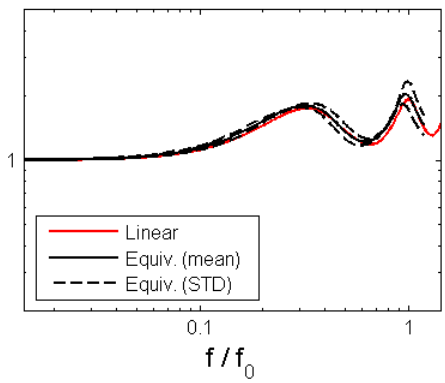

Equiv. Lin. TF (color coded by PGA_{RO})

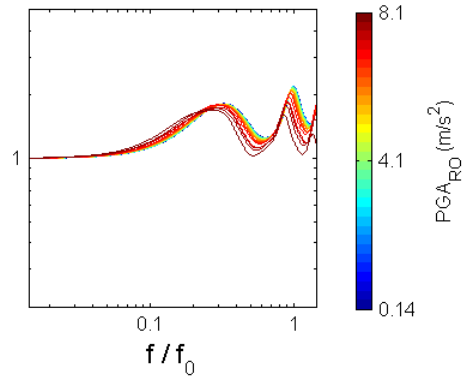

Non-linear Transfer Function

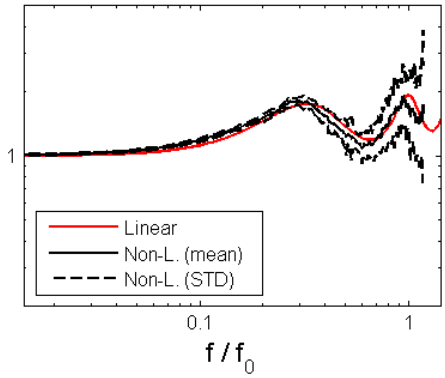

Non-linear TF (color coded by PGA_{RO})

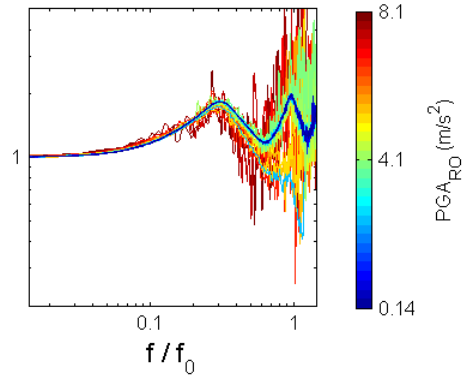

Equiv. Lin. TF (color coded by f_c)

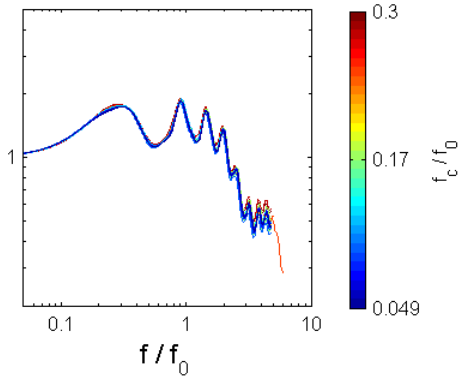

Non-linear TF (color coded by f_c)

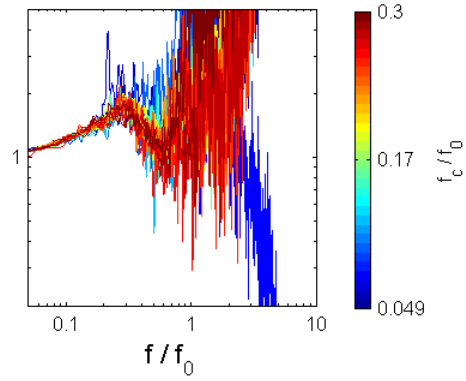

4.3.37 NC.HCABb

Depth (m)	Thickness (m)	V_s (m/s)	Damping ratio	Density (kg/m^3)
0	2.5	378	0.02	1800
2.5	3.5	574	0.02	1800
6	5	637	0.02	1800
11	7	640	0.02	1800
18	11	750	0.01	1800
29	21	1120	0.01	2000
50	5	1128.0	0.01	2000
55	5	1134.4	0.01	2000
60	5	1138.9	0.01	2000
65	5	1142.2	0.01	2000
70	5	1144.5	0.01	2000
75	5	1146.2	0.01	2000
80	5	1147.3	0.01	2000
85	5	1148.2	0.01	2000
90	5	1148.8	0.01	2000
95	5	1149.2	0.01	2000
100	–	1149.5	0.01	2000

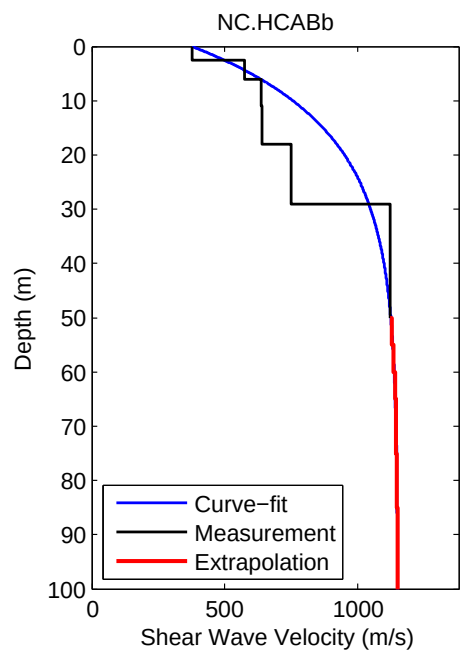

Linear Elastic Transfer Function

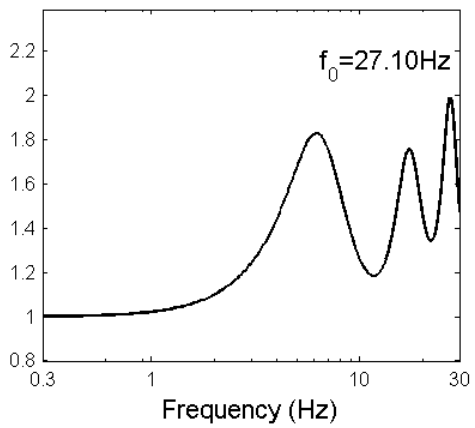

H/V Ratio – Sensor 450

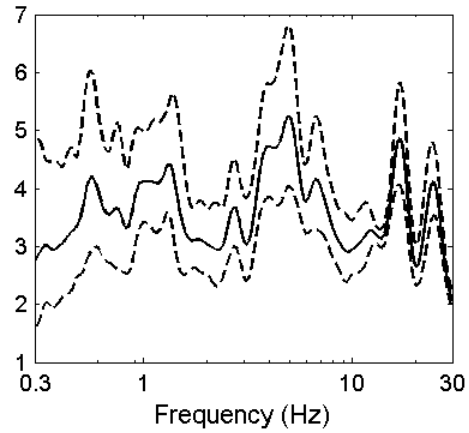

H/V Ratio – Sensor 507

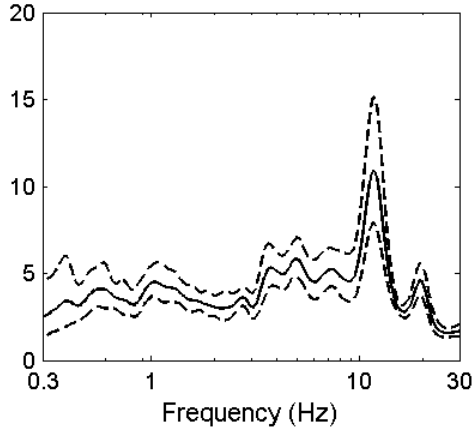

H/V Ratio – Sensor 453

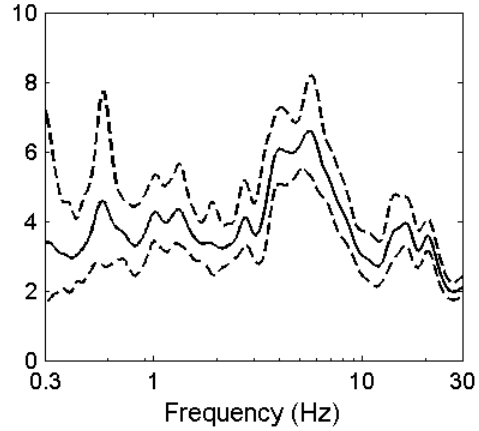

Equivalent Linear Transfer Function

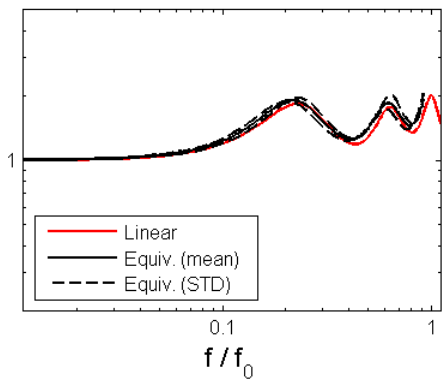

Equiv. Lin. TF (color coded by PGA_{RO})

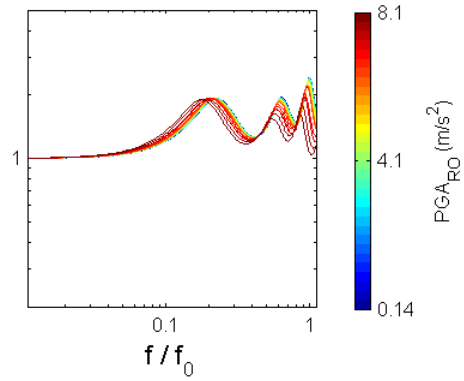

Non-linear Transfer Function

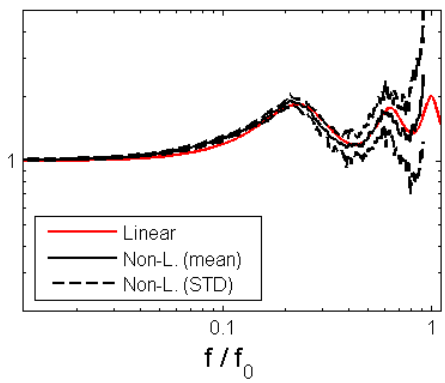

Non-linear TF (color coded by PGA_{RO})

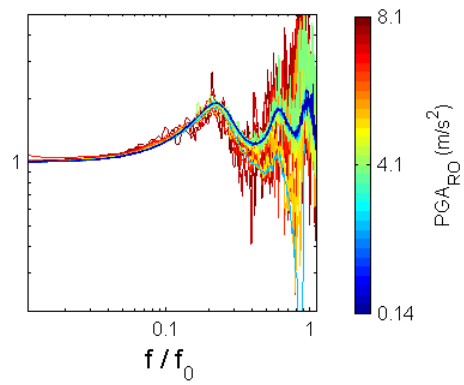

Equiv. Lin. TF (color coded by f_c)

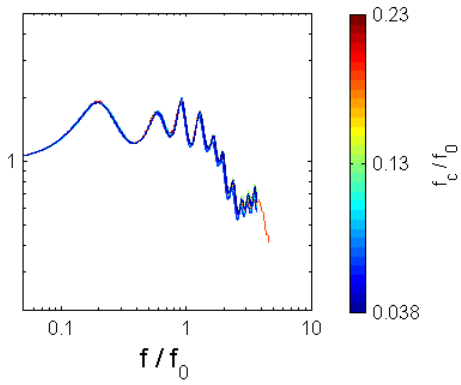

Non-linear TF (color coded by f_c)

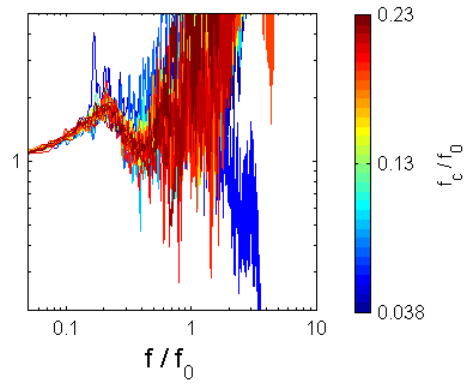

4.3.38 NC.JSFB

Depth (m)	Thickness (m)	V_s (m/s)	Damping ratio	Density (kg/m^3)
0	0.75	136	0.05	1600
0.75	1.25	269	0.02	1800
2	3	382	0.02	1800
5	4	442	0.02	1800
9	6	454	0.02	1800
15	8	474	0.02	1800
23	10	566	0.02	1800
33	7	708	0.02	1800
40	5	709.3	0.02	1800
45	5	727.4	0.02	1800
50	5	741.7	0.02	1800
55	5	752.8	0.01	1800
60	5	761.6	0.01	1800
65	5	768.5	0.01	1800
70	5	773.9	0.01	1800
75	5	778.2	0.01	1800
80	5	781.5	0.01	1800
85	5	784.1	0.01	1800
90	5	786.2	0.01	1800
95	5	787.8	0.01	1800
100	–	789.1	0.01	1800

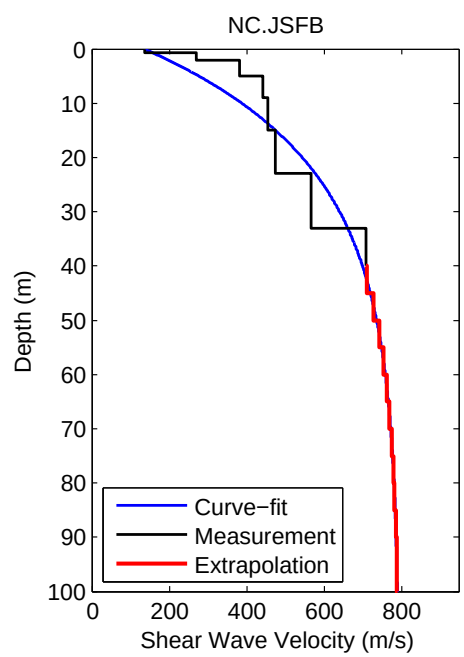

Linear Elastic Transfer Function

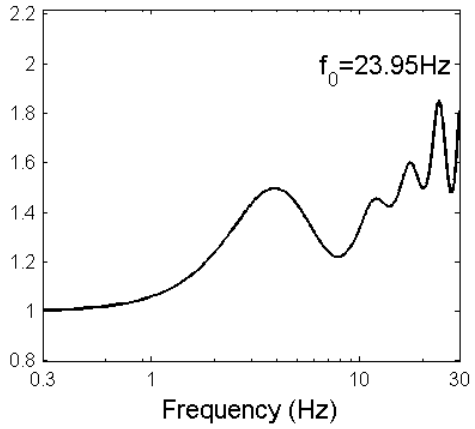

H/V Ratio – Sensor 450

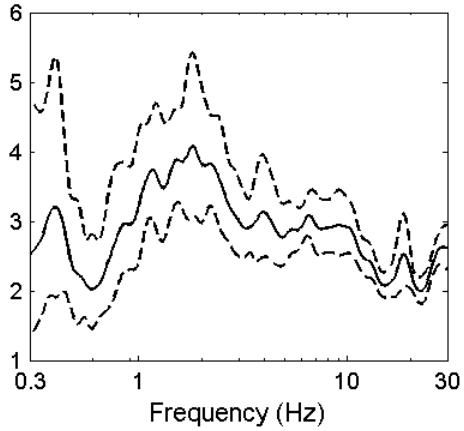

H/V Ratio – Sensor 453a

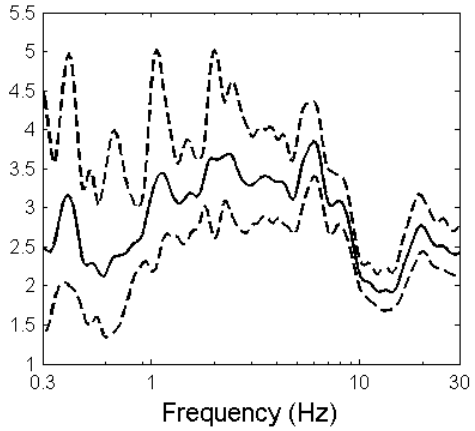

H/V Ratio – Sensor 453b

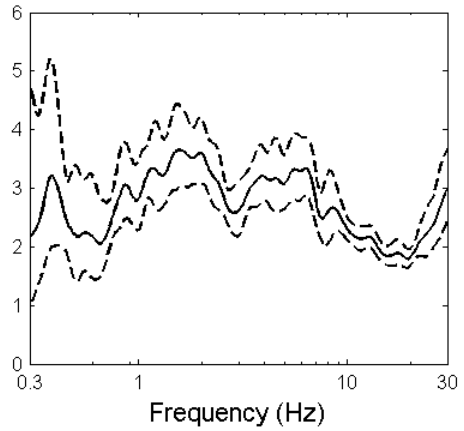

Equivalent Linear Transfer Function

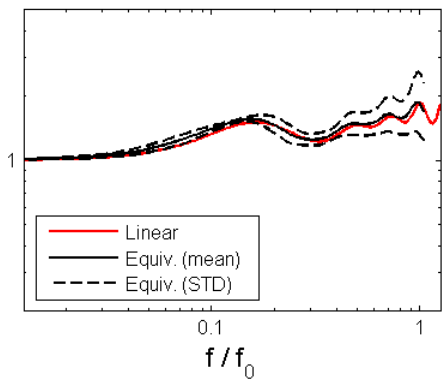

Equiv. Lin. TF (color coded by PGA_{RO})

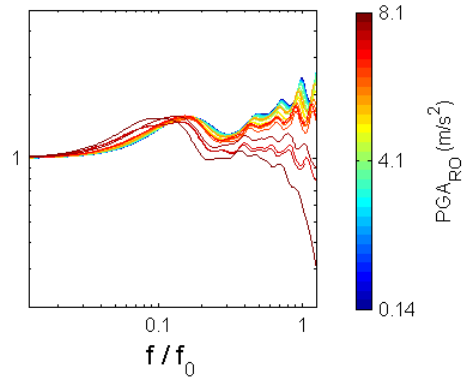

Non-linear Transfer Function

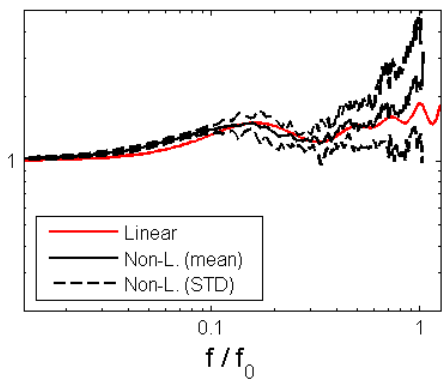

Non-linear TF (color coded by PGA_{RO})

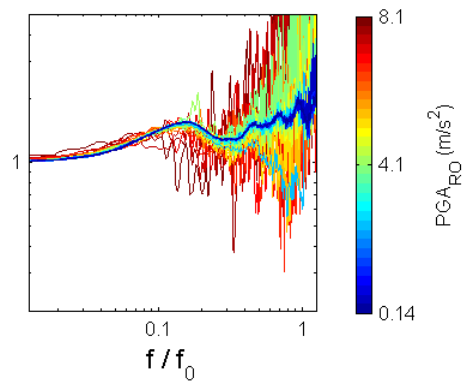

Equiv. Lin. TF (color coded by f_c)

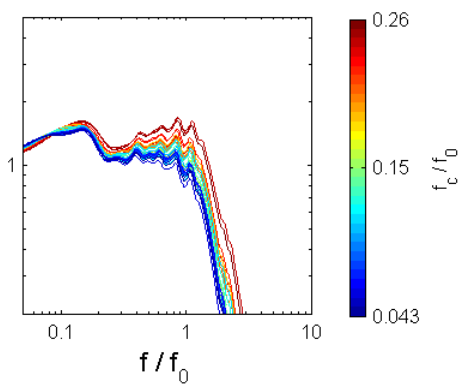

Non-linear TF (color coded by f_c)

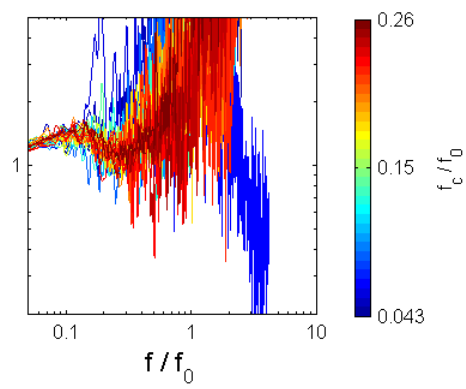

4.3.39 NC.PHOB

Depth (m)	Thickness (m)	V_s (m/s)	Damping ratio	Density (kg/m^3)
0	1	131	0.05	1600
1	2	289	0.02	1800
3	3	359	0.02	1800
6	6	371	0.02	1800
12	8	426	0.02	1800
20	10	455	0.02	1800
30	5	501	0.02	1800
35	5	545.7	0.02	1800
40	5	569.8	0.02	1800
45	5	589.9	0.02	1800
50	5	606.7	0.02	1800
55	5	620.8	0.02	1800
60	5	632.5	0.02	1800
65	5	642.4	0.02	1800
70	5	650.6	0.02	1800
75	5	657.5	0.02	1800
80	5	663.2	0.02	1800
85	5	668.0	0.02	1800
90	5	672.0	0.02	1800
95	5	675.4	0.02	1800
100	–	678.2	0.02	1800

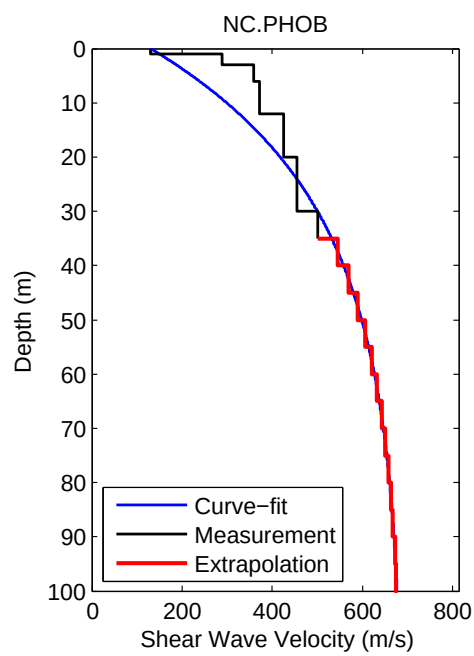

Linear Elastic Transfer Function

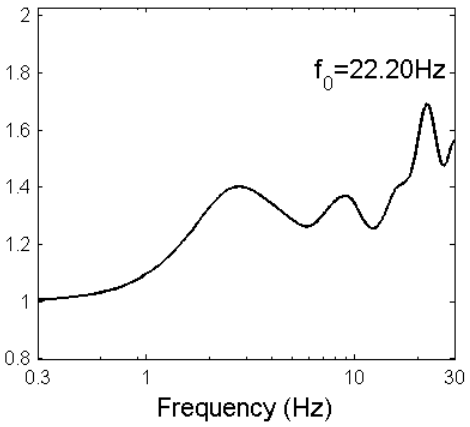

H/V Ratio – Sensor 450

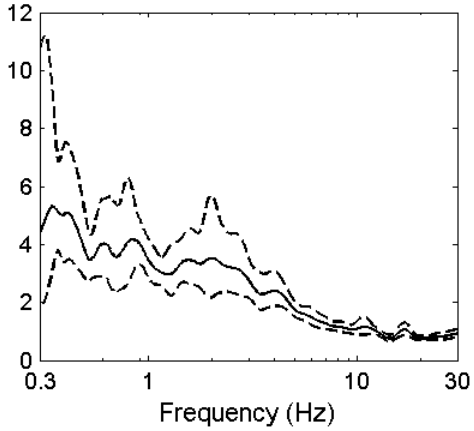

H/V Ratio – Sensor 507

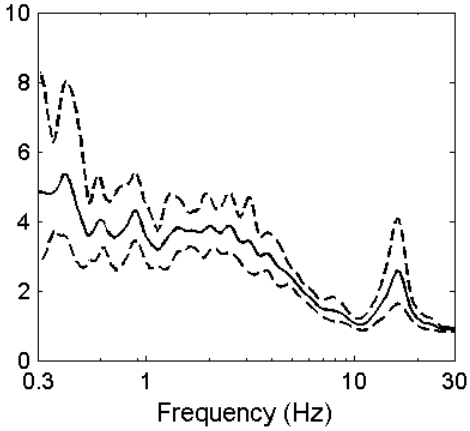

H/V Ratio – Sensor 453

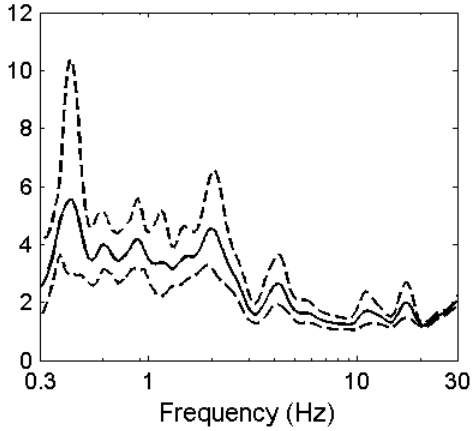

Equivalent Linear Transfer Function

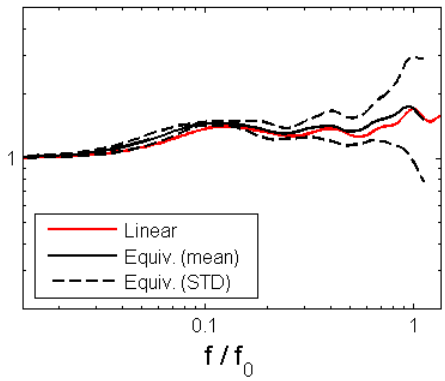

Equiv. Lin. TF (color coded by PGA_{RO})

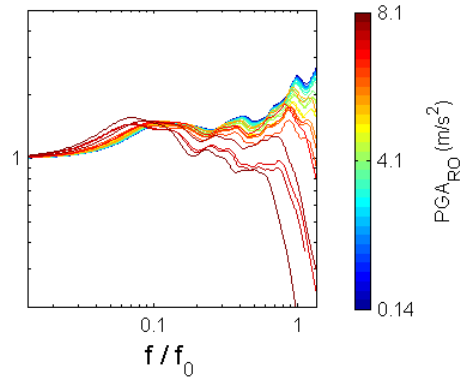

Non-linear Transfer Function

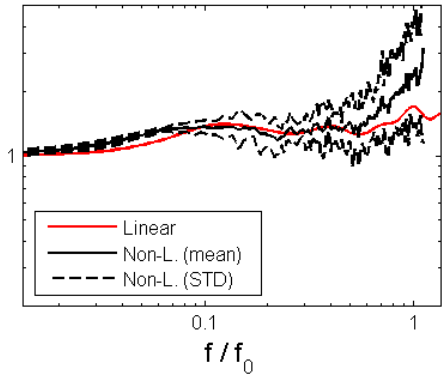

Non-linear TF (color coded by PGA_{RO})

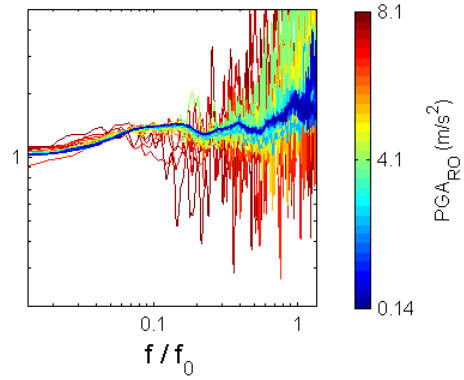

Equiv. Lin. TF (color coded by f_c)

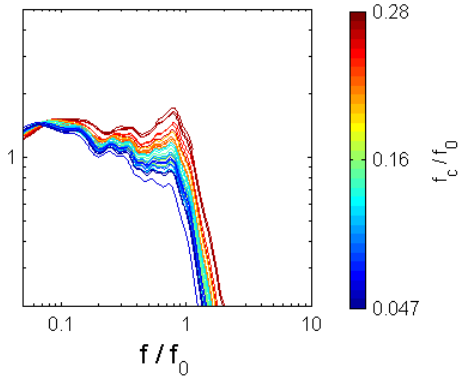

Non-linear TF (color coded by f_c)

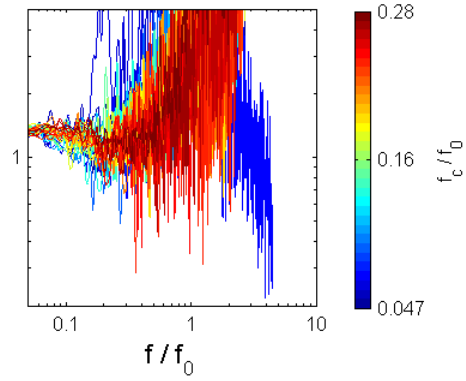

4.3.40 NC.PHSB

Depth (m)	Thickness (m)	V_s (m/s)	Damping ratio	Density (kg/m^3)
0	1	137	0.05	1600
1	2	210	0.05	1800
3	3	359	0.02	1800
6	4	405	0.02	1800
10	5	490	0.02	1800
15	7	539	0.02	1800
22	9	626	0.02	1800
31	–	796	0.01	1800

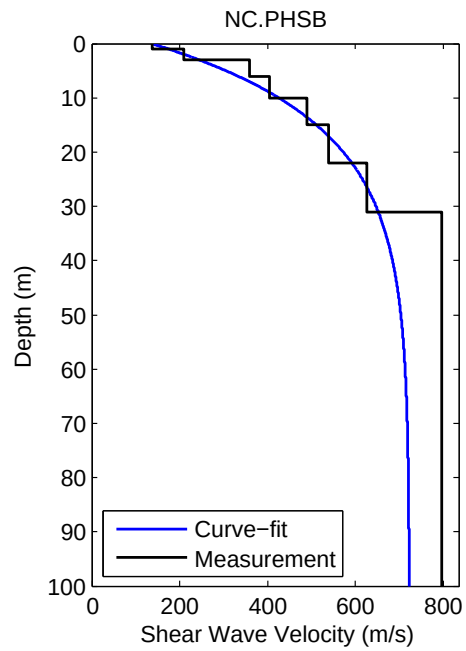

Linear Elastic Transfer Function

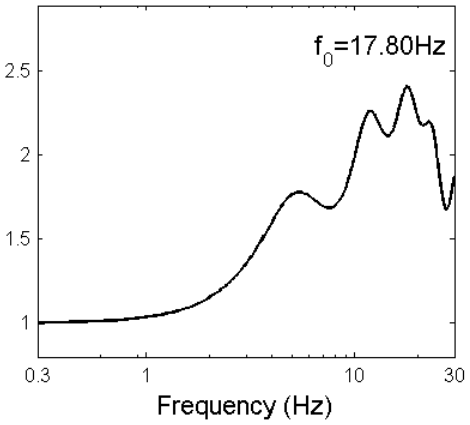

H/V Ratio – Sensor 453

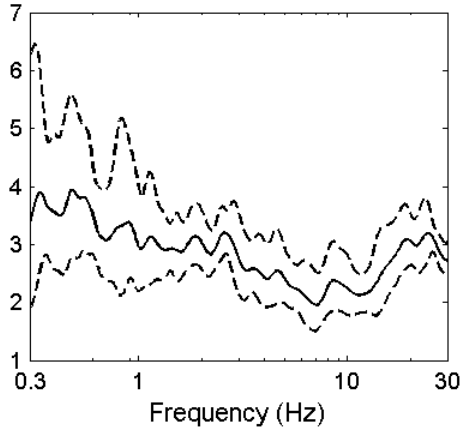

H/V Ratio – Sensor 507

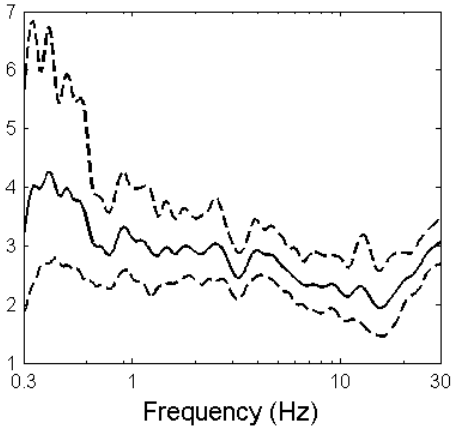

H/V Ratio – Sensor 507bis

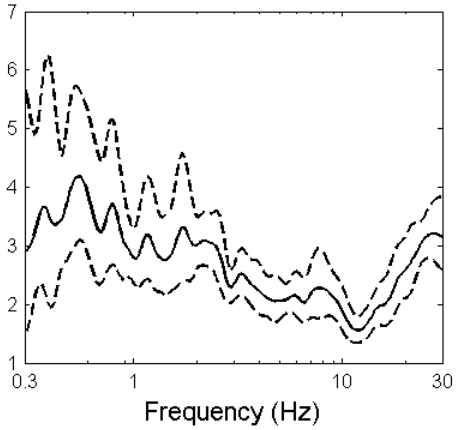

Equivalent Linear Transfer Function

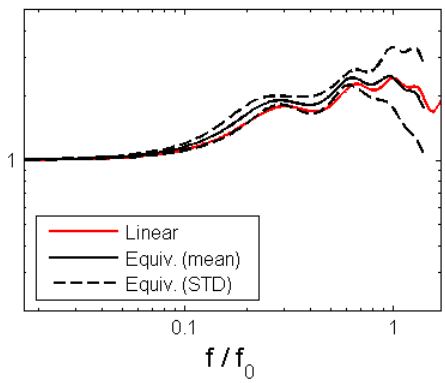

Equiv. Lin. TF (color coded by PGA_{RO})

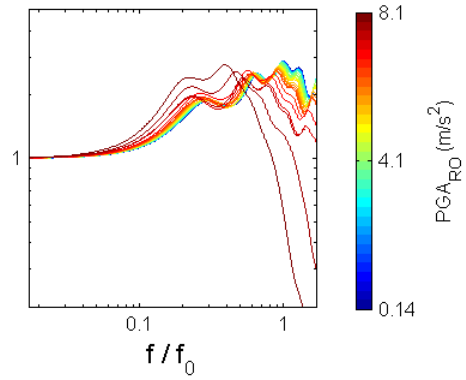

Non-linear Transfer Function

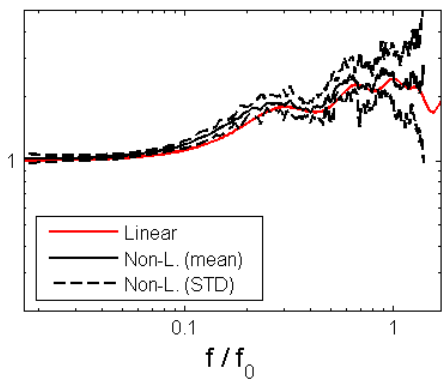

Non-linear TF (color coded by PGA_{RO})

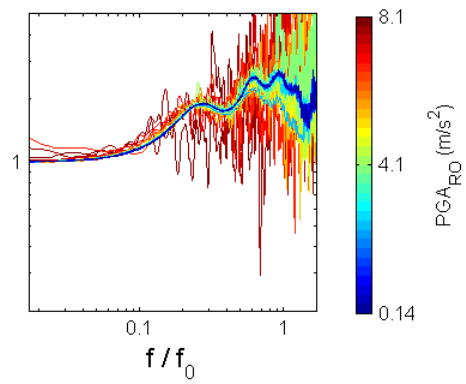

Equiv. Lin. TF (color coded by f_c)

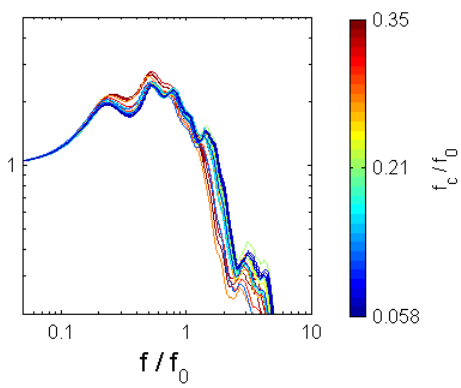

Non-linear TF (color coded by f_c)

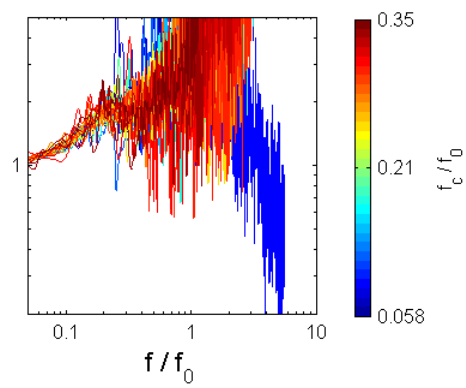

4.4 Class C/B

Class C/B sites include the following:

Site Code	V_{s30}-measured (m/s)	V_{s30}-adjusted (m/s)
CI.GLA	43	852
CI.HEC	726	768~795

4.4.1 CI.GLAa

Depth (m)	Thickness (m)	V_s (m/s)	Damping ratio	Density (kg/m^3)
0	1	221	0.05	1800
1	2	405	0.02	1800
3	3	634	0.02	1800
6	4	795	0.01	1800
10	6	891	0.01	2000
16	9	921	0.01	2000
25	5	1079	0.01	2000
30	5	1200.6	0.01	2000
35	5	1274.3	0.01	2000
40	5	1336.0	0.01	2000
45	5	1387.8	0.01	2000
50	5	1431.2	0.01	2000
55	5	1467.5	0.01	2000
60	5	1498.0	0.01	2000
65	5	1523.6	0.01	2000
70	5	1545.0	0.01	2000
75	5	1562.9	0.01	2000
80	5	1578.0	0.01	2000
85	5	1590.6	0.01	2000
90	5	1601.1	0.01	2000
95	5	1610.0	0.01	2000
100	–	1617.4	0.01	2000

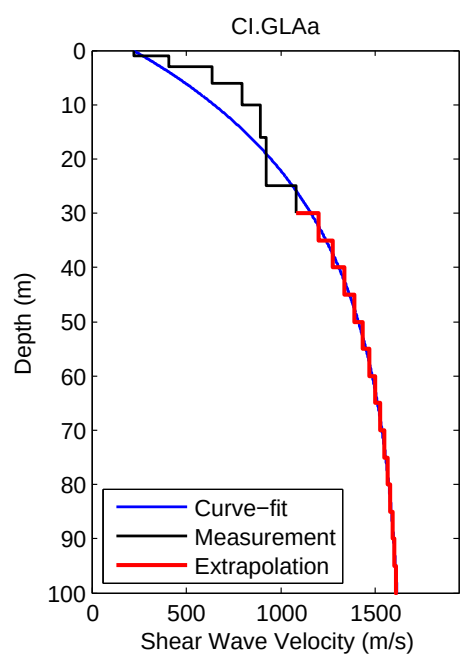

Linear Elastic Transfer Function

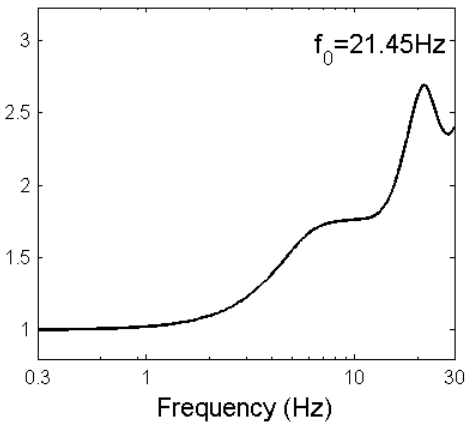

H/V Ratio – Sensor 450

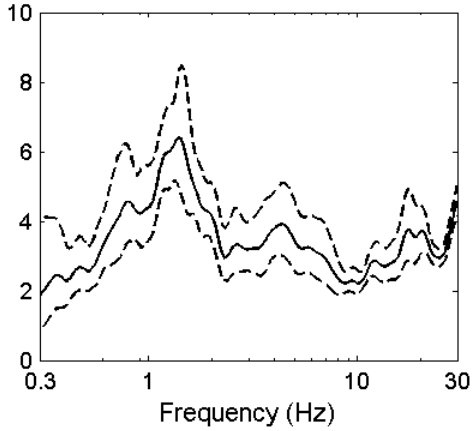

H/V Ratio – Sensor 507

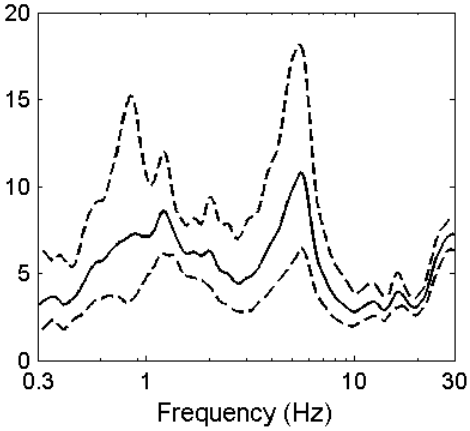

H/V Ratio – Sensor 453

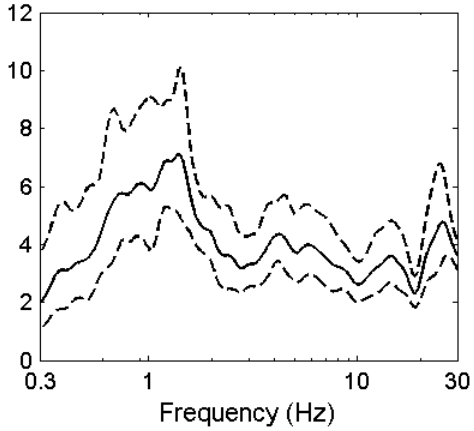

Equivalent Linear Transfer Function

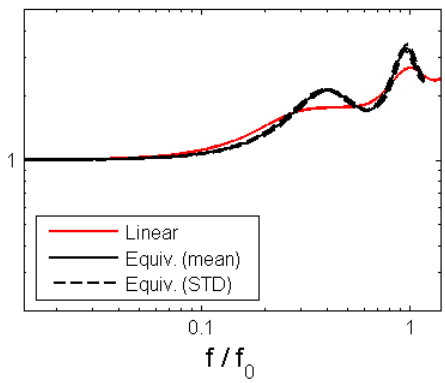

Equiv. Lin. TF (color coded by PGA_{RO})

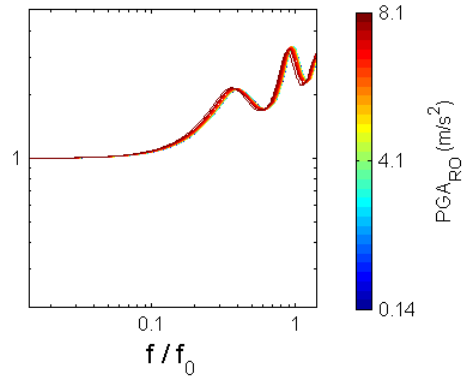

Non-linear Transfer Function

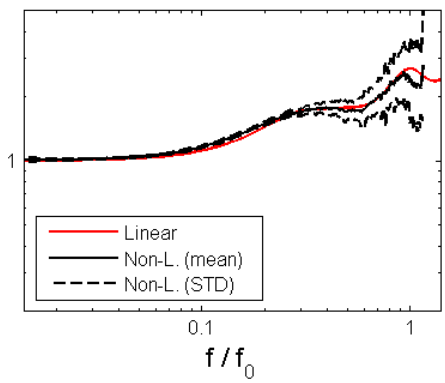

Non-linear TF (color coded by PGA_{RO})

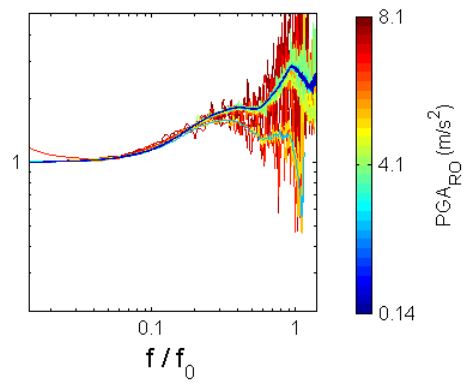

Equiv. Lin. TF (color coded by f_c)

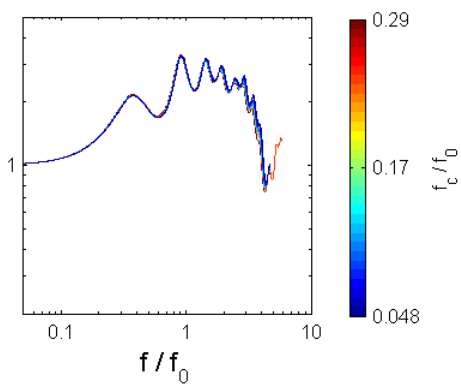

Non-linear TF (color coded by f_c)

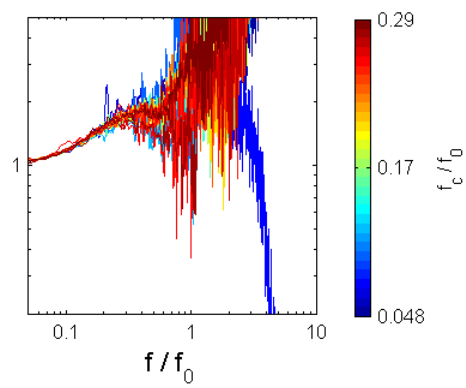

4.4.2 CI.GLAb

Depth (m)	Thickness (m)	V_s (m/s)	Damping ratio	Density (kg/m^3)
0	1	221	0.05	1800
1	2	405	0.02	1800
3	3	600	0.02	1800
6	4	700	0.02	1800
10	6	800	0.01	2000
16	9	925	0.01	2000
25	5	1100	0.01	2000
30	5	1188.6	0.01	2000
35	5	1262.6	0.01	2000
40	5	1325.0	0.01	2000
45	5	1377.4	0.01	2000
50	5	1421.5	0.01	2000
55	5	1458.7	0.01	2000
60	5	1489.9	0.01	2000
65	5	1516.2	0.01	2000
70	5	1538.3	0.01	2000
75	5	1557.0	0.01	2000
80	5	1572.6	0.01	2000
85	5	1585.8	0.01	2000
90	5	1596.9	0.01	2000
95	5	1606.2	0.01	2000
100	–	1614.1	0.01	2000

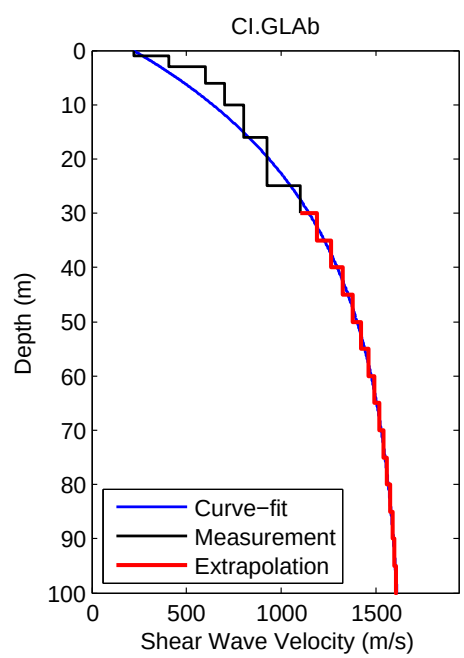

Linear Elastic Transfer Function

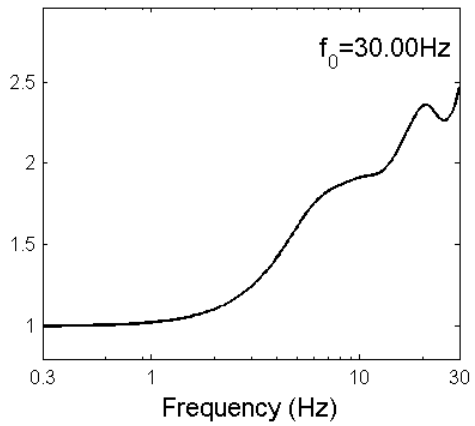

H/V Ratio – Sensor 450

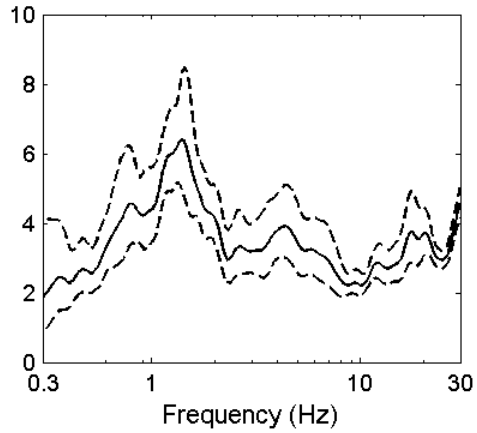

H/V Ratio – Sensor 507

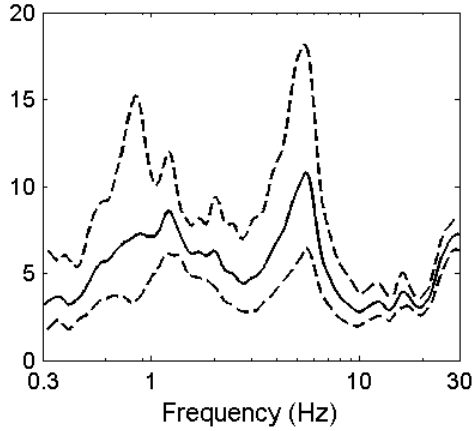

H/V Ratio – Sensor 453

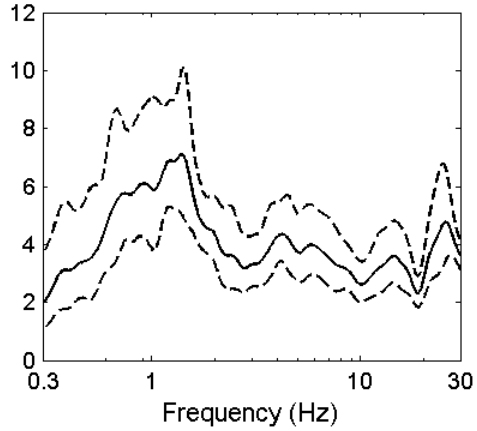

Equivalent Linear Transfer Function

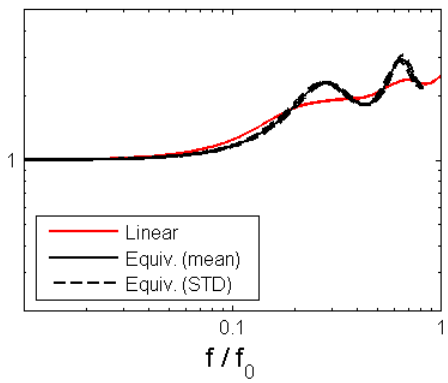

Equiv. Lin. TF (color coded by PGA_{RO})

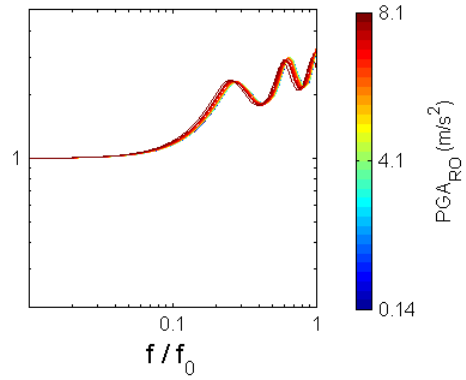

Non-linear Transfer Function

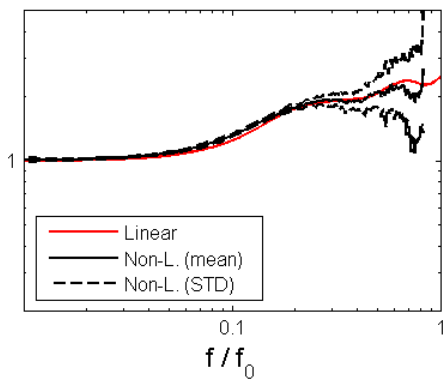

Non-linear TF (color coded by PGA_{RO})

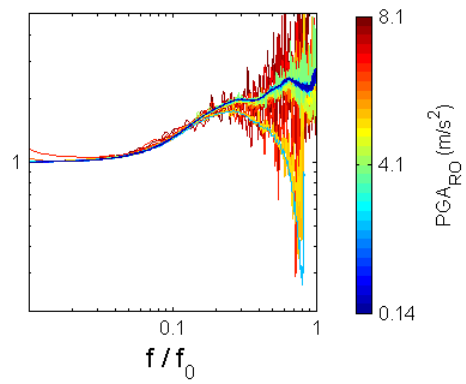

Equiv. Lin. TF (color coded by f_c)

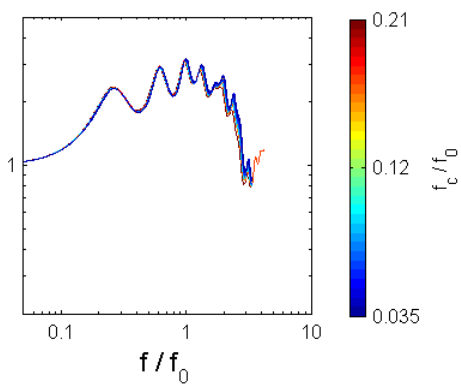

Non-linear TF (color coded by f_c)

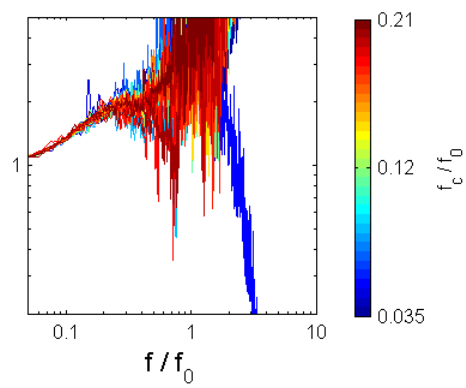

4.4.3 CI.GLAc

Depth (m)	Thickness (m)	V_s (m/s)	Damping ratio	Density (kg/m^3)
0	1	221	0.05	1800
1	2	405	0.02	1800
3	3	650	0.02	1800
6	4	925	0.01	2000
10	6	950	0.01	2000
16	9	975	0.01	2000
25	5	1050	0.01	2000
30	5	1224.2	0.01	2000
35	5	1297.1	0.01	2000
40	5	1357.6	0.01	2000
45	5	1407.9	0.01	2000
50	5	1449.7	0.01	2000
55	5	1484.5	0.01	2000
60	5	1513.4	0.01	2000
65	5	1537.4	0.01	2000
70	5	1557.4	0.01	2000
75	5	1574.0	0.01	2000
80	5	1587.8	0.01	2000
85	5	1599.3	0.01	2000
90	5	1608.8	0.01	2000
95	5	1616.7	0.01	2000
100	–	1623.3	0.01	2000

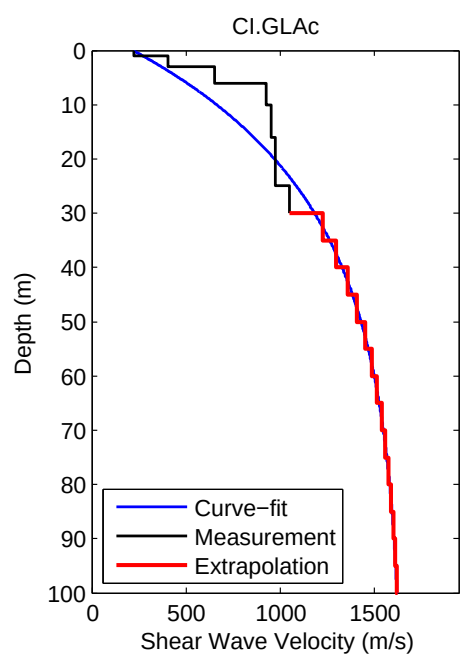

Linear Elastic Transfer Function

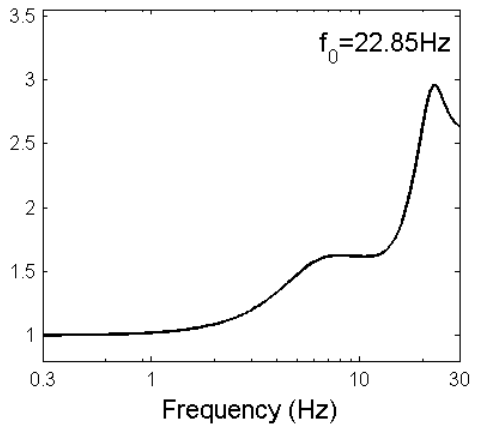

H/V Ratio – Sensor 450

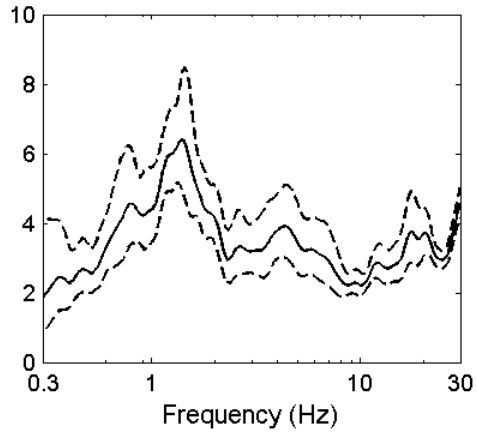

H/V Ratio – Sensor 507

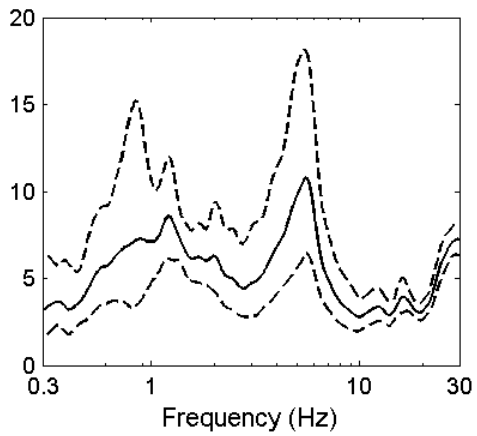

H/V Ratio – Sensor 453

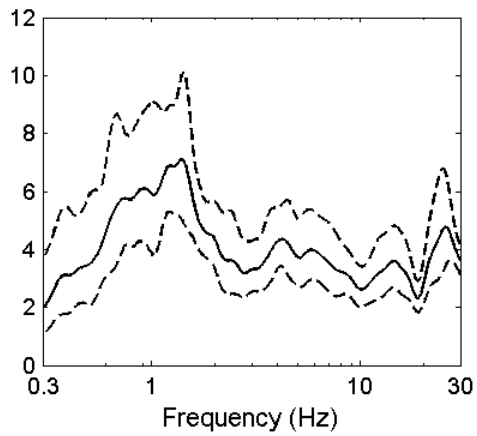

Equivalent Linear Transfer Function

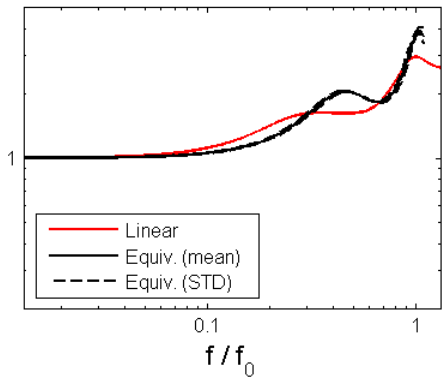

Equiv. Lin. TF (color coded by PGA_{RO})

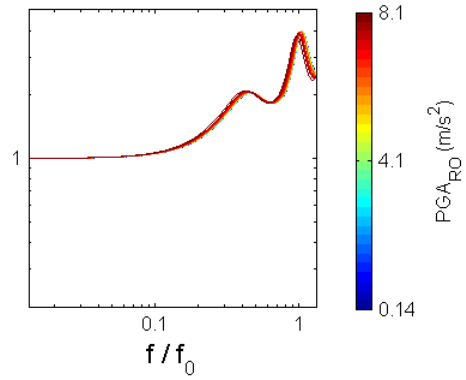

Non-linear Transfer Function

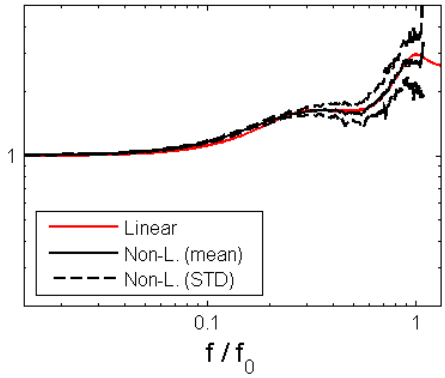

Non-linear TF (color coded by PGA_{RO})

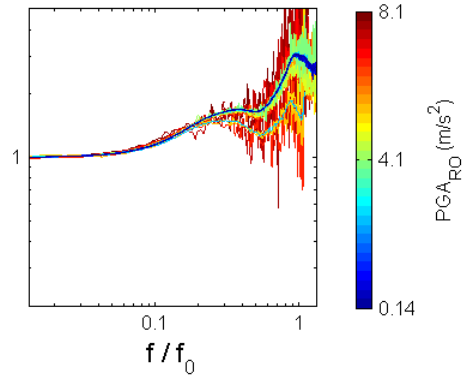

Equiv. Lin. TF (color coded by f_c)

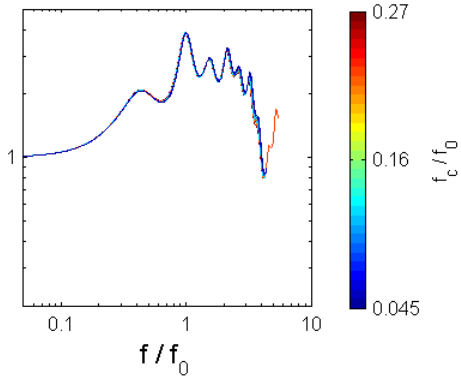

Non-linear TF (color coded by f_c)

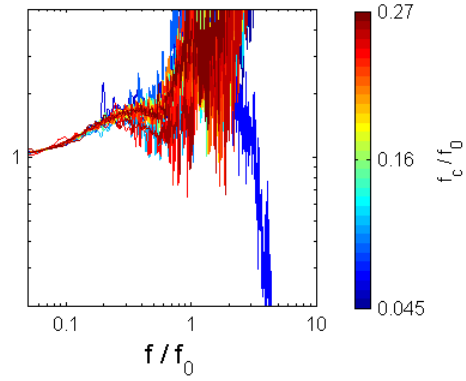

4.4.4 CI.GLAd

Depth (m)	Thickness (m)	V_s (m/s)	Damping ratio	Density (kg/m^3)
0	1	219	0.05	1800
1	2	394	0.02	1800
3	3	608	0.02	1800
6	4	769	0.01	1800
10	6	870	0.01	2000
16	9	907	0.01	2000
25	5	1066	0.01	2000
30	5	1183.8	0.01	2000
35	5	1258.1	0.01	2000
40	5	1320.7	0.01	2000
45	5	1373.4	0.01	2000
50	5	1417.9	0.01	2000
55	5	1455.3	0.01	2000
60	5	1486.9	0.01	2000
65	5	1513.5	0.01	2000
70	5	1535.9	0.01	2000
75	5	1554.7	0.01	2000
80	5	1570.6	0.01	2000
85	5	1584.0	0.01	2000
90	5	1595.3	0.01	2000
95	5	1604.9	0.01	2000
100	–	1612.9	0.01	2000

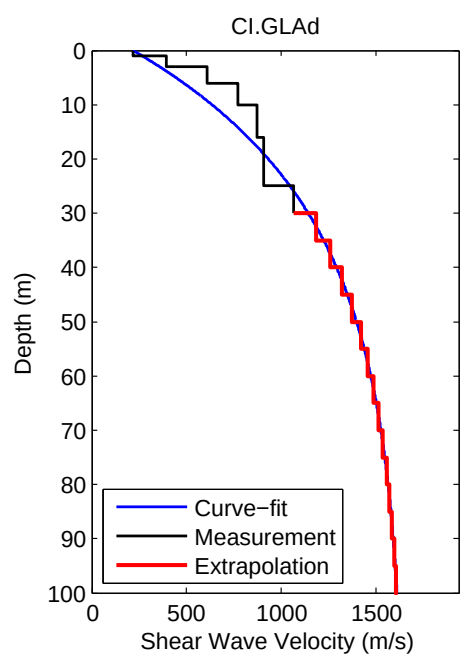

Linear Elastic Transfer Function

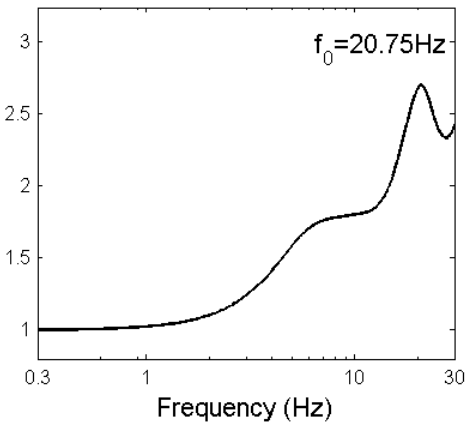

H/V Ratio – Sensor 450

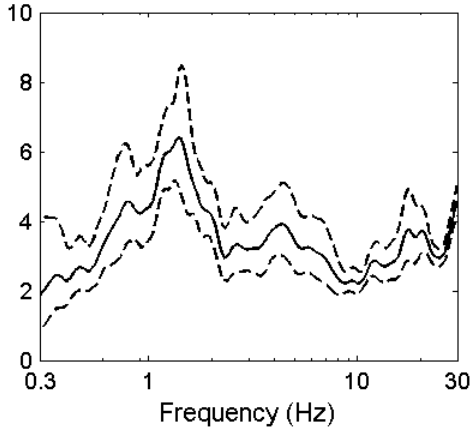

H/V Ratio – Sensor 507

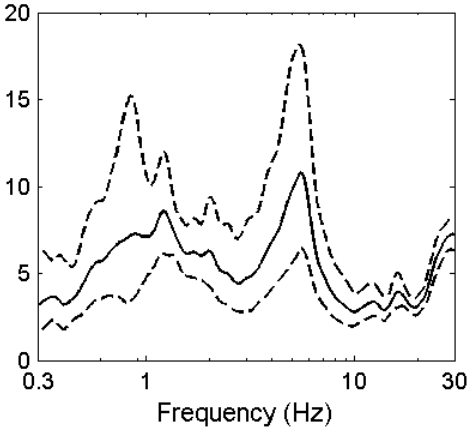

H/V Ratio – Sensor 453

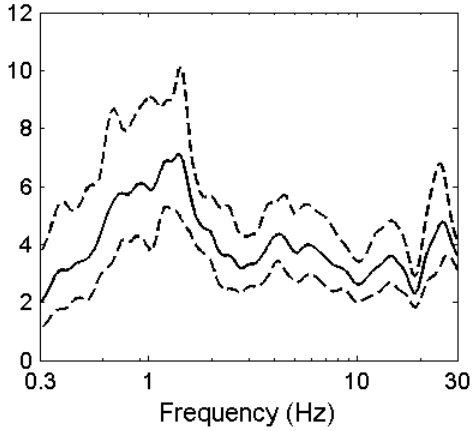

Equivalent Linear Transfer Function

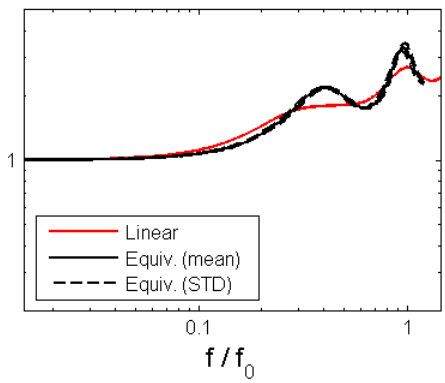

Equiv. Lin. TF (color coded by PGA_{RO})

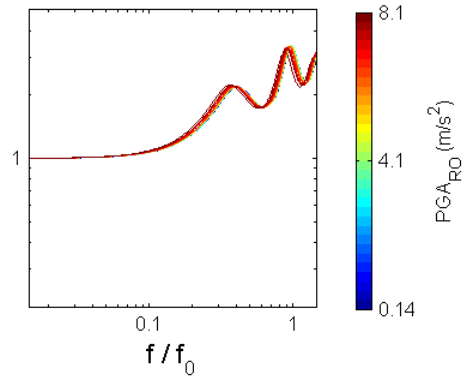

Non-linear Transfer Function

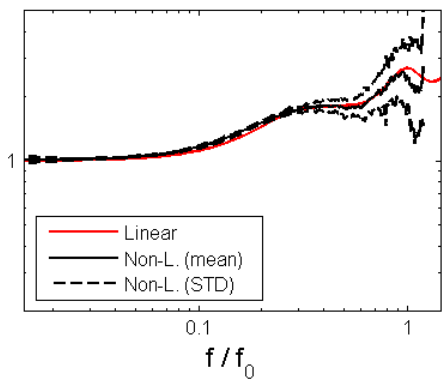

Non-linear TF (color coded by PGA_{RO})

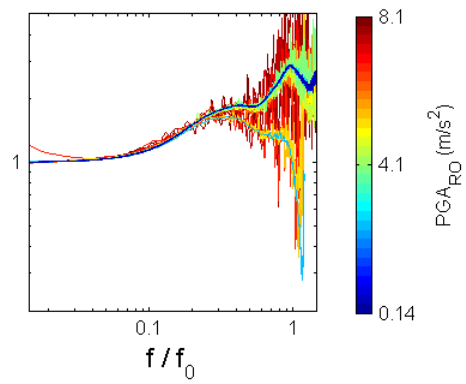

Equiv. Lin. TF (color coded by f_c)

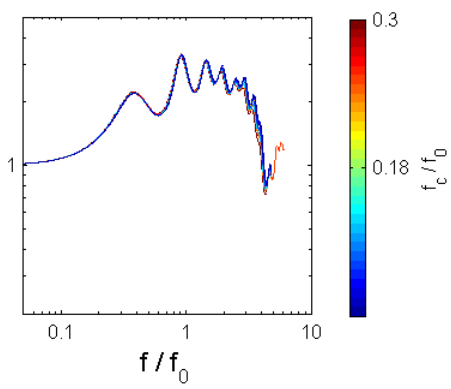

Non-linear TF (color coded by f_c)

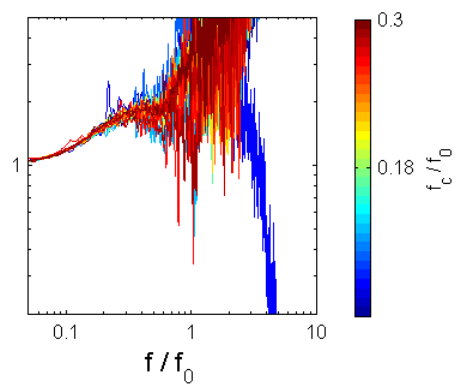

4.4.5 CI.HEC

Depth (m)	Thickness (m)	V_s (m/s)	Damping ratio	Density (kg/m^3)
0	1	225	0.05	1800
1	1.5	451	0.02	1800
2.5	9.5	812	0.01	2000
12	18	825	0.01	2000
30	10	1155	0.01	2000
40	5	1205.4	0.01	2000
45	5	1253.6	0.01	2000
50	5	1294.4	0.01	2000
55	5	1329.0	0.01	2000
60	5	1358.2	0.01	2000
65	5	1383.0	0.01	2000
70	5	1404.0	0.01	2000
75	5	1421.7	0.01	2000
80	5	1436.8	0.01	2000
85	5	1449.5	0.01	2000
90	5	1460.3	0.01	2000
95	5	1469.4	0.01	2000
100	–	1477.1	0.01	2000

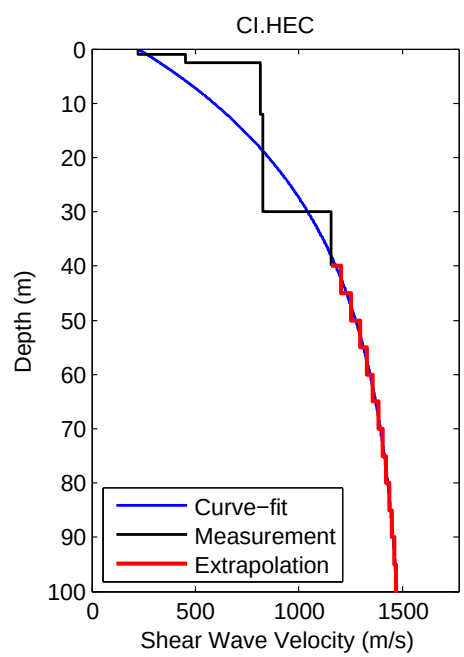

Linear Elastic Transfer Function

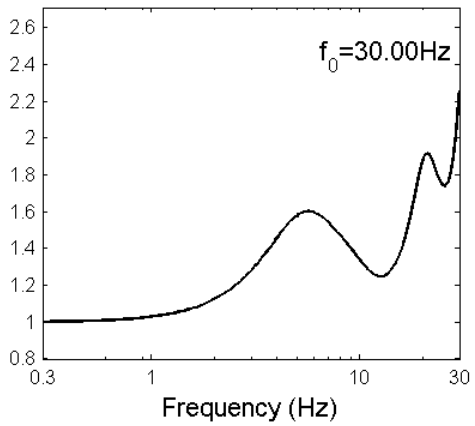

H/V Ratio – Sensor 450

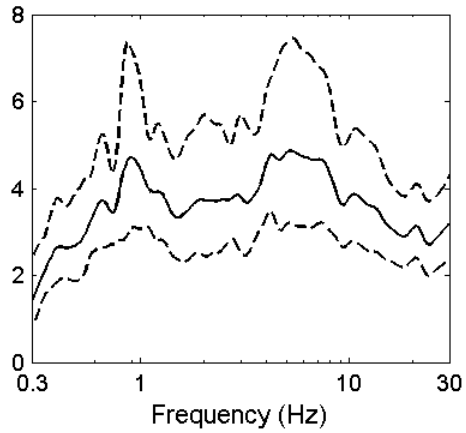

H/V Ratio – Sensor 507

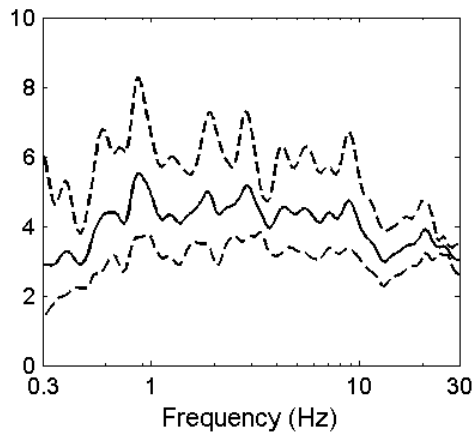

H/V Ratio – Sensor 453

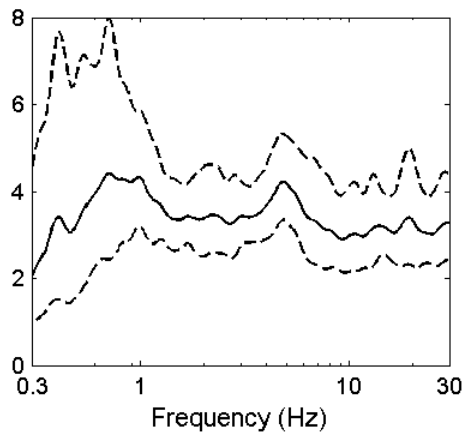

Equivalent Linear Transfer Function

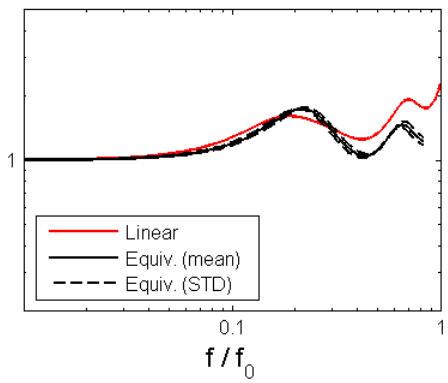

Equiv. Lin. TF (color coded by PGA_{RO})

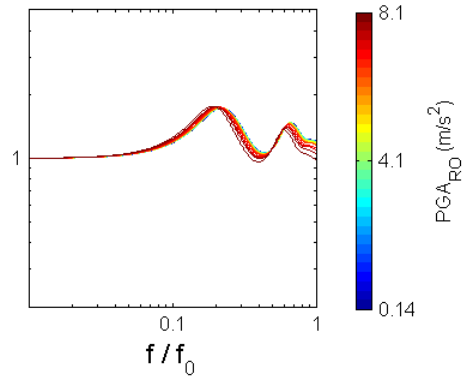

Non-linear Transfer Function

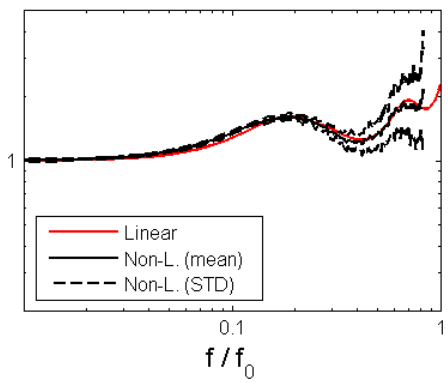

Non-linear TF (color coded by PGA_{RO})

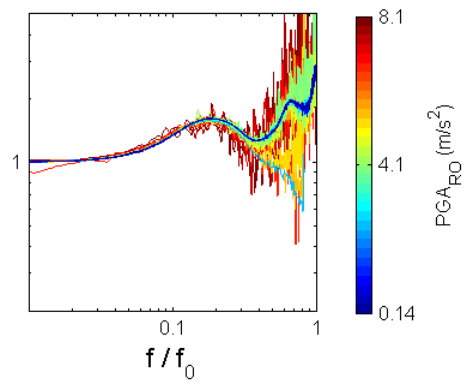

Equiv. Lin. TF (color coded by f_c)

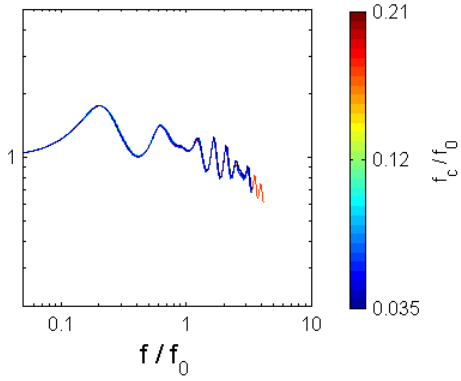

Non-linear TF (color coded by f_c)

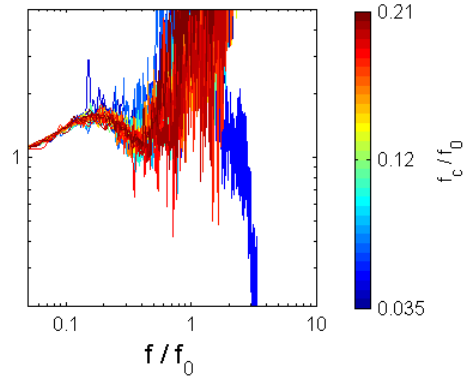

4.5 Class B

Class B sites include the following:

Site Code	V_{s30}-measured (m/s)	V_{s30}-adjusted (m/s)
CI.BEL	796	796
CI.IRM	981	1055

4.5.1 CI.BEL

Depth (m)	Thickness (m)	V_s (m/s)	Damping ratio	Density (kg/m^3)
0	2	505	0.02	1800
2	3	697	0.02	1800
5	5	802	0.01	2000
10	7	840	0.01	2000
17	9	851	0.01	2000
26	4	933	0.01	2000
30	5	996.7	0.01	2000
35	5	1042.1	0.01	2000
40	5	1082.1	0.01	2000
45	5	1117.2	0.01	2000
50	5	1148.1	0.01	2000
55	5	1175.3	0.01	2000
60	5	1199.2	0.01	2000
65	5	1220.3	0.01	2000
70	5	1238.7	0.01	2000
75	5	1255.0	0.01	2000
80	5	1269.3	0.01	2000
85	5	1281.9	0.01	2000
90	5	1292.9	0.01	2000
95	5	1302.7	0.01	2000
100	–	1311.2	0.01	2000

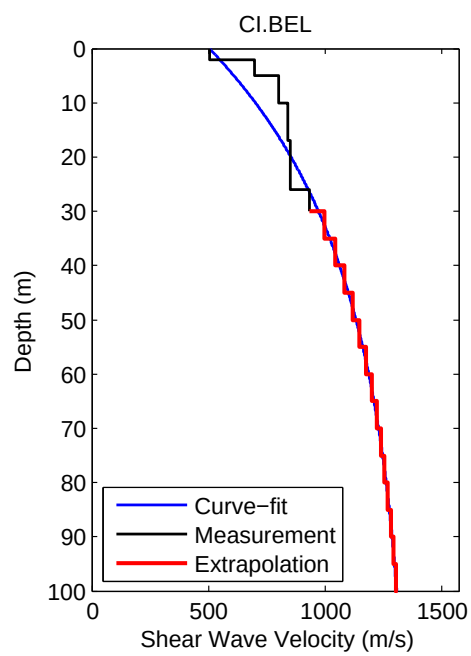

Linear Elastic Transfer Function

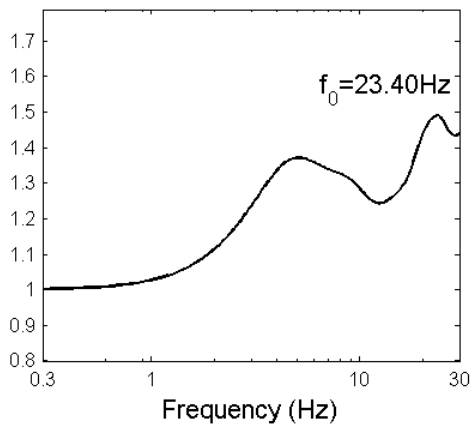

H/V Ratio – Sensor 450

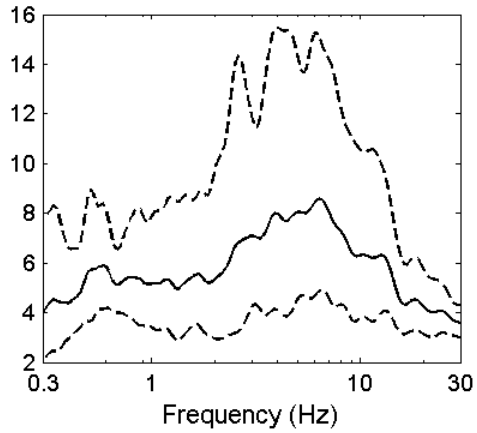

H/V Ratio – Sensor 507

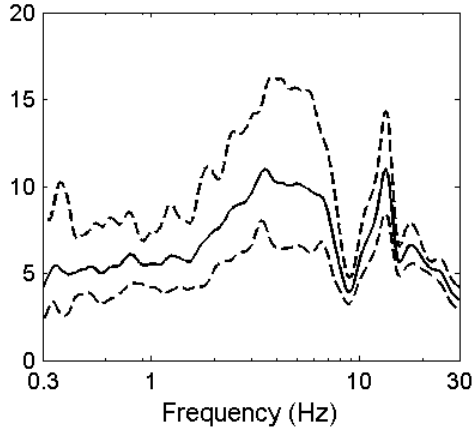

H/V Ratio – Sensor 453

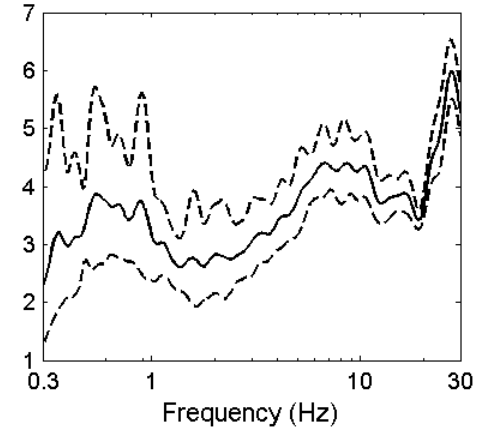

Equivalent Linear Transfer Function

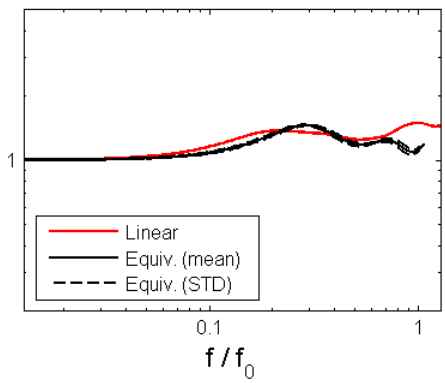

Equiv. Lin. TF (color coded by PGA_{RO})

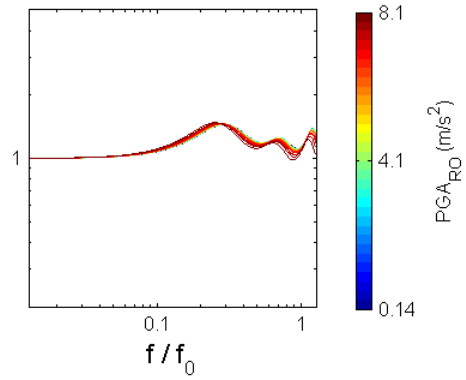

Non-linear Transfer Function

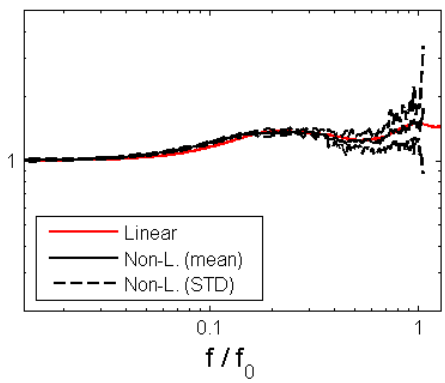

Non-linear TF (color coded by PGA_{RO})

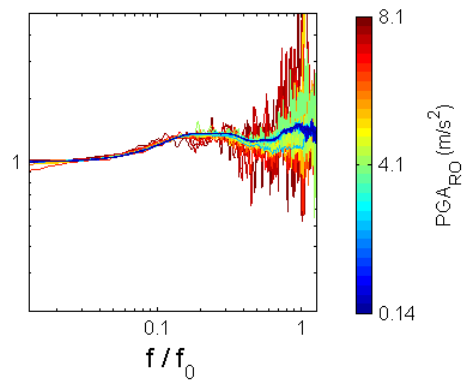

Equiv. Lin. TF (color coded by f_c)

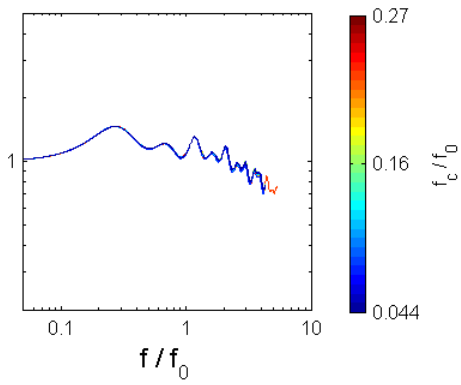

Non-linear TF (color coded by f_c)

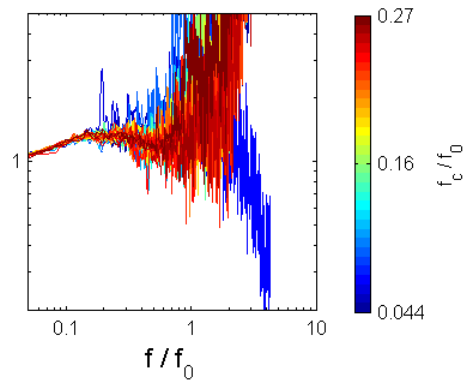

4.5.2 CI.IRM

Depth (m)	Thickness (m)	V_s (m/s)	Damping ratio	Density (kg/m^3)
0	1.5	350	0.02	1800
1.5	2.5	697	0.02	1800
4	3	884	0.01	2000
7	4	1085	0.01	2000
11	6	1133	0.01	2000
17	8	1197	0.01	2000
25	5	1373	0.01	2000
30	5	1485.1	0.01	2000
35	5	1553.3	0.01	2000
40	5	1607.7	0.01	2000
45	5	1651.0	0.01	2000
50	5	1685.5	0.01	2000
55	5	1713.0	0.01	2000
60	5	1734.8	0.01	2000
65	5	1752.3	0.01	2000
70	5	1766.2	0.01	2000
75	5	1777.2	0.01	2000
80	5	1786.0	0.01	2000
85	5	1793.1	0.01	2000
90	5	1798.7	0.01	2000
95	5	1803.1	0.01	2000
100	–	1806.7	0.01	2000

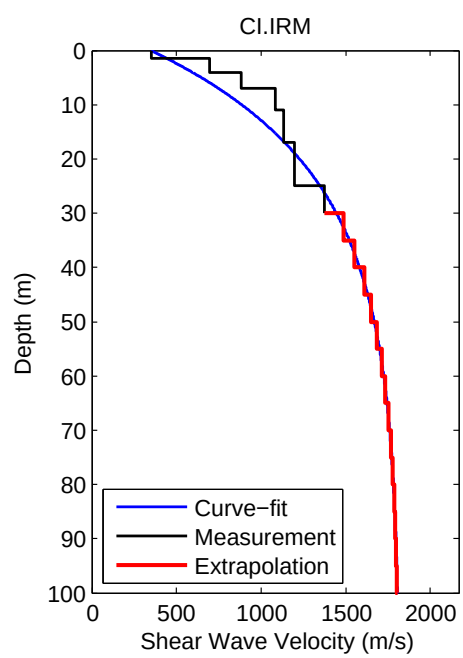

Linear Elastic Transfer Function

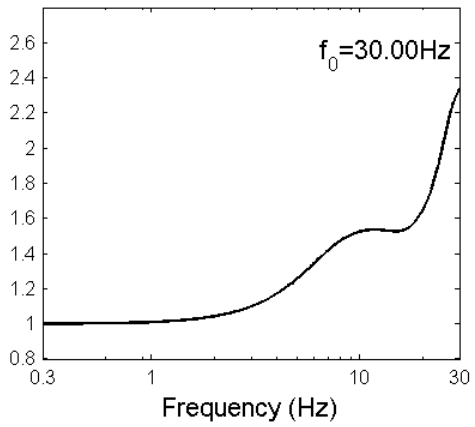

H/V Ratio – Sensor 450

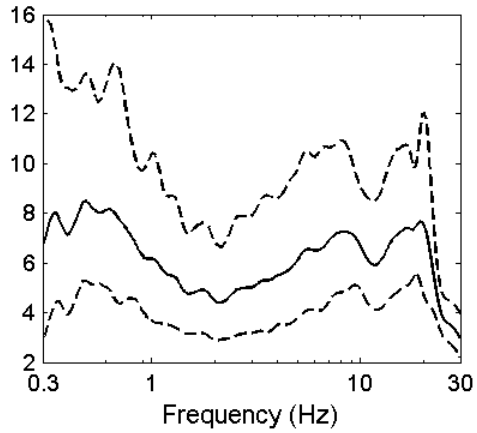

H/V Ratio – Sensor 507

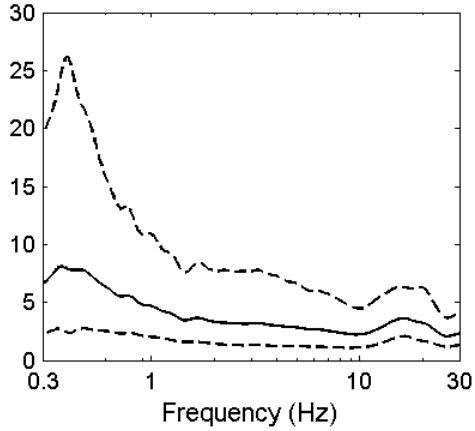

H/V Ratio – Sensor 453

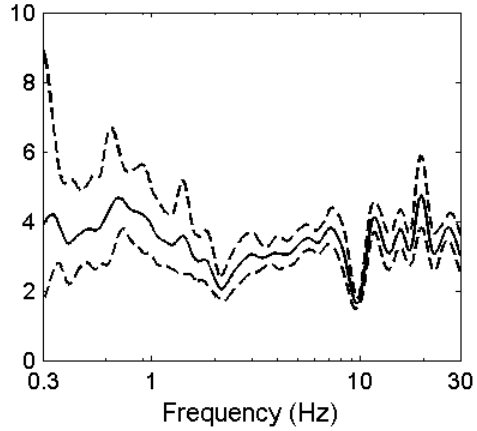

Equivalent Linear Transfer Function

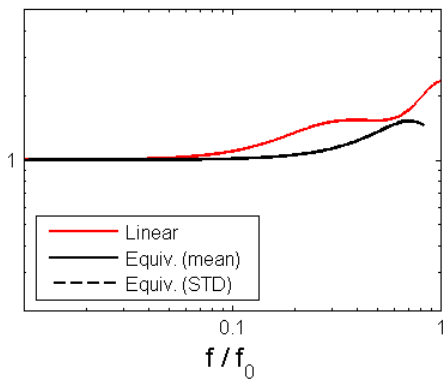

Equiv. Lin. TF (color coded by PGA_{RO})

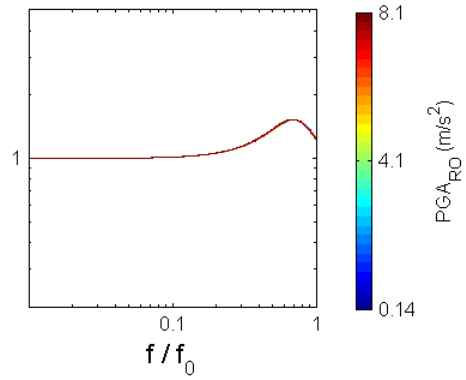

Non-linear Transfer Function

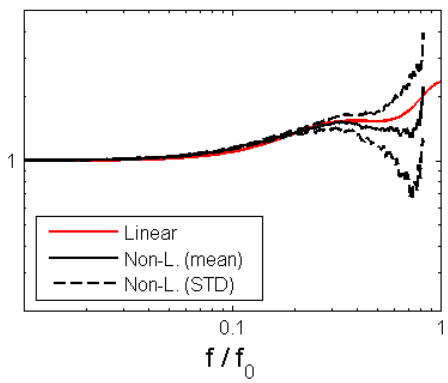

Non-linear TF (color coded by PGA_{RO})

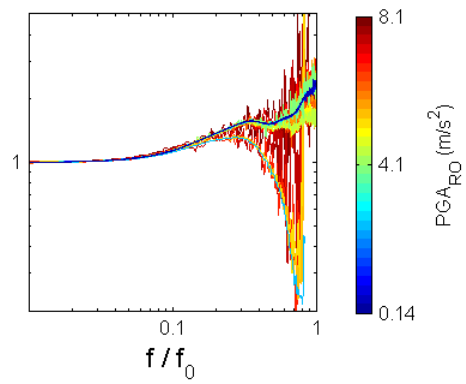

Equiv. Lin. TF (color coded by f_c)

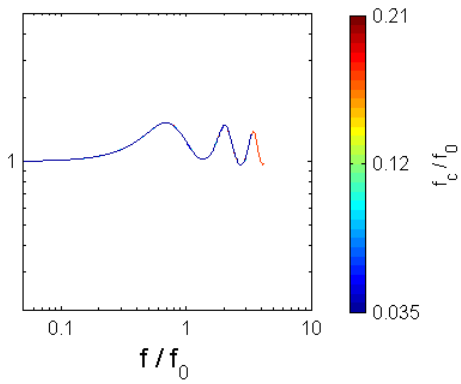

Non-linear TF (color coded by f_c)

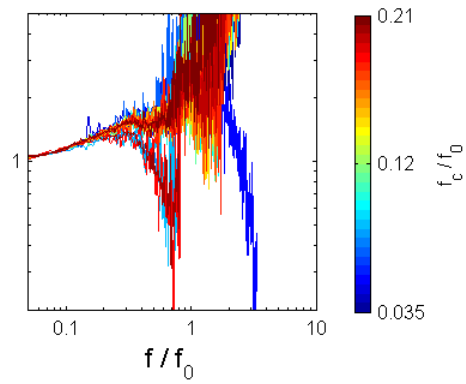

4.6 Class B/A

Class B/A sites include the following:

Site Code	V_{s30}-measured (m/s)	V_{s30}-adjusted (m/s)
CI.PDM	1399	1587

4.6.1 CI.PDM

Depth (m)	Thickness (m)	V_s (m/s)	Damping ratio	Density (kg/m^3)
0	3	472	0.02	1800
3	15	1739	0.01	2000
18	2	1861	0.01	2000
20	5	1879.2	0.01	2000
25	5	2044.3	0.01	2000
30	5	2177.0	0.01	2000
35	5	2283.6	0.01	2000
40	5	2369.4	0.01	2000
45	5	2438.3	0.01	2000
50	5	2493.7	0.01	2000
55	5	2538.2	0.01	2000
60	5	2574.0	0.01	2000
65	5	2602.8	0.01	2000
70	5	2625.9	0.01	2000
75	5	2644.5	0.01	2000
80	5	2659.4	0.01	2000
85	5	2671.4	0.01	2000
90	5	2681.0	0.01	2000
95	5	2688.8	0.01	2000
100	–	2695.0	0.01	2000

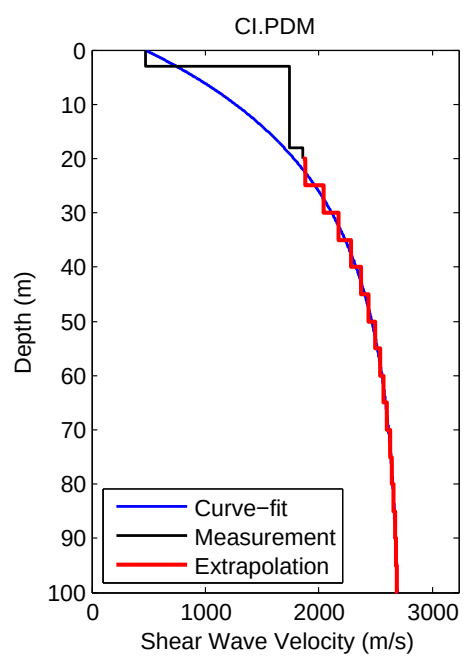

Linear Elastic Transfer Function

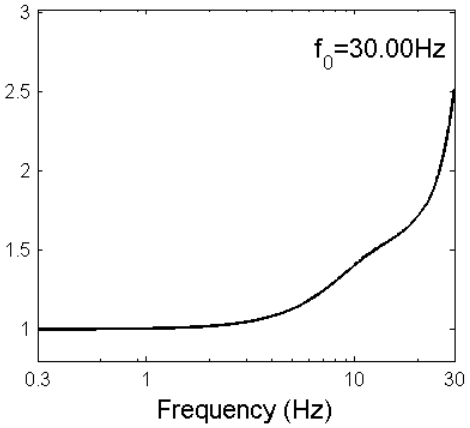

H/V Ratio – Sensor 450

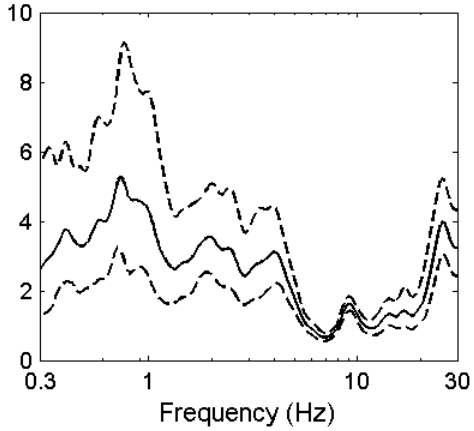

H/V Ratio – Sensor 507

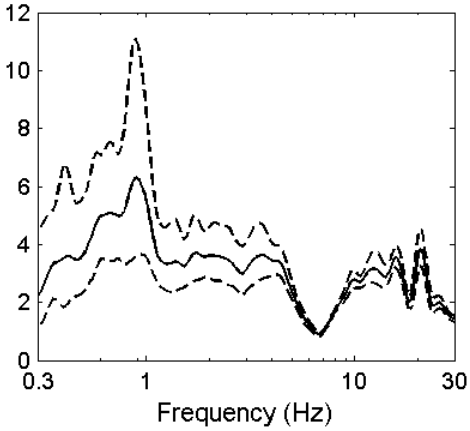

H/V Ratio – Sensor 453

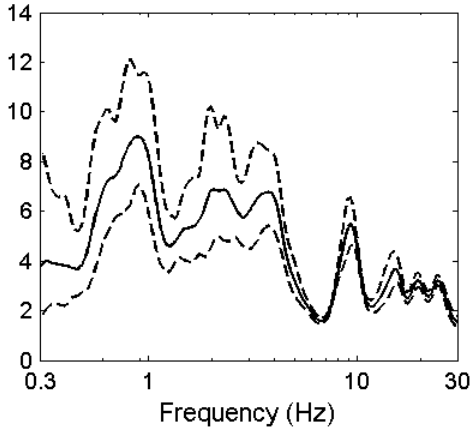

Equivalent Linear Transfer Function

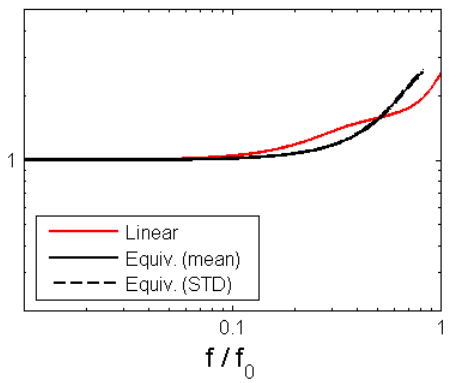

Equiv. Lin. TF (color coded by PGA_{RO})

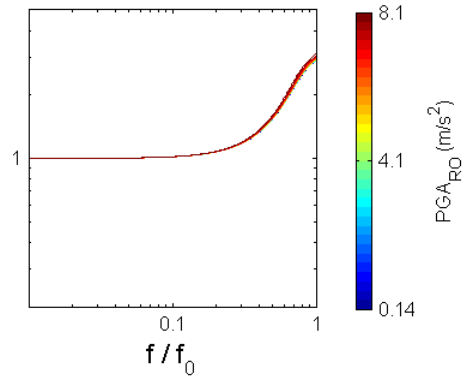

Non-linear Transfer Function

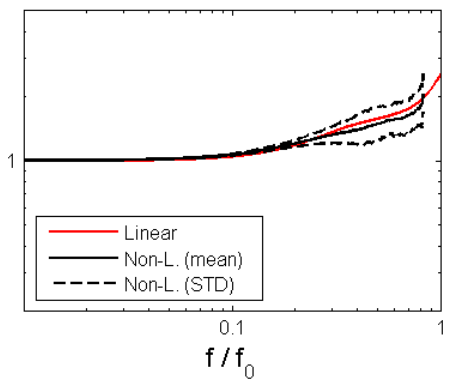

Non-linear TF (color coded by PGA_{RO})

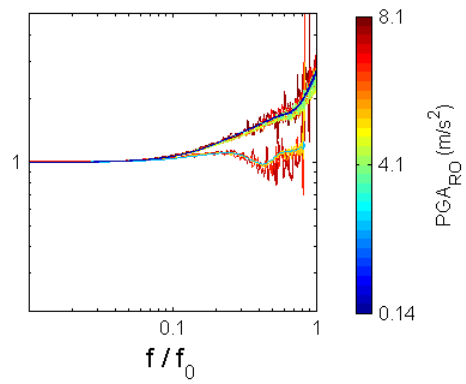

Equiv. Lin. TF (color coded by f_c)

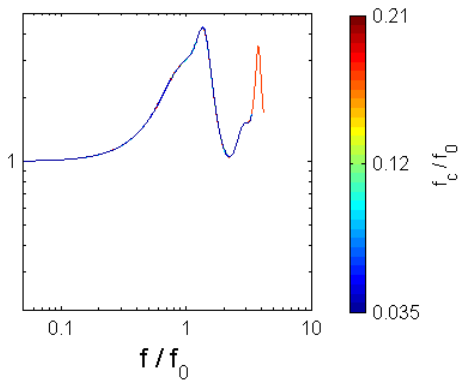
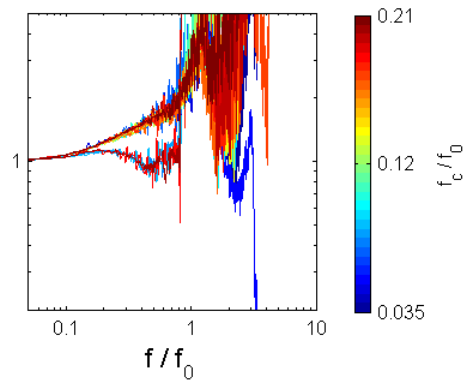
Non-linear TF (color coded by f_c)